Numerical investigation of spinal neuron facilitation with multi-electrode epidural stimulation

Thesis by
Jeffrey A. Edlund

In Partial Fulfillment of the Requirements for the
degree of
Doctor of Philosophy

CALIFORNIA INSTITUTE OF TECHNOLOGY
Pasadena, California

2019
Defended October 15, 2018

Jeffrey A. Edlund
ORCID: 0000-0003-3092-4493

ACKNOWLEDGEMENTS

Thank you to my wife Jian Yuan, my daughter Freyja, my family, and Jian Yuan's family for all their patience and support.

Thank you to my PhD advisor Professor Joel Burdick for his help, support, and feedback.

Special thank you to Ellen Feldman Novoseller for reading the entire thesis and giving valuable feedback.

Thank you to all my friends and colleagues at Caltech, especially Melissa Tanner, Ellen Feldman Novoseller, Greg Griffin, Tom Allen, and Tom Desautels.

Professor Reggie Edgerton and Parag Gad from UCLA provided valuable discussions.

I'd also like to acknowledge my former advisors and supervisors: Chris Adami, Issa Nesnas, Tom Prince, Massimo Tinto, Thomas Sterling, and Daniel Savarese.

A number of other people and friends have supported me in various ways: Alice, Athena Castro, Greg Fletcher, Daniel Castro, Serina Diniega, Jon, Kheang Yang, and more.

ABSTRACT

Approximately 1,275,000 people in the US have a spinal cord injury severe enough to cause some paralysis of the arms and/or legs. Epidural stimulation using implanted multi-electrode stimulating arrays over the lumbosacral spinal cord has recently shown promise in assisting individuals with severe spinal cord injuries to stand, walk, and even facilitate voluntary movement. Both animal model and human studies have shown that sub-threshold facilitation of motor recovery gives the best results. The underlying neural mechanisms by which sub-threshold epidural stimulation leads to motor recovery are incompletely known.

This thesis uses computational methods to study the *facilitation effect*. A neuron is facilitated if a sub-threshold synaptic input can cause a neuronal output under the influence of a stimulating electric field. The analysis in this thesis is based on a computational model of the epidural spinal stimulation process in the rat spinal cord. This model includes a time-domain finite element simulation (using COMSOL®) of the various tissues in the spinal cord with the appropriate anisotropic and frequency-dependent complex relative permittivities. The voltages obtained from the finite element simulations were used as the extracellular voltage in NEURON simulations.

A population of neurons was simulated under a wide variety of conditions. These simulations highlight the effect of neuron orientation, location, and synaptic timing as key parameters which influence facilitation.

This study indicates that regions of the spinal cord that have previously been ignored may be actively involved in motor recovery. These results may also enable the design of specialized epidural electrode arrays and the design of new stimulation protocols.

TABLE OF CONTENTS

LIST OF ILLUSTRATIONS

Number *Page*

c

LIST OF TABLES

Number *Page*

NOMENCLATURE

neurite. Any projection from the neuron cell body; a dendrite or an axon.

sub-threshold. In this thesis sub-threshold indicates that the electrical stimulation or the synaptic input does not cause neurotransmitter release from the neuron(s) simulated.

Chapter 1

INTRODUCTION

A survey conducted by the Christopher & Dana Reeve Foundation in 2008 (summarized in (Cahill, Fredine, and Zilberman, 2009)) revealed that approximately 1.9% of the population of the United States (5,596,000 people) reported some form of paralysis of their arms and legs. Stroke is the leading cause of paralysis (29% or 1,608,000 people) followed by spinal cord injury (SCI) (23% or 1,275,000 people). Work accidents (28%) and motor vehicle accidents (24%) are the leading causes of spinal cord injury followed by sporting and recreational accidents (16%). The average person with a SCI has been living with it for 15.6 years. It has been estimated that about 300,000 people of this population are confined to wheel chairs. It is this population that motivates this thesis.

While physical therapy is helpful for people with SCI, it is often insufficient to recover useful motor and autonomic function. In such cases, alternative treatments are sought. Epidural stimulation has recently shown promise as a therapy for SCI (Harkema et al., 2011). In this therapeutic approach, a multi-electrode array is implanted in the epidural space over either the cervical enlargement for quadriplegia patients or over the lumbosacral enlargement for paraplegics. A series of pulse trains are applied to selected electrodes in order to excite and *facilitate* the operation of the sensory motor feedback circuits that control limb activity. See Fig. 2.8 for an example of electrode placement.

The analysis in this thesis is most relevant to the motor complete paraplegic subpopulation, but the results should also benefit the treatment of motor complete quadriplegia. From a clinical perspective, paralysis is defined to be motor complete when no voluntary control of muscle is possible for the muscles which are inner-

vated by the spinal cord below the level of the injury. While the work in this thesis is most motivated by efforts to use epidural stimulation to recover motor function in complete paralysis, the results should be useful in cases of incomplete or partial paralysis.

In the absence of supraspinal input (from the brain) there is an upregulation of inhibitory receptors in the lumbosacral spinal cord after an SCI. Combined with the loss of supraspinal input, the lower limb motor control circuitry enters an inactive state. Without supraspinal input, Edgerton and colleagues (Edgerton et al., 2008; Courtine et al., 2009) discussed how pharmacological mechanisms (such as quipazine (a serotonin agonist)) and/or epidural stimulation can be used to modulate the physiological state of the spinal cord to facilitate locomotion or standing in response to signals from afferent fibers (sensory input). For both pharamcological mechanisms and epidural stimulation, the key to facilitation appears to be an application of the right amount of sub-threshold drug intervention and/or electrical stimulation. Too much of either can cause direct neuron activation independent of the state of the afferent inputs.

Studies in humans (Harkema et al., 2011) have shown similar responses (standing, walking, improvements to autonomic function) to epidural stimulation. However, in humans most of the injuries leave some supraspinal input intact, just not enough (in the case of clinically complete spinal injuries) to activate the spinal cord without external help (from epidural, transcutaneous, or other form of stimulation). It is unclear how much the remaining supraspinal input is involved with the standing and walking behaviors in spinally stimulated humans with SCI, but epidural stimulation has also been shown to facilitate voluntary leg movement in clinically complete subjects. Thus epidural stimulation is able to facilitate the spinal cord response to both afferent and weak supraspinal input. These studies (Edgerton et al., 2008; Harkema et al., 2011) have also shown that the optimal selection of the stimulat-

ing parameters (for example, the amplitude on each electrode, frequency, polarity, and pulse width) varies significantly across subjects, making it difficult to find the optimal stimulation parameters. All of these studies appear to work best with stimulation that is best described as sub-threshold. In experiments with live animals, that threshold is usually based on the observed level of muscle activity. Stimulation with magnitudes above direct motor stimulation is usually counter productive. In this thesis the threshold is based on neurotransmitter release. The mechanisms underlying the facilitation of motor function using epidural stimulation are at present poorly known. A better understanding of how epidural stimulation facilitates spinal cord function may allow us to build better electrode arrays (design, number of electrodes, location in the spinal cord, etc.), shape stimulating waveforms, and perhaps find better targeted drug therapy.

This thesis uses computational methods to study the facilitation of interneurons inside the spinal cord with glutamate receptive synapses as suggested in (Edgerton et al., 2008). In this thesis, facilitation is defined as a process which allows subthreshold synaptic inputs to control the output of the neuron (i.e. neurotransmitter release) in the presence of electrical stimulation. Table 1.1 summarizes the possible outcomes (neurotransmitter release, facilitated neurotransmitter release, or no neurotransmitter release) for varying amounts of stimulation and synaptic input. Existing computational studies have focused on direct activation of the dorsal afferent fibers as they enter the spinal cord (Capogrosso et al., 2013; J Ladenbauer et al., 2010), finding that the spinal interneurons are too difficult to activate. However, these simulations did not include synaptic input in a meaningful way or include active dendrites.

To study facilitation, I built a volume conductor model of the rat spinal cord, including an epidural electrode array and 3D models of interneurons with synaptic input, located at 66 locations throughout the cord in 6 different orientations. These

Table 1.1: This table summarizes the possible results of varying amounts of stimulation and synaptic input for a neuron in the spinal cord. Sub-threshold and super-threshold refer to the threshold of synaptic input or stimulation voltage necessary for a given neuron to release neurotransmitters. Neurotransmitter release in response to sub-threshold synaptic input can be facilitated by sub-threshold stimulation under certain conditions as seen in Chapter 5.

Synaptic input	Stimulation level	AP*	NT† release	Description
sub-threshold	None	no	no	sub-threshold synaptic input
None	sub-threshold	no	no	sub-threshold stimulation
super-threshold	None	yes	yes	neuron activated by synaptic input
None	super-threshold	maybe	yes	neuron activated by stimulation pulse
sub-threshold	sub-threshold	no	no	no facilitation
sub-threshold	sub-threshold	yes	yes	neuron activated by sub-threshold synaptic input facilitated by sub-threshold stimulation pulse

* Does an action potential (AP) occur in the neuron?
† Does the neuron release neurotransmitters (NT)?

neurons were exposed to 18 characteristic bipolar electrode combinations with both biphasic and monophasic stimulation waveforms to determine thresholds for neurotransmitter release with and without a varying amount of synaptic input. The timing between the synaptic input and the stimulation pulse was also varied to study the time sensitivity and optimality of the stimulation.

Stimulation thresholds for neurotransmitter release were found first in the case of epidural stimulation without synaptic input using stimulation voltage magnitudes of up to 10 V. After testing 28512 different neuron stimulation configurations (66 neuron locations, 6 axon orientations, 18 characteristic bipolar electrode pairs, 2 polarities, and 2 stimulation pulse shapes), the minimum amplitude of electrical stimulation required to raise the neuron's axon tip to above -10 mV and release neurotransmitters (based on (Destexhe, Mainen, and Sejnowski, 1994)) was found to be 2.75 V for monophasic stimulation and 3.25 V for biphasic stimulation. Plotting the maximum membrane voltage at the axon tip against $V_{static}^{\text{AxonTip}} - V_{static}^{\text{Soma}}$ (where $V_{static}^{\text{AxonTip}}$ and V_{static}^{Soma} are the extracellular voltages computed using a static volume conductor simulation at the axon tip and soma respectively) showed that this difference could be used to predict stimulation patterns that would cause neurotransmitter

release.

Next, simulations were conducted with a single sub-threshold synaptic input arriving at one of 10 locations on each neuron at times before, during, and after a sub-threshold stimulation pulse. Stimulation pulses of magnitude 5 V or less were tested with 8 sub-threshold synapse weights at locations in the middle of the distal dendrite and 3 synapse weights at the locations on the distal tips of the dendrites. Since both the synaptic input and the stimulation pulse are sub-threshold (i.e. do not cause the axon tip membrane voltage to go above $-10\,\mathrm{mV}$), the synaptic input is facilitated by the stimulation pulse if together they cause the axon tip membrane voltage to go above $-10\,\mathrm{mV}$. Windows of time in which facilitation occurs were found for many stimulation configurations and synapse weights. If the sub-threshold synaptic input is large enough, a 0.5 V stimulation pulse is enough to facilitate neurotransmitter release in some neurons. A greedy search for features which were able to identify stimulation configurations which cause facilitation found that $V_{static}^{\mathrm{Synapse}} - V_{static}^{\mathrm{Soma}}$ (the difference in the static voltage between the synapse location and the soma) and $V_{static}^{\mathrm{IS}} - V_{static}^{\mathrm{Soma}}$ (the difference in the static voltage between the initial segment of the axon and the soma) were able to separate 60-89% of the facilitated stimulation configurations from 21 out of 22 datasets (separated by synapse weight) and 42% in the remaining dataset.

This is the largest scale study of the facilitation effect. The facilitation effect is a function of many variables (timing, synapse weight, ion channel densities, neuron geometries, etc.). A large-scale computational campaign was helpful to identify the various phenomena (some of which are non-intuitive) and to organize the results into a smaller set of rules that would otherwise be difficult without such a large-scale study.

1.1 Review of existing literature

Much of the research into electrical stimulation of the spinal cord was initially motivated by success in using electrical stimulation of the spinal cord to temporarily stop or reduce chronic pain (Shealy, Mortimer, and Reswick, 1967; Hosobuchi, Adams, and Linchitz, 1977; Aló and Jan Holsheimer, 2002). Electrical stimulation of the spinal cord for reducing the pain associated with multiple sclerosis (MS) showed improvement in mobility, sensory function, and bladder function (Cook and Weinstein, 1973; Illis, Sedgwick, and Tallis, 1980). Two dimensional (B. Coburn, 1980) and then three dimensional (Barry Coburn and Sin, 1985) finite element volume conductor models of electrical stimulation of the spinal cord were conducted. The results of the 3D volume conductor simulations were used in combination with compartmental models of myelinated fibers (i.e. without soma or dendrite compartments) in the white matter of the spinal cord to predict firing thresholds (Barry Coburn, 1985). Efforts to use electrical stimulation of the spinal cord to activate or inactivate certain neurons/fibers while not interfering with other neurons lead to increased computer modeling of axon fibers in the spinal cord. In the field of spinal cord stimulation, this problem lead to more models of external electric stimulation of axons (mostly myelinated axons of different diameters in the white matter and dorsal roots) in uniform materials (B. Coburn, 1988; Rubinstein and Spelman, 1988; Rubinstein, 1991; Richardson, C. C. McIntyre, and W. M. Grill, 2000) and 3D volume conductor models (Struijk, Holsheimer, van Veen, et al., Jan./1991; J. Holsheimer and J. J Struijk, 1992; Struijk, Holsheimer, van der Heide, et al., Sept./1992; Johannes J. Struijk, Jan Holsheimer, and Boom, 1993; J Ladenbauer et al., 2010; Capogrosso et al., 2013; Lempka et al., 2015).

Most of these authors consider a neuron or fiber to be activated or recruited if an action potential is generated or travels a certain distance in the neuron. This definition can be problematic if the stimulation also blocks the axon potential from reaching

the axon tip, or if the axon tip is stimulated sufficiently to release neurotransmitters without an action potential. This will be discussed more in Chapters 3 and 4.

(Rattay, 1999) derived and proposed the activation function (which is proportional to the second derivative of the extracellular voltage along the axon) to predict whether a uniform neuron fiber will be stimulated (depolarized) or hyperpolarized without actually simulating neurons. This turned out not to be useful for the type of neurons simulated in this thesis. There is more discussion of this in Chapters 4 and 5.

In the last decade, a small number of papers used computational means to study epidural stimulation for SCI therapy. (C. C. McIntyre and Warren M Grill, 2002; Capogrosso et al., 2013) also modeled activation of motorneurons and interneurons in the gray matter of the spinal cord. Capogrosso et al. (2013) also included some limited simulations of a sub-threshold synapse, but they did not appear to study how this relates to facilitation. Other researchers have modeled sub-threshold external electrical stimulation of whole neurons (Tranchina and Nicholson, 1986). Ephaptic interactions between neurons (Holt and Koch, 1999; Gold et al., 2009; Anastassiou et al., 2011) are another sub-threshold phenomena.

Remme and Rinzel, 2011 looked at the role of active dendritic conductances in the propagation and summation of excitatory postsynaptic potentials (EPSPs) using a linear quasi-active approximation to membrane and ion channel dynamics. Their analysis showed that EPSPs are attenuated and sharpened by restorative ion channel currents, and amplified and broadened by regenerative ion channel currents. This analysis suggests that modeling active ion channels in the dendrites is important when EPSPs are modeled. Their analysis methods may also be useful for future work on understanding the effect of electrical stimulation on ion channels.

Spinal stimulation has also been investigated for reduction of the spasticity of-

ten seen in SCI. (ElBasiouny and Mushahwar, 2007) model suppression of excess synaptic inputs to spinal motoneurons using extracellularly applied electric fields. This thesis simulates facilitating synaptic input rather than interfering with it.

The style of the volume conductor model used in this thesis is most similar to that of (J Ladenbauer et al., 2010; Capogrosso et al., 2013). (Capogrosso et al., 2013) has enough similarities to the approach taken in this thesis to warrant a comparison. (Capogrosso et al., 2013) models square current pulses using static voltage simulations. This thesis uses time domain volume conductor simulations of Gaussian monophasic and biphasic voltage stimulation. (Capogrosso et al., 2013) assumes purely resistive materials with frequency independent conductivity. In this thesis, I pick the conductivity and real valued permittivity based on the largest frequency component of the stimulation waveform. Based on the analysis in Chapter 2, the conductivity of the gray matter and white matter used in (Capogrosso et al., 2013) is too high. The conductivity of the cerebrospinal fluid differs (2 nS vs 1.7 nS). The interneuron geometry differs significantly (they use scaled cat interneurons, I use a constructed geometry), the soma diameter is similar, but the axon diameter differs. They use a value of 2.5 µm for the diameter of the axon which comes from cat studies (Saywell et al., 2011), while I use a value of 0.8 µm from rat studies (Ostroumov, 2007; Nunes et al., 2017; Saliani et al., 2017). (Capogrosso et al., 2013) uses passive dendrites while I use an active model based on (Ostroumov, 2007). Both studies use a similar synapse model, although they do not state the weight of the synapse and appear to trigger the synapse based on the stimulation of a dorsal root rather than the general model of facilitation (with multiple values of synapse weights and time offset between the stimulation pulse and the synaptic event) used in this thesis. The paper concludes that epidural stimulation of interneurons in the spinal cord is unlikely, while this thesis concludes that facilitation of interneurons is possible.

The stimulation voltage ranges used in this thesis (0.25 V to 10 V) have been selected to cover the voltage range used experimentally by my colleagues at UCLA: 3 V (P. Gad et al., 2012), 5 V to 7 V (Desautels et al., 2015), 4 V (Parag Gad, Roy, Choe, Creagmile, et al., 2015), and 1 V to 8 V (Parag Gad, Roy, Choe, Zhong, et al., 2015).

1.2 Contributions of thesis

Rather than trying to solve the general problem of understanding how epidural electrical stimulation interacts with the complex network activity of neurons in the spinal cord, this thesis focuses on the problem of understanding through simulation how the activation of a single neuron (in many locations/orientations) may be facilitated by spinal stimulation in combination with an excitatory postsynaptic potential (EPSP) (either naturally occurring background activity or voluntarily induced). Hopefully these results will be useful in understanding how epidural stimulation can be used to facilitate recovery of motor movement.

The problem of facilitation is broken down into an investigation of how a single EPSP interacts with epidural stimulation. The EPSP in this example is assumed to be triggered by the release of neurotransmitters from an action potential in a presynaptic neuron. The action potential in the presynaptic neuron could have many possible sources, including: the brain, sensory neurons, baseline activity, and other facilitated or stimulated neurons. Building this simulation requires building a finite element volume conductor model of an epidural stimulation array in a rat spinal cord along with a model for the neurons in the spinal cord. After building these models, the two components of facilitation (synapse weight and stimulation voltage) must be understood separately before understanding the interaction.

- Chapter 2 develops a finite element geometrical and electrical model of a rat spinal cord based on MRI images of a rat spine. This chapter also includes a

discussion on choosing material properties based on the frequency spectrum of monophasic and biphasic stimulation waveforms.

- A model neuron is described in Chapter 3. The results of injecting current pulses into the model neuron are presented to allow comparison with other studies. The synapse weight necessary for a single presynaptic event to generate an EPSP event large enough to achieve neurotransmitter release from the axon tip was also determined. Synapse weights less than this amount allow for the possibility of facilitation rather than causing neurotransmitter release directly.

- Chapter 4 looks at the effect of epidural stimulation on neurons with no synaptic activity using the volume conductor simulations presented in Chapter 2 and the neuron models from Chapter 3. The locations of neurons electrically stimulated sufficiently to release neurotransmitters using an amplitude of less than 5 V of stimulation are presented in Tables 4.2 and 4.3. Results for neurotransmitter release using an amplitude of less than 10 V are presented graphically. Plots of the membrane voltage at the axon tip for all simulations vs the static extracellular voltage, the second derivative of the static extracellular voltage, and the difference in static extracellular voltage between the axon tip and the soma are presented. These show that the membrane voltage at the axon tip cannot be predicted from the second derivative of the static voltage or the static voltage at the axon tip directly. However, the difference in static extracellular voltage between the axon tip and the soma showed a clear relationship with neuron activation (neurotransmitter release).

- Chapter 5 pulls this all together with simulations of interneurons exposed to varying amounts of sub-threshold synaptic input at times before, during, and after a sub-threshold epidural stimulation pulse. Simulations included all

the stimulation configurations and neurons from Chapter 4 using 5 different magnitudes of stimulation voltage combined with 8 sub-threshold values of synapse weights for synapses located in the middle of each distal dendrite, and 3 sub-threshold values of synapse weights for synapses located at the distal tip of each dendrite.

- Examples of facilitation are shown for some of the neurons discussed in Chapter 4. These examples show facilitation can occur with synapse triggers both before and after the stimulation pulse, but there are time intervals during which facilitation takes less magnitude of stimulation and/or synapse weight. For the examples using biphasic stimulation, the least effort facilitation occurred if the synaptic input occurred 0 to 20 ms before the stimulation pulse. For the examples using monophasic stimulation, the least effort facilitation occurred either 0 to 20 ms before the stimulation pulse or 0 to about 20 ms after the stimulation pulse depending on the polarity of the stimulation. The particular timing of the least effort facilitation windows appears to depend on the value of some of the ion channel state variables near the synapse.
- Histograms and stacked bar charts are presented showing the number of neurons vs facilitation window size for each pairing of stimulation magnitude and synapse weight. These show a significant amount of facilitation at the largest magnitude (5 V) stimulation voltage and largest but sub-threshold synapse weight. There is a decrease in the size of the facilitation window, and number of neurons facilitated as either the magnitude of stimulation or synapse weight decreases. In general, monophasic stimulation causes more simulated facilitation than biphasic stimulation, with the exception of simulations with synapses located on the distal tips of the dendrites, 5 V of stimulation, and the largest

sub-threshold synapse weight (4.783 nS).

  - A greedy search was conducted to find a series of features in either the static volume conductor simulations or the stimulation only (no synaptic input) simulations that would allow separation of simulations that showed facilitation from those that did not. As in Chapter 4, features based on the difference in static voltage between particular locations on the neuron and the soma were best at separating simulation parameters that would result in facilitation from the rest. In particular, the difference in static voltage between the synapse location and the soma and the difference in static voltage between the initial segment and the soma were able to separate the most facilitated neuron simulations from the rest.

- Chapter 6 summarizes the main contributions of the thesis and suggests future work.

Chapter 2

FINITE ELEMENT MODELING OF A RAT SPINAL CORD

In this chapter, I will discuss applying finite element modeling to the problem of modeling epidural stimulation in the lumbar portion of a rat spinal cord. Briefly, magnetic resonance imaging (MRI) was used to obtain images of a rat spinal cord (Section 2.1). Tissue images were segmented and a transverse slice through the L1 vertebra was used to extrude a 3D spinal model which was coupled with electrodes in SolidWorks (Section 2.1.1). Stimulation waveforms were analyzed for their dominant frequency components (Section 2.1.3). Material properties (conductivity and permittivity) were determined (Section 2.1.4) using the main frequency component of each stimulation waveform. Section 2.2 describes a volume conductor simulation using the COMSOL environment. This section also uses spatial symmetries and translations in the bipolar electrode combinations in order to reduce the number of simulated combinations to 18. Section 2.2.2 briefly discusses computational details of running the simulations. Section 2.A presents a summary of conductivity and permittivity data from the literature.

2.1 Building the 3D volume conductor model

To provide a realistic simulation model, the geometry of the lumbosacral spinal cord and its surrounding tissue was derived from MRI scans of a rat. An adult female Sprague Dawley rat (a control animal from another lab already scheduled to be euthanized) was fixed with 4% paraformaldehyde. The legs, tail, and everything rostral from the T12 vertebra was removed. The remaining spinal cord and muscle tissue was soaked for about 6 days in 3% $K_2(Cr_2O_7)$ and 10-mM Gd-HP-DO3A following (Zhang et al., 2010). After soaking, it was placed in a solution containing

perfluoropolyether (Galden®) to maintain the staining. The sample was imaged in an 11.7 tesla MRI machine at the Caltech Center for Biological Imaging at a voxel resolution of 78 µm. Vertebrae T13, L1, L2, L3, and L4 were manually identified in the resulting scans and segmented by hand (labeling bone and the inside of the bone, see Figs. 2.1 and 2.2). Segmentation was done using the Matlab NIFTI[a] toolbox and the bioelectromagnetism Toolbox[b] to select regions of interest, and ITK-SNAP[c] (Yushkevich et al., 2006) to segment the regions. Custom Matlab code was then used to merge the segmentation labels back into a single 3D image.

2.1.1 2d extrusion model with embedded electrode array model

Rather than model the full 3D structure of the rat spine shown in Figs. 2.1 and 2.2, it was decided to model a 3 by 7 electrode array embedded in a 3D extrusion of a spinal cord MRI slice taken from the middle of the L1 vertebra. This simplified model reduced the complexity of the simulations while maintaining the applicability to the L1 region. The area of the spinal cord under the L1 vertebra is known (Parag Gad, Choe, et al., 2013) to contain the motor pools for the soleus, tibialis anterior, and medial gastrocnemius muscles.

The manual segmentation of a transverse spinal cord slice from the middle of the L1 vertebra can be seen in Fig. 2.3. Gray matter and white matter were clearly visible in in the MRI data. Some spinal roots and nerve fibers were visible in the Cerebrospinal fluid (CSF). Preliminary COMSOL simulations including the fibers as cylinders of white matter in the CSF showed minimal effect on the voltage distribution inside the spinal cord (white/gray matter), so these fibers were left out from the final simulation model. Epidural fat was not visible in the MRI images. During the surgical implantation of epidural electrodes in rat models, the epidural fat

[a] http://www.mathworks.com/matlabcentral/fileexchange/8797-tools-for-nifti-and-analyze-image

[b] http://eeg.sourceforge.net/bioelectromagnetism.html

[c] www.itksnap.org

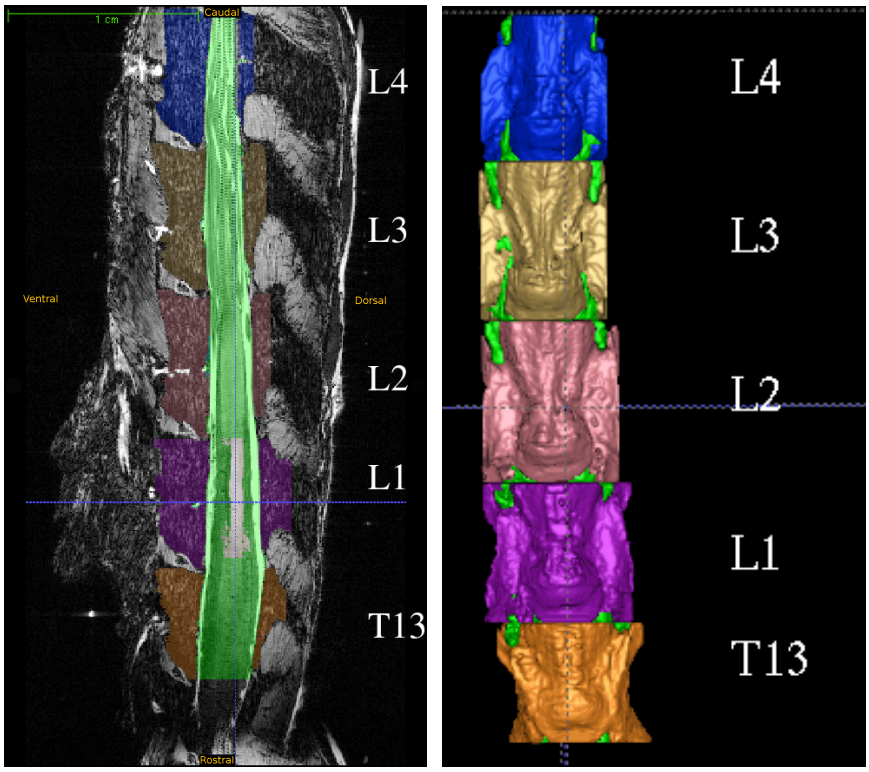

(a) Sagittal slice (b) 3D mesh of segmented vertebra

Figure 2.1: MRI data of the spinal cord of an adult female Sprague Dawley rat showing vertebra T13-L4. The vertebra are labeled with colors: L4, L3, L2, L1, and T13. The CSF, white matter, gray matter, and nerve fibers are labeled green except for the L1 gray matter which is uncolored. Subfigures: (a) shows a sagittal slice (down the middle of the spinal cord) with the dorsal direction to the right, the ventral direction to the left, the rostral direction to the top, and the caudal direction to the bottom of the page. (b) shows a 3D mesh representation of the segmented data.

is usually removed from the region that the electrode array will sit over. In other regions, the epidural fat would be next to vertebral bone, which has a conductivity more similar to epidural fat than to CSF. Therefore the epidural fat was left out of the simulation. Bone and muscle are also visible in the MRI slice. The gray matter, CSF, and bone can be modeled as isotropic. Muscles and white matter on the other hand have mostly parallel internal fibers which allow for increased conduction along the fibers and reduced conduction perpendicular to the fibers. In the spinal white matter, the myelinated axons run primarily along the rostral-caudal direction.

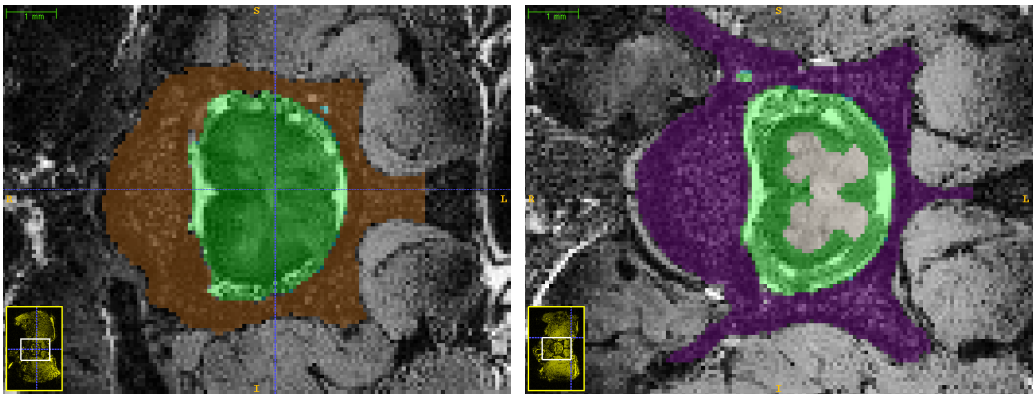

(a) T13 (b) L1

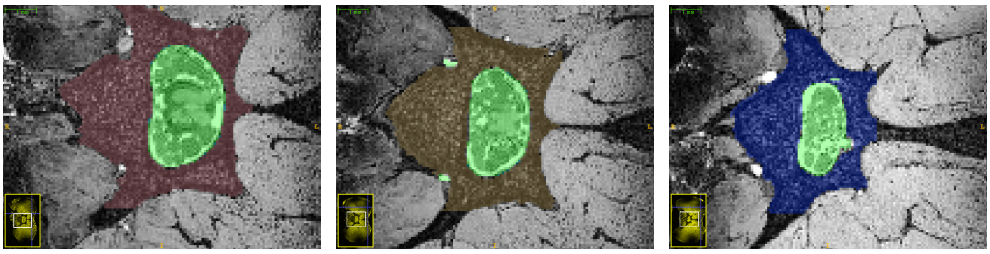

(c) L2 (d) L3 (e) L4

Figure 2.2: Transverse slices of the MRI data of the spinal cord of an adult female Sprague Dawley. Each subfigure shows a slice in the approximate middle of each vertebra: (a) T13 vertebra, (b) L1 vertebra, (c) L2 vertebra, (d) L3 vertebra, and (e) L4 vertebra. The CSF, white matter, gray matter, and nerve fibers are labeled green except for the L1 gray matter which is uncolored. The dorsal direction is to the right of the page.

For muscle fibers, the attachment of muscle to the vertebra is more complex, but appeared to mostly contain fibers parallel to the rostral-caudal axis in the region near the spinal cord.

This model will be used throughout the rest of the thesis and uses an x, y, z coordinate system defined such that:

- $+\hat{x}$ points to the animal's right side
- $-\hat{x}$ points to the animal's left side
- $+\hat{y}$ points in the dorsal direction
- $-\hat{y}$ points in the ventral direction

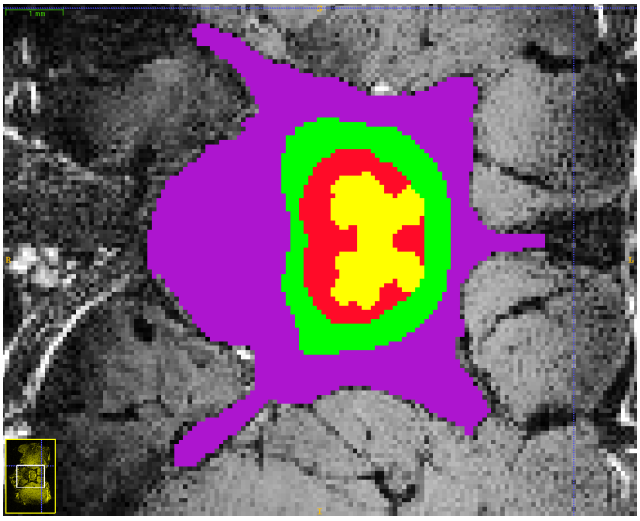

Figure 2.3: Transverse MRI slice of rat spinal cord from the middle of L1 vertebra. The dorsal direction is to the right of the page. Materials are labeled with colors: gray matter (yellow), white matter (red), cerebrospinal fluid (CSF)/roots/fibers (green), and bone (purple).

- $+\hat{z}$ points in the caudal direction
- $-\hat{z}$ points in the rostral direction

2.1.2 Electrical and physical model of epidural stimulating arrays

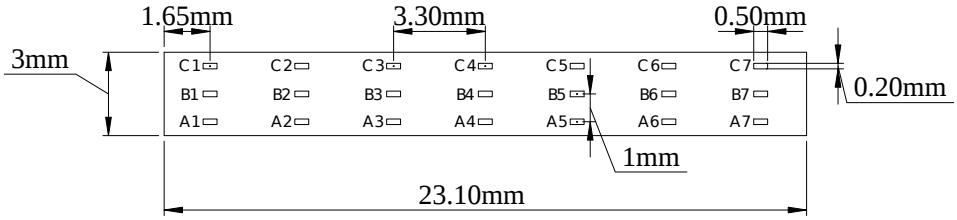

Figure 2.4: Dimensions of flat electrode array. The small (0.50 mm by 0.20 mm) rectangles are the platinum electrodes. See Table 2.1 for electrode labels and array orientation. Figures 4.1 and 4.2 show the labeled electrode array in the simulated spinal cord.

The parameters of the model's multi-electrode epidural stimulating array were based on those found in (Parag Gad, Choe, et al., 2013). Specifically, rectangular platinum electrodes (500 µm by 200 µm) spaced 1 mm laterally (when flat, center to center) and 3.3 mm rostral-caudally were modeled (when flat, center to center). Figure 2.4 shows the dimensions of the flat array. See Table 2.1 for electrode labels

Column Letters: A B C

row #					
1	A1	B1	C1	$\hat{z}\downarrow$	cranial↑
2	A2	B2	C2		
3	A3	B3	C3		
4	A4	B4	C4		
5	A5	B5	C5		
6	A6	B6	C6		
7	A7	B7	C7		caudal↓

$\hat{x} \rightarrow$
←left side right side→
$\odot$ $\hat{y}$, dorsal
$\otimes$ ventral

Table 2.1: This table shows the names of the electrodes and the orientation of the array in the spinal cord as if you are looking down at the back of the rat with its head pointed towards the top of the page. (Note that $\odot$ means that the dorsal direction is pointing out of the page and the $\otimes$ symbol indicates that the ventral direction is into the page.) Figures 4.1 and 4.2 show the labeled electrode array in the simulated spinal cord.

and array orientation. Figures 4.1 and 4.2 show the labeled electrode array in the simulated spinal cord. (See also Section 2.2.1 for discussion of electrode array combinations and combination naming.) Based on Figure 6 of (Parag Gad, Choe, et al., 2013), the center 5 rows of electrodes would cover the spinal region of L4, L5, L6, and S1. The parylene C backing of the electrode array is normally 20 µm thick (Parag Gad, Choe, et al., 2013). In order to simulate efficiently (and reduce the number of necessary mesh points), the parylene C thickness was chosen to be 40 µm and the electrode (platinum) thickness chosen to be 10 µm (normally 0.2 µm). A slice through the extruded model showing the thicker array can be seen in Figs. 2.6 and 2.7. The width of the curved portion of the parylene C next to the CSF was constrained to a path length of 3 mm (the actual width of the array), while the back of the array was allowed to be wider to compensate for the increased thickness.

In order to reduce the number of mesh points required in COMSOL, to avoid errors

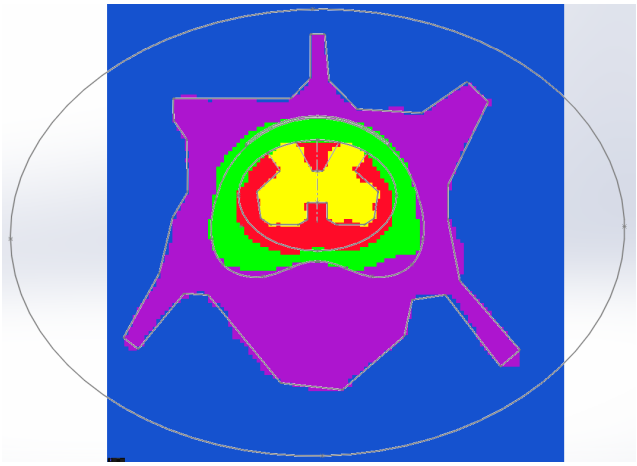

Figure 2.5: Sketch of the spinal cord geometry and electrode array on top of the segmented image. Regions in the segmented image are indicated by color: gray matter (yellow), white matter (red), CSF/roots/fibers (green), and bone (purple). See Figs. 2.6 and 2.7 for a better view of the electrode array after extrusion.

in COMSOL's meshing algorithms, and to remove the discretization of the MRI data, it was necessary to simplify the model geometry. Figure 2.5 shows a cross-section of the CAD (SolidWorks) sketch over the segmented MRI image before extrusion.

After extrusion, the electrode array model seen in Fig. 2.4 was wrapped and embossed onto the parylene C material to create holes for the electrodes. These holes were filled using constructive geometry. The result can be seen in Figs. 2.6 to 2.8.

2.1.3 Stimulation waveforms

Typically, electrical spinal stimulation uses monophasic square pulses (Parag Gad, Choe, et al., 2013), biphasic square pulses (Josef Ladenbauer, 2008), or biphasic square exponential pulses (Gill et al., 2018) where the exponential decay results from capacitive discharge. For this work, I will assume that the distance between multiple stimulation pulses is large enough that the voltage in the tissues returns to steady state for a long time relative to the pulse width so that each pulse can be analyzed separately.

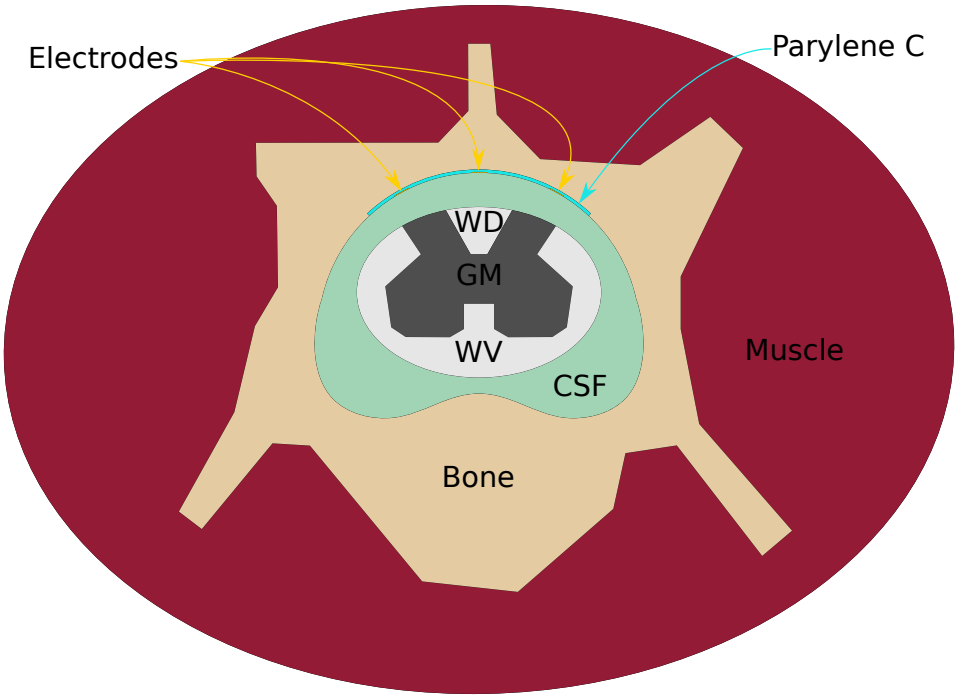

Figure 2.6: After the sketch in Fig. 2.5 was extruded to a length of 23.1 mm, 10 µm-thick electrodes were placed in the parylene. This figure shows a slice through one of the electrode rows. The cerebrospinal fluid is labeled CSF. The dorsal white matter, ventral white matter, and gray matter are labeled WD, WV, and GM respectively. See Fig. 2.7 for a close up view of the electrodes.

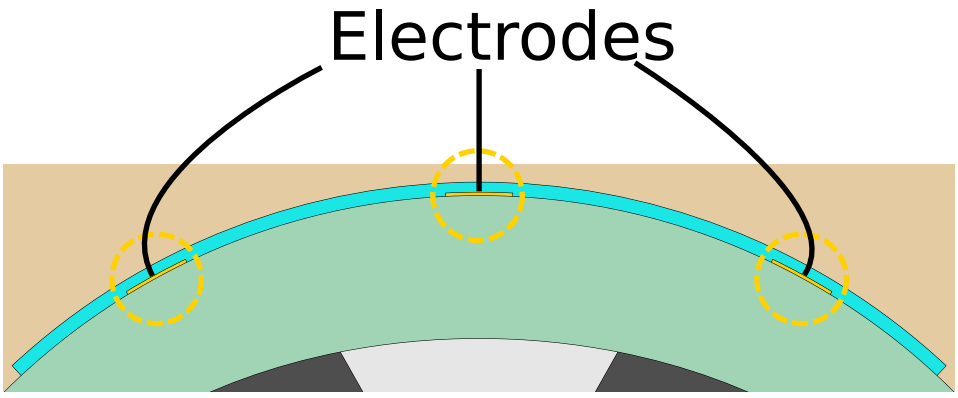

Figure 2.7: Close up view of the electrode array seen in Fig. 2.6. Electrodes are gold and indicated with dashed gold circles. The parylene C is colored cyan. See Fig. 2.6 for more details on the other materials.

Define a square monophasic pulse ($S_{\text{mono}}(t, w)$) centered at $t = 0$ with an amplitude of 1,

$$S_{\text{mono}}(t, w) = H\left(t + \frac{w}{2}\right) H\left(\frac{w}{2} - t\right), \tag{2.1}$$

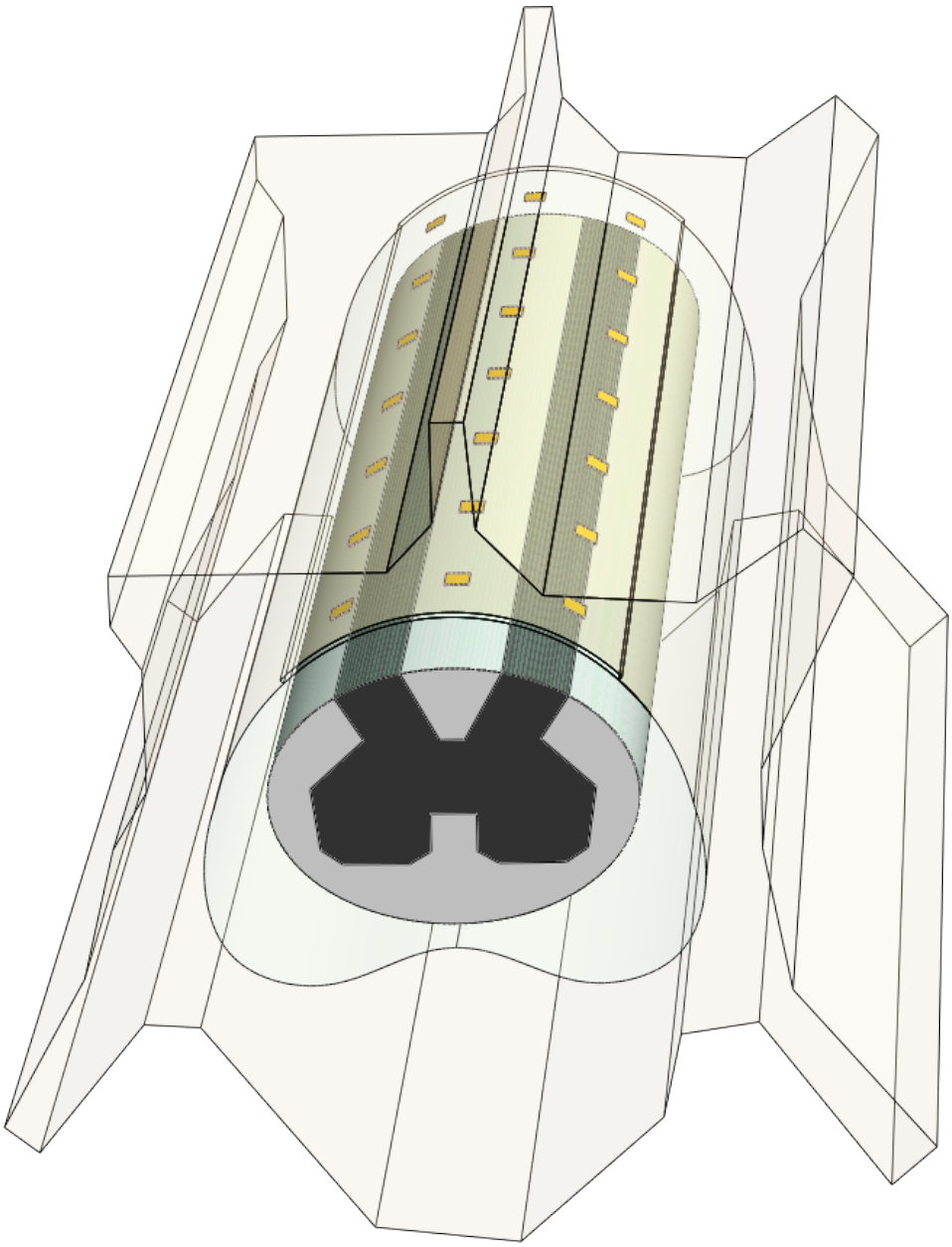

Figure 2.8: A partially transparent view of the model showing the placement of the 27 electrodes. See Figs. 2.6 and 2.7 for material labels.

where $H(.)$ is the Heaviside function, t is time in seconds, and w is the width of the pulse in seconds. Similarly, define a square biphasic pulse ($S_{\text{bi}}(t, w)$) centered at $t = 0$ with an amplitude of 1,

$$S_{\text{bi}}(t, w) = (2H(-t) - 1)H(t + w)H(w - t), \tag{2.2}$$

and a square exponential biphasic pulse ($S_{\text{SqExp}}(t, w)$) given by:

$$S_{\text{SqExp}}(t, w) = H(t + w)H(-t) - H(t)e^{-\frac{t}{w}}. \tag{2.3}$$

Plots of $S_{\text{mono}}(t, w)$, $S_{\text{bi}}(t, w)$, and $S_{\text{SqExp}}(t, w)$ can be seen in Figure (2.9) with $w = 200\,\mu\text{s}$.

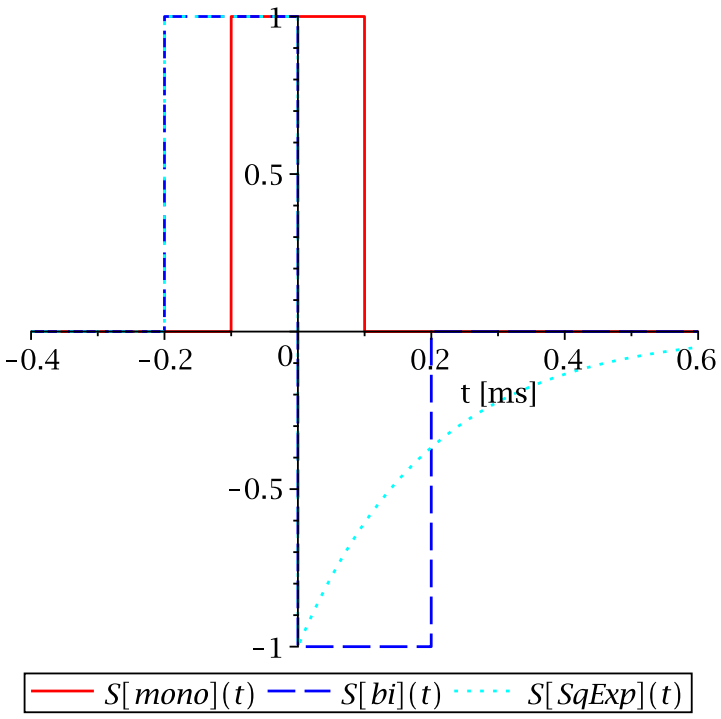

Figure 2.9: Plots of $S_{\text{mono}}(t, w = 200\,\mu\text{s})$, $S_{\text{bi}}(t, w = 200\,\mu\text{s})$, and $S_{\text{SqExp}}(t, w = 200\,\mu\text{s})$

The frequency content of the stimulation pulse is an important factor in simulating the electrical response of tissue to that stimulation pulse (as seen in Section 2.1.4). The Fourier transform ($\mathcal{F}$) can be used to convert an arbitrary time domain function $h(t)$ into a frequency domain function ($\tilde{h}(\omega)$) so that the power spectral density ($\tilde{h}^2(\omega)$) can be plotted. For this thesis, the Fourier transform ($\mathcal{F}$) is defined by:

$$\mathcal{F}(h(t)) = \int_{-\infty}^{\infty} h(t)e^{-i\omega t}dt = \tilde{h}(\omega), \tag{2.4}$$

and the inverse Fourier transform ($\mathcal{F}^{-1}$) is defined by:

$$\mathcal{F}^{-1}(\tilde{h}(\omega)) = \frac{1}{2\pi}\int_{-\infty}^{\infty}\tilde{h}(\omega)e^{i\omega t}d\omega = h(t), \tag{2.5}$$

where $\omega = 2\pi f$.

Using the above definitions, the Fourier transforms of these pulses are given by:

$$\mathcal{F}(S_{\text{mono}}(t,w)) = \tilde{S}_{\text{mono}}(f,w) = \frac{\sin(w\pi f)}{\pi f}, \tag{2.6}$$

$$\mathcal{F}(S_{\text{bi}}(t,w)) = \tilde{S}_{\text{bi}}(f,w) = 2i\frac{\sin^2(w\pi f)}{\pi f}, \tag{2.7}$$

and

$$\mathcal{F}(S_{\text{SqExp}}(t,w)) = \tilde{S}_{\text{SqExp}} = \frac{(2\pi fw - i)e^{i2\pi fw} - 4\pi fw + i}{2(i2\pi fw + 1)\pi f}. \tag{2.8}$$

Plots of $\tilde{S}^2_{\text{mono}}(f,w)$, $\tilde{S}^2_{\text{bi}}(f,w)$, and $\tilde{S}^2_{\text{SqExp}}(f,w)$ can be seen in Fig. 2.10 with $w = 200\,\mu\text{s}$.

These pulses have a broad frequency response due to the discontinuities. These discontinuities also make time-domain COMSOL simulations problematic without smoothing. In order to address both of these issues, a Gaussian was selected for a monophasic pulse (G_{mono}), and a normalized derivative of a Gaussian for a biphasic pulse (G_{bi}). In order to keep the pulses equivalent to the square monophasic and biphasic pulses, the amplitude and energy of the Gaussian pulses will be fixed to that of the equivalent square pulse. In this case, energy (E) is

$$E = \int_{-\infty}^{\infty}P(t)dt \tag{2.9}$$

where the power $P(t)$ is given by,

$$P(t) = I(t)V(t) = \frac{(V(t))^2}{R}, \tag{2.10}$$

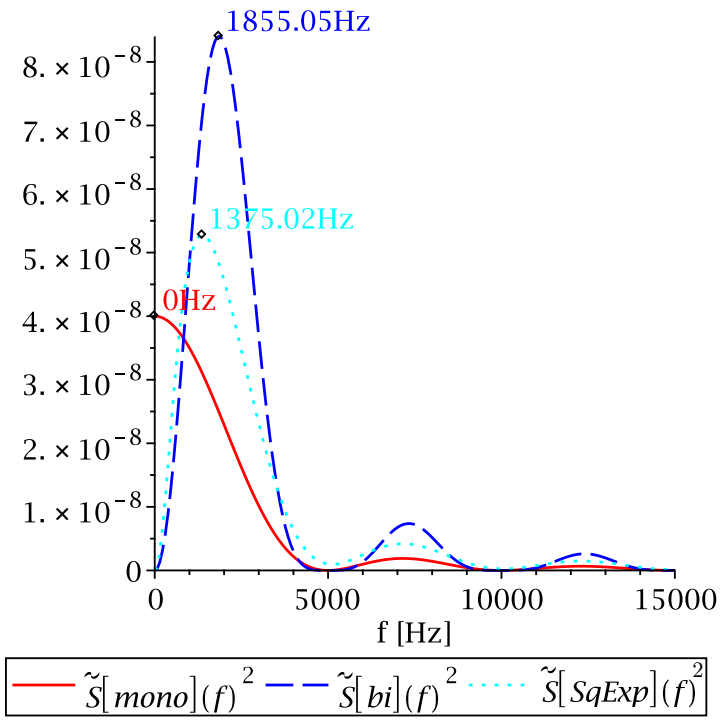

Figure 2.10: Plots of power spectral density for monophasic square pulse ($\tilde{S}^2_{\text{mono}}(f, w = 200\,\mu\text{s})$), biphasic square pulse ($\tilde{S}^2_{\text{bi}}(f, w = 200\,\mu\text{s})$), and biphasic square exponential ($\tilde{S}^2_{\text{SqExp}}(f, w = 200\,\mu\text{s})$).

$I(t) = V(t)/R$ is the current as a function of time, $V(t)$ is the voltage as a function of time, and R is a generalized resistance of the tissues. The amplitude of both square pulses is 1. The energy of the monophasic square pulse is:

$$E(S_{\text{mono}}(t, w)) = \frac{w}{R}, \tag{2.11}$$

and the energy of the biphasic square pulse is:

$$E(S_{\text{bi}}(t, w)) = \frac{2w}{R}. \tag{2.12}$$

First, define a Gaussian monophasic pulse ($G_{\text{mono}}(t, \varsigma_{\text{mono}})$) centered at $t = 0$ and

with an amplitude of $G_{\text{mono}}(0) = 1$,

$$G_{\text{mono}}(t, \varsigma_{\text{mono}}) = e^{\frac{-1}{2}\left(\frac{t}{\varsigma_{\text{mono}}}\right)^2}, \tag{2.13}$$

where ς_{mono} is a width parameter measured in seconds. The energy in this pulse is:

$$E(G_{\text{mono}}(t, \varsigma_{\text{mono}})) = \frac{\varsigma_{\text{mono}}\sqrt{\pi}}{R}. \tag{2.14}$$

So,

$$E(S_{\text{mono}}(t, w)) = E(G_{\text{mono}}(t, \varsigma_{\text{mono}})) \tag{2.15}$$

leads to:

$$\varsigma_{\text{mono}} = \frac{w}{\sqrt{\pi}}. \tag{2.16}$$

Similarly, define a Gaussian biphasic pulse ($G_{\text{bi}}(t) \propto \frac{d}{dt} G_{\text{mono}}(t)$) centered at $t = 0$ and normalized to a maximum amplitude of 1,

$$G_{\text{bi}}(t, \varsigma_{\text{bi}}) = \frac{-t}{\varsigma_{\text{bi}}} e^{\frac{1}{2}\left(1-\left(\frac{t}{\varsigma_{\text{bi}}}\right)^2\right)}. \tag{2.17}$$

The energy in this pulse is

$$E(G_{\text{bi}}(t, \varsigma_{\text{bi}})) = \frac{\varsigma_{\text{bi}}\sqrt{\pi}e}{2R}. \tag{2.18}$$

So

$$E(S_{\text{bi}}(t, w)) = E(G_{\text{mono}}(t, \varsigma_{\text{bi}})) \tag{2.19}$$

leads to:

$$\varsigma_{\text{bi}} = \frac{4w}{e\sqrt{\pi}}. \tag{2.20}$$

It can also be shown that the max and min amplitudes of the biphasic pulse occur at

$$t = \pm\varsigma_{\text{bi}}. \tag{2.21}$$

A square pulse width $w = 200\,\mu\text{s}$ corresponds in this normalization to $\varsigma_{\text{mono}} \approx 112.84\,\mu\text{s}$ and $\varsigma_{\text{bi}} \approx 166.04\,\mu\text{s}$. Plots of $G_{\text{mono}}(t, \varsigma_{\text{mono}})$ and $G_{\text{bi}}(t, \varsigma_{\text{bi}})$ can be found in Fig. 2.11.

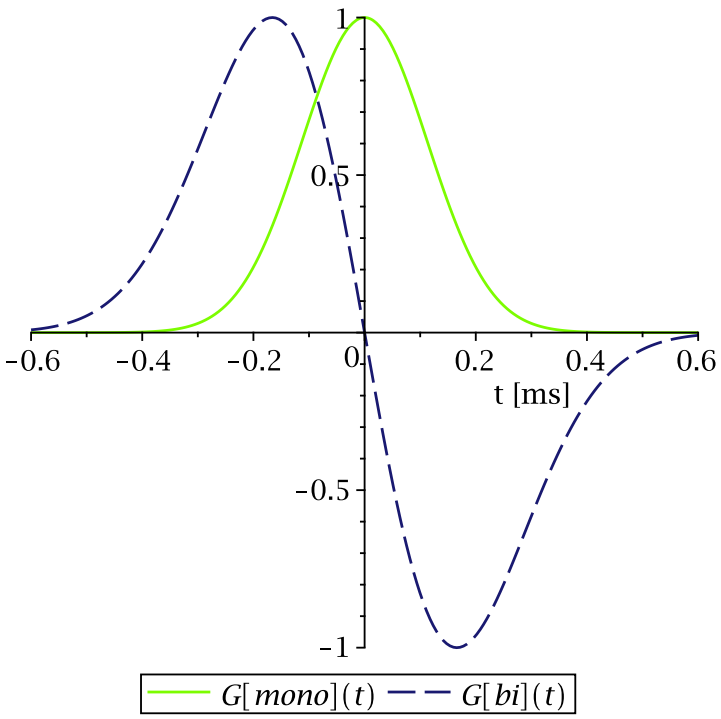

Figure 2.11: Plots of a Gaussian monophasic pulse $G_{\text{mono}}(t, \varsigma_{\text{mono}})$ and Gaussian biphasic pulse $G_{\text{bi}}(t, \varsigma_{\text{bi}})$. Where $\varsigma_{\text{mono}} \approx 112.84\,\mu\text{s}$ and $\varsigma_{\text{bi}} \approx 166.04\,\mu\text{s}$ cause $G_{\text{mono}}(t, \varsigma_{\text{mono}})$ and $G_{\text{bi}}(t, \varsigma_{\text{bi}})$ to have the same amount of power as a square pulse with width $w = 200\,\mu\text{s}$ and a biphasic square pulse with width $2w$ respectively.

The Fourier transforms of $G_{\text{bi,mono}}$ are given by:

$$\mathcal{F}(G_{\text{mono}}(t, \varsigma)) = \tilde{G}_{\text{mono}}(f, \varsigma) = \varsigma\sqrt{2\pi}e^{-2\pi^2 f^2 \varsigma^2} \tag{2.22}$$

and

$$\mathcal{F}(G_{\text{bi}}(t,\varsigma)) = \tilde{G}_{\text{bi}}(f,\varsigma) = 2\pi i\varsigma^2\sqrt{2\pi}fe^{\frac{1}{2}-2\pi^2f^2\varsigma^2}. \tag{2.23}$$

Plots of the power spectral density $\tilde{G}^2_{\text{mono}}(f,\varsigma_{\text{mono}})$ and $\tilde{G}^2_{\text{mono}}(f,\varsigma_{\text{bi}})$ can be seen in Fig. 2.12.

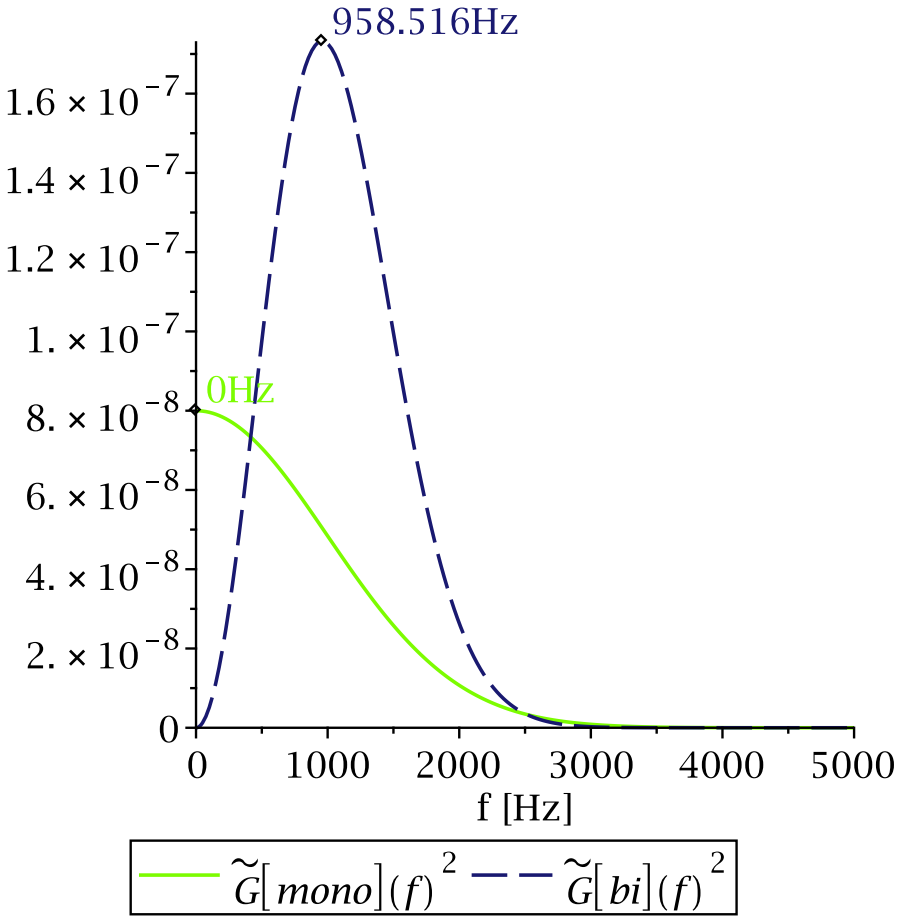

Figure 2.12: Plots of power spectral density for the monophasic Gaussian pulse $\tilde{G}_{\text{mono}}(f,\varsigma_{\text{mono}})$ and the biphasic Gaussian pulse $\tilde{G}_{\text{bi}}(f,\varsigma_{\text{bi}})$ used in this study

Unfortunately, time domain simulations in COMSOL only allow us to pick tissue electrical properties for a single frequency, so the frequencies with the most power are:

$$f^{\max}_{\text{mono}}(\varsigma) = \underset{f}{\text{argmax}}\,|\tilde{G}_{\text{mono}}(f,\varsigma)|^2 = 0 \tag{2.24}$$

and

$$f_{\text{bi}}^{\max}(\varsigma) = \underset{f}{\operatorname{argmax}} \, |\tilde{G}_{\text{bi}}(f, \varsigma)|^2 = \frac{1}{2\pi\varsigma}. \tag{2.25}$$

For the values of ς_{mono} and ς_{bi} found above, $f_{\text{mono}}^{\max} = 0$, and $f_{\text{bi}}^{\max} \approx 958.5\,\text{Hz}$.

2.1.4 Modeling tissues and electrode materials

In order to build a proper frequency-dependent simulation of epidural stimulation of the spinal cord, one must include key electrochemical properties of the affected materials, such as the relative permittivity and conductivity of the electrode array materials and biological tissues. While the relative permittivity is often referred to as the dielectric constant of the material, both conductivity and relative permittivity vary as a function of frequency and temperature. Data and 4-Cole-Cole model (K. S. Cole and R. H. Cole, 1941) fits from (C. Gabriel, 1996) will be used to model the relative permittivity and conductivity of biological tissue (Section 2.1.5.1). All materials other than muscle and white matter were modeled as isotropic materials. Data for Parylene C was taken from (Kahouli et al., 2012). The relative permittivity and conductivity of platinum were assumed to be constant in this frequency range and obtained from a CRC handbook (Chemical Rubber Company, 2012).

The rat body temperature is normally maintained between 37 °C and 38 °C (Gudjonsson, 1932), so where possible material properties have been obtained close to that temperature or adjusted for that temperature.

2.1.5 Tissues

For the model described in Section 2.1.1, it is necessary to know the frequency-dependent conductivity and relative permittivity for bone, grey matter, white matter, cerebro spinal fluid, and muscle. Additionally, the anisotropic conductivity for white matter and muscle must be taken into account.

The frequency-dependent conductivity and relative permittivity of general materials

vary with the polarizability of the material. The total polarizability of a material is the sum of the polarization of localized electrons (the electron cloud of individual atoms is distorted by the applied electric field, referred to as electronic polarizability), ionic polarizability (displacement of atoms attached with ionic bonds in response to an applied electric field), dipolar polarizability (reorientation of molecules in response to an applied electric field), and space charge polarization (long range motion of ions in response to an electric field). The polarization of a material is maximum at low frequencies when all of these types of polarization occur. See Figure 1 in (Leseal, 1982) for an overview. As the frequency of the electric field increases, the polarization decreases as the different types of polarization are unable to respond to the increased frequency. The frequency ranges at which this occurs are referred to as dispersion regions. Electronic polarizability is present at all frequencies. Ionic polarizability is limited by the speed of the displacement of the atoms and has a dispersion region around 10^{13}Hz (infrared). Dipolar polarizability is limited by the rotational speed of the dipoles and has a dispersion region around 10^{9}Hz (microwave). Space charge polarization depends on the speed of ions in the material and has a dispersion region around $10^{4} - 10^{5}$Hz (radio or lower).

In biological tissues, there are 3 commonly known dispersion regions (C. Gabriel, S. Gabriel, and Corthout, 1996): the low frequency α dispersion region associated with ionic diffusion, the β dispersion region (hundreds of kHz) associated with the polarization of cell membranes (which block the flow of ions), and the γ dispersion region (GHz) associated with the polarization of water. Other dispersion regions may exist in a particular type of tissue.

2.1.5.1 4-Cole-Cole model

The Cole-Cole model (K. S. Cole and R. H. Cole, 1941) is commonly used to fit measurements of the frequency-dependent isotropic complex relative permittivity

and conductivity of simple materials. For biological tissues it is common to use the Cole-Cole model with four dispersion regions. Three of these four dispersion regions may roughly fit the α, β, and γ regions described in Section 2.1.5, but the exact mechanisms of dispersion may differ in different types of tissues. The 4-Cole-Cole model is described by (De Geeter et al., 2012):

$$\epsilon_r(\omega) = \epsilon_\infty + \frac{\sigma_i}{i\omega\epsilon_0} + \sum_{n=1}^{4} \frac{\Delta\epsilon_n}{1 + (i\omega\tau_n)^{1-\alpha_n}}, \tag{2.26}$$

$$\sigma(\omega) = -\omega\epsilon_0 \Im(\epsilon_r(\omega)). \tag{2.27}$$

where $\epsilon_r(\omega)$ is the complex frequency-dependent relative permittivity, ϵ_∞ is the relative permittivity in the high-frequency limit, σ_i is the static conductivity arising from freely-moving charges (ions freely-moving in a liquid for example, the same ions involved in space charge polarization and the α dispersion), $i = \sqrt{-1}$, ω is the angular frequency (with units of rad/ sec), $\epsilon_0 = 8.854\,187\,817 \times 10^{-12}\,\mathrm{F\,m^{-1}}$ is the permittivity of free space[d], ($\Delta\epsilon_n$, τ_n, and α_n) are obtained by fitting experimental data, $\sigma(\omega)$ is the real valued conductivity, and $\Im(z)$ is the imaginary part of complex number z. Each term in the sum corresponds to one of the four dispersion regions.

Eqs. (2.26) and (2.27) run into non-physical numerical problems as $\omega \to 0$. These problems can be avoided by adopting the following definitions:

$$\epsilon_r(\omega) = \epsilon_\infty + \sum_{n=1}^{4} \frac{\Delta\epsilon_n}{1 + (i\omega\tau_n)^{1-\alpha_n}}, \tag{2.28}$$

$$\sigma(\omega) = \sigma_i - \omega\epsilon_0 \Im(\epsilon_r(\omega)). \tag{2.29}$$

The second term in Eq. (2.29) is the conduction from bound charges (i.e. electrons bound to molecules that are not free to move).

[d] http://physics.nist.gov/cgi-bin/cuu/Value?ep0

Gabriel et al. (C. Gabriel, 1996) found the Cole-Cole parameters for 44 biological materials (C. Gabriel and S. Gabriel, 1997) at 37 °C. Unfortunately, for some materials, in some frequency ranges, the values obtained from the 4-Cole-Cole equations can diverge significantly from nearby measured values. Fortunately, the raw data is also available for comparison (C. Gabriel and S. Gabriel, 1997). The 4-Cole-Cole parameters used in this thesis can be found in Table 2.2. Comparisons with the raw data can be found in Section 2.A. For muscle, the only available 4-Cole-Cole coefficients are for the transverse direction, even though data is available for both the parallel and transverse directions. Instead of attempting to fit the 4-Cole-Cole model to the data directly, the closest matching frequency data for "Ovine @ 37 degC" was used for the muscle.

Tissue Type	Bone (Cortical)	Grey Matter	White Matter	CSF
ϵ_∞	2.5	4	4	4
σ_i	0.02	0.02	0.02	2
$\Delta\epsilon_1$	10	45	32	65
τ_1 (ps)	13.263	7.958	7.958	7.958
α_1	0.2	0.1	0.1	0.1
$\Delta\epsilon_2$	180	400	100	40
τ_2 (ns)	79.577	15.915	7.958	1.592
α_2	0.2	0.15	0.1	0
$\Delta\epsilon_3$	5×10^3	2×10^5	4×10^4	0
τ_3 (us)	159.155	106.103	53.052	159.155
α_3	0.2	0.22	0.3	0
$\Delta\epsilon_4$	1×10^5	4.5×10^7	3.5×10^7	0
τ_4 (ms)	15.915	5.305	7.958	15.915
α_4	0	0	0.02	0

Table 2.2: Cole-Cole parameters

While there are some limited measurements of the anisotropic conductivity of CNS white matter (Ranck Jr. and BeMent, 1965), no one has measured the permittivity for white matter in both the parallel and transverse directions. For the simulations

in this thesis, I estimate the anisotropic conductivity and permittivity for the white matter using the diffusion tensor data in Table 2.3. This method assumes that ion diffusion is the dominant component of polarization at the frequencies used.

Define axes such that $+\hat{x}$ is in the right direction, $+\hat{y}$ is in the dorsal direction, and $+\hat{z}$ is in the caudal direction. This means that the eigenvectors are axis aligned such that $d_{trans} = d_{xx} = d_{yy}$, and $d_{parallel} = d_{zz}$, where $d_{\cdot}$ are the components of the diffusion tensor. Then, using the method described in (De Geeter et al., 2012), with the isotropic conductivity ($\sigma_{iso}(\omega)$) obtained from measurements or Eq. (2.29), I can obtain the conductivity in the transverse direction as follows:

$$\sigma_{trans}(\omega) = \frac{d_{trans}\sigma_{iso}(\omega)}{\sqrt[3]{d_{trans}^2 d_{parallel}}}. \tag{2.30}$$

Similarly, for the parallel direction:

$$\sigma_{parallel}(\omega) = \frac{d_{parallel}\sigma_{iso}(\omega)}{\sqrt[3]{d_{trans}^2 d_{parallel}}}. \tag{2.31}$$

Using the same method and the isotropic real relative permittivity ($\Re(\epsilon_r(\omega))_{iso}(\omega)$, where $\Re(z)$ is the real component of complex number z) again obtained from measurements or the real part of Eq. (2.28), I can obtain the real relative permittivity in the transverse direction:

$$\Re(\epsilon_r(\omega))_{trans} = \frac{d_{trans}\Re(\epsilon_r(\omega))_{iso}(\omega)}{\sqrt[3]{d_{trans}^2 d_{parallel}}}, \tag{2.32}$$

and the parallel direction

$$\Re(\epsilon_r(\omega))_{parallel} = \frac{d_{parallel}\Re(\epsilon_r(\omega))_{iso}(\omega)}{\sqrt[3]{d_{trans}^2 d_{parallel}}}. \tag{2.33}$$

Table 2.3: Diffusion tensor coefficients for rat spinal cord obtained from (Gulani et al., 1997).

Tissue Type	Measured diffusion coefficients (X $10^{-3}\frac{mm^2}{s}$)			
	d_{zz}	d_{xx}	d_{yy}	d_{xy}
Left Lateral Funiculus[a]	0.87 ± 0.04	0.23 ± 0.05	0.19 ± 0.04	−0.03 ± 0.05
Right Lateral Funiculus[a]	0.78 ± 0.03	0.18 ± 0.05	0.25 ± 0.04	−0.03 ± 0.05
Dorsal Columns[a]	1.01 ± 0.03	0.21 ± 0.03	0.25 ± 0.04	−0.06 ± 0.06
Gray Matter[a]	0.42 ± 0.02	0.44 ± 0.03	0.48 ± 0.03	−0.02 ± 0.03
Funiculus Avg[b]	0.825 ± 0.03	0.205 ± 0.04	0.22 ± 0.03	−0.03 ± 0.04

[a] (Gulani et al., 1997)
[b] Average of left and right lateral funiculus

2.1.6 Electrode array

Since the electrode array is made with parylene C and platinum traces, the conductivity ($\sigma(\omega)$) and relative permittivity ($\Re(\epsilon_r(\omega))$) of these materials are important to the modeling effort.

2.1.6.1 Parylene C

Data on the real part of the dielectric constant and the dissipation factor (D_F) were obtained from the as-deposited values at 25 °C in Figure 5 of Kahouli (2012) (Kahouli et al., 2012) and fit to a polynomial in $\Lambda = \log_{10}(fs)$.

$$\begin{aligned} D_F(\Lambda) =& 0.061018 - 2.912\times10^{-5}\Lambda - 0.0015511\Lambda^2 + 0.00089049\Lambda^3 - 0.00059251\Lambda^4 + 2.0756\times10^{-5}\Lambda^5 + 5.9074\times10^{-5}\Lambda^6 \\ & - 1.2942\times10^{-5}\Lambda^7 - 6.965\times10^{-8}\Lambda^8 + 2.5675\times10^{-7}\Lambda^9 - 1.9506\times10^{-8}\Lambda^{10} \end{aligned} \tag{2.34}$$

$$\begin{aligned} \Re(\epsilon_r(\Lambda)) =& 4.1276 - 0.28559\Lambda - 0.0078781\Lambda^2 - 0.0046379\Lambda^3 + 0.0054592\Lambda^4 + 0.0013196\Lambda^5 - 0.0024512\Lambda^6 \\ & + 0.0010473\Lambda^7 - 0.00021781\Lambda^8 + 2.2709\times10^{-5}\Lambda^9 - 9.492\times10^{-7}\Lambda^{10} \end{aligned} \tag{2.35}$$

The dissipation factor (D_F)[e] quantifies the dielectric's dissipation of electromag-

[e]The dissipation factor, D_F, is also called the loss tangent in some literature, usually with the notation $\tan\delta$.

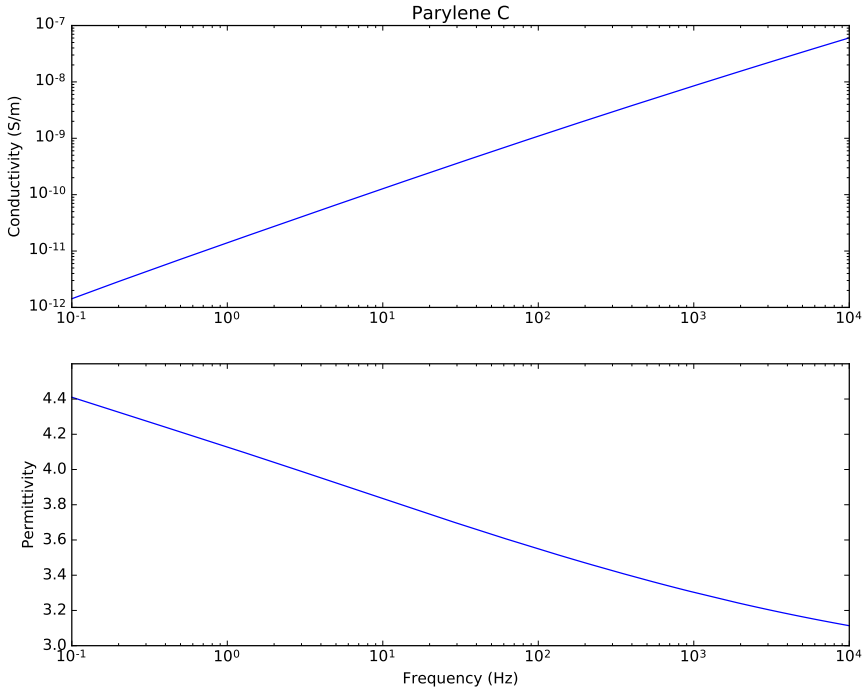

Figure 2.13: Conductivity and real relative permittivity for parylene C

netic energy as heat and is given by (Orfanidis, 2016):

$$D_F = \frac{\sigma_i - \omega\epsilon_0 \Im(\epsilon_r)}{\omega\epsilon_0 \Re(\epsilon_r)}. \tag{2.36}$$

The numerator in Eq. (2.36) can be recognized from Eq. (2.29), and so the following equation can be derived for conductivity:

$$\sigma(\omega) = D_F \omega\epsilon_0 \Re(\epsilon_r). \tag{2.37}$$

Based on Eqs. (2.34), (2.35) and (2.37), the conductivity and real relative permittivity of Parylene C are plotted in Fig. 2.13.

2.1.6.2 Platinum

The CRC Handbook of Chemistry and Physics (Chemical Rubber Company, 2012) lists the resistivity of platinum at 27 °C as $10.8 \times 10^{-8}\,\Omega\,\mathrm{m}$. This gives a conductivity of $\sigma = 9.26 \times 10^{6}\,\mathrm{S\,m^{-1}}$. The real part of the relative permittivity was set to 1 as is customary for metals. These values are assumed to be fairly frequency-independent below optical frequencies (Scheffler et al., 2005).

2.1.7 Materials Summary

Table 2.4: Conductivity values with units $\mathrm{S\,m^{-1}}$

Material	$\sigma^{0\,\mathrm{Hz}}_{parallel}$	$\sigma^{0\,\mathrm{Hz}}_{transverse}$
Bone	0.02	
CSF	2	
Gray matter	0.02	
Muscle	0.24[a]	0.22[a]
Parylene C	1.42×10^{-12}[b]	
Platinum	9259259.25926	
WM (Dorsal Columns)	0.054	0.012
WM (Lateral & Ventral Funiculus)	0.049	0.013
Material	$\sigma^{958.5\,\mathrm{Hz}}_{parallel}$	$\sigma^{958.5\,\mathrm{Hz}}_{transverse}$
Bone	0.02	
CSF	2	
Gray matter	0.099	
Muscle	0.52[c]	0.34[c]
Parylene C	8.20×10^{-9}[d]	
Platinum	9259259.25926	
WM (Dorsal Columns)	0.17	0.038
WM (Lateral & Ventral Funiculus)	0.15	0.040

[a] f=10.0 Hz (closest frequency for ovine @37 degC muscle data)
[b] f=0.1 Hz (closest frequency for parylene C data)
[c] f=1000.0 Hz (closest frequency for ovine @37 degC muscle data)
[d] f=959.0 Hz (closest frequency for parylene C data)

2.2 COMSOL simulations

A Matlab program was written using the COMSOL Matlab interface to import the SolidWorks model, label the various materials in the model, and set the ma-

Table 2.5: Real relative permittivity values (unit less)

Material	$er^{0\,\mathrm{Hz}}_{parallel}$	$er^{0\,\mathrm{Hz}}_{transverse}$
Bone	110000	
CSF	110	
Gray matter	45000000	
Muscle	83000000[a]	41000000[a]
Parylene C	4.410[b]	
Platinum	1	
WM (Dorsal Columns)	94000000	21000000
WM (Lateral & Ventral Funiculus)	87000000	22000000
Material	$er^{958.5\,\mathrm{Hz}}_{parallel}$	$er^{958.5\,\mathrm{Hz}}_{transverse}$
Bone	2800	
CSF	110	
Gray matter	170000	
Muscle	1200000[c]	590000[c]
Parylene C	3.307[d]	
Platinum	1	
WM (Dorsal Columns)	190000	44000
WM (Lateral & Ventral Funiculus)	180000	46000

[a] f=10.0 Hz (closest frequency for ovine @37 degC muscle data)
[b] f=0.1 Hz (closest frequency for parylene C data)
[c] f=1000.0 Hz (closest frequency for ovine @37 degC muscle data)
[d] f=959.0 Hz (closest frequency for parylene C data)

terial properties as summarized in Tables 2.4 and 2.5. The mesh was set to "Extra fine" and can be seen in Fig. 2.14. The outside boundaries (extruded oval shaped) were set to be insulating (Neumann boundary condition), i.e. no current passing through them. For active electrodes, the voltage of the back surface of the electrode was set to the stimulating waveform (Dirichlet boundary condition). No voltage or current restrictions were placed on the non-active electrodes. Static (time invariant inputs) simulations were used for comparison and testing purposes. For time domain simulations, the time step (Δt) was set to 0.01 ms and solved for time $t_{bi,mono} = -10\varsigma_{bi,mono} \cdots + 10\varsigma_{bi,mono}$. For biphasic stimulation, $\varsigma_{bi} = 0.166\,04$ ms so the COMSOL simulation was run from simulation time $t_{bi} = -1.6604$ ms to $t_{bi} = 1.6604$ ms. For monophasic stimulation, $\varsigma_{mono} = 0.112\,84$ ms so the COM-

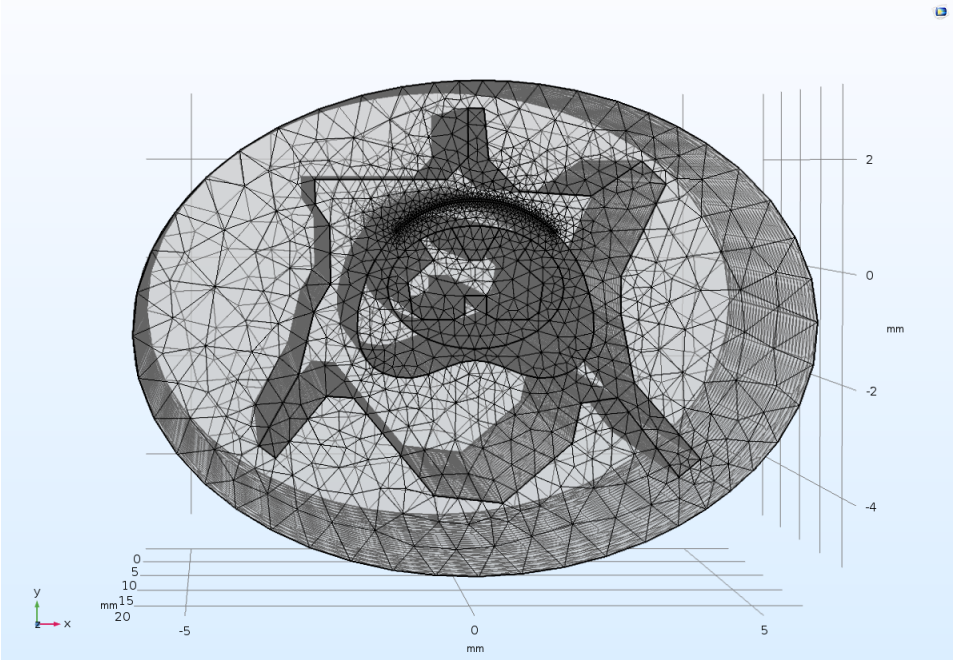

Figure 2.14: The finite element mesh used in all the volume conductor simulations.

SOL simulation was run from simulation time $t_{mono} = -1.1284$ ms to 1.1284 ms. After the simulations were complete, voltage time series were extracted from points corresponding to each segment of the neurons as will be described in Chapter 3.

2.2.1 Stimulation patterns

Although more complex patterns of the active stimulating electrodes are possible and have been used in humans (Harkema et al., 2011), for this thesis I will only consider bipolar combinations of electrodes. Each combination will be referred to by a name consisting of [positive electrode name][p for positive sign][negative electrode name][n for negative sign]. Each name implies a pair of equations. For example, combination A2pC5n means that the stimulation voltage on the back surface of the A2 and C5 electrodes are defined, respectively, by:

$$V_s^{\mathrm{A2}} = V_S G(t) \tag{2.38}$$

$$V_s^{\mathrm{C5}} = -V_S G(t), \tag{2.39}$$

where V_s is the stimulation scale factor (can be positive or negative with units of volts), and $G(t)$ is the stimulation shape function (either $G_{bi}(t)$ for biphasic stimulation or $G_{mono}(t)$ for monophasic stimulation (see Section 2.1.3 for definitions)). Electrodes not referenced in the combination name are simulated as floating. See Table 2.1 for electrode labels and array orientation. Figures 4.1 and 4.2 show the labeled electrode array in the simulated spinal cord.

The COMSOL simulations are linear so all simulations can be done with $V_s = 1\,\mathrm{V}$ and the output scaled for other voltages. For the electrode array described in Section 2.1.1 (3 columns and 7 rows), there are 210 unique bipolar combinations (considering that the combination A1pB1n ($V_s^{\mathrm{A1}} = V_S G(t)$, $V_s^{\mathrm{B1}} = -V_S G(t)$) is a scalar multiple of B1pA1n ($V_s^{\mathrm{B1}} = V_S G(t)$, $V_s^{\mathrm{A1}} = -V_S G(t)$). Since the model is an extrusion, the combinatorial number of simulations necessary can be reduced if translations of combinations of electrodes along the $\hat{z}$ direction result in the same output. To test this, I will compute stationary simulations for all three possible single row combinations (ANpBNn, ANpCNn, BNpCNn) for each row N and compare extracted voltage points under that row with the center row. Extracted points correspond to each segment in the neurons described in Chapter 3 (including all 6 axons directions). Figure 4.2 shows the locations of these neurons with the axons in the $-\hat{x}$ direction. The histogram results in Fig. 2.15 show that there are edge effects in rows 1 and 7. However, translations along the $\hat{z}$ axis between rows 2-6 result in nearly the same output. In this thesis, I will only consider combinations ignoring rows 1 and 7 to avoid edge effects.

Although the spinal cord model is not completely symmetric across the $x = 0$ plane (the bone and muscle geometry captured from the MRI data are not symmetric), it would be useful to test the difference between mirrored combinations. If the difference is small, then symmetry about the mid-line can be used to reduce the required number of simulations. The histogram of the difference between combina-

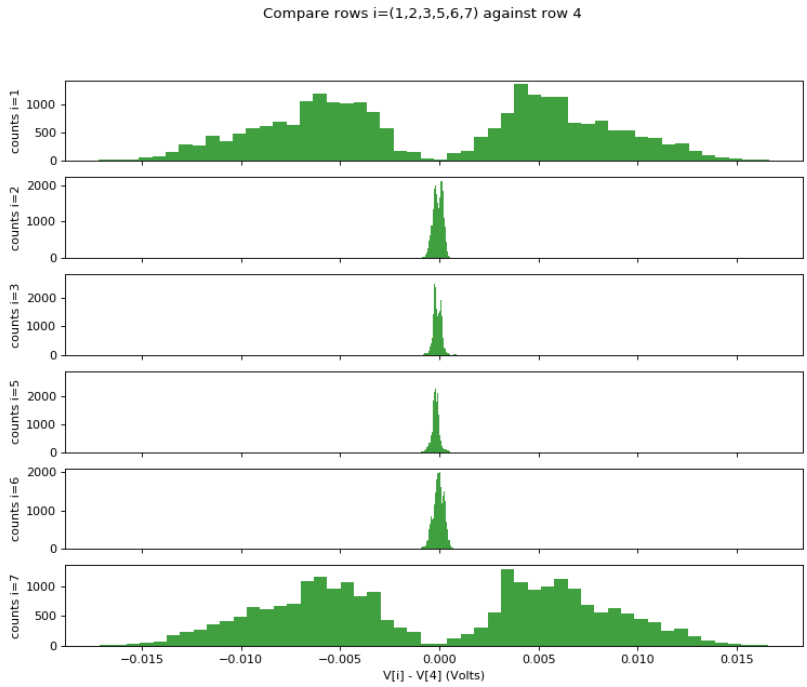

Figure 2.15: Comparison of combination translations along the $\hat{z}$ axis. Note the edge effects in row 1 and 7. The histogram includes all three single row combinations (ANpBNn,ANpCNn,BNpCNn) (where N is the row number) and stationary simulations run at $f_{\text{mono}}^{\text{max}} = 0\,\text{Hz}$ and $f_{\text{bi}}^{\text{max}} \approx 958.5\,\text{Hz}$.

tion A4pB4n and the mirrored output from B4nC4p can be seen in Fig. 2.16. These results show that there is a mean difference of 0.229 mV between these simulations. The maximum difference between these simulations was 1.49 mV. If these simulations are scaled by a factor of ±10 to reach maximum stimulation voltages of ±10 V, these differences would also be scaled by the same factor. This gives some idea of how much the results might change with differing physical geometry. While future studies may explore these geometry effects, the low differences support the use of symmetry.

Table 2.6 shows the number of unique bipolar combinations given different numbers of rows and different sets of assumptions. Given the previous discussion, edge rows are not used due to edge effects (5 active rows). Allowing $\hat{z}$ translations and mirroring across both the x=0 and z=0 planes yields 18 unique bipolar simulations:

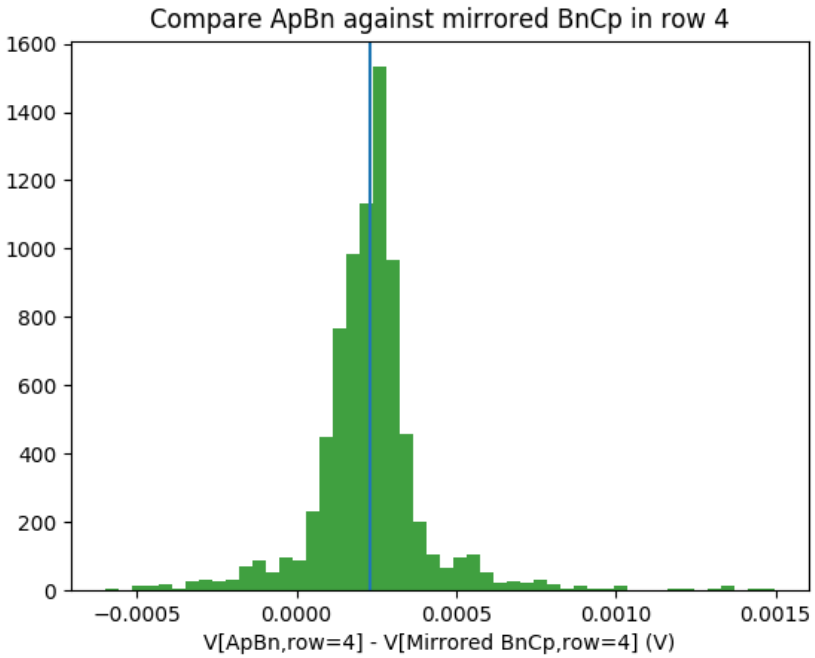

Figure 2.16: Comparison of combination ($A4 = 1V, B4 = -1V$) with mirrored combination ($C4 = 1V, B4 = -1V$). The mean difference is 0.229 mV (indicated by vertical line) and the maximum difference was 1.49 mV. The histogram includes stationary simulations run at $f_{\text{mono}}^{\text{max}} = 0\,\text{Hz}$ and $f_{\text{bi}}^{\text{max}} \approx 958.5\,\text{Hz}$.

A2pA6n, A2pB6n, A2pC6n, A3pA5n, A3pA6n, A3pB5n, A3pB6n, A3pC5n, A3pC6n, A4pA5n, A4pB4n, A4pB5n, A4pC4n, A4pC5n, B2pB6n, B3pB5n, B3pB6n, and B4pB5n.

Table 2.6: Number of unique bipolar combinations

# of rows	all bipolar	A	B	C	D
1	3	3	3	2	2
2	15	12	9	7	6
3	36	21	15	12	10
4	66	30	21	17	14
5	105	39	27	22	18
6	153	48	33	27	22
7	210	57	39	32	26

[A] allowing $\hat{z}$ translations
[B] allowing $\hat{z}$ translations and mirroring across the z=0 plane
[C] allowing $\hat{z}$ translations and mirroring across the x=0 plane
[D] allowing $\hat{z}$ translations and mirroring across both the x=0 and z=0 planes

2.2.2 Computational details

Simulations were conducted using COMSOL 5.1 and MATLAB R2012a on a machine with 94G RAM and dual Intel® Xeon® X5550 CPUs operating at 2.67GHz. Each biphasic simulation (i.e. one combination) on average took 5.5 ± 0.2 hours. Each monophasic simulation on average took 2.8 ± 0.1 hours. For the biphasic stimulation, the time series extraction on average took 4.73 ± 0.07 minutes for each combination. For monophasic, the same extraction took on average 3.22 ± 0.3 minutes.

2.3 Summary

In this chapter, I discussed the finite element model of the rat lumbosacral spinal cord and electrode array that will be used in the rest of the thesis. The geometry of the finite element model was derived from an extrusion of a transverse slice of an MRI image of the L1 vertebra. Stimulation waveforms were analyzed for their dominant frequency components, and material properties (conductivity and permittivity) were selected using the main frequency component of each stimulation waveform. The finite element model was validated by comparing extracted voltage values for translated single row combinations and mirrored combinations which should result in the same voltage potentials.

2.A Appendix: Conductivity and relative permittivity measurements from literature compared with 4-cole-cole fits

Conductivity and relative permittivity measurements for bone, CSF, gray matter, muscle, and isotropic white matter from a variety of animals and original authors were obtained from (C. Gabriel and S. Gabriel, 1997). 4-Cole-Cole parameters for these materials were also obtained from the same source. Conductivity values from (Josef Ladenbauer, 2008) were also obtained for comparison.

The collected data for muscle is presented in Fig. 2.17. Parameters for a 4-Cole-

Cole fit are only available for transverse muscle even though data is available for parallel muscle. At frequencies below 1 kHz, there is about an order of magnitude variation in the conductivity and 2 orders of magnitude in the permittivity variation. There also appears to be significant differences in the amount of anisotropy found in the different studies.

The collected data for bone is presented in Fig. 2.18. It shows variation of 2 orders of magnitude in both conductivity and relative permittivity below 1 kHz, depending on the type of bone and the animal source.

Figure 2.19 plots the very limited data available for cerebro spinal fluid (CSF). The value that Ladenbauer used for the CSF ($1.7\,\mathrm{S\,m^{-1}}$ @ 1000 Hz) is certainly closer in frequency to the dominant frequencies of the stimulation waveforms used in this thesis than the data used for the 4-Cole-Cole fit, but the corresponding relative permittivity was not available, so the value ($2\,\mathrm{S\,m^{-1}}$) obtained from the 4-Cole-Cole fit was used instead.

Figure 2.20 presents the conductivity and permittivity of white matter. At high frequencies the conductivity and permittivity of white matter appears to be conserved across species and studies. The values of conductivity used in (Josef Ladenbauer, 2008) (from a cat) appear to be significantly larger than those found by Gabriel et al. in a sheep.

Figure 2.21 shows the collected data for gray matter. The grey matter values appear to have minimal variation across species and samples at high frequencies. The conductivity of grey matter used in (Josef Ladenbauer, 2008) also seems high compared with the values Gabriel et al. found in a sheep.

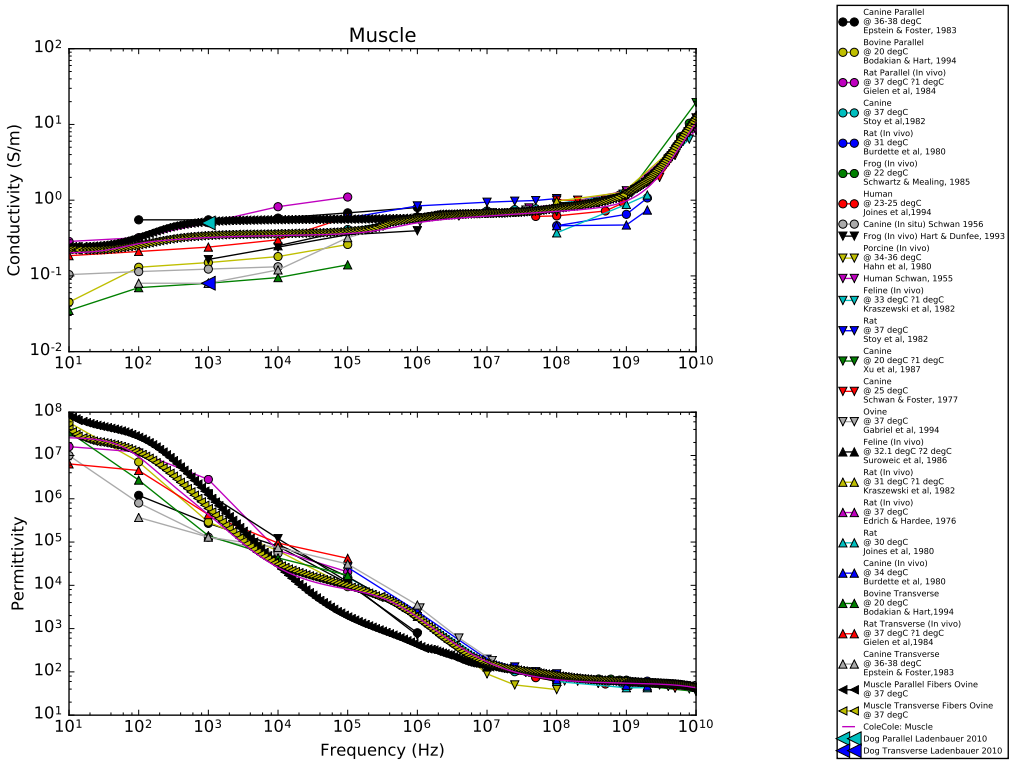

Figure 2.17: Data and Cole-Cole fits for Muscle. The 4-Cole-Cole fit is only for transverse muscle even though data is available for both parallel and transverse. Data from (C. Gabriel and S. Gabriel, 1997) and (Josef Ladenbauer, 2008).

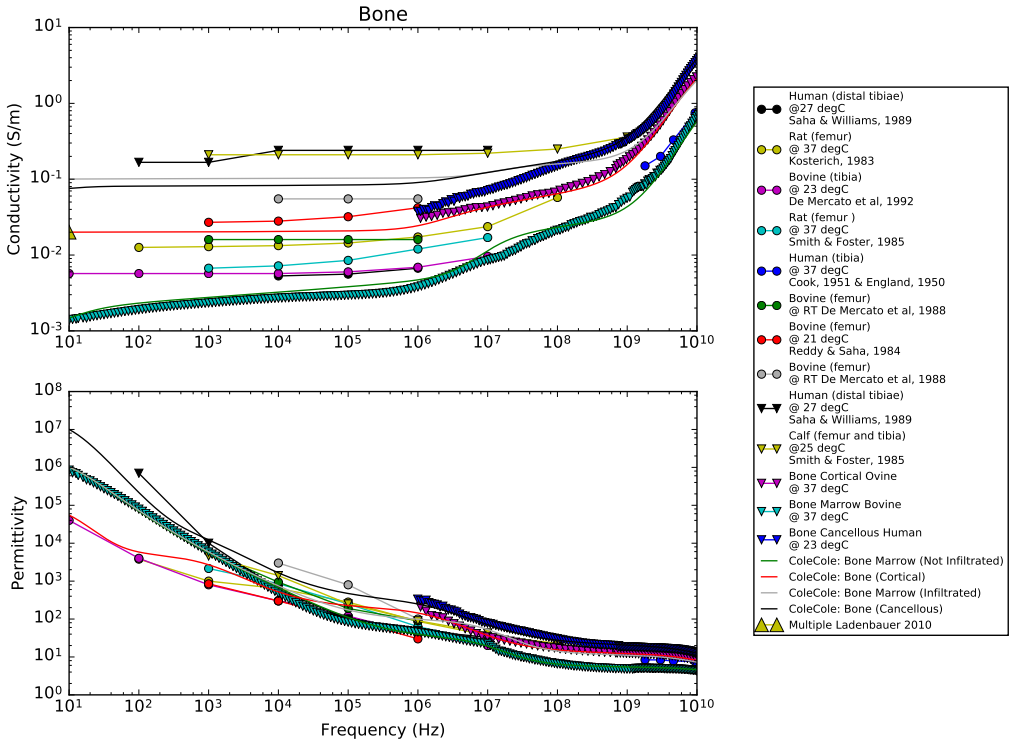

Figure 2.18: Data and Cole-Cole fits for bone. Data from (C. Gabriel and S. Gabriel, 1997) and (Josef Ladenbauer, 2008).

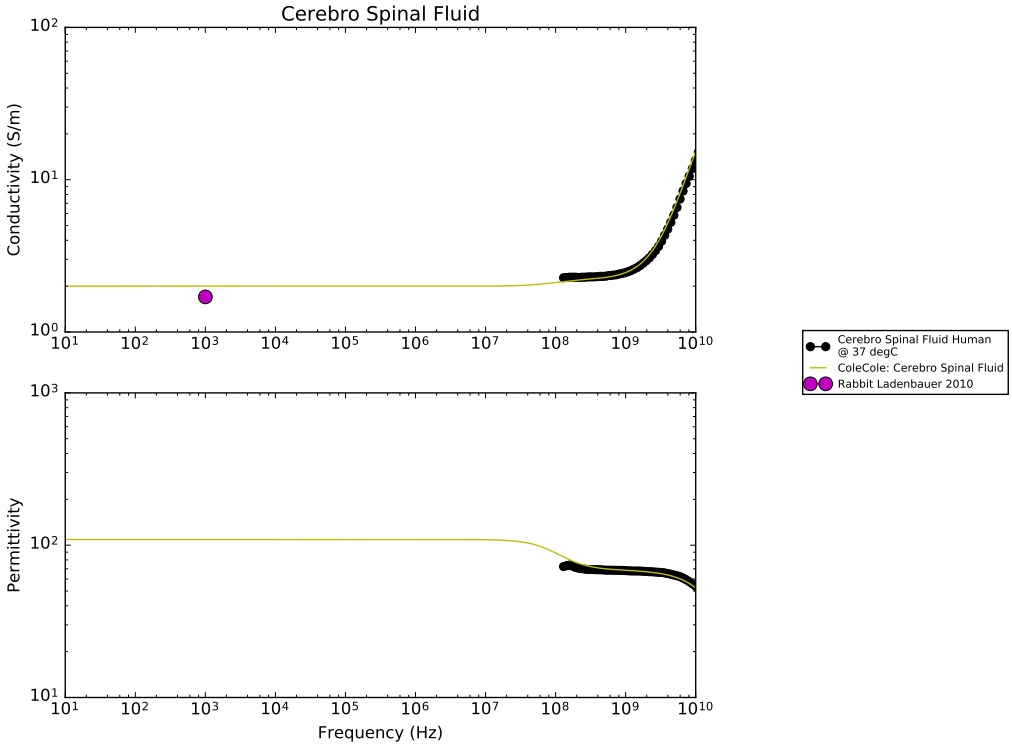

Figure 2.19: Data and Cole-Cole fits for cerebro spinal fluid (CSF). Data from (C. Gabriel and S. Gabriel, 1997) and (Josef Ladenbauer, 2008).

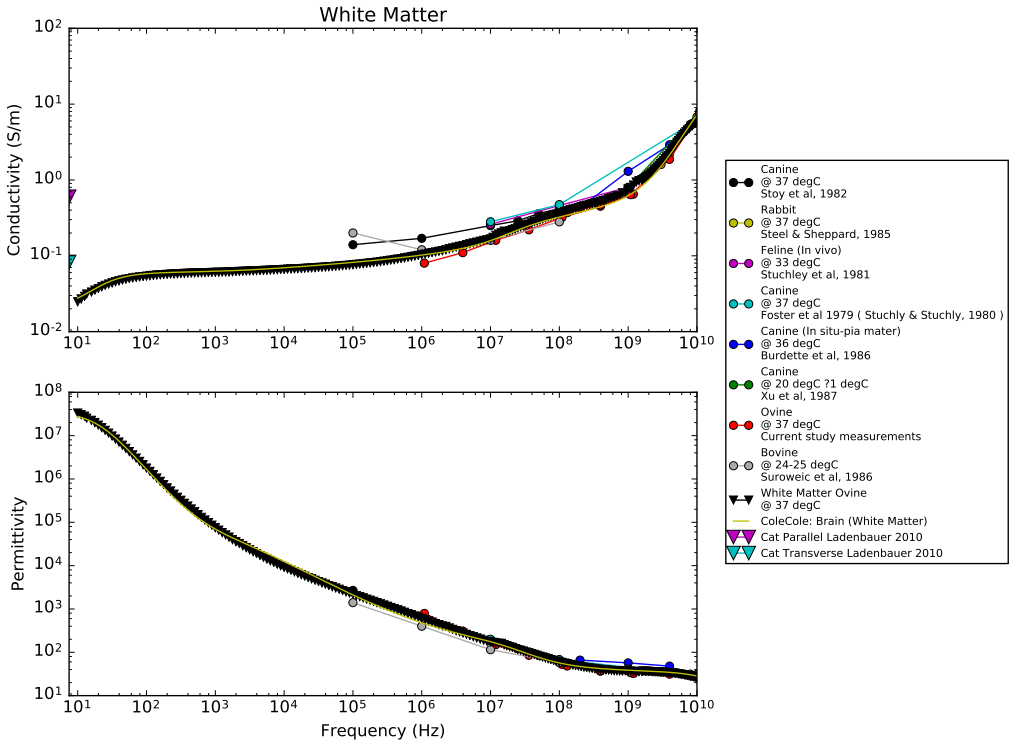

Figure 2.20: Data and Cole-Cole fits for isotropic white matter. Data from (C. Gabriel and S. Gabriel, 1997) and (Josef Ladenbauer, 2008).

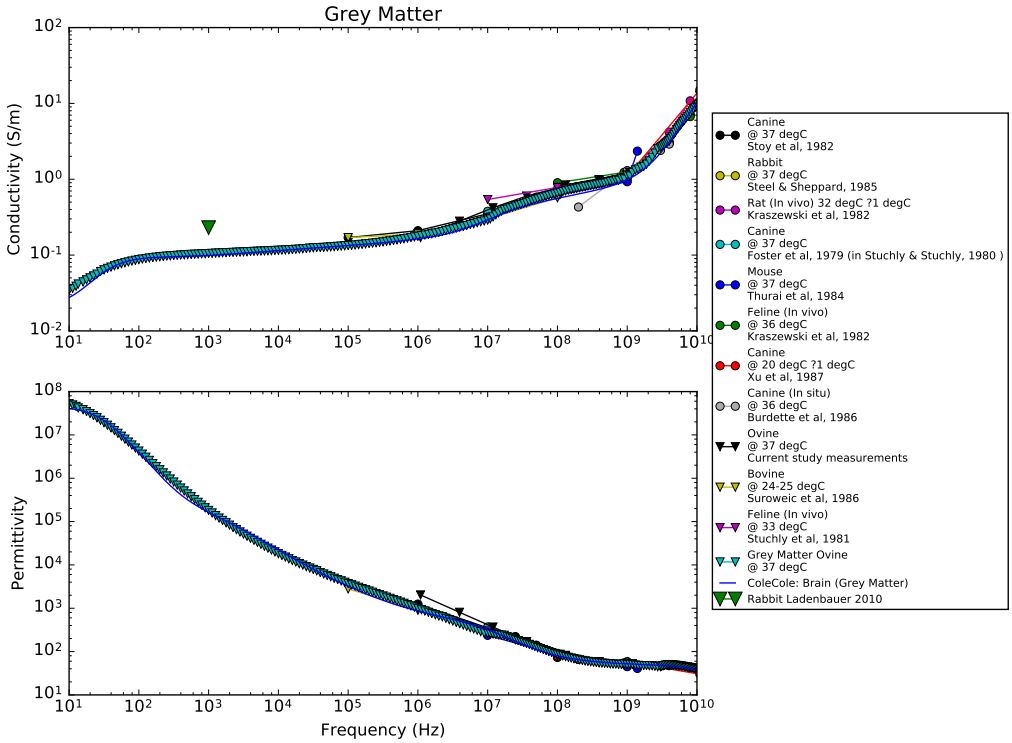

Figure 2.21: Data and Cole-Cole fits for gray matter. Data from (C. Gabriel and S. Gabriel, 1997) and (Josef Ladenbauer, 2008).

Chapter 3

BUILDING A NEURON MODEL OF A RAT SPINAL INTERNEURON

The previous chapter showed how simulation could be used to obtain a time series of the extracellular voltage, V_e, in a volume conductor model as a function of time for various electrode combinations. This chapter will discuss a computational model for a rat spinal interneuron. In the next chapters, the extracellular voltage from the volume conductor model will be applied to this neuron model to study the effect of epidural stimulation on neurons in the spinal cord. In particular, I will study if particular patterns of extracellular voltage from the epidural stimulation process can cause or facilitate the release of neurotransmitters from the tip of the axon.

The simulations of neuron dynamics used in this thesis are performed using NEURON version 7.3 (Michael L. Hines and Nicholas T. Carnevale, 1997). NEURON is a compartmental model neuron simulator. It simulates biological neurons by dividing each neuron into groups of compartments, called sections, which have similar membrane properties but may differ in diameter. The compartments in each section are referred to as segments and each may have a different diameter and 3D position. This thesis will not cover the background behind NEURON or compartmental modeling in detail. Readers unfamiliar with this material are encouraged to read (Michael L. Hines and Nicholas T. Carnevale, 1997). I will only cover the details necessary to reproduce the results reported in this thesis using the NEURON simulator.

Section 3.1 covers the neuron electrical properties which are used in the simulations. These properties are based on (Ostroumov, 2007). The model includes

sodium channels (INa), potassium fast channels (IK_A), and potassium delayed rectifier channels (IK_{dr}). In particular, the dendrites include sodium channels and potassium delayed rectifier channels, which means that the model described in this chapter includes active dendrites (dendrites with a non-linear response) rather than the passive dendrite model used in (Capogrosso et al., 2013). This section also discusses how the ion channels are modeled.

Section 3.2 covers the construction of a simple neuron model with 5 dendrites (with proximal and distal sections), a soma, and an axon (with axon hillock (AH), initial segment (IS), and axon proper sections). A simple constructed neuron model based on parameters from (Thurbon et al., 1998) and (Ostroumov, 2007) was chosen because of the difficulties in obtaining accurate 3D models of rat spinal interneurons and the increased computational demands of a complex model. It is hoped that results from this study will inspire further studies with more realistic neuron models.

Section 3.3 discusses models of neurotransmitter release from the axon tip due to neuron membrane activity (Section 3.3.2) and a synapse model (Section 3.3.1). In this thesis, a synapse is artificially triggered at specific times but would normally be triggered by neurotransmitters released by another neuron.

The simple neuron model is characterized in Section 3.4 so that it can be compared with neuron models and experimental data in other papers. Section 3.4.1 describes how the resting potential of the neuron was found. Section 3.4.2 describes the results of injecting 0.1 ms square current pulses into the neuron at each segment of the neuron. Section 3.4.3 finds the synapse weight thresholds for synapses placed in the interval from the soma to the distal tip of a dendrite. Sub-threshold synapse weights based on these thresholds are used in combination with sub-threshold stimulation to study facilitation in Chapter 5.

3.1 Model neuron properties

The membrane of a neuron cell is composed of a bilayer of lipid molecules which acts as an insulator. Various proteins are embedded in the lipid layers. Some of these proteins form ion channels which allow electrically charged ions to pass through the membrane. Many of these ion channels selectively allow only certain ions through in response to factors such as: membrane voltage, interactions with molecules outside or inside the cell, or the internal state of the ion channel. Other proteins in the membrane form ion pumps which push specific ions against the diffusion gradient to maintain the resting state of the neuron. The NEURON simulator models the ion pumps as a generalized leakage current across the membrane resistance (R_m) and a passive reversal potential (e_{pas}). Figure 3.1 shows the circuit representation of NEURON's model of a single compartment (segment) of a neuron.

The following properties of the neuron membrane were the same for all neuron sections used in the simulations and were taken from (Ostroumov, 2007):

- $e_{pas} = -70\,\text{mV}$ (the reversal potential of the uniformly distributed leakage current)
- $e_{na} = 50.0\,\text{mV}$ (the reversal potential of Na+ ions)
- $e_k = -77.0\,\text{mV}$ (the reversal potential of K+ ions)
- $C_m = 2.4\,\mu\text{F}\,\text{cm}^{-2}$ (the specific membrane capacitance)
- $R_m = 5300\,\Omega\,\text{cm}^2$ (the membrane resistance)
- $R_a = 87\,\Omega\,\text{cm}$ (the axial resistance)
- $R_{xraxial} = 1 \times 10^9\,\text{M}\Omega\,\text{cm}^{-1}$ (the resistance of the extracellular medium along the axial direction, value is the NEURON default)

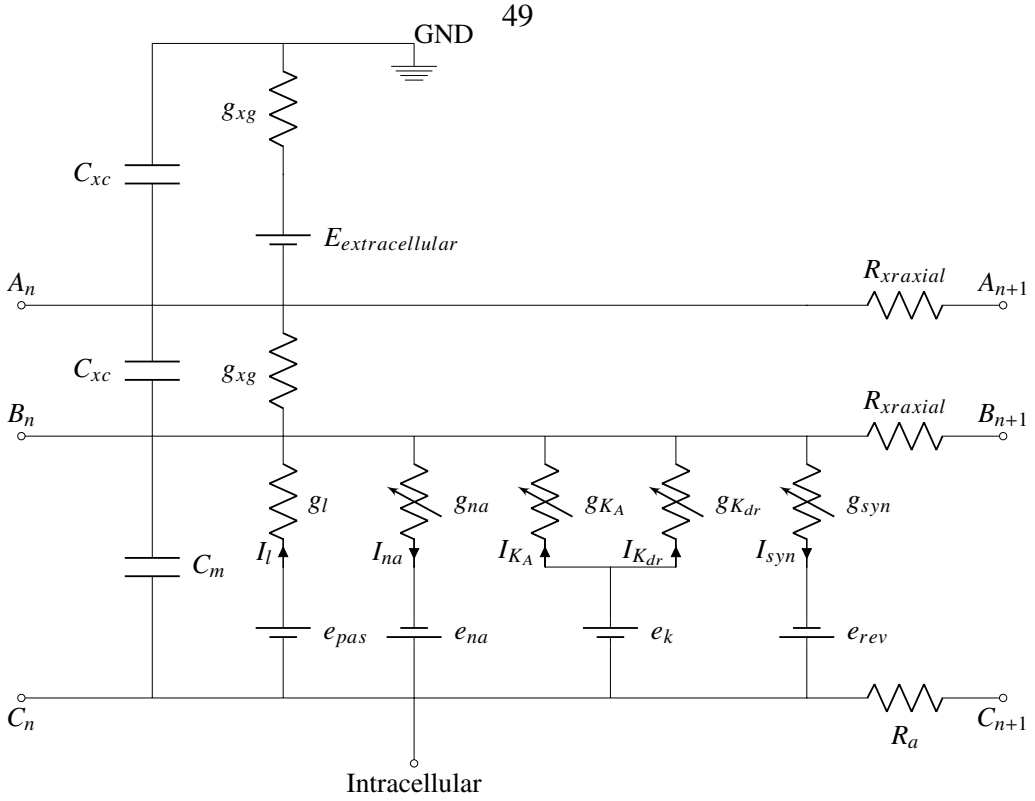

Figure 3.1: Neuron compartment circuit model for arbitrary compartment n including all modeled ion channels, a synapse, and extracellular voltage ($E_{extracellular}$). Points (A_n,B_n,C_n) connect to the corresponding points on the right hand side of compartment $n-1$. Starting from the bottom and going left to right,the components in the circuit are: the passive properties of the compartment which are modeled by the following components in the bottom left: the membrane capacitance (C_m), the membrane leakage conductance (g_l), and the reversal potential of the leakage current (e_{pas}). To the right of that is the sodium channel with variable conductance g_{na} (given by Eq. (3.1)) and e_{na} which is the reversal potential of Na^+ ions. To the right of that is the fast potassium channel with variable conductance g_{K_A} (given by Eq. (3.2)) and e_k which is the reversal potential of K^+ ions. The potassium delayed rectifier conductance ($g_{K_{dr}}$) is also connected to e_k and is given by Eq. (3.3). The synapse channel (only present if the compartment has a synapse attached) consists of the variable synaptic conductance g_{syn} (given by Eq. (3.5)) and the reversal potential of the synapse (e_{rev}). The axial resistance inside the neuron is modeled by resistance R_a. The upper portion of the circuit is the extracellular voltage mechanism of NEURON and is described in more detail in the NEURON documentation. $R_{xraxial}$ is the resistance of the extracellular medium along the axial direction. g_{xg} is the conductance of the extracellular medium between the extracellular potential and the membrane surface. C_{xc} is the capacitance of the extracellular medium (by default $C_{xc} = 0$ indicating an open circuit). $e_{extracellular}$ is the extracellular voltage which is obtained from the volume conductor models. Points (A_{n+1},B_{n+1},C_{n+1}) connect to the corresponding points in the next compartment ($n+1$).

- $g_{xg} = 1 \times 10^9\,\mathrm{S\,cm^{-2}}$ (the conductance of the extracellular medium between the extracellular potential and the membrane surface, value is the NEURON default)

- $C_{xc} = 0\,\mu\mathrm{F\,cm^{-2}}$ (the capacitance of the extracellular medium, value is the NEURON default)

The active ion channels (sodium channel, potassium fact channel, and potassium delayed rectifier channel) were taken from (Ostroumov, 2007). The maximum conductances of each channel in each section type are summarized in Table 3.1. The conductance of the sodium channel is given by:

$$g_{na} = g_{na,max} m_{ina}^3 h_{ina} \tag{3.1}$$

where $g_{na,max}$ is the maximum conductance of the channel given in Table 3.1, m_{ina} is the state variable of activation, and h_{ina} is the state variable of inactivation. The conductance of the potassium fast channel is given by:

$$g_{k_A} = g_{K_A,max} m_{ika}^4 h_{ika} \tag{3.2}$$

where $g_{K_A,max}$ is the maximum conductance of the channel given in Table 3.1, m_{ika} is the state variable of activation, and h_{ika} is the state variable of inactivation. The conductance of the potassium delayed rectifier channel is given by:

$$g_{k_{dr}} = g_{K_{dr},max} m_{ikdr}^4 \tag{3.3}$$

where $g_{K_{dr},max}$ is the maximum conductance of the channel given in Table 3.1 and m_{ikdr} is the state variable of activation. More detailed discussion of these channels can be found in (Safronov, Wolff, and Vogel, 2000). NEURON mod files for these

channels were obtained from Senselab model 138273[a]. Neurons were simulated at 37 °C using a timestep of 0.01 ms.

Table 3.1: Simple neuron ion channel conductances: the maximum conductances of the sodium channel ($g_{na,max}$), potassium fast channel ($g_{K_A,max}$), and potassium delayed rectifier channel ($g_{K_{dr},max}$) for each section type.

SectionType	$g_{na,max}$ (Ω^{-1} cm^{-2})	$g_{K_A,max}$ (Ω^{-1} cm^{-2})	$g_{K_{dr},max}$ (Ω^{-1} cm^{-2})
Soma	0.113	0.218	0.029
Proximal	0.003	0	0.001
Distal	0.003	0	0.001
AH	0.7	0	0.11
IS	0.7	0	0.11
AxonProper	0.012	0	0.04

From (Ostroumov, 2007)

3.2 Model neuron physical geometry

Detailed 3D models of neurons in the rat spinal cord are still very limited. Some researchers (Capogrosso et al., 2013) use the dendritic tree and soma from cat spinal neurons after resizing it and adding an axon. That is one possible solution, but it is unclear how similar these neurons are to the neurons in the rat spinal cord. More complex neuron models also require more computational resources. I chose to instead construct a simple neuron with parameters approximately matching those of (Thurbon et al., 1998) and (Ostroumov, 2007). It is my hope that using this simple neuron model at many locations, orientations, and stimulation configurations will compensate for the lack of a more complex model and perhaps give more general results.

Based on the morphological data in (Thurbon et al., 1998) the mean number of neurites in ventral horn neurons is 5.50 with sampled range from 3 to 8. Without additional data, I am assuming that the distribution in the dorsal horn is about the same and picking 6 neurites for the model. This also makes it easy to distribute

[a] https://senselab.med.yale.edu/modeldb/ShowModel.cshtml?model=138273&file=/NeuroMorph/Motoneuron-MorphoLogy/neuron/

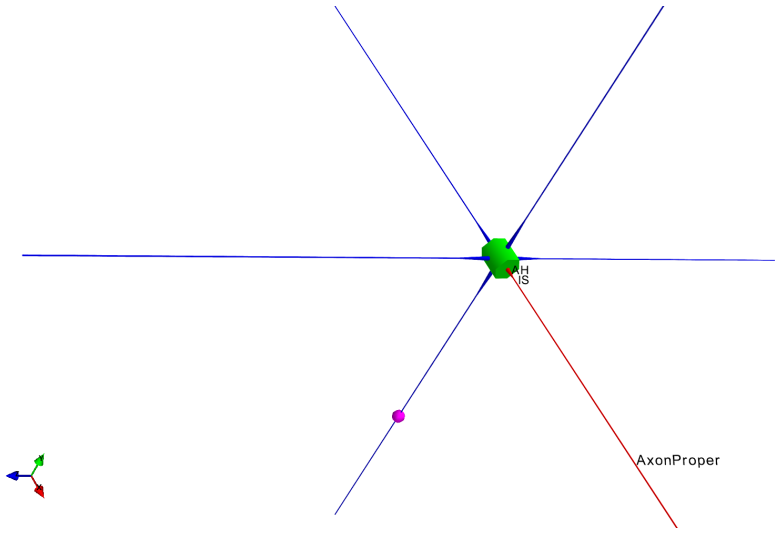

Figure 3.2: Model neuron showing dendrites (blue), soma (green), axon (red), and synapse location (pink ball). The synapse is shown here in the middle of one of the distal sections of the dendrites. This is one of the 5 possible location "A"s indicated in Fig. 3.3.

the neurites along the 6 Euclidean axis directions ($-\hat{x}$, $+\hat{x}$, $-\hat{y}$, $+\hat{y}$, $-\hat{z}$, and $+\hat{z}$) in an x-y-z coordinate system as described in Section 2.1.1. Based on the soma surface areas in (Thurbon et al., 1998), the mean spherical soma equivalent has a diameter of 25 µm and a range from 15.8 µm to 31.8 µm. A soma diameter of 20 µm was chosen to be in this range and match the model used in Table 2 of (Ostroumov, 2007). The total length of each neurite was chosen to be 290 µm to be approximately consistent with Figure 6 in (Thurbon et al., 1998). This means that each neuron fits inside a sphere with radius 300 µm.

The axon was modeled as 3 sections (listed proximal-distal from the soma), an axon hillock (AH) (with length 8 µm and a diameter varying linearly from 3 µm at the soma to 0.8 µm on the distal end), an initial segment (IS) (with a length of 10 µm and a constant diameter of 0.8 µm), and the axon proper (with a length of 272 µm[b] and a constant diameter of 0.8 µm). All of the axon parameters were taken from (Ostroumov, 2007) Section 3.2 except for the axon proper length which was chosen

[b] $(300 - 20/2 - 8 - 10)\mu m$

to match the total neurite size. The width of the axon is also supported by (Nunes et al., 2017; Saliani et al., 2017).

Each dendrite in the model consists of a proximal section (with length 25 µm, from Ostroumov 2007, Section 3.5) and a diameter varying linearly from 3 µm (consistent with AH diam and Ostroumov 2007 fig 2 (c) (1 dendritic end branch)) at the soma to 0.8 µm on the distal end) and a distal section (with length 265 µm[c] and constant diameter of 0.8 µm). The diameter of the distal section of the dendrite was selected based on the average diameter of a dendrite ((0.78 ± 0.05) µm) in (Thurbon et al., 1998) Table 3. The average diameter of a dendrite was calculated using $\frac{A_D}{\pi l_{Tot}}$ where A_D is the total membrane surface area in µm^2 and l_{Tot} is the total dendritic path length in µm. The physical parameters for this simple neuron are summarized in Table 3.2.

The total surface area for the soma (1256.6 µm^2), axon (823.1 µm^2), and dendrites (4115.5 µm^2) are in the distribution indicated in the sampling of neurons given in (Thurbon et al., 1998) Table 3.

Using the "d_lambda" rule from (M. L. Hines and N. T. Carnevale, 2001) and found at https://www.neuron.yale.edu/neuron/static/docs/d_lambda/d_lambda.html, the number of compartmental segments for the soma, proximal dendrite, axon hillock, and initial segment sections were each respectively set to 1. Similarly, the distal dendrites and the axon proper sections were set to have 17 segments. Please note that in this thesis, segments are numbered starting at 0, so the segments in the Distal dendrite or the AxonProper would be numbered [0, 1, 2, 3, 4, 5, 6, 7, 8, 9, 10, 11, 12, 13, 14, 15, 16], where segment 0 is closest to the soma, segment 8 is in the middle of the section, and segment 16 is at the distal tip.

[c] (300 − 20/2 − 25)µm

Table 3.2: Simple neuron physical parameters

SectionType	length (μm)	proximal diam (μm)	distal diam (μm)
soma	20	20	20
proximal dendrite	25[*]	3[†]	0.8[‡]
distal dendrite	265[§]	0.8[‡]	0.8[‡]
axon hillock	8[¶]	3[¶]	0.8[‡]
IS	10[¶]	0.8[‡]	0.8[‡]
AxonProper	272[‖]	0.8[¶]	0.8[¶]

[*] (Ostroumov, 2007) Section 3.5
[†] Consistent with AH and (Ostroumov, 2007) fig 2 (c) (1 dendritic end branch)
[‡] Calculated from Thurbon 1998 Table 3 using average diameter of a dendrite = $\frac{A_D}{\pi l_{Tot}}$ where A_D is the total membrane surface area in μm^2, and l_{Tot} is the total dendritic path length in μm. The average diameter of a dendrite was (0.78 ± 0.18) μm.
[§] 300 − 20/2 − 25
[¶] (Ostroumov, 2007) Section 3.2 also consistent with ‡ and (Nunes et al., 2017)
[‖] 300 − 20/2 − 8 − 10

Table 3.3: Simple neuron segments based on "d_lambda" rule from (M. L. Hines and N. T. Carnevale, 2001)

SectionType	number of segments
Soma	1
Proximal	1
Distal	17
AH	1
IS	1
AxonProper	17

3.3 Neurotransmitter models

In a biological neural system, information enters a post-synaptic neuron when a pre-synaptic neuron releases neurotransmitters which bind to ligand-gated ion channels on the post-synaptic neuron. The ligand-gated ion channels then open and cause a post-synaptic potential (PSP). In the case of an excitatory synapse, this is referred to as an excitatory post-synaptic potential (EPSP). If the sum of the PSPs (both inhibitory and excitatory) in the neuron increases the potential above a certain threshold value, an action potential occurs. If the action potential reaches the

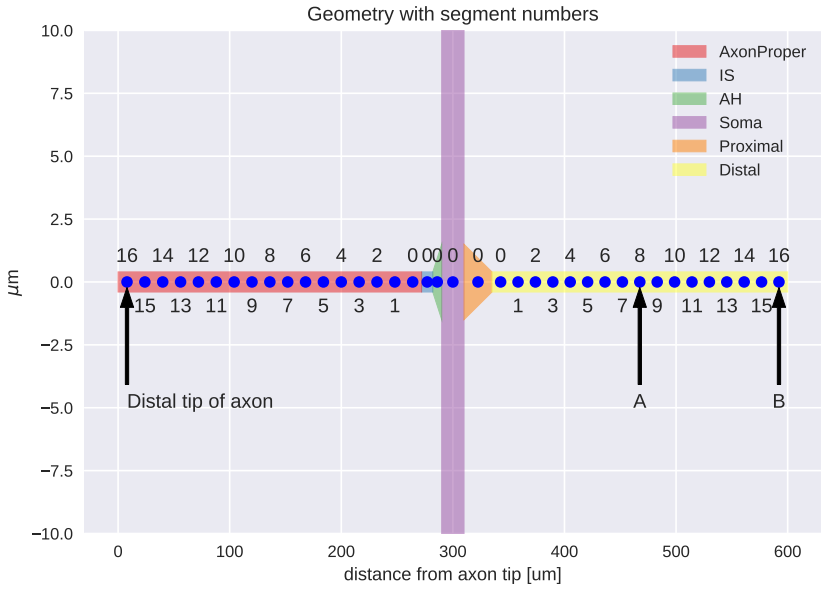

Figure 3.3: This figure shows the sections of the model neuron from the axon tip on the left side to the distal tip of one of the dendrites on the right side. Only one of the 5 dendrites is shown (since the rest only differ in orientation). Each section type is labeled by color (see legend). The diameter of the various sections is indicated by the size of the section on the vertical axis and the length of each section on the horizontal axis. The horizontal axis also indicates the path length distance from the axon tip. The center of each segment inside each section is indicated by a blue circle and labeled with a black number. The distal tip of the axon is labeled. Location "A" is in the middle of the distal section of the dendrite with segment number 8. Location "B" is at the distal tip of the distal section of the dendrite with segment number 16. These locations will be used for probe points in Chapters 3 to 5 and synapse locations in Chapters 3 and 5. Note that because there are 5 dendrites, there are 5 location "A"s and 5 location "B"s on each neuron. These will be distinguished (if it matters) by indicating the orientation of the dendrite the location is on. See Fig. 3.2 for a 3D view of the entire neuron.

axon tip, usually the membrane voltage at the axon tip is raised sufficiently for neurotransmitters to be released from the axon tip and communicate with the next cell.

Studying the facilitation of information transmission in neurons requires models for the synaptic current generated when the neurotransmitters are received, the neuron processes the input, and neurotransmitter is released.

3.3.1 Synapse model: Exp2Syn

The current through a synapse after the synapse is triggered by neurotransmitters from the presynaptic cell was modeled using the Exp2Syn[d] synapse model. The Exp2Syn consists of a trans-membrane current (Santos et al., 2009):

$$I_{syn} = g_{syn} * (V_{m@syn} - E_{\text{Rev}}) \tag{3.4}$$

where

$$g_{syn} = \frac{\tau_D}{\tau_D - \tau_R} * (e^{\frac{-t}{\tau_D}} - e^{\frac{-t}{\tau_R}}) * g_M, \tag{3.5}$$

τ_D is the conductance decay time constant, τ_R is the conductance rise time constant, g_M is the maximum synapse conductance (also referred to as the synaptic weight), V_m is the membrane voltage at the synapse location, and E_{Rev} is the reversal potential. In this thesis, $\tau_R = 0.5\,\text{ms}$, $\tau_D = 5\,\text{ms}$, and $E_{\text{Rev}} = 0$. These values correspond to excitatory glutamatergic synapses formed by interneurons in the substantia gelatinosa in the rat spinal cord and were obtained from (Santos et al., 2009).

Each time that an excitatory synapse is triggered (by neurotransmitters from a presynaptic neuron in a real biological system or by a trigger event in simulation) the time-varying trans-membrane current I_{syn} gives rise to a change in the membrane voltage at the synapse and the rest of the cell. As mentioned previously, this change in membrane voltage is referred to as an excitatory post-synaptic potential or EPSP. Each EPSP depends indirectly on the entire state of the neuron, since the tran-membrane current (I_{syn}) is dependent on the membrane current at the synapse ($V_{m@syn}$). $V_{m@syn}$ is in turn dependent (indirectly) on the state of the entire neuron (V_m, V_e, and ion channel states). One or more of these EPSPs can combine to

[d] https://www.neuron.yale.edu/neuron/static/py_doc/modelspec/programmatic/mechanisms/mech.html#Exp2Syn

cause enough of an increase in the membrane potential at the axon tip to activate the neuron and cause the release of neurotransmitters.

3.3.2 Neurotransmitter release

Most other stimulation literature uses recruitment/activation definitions similar to "considered recruited if the resulting depolarization elicited an action potential that traveled along the efferent axon" (Capogrosso et al., 2013) or "propagating action potentials were initiated" (J Ladenbauer et al., 2010). Unfortunately, when dealing with electrical stimulation of neurons, these definitions can be ambiguous. For example, an action potential may be generated near the soma but not reach the axon tip with sufficient potential to cause neurotransmitter release because the external stimulating field can quench activity further down the axon. The opposite can also occur, where no action potential is generated but the membrane voltage at the axon tip is raised by stimulation above the amount necessary to release neurotransmitters. For information to be transmitted to the next post-synaptic neuron, the release of neurotransmitters is required, while action potentials may not be.

While neurotransmitter release could be modeled using kinetic models as in (Destexhe, Mainen, and Sejnowski, 1994), this thesis study uses Equation (37) from (Destexhe, Mainen, and Sejnowski, 1994) to model this process:

$$[L](V_{pre}) = \frac{L_{\max}}{1 + \exp(-(V_{pre} - V_p)/K_p)} \tag{3.6}$$

where $[L]$ is the concentration of an arbitrary neurotransmitter L, V_{pre} is the presynaptic membrane voltage measured in the axon tip, $L_{\max} = 2.84\,\text{mM}$ is the maximum concentration of neurotransmitter in the synaptic cleft, $V_p = 2\,\text{mV}$, and $K_p = 5\,\text{mV}$. This equation is plotted in Fig. 3.4. For the purposes of this thesis, a neuron is considered to have released neurotransmitters if the membrane voltage on the distal tip of the axon goes above $-10\,\text{mV}$, and in this case, will be referred to as

an *active* neuron.

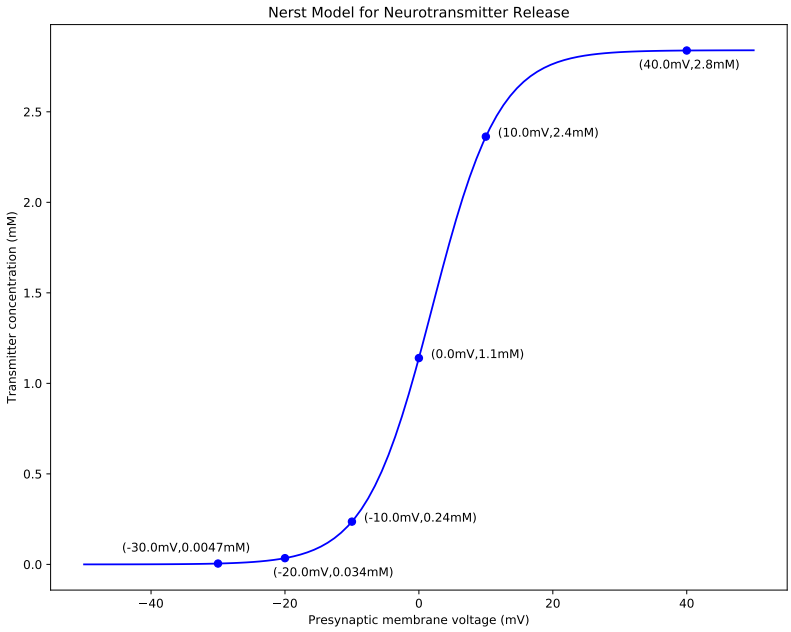

Figure 3.4: Amount of neurotransmitter released (in millimolar concentration) as a function of membrane voltage (in mV) from Eq. (3.6).

3.4 Neuron characterization

In order to better understand the behavior of the simple neuron model and to benchmark the model against other known results, computational experiments were conducted to determine the resting potential, the firing threshold of the neuron in response to current pulse injection, and the firing threshold in response to synapse firing.

3.4.1 Resting potential of model neuron

Six neuron models were generated with their axons lying respectively along the $-\hat{x}$, $+\hat{x}$, $-\hat{y}$, $+\hat{y}$, $-\hat{z}$, and $+\hat{z}$ directions, i.e. an axon located along the $+\hat{x}$ direction has its distal tip located in a more positive x-coordinate than the soma. The initial membrane voltage (V_m) in all segments of all sections of the neurons was set to

$v_{init} = -70\,\text{mV}$ at $t = 0$. Then a NEURON simulation is executed for 800 ms (without an external electric field or synapses firing) until the simulated neuron's membrane voltage reaches steady state. The state of each neuron model at steady state was saved so that it could be reloaded to save computational time for future simulations. The resting membrane voltage at the end of these simulations can be seen in Fig. 3.5.

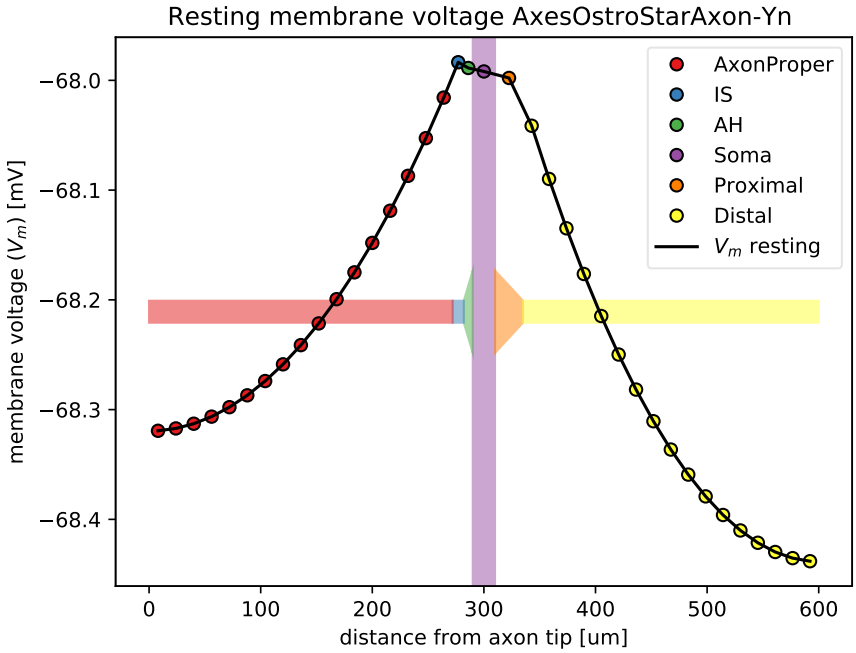

Figure 3.5: The resting membrane voltage (V_m) for each segment along the model neuron's axon, soma, and a single dendrite after 800 ms of simulation time with no external inputs. The colored polygons show where the neuron model sections are and their relative diameters. Since all five dendrites in the model have an identical resting membrane voltage distribution as a function of distance from the soma, only one result is plotted.

3.4.2 Current injection

One way to validate the neuron model used in this thesis is to compare the response of the neuron to a known experimental configuration used in other papers. The (Ostroumov, 2007) paper contains 2 current injection studies where increasing amplitudes of square current pulses (width = 0.1 ms in Figure 4(c) and width 5 ms in Figure 4(d)[e]) are injected into the soma until one of them causes the membrane voltage at the soma to exceed -10 mV. The results for the simple neuron model, a modified simple neuron model with thicker dendrites, and the data from (Ostroumov, 2007) are summarized in Table 3.4. The model presented in (Ostroumov, 2007) requires between 2.4 to 2.95 times more current for a 5 ms pulse and 3 to 4.3 times more current for a 0.1 ms pulse compared with the simple model presented in this chapter. As seen in Table 3.4, the simple model used in this thesis has a smaller surface area than the model neuron presented in (Ostroumov, 2007). In order to see how much these thresholds depend on the surface area of the dendrites, a modified model neuron was created with the diameter of the distal dendrites increased by a factor of 2 (so that the diameter is now 1.6 µm). With this change, the (Ostroumov, 2007) model requires 1-1.11 times the current for the 5 ms pulse and 1.3-1.8 for the 0.1 ms pulse compared with the modified simple neuron model. Note that the wide range of scale factors presented here is due to the lack of specificity in the threshold values in (Ostroumov, 2007). It appears based on this test that the additional current required to reach threshold can be explained by the increased surface area of the Ostroumov model. Since neurons with smaller and larger surface areas have been found in the rat spinal cord (see Table 3 in (Thurbon et al., 1998)), it appears based on this test that the simple model neuron used in this thesis has properties similar to neurons in the rat spinal cord.

[e]Note that unfortunately (Ostroumov, 2007) Figure 4(c) incorrectly labels the current pulses in mA instead of µA, and Figure 4(d) incorrectly shows amplitude of the current pulse as 5 nA instead of 0.5 nA as described in the caption.

Additional plots and discussion of the effects of current injection can be found in Section 3.A.

Table 3.4: Current injection thresholds necessary for a current pulse with a width of 0.1 ms (⎍ column) or 5 ms (⎍ column) injected into the soma to cause the soma's membrane voltage to exceed −10 mV. Three neuron models are presented: the simple neuron model used in the rest of the thesis, a modified version of the simple neuron with dendrites that are twice as thick, and the data from (Ostroumov, 2007) for comparison. Columns A_S, A_A, and A_D are the surface area of the soma, axon, and all the dendrites respectively.

Model	A_S (μm^2)	A_A (μm^2)	A_D (μm^2)	0.1 ms ⎍ threshold*	5 ms ⎍ threshold*
Simple	1256.6	823.1	4115.5	6.944nA	0.169nA
Simple with distal dendrite diam=1.6 μm	1256.6	823.1	7759.7	15.929nA	0.447nA
(Ostroumov, 2007) model	1305 ± 21	1350†	7514 ± 74	30nA	0.5nA

* Amplitude of current pulse required to for the membrane voltage at the soma to exceed −10 mV.
† Calculated based on an axon 500 μm long with the parameters in the paper.
For the thresholds calculated using the simple neuron model and the modified simple neuron model, reducing the value given in the table by 0.001 nA causes the membrane voltage at the soma to be less then −10 mV.

3.4.3 Synapse Thresholds

In a real biological system without electrical stimulation, one or more EPSPs from one or more synapses would combine to trigger an action potential. There is little data on the maximum conductance (g_M) of synapses in the rat spinal cord. Santos et al. (2009) use values between 0.02 nS and 0.23 nS without reference to actual measurements. In order to simplify the facilitation study in Chapter 5, I have assumed that either some neurons exist in the spinal cord with synapses with near threshold weights or that multiple active synapses (perhaps with highly synchronous input) resulting in a near threshold potential can be approximated by a single near threshold potential.

I used linear extrapolation combined with a binary search to bracket the synapse weights necessary for a single synapse positioned at locations from the soma to the distal tip of a dendrite to cause the membrane voltage at the axon tip to just exceed values −60 mV to 10 mV in steps of 10 mV. The results of this search can be seen in Fig. 3.6. The difference in synapse weight to achieve a membrane voltage of −50 mV is very close to that needed to achieve 0 mV. For the synapse weights found and shown in Fig. 3.6, Fig. 3.7 shows the amount of time necessary for the axon tip membrane voltage to reach the target voltage. Signals with a peak membrane

voltage at the axon tip of $-20\,\text{mV}$, $-30\,\text{mV}$, and $-40\,\text{mV}$ take the longest time for the peak of the signal to reach the axon tip.

The membrane voltage at the axon tip as a function of synaptic weight for synapses located at the middle and distal tip of the distal dendrite section can be found in Figs. 3.8 and 3.11 respectively. Specific sub-threshold synapse weights have been marked with red vertical lines on these figures for use in the facilitation studies in Chapter 5. The largest selected synapse weights can also be seen in Figs. 3.9 and 3.12, which are close ups of Figs. 3.8 and 3.11. These figures also show that very small differences in synapse weight can cause the axon tip membrane voltage to increase from $-50\,\text{mV}$ to $0\,\text{mV}$.

The response of the neuron (membrane voltage and ion-channel state variables) to input at a synapse located in the middle of the distal dendrite section when triggered with synapse weight of $3.45\,\text{nS}$ can be found in Fig. 3.10. A similar plot for a synapse located at the distal dendrite tip with synapse weight of $4.783\,\text{nS}$ can be found in Fig. 3.13. These plots are provided for comparison to similar plots in Chapters 4 and 5.

Synapse weight thresholds for membrane voltages on the soma are presented in Section 3.B for possible comparison with soma patch clamp data.

Additional simulations with passive dendrites, active dendrites with double the diameter, and passive dendrites with an axon with double the diameter all required a larger synapse weight to cause neurotransmitter release. Simulations with passive dendrites required significantly larger synaptic weights.

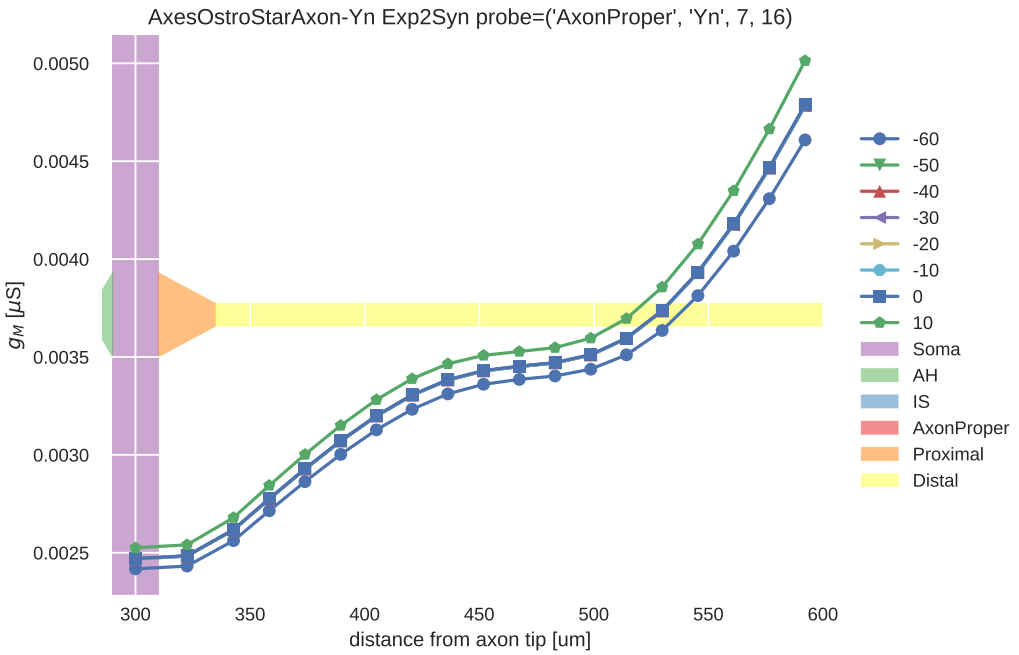

Figure 3.6: Synapse weight (g_M) (y-axis in µS) necessary for a synapse at that distance (x-axis in µm) from the axon tip to cause the specified membrane voltage (see legend: -60 mV to 10 mV in steps of 10 mV) at the axon tip after a single synapse event. Note that as the synapse location is farther from the soma, the synapse weight necessary to cause a given membrane voltage at the axon tip increases. Lines and symbols for -50 mV through 0 mV are plotted on top of each other.

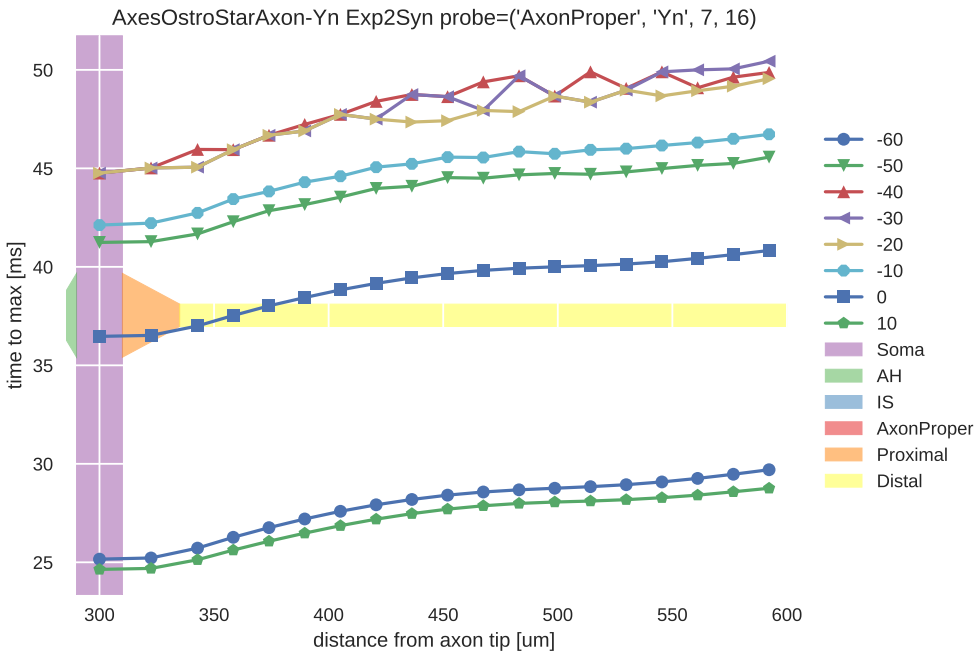

Figure 3.7: The time required for the axon tip to reach maximum membrane voltage (y-axis in µs) when a synapse triggered at that distance from the axon tip (x-axis) with the synapse weight necessary (see Fig. 3.6) to reach the specified membrane voltage (see legend) is triggered.

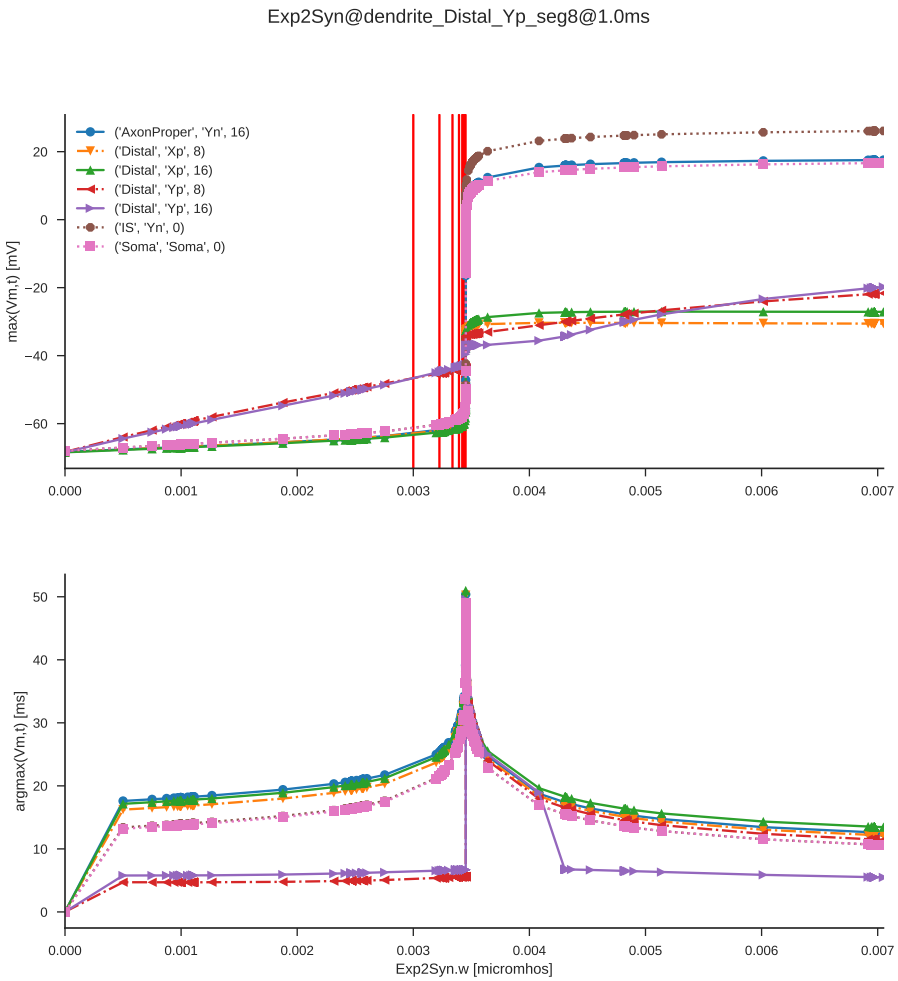

Figure 3.8: Maximum membrane voltage (top) and time to reach that maximum (from simulation start (synapse fire starts at 1ms)) (bottom) at probe locations (see legend) in the neuron when a synapse fires in the middle of the distal section of one of the dendrites. Red vertical lines mark synapse weight values ([3.45, 3.443, 3.436, 3.422, 3.394, 3.337, 3.225, and 3] nS) used for facilitation in Chapter 5. Top and bottom plots share the same x-axis.

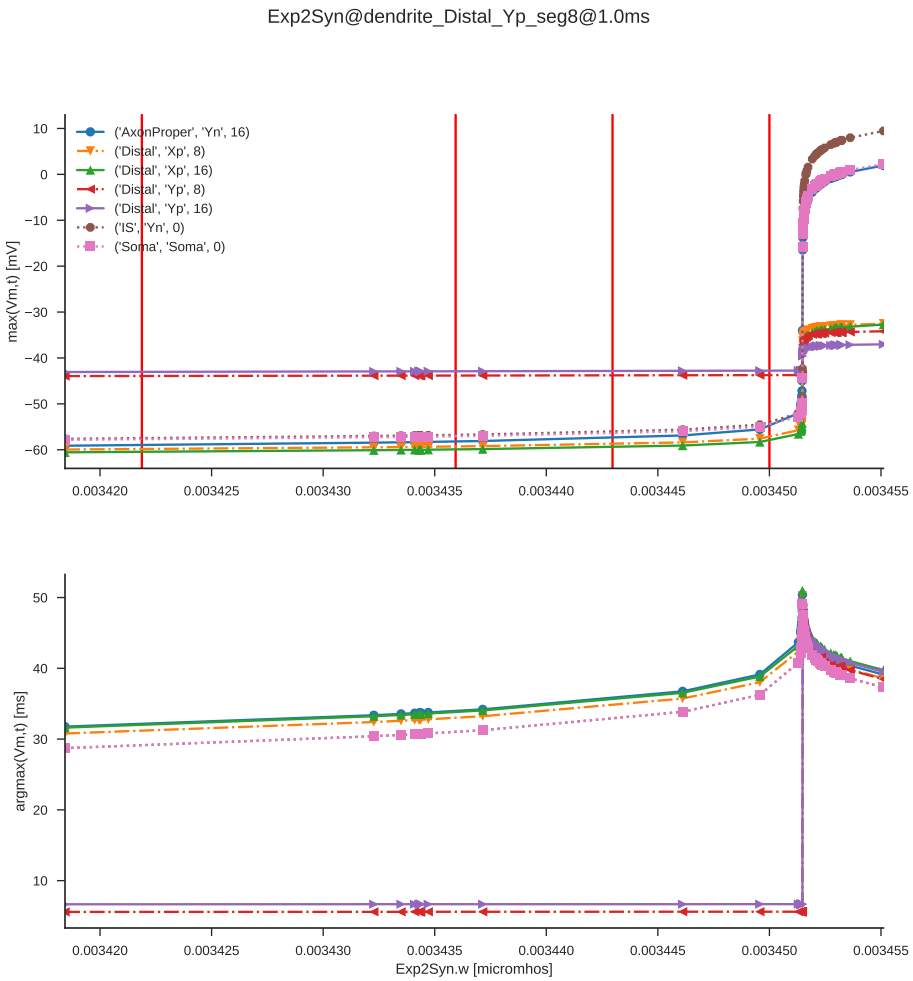

Figure 3.9: A close up of Fig. 3.8 showing the largest 4 facilitation synapse weights. Maximum membrane voltage (top) and time to reach that maximum (from simulation start (synapse fire starts at 1ms)) (bottom) at probe locations (see legend) in the neuron when a synapse fires in the middle of the distal section of one of the dendrites. Red vertical lines mark synapse weight values ([3.45, 3.443, 3.436, 3.422] nS) used for facilitation in Chapter 5.

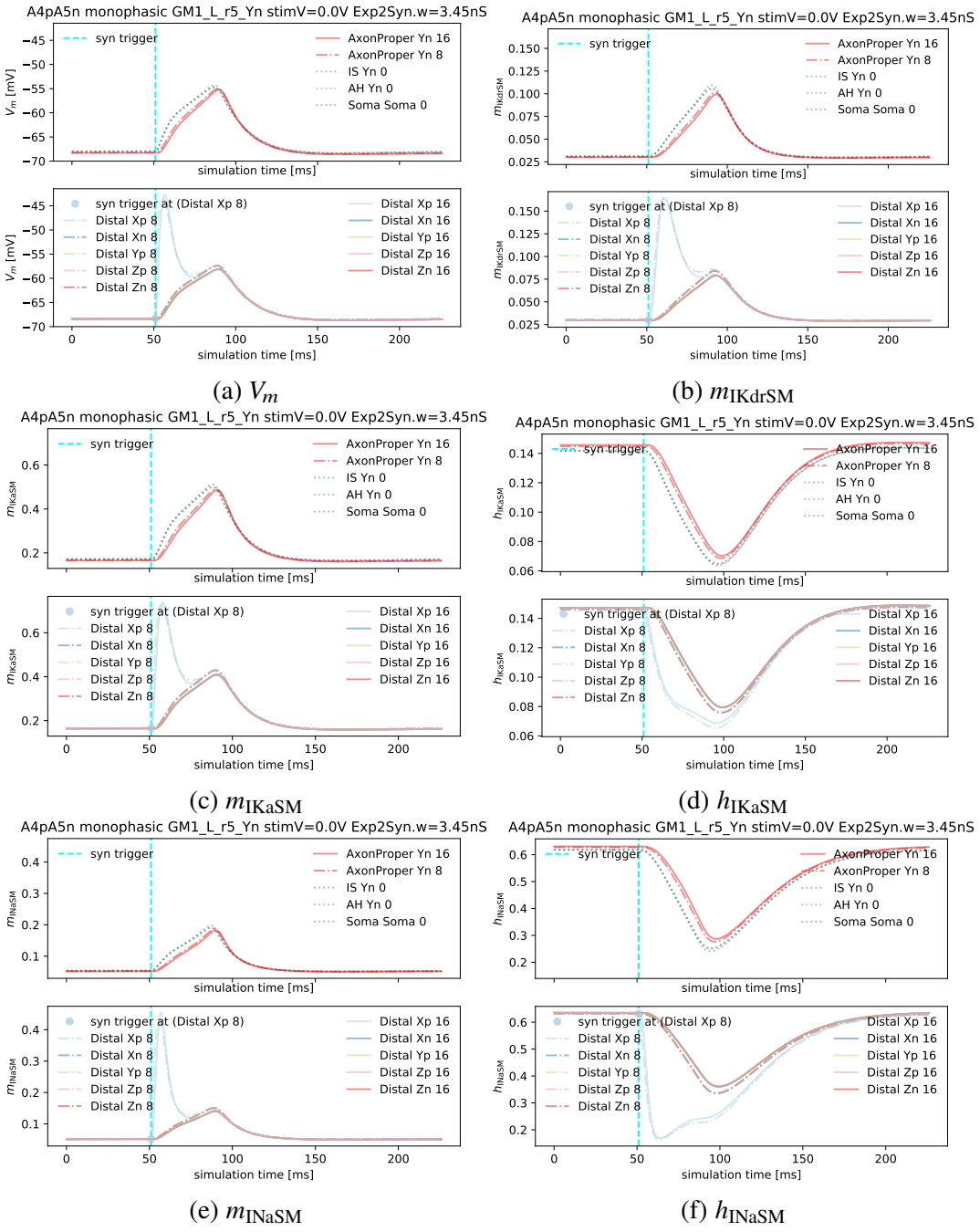

(a) V_m (b) m_{IKdrSM}

(c) m_{IKaSM} (d) h_{IKaSM}

(e) m_{INaSM} (f) h_{INaSM}

Figure 3.10: Time series of the internal state of the neuron model after a single EPSP was triggered at a synapse located in the middle of a distal dendrite section with a synaptic weight of 3.45 nS. Each subplot plots a different variable ((a) V_m, (b) m_{IKdrSM}, (c) m_{IKaSM}, (d) h_{IKaSM}, (e) m_{INaSM}, and (f) h_{INaSM}) against simulation time (ms) for probes on axon-soma (a through f top) and dendrites (a through f bottom).

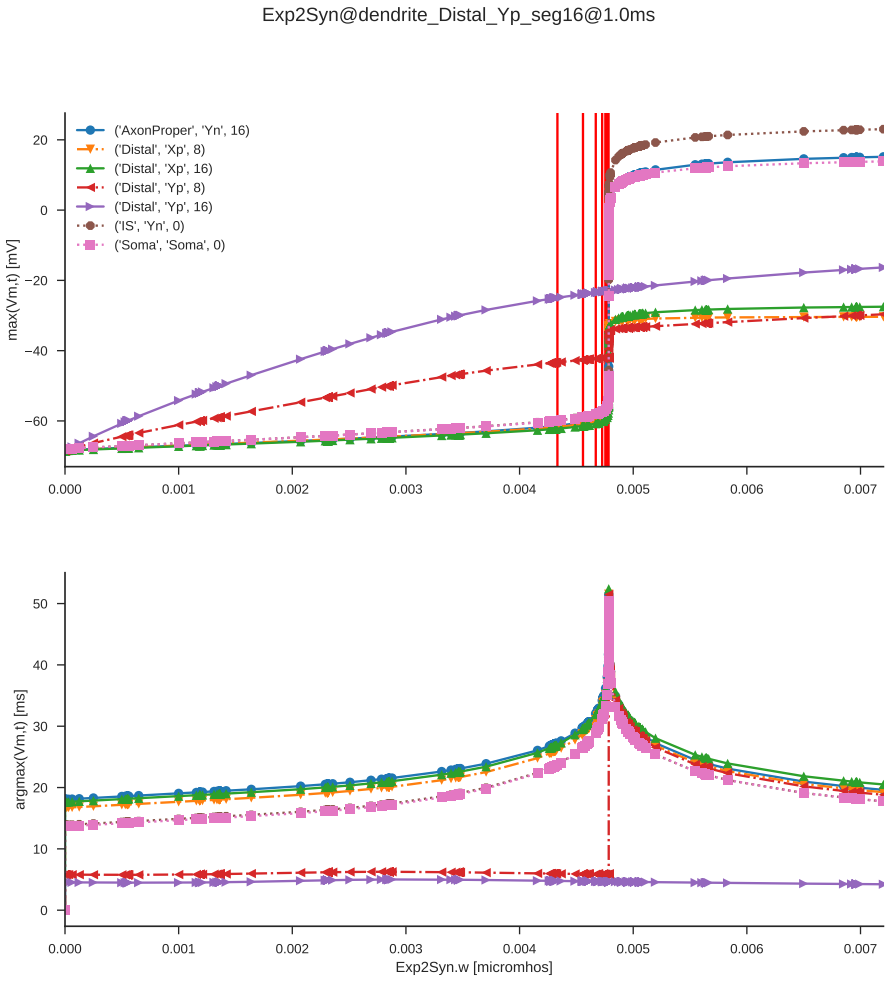

Figure 3.11: Maximum membrane voltage (top) and time to reach that maximum (from simulation start (synapse fire starts at 1ms)) (bottom) at probe locations (see legend) in the neuron when a synapse fires at the distal tip of one of the dendrites. Red vertical lines mark synapse weight values ([4.783, 4.776, and 4.769] nS) used for facilitation in Chapter 5. Top and bottom plots share the same x-axis.

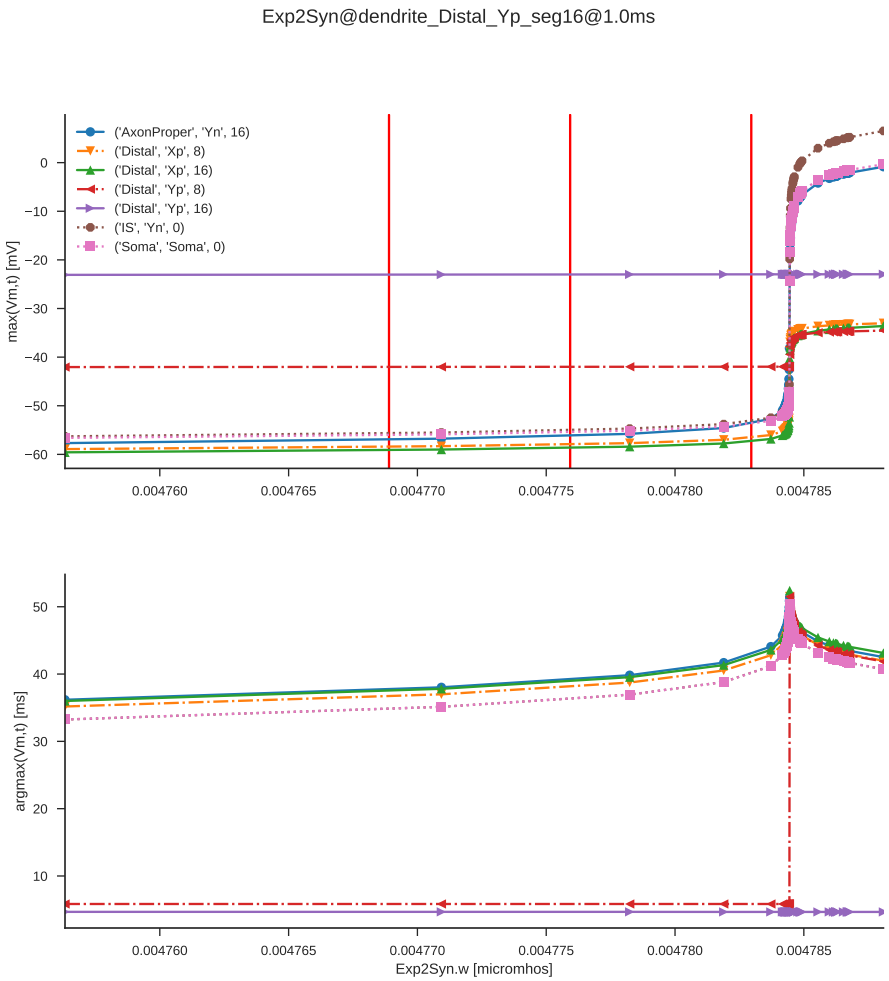

Figure 3.12: A close up of Fig. 3.11 showing the largest 3 facilitation synapse weights. Maximum membrane voltage (top) and time to reach that maximum (from simulation start (synapse fire starts at 1ms)) (bottom) at probe locations (see legend) in the neuron when a synapse fires at the distal tip of one of the dendrites. Red vertical lines mark synapse weight values ([4.783, 4.776, and 4.769] nS) used for facilitation in Chapter 5.

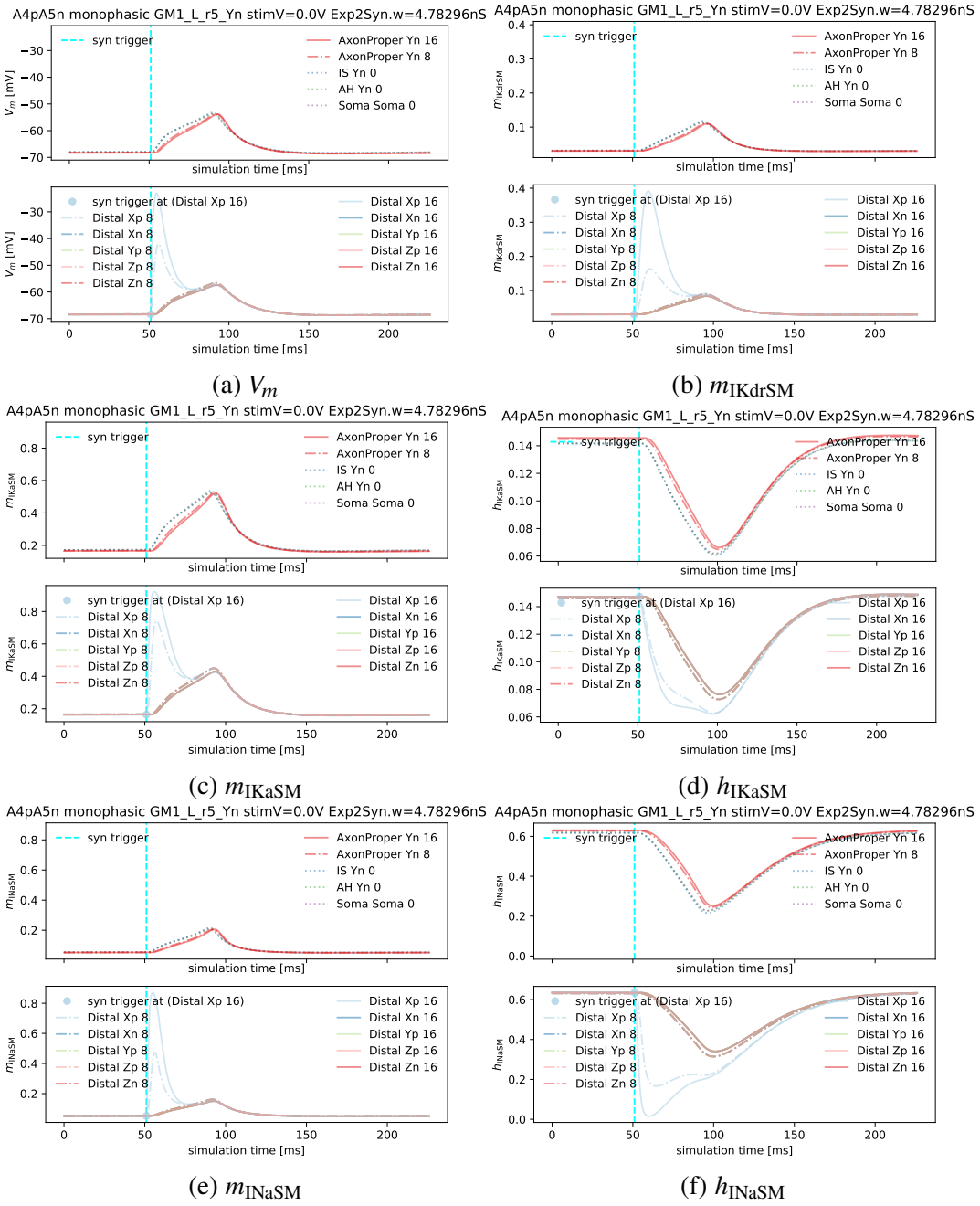

(a) V_m (b) m_{IKdrSM}

(c) m_{IKaSM} (d) h_{IKaSM}

(e) m_{INaSM} (f) h_{INaSM}

Figure 3.13: Time series of the internal state of the neuron model after a single EPSP was triggered at a synapse located at the distal tip of a dendrite with a weight of 4.78 nS. Each subplot plots a different variable ((a) V_m, (b) m_{IKdrSM}, (c) m_{IKaSM}, (d) h_{IKaSM}, (e) m_{INaSM}, and (f) h_{INaSM}) against simulation time (ms) for probes on axon-soma (a through f top) and dendrites (a through f bottom).

3.5 Error discussion

It is important to try to quantify the possible sources of errors in any experiment or simulation. Based on the modeling methods introduced in Chapters 2 and 3, I can divide the possible sources of error into geometric errors, biophysical parameter errors, and numerical computational errors.

There are a number of these possible types of errors in the volume conductor model. Although I used a transverse slice from an MRI of a rat spine as the basis for the model extrusion, the detailed segmental variations in the lumbosacral spinal cord were not taken into account. None of the issues studied in this thesis are dependent upon specific properties or functions of particular spinal segments. The electrode array used in these simulations is based on an actual array (Parag Gad, Choe, et al., 2013) used in rats, but placement in individual subjects might differ in minor ways.

A number of biophysical parameters are used in the volume conductor simulation. The conductivity and permittivity of the parylene C and platinum are known to a fairly high precision and are unlikely to change the results. For the tissues in the volume conductor model, I have collected the best frequency dependent values of conductivity and permittivity from multiple sources. Rarely is the frequency dependent nature of these parameters taken into account. Incorporating this frequency dependence should reduce the effective error in the simulated results, but the fact remains that these values are going to vary across subjects. Changes in these values would likely change the depth and shape of the electrical penetration in the spinal cord. These would likely cause minor differences in the stimulation thresholds (Chapter 4) and facilitation amounts (Chapter 5).

The volume conductor simulations depend on finite-element meshing techniques and computational approaches. Boundary effects in the model were tested in Section 2.2.1 and found to be minimal after avoiding rows 1 and 7. Boundary effects

with the electrode surfaces are believed to be minimal a small distance away from the electrodes and were also minimized by controlling the voltage of the back surface of the electrode rather than the front surface. Meshing errors are also possible, but were minimized by looking at the mesh quality as calculated by COMSOL and tested by comparing voltages for translated and reflected electrode combinations which should result in the same voltage potentials (Section 2.2.1).

My goal for the neuron model was not to study one particular neuron, but to use a nominal model whose surface area and size falls into the distribution of neurons in the rat spinal cord (Thurbon et al., 1998). That being said, it is possible that particular geometrical features not included in this model may react differently to stimulation. I have tried to minimize these effects by testing these neurons in many locations, orientations, and electrode combinations.

For the biophysical parameters of the neuron model, the key membrane biophysical parameters are membrane capacitance, membrane resistance, and the ion channel densities. While ion channel densities may vary across neuron types, the values that I selected were taken from studies based using mostly rat spinal neurons.

There may also be errors due to the compartmental modeling of the neurons. I have tried to address these issues by following the d_lambda rule (M. L. Hines and N. T. Carnevale, 2001).

In this model, I have assumed that the external electric field is not modified by the neurons. This assumption (while widely used) is not completely correct (Ye and Steiger, 2015) and may lead to minor errors.

I have tried to present the sources of errors here and the decisions taken to mitigate them. Since the errors in many of these parameters are not well understood, it is difficult to place precise error bars on the results of the ensuing chapters. The effects of these errors can be practically interpreted in terms of perturbations to

the electric and current density distributions in the volume conductor model. The use of many different neuron locations, orientations, and electrode combinations should minimize the effect of these errors on the interpretation of the results of these simulations.

The main point of this thesis is to show that facilitation of interneurons is possible under a variety of stimulating conditions. The subsequent chapters will find thresholds for activation and facilitation under a variety of stimulating conditions, and I believe that these errors would perturb these thresholds and only alter the spatial boundaries of the facilitation effect, and not the existence of this important phenomenon.

3.6 Summary

In this chapter, I described the electrical and geometrical properties of a model neuron that will be used in the rest of the thesis. The geometrical values (surface areas, diameters, number of neurites, etc.) are within the distribution of values for rat spinal cord neurons found in (Thurbon et al., 1998) Table 3. A study of current injection at the soma showed that less current was required compared to the model used in (Ostroumov, 2007), but that this decrease was likely due to the larger surface area of the Ostroumov model.

Rather than using the presence of action potentials on the axon, even for a brief time as a measure of neuron recruitment, I used the principle that neurons transmit information with the release of neurotransmitters from the axon tip. This principle in combination with the work of Destexhe and colleagues (Destexhe, Mainen, and Sejnowski, 1994) simplified the analysis and removed ambiguity. Based on this analysis, a neuron is judged to be active and to have released neurotransmitters if the membrane voltage at the axon tip exceeds $-10\,\mathrm{mV}$.

A synapse model was introduced, and sub-threshold weight values were found for

synapse locations at the middle and distal tip of the distal section of the dendrites. These will be used for the facilitation studies in Chapter 5.

3.A Appendix: Current injection

In Section 3.4.2, thresholds for a 0.1 ms and a 5 ms square current pulse were determined for comparison with (Ostroumov, 2007) and other papers. In this appendix, related figures for the 0.1 ms pulse are presented for reference. Please see the attached captions for explanations.

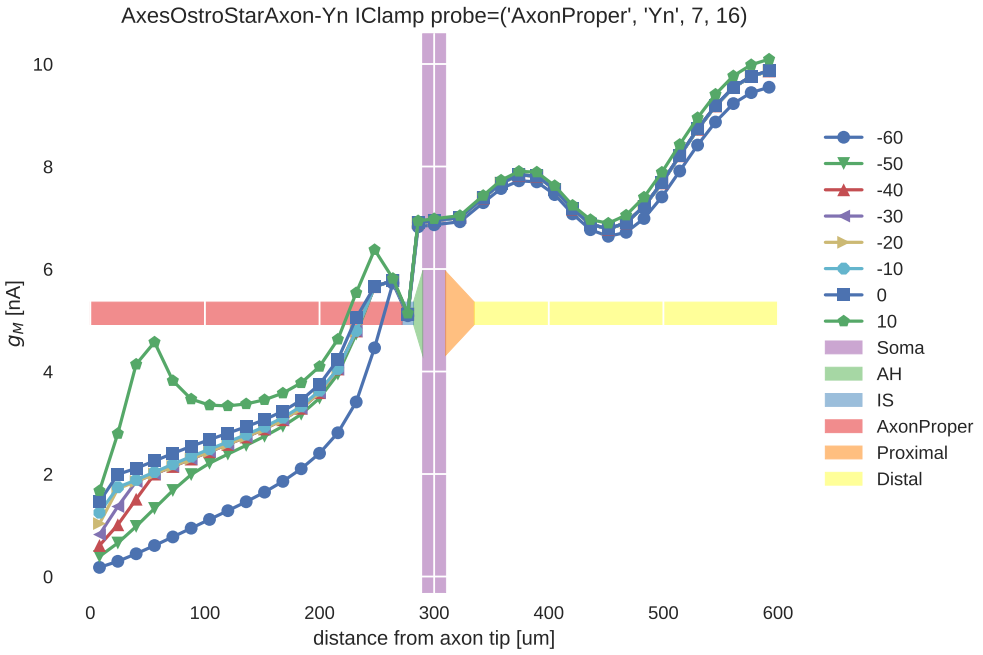

Figure 3.14: Current amplitude (y-axis in nA) necessary for a single square current pulse 0.1 ms long injected at that distance (x-axis in µm) from the axon tip to cause the specified membrane voltage (see legend: −60 mV to 10 mV in steps of 10 mV) at the axon tip.

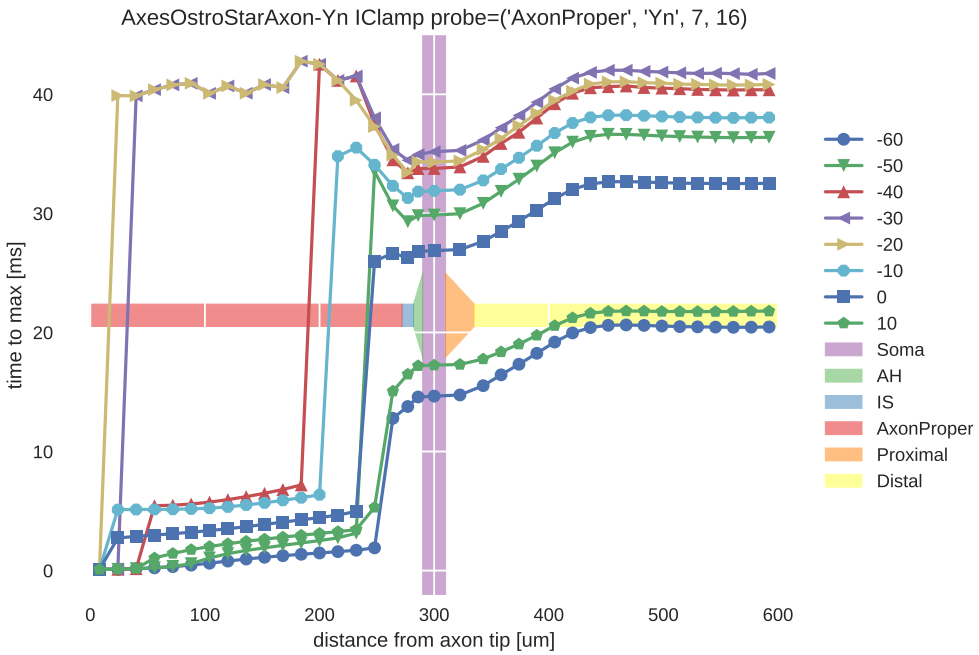

Figure 3.15: The time required for the axon tip to reach maximum membrane voltage (y-axis in µs) when a 0.1 ms square current pulse is injected at that distance from the axon tip (x-axis) with the current necessary (see Fig. 3.6) to reach the specified membrane voltage (see legend).

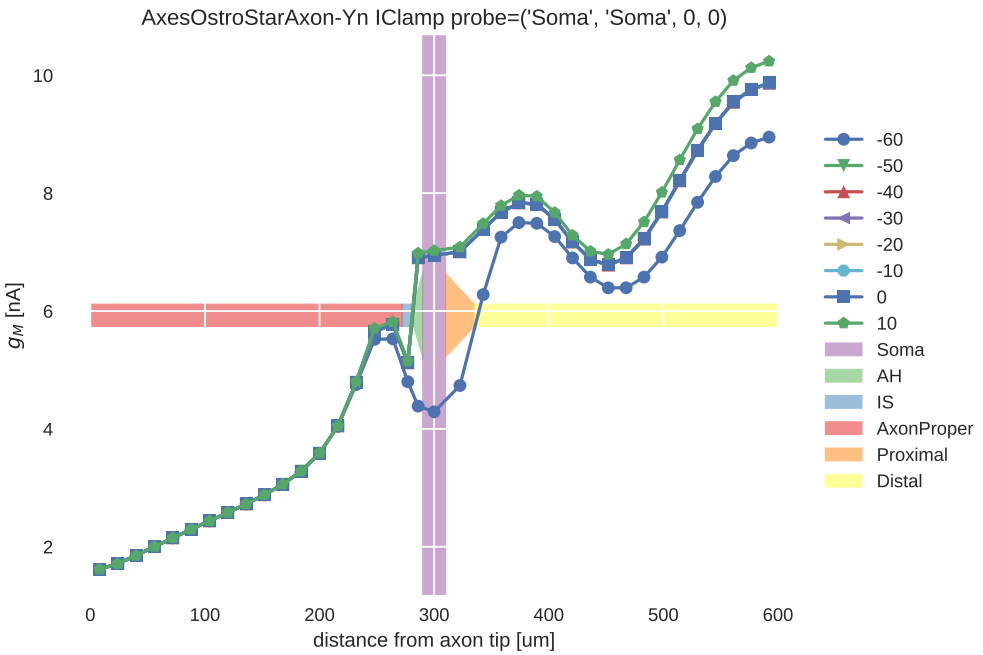

Figure 3.16: Current amplitude (y-axis in nA) necessary for a single square current pulse 0.1 ms long injected at that distance (x-axis in µm) from the axon tip to cause the specified membrane voltage (see legend: −60 mV to 10 mV in steps of 10 mV) at the soma.

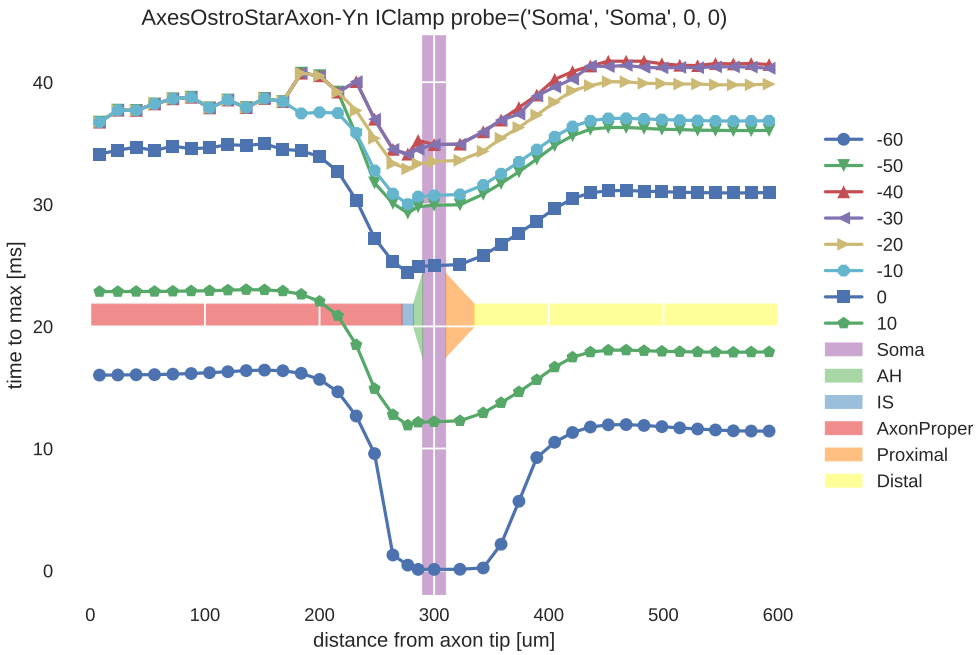

Figure 3.17: The time required for the soma to reach maximum membrane voltage (y-axis in µs) when a 0.1 ms square current pulse is injected at that distance from the axon tip (x-axis) with the current necessary (see Fig. 3.16) to reach the specified membrane voltage (see legend).

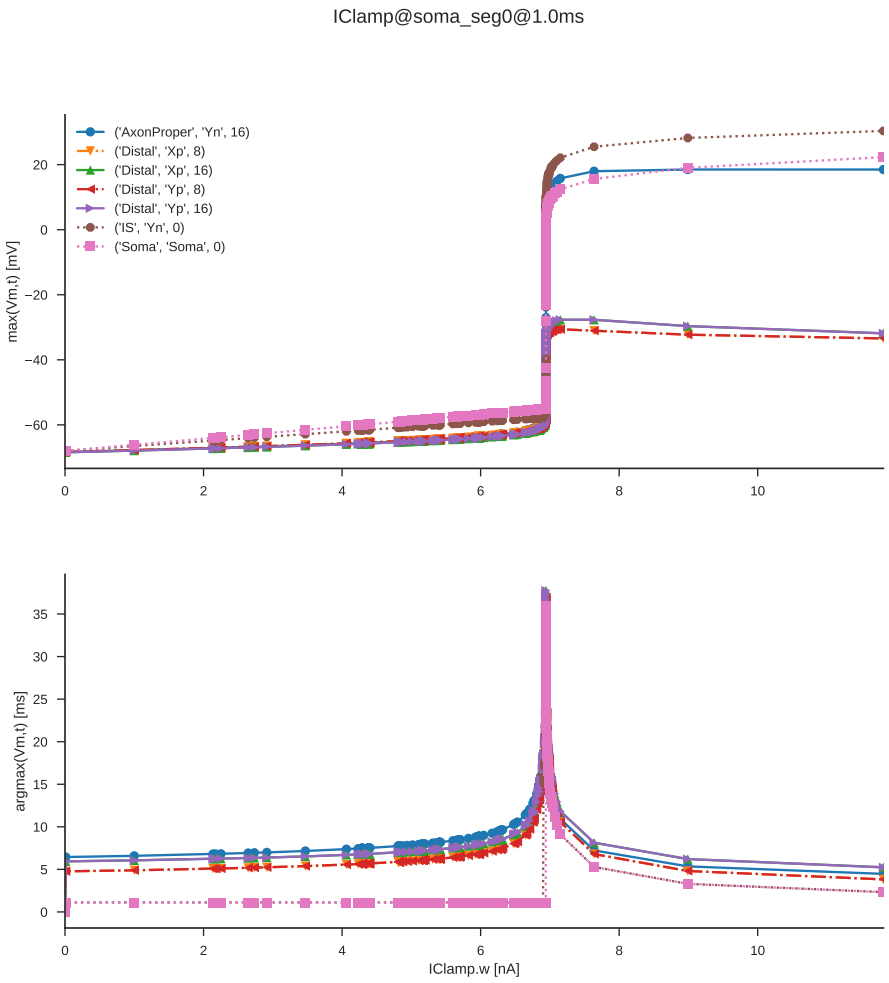

Figure 3.18: Maximum membrane voltage vs the amplitude of a 0.1 ms square current pulse injected at the soma (top) and time to reach that maximum (from simulation start (pulse occurs at 1ms)) vs injected current (bottom). Each colored line corresponds to a probe location labeled by (section type, axis direction, segment number). This figure corresponds to the threshold of 6.944nA for the simple neuron model given in Table 3.4.

3.B Appendix: synapse thresholds at the soma for comparison

It is usually easier to measure the membrane voltage of a real neuron at the soma rather than at the distal tip of an axon. For that reason, I repeated the analysis given in Section 3.4.3 for soma membrane voltages of −60 mV to 10 mV in steps of 10 mV. Again, linear extrapolation combined with a binary search was used to bracket the synapse weights necessary for a single synapse located at locations from the soma to the distal tip of a dendrite to cause the membrane voltage at the soma to just exceed the specified membrane voltages.

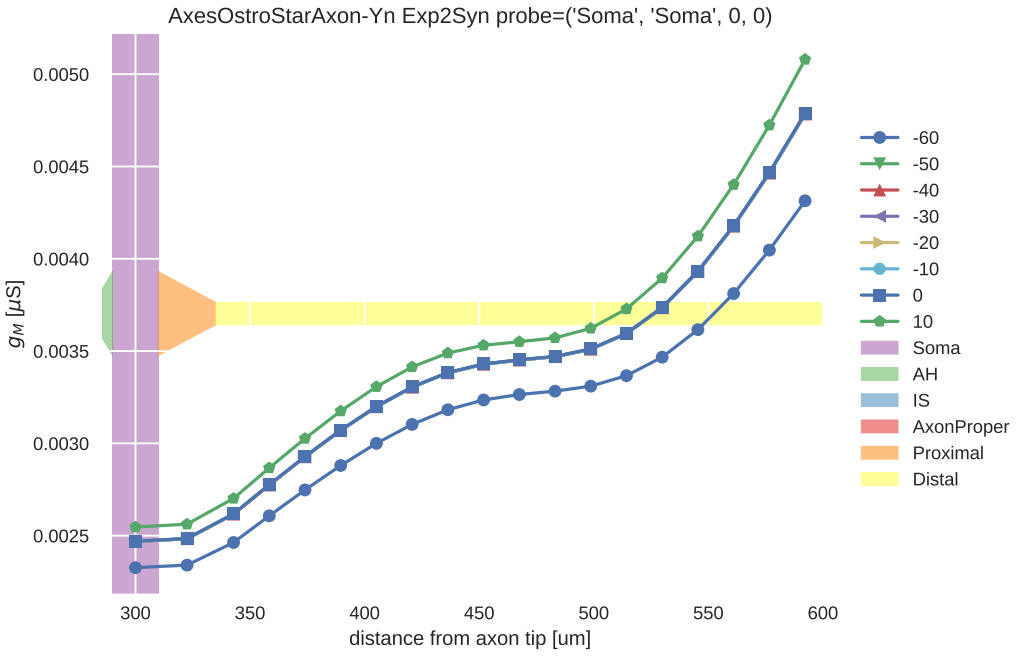

Figure 3.19: Synapse weight (g_M) (y-axis in µS) necessary for a synapse at that distance (x-axis in µm) from the axon tip to cause the specified membrane voltage (see legend: −60 mV to 10 mV in steps of 10 mV) at the soma after a single synapse event. Note that as the synapse location is farther from the soma, the synapse weight necessary to cause a given membrane voltage at the soma increases. Lines and symbols for −50 mV through 0 mV are plotted on top of each other.

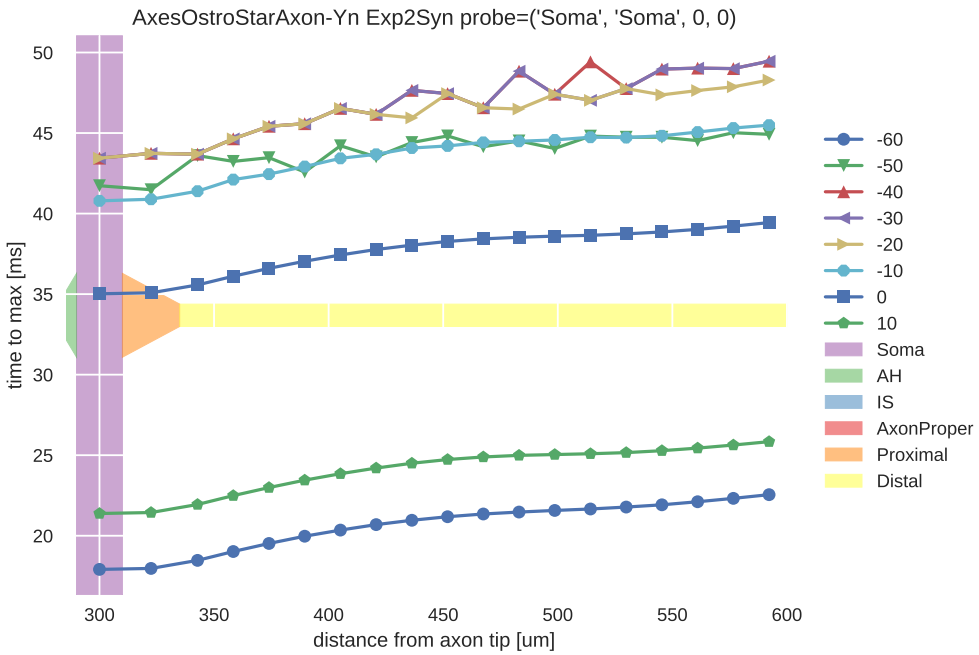

Figure 3.20: The time required for the soma to reach maximum membrane voltage (y-axis in µs) when a synapse triggered at that distance from the axon tip (x-axis) with the synapse weight necessary (see Fig. 3.19) to reach the specified membrane voltage (see legend) is triggered.

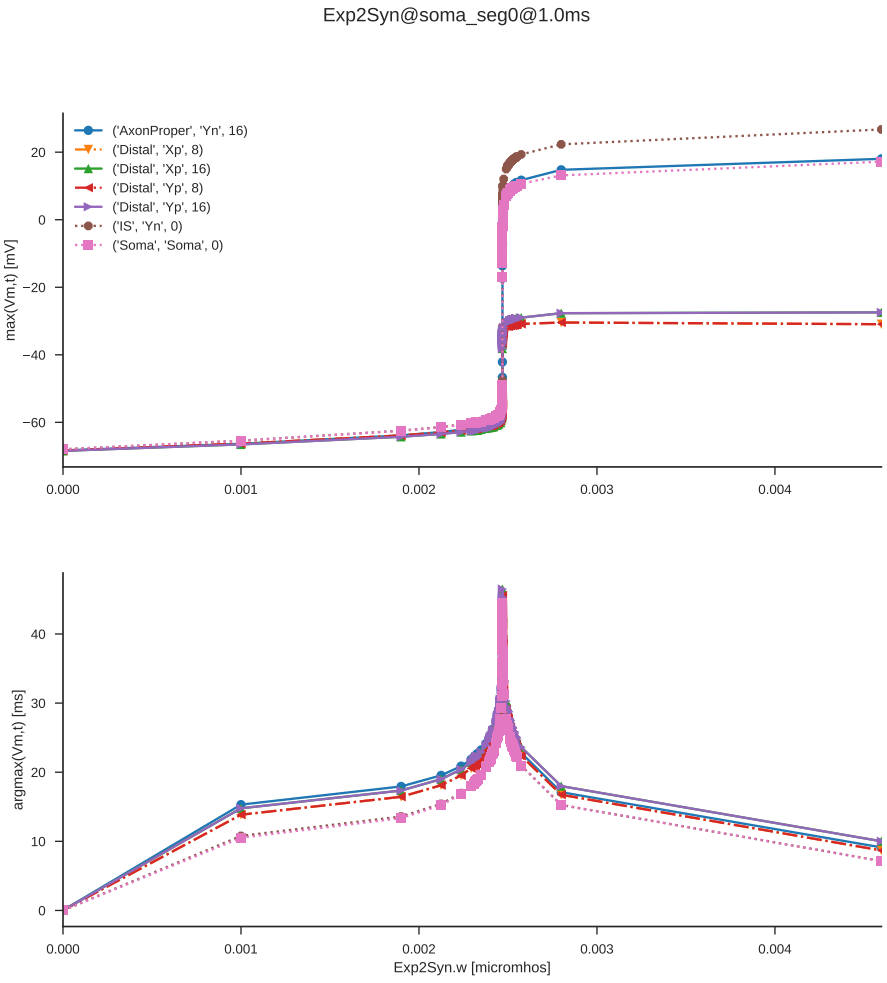

Figure 3.21: Maximum membrane voltage (top) and time to reach that maximum (from simulation start (synapse fire starts at 1ms)) (bottom) at probe locations (see legend) in the neuron when a synapse located on the soma is triggered. Top and bottom plots share the same x-axis.

Chapter 4

ACTIVATING NEURONS USING EPIDURAL STIMULATION IN THE ABSENCE OF EXCITATORY POSTSYNAPTIC POTENTIALS (EPSPS)

This chapter looks at the effect of epidural stimulation on spinal neurons when there is no synaptic input. Specifically, this chapter looks for the stimulation conditions in which epidural stimulation causes neuronal activation (release of neurotransmitters). The next chapter will build upon these results in order to look how epidural stimulation facilitates neuron activation when a single EPSP occurs at a synaptic input. This computational study uses the volume conductor model presented in Chapter 2 and the neuron models from Chapter 3. Although epidural stimulation is often used with a sequence of stimulation pulses, this thesis focuses on understanding the response to a single stimulation pulse. If the stimulation pulses are sufficiently far apart in time, the single pulse analysis is a useful simplification, otherwise complex interactions between pulse responses may occur.

As described in Chapter 2, volume conductor simulations for both biphasic and monophasic stimulation (1 V peak voltage amplitude) were computed for the 18 electrode pair combinations listed in Section 2.2.1. Section 4.1 discusses the location of simulated neurons in these simulations, and Section 4.2 discusses the extraction of the extracellular voltage time series from the volume conductor studies for application to simulated neurons. Section 4.3 discusses and plots the total number of active neurons broken down by stimulation type, neuron dorsal-ventral location, and axon orientation. Section 4.4 compares the effect of monophasic and biphasic stimulation on the membrane voltage at a number of probe locations as a function of stimulation voltage. Section 4.5 looks at the simulations using ≤ 5 V which re-

sult in the axon tip having a membrane voltage of $> -10\,\text{mV}$ which, based on the discussion in Section 3.3.2, is believed to release neurotransmitters and is referred to as an *active* neuron. The stimulation voltage required to activate a neuron will be important in the next chapter because facilitation of neuron activation with an EPSP should ideally occur using stimulation less than that required to activate a neuron without EPSPs. Section 4.5.1 examines active neurons with monophasic stimulation. Section 4.5.2 examines active neurons under biphasic stimulation. Section 4.6 looks at ways of predicting neuron activation from static volume conductor simulations. Section 4.A shows the locations and orientations of activated neurons in the spinal cord for all 18 characteristic bipolar combinations.

These studies yield some interesting results, such as the fact that monophasic stimulation is much more likely to lead to a non-linear membrane voltage response between the stimulation voltage and the membrane voltage at the axon tip. Biphasic stimulation is more likely to maintain a linear relationship between stimulation voltage and membrane voltage at the axon tip (without synaptic input). This means that researchers using monophasic stimulation should expect a non-linear activation profile when increasing stimulation voltage. Section 4.6 may also be of particular interest because it shows that neuron activation can be predicted from the difference in the static simulated voltage between the axon tip and the soma.

4.1 Locations of simulated neurons

First, recall from Section 2.2.1 that:

- $+\hat{z}$ points in the caudal direction and increasing electrode array row number.
- $-\hat{z}$ points in the rostral direction and decreasing array row number.
- $+\hat{y}$ points in the dorsal direction.
- $-\hat{y}$ points in the ventral direction.

- $+\hat{x}$ points to the animals right side and towards the C column.
- $-\hat{x}$ points to the animals left side and towards the A column.

In order to simulate a representative set of neurons in the spinal cord, 3 soma positions labeled GM1 (most dorsal), GM2 (most ventral), and GM3 (between GM1 and GM2), were chosen in the (x, y) transverse plane, such that the entire neuron remained inside the gray matter and the neurites spanned most of the gray matter. These 3 soma positions were mirrored across the (y, z) sagittal plane (see Fig. 4.1). z positions were then selected to place neurons directly under and halfway between each row of electrodes, as seen in Fig. 4.2. As seen in Fig. 4.2, the rows of electrodes are numbered 1 through 7. Neurons located directly under a row of electrodes are labeled with "r[row number]". Neurons located between 2 rows are labeled with "r[smaller row number]and[larger row number]".

This distribution of neuron models allows simulation of the influence of stimulation on neurons at varying depth and rostral-caudal position in the spinal cord. All six neuron models (with the axon along the $-\hat{x}$, $+\hat{x}$, $-\hat{y}$, $+\hat{y}$, $-\hat{z}$, and $+\hat{z}$ directions) were placed at each of the soma positions and the position of each neuron segment (center of each modeled compartment) recorded to allow voltage time series extraction from the volume conductor models.

In this thesis, a specific neuron can be referenced by "GM[1, 2, or 3]" (the neuron's dorsal-ventral position and part of the left-right position), [L or R] (whether it's on the left or right of the spinal cord), row specification ("r[row number]" or between electrode rows "r[smaller row number]and[larger row number]"), and an orientation ($-\hat{x}$, $+\hat{x}$, $-\hat{y}$, $+\hat{y}$, $-\hat{z}$, and $+\hat{z}$). Sometimes the orientation will be referred to as (Xn, Xp, Yn, Yp, Zn, and Zp). For example, GM1_L_r2and3_Xp would indicate a neuron location in the left dorsal horn of the gray matter between electrode rows 2 and 3 with an axon pointing in the $+\hat{x}$ direction. GM2_R_r5_Zn would indicate a

neuron location in the right ventral horn of the gray matter under electrode rows 5 with an axon pointing in the $-\hat{z}$ direction.

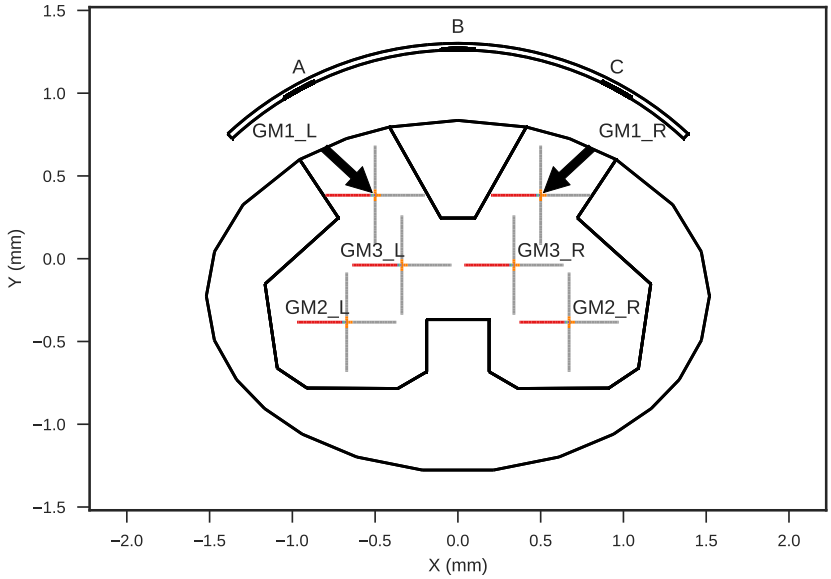

Figure 4.1: soma-positions

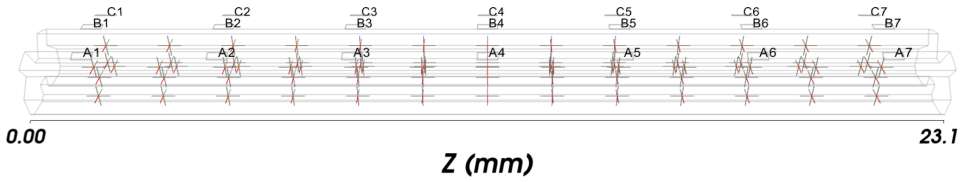

Figure 4.2: Locations of neurons in the simulated spine (with the axon (red) along the $-\hat{x}$ direction). Axis units are in mm.

4.2 Extracellular voltage and neuron simulations

The volume conductor model was discussed in Chapter 2. The monophasic and biphasic stimulation waveforms were discussed in Section 2.1.3. Specifically, the monophasic Gaussian pulse was defined in Eq. (2.13) and the biphasic Gaussian derivative pulse was defined in Eq. (2.17). The 18 stimulation patterns were discussed in Section 2.2.1. For reference, the stimulation parameters for monophasic and biphasic Gaussian stimulation are summarized in Table 4.1.

Table 4.1: Volume conductor simulation parameters. ς is the width parameter used in the monophasic (Eq. (2.13)) and biphasic (Eq. (2.17)) stimulation waveforms. $f^{\max}$ is the dominate frequency of a single stimulation pulse. This frequency was used to determine the material properties in Tables 2.4 and 2.5. The volume conductor simulation was run from $-t_{mag}$ to t_{mag} in steps with stepsize Δt.

	Biphasic	Monophasic
ς	166.04 µ sec	112.84 µ sec
$f^{\max}$	958.5 Hz	0 Hz
t_{mag}	1.66 ms	1.12 ms
Δt	0.01 ms	0.01 ms

For each of the six neuron models and each of the 18 electrode combinations, the extracellular voltage was extracted from the volume conductor simulations for each segment in each neuron and saved to an HDF5 file. As described in Section 2.2.1, the COMSOL volume conductor simulations are linear in the applied voltage, so that scalar multiples of the 6*18 datasets can then be used to derive the extracellular voltages that are applied to the neuron models.

For each type of stimulation (monophasic and biphasic) and electrode pair combination, there are (6 neuron locations for each constant z plane) * (6 geometry types) * (5 z planes under electrode rows +6 z planes between electrode rows (ignoring neurons under rows 1 and 7)) * (2 positive and negative voltage amplitude) = 792 simulation configurations. This means that there are a total of 792 * (18 combinations) * (2 stimulation types) = 28512 total simulation configurations. NEURON simulations were run with stimulation voltages from 0 V to 10 V in steps of 250 mV (yielding 40 unique simulations). The work in this chapter therefore required a

minimum of 792 * 18 * 2 * 40 = 1,140,480 NEURON simulations. Each NEURON simulation simulated 151.0 ms of time using a timestep of 0.01 ms. The stimulation pulse was started 1 ms of simulation time after the saved steady state was loaded. During the NEURON simulations, maximum and minimum membrane voltages were recorded at several locations (axon proper distal tip (seg=16), axon proper middle (seg=8), initial segment ("IS", seg=0), axon hillock ("AH",seg=0), soma (seg=0), distal tip of distal dendrite (seg=16), and the middle of distal dendrite (seg=8). (See Fig. 3.3 for probe locations.)

4.3 Active neurons for monophasic and biphasic stimulation

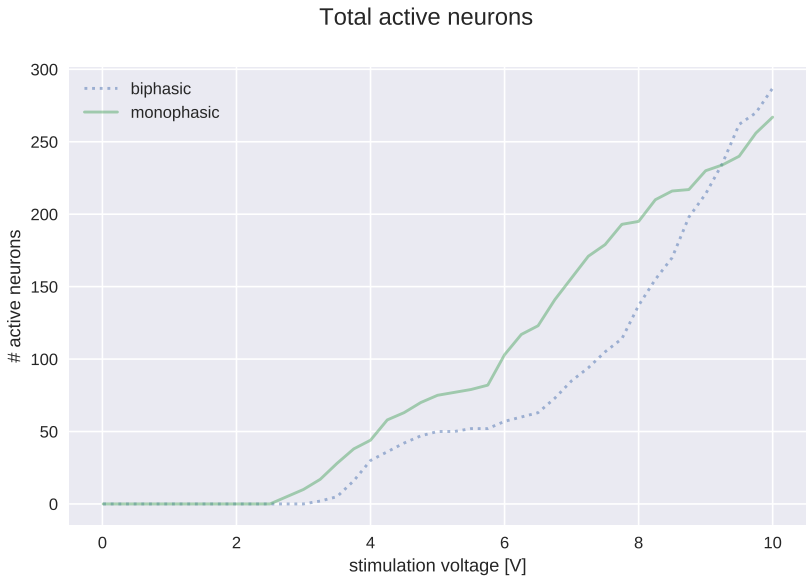

Figure 4.3: The total number of active neurons (neurons with axon tip membrane voltage > -10 mV) for all 18 bipolar stimulation combinations (listed in Section 2.2.1), all neuron locations, and all 6 axon orientations. For each type of stimulation and stimulation voltage magnitude, 14,256 neurons were tested.

As discussed in Section 3.3.2, a neuron is considered *active* (and to have released neurotransmitters) if the membrane voltage on the distal tip of the axon goes above -10 mV. The number of active neurons as a function of stimulation voltage for both biphasic and monophasic stimulation is plotted in Fig. 4.3. From this plot, it appears that monophasic stimulation activates more neurons at lower stimulation

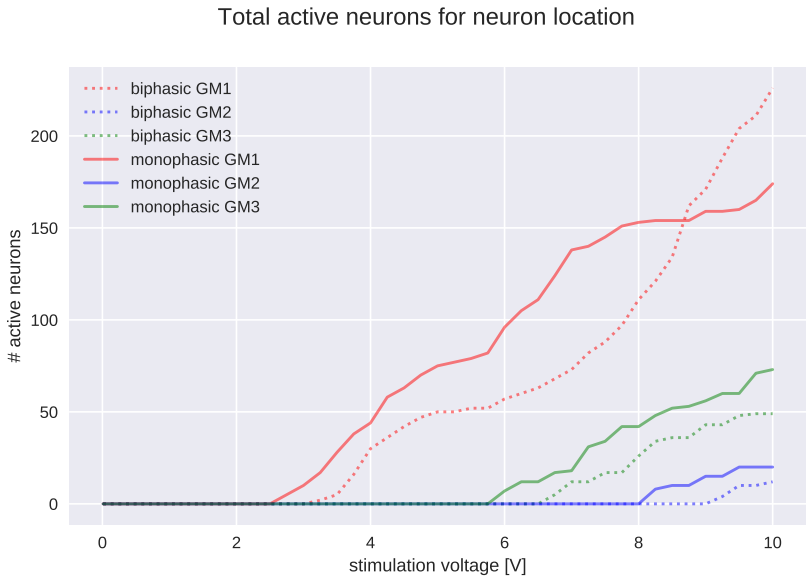

Figure 4.4: The total number of active neurons (neurons with axon tip membrane voltage $> -10\,\text{mV}$ in response to stimulation, as plotted in Fig. 4.3) separated by location in the transverse plane, for all 18 bipolar stimulation combinations (listed in Section 2.2.1), all neuron locations, and all 6 axon orientations. Note that GM1 is most dorsal, GM2 is most ventral, and GM3 is in between. For each type of stimulation, stimulation voltage magnitude, and position in the transverse plane, 4,752 neurons were tested.

magnitudes, but this reverses at higher stimulation magnitudes. Figure 4.4 shows that neurons closer to the electrodes are most easily activated. Figure 4.5 shows the total number of active neurons for each axon orientation. Over-all, more axons pointing in the $+\hat{y}$ direction are activated (likely because the axon tip is closer to the electrodes). Total active neurons by electrode combination can be seen in Fig. 4.6. The neurons activated by each electrode combination can also be seen in the spinal cord in figures in Section 4.A.

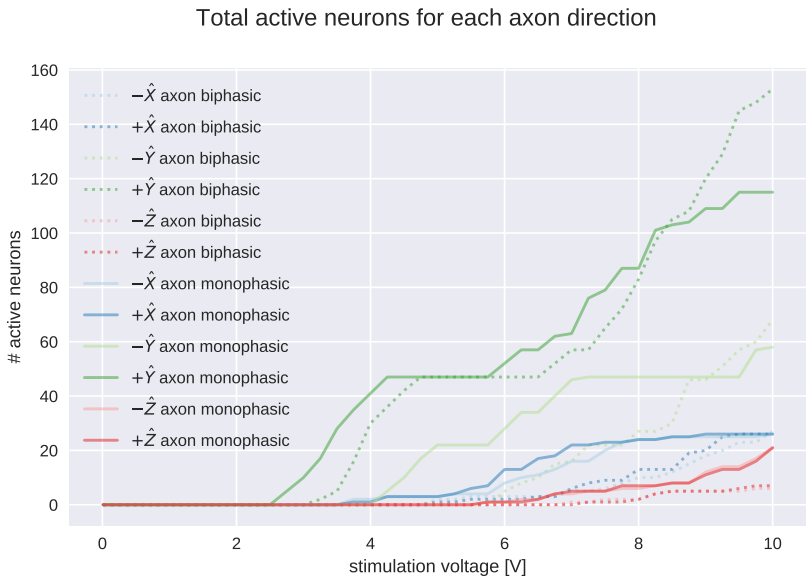

Figure 4.5: The total number of active neurons (neurons with axon tip membrane voltage $> -10\,\text{mV}$ in response to stimulation, as plotted in Fig. 4.3) separated by axon orientation, for all 18 bipolar stimulation combinations (listed in Section 2.2.1) and all neuron locations. Axons are labeled by the direction of the distal tip from the soma. Note that axons pointing in the $+\hat{y}$ direction are the easiest to activate, followed by $-\hat{y}$ with monophasic stimulation. For each type of stimulation, stimulation voltage magnitude, and axon orientation, 2,376 neurons were tested.

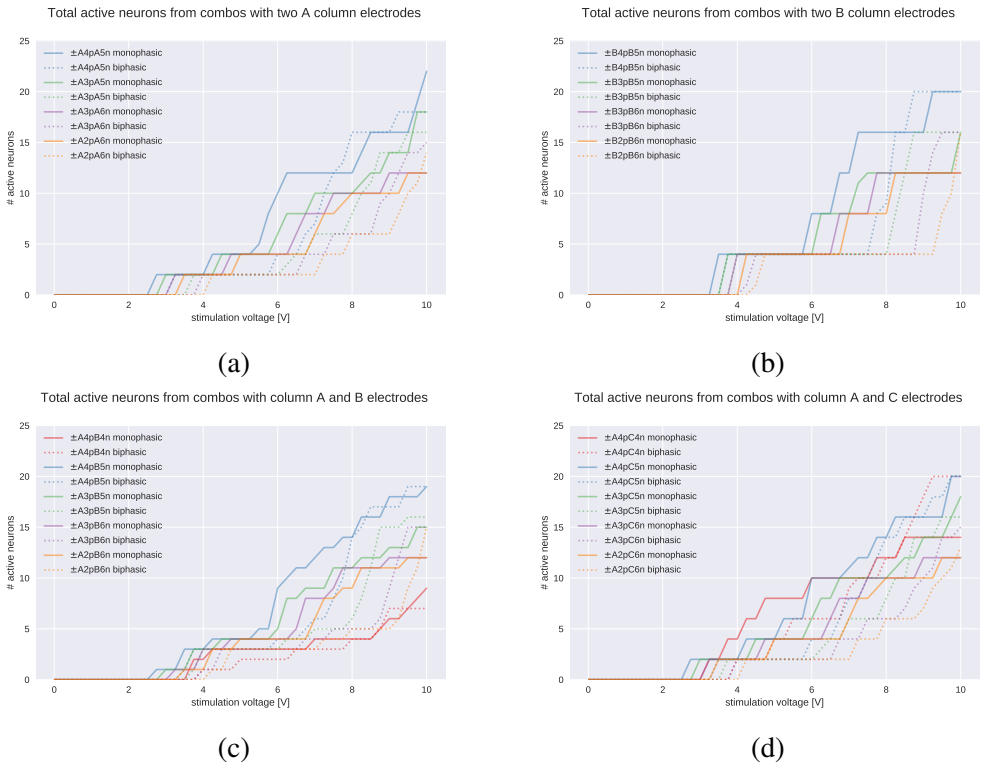

Figure 4.6: The total number of active neurons (neurons with axon tip membrane voltage $> -10\,\text{mV}$ in response to stimulation, as plotted in Fig. 4.3) separated by electrode combination for all neuron locations and all 6 axon orientations. Each sub-figure plots a subset of the combinations: (a) all combinations that have both active electrodes in the A column, (b) all combinations with both active electrodes in the B column, (c) combinations with one A electrode and one B electrode, and (d) combinations with one A electrode and one C electrode. 792 neurons were tested at each stimulation magnitude (x-axis) for each combination.

4.4 Comparison of membrane voltage distribution for monophasic and biphasic stimulation

The previous section looked at counts of active neurons as a function of stimulation voltage. For understanding the process of *facilitation* in the next chapter, it is important to understand how other parts of the neurons respond to stimulation. Figures 4.7 to 4.13 show 2d histograms of the number of neurons with a maximum membrane voltage in mV (y-axis) at probe locations (one for each figure) plotted against stimulation voltage in mV (x-axis) for all neuron locations and all 18 bipolar stimulation combinations using monophasic stimulation (top plot) and biphasic stimulation (bottom plot). The colored dots in each figure represent neuron parameters whose axon tip has a maximum membrane voltage greater than $-10\,\text{mV}$ (referred to in this thesis as activation) using less than or equal to 5 V of stimulation. The color of each dot indicates the lowest magnitude of stimulation required to activate that neuron (see right colorbar). The color of these dots is consistent across stimulation voltages and plots with the same stimulation type. Comparing the location of dots in each plot allows one to determine the maximum membrane voltage at each probe location for neurons that are activated using less than 5 V magnitude of stimulation.

Starting with the distal tip of the axon (seg=16) in Fig. 4.7, there are visibly different responses from biphasic and monophasic stimulation. The monophasic response is clearly non-linear with respect to stimulation magnitude and yields a non-continuous response in some neurons starting around 2750 mV of stimulation. This non-linearity means that for most of the active neurons, the maximum membrane voltage at the axon tip jumps from $-30\,\text{mV}$ to above $-10\,\text{mV}$ with a small change in stimulation input. The biphasic response is almost completely linear except for a small region above 8000 mV of stimulation and around 20 mV of membrane voltage. Also note that the maximum membrane voltage resulting from biphasic

stimulation (for a given stimulation amplitude) is larger than that of the equivalent monophasic stimulation, except for the beginning of the nonlinear response curve (between 2750 mV of stimulation and 4000 mV of stimulation).

In the middle of the axon (seg=8), as seen in Fig. 4.8, the maximum membrane voltage's response to monophasic stimulation continues to show the non-continuous jump behavior seen at the axon tip. The biphasic stimulation response continues to be mostly linear, but the non-continuous response above 8 V of stimulation is clearly visible in the Fig. 4.8b.

The maximum membrane voltages (or "probes") in the initial segment (IS) of the axon show a similar response (seen in Fig. 4.9) to that of the middle of the axon. However, in the monophasic response (top), some of the active neurons show a reduction in max membrane voltage starting at 9250 mV of stimulation. The axon hillock (Fig. 4.10) and soma (Fig. 4.11) show a similar response to that of the IS, except that most of the soma response is reduced to a membrane voltage below -60 mV, likely because the soma has a much larger membrane surface area.

Figure 4.12 shows the maximum membrane voltage response in the middle of the distal dendrites (seg=8). The response to monophasic stimulation shows at least two types of responses: the maximum membrane voltages of the active neurons jump to around -31 mV and increase continuously from there (with a few exceptions). The maximum membrane voltages of other neurons seem to increase continuously with increasing stimulus, but not linearly. The maximum membrane response to biphasic stimuli in the middle of the distal dendrite is lower than the monophasic response and is mostly continuous and linear (with the exception starting at 8 V of stimulation) with respect to increasing stimulation voltage.

The maximum membrane voltage response of the distal tips of the dendrites (seg=16) to monophasic and biphasic stimulation can be seen in Fig. 4.13. For

biphasic stimulation, the 2D-histogram of maximum membrane voltages appears to be almost identical to the histogram of biphasic responses at the axon tip Fig. 4.7 (bottom). The maximum monophasic response is less than that of the biphasic response and shows some discontinuous behavior (jump to around -27 mV for active neurons). The discontinuous behavior is likely due to orthodromic propagation of an action potential into the dendrites.

The membrane voltage in the dendrites will be discussed more in the next chapter in regards to facilitation.

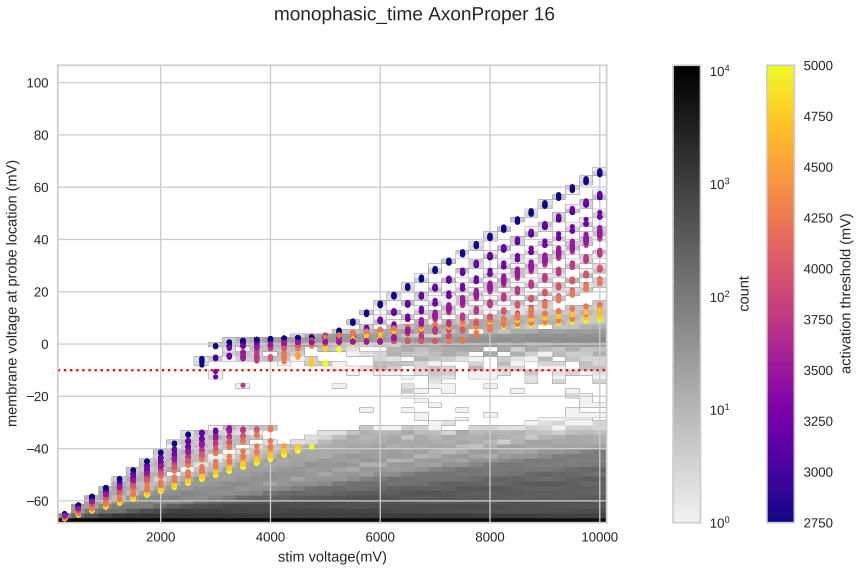

(a) monophasic

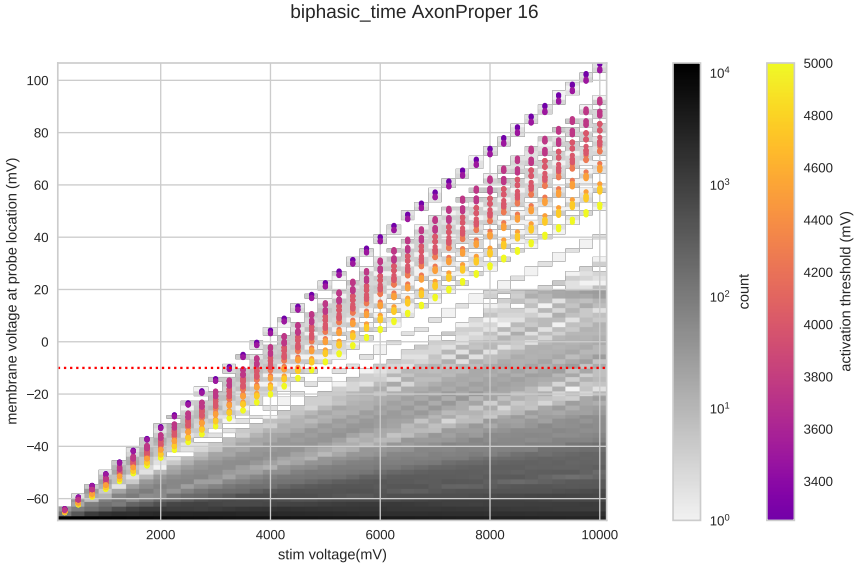

(b) biphasic

Figure 4.7: Maximum membrane voltage in mV at the axon distal tip (segment 16) (y-axis) plotted against stimulation voltage in mV (x-axis) for all neuron locations and all 18 electrode pair combinations using monophasic stimulation (top plot) and biphasic stimulation (bottom plot). The gray rectangles are a 2d histogram of the number of simulated neurons exhibiting given the voltage level (see gray colorbar). The colored dots represent neurons selected because their axon tip has a membrane voltage greater than -10 mV (referred to in this thesis as activation) using less than or equal to 5 V of stimulation. The color of each dot indicates the lowest magnitude of stimulation voltage required to activate that neuron (see right colorbar). The red dotted horizontal line indicates the activation threshold (dots and gray rectangles above this line indicate activated neurons).

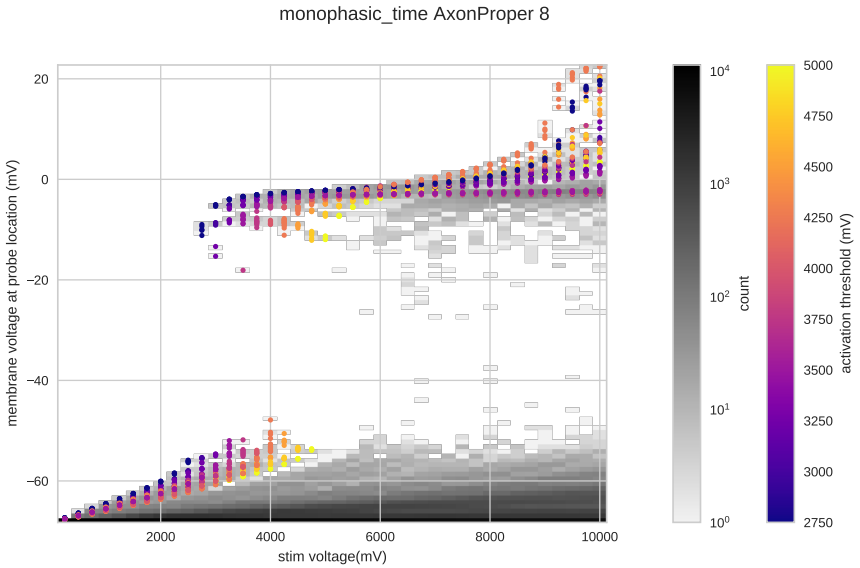

(a) monophasic

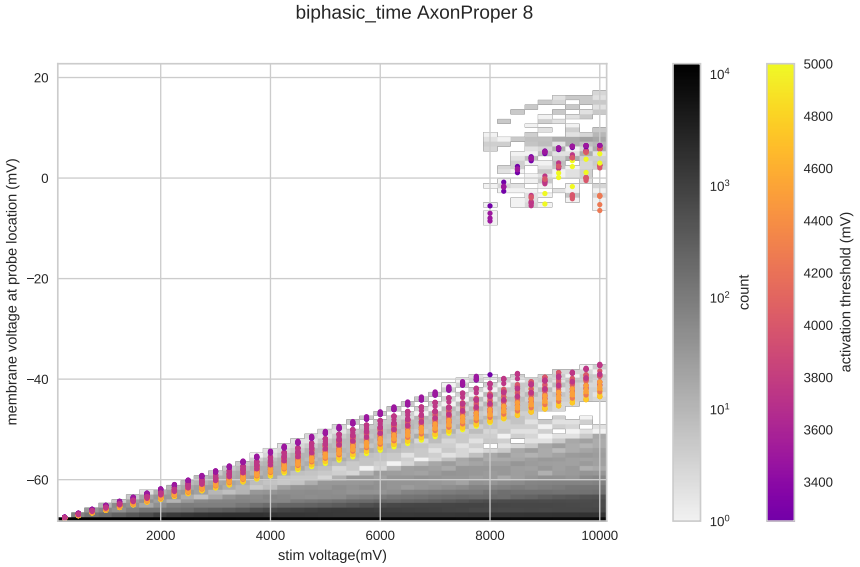

(b) biphasic

Figure 4.8: Maximum membrane voltage in mV at the axon proper middle (segment 8) (y-axis) plotted against stimulation voltage in mV (x-axis) for all neuron locations and all 18 electrode pair combinations using monophasic stimulation (top plot) and biphasic stimulation (bottom plot). The gray rectangles are a 2d histogram of the number of simulated neurons exhibiting given the voltage level (see gray colorbar). The colored dots represent neurons selected because their axon tip has a membrane voltage greater than −10 mV (referred to in this thesis as activation) using less than or equal to 5 V of stimulation. The color of each dot indicates the lowest magnitude of stimulation voltage required to activate that neuron (see right colorbar).

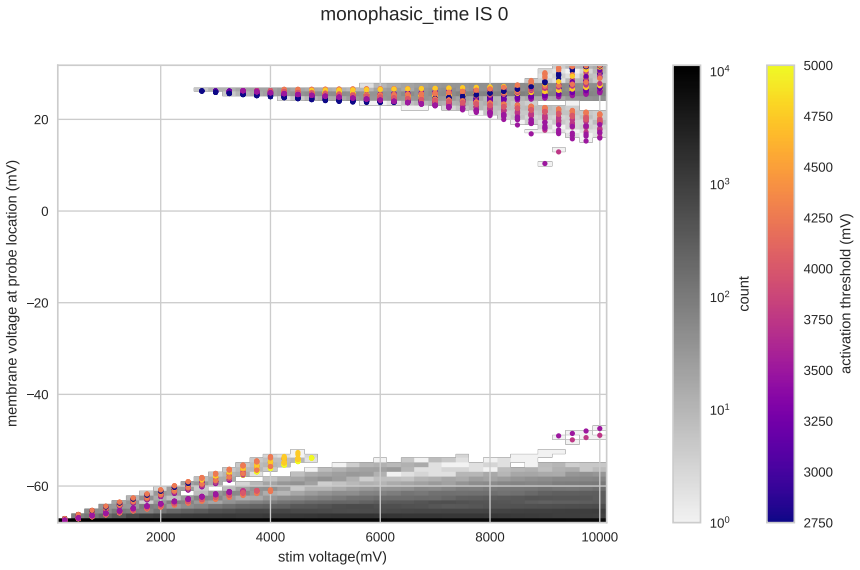

(a) monophasic

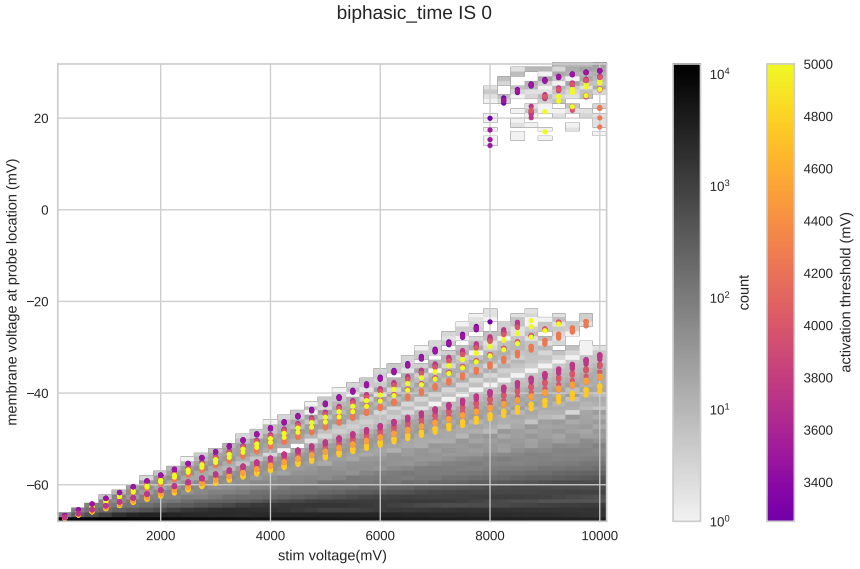

(b) biphasic

Figure 4.9: Maximum membrane voltage in mV at the initial segment (segment 0) (y-axis) plotted against stimulation voltage in mV (x-axis) for all neuron locations and all 18 electrode pair combinations using monophasic stimulation (top plot) and biphasic stimulation (bottom plot). The gray rectangles are a 2d histogram of the number of simulated neurons exhibiting given the voltage level (see gray colorbar). The colored dots represent neurons selected because their axon tip has a membrane voltage greater than −10 mV (referred to in this thesis as activation) using less than or equal to 5 V of stimulation. The color of each dot indicates the lowest magnitude of stimulation voltage required to activate that neuron (see right colorbar).

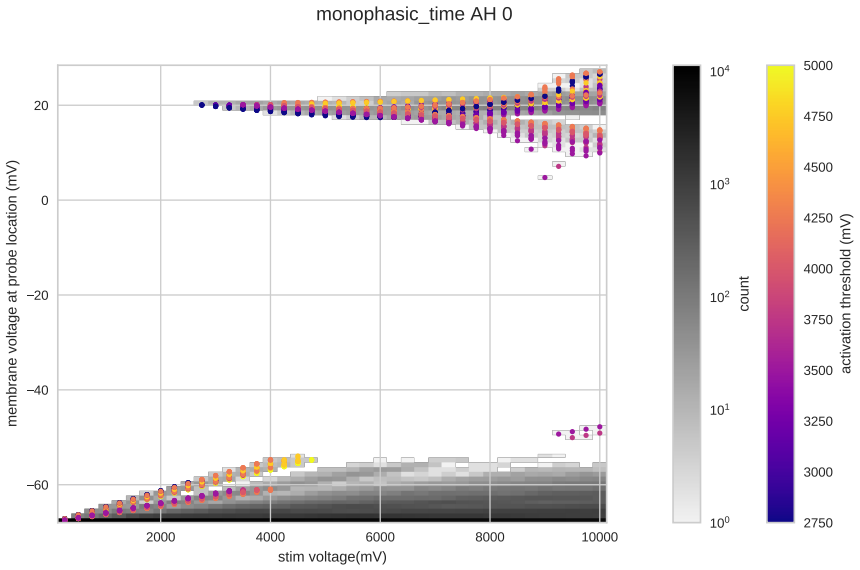

(a) monophasic

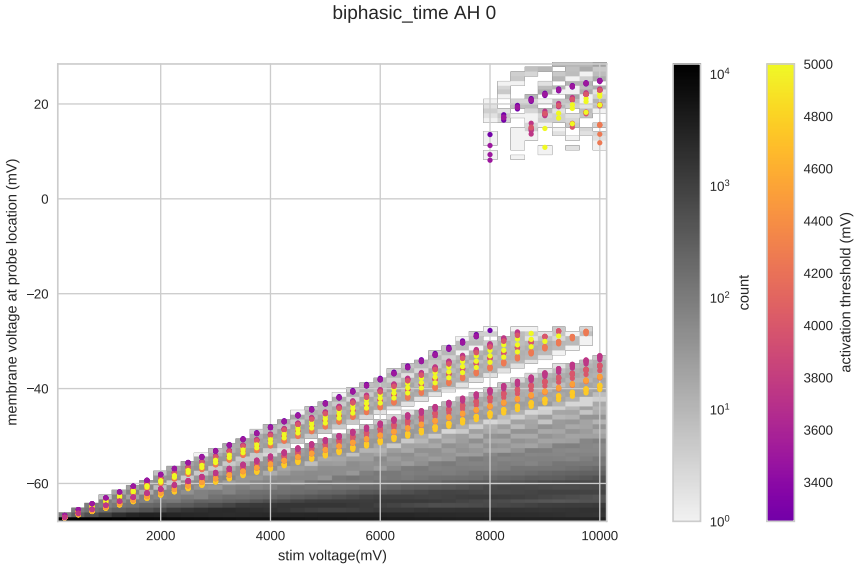

(b) biphasic

Figure 4.10: Maximum membrane voltage in mV at the axon hillock (segment 0) (y-axis) plotted against stimulation voltage in mV (x-axis) for all neuron locations and all 18 electrode pair combinations using monophasic stimulation (top plot) and biphasic stimulation (bottom plot). The gray rectangles are a 2d histogram of the number of simulated neurons exhibiting given the voltage level (see gray colorbar). The colored dots represent neurons selected because their axon tip has a membrane voltage greater than -10 mV (referred to in this thesis as activation) using less than or equal to 5 V of stimulation. The color of each dot indicates the lowest magnitude of stimulation voltage required to activate that neuron (see right colorbar).

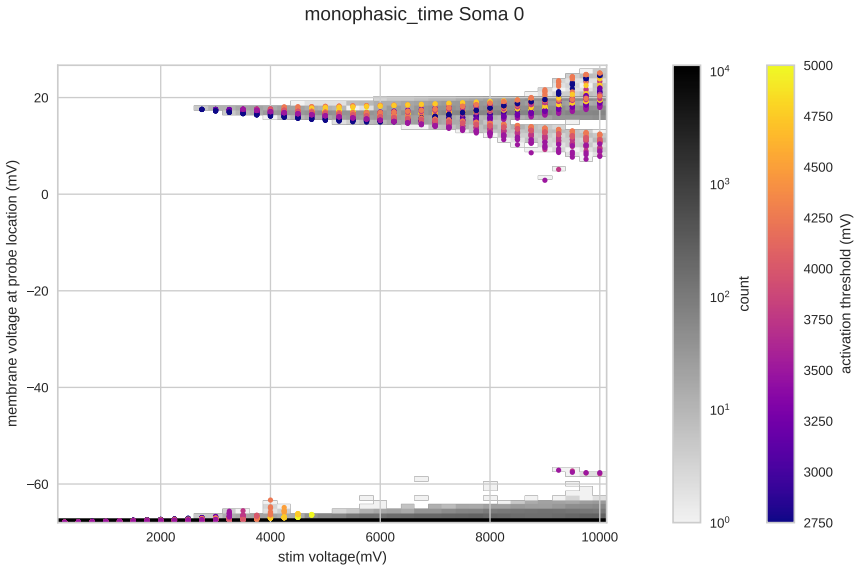

(a) monophasic

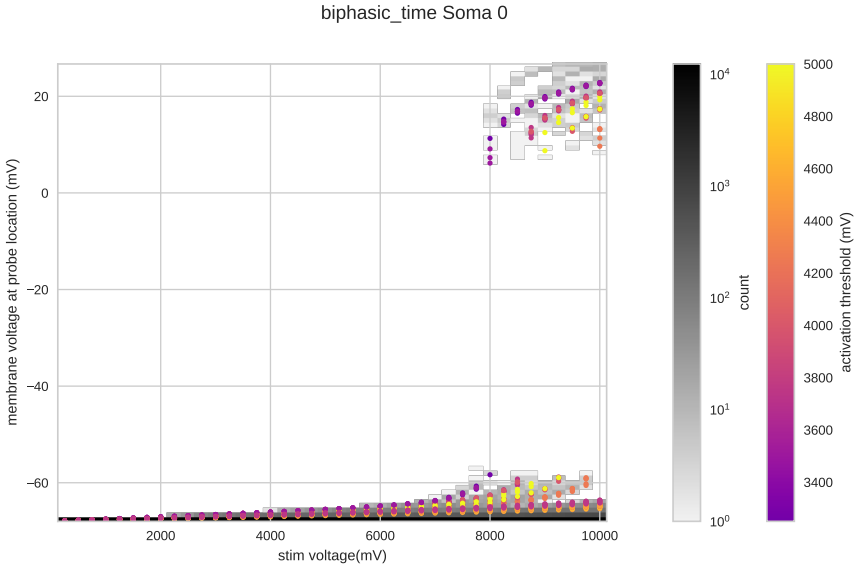

(b) biphasic

Figure 4.11: Maximum membrane voltage in mV at the soma (segment 0) (y-axis) plotted against stimulation voltage in mV (x-axis) for all neuron locations and all 18 electrode pair combinations using monophasic stimulation (top plot) and biphasic stimulation (bottom plot). The gray rectangles are a 2d histogram of the number of simulated neurons exhibiting given the voltage level (see gray colorbar). The colored dots represent neurons selected because their axon tip has a membrane voltage greater than -10 mV (referred to in this thesis as activation) using less than or equal to 5 V of stimulation. The color of each dot indicates the lowest magnitude of stimulation voltage required to activate that neuron (see right colorbar).

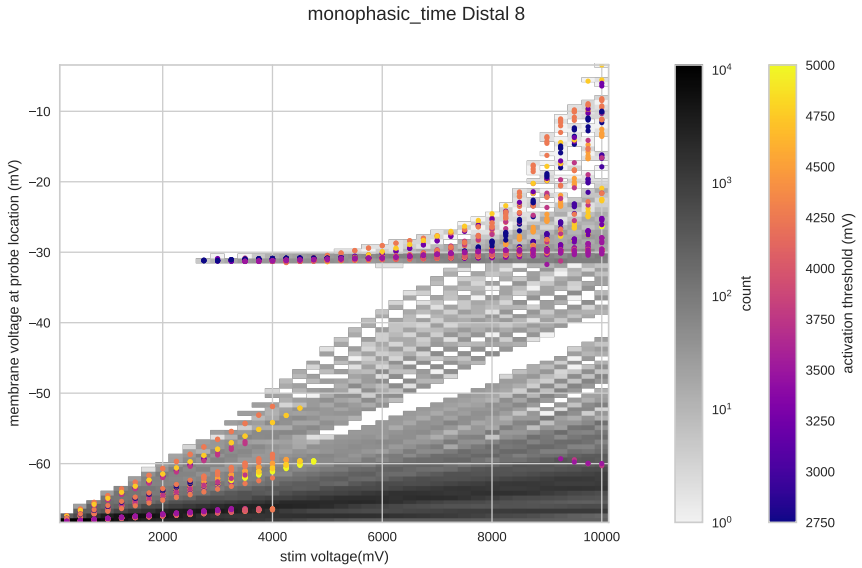

(a) monophasic

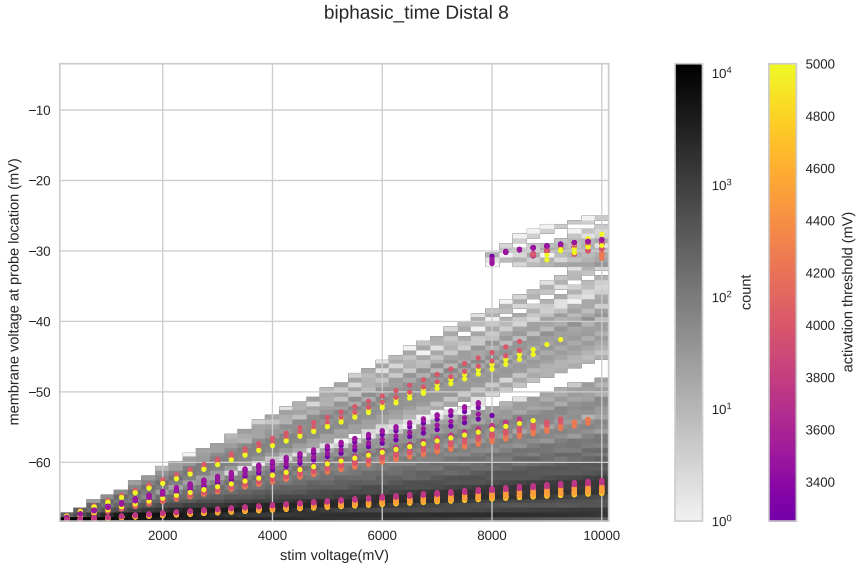

(b) biphasic

Figure 4.12: Maximum membrane voltage in mV at the distal dendrite middle (segment 8) (y-axis) plotted against stimulation voltage in mV (x-axis) for all neuron locations and all 18 electrode pair combinations using monophasic stimulation (top plot) and biphasic stimulation (bottom plot). The gray rectangles are a 2d histogram of the number of simulated neurons exhibiting given the voltage level (see gray colorbar). The colored dots represent neurons selected because their axon tip has a membrane voltage greater than −10 mV (referred to in this thesis as activation) using less than or equal to 5 V of stimulation. The color of each dot indicates the lowest magnitude of stimulation voltage required to activate that neuron (see right colorbar).

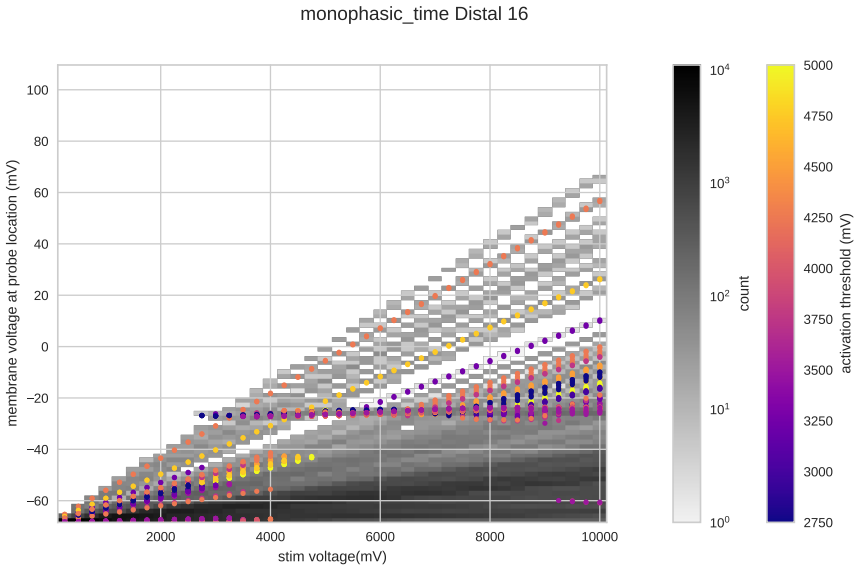

(a) monophasic

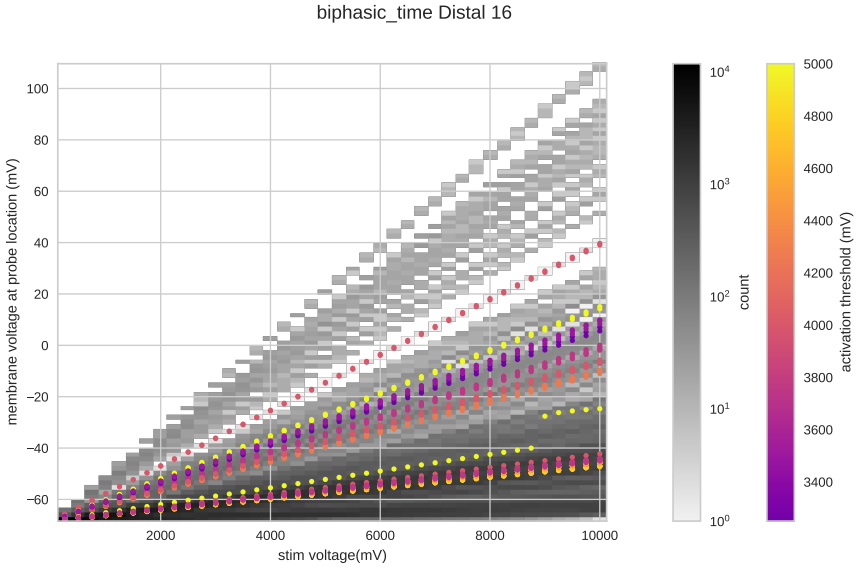

(b) biphasic

Figure 4.13: Maximum membrane voltage in mV at the distal dendrite tip (segment 16) (y-axis) plotted against stimulation voltage in mV (x-axis) for all neuron locations and all 18 electrode pair combinations using monophasic stimulation (top plot) and biphasic stimulation (bottom plot). The gray rectangles are a 2d histogram of the number of simulated neurons exhibiting given the voltage level (see gray colorbar). The colored dots represent neurons selected because their axon tip has a membrane voltage greater than −10 mV (referred to in this thesis as activation) using less than or equal to 5 V of stimulation. The color of each dot indicates the lowest magnitude of stimulation voltage required to activate that neuron (see right colorbar).

4.5 Neurotransmitter release with $\leq 5\,\mathrm{V}$ of stimulation

This section will analyze those combinations of stimuli and neuron configurations that lead to the release of neurotransmitters when using stimulation amplitudes of less than or equal to 5 V. This range of stimulation voltage has a limited amount of neuron activation without synaptic input and will also be used to look for facilitation in the next chapter. These neurons/simulations were plotted as colored dots on Figs. 4.7 to 4.13. As discussed in Section 3.3.2, a model neuron is considered to be *active* and to have released neurotransmitters if the membrane voltage (V_m) at the distal end of the axon tip goes above $-10\,\mathrm{mV}$ in response to the external stimulation.

4.5.1 Monophasic stimulation

The active neurons for all stimulus combinations using no more than 5 V of monophasic stimulation are listed in Table 4.2. Recall from Section 2.2.1 that electrode pair combinations are denoted by the notation [column letter][row number][p for +1V or n for -1V] repeated for each active electrode. In this thesis, nonactive electrodes have a floating voltage. The simulation shows that under these conditions, all of the active neurons are in the GM1 level (closest to the dorsal side of the spinal cord). All of the active axons point towards the negative electrode or away from the positive electrode (see also figures of Section 4.A.1). This implies that it is easier to activate the neuron if the axon tip has a lower extracellular voltage than the soma and other parts of the neuron. This fact is supported by the rest of the monophasic stimulation data (see Fig. 4.22) and is discussed in more detail in Section 4.6. Of the 75 active neurons, 44 had axons pointing in the $+\hat{y}$ direction near negative electrodes, 21 had axons pointing in the $-\hat{y}$ direction near positive electrodes, and 10 were inside a single row combination (3 with axons pointing in the $-\hat{x}$ direction, 3 with axons pointing in the $+\hat{x}$ direction, 1 with an axon pointing in the $-\hat{y}$ direction, and 3 with axons pointing in the $+\hat{y}$ direction) that also follows

the "axon points to the negative electrode or away from the positive electrode" rule. Also note that the stimulation voltage necessary to raise the membrane voltage of the IS probe above $-20\,\text{mV}$ is close to the stimulation voltage needed to activate the axon tip. This indicates that a significant portion of the cell is involved in the generation of the action potential, not just the tip of the axon.

Table 4.2: Monophasic simulations which result in the membrane voltage of the axon tip being above $-10\,\text{mV}$ ($V_m > -10\,\text{mV}$) while the stimulation voltage is below an amplitude of $5\,\text{V}$ ($|V_{stim}| < 5\,\text{V}$). The combo column indicates which electrodes are active. (Recall from Section 2.2.1 that electrode combinations use the notation [column letter][row number][p for +1V or n for -1V] repeated for each active electrode.) Nonactive electrodes are floating. A value of -1 in the sign column reverses the sign of the electrodes in the combination. The side, row, and dorsal-ventral columns indicate the location of the neuron. The axon column indicates the direction of the distal tip of the axon from the soma. In this table, column A16 captures the magnitude of the stimulation voltage necessary to cause the membrane voltage at the axon tip (segment 16) to exceed $-10\,\text{mV}$. Column S-A16 tabulates the additional amount of stimulation necessary to cause the soma membrane voltage to exceed $-10\,\text{mV}$. Columns D8-A16 and D16-A16 are the additional amount of stimulation (beyond that in column A16) necessary to cause the membrane voltage of the middle (seg=8) and distal tip (seg=16) of the distal dendrite respectively to exceed $-40\,\text{mV}$.

combo	sign	side	row	dorsal-ventral	axon	A16	S-A16	D8-A16	D16-A16
A2pA6n	-1	L	r2	GM1	Yp	3500	0	0	0
			r6		Yn	5000	0	0	0
	1		r2			5000	0	0	0
			r6		Yp	3500	0	0	0
A2pB6n	-1		r2			3500	0	0	0
	1				Yn	5000	0	0	0
			r6		Yp	4250	0	0	0
		R				4250	0	0	0
A2pC6n	-1	L	r2			3500	0	0	0
		R	r6		Yn	5000	0	0	0
	1	L	r2			5000	0	0	0
		R	r6		Yp	3500	0	0	0
A3pA5n	-1	L	r3			3000	0	0	0
			r5		Yn	4500	0	0	0

Continued on next page

Continued from previous page

combo	sign	side	row	dorsal-ventral	axon	A16	S-A16	D8-A16	D16-A16
	1		r3			4500	0	0	0
			r5		Yp	3000	0	0	0
A3pA6n	-1		r3			3250	0	0	0
			r6		Yn	4750	0	0	0
	1		r3			4750	0	0	0
			r6		Yp	3250	0	0	0
A3pB5n	-1		r3			3000	0	0	0
	1				Yn	4500	0	0	0
			r5		Yp	3750	0	0	0
		R				3750	0	0	0
A3pB6n	-1	L	r3			3250	0	0	0
	1				Yn	4750	0	0	0
			r6		Yp	4000	0	0	0
		R				4000	0	0	0
A3pC5n	-1	L	r3			3000	0	0	0
		R	r5		Yn	4500	0	0	0
	1	L	r3			4500	0	0	0
		R	r5		Yp	3000	0	0	0
A3pC6n	-1	L	r3			3250	0	0	0
		R	r6		Yn	4750	0	0	0
	1	L	r3			4750	0	0	0
		R	r6		Yp	3250	0	0	0
A4pA5n	-1	L	r4			2750	0	0	0
			r5		Yn	4250	0	0	0
	1		r4			4250	0	0	0
			r5		Yp	2750	0	0	0
A4pB4n	-1		r4		Xn	3750	0	0	0
	1				Xp	4250	0	0	0
		R			Yp	3750	-250	-250	-250
A4pB5n	-1	L				2750	0	0	0
	1				Yn	4250	0	0	0
			r5		Yp	3500	0	0	0
		R				3500	0	0	0
A4pC4n	-1	L	r4		Xn	4250	0	0	-1750
					Yp	3250	-250	-250	-250
		R			Xn	3750	0	0	0

Continued on next page

Continued from previous page

combo	sign	side	row	dorsal-ventral	axon	A16	S-A16	D8-A16	D16-A16
					Yn	4750	0	0	-1500
	1	L			Xp	3750	0	0	0
					Yn	4750	0	0	-1500
		R			Xp	4250	0	0	-1750
					Yp	3250	-250	-250	-250
A4pC5n	-1	L				2750	0	0	0
		R	r5		Yn	4250	0	0	0
	1	L	r4			4250	0	0	0
		R	r5		Yp	2750	0	0	0
B2pB6n	-1	L	r2			4250	0	0	0
		R				4250	0	0	0
	1	L	r6			4250	0	0	0
		R				4250	0	0	0
B3pB5n	-1	L	r3			3750	0	0	0
		R				3750	0	0	0
	1	L	r5			3750	0	0	0
		R				3750	0	0	0
B3pB6n	-1	L	r3			4000	0	0	0
		R				4000	0	0	0
	1	L	r6			4000	0	0	0
		R				4000	0	0	0
B4pB5n	-1	L	r4			3500	0	0	0
		R				3500	0	0	0
	1	L	r5			3500	0	0	0
		R				3500	0	0	0

The minimum amount of monophasic stimulation to activate a neuron was 2750 mV. A total of five neurons were activated at that stimulation level using combinations ±A4pA5n, -A4pB5n, and ±A4pC5n. All of the active neurons were directly under the negative electrode.

The membrane voltage as a function of time for all segments of the neuron located at GM1_L_r5 with an axon pointing in the $+\hat{y}$ direction exposed to 2750 mV of monophasic stimulation using combination A4pA5n is plotted in Fig. 4.14. Note that the action potential starts at the axon tip and travels in the antidromic direction until it reaches the initial segment (IS). Then an orthodromic conduction occurs (back towards the axon tip) but is diminished in strength by the time it reaches the axon tip. All of the neurons activated using less than or equal to 10 V of monophasic stimulation show similar behavior (in some cases the second conduction merges with the first). Figure 4.15 shows the membrane voltage for the probe locations as a function of stimulation voltage. In this case, the axon tip has the highest membrane voltage when the stimulation voltage is below the level required to "activate" (i.e. membrane voltage at the axon tip goes above -10 mV) the neuron. This is not always the case. In some of the simulated neurons, a dendrite tip is most stimulated. The bottom plot of Fig. 4.15 also confirms that the axon tip reaches maximum membrane voltage first, followed by the axon middle, then the AH, IS, and soma at the same time.

4.5.2 Biphasic stimulation

The active neurons (with axon tip membrane voltage > -10 mV) for all combinations using no more than 5 V of biphasic stimulation are listed in Table 4.3. Similar to the monophasic simulation seen in Table 4.2, all of the active neurons are in the GM1 layer. Of the 50 active neurons (25 fewer than monophasic), 44 had axons pointing in the $+\hat{y}$ direction and were located near electrodes whose biphasic stim-

ulation has a leading edge which is negative. The other 6 active neurons (2 with axons pointing in the $-\hat{x}$ direction, 1 with an axon pointing in the $+\hat{x}$ direction, and 3 with axons pointing in the $+\hat{y}$ direction) are stimulated by electrodes in a single row and have axons that point towards the electrode whose biphasic stimulation has a leading edge which is negative.

All of the active neurons were positioned directly under the electrode with the negative leading edge. Note that it takes a substantially larger stimulation voltage for the Initial Segment (IS) to be involved (at least 4V). This suggests that biphasic stimulation of neurons in the spinal cord (without additional synapse involvement) does not usually involve the whole cell. This can also be seen in the biphasic plots in Figs. 4.7 to 4.13.

Table 4.3: Biphasic simulations which result in the membrane voltage of the axon tip being above $-10\,\text{mV}$ ($V_m > -10\,\text{mV}$) while the stimulation voltage is below an amplitude of $5\,\text{V}$ ($|V_{stim}| < 5\,\text{V}$). The combo column indicates which electrodes are active. (Recall from Section 2.2.1 that electrode combinations use the notation [column letter][row number][p for +1V or n for -1V] repeated for each active electrode.) Nonactive electrodes are floating. A value of -1 in the sign column reverses the sign of the electrodes in the combination. The side, row, and dorsal-ventral columns indicate the location of the neuron. The axon column indicates the direction of the distal tip of the axon from the soma. In this table, column A16 captures the magnitude of the stimulation voltage necessary to cause the membrane voltage at the axon tip (segment 16) to exceed $-10\,\text{mV}$. Column S-A16 tabulates the additional amount of stimulation necessary to cause the soma membrane voltage to exceed $-10\,\text{mV}$. Columns D8-A16 and D16-A16 are the additional amount of stimulation (beyond that in column A16) necessary to cause the membrane voltage in the middle (seg=8) or distal tip (seg=16) of one of the distal dendrites respectively to exceed $-40\,\text{mV}$. A value of OSR means Outside Search Range (i.e. more than $\pm 10\,\text{V}$ of stimulation is necessary).

combo	sign	side	row	dorsal-ventral	axon	A16	S-A16	D8-A16	D16-A16
A2pA6n	-1	L	r2	GM1	Yp	4250	5750	5750	750
	1		r6			4250	5750	5750	750
A2pB6n	-1		r2			4250	5750	5750	750

Continued on next page

Continued from previous page

combo	sign	side	row	dorsal-ventral	axon	A16	S-A16	D8-A16	D16-A16
	1		r6			4750	OSR	OSR	OSR
		R				4750	OSR	OSR	OSR
A2pC6n	-1	L	r2			4250	5750	5750	750
	1	R	r6			4250	5750	5750	750
A3pA5n	-1	L	r3			3750	5000	5000	750
	1		r5			3750	5000	5000	500
A3pA6n	-1		r3			4000	5500	5500	750
	1		r6			4000	5500	5500	750
A3pB5n	-1		r3			3750	5000	5000	750
	1		r5			4000	OSR	OSR	OSR
		R				4000	OSR	OSR	OSR
A3pB6n	-1	L	r3			4000	5500	5500	750
	1		r6			4500	OSR	OSR	OSR
		R				4500	OSR	OSR	OSR
A3pC5n	-1	L	r3			3750	5000	5000	750
	1	R	r5			3750	5000	5000	500
A3pC6n	-1	L	r3			4000	5500	5500	750
	1	R	r6			4000	5500	5500	750
A4pA5n	-1	L	r4			3250	4750	4750	750
	1		r5			3250	5000	5000	750
A4pB4n	-1		r4		Xn	5000	4000	4000	4000
	1	R			Yp	4000	OSR	OSR	OSR
A4pB5n	-1	L				3500	4500	4500	250
	1		r5			3750	OSR	OSR	OSR
		R				3750	OSR	OSR	OSR
A4pC4n	-1	L	r4			4000	4750	4750	-1250
		R			Xn	5000	4500	4500	-1500
	1	L			Xp	5000	4000	4000	-1500
		R			Yp	4000	4750	4750	-1250
A4pC5n	-1	L				3500	4500	4500	250
	1	R	r5			3500	4500	4500	250
B2pB6n	-1	L	r2			4500	OSR	OSR	OSR
		R				4750	OSR	OSR	OSR
	1	L	r6			4750	OSR	OSR	OSR
		R				4750	OSR	OSR	OSR
B3pB5n	-1	L	r3			4000	OSR	OSR	OSR

Continued on next page

Continued from previous page

combo	sign	side	row	dorsal-ventral	axon	A16	S-A16	D8-A16	D16-A16
		R				4000	OSR	OSR	OSR
	1	L	r5			4000	OSR	OSR	OSR
		R				4000	OSR	OSR	OSR
B3pB6n	-1	L	r3			4250	OSR	OSR	OSR
		R				4500	OSR	OSR	OSR
	1	L	r6			4500	OSR	OSR	OSR
		R				4500	OSR	OSR	OSR
B4pB5n	-1	L	r4			3750	OSR	OSR	OSR
		R				3750	OSR	OSR	OSR
	1	L	r5			3750	OSR	OSR	OSR
		R				3750	OSR	OSR	OSR

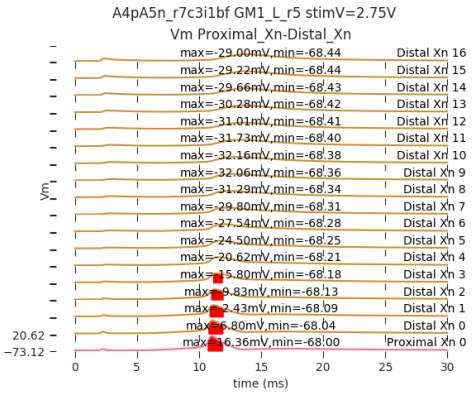

(a) Proximal_Xn-Distal_Xn

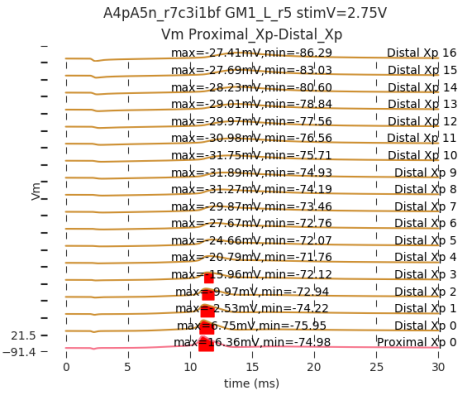

(b) Proximal_Xp-Distal_Xp

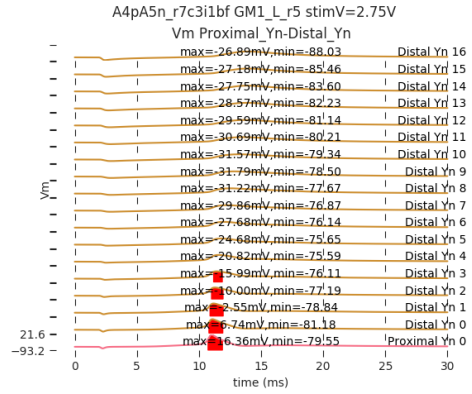

(c) Proximal_Yn-Distal_Yn

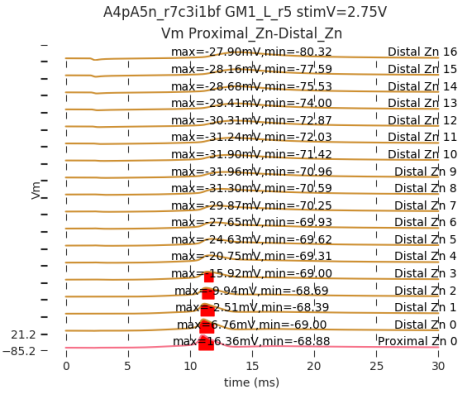

(d) Proximal_Zn-Distal_Zn

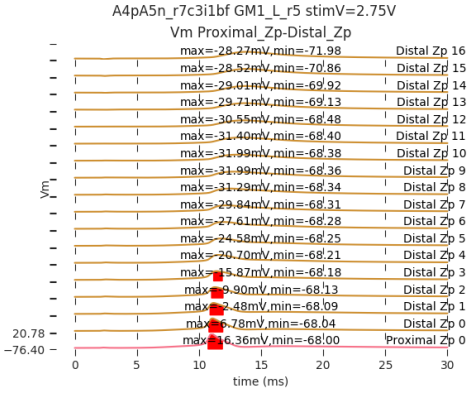

(e) Proximal_Zp-Distal_Zp

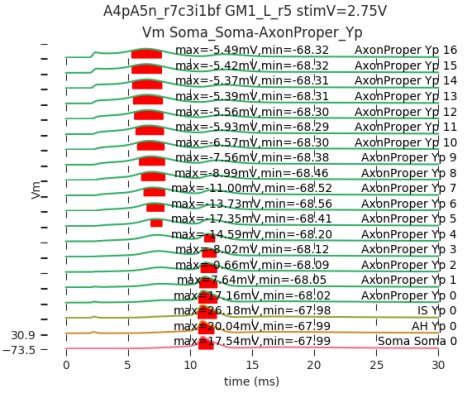

(f) Soma_Soma-AxonProper_Yp

Figure 4.14: Membrane voltage (V_m) vs time, for a neuron with axon pointing towards Yp located at GM1_L_r5 exposed to 2.75 V of monophasic stimulation using combination A4pA5n. Each subfigure (a-f) plots V_m on a each segment of a different neurite: (a) $-\hat{x}$ dendrite, (b) $+\hat{x}$ dendrite, (c) $-\hat{y}$ dendrite, (d) $-\hat{z}$ dendrite, (e) $+\hat{z}$ dendrite, and (f) $+\hat{y}$ axon + soma. For each subfigure (a-f): The horizontal axis is the simulation time in ms. Each segment plot is labeled on the right side with (section type, orientation, segment number). The range of the vertical axis for the segment plots is indicated in the lower left corner. The minimum and maximum V_m for each segment is in the middle of each segment plot. Red areas under each segment plot indicate time periods in which V_m at that segment exceeds -10 mV.
Subfigure (f) shows an antidromic action potential starting at the axon tip followed by an orthodromic action potential starting at the IS. The second action potential fails to cause neurotransmitter release most likely because of the refractory period of the axon.

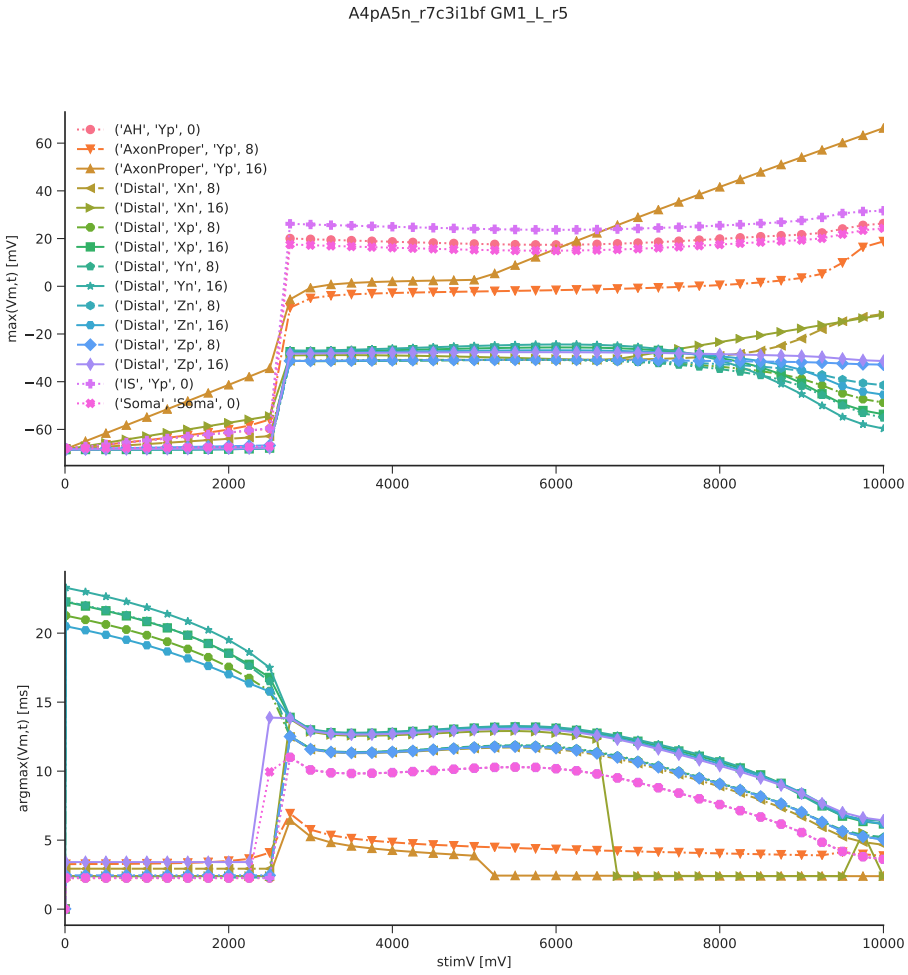

Figure 4.15: (top): Membrane voltage (in mV) at different locations on a simulated neuron as a function of stimulation voltage (in mV, axis shared with bottom plot) for monophasic stimulation with combination A4pA5n, location GM1_L_r5, and axon in the $+\hat{y}$ direction. This is one of the configurations that results in neuron activation with the minimum amount of monophasic stimulation (in this case 2.75 V). The legend labels in the top plot are in the format (section type, orientation, segment number). See Fig. 3.3 for segment number locations by section type. Note that the axon tip (AxonProper, Yp, 16) is most stimulated compared to other probe locations if the stimulation voltage amplitude is less than 2.75 V. (bottom): The time of the maximum membrane voltage (in ms) for each probe vs stimulation voltage (in mV). The time of the maximum membrane voltage helps explain which parts of the neuron reach maximum first. Note that the stimulation pulse starts at 1 ms and peaks at 2.12 ms.

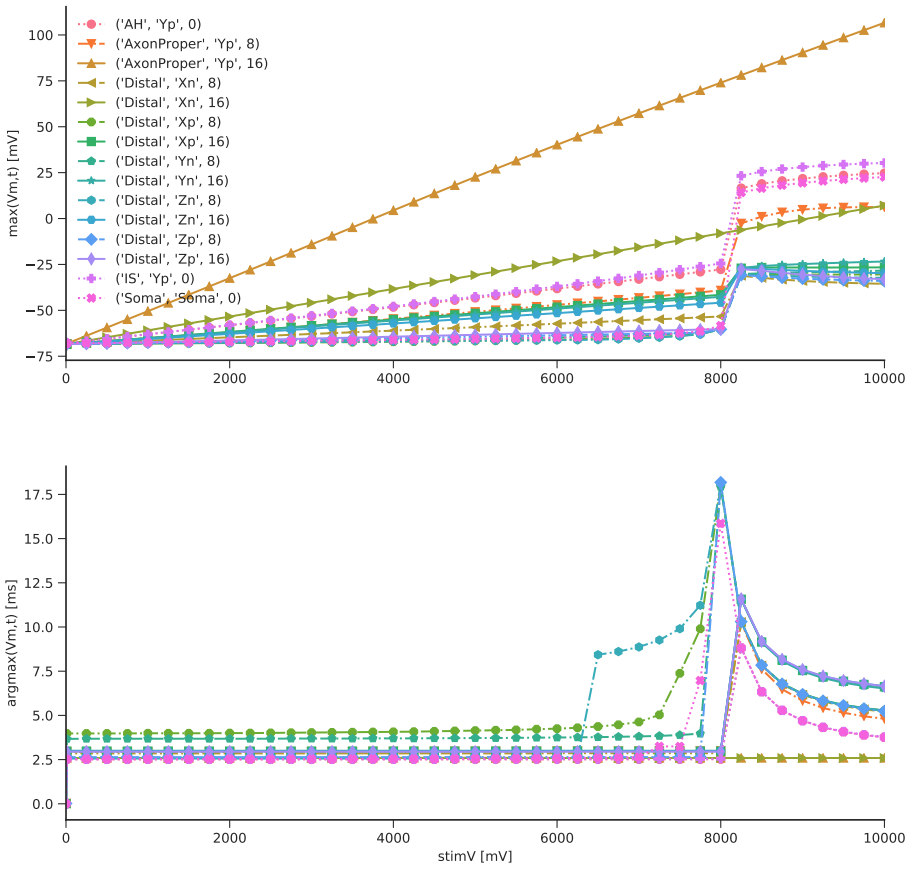

Figure 4.16: (top): Membrane voltage (in mV) at different locations on a simulated neuron as a function of stimulation voltage (in mV, axis shared with bottom plot) for biphasic stimulation with combination A4pA5n, location GM1_L_r5, and axon in the $+\hat{y}$ direction. This is the same configuration as in Fig. 4.15, except biphasic instead of monophasic stimulation. This is one of the configurations that results in neuron activation with the minimum amount of biphasic stimulation (in this case 3.25 V). The legend labels in the top plot are in the format (section type, orientation, segment number). See Fig. 3.3 for segment number locations by section type. Note that the axon tip (AxonProper, 'Yp' ,16) is most stimulated compared to other probe locations and linear as expected from Fig. 4.7b. (bottom): The time of the maximum membrane voltage (in ms) for each probe vs stimulation voltage (in mV). The time of the maximum membrane voltage helps explain which parts of the neuron reach maximum first. Note that the stimulation pulse starts at 1 ms the middle of the pulse is at 2.66 ms and the maximum amplitudes of the pulse occur at 2.66 ms ± 0.16 ms. The first maximum amplitude occurs at 2.5 ms and the maximum in the axon proper tip, and the $-\hat{x}$ distal dendrite tip occurs very shortly after.

Table 4.4: Biphasic simulations which result in an orthodromic action potential using less than 10V of biphasic stimulation. The simulation voltage necessary (V_{stim}) is listed in volts.

combo	sign	side	row	dorsal-ventral	axon	V_{stim}
A2pA6n	1	L	r6	GM1	Yn	10.0
A2pA6n	-1	L	r2	GM1	Yn	9.75
A2pB6n	-1	L	r2	GM1	Yn	9.75
A2pC6n	1	R	r6	GM1	Yn	10.0
A2pC6n	-1	L	r2	GM1	Yn	9.75
A3pA5n	1	L	r5	GM1	Yn	8.75
A3pA5n	-1	L	r3	GM1	Yn	8.75
A3pA6n	1	L	r6	GM1	Yn	9.25
A3pA6n	-1	L	r3	GM1	Yn	9.5
A3pB5n	-1	L	r3	GM1	Yn	8.75
A3pB6n	-1	L	r3	GM1	Yn	9.5
A3pC5n	1	R	r5	GM1	Yn	8.75
A3pC5n	-1	L	r3	GM1	Yn	8.75
A3pC6n	1	R	r6	GM1	Yn	9.25
A3pC6n	-1	L	r3	GM1	Yn	9.5
A4pA5n	1	L	r5	GM1	Yn	8.0
A4pA5n	-1	L	r4	GM1	Yn	8.0
A4pB4n	1	L	r4	GM1	Xn	9.0
A4pB4n	-1	L	r4	GM1	Xp	8.75
A4pB5n	-1	L	r4	GM1	Yn	8.0

Continued on next page

Continued from previous page

combo	sign	side	row	dorsal-ventral	axon	V_{stim}
A4pC4n	1	L	r4	GM1	Xn	9.0
A4pC4n	1	L	r4	GM1	Yp	8.5
A4pC4n	1	R	r4	GM1	Xn	9.25
A4pC4n	1	R	r4	GM1	Yn	8.75
A4pC4n	-1	L	r4	GM1	Xp	9.0
A4pC4n	-1	L	r4	GM1	Yn	8.5
A4pC4n	-1	R	r4	GM1	Xp	9.25
A4pC4n	-1	R	r4	GM1	Yp	8.75
A4pC5n	1	R	r5	GM1	Yn	8.0
A4pC5n	-1	L	r4	GM1	Yn	8.0

The minimum amount of biphasic stimulation magnitude to activate a neuron was 3250 mV (500 mV more than monophasic). Two neurons were activated at that stimulation level using combinations ±A4pA5n (A4pA5n means electrode A4 has a positive leading edge of the biphasic stimulation and A5 has a negative leading edge. -A4pA5n means electrode A4 has the negative leading edge and A5 the positive leading edge). One of these neurons happens to be the same neuron examined with monophasic stimulation in Figs. 4.14 and 4.15. The membrane voltage as a function of time for all segments with 3.25 V of biphasic stimulation (just enough to activate the neuron), combination A4pA5n, axon along the $+\hat{y}$ direction, location GM1_L_r5 (most dorsal, left side, row 5) is plotted in Fig. 4.17. In this case, the axon tip is activated, but when the voltage is reversed, the cell returns to resting potential and no action potential is formed. The linear nature of this response to stimulation voltage below 8 V of stimulation can be seen in Fig. 4.16. It is impor-

tant to remember that although the membrane voltage returns to resting potential in a short time frame, the state of the ion channels and ion concentrations inside the cell may take longer to return to steady state and could help or hinder facilitation, as will be studied in the next chapter.

As seen in Figs. 4.7 to 4.13, the response of other neurons to stimulation is also mostly linear below 8 V. Those neurons with a non-linear action-potential-like response in the axon tip are listed in Table 4.4. One or more of the dendrites in these neurons are strongly stimulated, and this effect seems to generate an orthodromic action potential starting at the IS. One example of an orthodromic action potential occurs using 8 V biphasic stimulation, combination A4pA5n, location GM1_L_r5 (most dorsal, left side, row 5)), but with the axon along the $-\hat{y}$ direction instead of the $+\hat{y}$ direction in the previous examples. The membrane voltage as a function of time can be seen in Fig. 4.18. Although many parts of the cell are hyperpolarized (have a lower membrane voltage) and depolarized (higher membrane voltage) compared to resting potential at different times in the simulation, the $+\hat{y}$ direction is notably strongly depolarized and the $-\hat{x}$ dendrite moderately depolarized compared to the other dendrites. This can also be seen in as a function of stimulation voltage in Fig. 4.19 where the $+\hat{y}$ and $-\hat{x}$ dendrites are most depolarized at stimulation voltages less than 8 V.

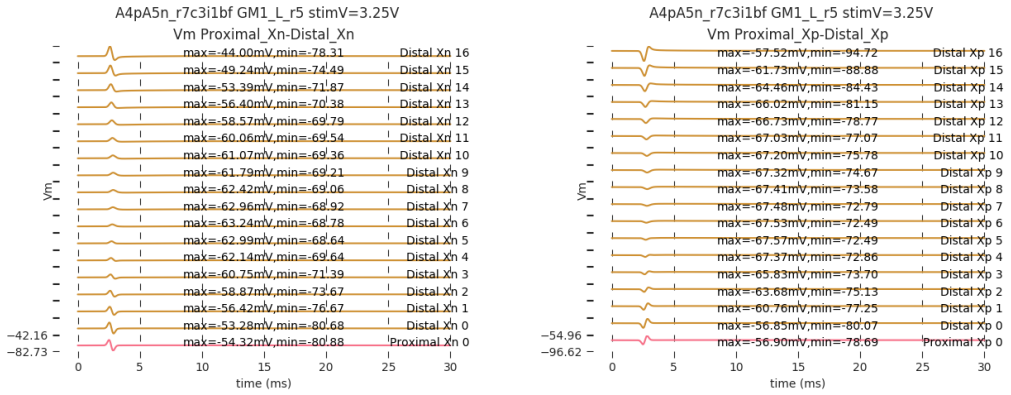

(a) Proximal_Xn-Distal_Xn

(b) Proximal_Xp-Distal_Xp

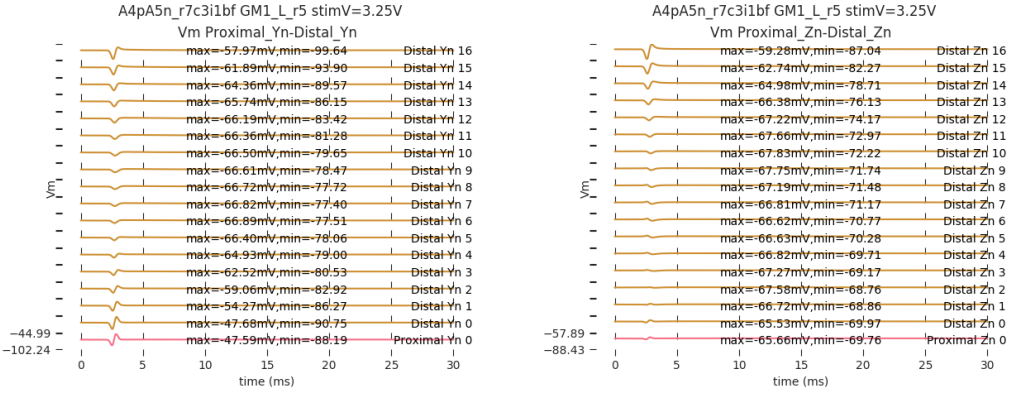

(c) Proximal_Yn-Distal_Yn

(d) Proximal_Zn-Distal_Zn

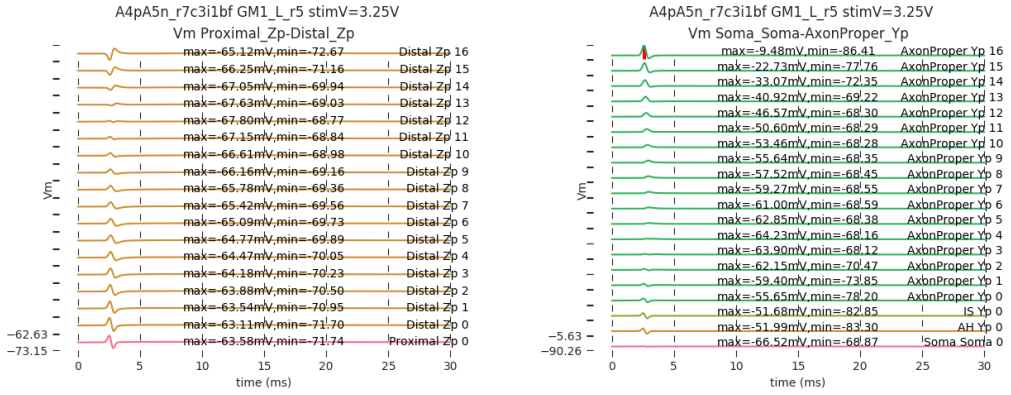

(e) Proximal_Zp-Distal_Zp

(f) Soma_Soma-AxonProper_Yp

Figure 4.17: Membrane voltage (V_m) vs time, for a neuron with axon pointing towards Yp located at GM1_L_r5 exposed to 3.25 V of biphasic stimulation using combination A4pA5n. Each subfigure (a-f) plots V_m on each segment of a different neurite: (a) $-\hat{x}$ dendrite, (b) $+\hat{x}$ dendrite, (c) $-\hat{y}$ dendrite, (d) $-\hat{z}$ dendrite, (e) $+\hat{z}$ dendrite, and (f) $+\hat{y}$ axon + soma. For each subfigure (a-f): The horizontal axis is the simulation time in ms. Each segment plot is labeled on the right side with (section type, orientation, segment number). The range of the vertical axis for the segment plots is indicated in the lower left corner. The minimum and maximum V_m for each segment are in the middle of each segment plot. Red areas under each segment plot indicate time periods in which V_m at that segment exceeds −10 mV.
Subfigure (f) shows that no action potential occurs, and instead the stimulation pulse causes V_m at the axon tip to exceed −10 mV (and release neurotransmitters) directly.

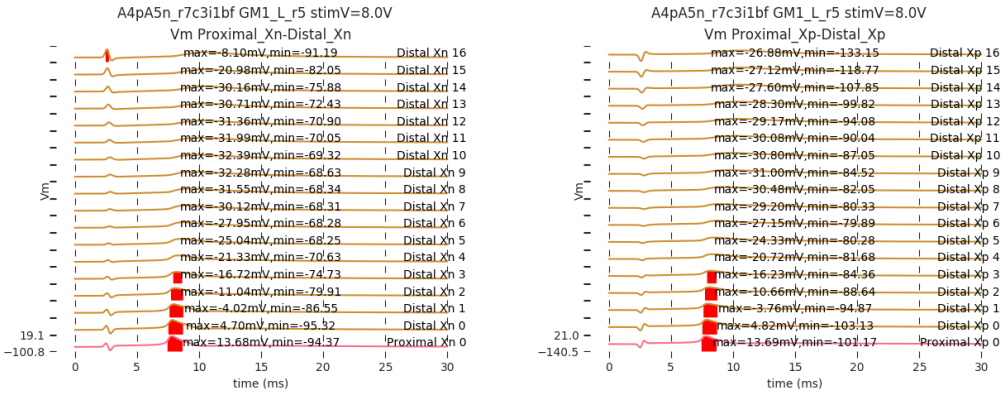

(a) Proximal_Xn-Distal_Xn

(b) Proximal_Xp-Distal_Xp

(c) Proximal_Yp-Distal_Yp

(d) Proximal_Zn-Distal_Zn

(e) Proximal_Zp-Distal_Zp

(f) Soma_Soma-AxonProper_Yn

Figure 4.18: Membrane voltage (V_m) vs time, for a neuron with axon pointing towards Yn located at GM1_L_r5 exposed to 8.0 V of biphasic stimulation using combination A4pA5n.
Each subfigure (a-f) plots V_m on each segment of a different neurite: (a) $-\hat{x}$ dendrite, (b) $+\hat{x}$ dendrite, (c) $+\hat{y}$ dendrite, (d) $-\hat{z}$ dendrite, (e) $+\hat{z}$ dendrite, and (f) $-\hat{y}$ axon + soma. For each subfigure (a-f): The horizontal axis is the simulation time in ms. Each segment plot is labeled on the right side with (section type, orientation, segment number). The range of the vertical axis for the segment plots is indicated in the lower left corner. The minimum and maximum V_m for each segment are in the middle of each segment plot. Red areas under each segment plot indicate time periods in which V_m at that segment exceeds -10 mV.
Subfigure (f) shows an orthodromic action potential starting at the IS traveling to the axon tip and causing neurotransmitter release.

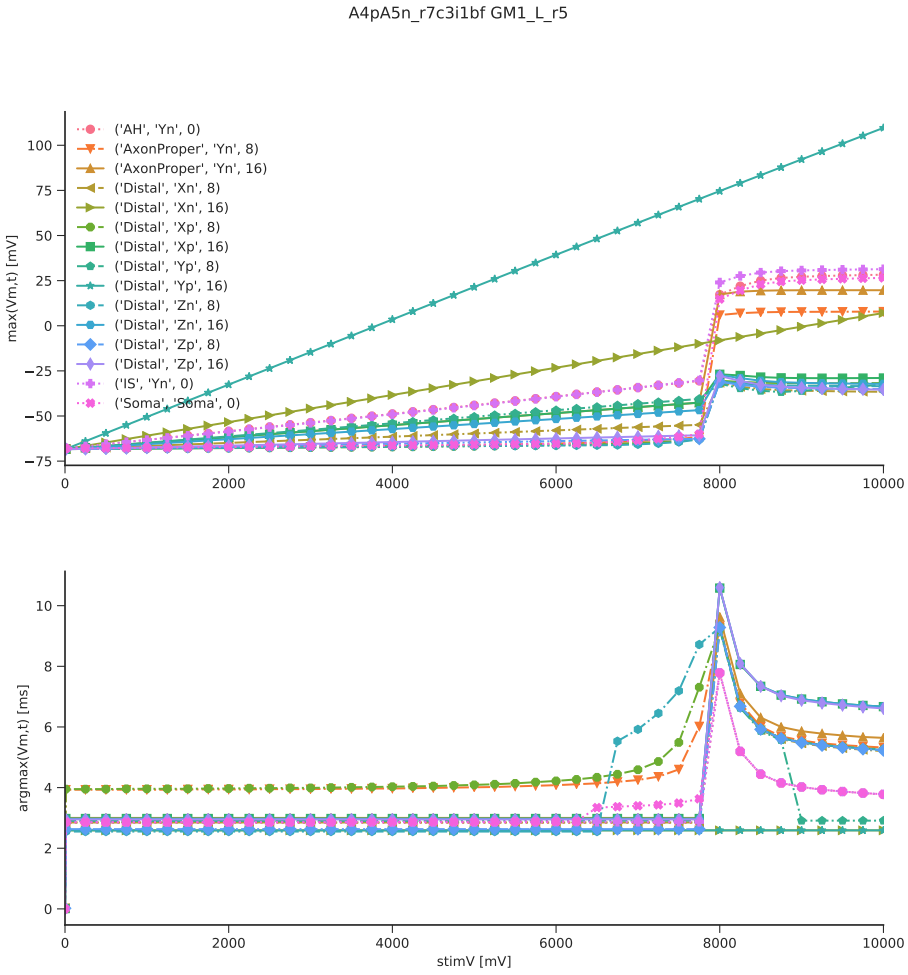

Figure 4.19: (top): Membrane voltage (in mV) as a function of stimulation voltage (in mV, axis shared with bottom plot) for biphasic stimulation with combination A4pA5n, location GM1_L_r5, and axon in the $-\hat{y}$ direction. This is the same configuration as in Fig. 4.16 except the axon is in the $-\hat{y}$ direction. This configuration results in an orthodromic action potential starting at the initial segment (IS) with 8 V of stimulation. This is one of the few neurons in Fig. 4.7b with a nonlinear response in the axon tip above 8 V. The legend labels in the top plot are in the format (section type, orientation, segment number). See Fig. 3.3 for segment number locations by section type. (bottom): The time of the maximum membrane voltage (in ms) for each probe vs stimulation voltage (in mV). The time of the maximum membrane voltage helps explain which parts of the neuron reach maximum first. Note that the stimulation pulse starts at 1 ms the middle of the pulse is at 2.66 ms and the maximum amplitudes of the pulse occur at 2.66 ms $\pm$ 0.16 ms. The first maximum amplitude occurs at 2.5 ms and the maximum in the $+\hat{y}$ distal dendrite tip occurs very shortly after.

4.6 Predicting neuron activation

The computational cost of running time-domain finite element simulations and NEURON simulations limits the number of simulations possible. A less computationally intensive method for predicting whether a particular configuration of electrodes would activate a particular neuron would make it easier to tailor electrode arrays and stimulation for particular applications and subjects. In this section, I explore a few possibilities for predicting activation based on static volume conductor simulations.

The second spatial derivative of the static voltage [a] is often used as a proxy for activation. Figure 4.20 shows that the second spatial derivative of the static voltage (V_{static}) along a vector pointing towards the soma cannot be used to separate active neurons from non-active neurons. Figure 4.21 shows that a wide range of extracellular voltages result in the axon tip membrane voltage going above $-10\,\text{mV}$, so that cannot be used either. However, the results in Section 4.5.1 hinted that perhaps the difference in the extracellular voltage between the axon tip and the soma could be used to predict neuron activation. Figure 4.22 shows the static voltage at the axon tip ($V_{static}^{\text{AxonTip}}$) minus the static voltage at the soma (V_{static}^{Soma}) plotted against the membrane voltage at the axon tip (V_m^{AxonTip}). This estimate of the first spatial derivative is useful to separate activated neurons from non-activated neurons. For this dataset and monophasic stimulation, the neuron is guaranteed to be active if $V_{static}^{\text{AxonTip}} - V_{static}^{\text{Soma}} < -373\,\text{mV}$ and guaranteed not active if $-279\,\text{mV} < V_{static}^{\text{AxonTip}} - V_{static}^{\text{Soma}}$. These equations match the "axon points to the negative electrode or away from the positive electrode" rule mentioned in Section 4.5.1 for monophasic stimulation. For biphasic stimulation, the neuron is guaranteed to be active if $V_{static}^{\text{AxonTip}} - V_{static}^{\text{Soma}} < -492\,\text{mV}$ or $V_{static}^{\text{AxonTip}} - V_{static}^{\text{Soma}} > 872\,\text{mV}$. The neuron is guaranteed not active if $-290\,\text{mV} < V_{static}^{\text{AxonTip}} - V_{static}^{\text{Soma}} < 580\,\text{mV}$. Using biphasic

[a] referred to in some of the literature as the activating function (Rattay, 1999)

stimulation, it takes less magnitude of stimulation voltage to activate a neuron if the electrode with the negative leading edge is closer to the axon tip and further away from the soma. This generally results in the axon tip exceeding −10 mV but no cell wide action potential. If instead there is an electrode with a positive leading edge closer to the axon tip and further from the soma, then it takes a larger magnitude of stimulation voltage, but the stimulation first affects the membrane voltage in one or more of the dendrites before an orthodromic action potential occurs.

While the numerical values in the above rules are likely to change for different neurons (geometry, ion channel density, etc.), this study shows that features similar to $V_{static}^{\text{AxonTip}} - V_{static}^{\text{Soma}}$ could be useful for estimating when electrically stimulated neurons would be activated without running large numbers of NEURON simulations. The success of these simple rules based on static features for separating active neurons from inactive neurons also shows that the geometry of the stimulation field plays a critical role.

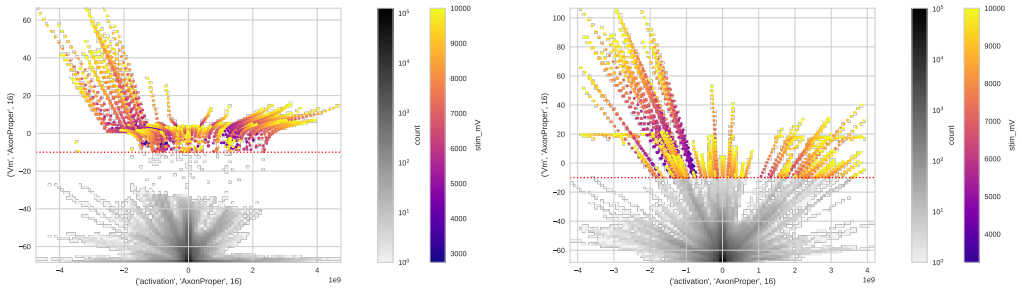

(a) monophasic activation

(b) biphasic activation

Figure 4.20: Maximum membrane voltage in mV at the axon distal tip (segment 16) (y-axis) plotted against the second spatial derivative of the static extracellular voltage V_e along a vector pointing towards the soma at the axon distal tip (x-axis) for all neuron locations and all 18 electrode pair combinations using monophasic stimulation (left plot) and biphasic stimulation (right plot). The gray rectangles are a 2d histogram of the number of neurons (see gray colorbar). The colored dots are active neurons (axon tip has a membrane voltage greater than −10 mV) and are colored based on the stimulation voltage (see right colorbar). The red dotted horizontal line indicates the activation threshold (dots and gray rectangles above this line indicate activated neurons).

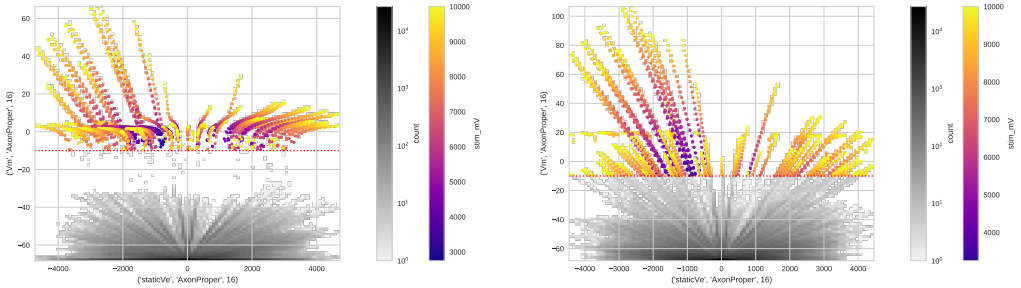

(a) monophasic static V_e (b) biphasic static V_e

Figure 4.21: Maximum membrane voltage in mV at the axon distal tip (segment 16) (y-axis) plotted against the static extracellular voltage at the axon distal tip (x-axis) for all neuron locations and all 18 electrode pair combinations using monophasic stimulation (left plot) and biphasic stimulation (right plot). The gray rectangles are a 2d histogram of the number of neurons (see gray colorbar). The colored dots are active neurons (axon tip has a membrane voltage greater than -10 mV) and are colored based on the stimulation voltage (see right colorbar). The red dotted horizontal line indicates the activation threshold (dots and gray rectangles above this line indicate activated neurons).

4.7 Discussion

Based on simulations, both biphasic and monophasic stimulation (without additional synaptic input) can cause the membrane voltage in the axon tip of interneurons in the spinal cord to go above -10 mV, and therefore release neurotransmitters, using less than 5 V of stimulation (minimum of 2.75 V for monophasic and 3.25 V for biphasic). This is in the same range of voltages that are used in actual epidural stimulation experiments with rats (3 V (P. Gad et al., 2012), 5 V to 7 V (Desautels et al., 2015), 4 V (Parag Gad, Roy, Choe, Creagmile, et al., 2015), and 1 V to 8 V (Parag Gad, Roy, Choe, Zhong, et al., 2015)). Monophasic stimulation resulted in antidromic action potentials and biphasic stimulation resulted in no action potentials inside the cell at stimulation voltages of < 8 V (even if the tip of the axon went above -10 mV, which is considered to be enough to release neurotransmitters into the presynaptic cleft), but a few neurons generated orthodromic action potentials at stimulation voltages ≥ 8 V. Simple rules using the difference in static voltage at

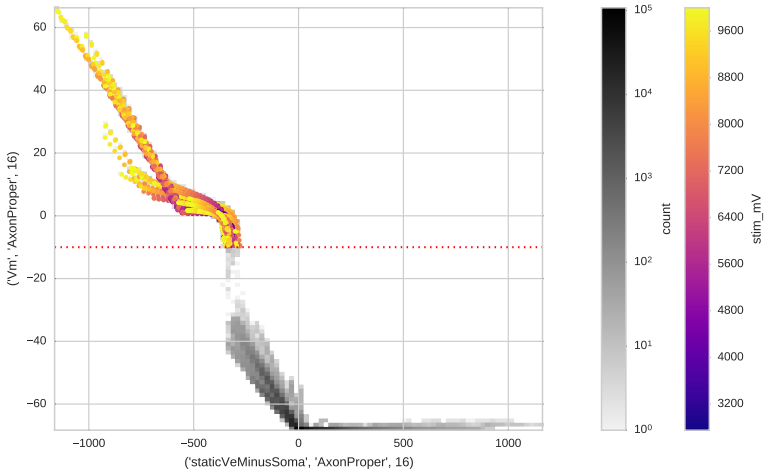

(a) monophasic

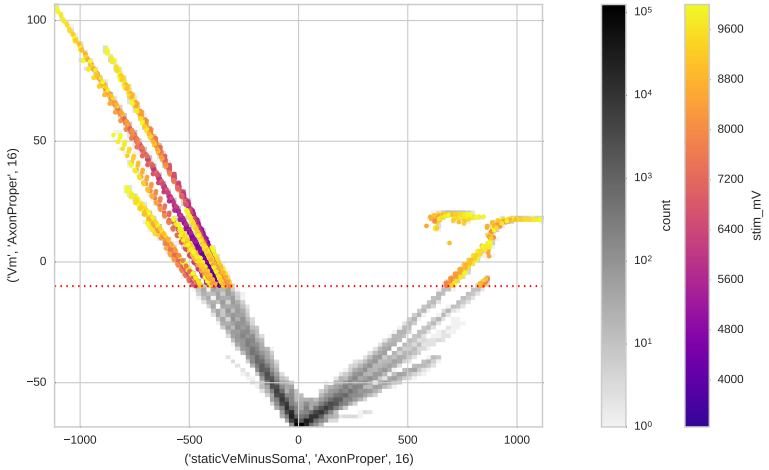

(b) biphasic

Figure 4.22: Maximum membrane voltage in mV at the axon distal tip (segment 16) (y-axis) plotted against the static extracellular voltage at the axon distal tip minus the static extracellular voltage at the soma (x-axis) for all neuron locations and all 18 electrode pair combinations using monophasic stimulation (top plot) and biphasic stimulation (bottom plot). The gray rectangles are a 2d histogram of the number of neurons (see gray colorbar). The colored dots are active neurons (axon tip has a membrane voltage greater than −10 mV) and are colored based on the stimulation voltage (see right colorbar). The red dotted horizontal line indicates the activation threshold (dots and gray rectangles above this line indicate activated neurons).

the axon and the soma were found that could be useful for predicting neuron activation without costly time-domain simulations. This would allow faster design of

stimulation protocols for particular applications and/or subjects.

Additional simulations of the neurons that are activated using a magnitude of stimulation of 5 V or less (listed in Tables 4.2 and 4.3) using passive dendrites instead of active dendrites found little change in the amount of stimulation necessary to activate the neurons. This implies that these neurons are mostly activated by stimulation of the axon.

Most existing studies would stop here and completely ignore the possibility of the interaction of synaptic input in the spinal cord with the stimulation pulses. The next chapter will examine how epidural stimulation can facilitate synaptic input to generate neurotransmitter release.

4.A Appendix: Stimulation Thresholds

This appendix contains figures showing which axons are activated (axon tip membrane voltage $\geq -10\,\text{mV}$) using $\leq 10\,\text{V}$ of stimulation voltage magnitude. Each figure shows the results for one of the 18 bipolar combinations listed in Section 2.2.1 with either a positive or a negative voltage and either monophasic or biphasic stimulation (36 plots for monophasic and 36 plots for biphasic). Please note that in each of the plots, the spinal cord is oriented such that the head of the rat would be outside the lower left corner and the tail of the rat would be beyond the upper right corner. In each plot, the active electrodes are labeled by name and a "+" symbol if they have a positive initial phase or a "-" symbol if they have a negative initial phase. The electrode labels are also colored blue for negative and red for positive. The soma, AH, IS, and AP are displayed as red lines for those neurons whose axon tip membrane voltage exceeds $-10\,\text{mV}$ with no more than $10\,\text{V}$ of stimulation. Since 6 neurons are plotted at the same location, dendrites are not displayed. The color of the cube at each axon tip indicates stimulation voltages required for axon tip to reach $V_m > -10\,\text{mV}$. A list of the active neurons is included in each caption as a location, orientation (Yp=$+\hat{y}$, Yn=$-\hat{y}$, etc), and the threshold to cause that neuron to activate in Volts.

4.A.1 Monophasic

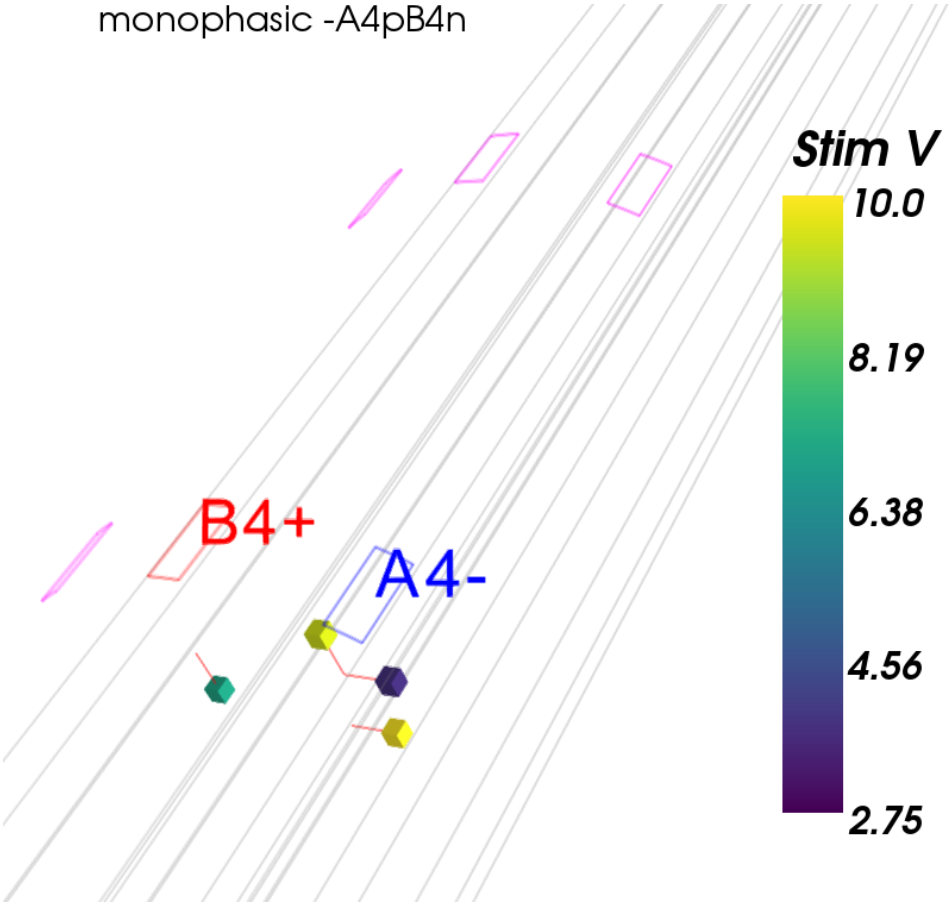

Figure 4.23: Monophasic stimulation using combination -A4pB4n. Electrode B4 has a positive phase and is labeled red. Electrode A4 has a negative phase and is labeled blue. All other electrodes are floating and labeled purple. Soma, AH, IS, and AP are displayed as red lines for those neurons whose axon tip membrane voltage exceeds −10 mV with no more than 10 V of stimulation. Dendrites are not displayed. The color of the cube at each axon tip indicates stimulation voltages required for axon tip to reach $V_m > -10$ mV. List of location, axon direction, and threshold: (GM1_L_r4, Yp, 9.5 V), (GM1_L_r4, Xn, 3.75 V), (GM3_L_r4, Xn, 10.0 V), and (GM1_R_r4, Yn, 7.0 V).

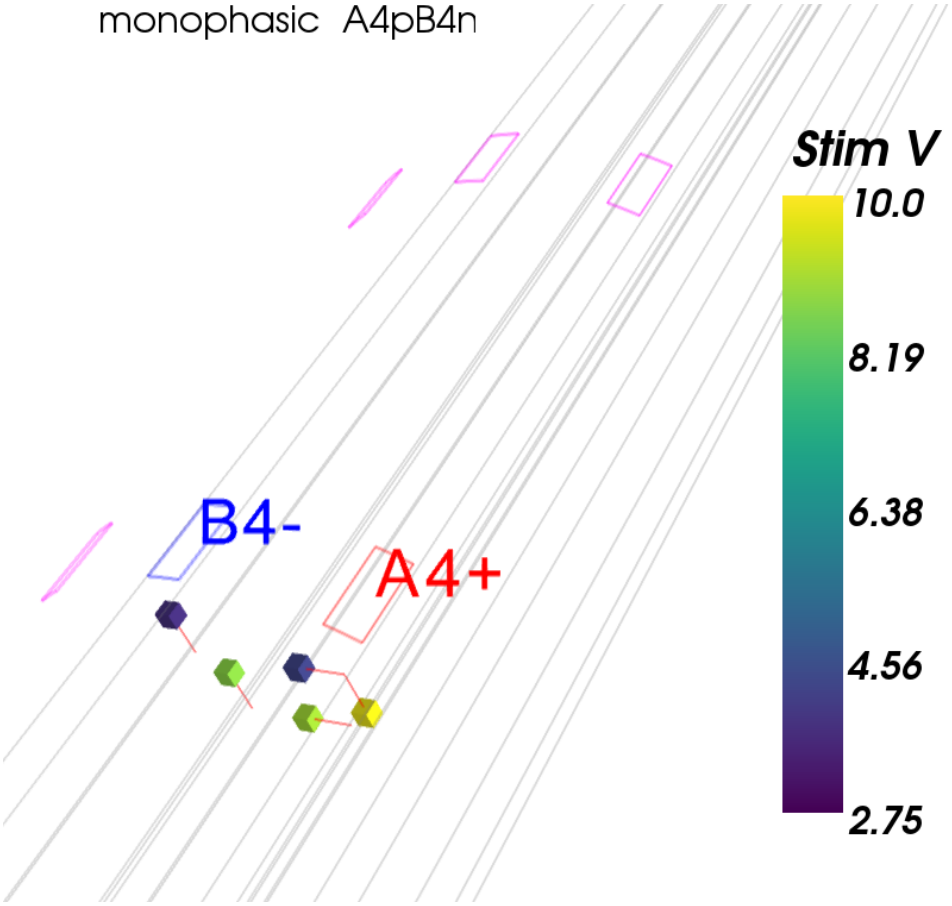

Figure 4.24: Monophasic stimulation using combination A4pB4n. Electrode A4 has a positive phase and is labeled red. Electrode B4 has a negative phase and is labeled blue. All other electrodes are floating and labeled purple. Soma, AH, IS, and AP are displayed as red lines for those neurons whose axon tip membrane voltage exceeds −10 mV with no more than 10 V of stimulation. Dendrites are not displayed. The color of the cube at each axon tip indicates stimulation voltages required for axon tip to reach $V_m > -10$ mV. List of location, axon direction, and threshold: (GM1_R_r4, Yp, 3.75 V), (GM3_R_r4, Yp, 8.75 V), (GM1_L_r4, Xp, 4.25 V), (GM3_L_r4, Xp, 9.0 V), and (GM1_L_r4, Yn, 9.75 V).

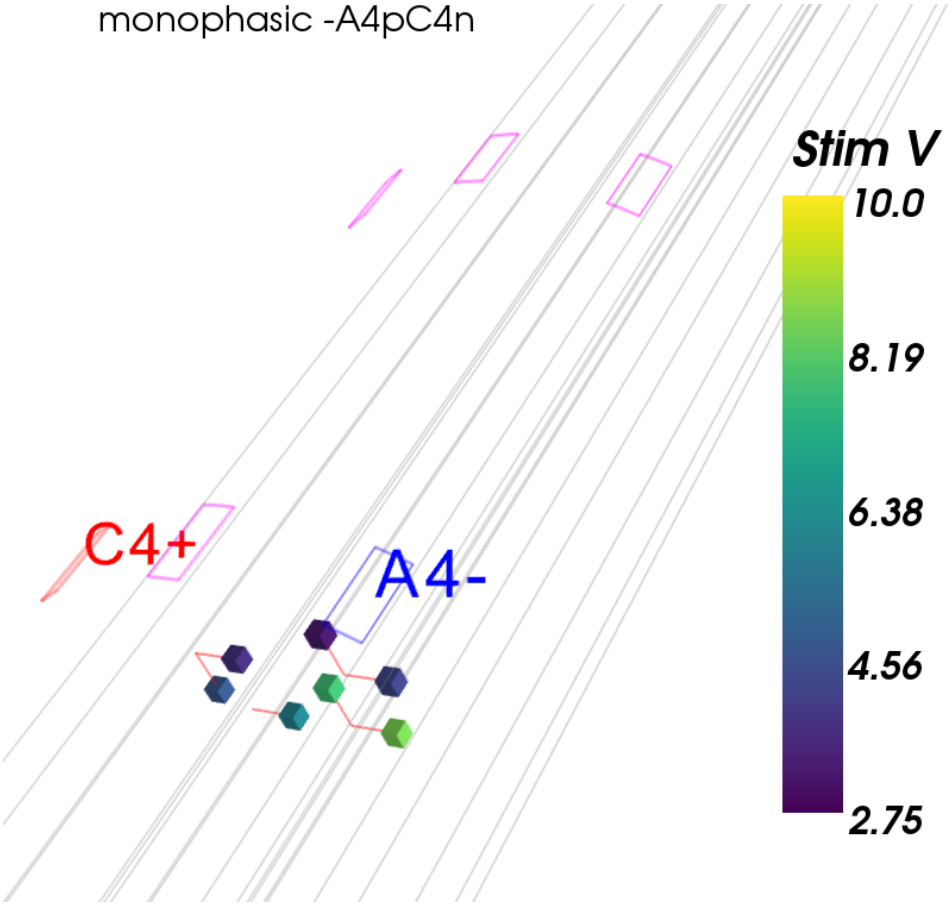

Figure 4.25: Monophasic stimulation using combination -A4pC4n. Electrode C4 has a positive phase and is labeled red. Electrode A4 has a negative phase and is labeled blue. All other electrodes are floating and labeled purple. Soma, AH, IS, and AP are displayed as red lines for those neurons whose axon tip membrane voltage exceeds −10 mV with no more than 10 V of stimulation. Dendrites are not displayed. The color of the cube at each axon tip indicates stimulation voltages required for axon tip to reach $V_m > -10$ mV. List of location, axon direction, and threshold: (GM1_L_r4, Yp, 3.25 V), (GM3_L_r4, Yp, 7.75 V), (GM1_L_r4, Xn, 4.25 V), (GM1_R_r4, Xn, 3.75 V), (GM3_L_r4, Xn, 8.5 V), (GM3_R_r4, Xn, 6.0 V), and (GM1_R_r4, Yn, 4.75 V).

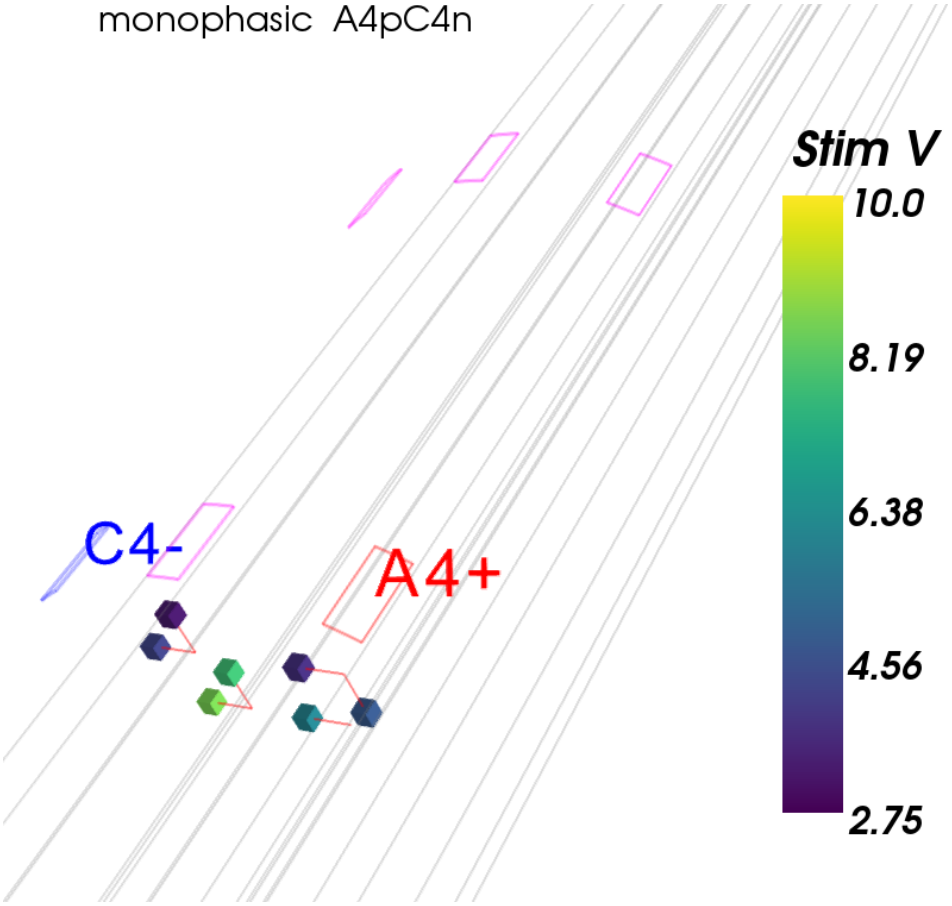

Figure 4.26: Monophasic stimulation using combination A4pC4n. Electrode A4 has a positive phase and is labeled red. Electrode C4 has a negative phase and is labeled blue. All other electrodes are floating and labeled purple. Soma, AH, IS, and AP are displayed as red lines for those neurons whose axon tip membrane voltage exceeds −10 mV with no more than 10 V of stimulation. Dendrites are not displayed. The color of the cube at each axon tip indicates stimulation voltages required for axon tip to reach $V_m > -10$ mV. List of location, axon direction, and threshold: (GM1_R_r4, Yp, 3.25 V), (GM3_R_r4, Yp, 7.75 V), (GM1_L_r4, Xp, 3.75 V), (GM1_R_r4, Xp, 4.25 V), (GM3_L_r4, Xp, 6.0 V), (GM3_R_r4, Xp, 8.5 V), and (GM1_L_r4, Yn, 4.75 V).

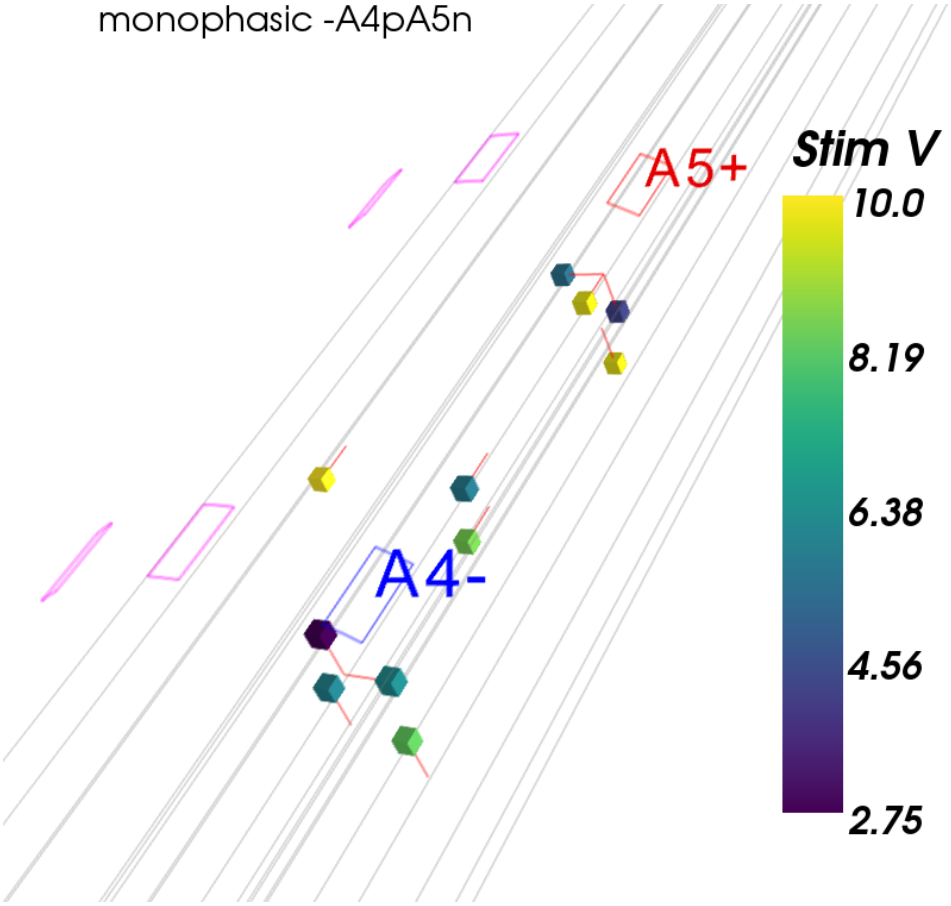

Figure 4.27: Monophasic stimulation using combination -A4pA5n. Electrode A5 has a positive phase and is labeled red. Electrode A4 has a negative phase and is labeled blue. All other electrodes are floating and labeled purple. Soma, AH, IS, and AP are displayed as red lines for those neurons whose axon tip membrane voltage exceeds $-10\,\text{mV}$ with no more than $10\,\text{V}$ of stimulation. Dendrites are not displayed. The color of the cube at each axon tip indicates stimulation voltages required for axon tip to reach $V_m > -10\,\text{mV}$. List of location, axon direction, and threshold: (GM1_L_r5, Zn, 9.75 V), (GM1_L_r4and5, Zn, 5.75 V), (GM3_L_r4and5, Zn, 8.5 V), (GM1_R_r4and5, Zn, 10.0 V), (GM1_L_r4, Yp, 2.75 V), (GM3_L_r4, Yp, 6.0 V), (GM2_L_r4, Yp, 8.25 V), (GM1_L_r5, Xp, 5.5 V), (GM1_L_r4, Xn, 6.25 V), (GM1_L_r5, Yn, 4.25 V), and (GM3_L_r5, Yn, 9.75 V).

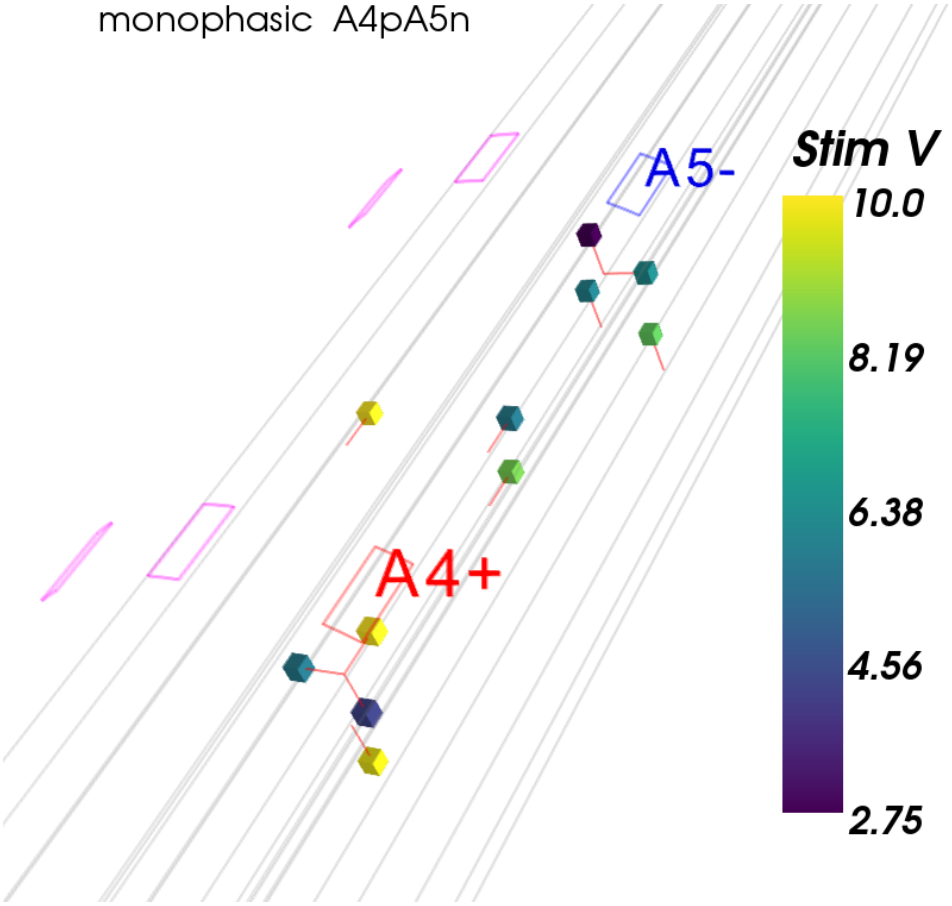

Figure 4.28: Monophasic stimulation using combination A4pA5n. Electrode A4 has a positive phase and is labeled red. Electrode A5 has a negative phase and is labeled blue. All other electrodes are floating and labeled purple. Soma, AH, IS, and AP are displayed as red lines for those neurons whose axon tip membrane voltage exceeds −10 mV with no more than 10 V of stimulation. Dendrites are not displayed. The color of the cube at each axon tip indicates stimulation voltages required for axon tip to reach $V_m > -10$ mV. List of location, axon direction, and threshold: (GM1_L_r5, Yp, 2.75 V), (GM3_L_r5, Yp, 6.0 V), (GM2_L_r5, Yp, 8.25 V), (GM1_L_r4, Xp, 5.75 V), (GM1_L_r5, Xn, 6.25 V), (GM1_L_r4, Yn, 4.25 V), (GM3_L_r4, Yn, 9.75 V), (GM1_L_r4, Zp, 10.0 V), (GM1_L_r4and5, Zp, 5.75 V), (GM3_L_r4and5, Zp, 8.5 V), and (GM1_R_r4and5, Zp, 10.0 V).

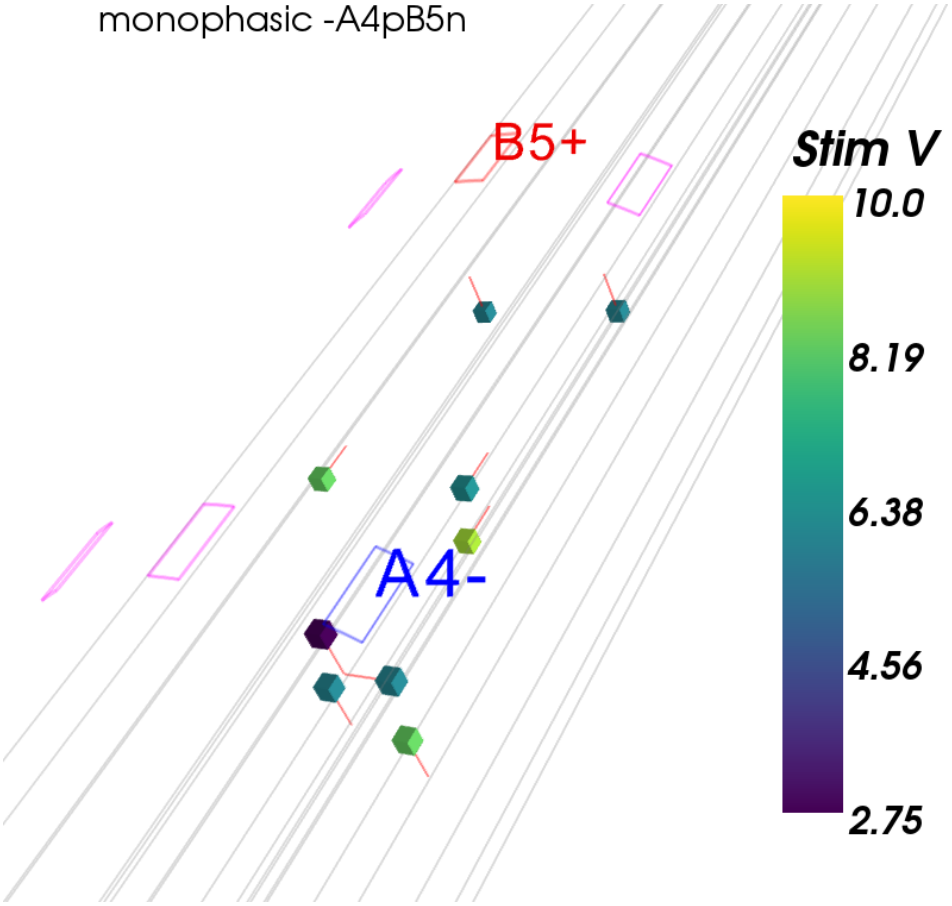

Figure 4.29: Monophasic stimulation using combination -A4pB5n. Electrode B5 has a positive phase and is labeled red. Electrode A4 has a negative phase and is labeled blue. All other electrodes are floating and labeled purple. Soma, AH, IS, and AP are displayed as red lines for those neurons whose axon tip membrane voltage exceeds $-10\,\text{mV}$ with no more than $10\,\text{V}$ of stimulation. Dendrites are not displayed. The color of the cube at each axon tip indicates stimulation voltages required for axon tip to reach $V_m > -10\,\text{mV}$. List of location, axon direction, and threshold: (GM1_L_r4and5, Zn, 6.25 V), (GM1_R_r4and5, Zn, 8.25 V), (GM3_L_r4and5, Zn, 9.0 V), (GM1_L_r4, Yp, 2.75 V), (GM3_L_r4, Yp, 6.0 V), (GM2_L_r4, Yp, 8.25 V), (GM1_L_r4, Xn, 6.0 V), (GM1_R_r5, Yn, 6.0 V), and (GM1_L_r5, Yn, 6.0 V).

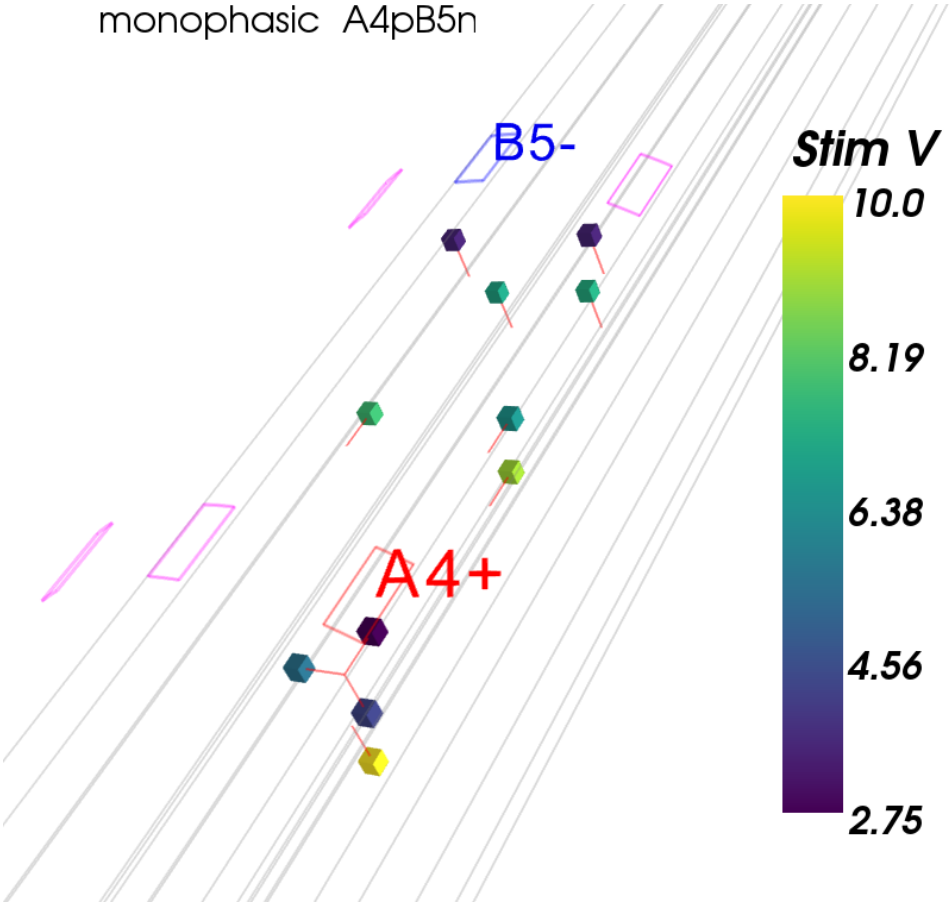

Figure 4.30: Monophasic stimulation using combination A4pB5n. Electrode A4 has a positive phase and is labeled red. Electrode B5 has a negative phase and is labeled blue. All other electrodes are floating and labeled purple. Soma, AH, IS, and AP are displayed as red lines for those neurons whose axon tip membrane voltage exceeds −10 mV with no more than 10 V of stimulation. Dendrites are not displayed. The color of the cube at each axon tip indicates stimulation voltages required for axon tip to reach $V_m > -10$ mV. List of location, axon direction, and threshold: (GM1_R_r5, Yp, 3.5 V), (GM1_L_r5, Yp, 3.5 V), (GM3_R_r5, Yp, 7.0 V), (GM3_L_r5, Yp, 7.25 V), (GM1_L_r4, Xp, 5.5 V), (GM1_L_r4, Yn, 4.25 V), (GM3_L_r4, Yn, 10.0 V), (GM1_L_r4, Zp, −1.0 V), (GM1_L_r4and5, Zp, 6.5 V), (GM1_R_r4and5, Zp, 7.75 V), and (GM3_L_r4and5, Zp, 9.0 V).

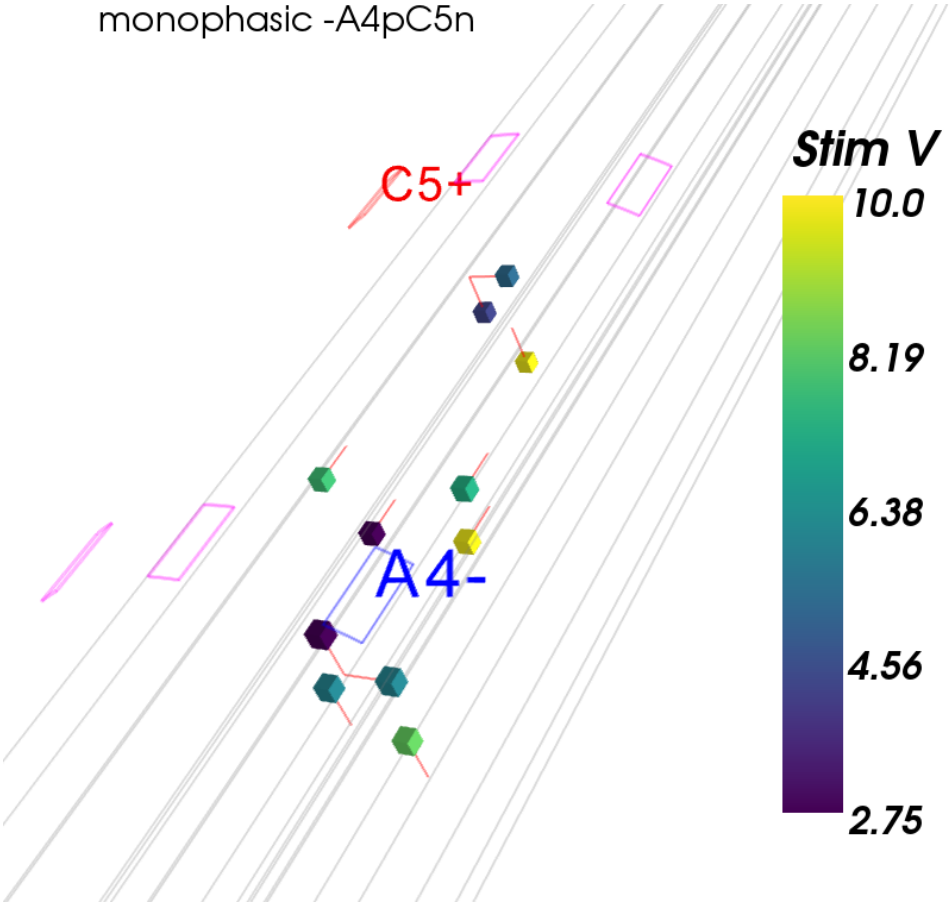

Figure 4.31: Monophasic stimulation using combination -A4pC5n. Electrode C5 has a positive phase and is labeled red. Electrode A4 has a negative phase and is labeled blue. All other electrodes are floating and labeled purple. Soma, AH, IS, and AP are displayed as red lines for those neurons whose axon tip membrane voltage exceeds -10 mV with no more than 10 V of stimulation. Dendrites are not displayed. The color of the cube at each axon tip indicates stimulation voltages required for axon tip to reach $V_m > -10$ mV. List of location, axon direction, and threshold: (GM1_L_r4and5, Zn, 7.25 V), (GM3_L_r4and5, Zn, 9.75 V), (GM1_R_r4and5, Zn, 7.75 V), (GM3_R_r4and5, Zn, -1.0 V), (GM1_L_r4, Yp, 2.75 V), (GM3_L_r4, Yp, 6.0 V), (GM2_L_r4, Yp, 8.25 V), (GM1_L_r4, Xn, 6.0 V), (GM1_R_r5, Xn, 5.25 V), (GM1_R_r5, Yn, 4.25 V), and (GM3_R_r5, Yn, 9.75 V).

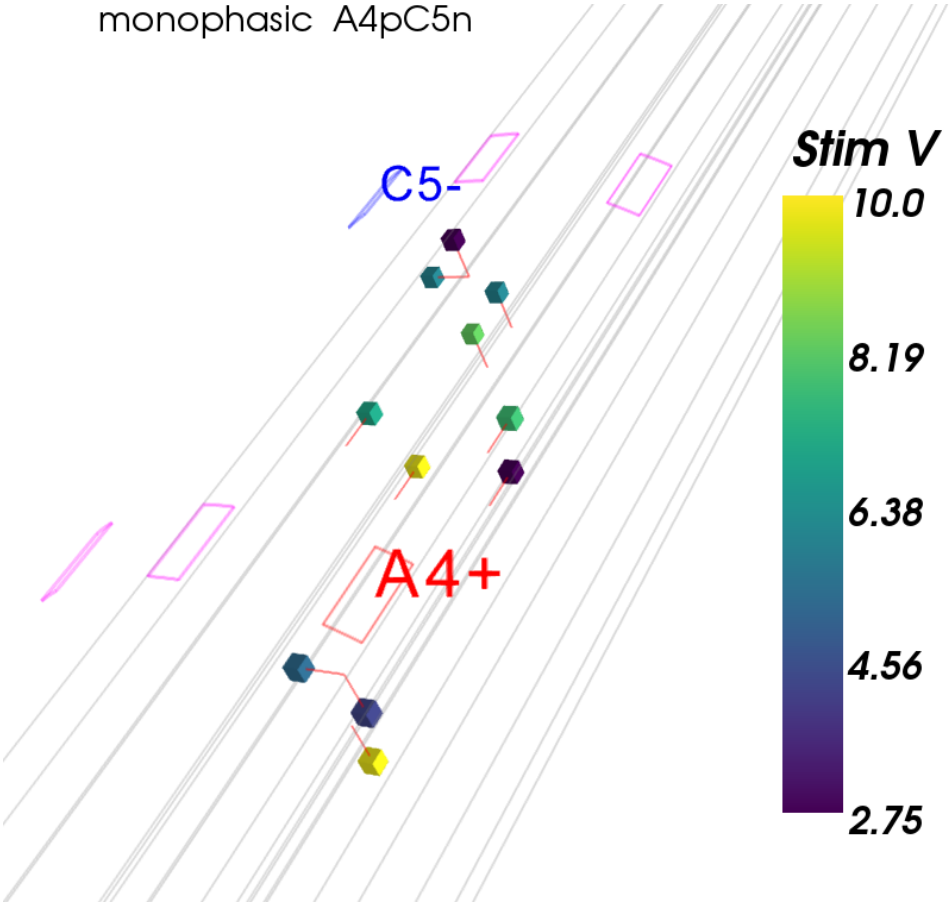

Figure 4.32: Monophasic stimulation using combination A4pC5n. Electrode A4 has a positive phase and is labeled red. Electrode C5 has a negative phase and is labeled blue. All other electrodes are floating and labeled purple. Soma, AH, IS, and AP are displayed as red lines for those neurons whose axon tip membrane voltage exceeds −10 mV with no more than 10 V of stimulation. Dendrites are not displayed. The color of the cube at each axon tip indicates stimulation voltages required for axon tip to reach $V_m > -10$ mV. List of location, axon direction, and threshold: (GM1_R_r5, Yp, 2.75 V), (GM3_R_r5, Yp, 6.0 V), (GM2_R_r5, Yp, 8.25 V), (GM1_L_r4, Xp, 5.25 V), (GM1_R_r5, Xp, 6.0 V), (GM1_L_r4, Yn, 4.25 V), (GM3_L_r4, Yn, 9.75 V), (GM1_L_r4and5, Zp, 7.75 V), (GM3_L_r4and5, Zp, −1.0 V), (GM1_R_r4and5, Zp, 7.0 V), and (GM3_R_r4and5, Zp, 9.75 V).

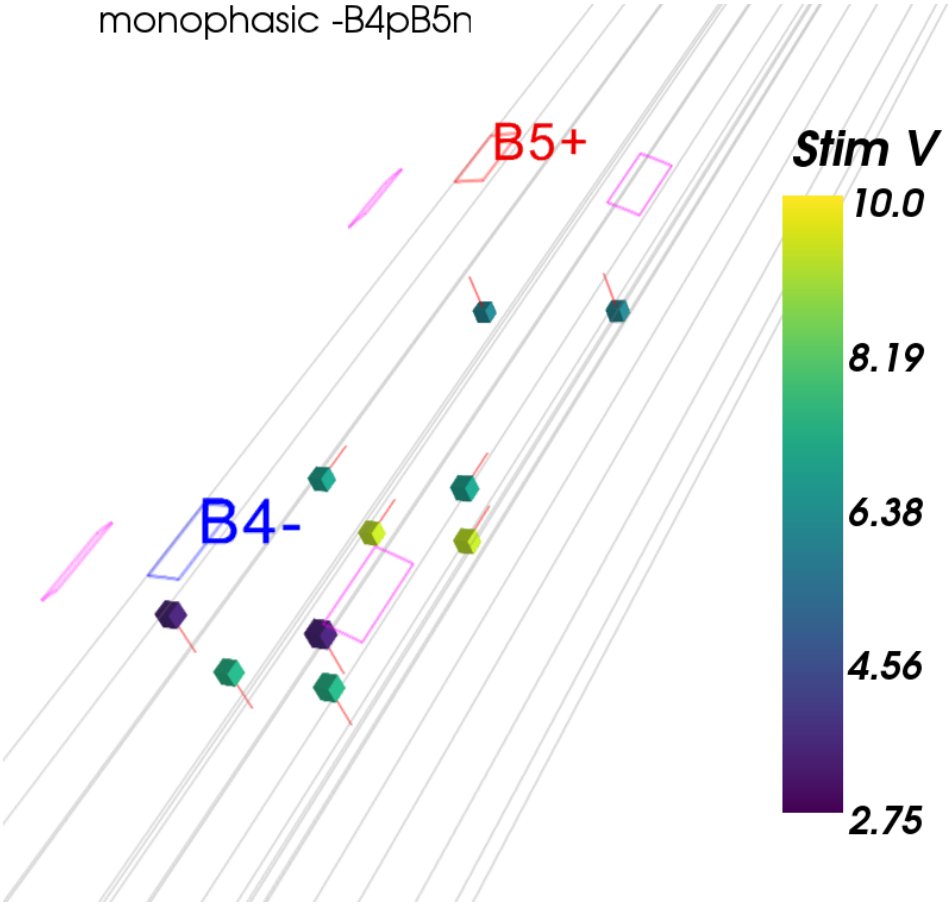

Figure 4.33: Monophasic stimulation using combination -B4pB5n. Electrode B5 has a positive phase and is labeled red. Electrode B4 has a negative phase and is labeled blue. All other electrodes are floating and labeled purple. Soma, AH, IS, and AP are displayed as red lines for those neurons whose axon tip membrane voltage exceeds $-10\,\text{mV}$ with no more than $10\,\text{V}$ of stimulation. Dendrites are not displayed. The color of the cube at each axon tip indicates stimulation voltages required for axon tip to reach $V_m > -10\,\text{mV}$. List of location, axon direction, and threshold: (GM1_R_r4and5, Zn, 6.75 V), (GM1_L_r4and5, Zn, 6.75 V), (GM3_L_r4and5, Zn, 9.25 V), (GM3_R_r4and5, Zn, 9.25 V), (GM1_L_r4, Yp, 3.5 V), (GM1_R_r4, Yp, 3.5 V), (GM3_R_r4, Yp, 7.25 V), (GM3_L_r4, Yp, 7.25 V), (GM1_L_r5, Yn, 6.0 V), and (GM1_R_r5, Yn, 6.0 V).

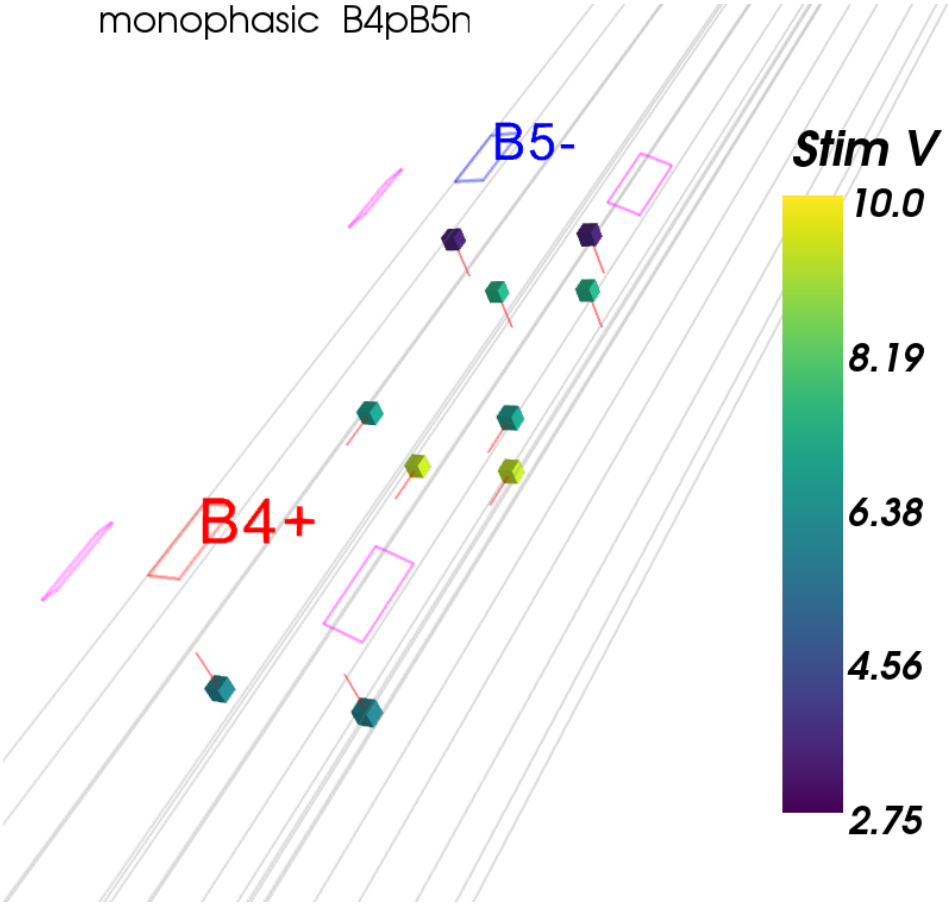

Figure 4.34: Monophasic stimulation using combination B4pB5n. Electrode B4 has a positive phase and is labeled red. Electrode B5 has a negative phase and is labeled blue. All other electrodes are floating and labeled purple. Soma, AH, IS, and AP are displayed as red lines for those neurons whose axon tip membrane voltage exceeds −10 mV with no more than 10 V of stimulation. Dendrites are not displayed. The color of the cube at each axon tip indicates stimulation voltages required for axon tip to reach $V_m > -10$ mV. List of location, axon direction, and threshold: (GM1_L_r5, Yp, 3.5 V), (GM1_R_r5, Yp, 3.5 V), (GM3_L_r5, Yp, 7.25 V), (GM3_R_r5, Yp, 7.25 V), (GM1_L_r4, Yn, 6.0 V), (GM1_R_r4, Yn, 6.0 V), (GM1_R_r4and5, Zp, 6.75 V), (GM1_L_r4and5, Zp, 6.75 V), (GM3_L_r4and5, Zp, 9.25 V), and (GM3_R_r4and5, Zp, 9.25 V).

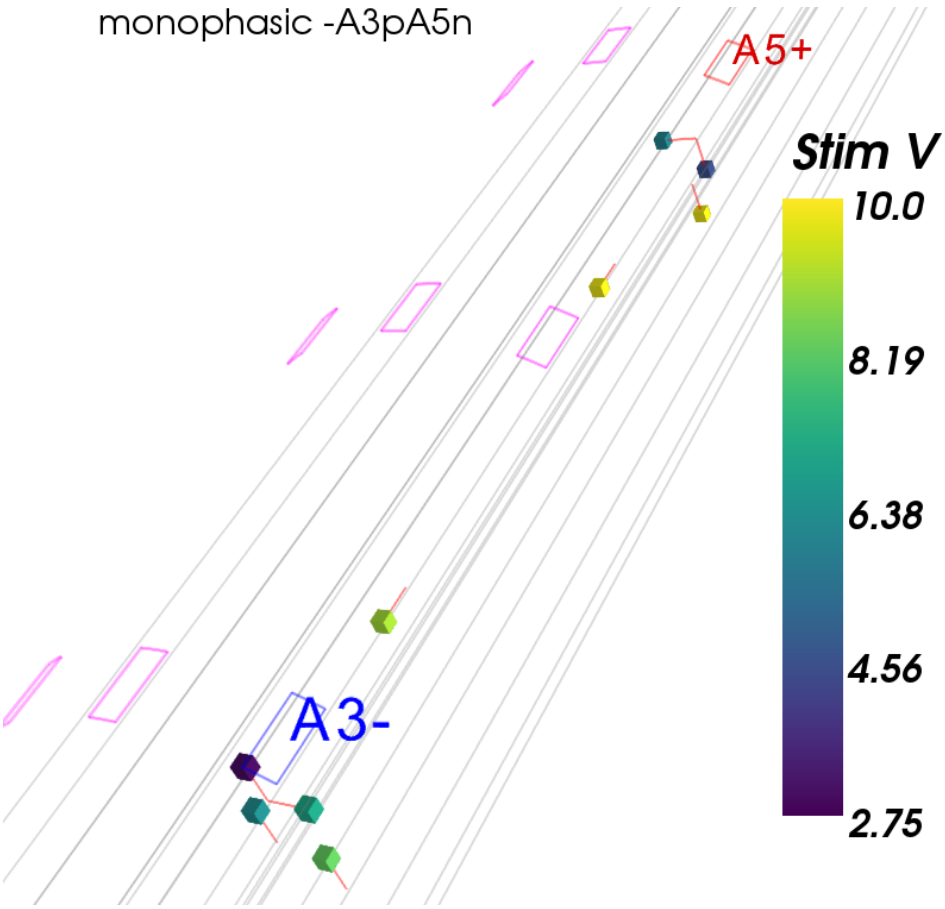

Figure 4.35: Monophasic stimulation using combination -A3pA5n. Electrode A5 has a positive phase and is labeled red. Electrode A3 has a negative phase and is labeled blue. All other electrodes are floating and labeled purple. Soma, AH, IS, and AP are displayed as red lines for those neurons whose axon tip membrane voltage exceeds $-10\,\text{mV}$ with no more than $10\,\text{V}$ of stimulation. Dendrites are not displayed. The color of the cube at each axon tip indicates stimulation voltages required for axon tip to reach $V_m > -10\,\text{mV}$. List of location, axon direction, and threshold: (GM1_L_r3and4, Zn, 9.0 V), (GM1_L_r4and5, Zn, 9.75 V), (GM1_L_r3, Yp, 3.0 V), (GM3_L_r3, Yp, 6.25 V), (GM2_L_r3, Yp, 8.25 V), (GM1_L_r5, Xp, 6.0 V), (GM1_L_r3, Xn, 7.0 V), (GM1_L_r5, Yn, 4.5 V), and (GM3_L_r5, Yn, 9.75 V).

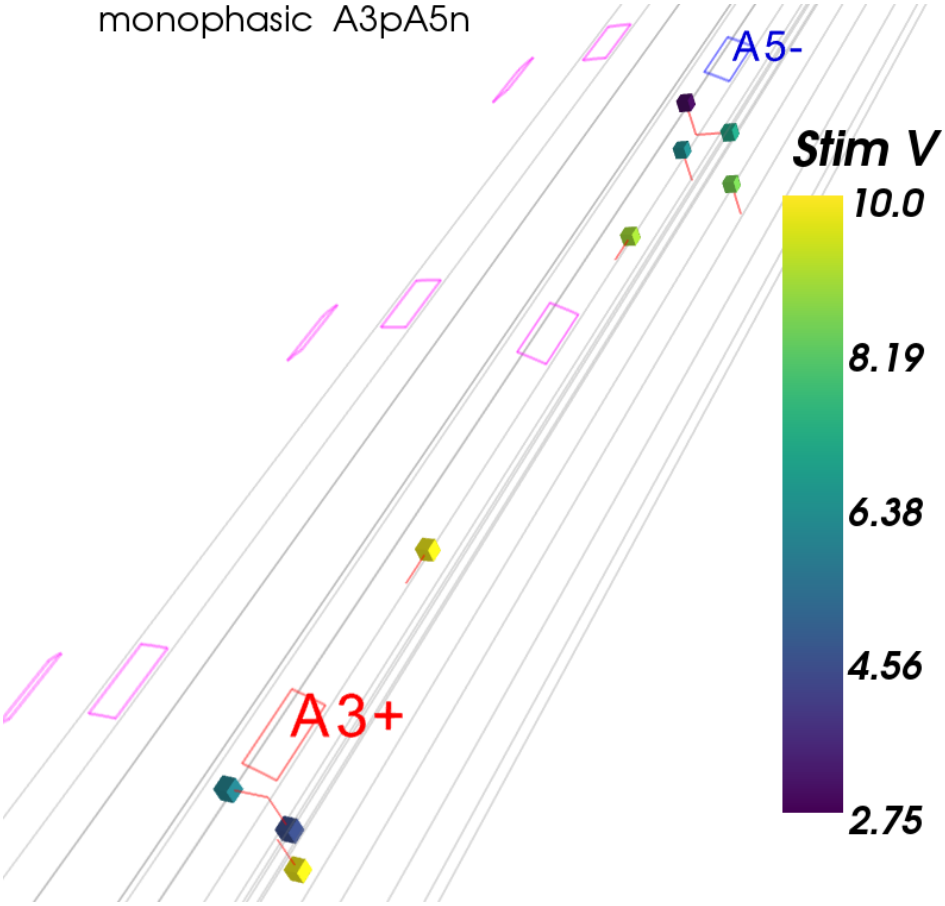

Figure 4.36: Monophasic stimulation using combination A3pA5n. Electrode A3 has a positive phase and is labeled red. Electrode A5 has a negative phase and is labeled blue. All other electrodes are floating and labeled purple. Soma, AH, IS, and AP are displayed as red lines for those neurons whose axon tip membrane voltage exceeds −10 mV with no more than 10 V of stimulation. Dendrites are not displayed. The color of the cube at each axon tip indicates stimulation voltages required for axon tip to reach $V_m > -10$ mV. List of location, axon direction, and threshold: (GM1_L_r5, Yp, 3.0 V), (GM3_L_r5, Yp, 6.25 V), (GM2_L_r5, Yp, 8.5 V), (GM1_L_r3, Xp, 6.0 V), (GM1_L_r5, Xn, 7.0 V), (GM1_L_r3, Yn, 4.5 V), (GM3_L_r3, Yn, 9.75 V), (GM1_L_r3and4, Zp, 9.75 V), and (GM1_L_r4and5, Zp, 9.0 V).

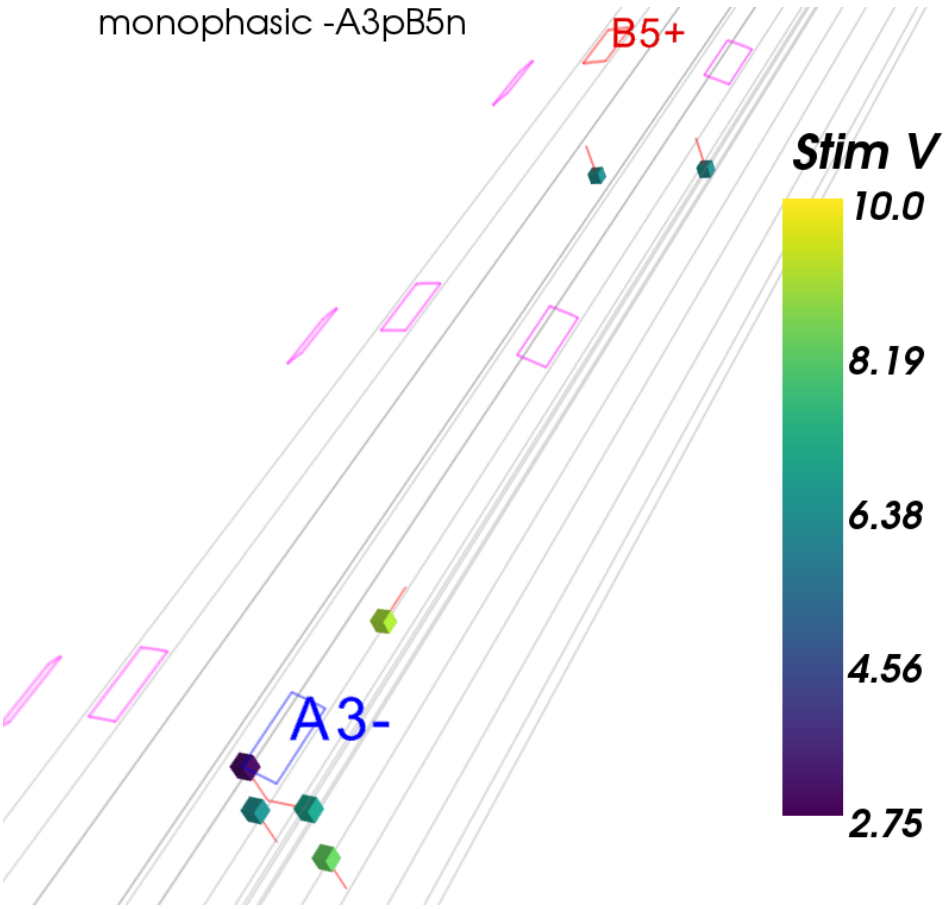

Figure 4.37: Monophasic stimulation using combination -A3pB5n. Electrode B5 has a positive phase and is labeled red. Electrode A3 has a negative phase and is labeled blue. All other electrodes are floating and labeled purple. Soma, AH, IS, and AP are displayed as red lines for those neurons whose axon tip membrane voltage exceeds -10 mV with no more than 10 V of stimulation. Dendrites are not displayed. The color of the cube at each axon tip indicates stimulation voltages required for axon tip to reach $V_m > -10$ mV. List of location, axon direction, and threshold: (GM1_L_r3and4, Zn, 9.0 V), (GM1_L_r3, Yp, 3.0 V), (GM3_L_r3, Yp, 6.25 V), (GM2_L_r3, Yp, 8.25 V), (GM1_L_r3, Xn, 6.75 V), (GM1_R_r5, Yn, 6.25 V), and (GM1_L_r5, Yn, 6.25 V).

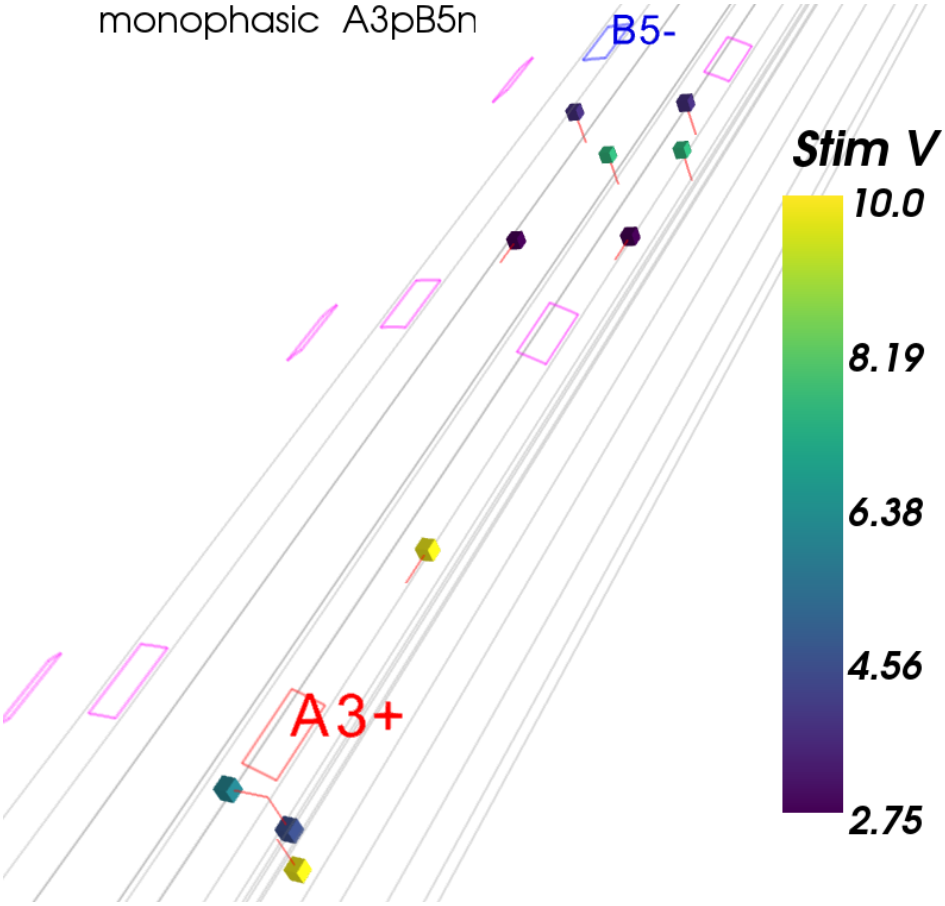

Figure 4.38: Monophasic stimulation using combination A3pB5n. Electrode A3 has a positive phase and is labeled red. Electrode B5 has a negative phase and is labeled blue. All other electrodes are floating and labeled purple. Soma, AH, IS, and AP are displayed as red lines for those neurons whose axon tip membrane voltage exceeds −10 mV with no more than 10 V of stimulation. Dendrites are not displayed. The color of the cube at each axon tip indicates stimulation voltages required for axon tip to reach $V_m > -10$ mV. List of location, axon direction, and threshold: (GM1_R_r5, Yp, 3.75 V), (GM1_L_r5, Yp, 3.75 V), (GM3_R_r5, Yp, 7.5 V), (GM3_L_r5, Yp, 7.5 V), (GM1_L_r3, Xp, 6.0 V), (GM1_L_r3, Yn, 4.5 V), (GM3_L_r3, Yn, 9.75 V), (GM1_L_r3and4, Zp, 9.75 V), (GM1_R_r4and5, Zp, −1.0 V), and (GM1_L_r4and5, Zp, −1.0 V).

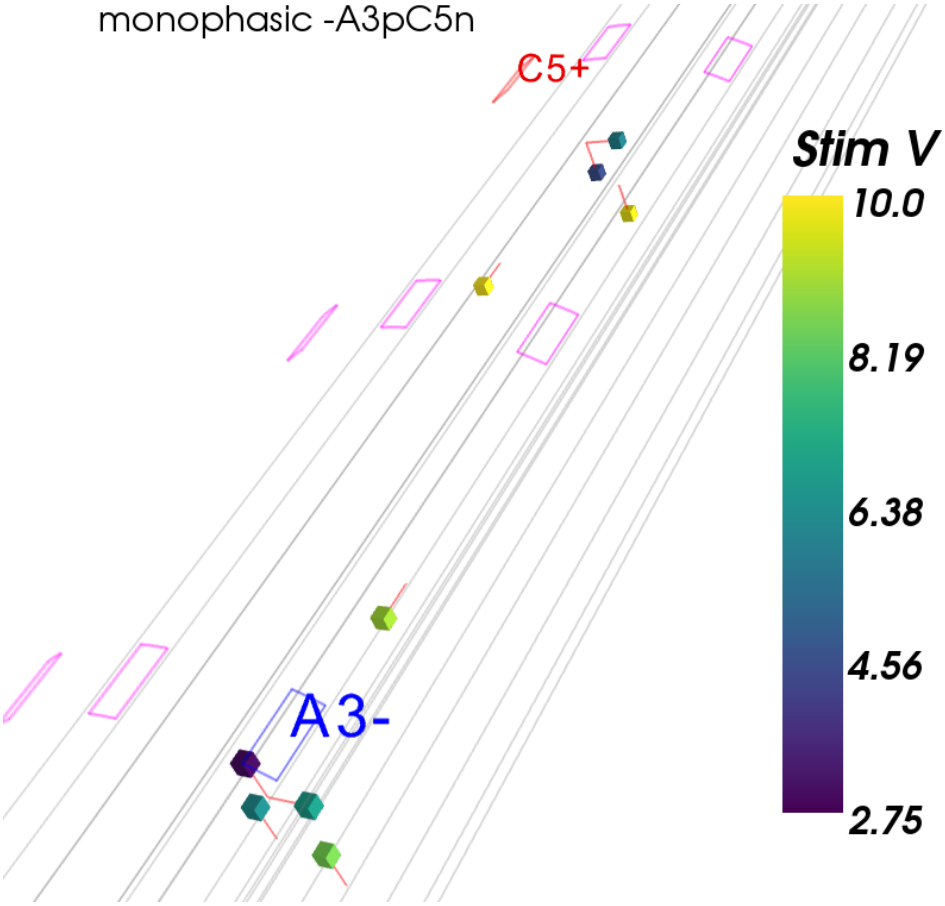

Figure 4.39: Monophasic stimulation using combination -A3pC5n. Electrode C5 has a positive phase and is labeled red. Electrode A3 has a negative phase and is labeled blue. All other electrodes are floating and labeled purple. Soma, AH, IS, and AP are displayed as red lines for those neurons whose axon tip membrane voltage exceeds −10 mV with no more than 10 V of stimulation. Dendrites are not displayed. The color of the cube at each axon tip indicates stimulation voltages required for axon tip to reach $V_m > -10$ mV. List of location, axon direction, and threshold: (GM1_L_r3and4, Zn, 9.0 V), (GM1_R_r4and5, Zn, 10.0 V), (GM1_L_r3, Yp, 3.0 V), (GM3_L_r3, Yp, 6.25 V), (GM2_L_r3, Yp, 8.5 V), (GM1_L_r3, Xn, 6.75 V), (GM1_R_r5, Xn, 6.0 V), (GM1_R_r5, Yn, 4.5 V), and (GM3_R_r5, Yn, 9.75 V).

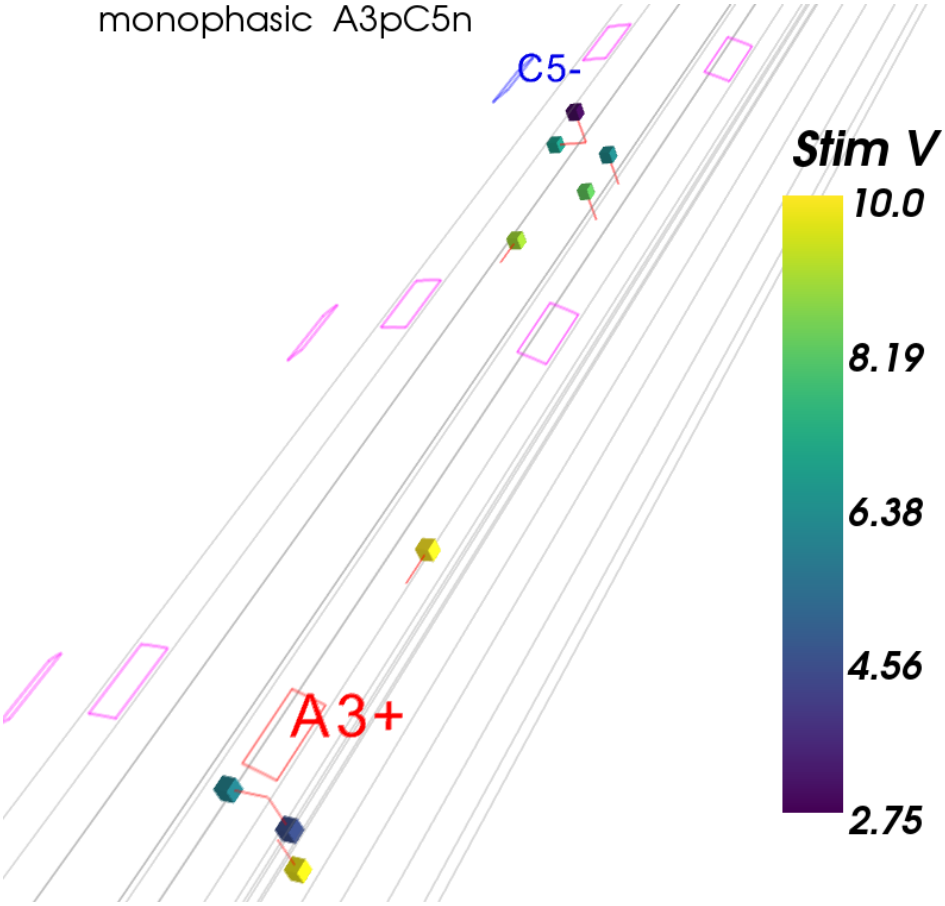

Figure 4.40: Monophasic stimulation using combination A3pC5n. Electrode A3 has a positive phase and is labeled red. Electrode C5 has a negative phase and is labeled blue. All other electrodes are floating and labeled purple. Soma, AH, IS, and AP are displayed as red lines for those neurons whose axon tip membrane voltage exceeds $-10\,\text{mV}$ with no more than $10\,\text{V}$ of stimulation. Dendrites are not displayed. The color of the cube at each axon tip indicates stimulation voltages required for axon tip to reach $V_m > -10\,\text{mV}$. List of location, axon direction, and threshold: (GM1_R_r5, Yp, 3.0 V), (GM3_R_r5, Yp, 6.25 V), (GM2_R_r5, Yp, 8.25 V), (GM1_L_r3, Xp, 6.0 V), (GM1_R_r5, Xp, 6.75 V), (GM1_L_r3, Yn, 4.5 V), (GM3_L_r3, Yn, 9.75 V), (GM1_L_r3and4, Zp, 10.0 V), and (GM1_R_r4and5, Zp, 9.0 V).

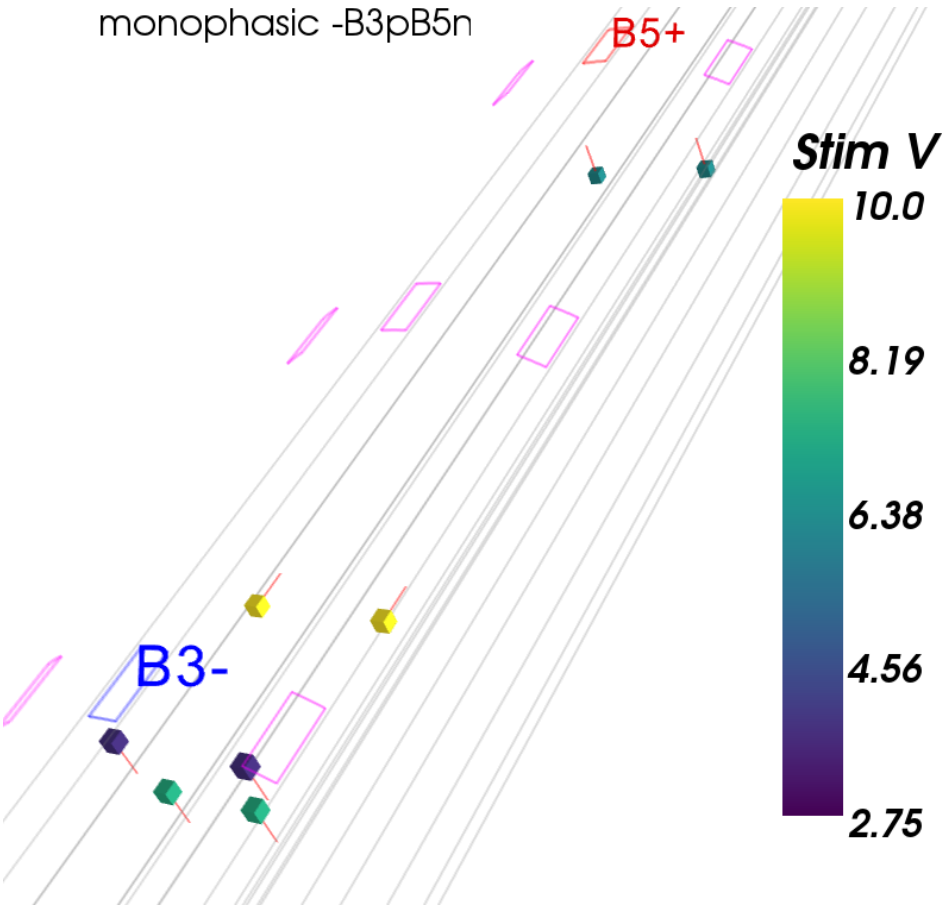

Figure 4.41: Monophasic stimulation using combination -B3pB5n. Electrode B5 has a positive phase and is labeled red. Electrode B3 has a negative phase and is labeled blue. All other electrodes are floating and labeled purple. Soma, AH, IS, and AP are displayed as red lines for those neurons whose axon tip membrane voltage exceeds $-10\,\text{mV}$ with no more than $10\,\text{V}$ of stimulation. Dendrites are not displayed. The color of the cube at each axon tip indicates stimulation voltages required for axon tip to reach $V_m > -10\,\text{mV}$. List of location, axon direction, and threshold: (GM1_L_r3and4, Zn, 10.0 V), (GM1_R_r3and4, Zn, 10.0 V), (GM1_L_r3, Yp, 3.75 V), (GM1_R_r3, Yp, 3.75 V), (GM3_L_r3, Yp, 7.25 V), (GM3_R_r3, Yp, 7.25 V), (GM1_L_r5, Yn, 6.25 V), and (GM1_R_r5, Yn, 6.25 V).

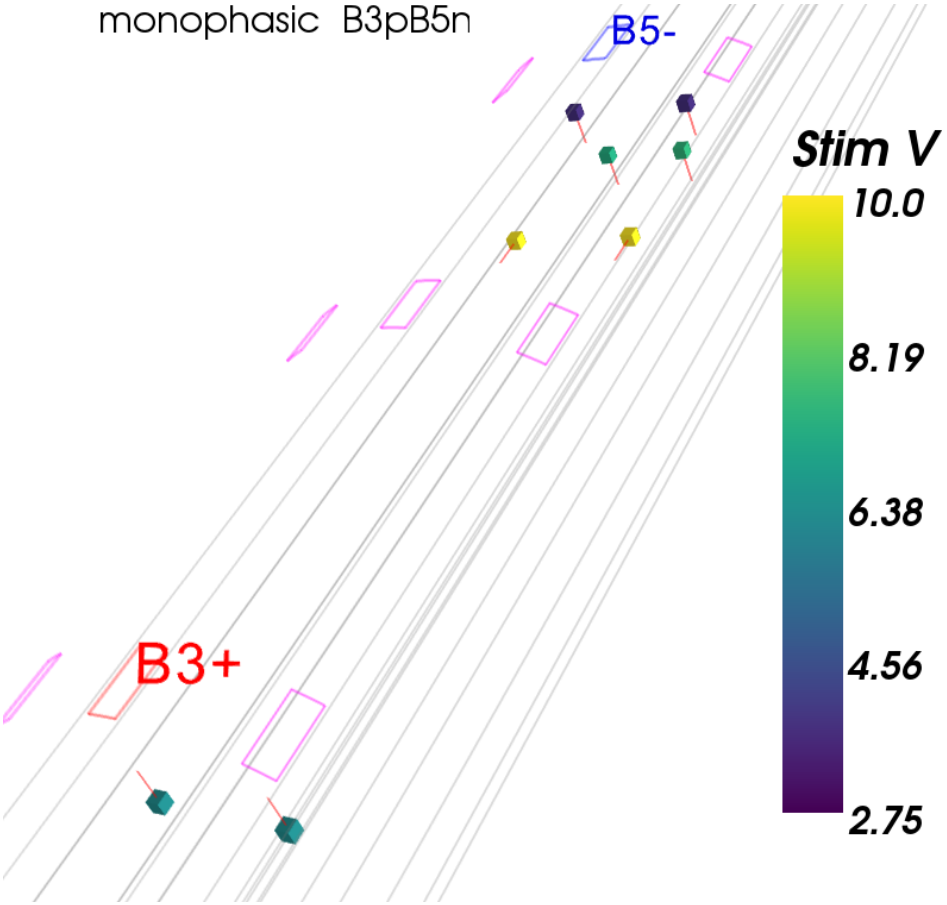

Figure 4.42: Monophasic stimulation using combination B3pB5n. Electrode B3 has a positive phase and is labeled red. Electrode B5 has a negative phase and is labeled blue. All other electrodes are floating and labeled purple. Soma, AH, IS, and AP are displayed as red lines for those neurons whose axon tip membrane voltage exceeds −10 mV with no more than 10 V of stimulation. Dendrites are not displayed. The color of the cube at each axon tip indicates stimulation voltages required for axon tip to reach $V_m > -10$ mV. List of location, axon direction, and threshold: (GM1_L_r5, Yp, 3.75 V), (GM1_R_r5, Yp, 3.75 V), (GM3_L_r5, Yp, 7.5 V), (GM3_R_r5, Yp, 7.25 V), (GM1_L_r3, Yn, 6.25 V), (GM1_R_r3, Yn, 6.25 V), (GM1_L_r4and5, Zp, 10.0 V), and (GM1_R_r4and5, Zp, 10.0 V).

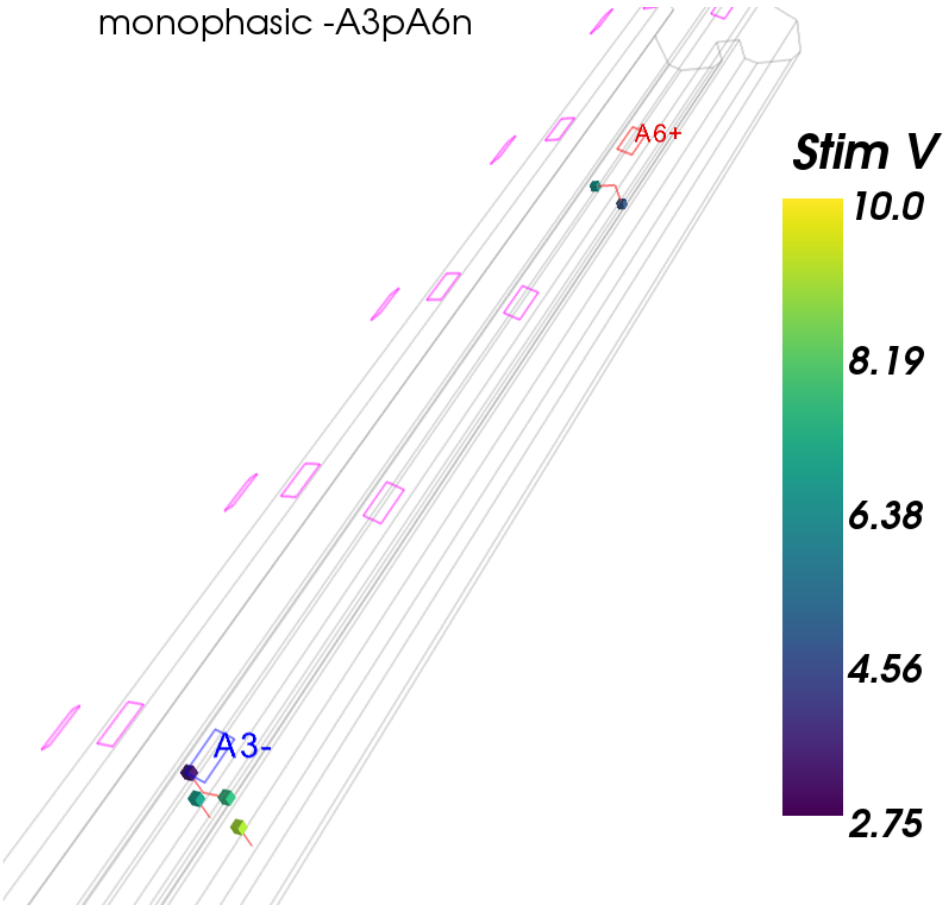

Figure 4.43: Monophasic stimulation using combination -A3pA6n. Electrode A6 has a positive phase and is labeled red. Electrode A3 has a negative phase and is labeled blue. All other electrodes are floating and labeled purple. Soma, AH, IS, and AP are displayed as red lines for those neurons whose axon tip membrane voltage exceeds −10 mV with no more than 10 V of stimulation. Dendrites are not displayed. The color of the cube at each axon tip indicates stimulation voltages required for axon tip to reach $V_m > -10$ mV. List of location, axon direction, and threshold: (GM1_L_r3, Yp, 3.25 V), (GM3_L_r3, Yp, 6.75 V), (GM2_L_r3, Yp, 9.0 V), (GM1_L_r6, Xp, 6.5 V), (GM1_L_r3, Xn, 7.5 V), and (GM1_L_r6, Yn, 4.75 V).

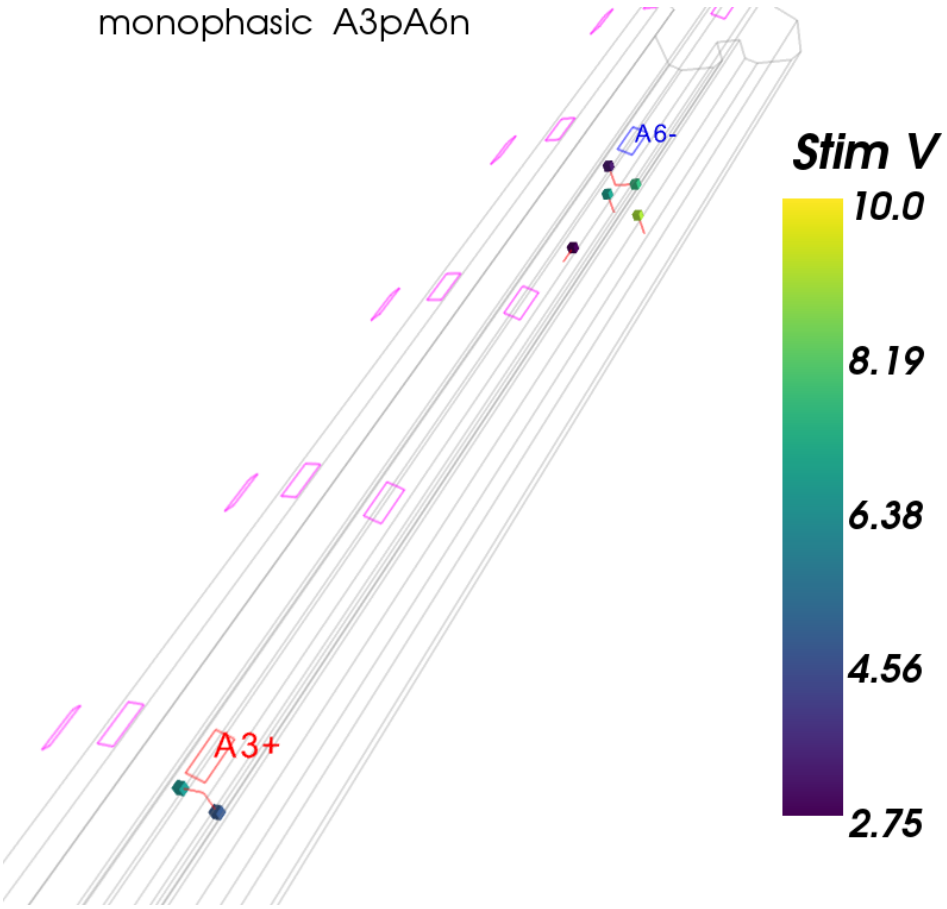

Figure 4.44: Monophasic stimulation using combination A3pA6n. Electrode A3 has a positive phase and is labeled red. Electrode A6 has a negative phase and is labeled blue. All other electrodes are floating and labeled purple. Soma, AH, IS, and AP are displayed as red lines for those neurons whose axon tip membrane voltage exceeds −10 mV with no more than 10 V of stimulation. Dendrites are not displayed. The color of the cube at each axon tip indicates stimulation voltages required for axon tip to reach $V_m > -10$ mV. List of location, axon direction, and threshold: (GM1_L_r6, Yp, 3.25 V), (GM3_L_r6, Yp, 6.75 V), (GM2_L_r6, Yp, 9.0 V), (GM1_L_r3, Xp, 6.5 V), (GM1_L_r6, Xn, 7.5 V), (GM1_L_r3, Yn, 4.75 V), and (GM1_L_r5and6, Zp, −1.0 V).

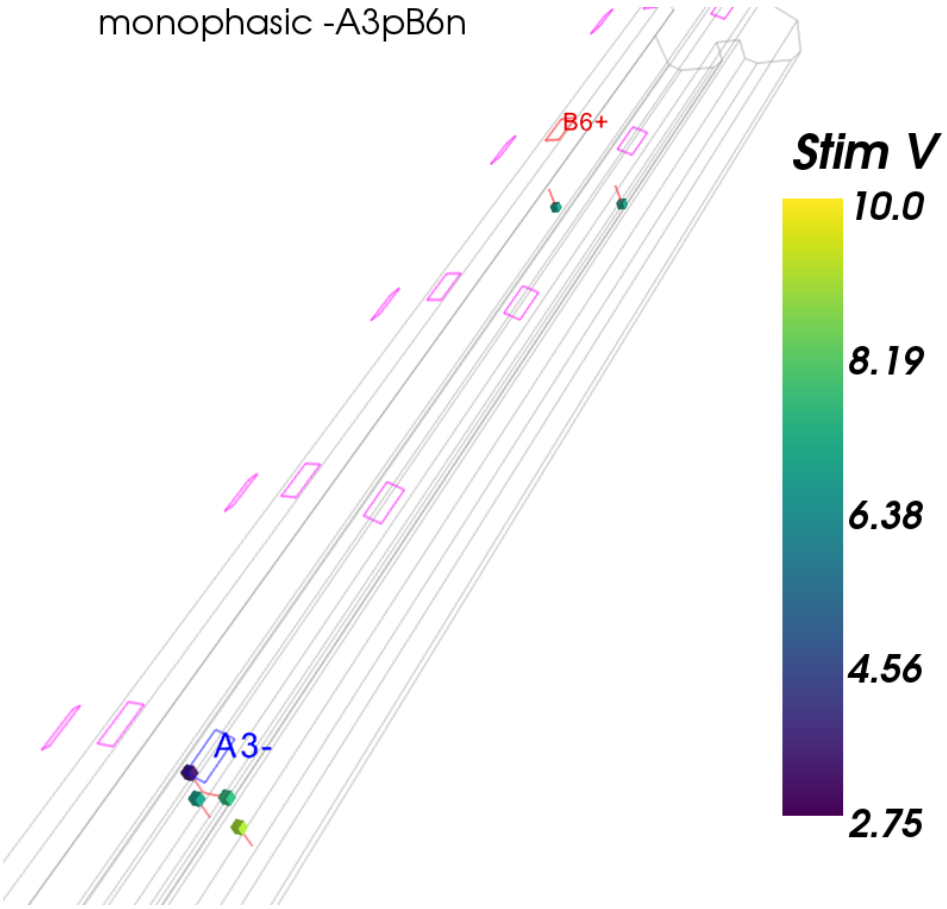

Figure 4.45: Monophasic stimulation using combination -A3pB6n. Electrode B6 has a positive phase and is labeled red. Electrode A3 has a negative phase and is labeled blue. All other electrodes are floating and labeled purple. Soma, AH, IS, and AP are displayed as red lines for those neurons whose axon tip membrane voltage exceeds −10 mV with no more than 10 V of stimulation. Dendrites are not displayed. The color of the cube at each axon tip indicates stimulation voltages required for axon tip to reach $V_m > -10$ mV. List of location, axon direction, and threshold: (GM1_L_r3, Yp, 3.25 V), (GM3_L_r3, Yp, 6.75 V), (GM2_L_r3, Yp, 9.0 V), (GM1_L_r3, Xn, 7.5 V), (GM1_R_r6, Yn, 6.75 V), and (GM1_L_r6, Yn, 6.75 V).

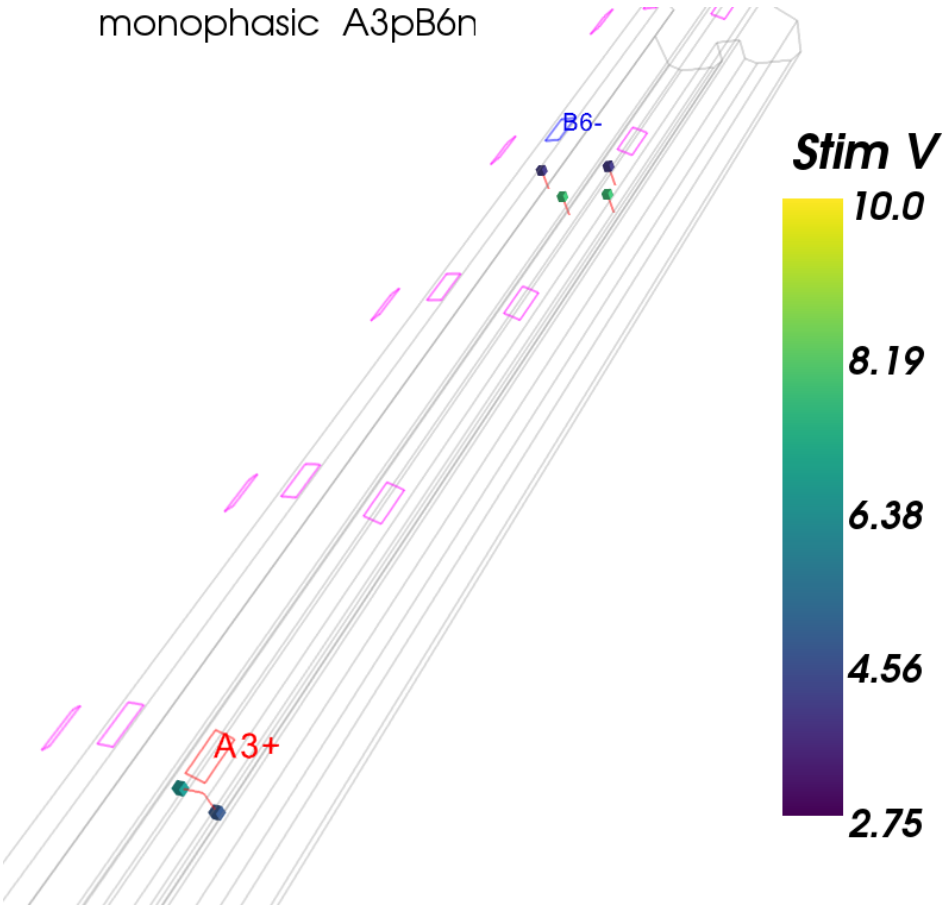

Figure 4.46: Monophasic stimulation using combination A3pB6n. Electrode A3 has a positive phase and is labeled red. Electrode B6 has a negative phase and is labeled blue. All other electrodes are floating and labeled purple. Soma, AH, IS, and AP are displayed as red lines for those neurons whose axon tip membrane voltage exceeds −10 mV with no more than 10 V of stimulation. Dendrites are not displayed. The color of the cube at each axon tip indicates stimulation voltages required for axon tip to reach $V_m > -10$ mV. List of location, axon direction, and threshold: (GM1_R_r6, Yp, 4.0 V), (GM1_L_r6, Yp, 4.0 V), (GM3_L_r6, Yp, 7.75 V), (GM3_R_r6, Yp, 7.75 V), (GM1_L_r3, Xp, 6.5 V), and (GM1_L_r3, Yn, 4.75 V).

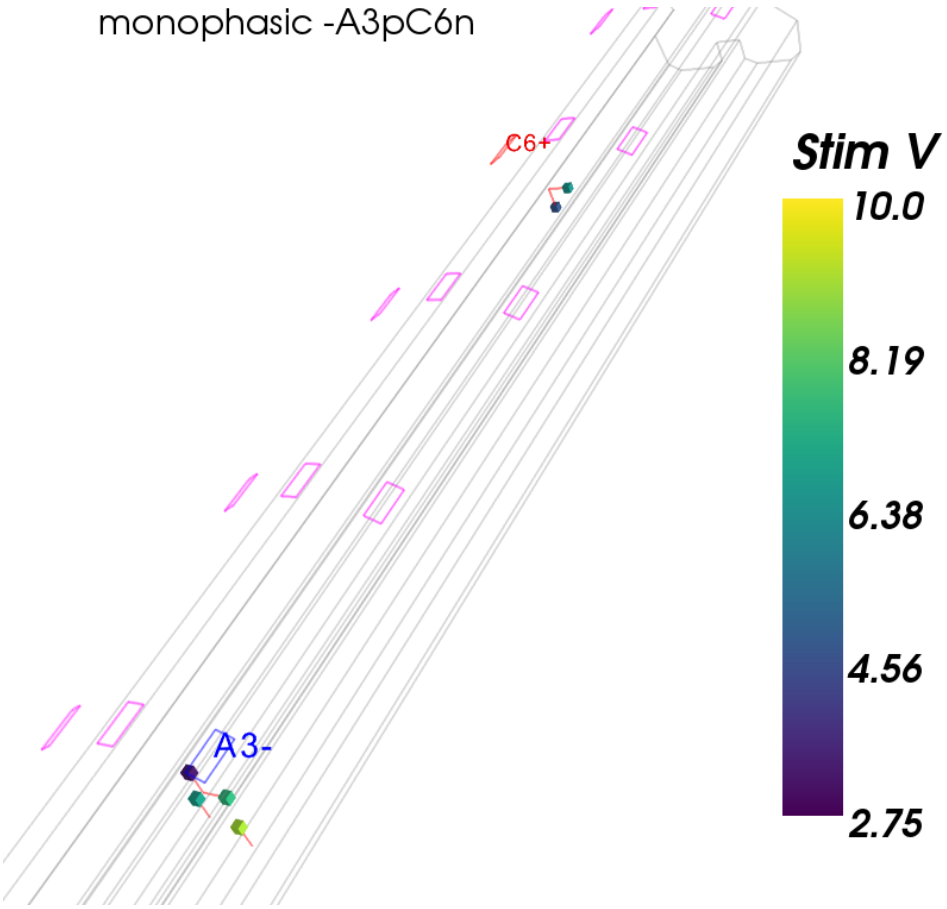

Figure 4.47: Monophasic stimulation using combination -A3pC6n. Electrode C6 has a positive phase and is labeled red. Electrode A3 has a negative phase and is labeled blue. All other electrodes are floating and labeled purple. Soma, AH, IS, and AP are displayed as red lines for those neurons whose axon tip membrane voltage exceeds −10 mV with no more than 10 V of stimulation. Dendrites are not displayed. The color of the cube at each axon tip indicates stimulation voltages required for axon tip to reach $V_m > -10$ mV. List of location, axon direction, and threshold: (GM1_L_r3, Yp, 3.25 V), (GM3_L_r3, Yp, 6.75 V), (GM2_L_r3, Yp, 9.0 V), (GM1_L_r3, Xn, 7.5 V), (GM1_R_r6, Xn, 6.5 V), and (GM1_R_r6, Yn, 4.75 V).

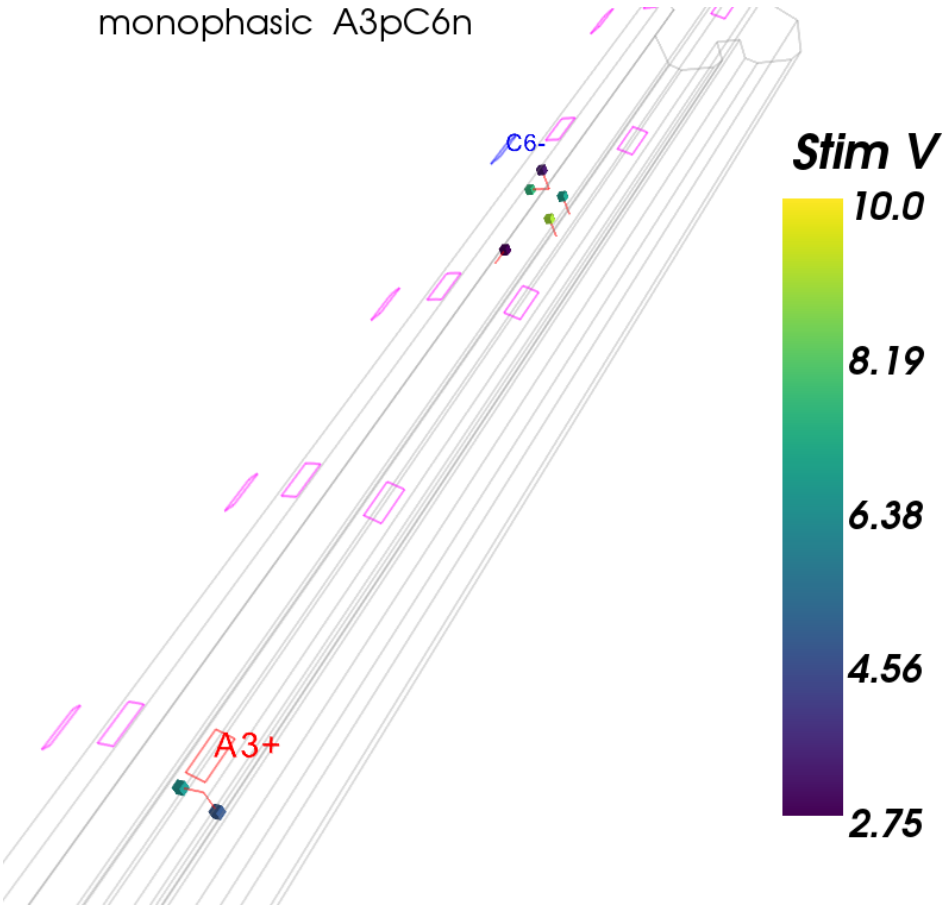

Figure 4.48: Monophasic stimulation using combination A3pC6n. Electrode A3 has a positive phase and is labeled red. Electrode C6 has a negative phase and is labeled blue. All other electrodes are floating and labeled purple. Soma, AH, IS, and AP are displayed as red lines for those neurons whose axon tip membrane voltage exceeds −10 mV with no more than 10 V of stimulation. Dendrites are not displayed. The color of the cube at each axon tip indicates stimulation voltages required for axon tip to reach $V_m > -10$ mV. List of location, axon direction, and threshold: (GM1_R_r6, Yp, 3.25 V), (GM3_R_r6, Yp, 6.75 V), (GM2_R_r6, Yp, 9.0 V), (GM1_L_r3, Xp, 6.5 V), (GM1_R_r6, Xp, 7.5 V), (GM1_L_r3, Yn, 4.75 V), and (GM1_R_r5and6, Zp, −1.0 V).

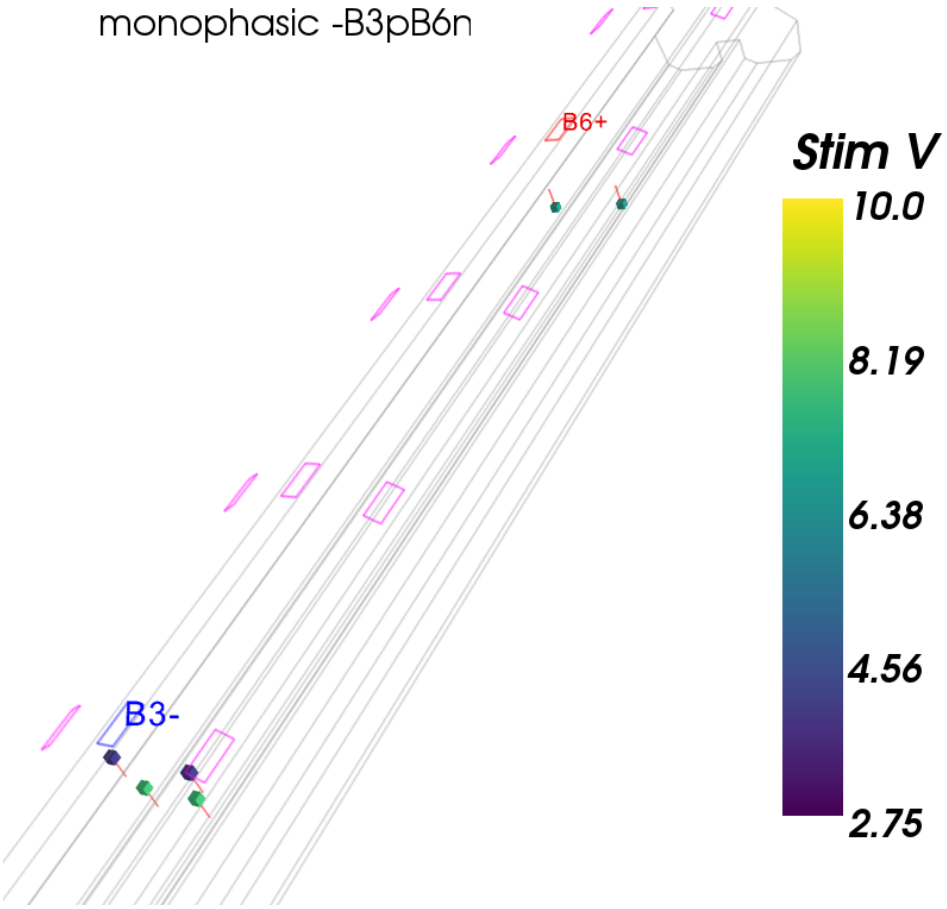

Figure 4.49: Monophasic stimulation using combination -B3pB6n. Electrode B6 has a positive phase and is labeled red. Electrode B3 has a negative phase and is labeled blue. All other electrodes are floating and labeled purple. Soma, AH, IS, and AP are displayed as red lines for those neurons whose axon tip membrane voltage exceeds −10 mV with no more than 10 V of stimulation. Dendrites are not displayed. The color of the cube at each axon tip indicates stimulation voltages required for axon tip to reach $V_m > -10$ mV. List of location, axon direction, and threshold: (GM1_L_r3, Yp, 4.0 V), (GM1_R_r3, Yp, 4.0 V), (GM3_L_r3, Yp, 7.75 V), (GM3_R_r3, Yp, 7.75 V), (GM1_L_r6, Yn, 6.75 V), and (GM1_R_r6, Yn, 6.75 V).

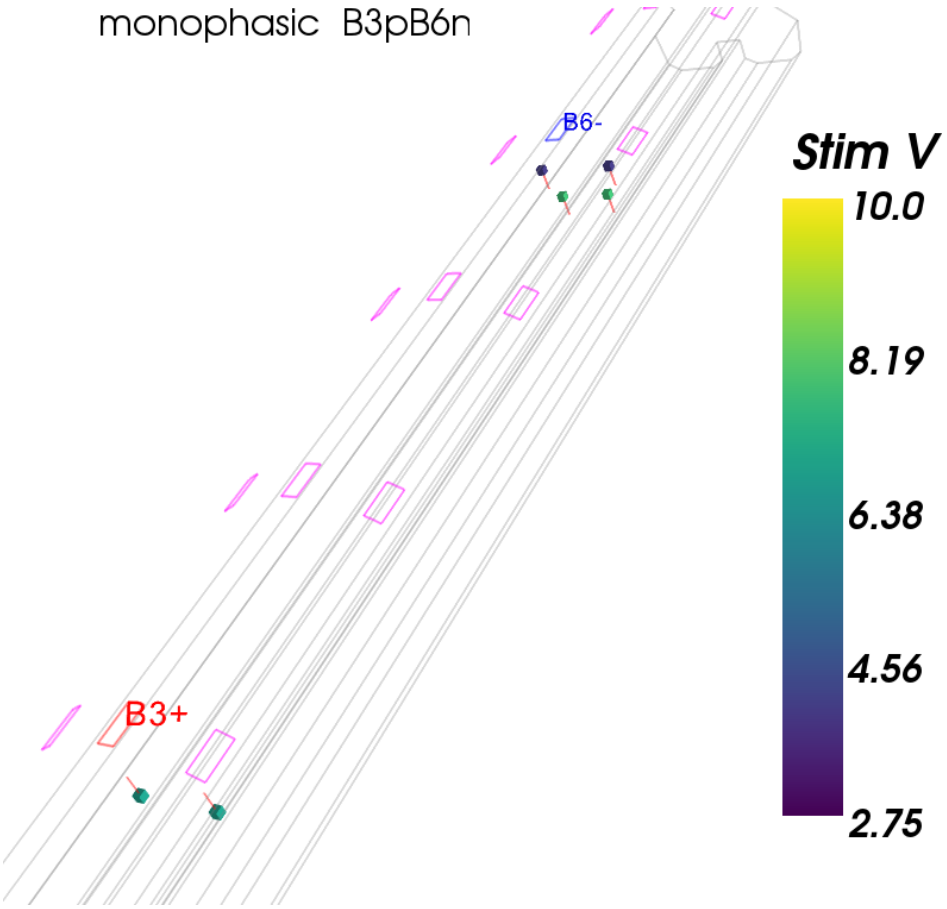

Figure 4.50: Monophasic stimulation using combination B3pB6n. Electrode B3 has a positive phase and is labeled red. Electrode B6 has a negative phase and is labeled blue. All other electrodes are floating and labeled purple. Soma, AH, IS, and AP are displayed as red lines for those neurons whose axon tip membrane voltage exceeds −10 mV with no more than 10 V of stimulation. Dendrites are not displayed. The color of the cube at each axon tip indicates stimulation voltages required for axon tip to reach $V_m > -10$ mV. List of location, axon direction, and threshold: (GM1_L_r6, Yp, 4.0 V), (GM1_R_r6, Yp, 4.0 V), (GM3_L_r6, Yp, 7.75 V), (GM3_R_r6, Yp, 7.75 V), (GM1_L_r3, Yn, 6.75 V), and (GM1_R_r3, Yn, 6.75 V).

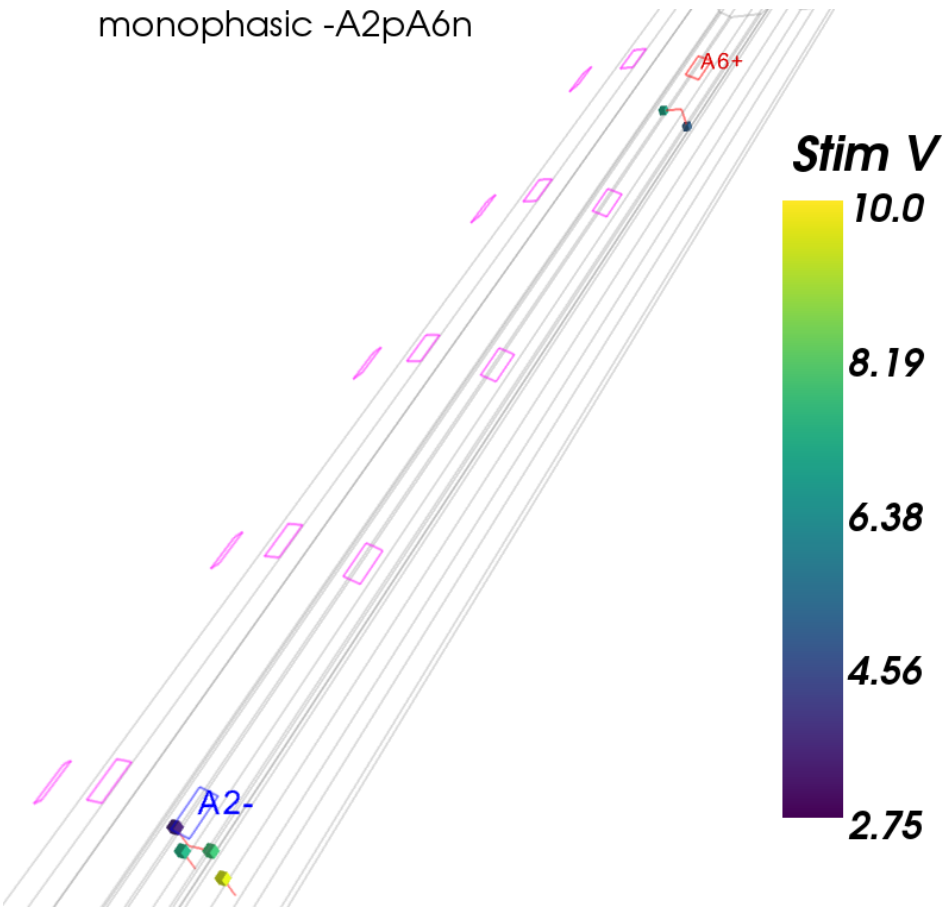

Figure 4.51: Monophasic stimulation using combination -A2pA6n. Electrode A6 has a positive phase and is labeled red. Electrode A2 has a negative phase and is labeled blue. All other electrodes are floating and labeled purple. Soma, AH, IS, and AP are displayed as red lines for those neurons whose axon tip membrane voltage exceeds −10 mV with no more than 10 V of stimulation. Dendrites are not displayed. The color of the cube at each axon tip indicates stimulation voltages required for axon tip to reach $V_m > -10$ mV. List of location, axon direction, and threshold: (GM1_L_r2, Yp, 3.5 V), (GM3_L_r2, Yp, 7.25 V), (GM2_L_r2, Yp, 9.5 V), (GM1_L_r6, Xp, 7.0 V), (GM1_L_r2, Xn, 7.75 V), and (GM1_L_r6, Yn, 5.0 V).

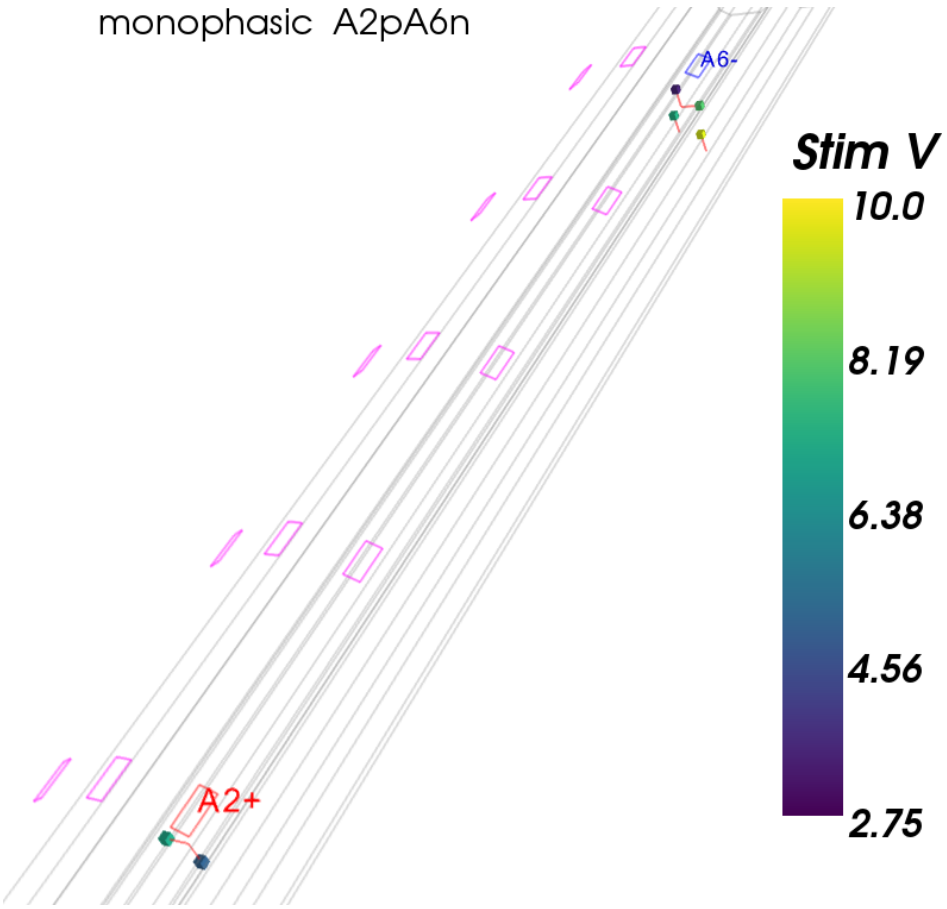

Figure 4.52: Monophasic stimulation using combination A2pA6n. Electrode A2 has a positive phase and is labeled red. Electrode A6 has a negative phase and is labeled blue. All other electrodes are floating and labeled purple. Soma, AH, IS, and AP are displayed as red lines for those neurons whose axon tip membrane voltage exceeds −10 mV with no more than 10 V of stimulation. Dendrites are not displayed. The color of the cube at each axon tip indicates stimulation voltages required for axon tip to reach $V_m > -10$ mV. List of location, axon direction, and threshold: (GM1_L_r6, Yp, 3.5 V), (GM3_L_r6, Yp, 7.25 V), (GM2_L_r6, Yp, 9.5 V), (GM1_L_r2, Xp, 7.0 V), (GM1_L_r6, Xn, 8.0 V), and (GM1_L_r2, Yn, 5.0 V).

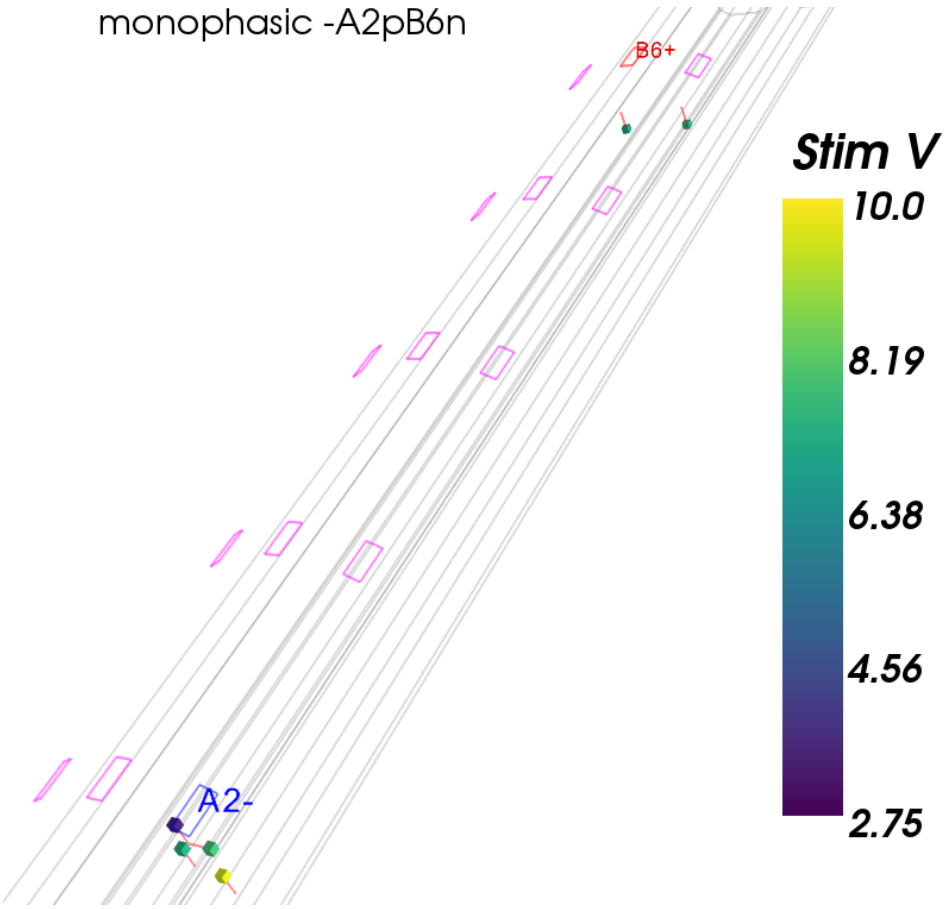

Figure 4.53: Monophasic stimulation using combination -A2pB6n. Electrode B6 has a positive phase and is labeled red. Electrode A2 has a negative phase and is labeled blue. All other electrodes are floating and labeled purple. Soma, AH, IS, and AP are displayed as red lines for those neurons whose axon tip membrane voltage exceeds −10 mV with no more than 10 V of stimulation. Dendrites are not displayed. The color of the cube at each axon tip indicates stimulation voltages required for axon tip to reach $V_m > -10$ mV. List of location, axon direction, and threshold: (GM1_L_r2, Yp, 3.5 V), (GM3_L_r2, Yp, 7.25 V), (GM2_L_r2, Yp, 9.5 V), (GM1_L_r2, Xn, 7.75 V), (GM1_L_r6, Yn, 7.25 V), and (GM1_R_r6, Yn, 7.0 V).

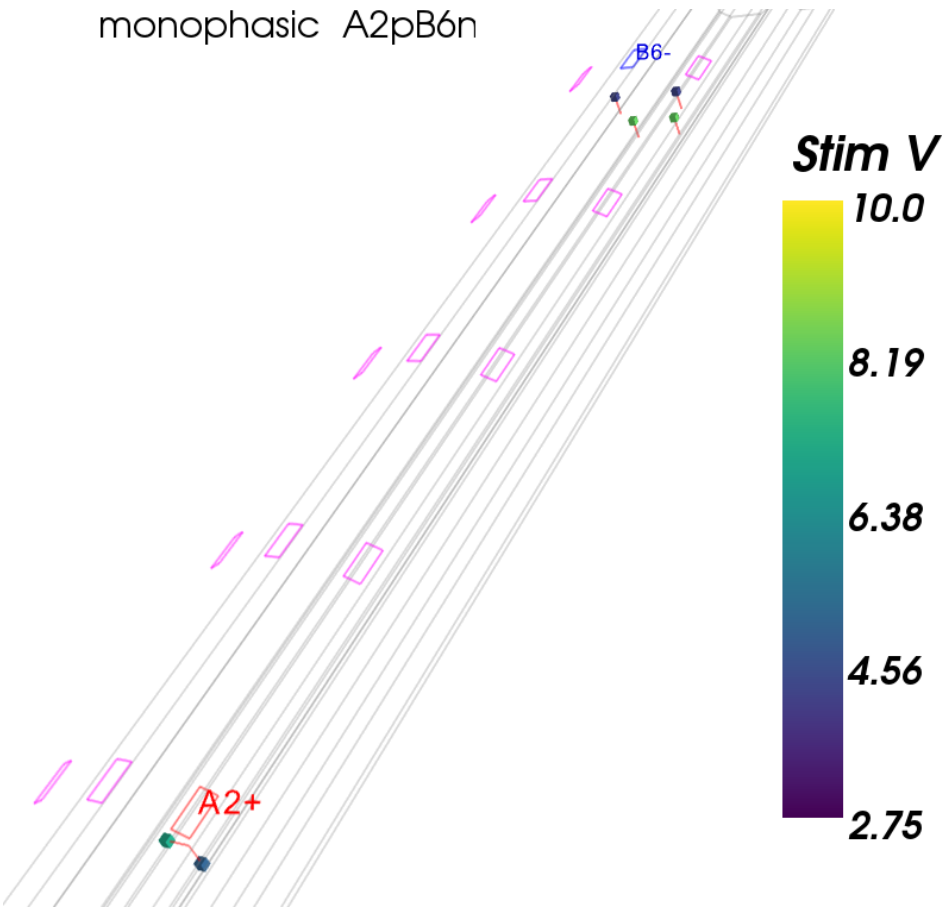

Figure 4.54: Monophasic stimulation using combination A2pB6n. Electrode A2 has a positive phase and is labeled red. Electrode B6 has a negative phase and is labeled blue. All other electrodes are floating and labeled purple. Soma, AH, IS, and AP are displayed as red lines for those neurons whose axon tip membrane voltage exceeds −10 mV with no more than 10 V of stimulation. Dendrites are not displayed. The color of the cube at each axon tip indicates stimulation voltages required for axon tip to reach $V_m > -10$ mV. List of location, axon direction, and threshold: (GM1_L_r6, Yp, 4.25 V), (GM1_R_r6, Yp, 4.25 V), (GM3_L_r6, Yp, 8.25 V), (GM3_R_r6, Yp, 8.25 V), (GM1_L_r2, Xp, 7.0 V), and (GM1_L_r2, Yn, 5.0 V).

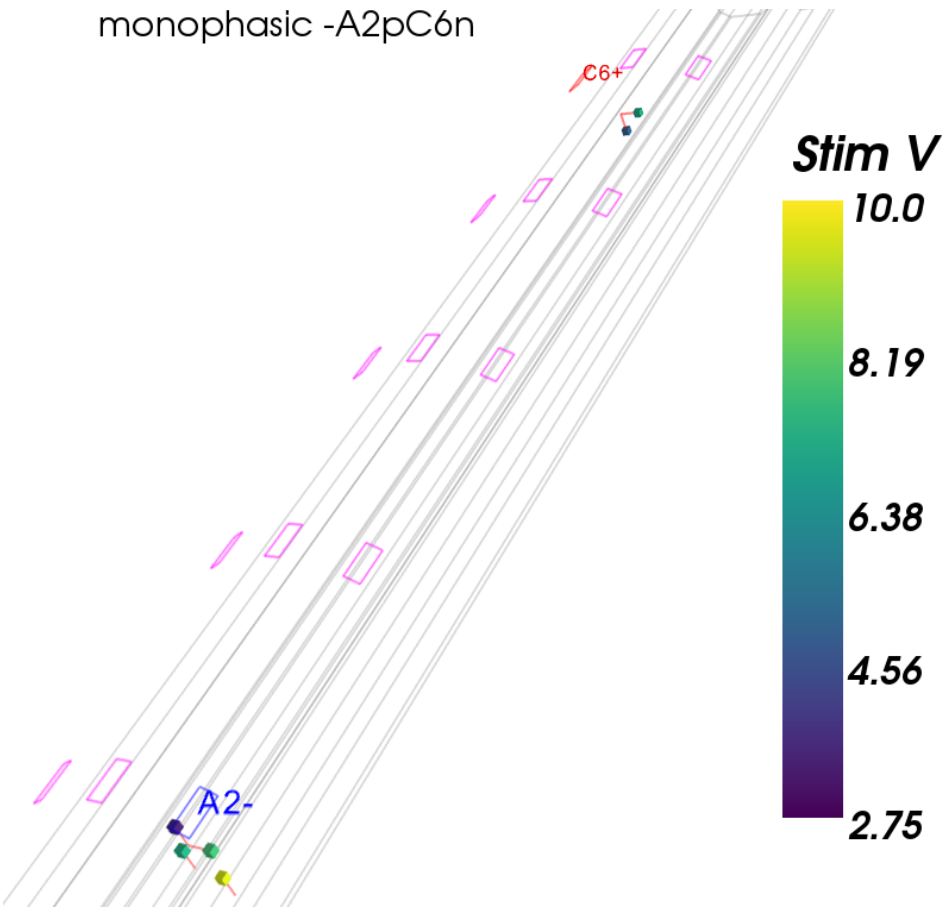

Figure 4.55: Monophasic stimulation using combination -A2pC6n. Electrode C6 has a positive phase and is labeled red. Electrode A2 has a negative phase and is labeled blue. All other electrodes are floating and labeled purple. Soma, AH, IS, and AP are displayed as red lines for those neurons whose axon tip membrane voltage exceeds −10 mV with no more than 10 V of stimulation. Dendrites are not displayed. The color of the cube at each axon tip indicates stimulation voltages required for axon tip to reach $V_m > -10$ mV. List of location, axon direction, and threshold: (GM1_L_r2, Yp, 3.5 V), (GM3_L_r2, Yp, 7.25 V), (GM2_L_r2, Yp, 9.5 V), (GM1_L_r2, Xn, 7.75 V), (GM1_R_r6, Xn, 7.0 V), and (GM1_R_r6, Yn, 5.0 V).

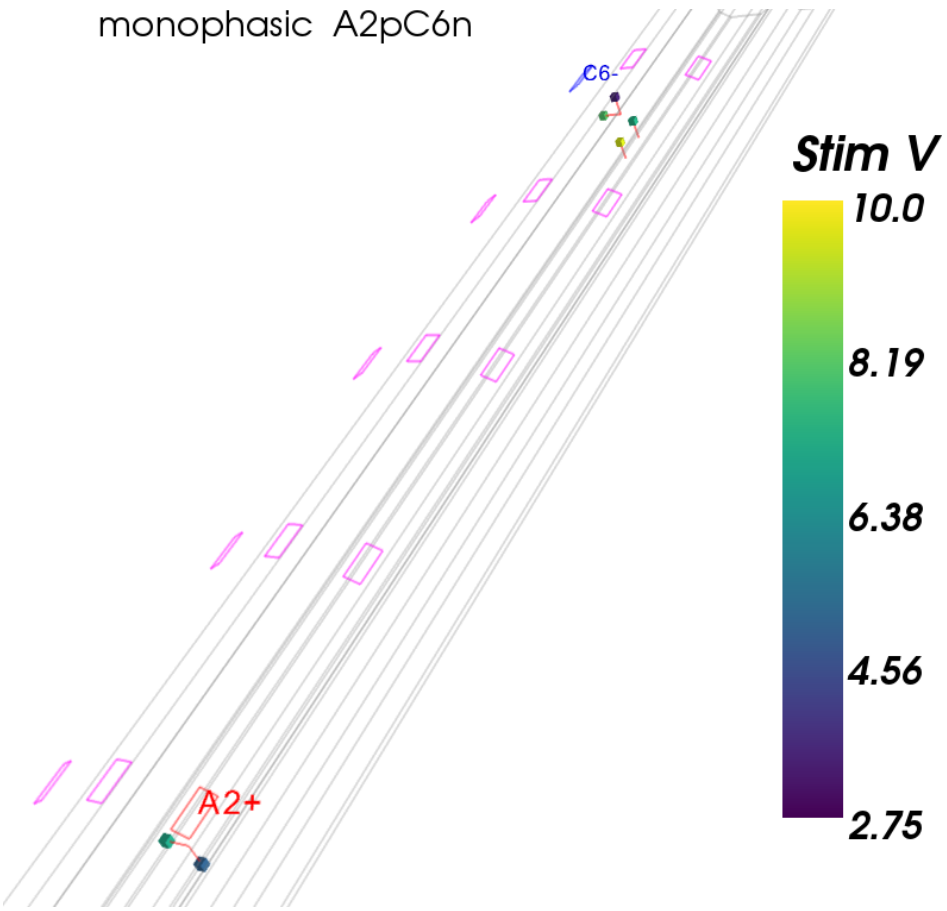

Figure 4.56: Monophasic stimulation using combination A2pC6n. Electrode A2 has a positive phase and is labeled red. Electrode C6 has a negative phase and is labeled blue. All other electrodes are floating and labeled purple. Soma, AH, IS, and AP are displayed as red lines for those neurons whose axon tip membrane voltage exceeds −10 mV with no more than 10 V of stimulation. Dendrites are not displayed. The color of the cube at each axon tip indicates stimulation voltages required for axon tip to reach $V_m > -10$ mV. List of location, axon direction, and threshold: (GM1_R_r6, Yp, 3.5 V), (GM3_R_r6, Yp, 7.25 V), (GM2_R_r6, Yp, 9.5 V), (GM1_L_r2, Xp, 7.0 V), (GM1_R_r6, Xp, 8.0 V), and (GM1_L_r2, Yn, 5.0 V).

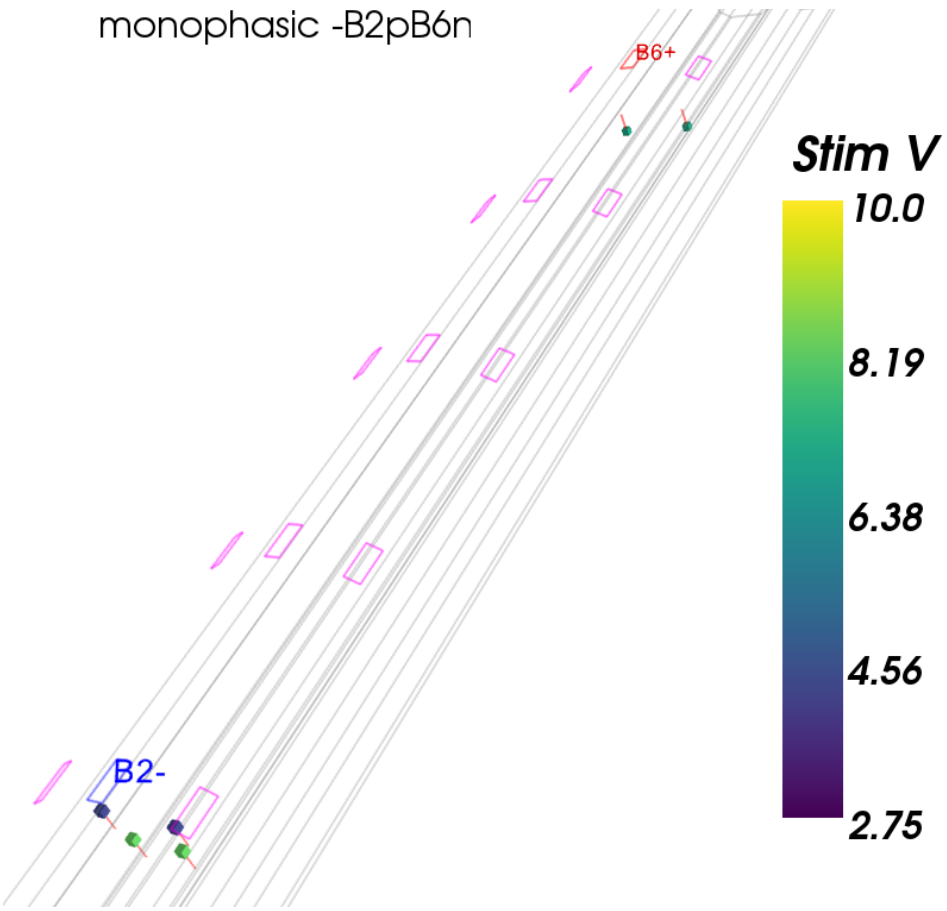

Figure 4.57: Monophasic stimulation using combination -B2pB6n. Electrode B6 has a positive phase and is labeled red. Electrode B2 has a negative phase and is labeled blue. All other electrodes are floating and labeled purple. Soma, AH, IS, and AP are displayed as red lines for those neurons whose axon tip membrane voltage exceeds −10 mV with no more than 10 V of stimulation. Dendrites are not displayed. The color of the cube at each axon tip indicates stimulation voltages required for axon tip to reach $V_m > -10$ mV. List of location, axon direction, and threshold: (GM1_L_r2, Yp, 4.25 V), (GM1_R_r2, Yp, 4.25 V), (GM3_L_r2, Yp, 8.25 V), (GM3_R_r2, Yp, 8.25 V), (GM1_L_r6, Yn, 7.0 V), and (GM1_R_r6, Yn, 7.0 V).

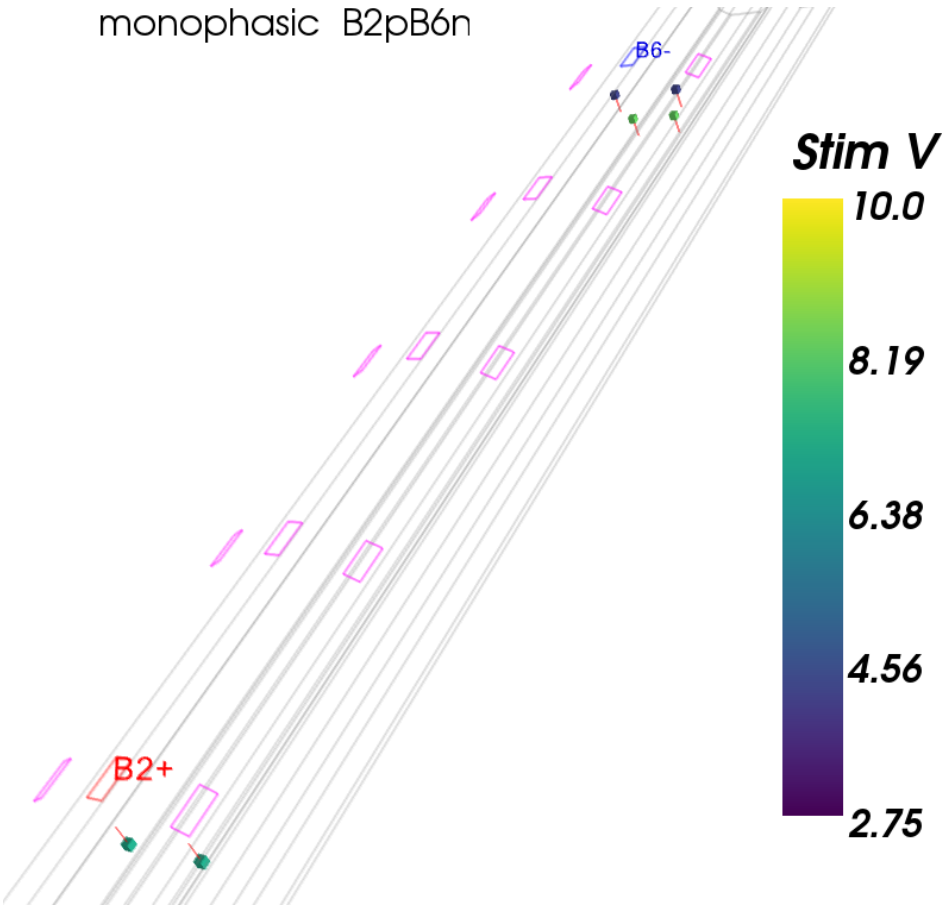

Figure 4.58: Monophasic stimulation using combination B2pB6n. Electrode B2 has a positive phase and is labeled red. Electrode B6 has a negative phase and is labeled blue. All other electrodes are floating and labeled purple. Soma, AH, IS, and AP are displayed as red lines for those neurons whose axon tip membrane voltage exceeds −10 mV with no more than 10 V of stimulation. Dendrites are not displayed. The color of the cube at each axon tip indicates stimulation voltages required for axon tip to reach $V_m > -10$ mV. List of location, axon direction, and threshold: (GM1_L_r6, Yp, 4.25 V), (GM1_R_r6, Yp, 4.25 V), (GM3_L_r6, Yp, 8.25 V), (GM3_R_r6, Yp, 8.25 V), (GM1_L_r2, Yn, 7.0 V), and (GM1_R_r2, Yn, 7.0 V).

4.A.2 Biphasic

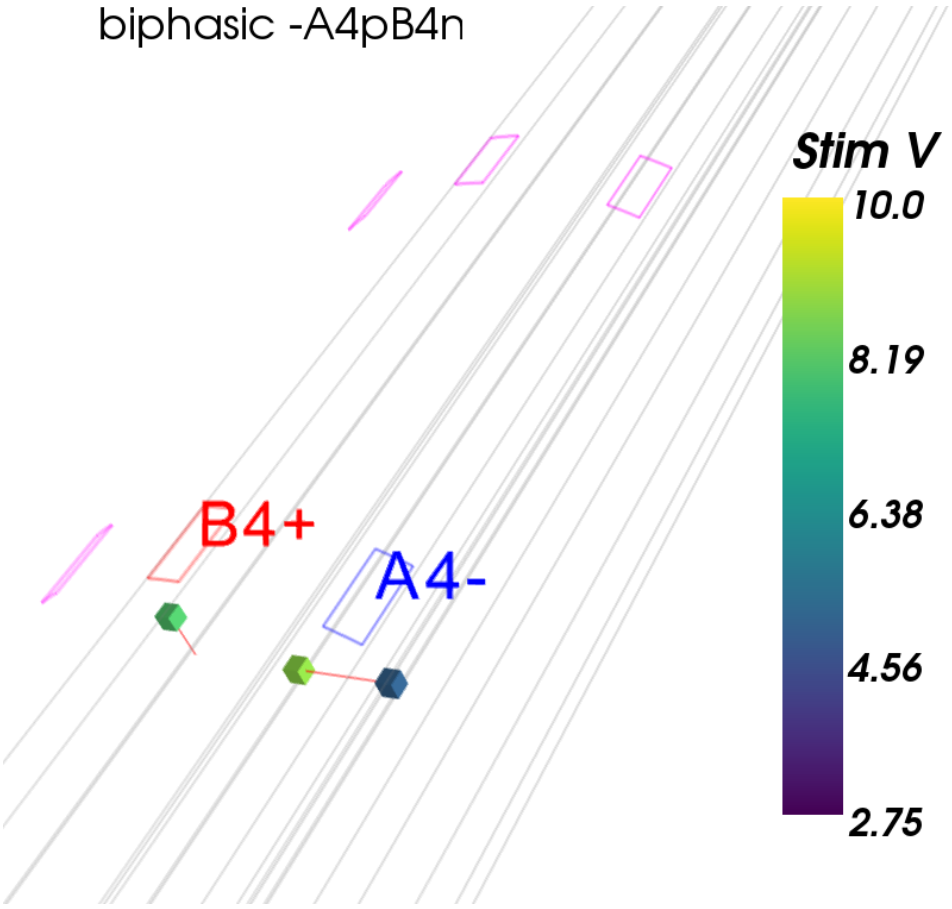

Figure 4.59: Biphasic stimulation using combination -A4pB4n. Electrode B4 has a positive phase first followed by a negative phase and is labeled red. Electrode A4 has a negative phase first followed by a positive phase and is labeled blue. All other electrodes are floating and labeled purple. Soma, AH, IS, and AP are displayed as red lines for those neurons whose axon tip membrane voltage exceeds −10 mV with no more than 10 V of stimulation. Dendrites are not displayed. The color of the cube at each axon tip indicates stimulation voltages required for axon tip to reach $V_m > -10$ mV. List of location, axon direction, and threshold: (GM1_R_r4, Yp, 8.0 V), (GM1_L_r4, Xp, 8.75 V), and (GM1_L_r4, Xn, 5.0 V).

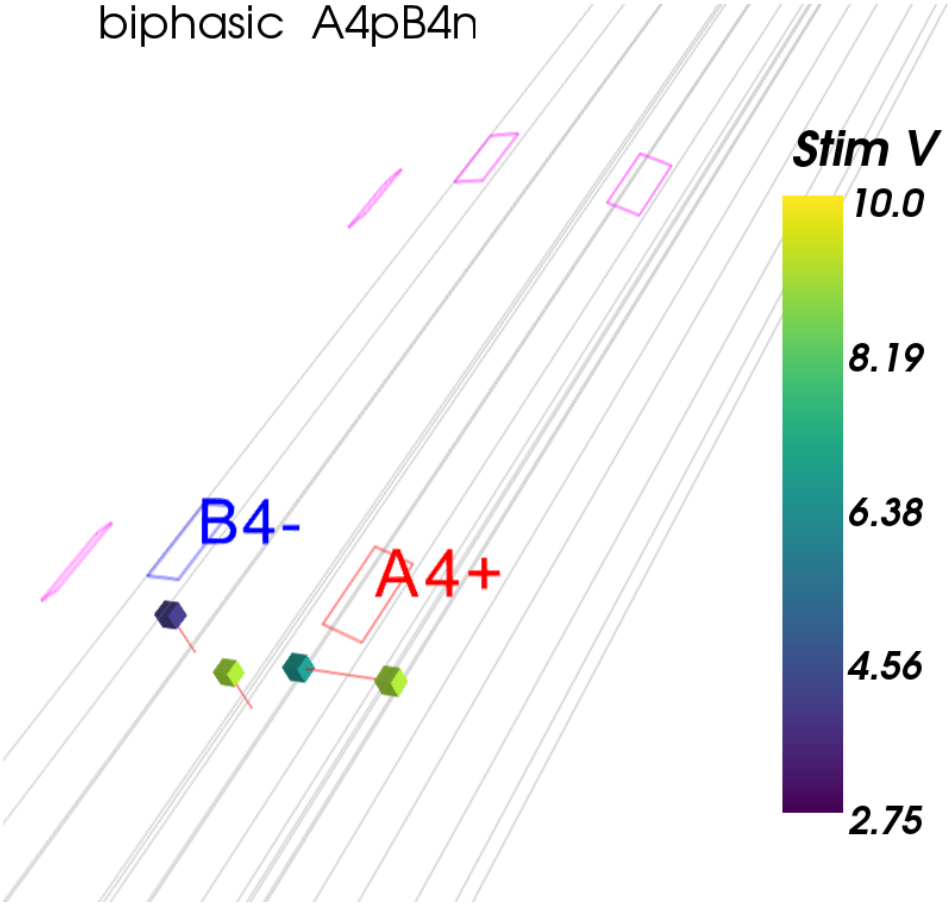

Figure 4.60: Biphasic stimulation using combination A4pB4n. Electrode A4 has a positive phase first followed by a negative phase and is labeled red. Electrode B4 has a negative phase first followed by a positive phase and is labeled blue. All other electrodes are floating and labeled purple. Soma, AH, IS, and AP are displayed as red lines for those neurons whose axon tip membrane voltage exceeds $-10\,\text{mV}$ with no more than $10\,\text{V}$ of stimulation. Dendrites are not displayed. The color of the cube at each axon tip indicates stimulation voltages required for axon tip to reach $V_m > -10\,\text{mV}$. List of location, axon direction, and threshold: (GM1_R_r4, Yp, $4.0\,\text{V}$), (GM3_R_r4, Yp, $9.0\,\text{V}$), (GM1_L_r4, Xp, $6.5\,\text{V}$), and (GM1_L_r4, Xn, $9.0\,\text{V}$).

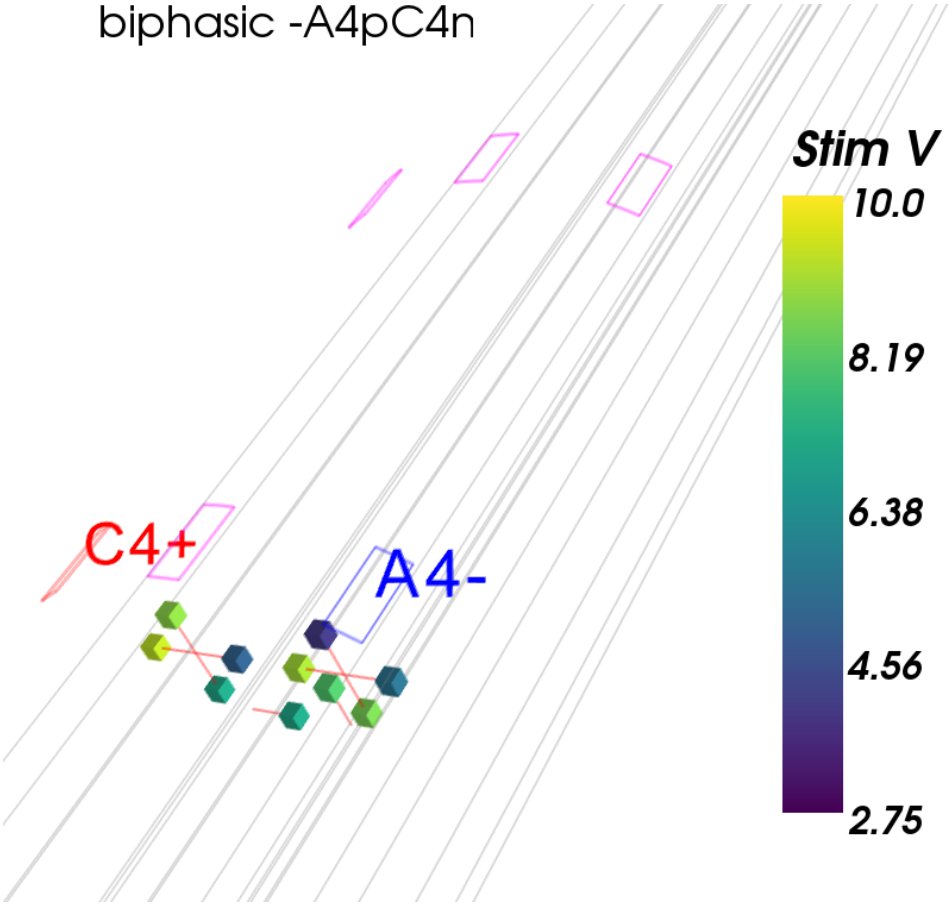

Figure 4.61: Biphasic stimulation using combination -A4pC4n. Electrode C4 has a positive phase first followed by a negative phase and is labeled red. Electrode A4 has a negative phase first followed by a positive phase and is labeled blue. All other electrodes are floating and labeled purple. Soma, AH, IS, and AP are displayed as red lines for those neurons whose axon tip membrane voltage exceeds $-10\,\text{mV}$ with no more than $10\,\text{V}$ of stimulation. Dendrites are not displayed. The color of the cube at each axon tip indicates stimulation voltages required for axon tip to reach $V_m > -10\,\text{mV}$. List of location, axon direction, and threshold: (GM1_L_r4, Yp, 4.0 V), (GM1_R_r4, Yp, 8.75 V), (GM3_L_r4, Yp, 8.0 V), (GM1_L_r4, Xp, 9.0 V), (GM1_R_r4, Xp, 9.25 V), (GM1_L_r4, Xn, 5.5 V), (GM1_R_r4, Xn, 5.0 V), (GM3_R_r4, Xn, 7.0 V), (GM1_L_r4, Yn, 8.5 V), and (GM1_R_r4, Yn, 7.0 V).

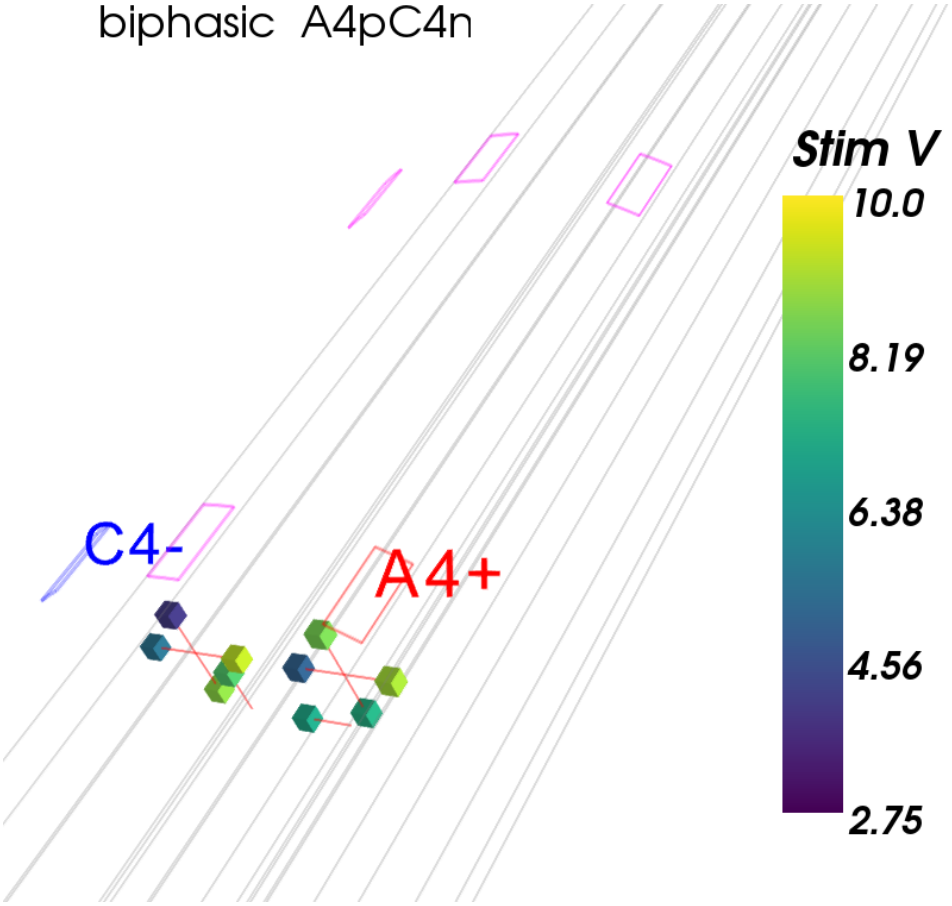

Figure 4.62: Biphasic stimulation using combination A4pC4n. Electrode A4 has a positive phase first followed by a negative phase and is labeled red. Electrode C4 has a negative phase first followed by a positive phase and is labeled blue. All other electrodes are floating and labeled purple. Soma, AH, IS, and AP are displayed as red lines for those neurons whose axon tip membrane voltage exceeds −10 mV with no more than 10 V of stimulation. Dendrites are not displayed. The color of the cube at each axon tip indicates stimulation voltages required for axon tip to reach $V_m > -10$ mV. List of location, axon direction, and threshold: (GM1_L_r4, Yp, 8.5 V), (GM1_R_r4, Yp, 4.0 V), (GM3_R_r4, Yp, 8.0 V), (GM1_L_r4, Xp, 5.0 V), (GM1_R_r4, Xp, 5.5 V), (GM3_L_r4, Xp, 7.0 V), (GM1_L_r4, Xn, 9.0 V), (GM1_R_r4, Xn, 9.25 V), (GM1_L_r4, Yn, 7.25 V), and (GM1_R_r4, Yn, 8.75 V).

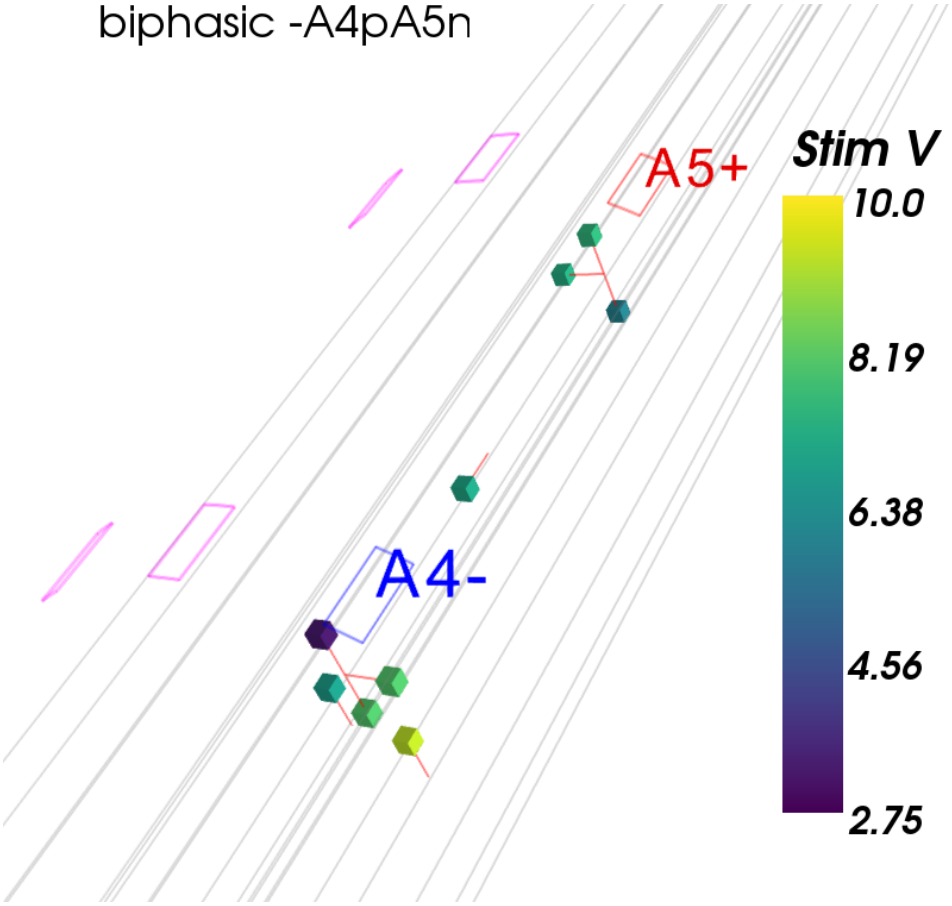

Figure 4.63: Biphasic stimulation using combination -A4pA5n. Electrode A5 has a positive phase first followed by a negative phase and is labeled red. Electrode A4 has a negative phase first followed by a positive phase and is labeled blue. All other electrodes are floating and labeled purple. Soma, AH, IS, and AP are displayed as red lines for those neurons whose axon tip membrane voltage exceeds −10 mV with no more than 10 V of stimulation. Dendrites are not displayed. The color of the cube at each axon tip indicates stimulation voltages required for axon tip to reach $V_m > -10$ mV. List of location, axon direction, and threshold: (GM1_L_r4and5, Zn, 7.0 V), (GM1_L_r4, Yp, 3.25 V), (GM1_L_r5, Yp, 7.5 V), (GM3_L_r4, Yp, 6.75 V), (GM2_L_r4, Yp, 9.25 V), (GM1_L_r5, Xp, 7.25 V), (GM1_L_r4, Xn, 8.0 V), (GM1_L_r4, Yn, 8.0 V), and (GM1_L_r5, Yn, 6.0 V).

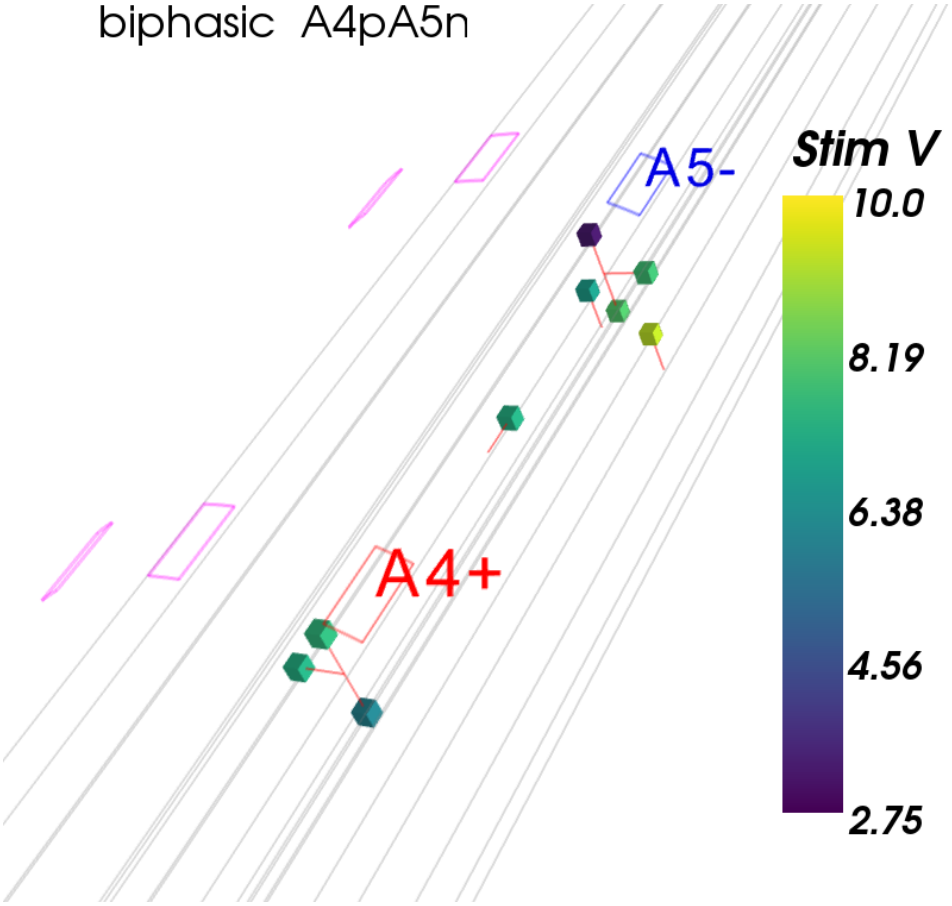

Figure 4.64: Biphasic stimulation using combination A4pA5n. Electrode A4 has a positive phase first followed by a negative phase and is labeled red. Electrode A5 has a negative phase first followed by a positive phase and is labeled blue. All other electrodes are floating and labeled purple. Soma, AH, IS, and AP are displayed as red lines for those neurons whose axon tip membrane voltage exceeds −10 mV with no more than 10 V of stimulation. Dendrites are not displayed. The color of the cube at each axon tip indicates stimulation voltages required for axon tip to reach $V_m > -10$ mV. List of location, axon direction, and threshold: (GM1_L_r4, Yp, 7.5 V), (GM1_L_r5, Yp, 3.25 V), (GM3_L_r5, Yp, 6.75 V), (GM2_L_r5, Yp, 9.25 V), (GM1_L_r4, Xp, 7.25 V), (GM1_L_r5, Xn, 7.75 V), (GM1_L_r4, Yn, 6.0 V), (GM1_L_r5, Yn, 8.0 V), and (GM1_L_r4and5, Zp, 7.25 V).

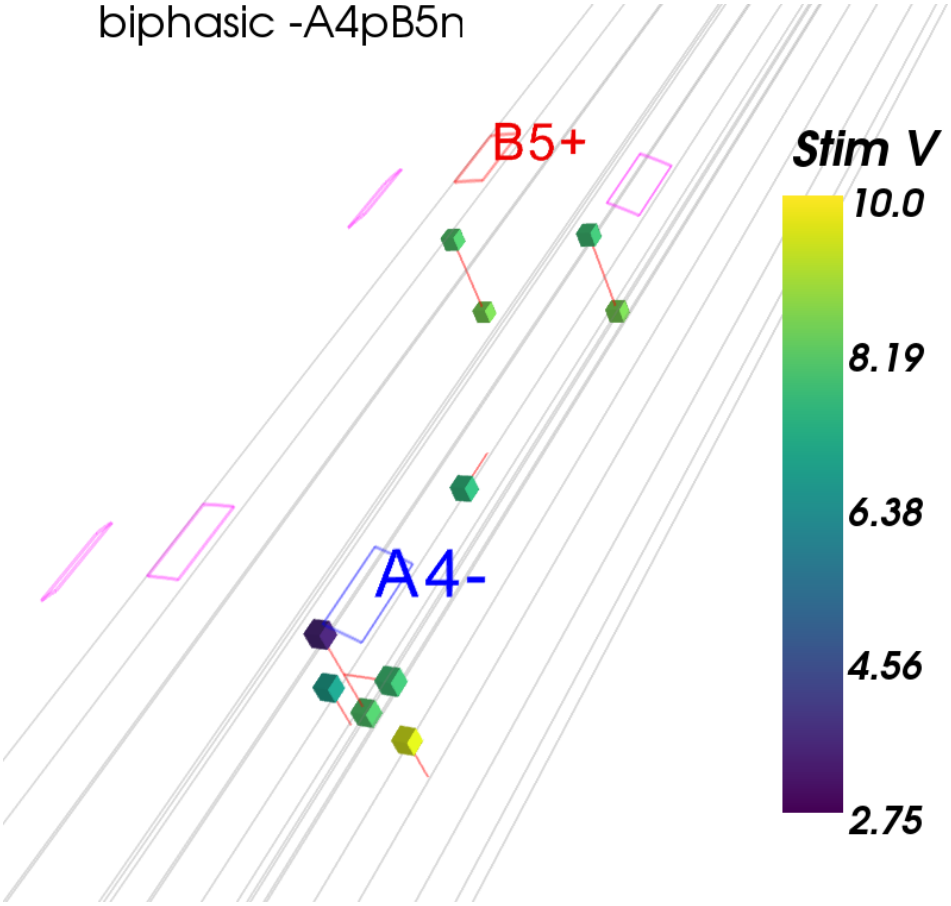

Figure 4.65: Biphasic stimulation using combination -A4pB5n. Electrode B5 has a positive phase first followed by a negative phase and is labeled red. Electrode A4 has a negative phase first followed by a positive phase and is labeled blue. All other electrodes are floating and labeled purple. Soma, AH, IS, and AP are displayed as red lines for those neurons whose axon tip membrane voltage exceeds −10 mV with no more than 10 V of stimulation. Dendrites are not displayed. The color of the cube at each axon tip indicates stimulation voltages required for axon tip to reach $V_m > -10$ mV. List of location, axon direction, and threshold: (GM1_L_r4and5, Zn, 7.5 V), (GM1_L_r4, Yp, 3.5 V), (GM1_R_r5, Yp, 8.0 V), (GM1_L_r5, Yp, 7.75 V), (GM3_L_r4, Yp, 6.75 V), (GM2_L_r4, Yp, 9.5 V), (GM1_L_r4, Xn, 7.75 V), (GM1_L_r4, Yn, 8.0 V), (GM1_R_r5, Yn, 8.5 V), and (GM1_L_r5, Yn, 8.5 V).

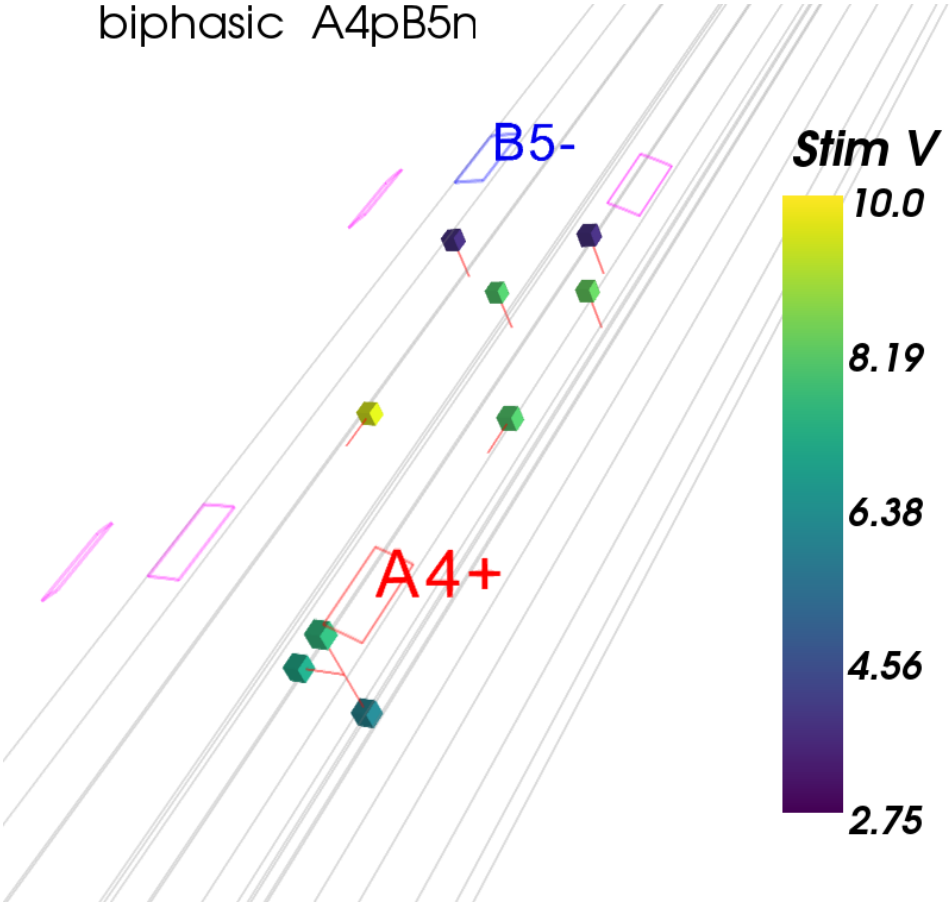

Figure 4.66: Biphasic stimulation using combination A4pB5n. Electrode A4 has a positive phase first followed by a negative phase and is labeled red. Electrode B5 has a negative phase first followed by a positive phase and is labeled blue. All other electrodes are floating and labeled purple. Soma, AH, IS, and AP are displayed as red lines for those neurons whose axon tip membrane voltage exceeds −10 mV with no more than 10 V of stimulation. Dendrites are not displayed. The color of the cube at each axon tip indicates stimulation voltages required for axon tip to reach $V_m > -10$ mV. List of location, axon direction, and threshold: (GM1_L_r4, Yp, 7.5 V), (GM1_R_r5, Yp, 3.75 V), (GM1_L_r5, Yp, 3.75 V), (GM3_R_r5, Yp, 8.0 V), (GM3_L_r5, Yp, 8.25 V), (GM1_L_r4, Xp, 7.0 V), (GM1_L_r4, Yn, 6.0 V), (GM1_L_r4and5, Zp, 8.0 V), and (GM1_R_r4and5, Zp, 9.5 V).

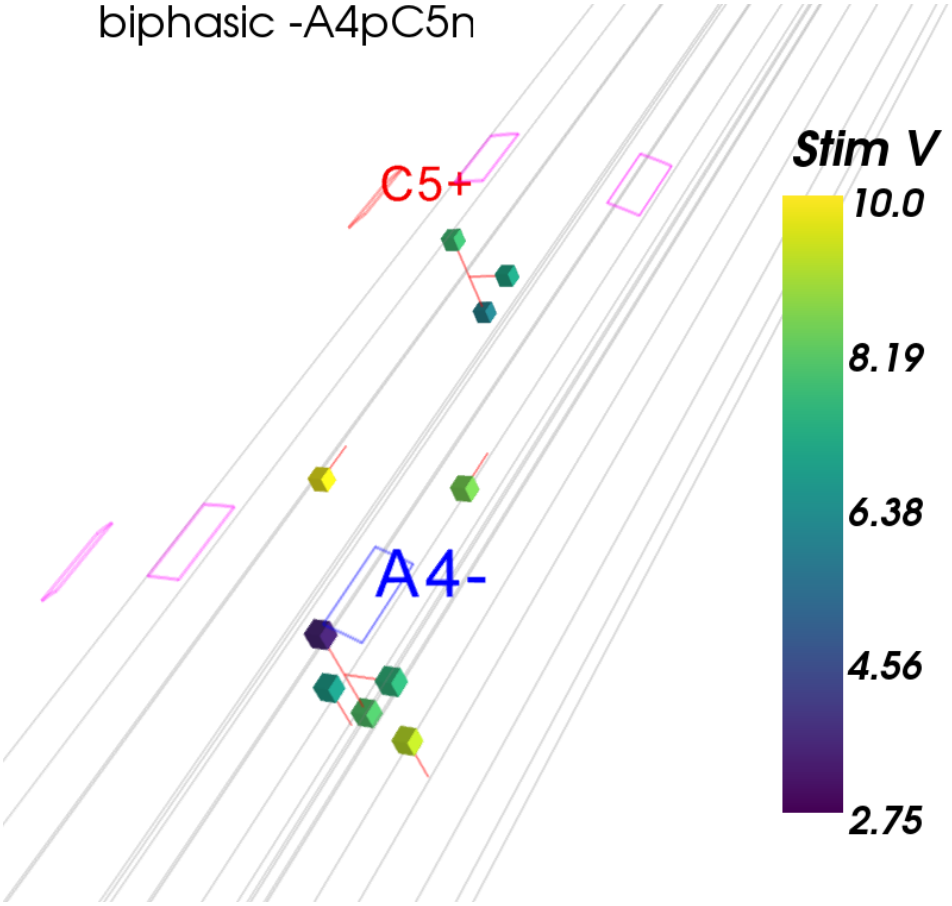

Figure 4.67: Biphasic stimulation using combination -A4pC5n. Electrode C5 has a positive phase first followed by a negative phase and is labeled red. Electrode A4 has a negative phase first followed by a positive phase and is labeled blue. All other electrodes are floating and labeled purple. Soma, AH, IS, and AP are displayed as red lines for those neurons whose axon tip membrane voltage exceeds −10 mV with no more than 10 V of stimulation. Dendrites are not displayed. The color of the cube at each axon tip indicates stimulation voltages required for axon tip to reach $V_m > -10$ mV. List of location, axon direction, and threshold: (GM1_L_r4and5, Zn, 8.5 V), (GM1_R_r4and5, Zn, 9.75 V), (GM1_L_r4, Yp, 3.5 V), (GM1_R_r5, Yp, 7.75 V), (GM3_L_r4, Yp, 6.75 V), (GM2_L_r4, Yp, 9.25 V), (GM1_L_r4, Xn, 7.5 V), (GM1_R_r5, Xn, 7.0 V), (GM1_L_r4, Yn, 8.0 V), and (GM1_R_r5, Yn, 6.0 V).

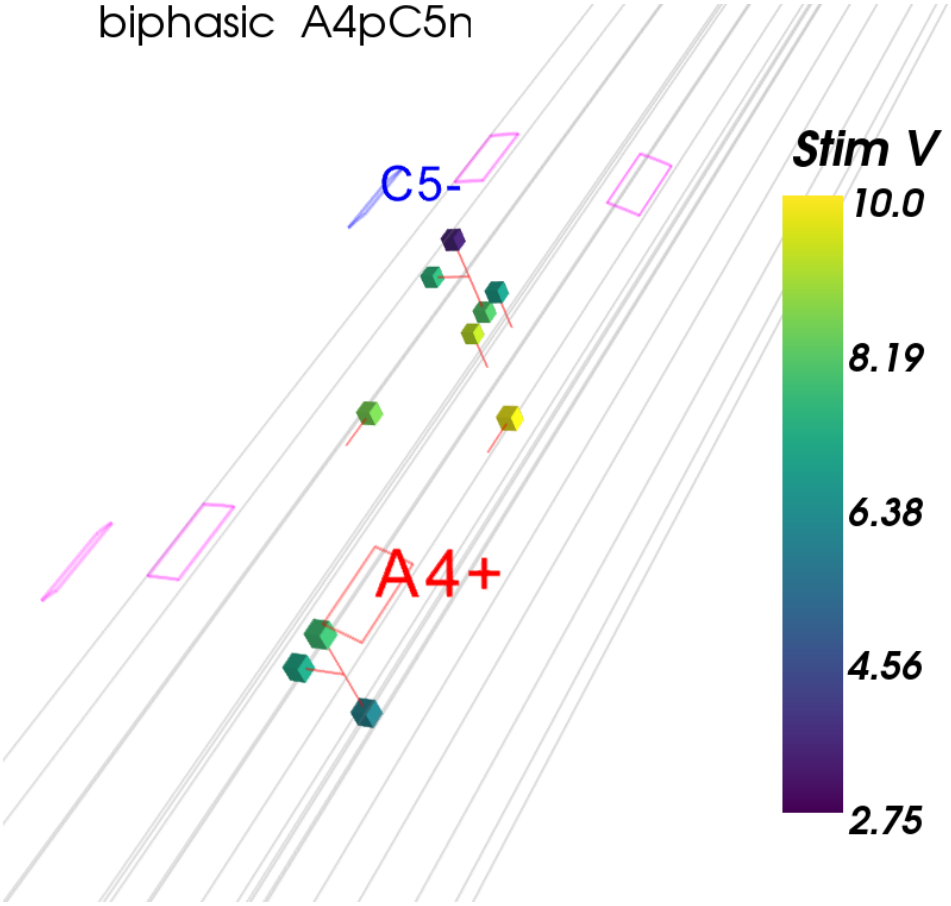

Figure 4.68: Biphasic stimulation using combination A4pC5n. Electrode A4 has a positive phase first followed by a negative phase and is labeled red. Electrode C5 has a negative phase first followed by a positive phase and is labeled blue. All other electrodes are floating and labeled purple. Soma, AH, IS, and AP are displayed as red lines for those neurons whose axon tip membrane voltage exceeds $-10\,\text{mV}$ with no more than $10\,\text{V}$ of stimulation. Dendrites are not displayed. The color of the cube at each axon tip indicates stimulation voltages required for axon tip to reach $V_m > -10\,\text{mV}$. List of location, axon direction, and threshold: (GM1_L_r4, Yp, 7.75 V), (GM1_R_r5, Yp, 3.5 V), (GM3_R_r5, Yp, 6.75 V), (GM2_R_r5, Yp, 9.25 V), (GM1_L_r4, Xp, 7.0 V), (GM1_R_r5, Xp, 7.5 V), (GM1_L_r4, Yn, 6.0 V), (GM1_R_r5, Yn, 8.0 V), (GM1_L_r4and5, Zp, 9.75 V), and (GM1_R_r4and5, Zp, 8.5 V).

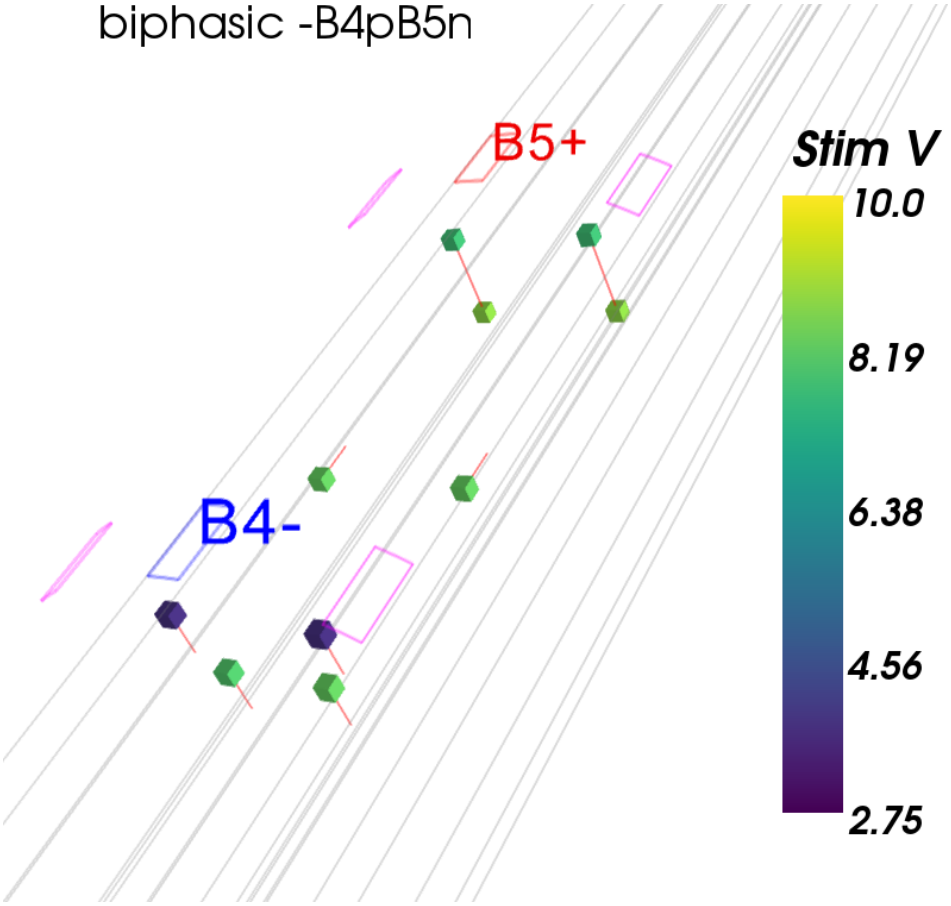

Figure 4.69: Biphasic stimulation using combination -B4pB5n. Electrode B5 has a positive phase first followed by a negative phase and is labeled red. Electrode B4 has a negative phase first followed by a positive phase and is labeled blue. All other electrodes are floating and labeled purple. Soma, AH, IS, and AP are displayed as red lines for those neurons whose axon tip membrane voltage exceeds -10 mV with no more than 10 V of stimulation. Dendrites are not displayed. The color of the cube at each axon tip indicates stimulation voltages required for axon tip to reach $V_m > -10$ mV. List of location, axon direction, and threshold: (GM1_R_r4and5, Zn, 8.25 V), (GM1_L_r4and5, Zn, 8.25 V), (GM1_L_r4, Yp, 3.75 V), (GM1_R_r4, Yp, 3.75 V), (GM1_L_r5, Yp, 7.75 V), (GM1_R_r5, Yp, 7.75 V), (GM3_R_r4, Yp, 8.0 V), (GM3_L_r4, Yp, 8.25 V), (GM1_L_r5, Yn, 8.75 V), and (GM1_R_r5, Yn, 8.75 V).

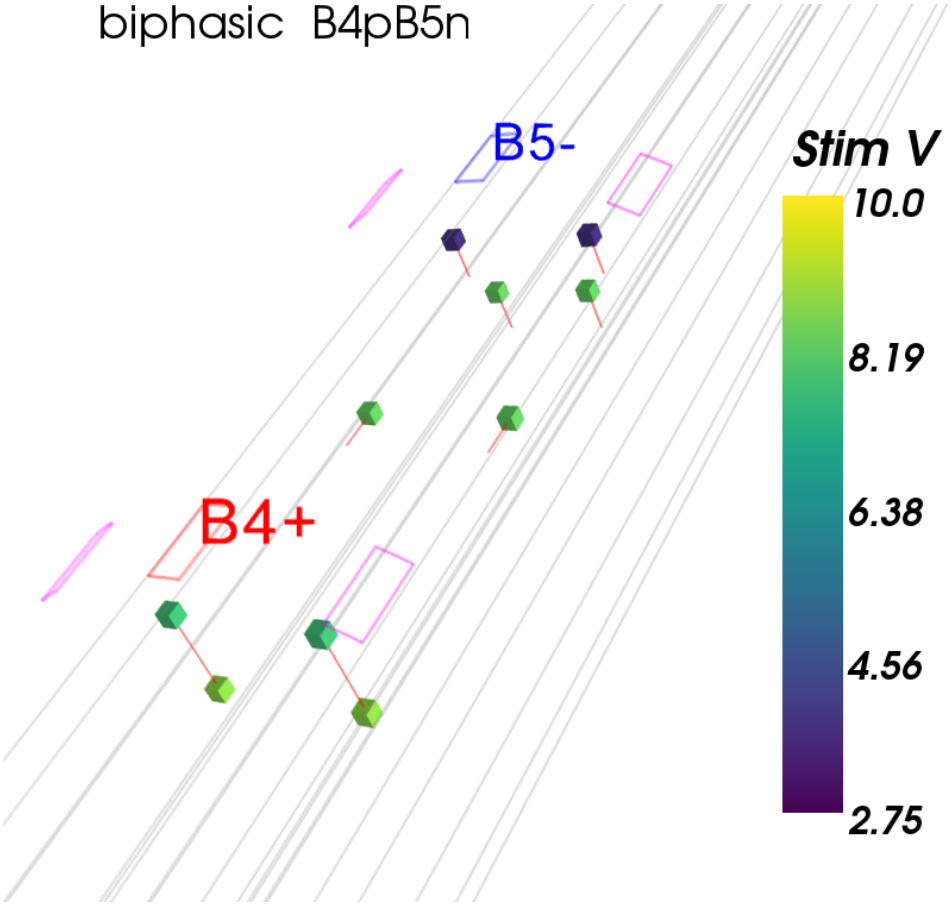

Figure 4.70: Biphasic stimulation using combination B4pB5n. Electrode B4 has a positive phase first followed by a negative phase and is labeled red. Electrode B5 has a negative phase first followed by a positive phase and is labeled blue. All other electrodes are floating and labeled purple. Soma, AH, IS, and AP are displayed as red lines for those neurons whose axon tip membrane voltage exceeds $-10\,\text{mV}$ with no more than $10\,\text{V}$ of stimulation. Dendrites are not displayed. The color of the cube at each axon tip indicates stimulation voltages required for axon tip to reach $V_m > -10\,\text{mV}$. List of location, axon direction, and threshold: (GM1_L_r4, Yp, 7.75 V), (GM1_R_r4, Yp, 7.75 V), (GM1_L_r5, Yp, 3.75 V), (GM1_R_r5, Yp, 3.75 V), (GM3_L_r5, Yp, 8.25 V), (GM3_R_r5, Yp, 8.25 V), (GM1_L_r4, Yn, 8.75 V), (GM1_R_r4, Yn, 8.75 V), (GM1_R_r4and5, Zp, 8.25 V), and (GM1_L_r4and5, Zp, 8.25 V).

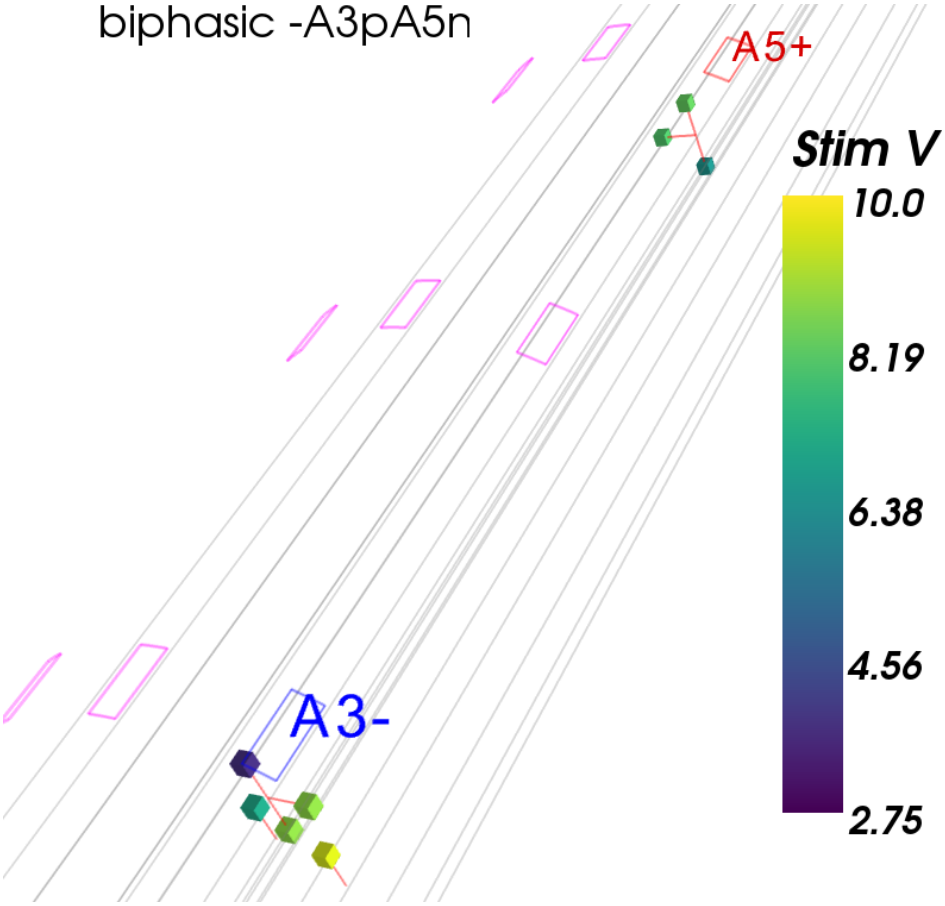

Figure 4.71: Biphasic stimulation using combination -A3pA5n. Electrode A5 has a positive phase first followed by a negative phase and is labeled red. Electrode A3 has a negative phase first followed by a positive phase and is labeled blue. All other electrodes are floating and labeled purple. Soma, AH, IS, and AP are displayed as red lines for those neurons whose axon tip membrane voltage exceeds −10 mV with no more than 10 V of stimulation. Dendrites are not displayed. The color of the cube at each axon tip indicates stimulation voltages required for axon tip to reach $V_m > -10$ mV. List of location, axon direction, and threshold: (GM1_L_r3, Yp, 3.75 V), (GM1_L_r5, Yp, 8.25 V), (GM3_L_r3, Yp, 7.0 V), (GM2_L_r3, Yp, 9.5 V), (GM1_L_r5, Xp, 8.0 V), (GM1_L_r3, Xn, 8.75 V), (GM1_L_r3, Yn, 8.75 V), and (GM1_L_r5, Yn, 6.5 V).

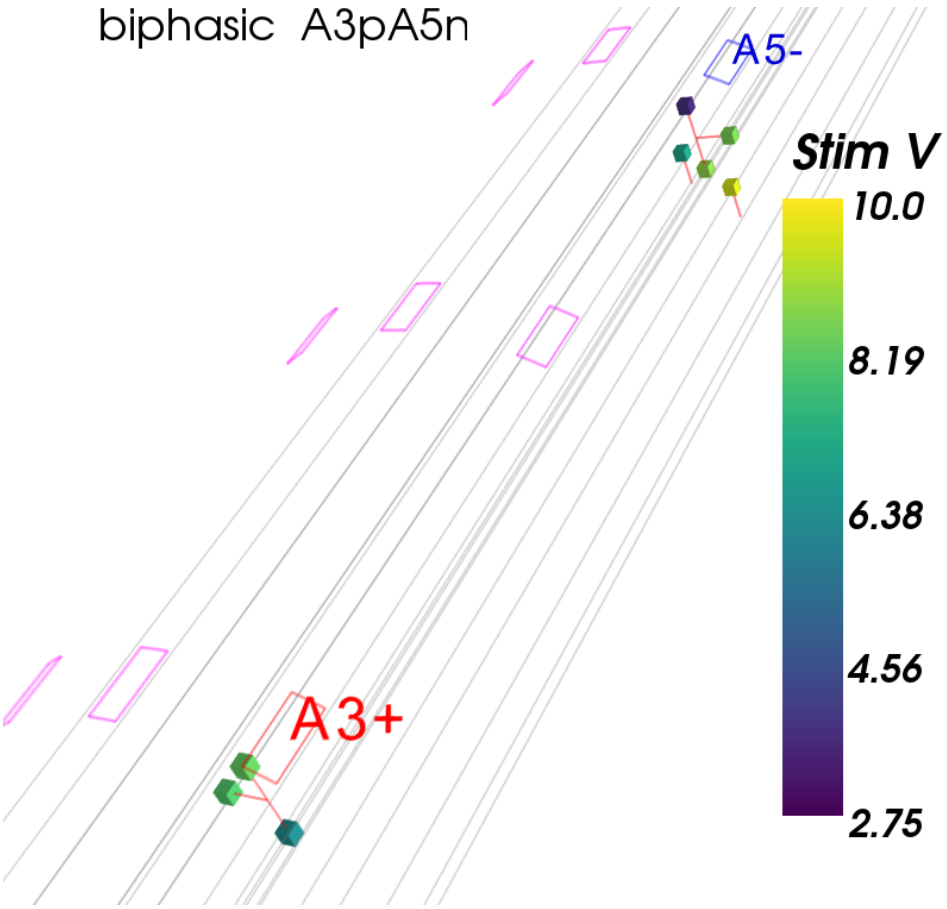

Figure 4.72: Biphasic stimulation using combination A3pA5n. Electrode A3 has a positive phase first followed by a negative phase and is labeled red. Electrode A5 has a negative phase first followed by a positive phase and is labeled blue. All other electrodes are floating and labeled purple. Soma, AH, IS, and AP are displayed as red lines for those neurons whose axon tip membrane voltage exceeds −10 mV with no more than 10 V of stimulation. Dendrites are not displayed. The color of the cube at each axon tip indicates stimulation voltages required for axon tip to reach $V_m > -10$ mV. List of location, axon direction, and threshold: (GM1_L_r3, Yp, 8.25 V), (GM1_L_r5, Yp, 3.75 V), (GM3_L_r5, Yp, 7.0 V), (GM2_L_r5, Yp, 9.5 V), (GM1_L_r3, Xp, 8.0 V), (GM1_L_r5, Xn, 8.5 V), (GM1_L_r3, Yn, 6.25 V), and (GM1_L_r5, Yn, 8.75 V).

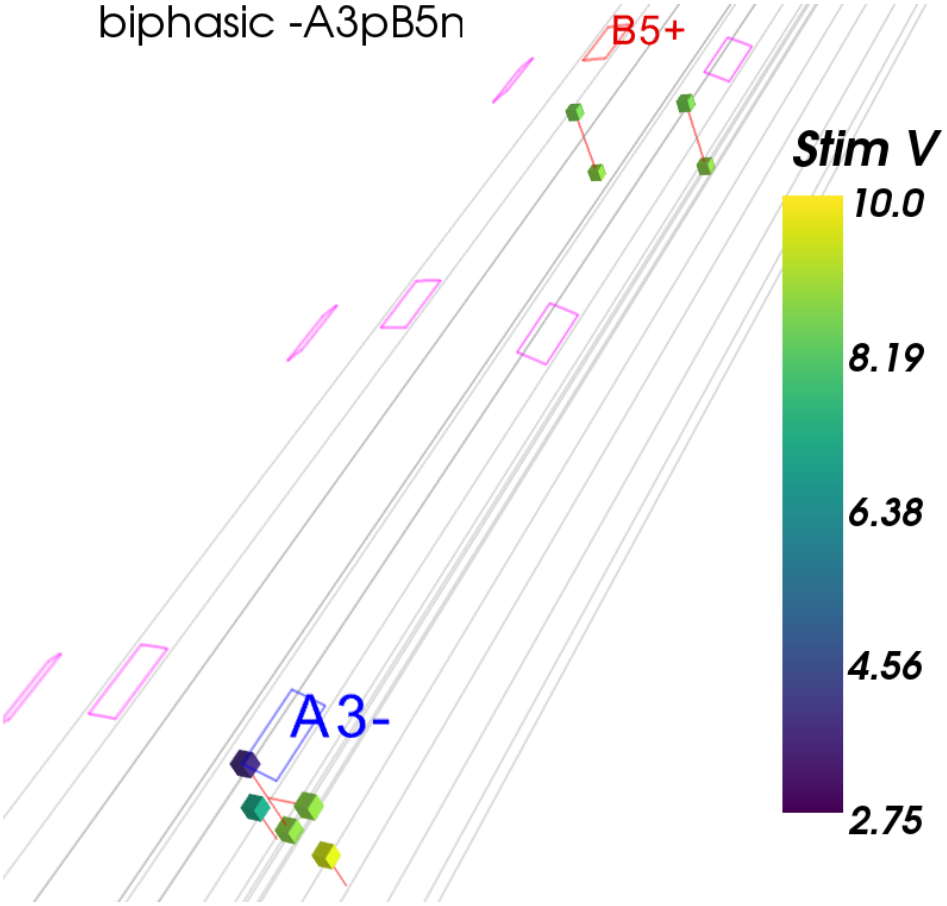

Figure 4.73: Biphasic stimulation using combination -A3pB5n. Electrode B5 has a positive phase first followed by a negative phase and is labeled red. Electrode A3 has a negative phase first followed by a positive phase and is labeled blue. All other electrodes are floating and labeled purple. Soma, AH, IS, and AP are displayed as red lines for those neurons whose axon tip membrane voltage exceeds $-10\,\text{mV}$ with no more than $10\,\text{V}$ of stimulation. Dendrites are not displayed. The color of the cube at each axon tip indicates stimulation voltages required for axon tip to reach $V_m > -10\,\text{mV}$. List of location, axon direction, and threshold: (GM1_L_r3, Yp, 3.75 V), (GM1_R_r5, Yp, 8.5 V), (GM1_L_r5, Yp, 8.5 V), (GM3_L_r3, Yp, 7.0 V), (GM2_L_r3, Yp, 9.5 V), (GM1_L_r3, Xn, 8.75 V), (GM1_L_r3, Yn, 8.75 V), (GM1_R_r5, Yn, 8.75 V), and (GM1_L_r5, Yn, 8.75 V).

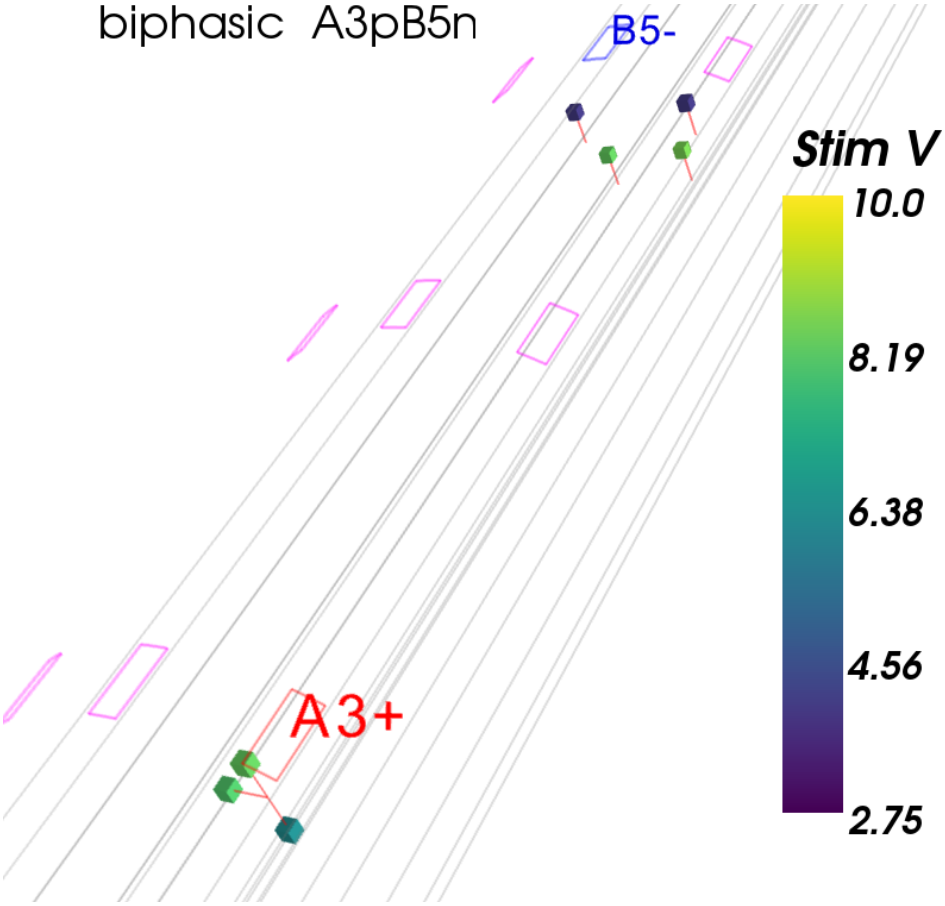

Figure 4.74: Biphasic stimulation using combination A3pB5n. Electrode A3 has a positive phase first followed by a negative phase and is labeled red. Electrode B5 has a negative phase first followed by a positive phase and is labeled blue. All other electrodes are floating and labeled purple. Soma, AH, IS, and AP are displayed as red lines for those neurons whose axon tip membrane voltage exceeds −10 mV with no more than 10 V of stimulation. Dendrites are not displayed. The color of the cube at each axon tip indicates stimulation voltages required for axon tip to reach $V_m > -10$ mV. List of location, axon direction, and threshold: (GM1_L_r3, Yp, 8.25 V), (GM1_R_r5, Yp, 4.0 V), (GM1_L_r5, Yp, 4.0 V), (GM3_R_r5, Yp, 8.25 V), (GM3_L_r5, Yp, 8.5 V), (GM1_L_r3, Xp, 8.0 V), and (GM1_L_r3, Yn, 6.25 V).

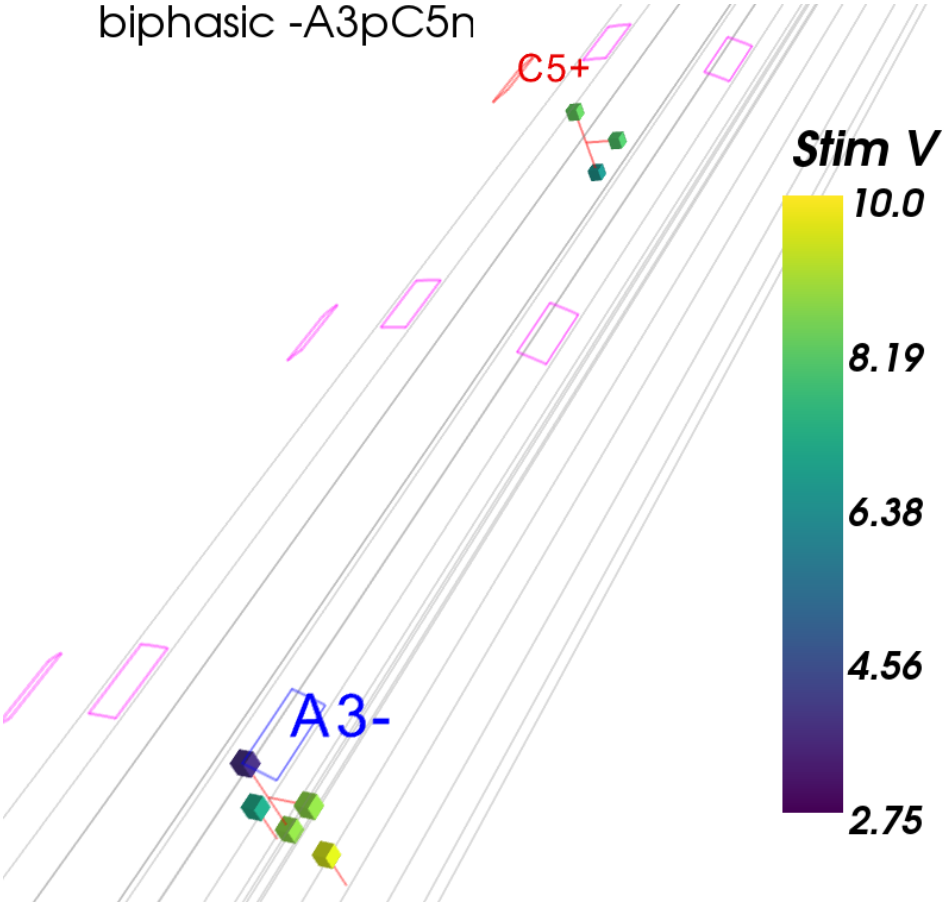

Figure 4.75: Biphasic stimulation using combination -A3pC5n. Electrode C5 has a positive phase first followed by a negative phase and is labeled red. Electrode A3 has a negative phase first followed by a positive phase and is labeled blue. All other electrodes are floating and labeled purple. Soma, AH, IS, and AP are displayed as red lines for those neurons whose axon tip membrane voltage exceeds −10 mV with no more than 10 V of stimulation. Dendrites are not displayed. The color of the cube at each axon tip indicates stimulation voltages required for axon tip to reach $V_m > -10$ mV. List of location, axon direction, and threshold: (GM1_L_r3, Yp, 3.75 V), (GM1_R_r5, Yp, 8.25 V), (GM3_L_r3, Yp, 7.0 V), (GM2_L_r3, Yp, 9.5 V), (GM1_L_r3, Xn, 8.75 V), (GM1_R_r5, Xn, 8.0 V), (GM1_L_r3, Yn, 8.75 V), and (GM1_R_r5, Yn, 6.5 V).

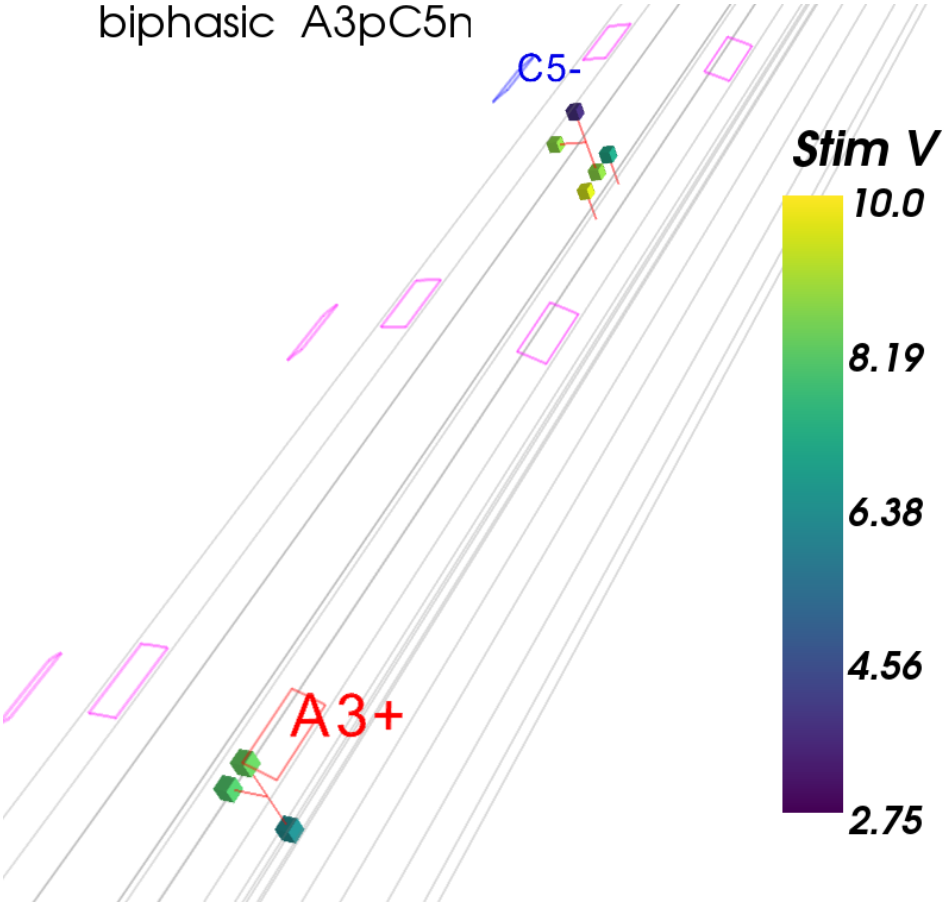

Figure 4.76: Biphasic stimulation using combination A3pC5n. Electrode A3 has a positive phase first followed by a negative phase and is labeled red. Electrode C5 has a negative phase first followed by a positive phase and is labeled blue. All other electrodes are floating and labeled purple. Soma, AH, IS, and AP are displayed as red lines for those neurons whose axon tip membrane voltage exceeds −10 mV with no more than 10 V of stimulation. Dendrites are not displayed. The color of the cube at each axon tip indicates stimulation voltages required for axon tip to reach $V_m > -10$ mV. List of location, axon direction, and threshold: (GM1_L_r3, Yp, 8.25 V), (GM1_R_r5, Yp, 3.75 V), (GM3_R_r5, Yp, 7.0 V), (GM2_R_r5, Yp, 9.5 V), (GM1_L_r3, Xp, 8.0 V), (GM1_R_r5, Xp, 8.75 V), (GM1_L_r3, Yn, 6.25 V), and (GM1_R_r5, Yn, 8.75 V).

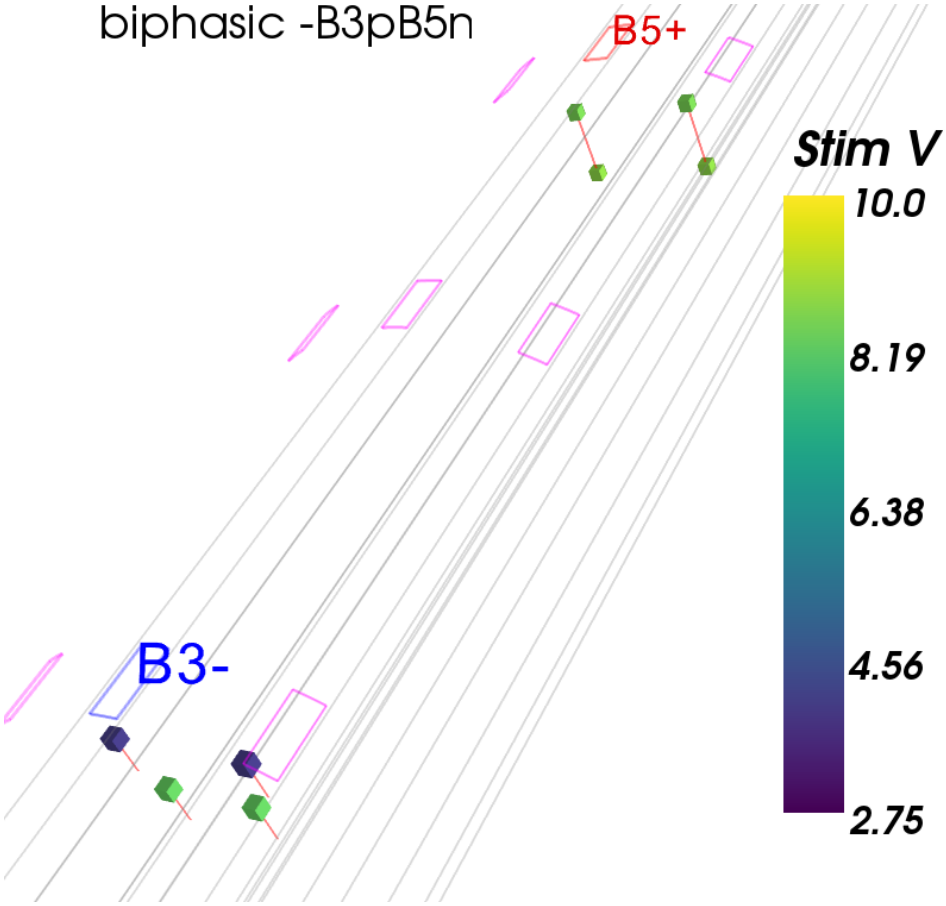

Figure 4.77: Biphasic stimulation using combination -B3pB5n. Electrode B5 has a positive phase first followed by a negative phase and is labeled red. Electrode B3 has a negative phase first followed by a positive phase and is labeled blue. All other electrodes are floating and labeled purple. Soma, AH, IS, and AP are displayed as red lines for those neurons whose axon tip membrane voltage exceeds −10 mV with no more than 10 V of stimulation. Dendrites are not displayed. The color of the cube at each axon tip indicates stimulation voltages required for axon tip to reach $V_m > -10$ mV. List of location, axon direction, and threshold: (GM1_L_r3, Yp, 4.0 V), (GM1_R_r3, Yp, 4.0 V), (GM1_L_r5, Yp, 8.5 V), (GM1_R_r5, Yp, 8.5 V), (GM3_L_r3, Yp, 8.25 V), (GM3_R_r3, Yp, 8.25 V), (GM1_L_r5, Yn, 8.75 V), and (GM1_R_r5, Yn, 8.75 V).

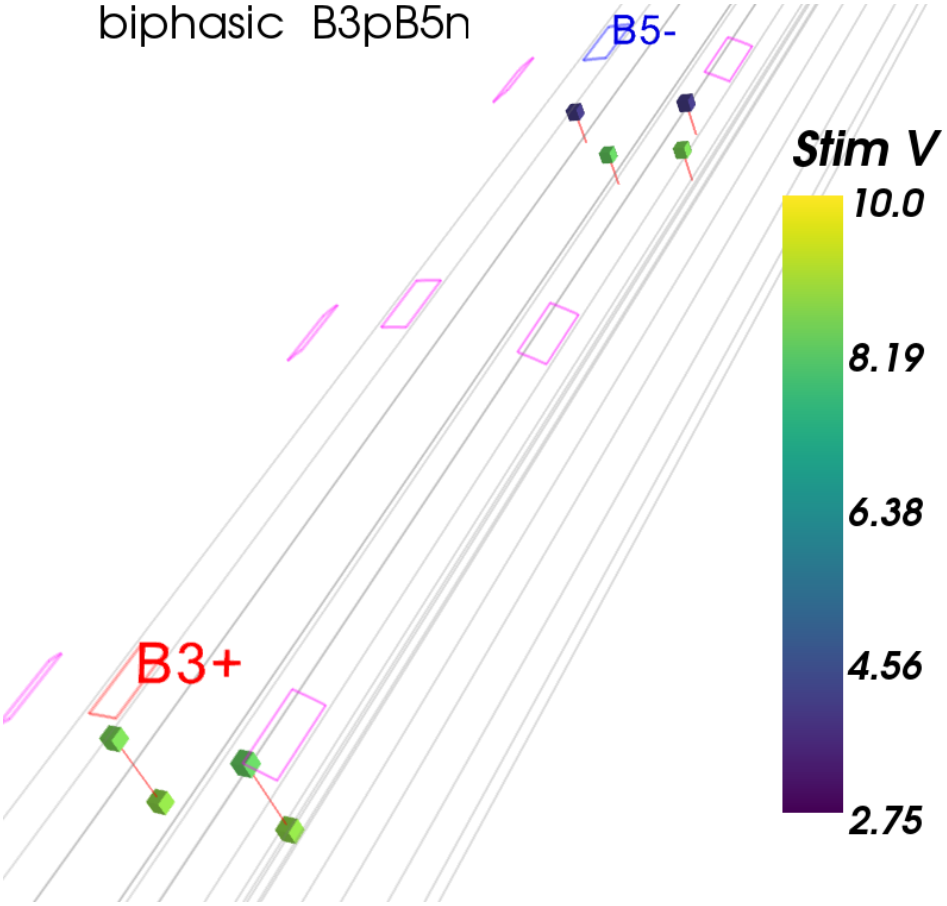

Figure 4.78: Biphasic stimulation using combination B3pB5n. Electrode B3 has a positive phase first followed by a negative phase and is labeled red. Electrode B5 has a negative phase first followed by a positive phase and is labeled blue. All other electrodes are floating and labeled purple. Soma, AH, IS, and AP are displayed as red lines for those neurons whose axon tip membrane voltage exceeds $-10\,\text{mV}$ with no more than $10\,\text{V}$ of stimulation. Dendrites are not displayed. The color of the cube at each axon tip indicates stimulation voltages required for axon tip to reach $V_m > -10\,\text{mV}$. List of location, axon direction, and threshold: (GM1_L_r3, Yp, 8.25 V), (GM1_R_r3, Yp, 8.5 V), (GM1_L_r5, Yp, 4.0 V), (GM1_R_r5, Yp, 4.0 V), (GM3_L_r5, Yp, 8.5 V), (GM3_R_r5, Yp, 8.25 V), (GM1_L_r3, Yn, 8.75 V), and (GM1_R_r3, Yn, 8.75 V).

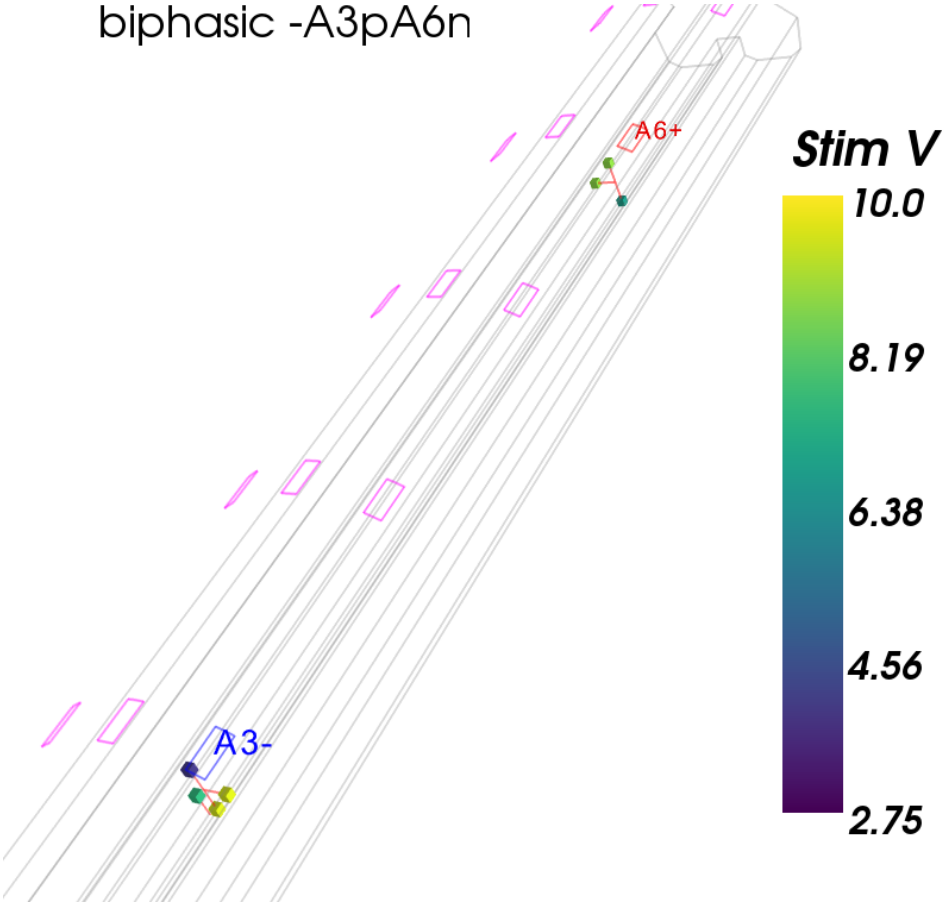

Figure 4.79: Biphasic stimulation using combination -A3pA6n. Electrode A6 has a positive phase first followed by a negative phase and is labeled red. Electrode A3 has a negative phase first followed by a positive phase and is labeled blue. All other electrodes are floating and labeled purple. Soma, AH, IS, and AP are displayed as red lines for those neurons whose axon tip membrane voltage exceeds −10 mV with no more than 10 V of stimulation. Dendrites are not displayed. The color of the cube at each axon tip indicates stimulation voltages required for axon tip to reach $V_m > -10$ mV. List of location, axon direction, and threshold: (GM1_L_r3, Yp, 4.0 V), (GM1_L_r6, Yp, 8.75 V), (GM3_L_r3, Yp, 7.5 V), (GM1_L_r6, Xp, 8.75 V), (GM1_L_r3, Xn, 9.5 V), (GM1_L_r3, Yn, 9.5 V), and (GM1_L_r6, Yn, 6.75 V).

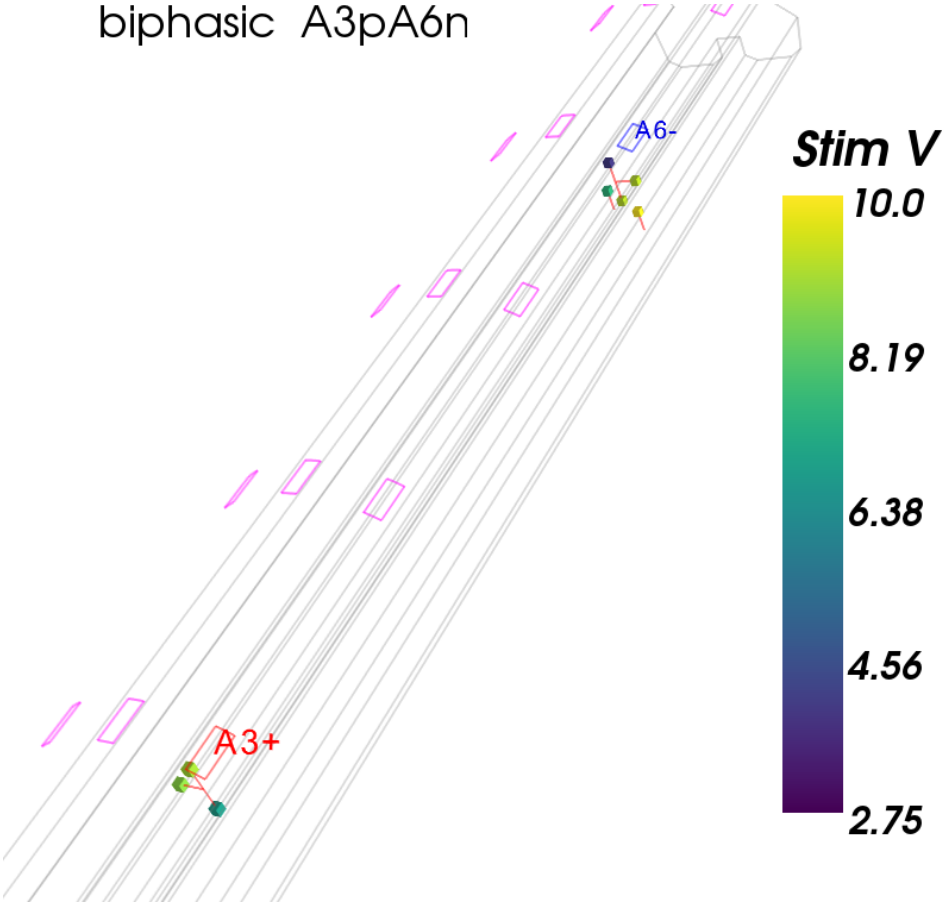

Figure 4.80: Biphasic stimulation using combination A3pA6n. Electrode A3 has a positive phase first followed by a negative phase and is labeled red. Electrode A6 has a negative phase first followed by a positive phase and is labeled blue. All other electrodes are floating and labeled purple. Soma, AH, IS, and AP are displayed as red lines for those neurons whose axon tip membrane voltage exceeds −10 mV with no more than 10 V of stimulation. Dendrites are not displayed. The color of the cube at each axon tip indicates stimulation voltages required for axon tip to reach $V_m > -10$ mV. List of location, axon direction, and threshold: (GM1_L_r3, Yp, 9.0 V), (GM1_L_r6, Yp, 4.0 V), (GM3_L_r6, Yp, 7.5 V), (GM2_L_r6, Yp, 10.0 V), (GM1_L_r3, Xp, 8.75 V), (GM1_L_r6, Xn, 9.25 V), (GM1_L_r3, Yn, 6.75 V), and (GM1_L_r6, Yn, 9.25 V).

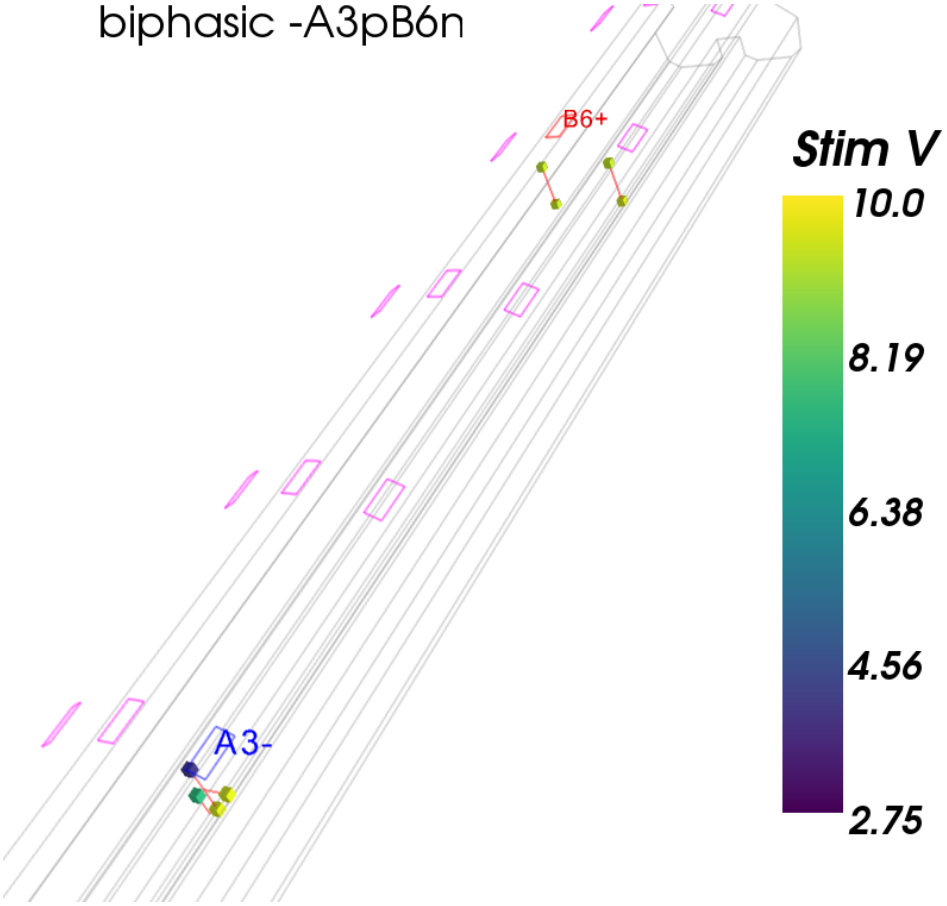

Figure 4.81: Biphasic stimulation using combination -A3pB6n. Electrode B6 has a positive phase first followed by a negative phase and is labeled red. Electrode A3 has a negative phase first followed by a positive phase and is labeled blue. All other electrodes are floating and labeled purple. Soma, AH, IS, and AP are displayed as red lines for those neurons whose axon tip membrane voltage exceeds −10 mV with no more than 10 V of stimulation. Dendrites are not displayed. The color of the cube at each axon tip indicates stimulation voltages required for axon tip to reach $V_m > -10$ mV. List of location, axon direction, and threshold: (GM1_L_r3, Yp, 4.0 V), (GM1_R_r6, Yp, 9.25 V), (GM1_L_r6, Yp, 9.25 V), (GM3_L_r3, Yp, 7.5 V), (GM1_L_r3, Xn, 9.5 V), (GM1_L_r3, Yn, 9.5 V), (GM1_R_r6, Yn, 9.25 V), and (GM1_L_r6, Yn, 9.5 V).

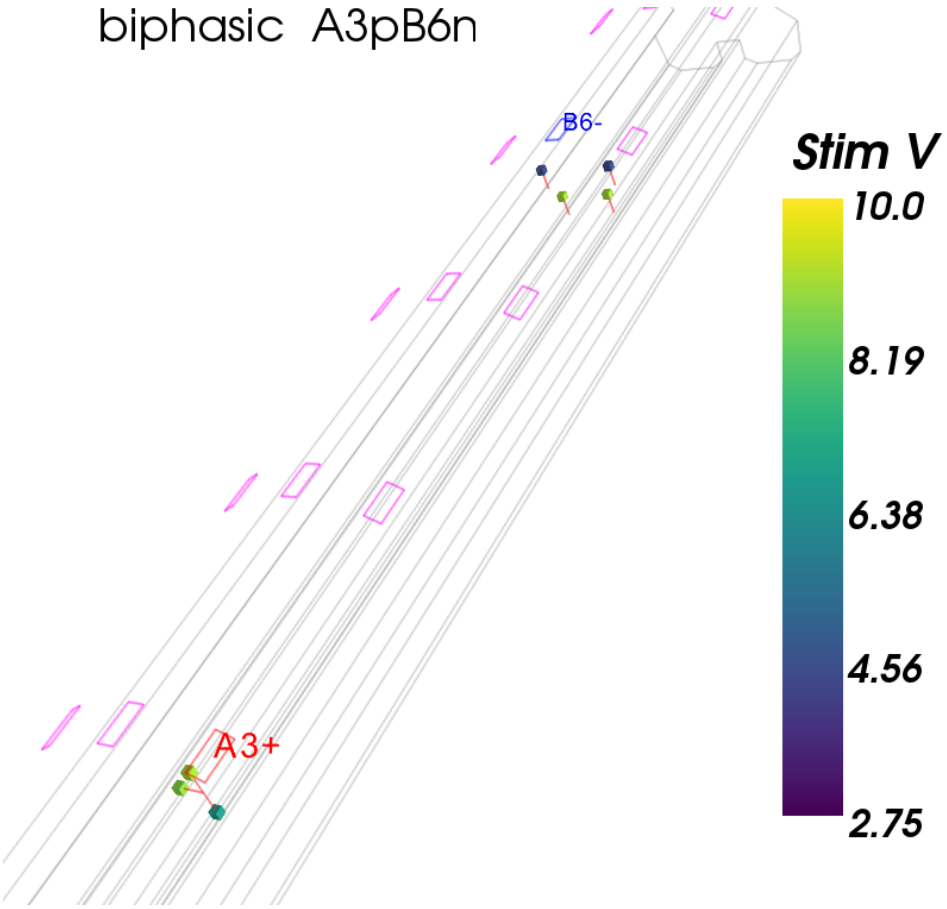

Figure 4.82: Biphasic stimulation using combination A3pB6n. Electrode A3 has a positive phase first followed by a negative phase and is labeled red. Electrode B6 has a negative phase first followed by a positive phase and is labeled blue. All other electrodes are floating and labeled purple. Soma, AH, IS, and AP are displayed as red lines for those neurons whose axon tip membrane voltage exceeds -10 mV with no more than 10 V of stimulation. Dendrites are not displayed. The color of the cube at each axon tip indicates stimulation voltages required for axon tip to reach $V_m > -10$ mV. List of location, axon direction, and threshold: (GM1_L_r3, Yp, 9.0 V), (GM1_R_r6, Yp, 4.5 V), (GM1_L_r6, Yp, 4.5 V), (GM3_L_r6, Yp, 9.0 V), (GM3_R_r6, Yp, 9.0 V), (GM1_L_r3, Xp, 8.75 V), and (GM1_L_r3, Yn, 6.75 V).

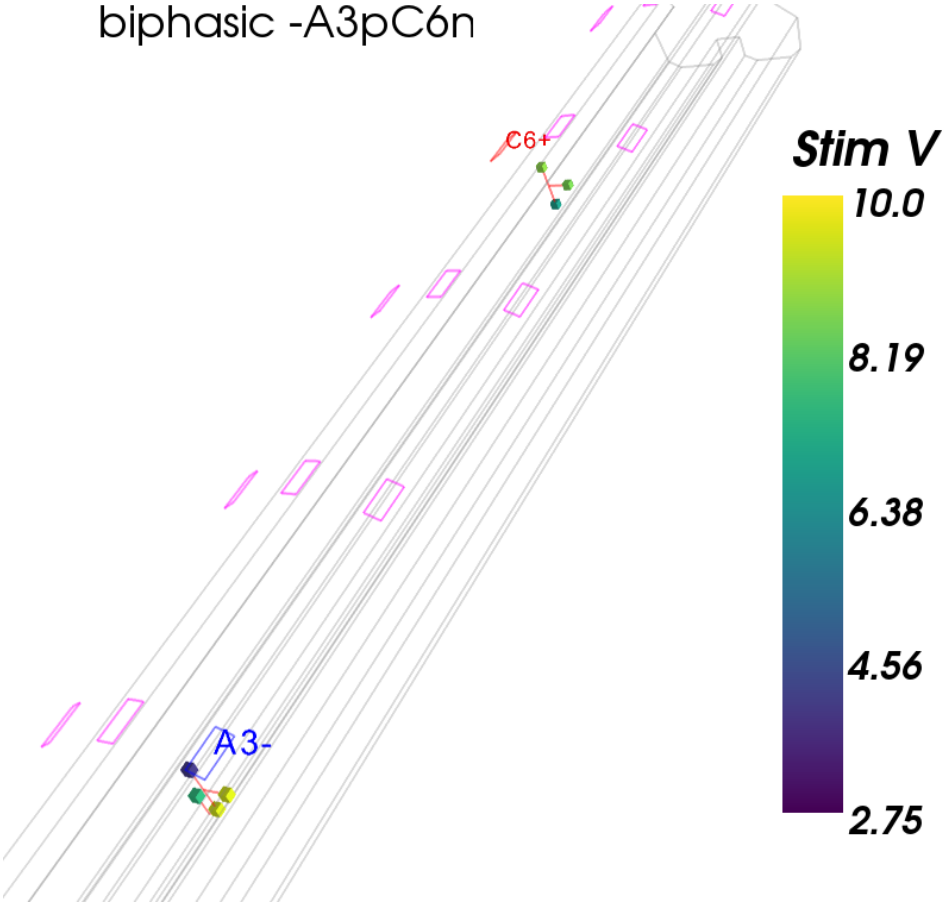

Figure 4.83: Biphasic stimulation using combination -A3pC6n. Electrode C6 has a positive phase first followed by a negative phase and is labeled red. Electrode A3 has a negative phase first followed by a positive phase and is labeled blue. All other electrodes are floating and labeled purple. Soma, AH, IS, and AP are displayed as red lines for those neurons whose axon tip membrane voltage exceeds −10 mV with no more than 10 V of stimulation. Dendrites are not displayed. The color of the cube at each axon tip indicates stimulation voltages required for axon tip to reach $V_m > -10$ mV. List of location, axon direction, and threshold: (GM1_L_r3, Yp, 4.0 V), (GM1_R_r6, Yp, 8.75 V), (GM3_L_r3, Yp, 7.5 V), (GM1_L_r3, Xn, 9.5 V), (GM1_R_r6, Xn, 8.5 V), (GM1_L_r3, Yn, 9.5 V), and (GM1_R_r6, Yn, 6.75 V).

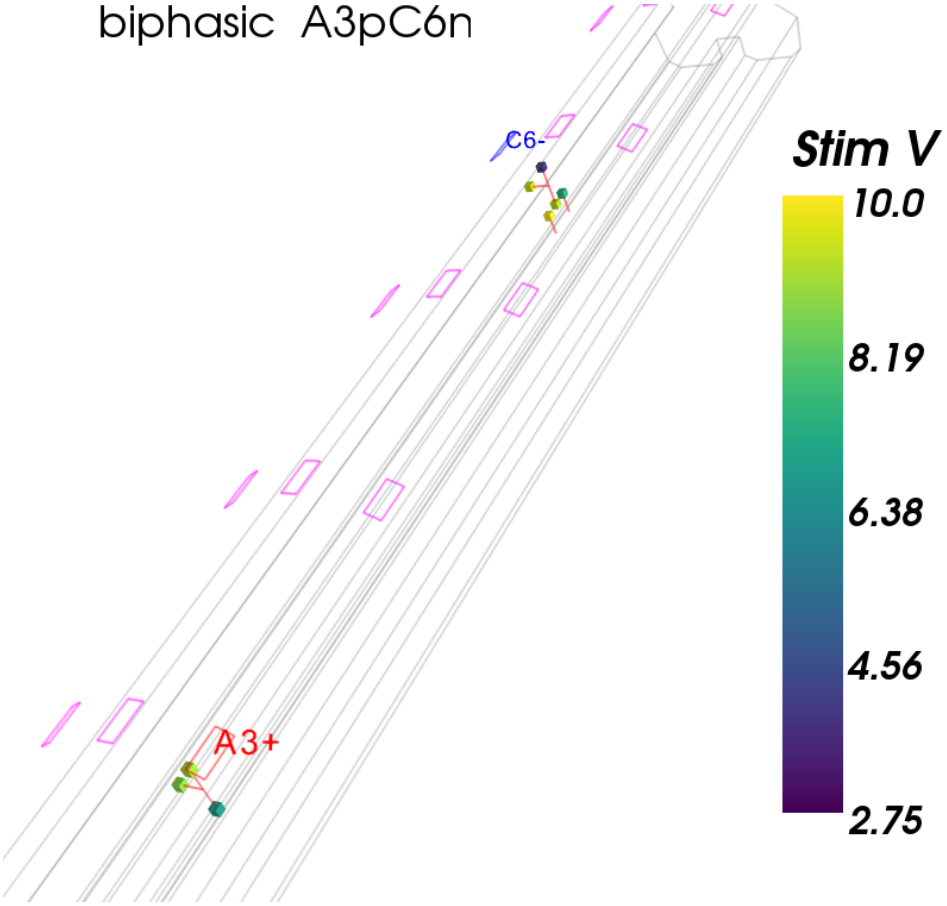

Figure 4.84: Biphasic stimulation using combination A3pC6n. Electrode A3 has a positive phase first followed by a negative phase and is labeled red. Electrode C6 has a negative phase first followed by a positive phase and is labeled blue. All other electrodes are floating and labeled purple. Soma, AH, IS, and AP are displayed as red lines for those neurons whose axon tip membrane voltage exceeds −10 mV with no more than 10 V of stimulation. Dendrites are not displayed. The color of the cube at each axon tip indicates stimulation voltages required for axon tip to reach $V_m > -10$ mV. List of location, axon direction, and threshold: (GM1_L_r3, Yp, 9.0 V), (GM1_R_r6, Yp, 4.0 V), (GM3_R_r6, Yp, 7.5 V), (GM2_R_r6, Yp, 10.0 V), (GM1_L_r3, Xp, 8.75 V), (GM1_R_r6, Xp, 9.5 V), (GM1_L_r3, Yn, 6.75 V), and (GM1_R_r6, Yn, 9.25 V).

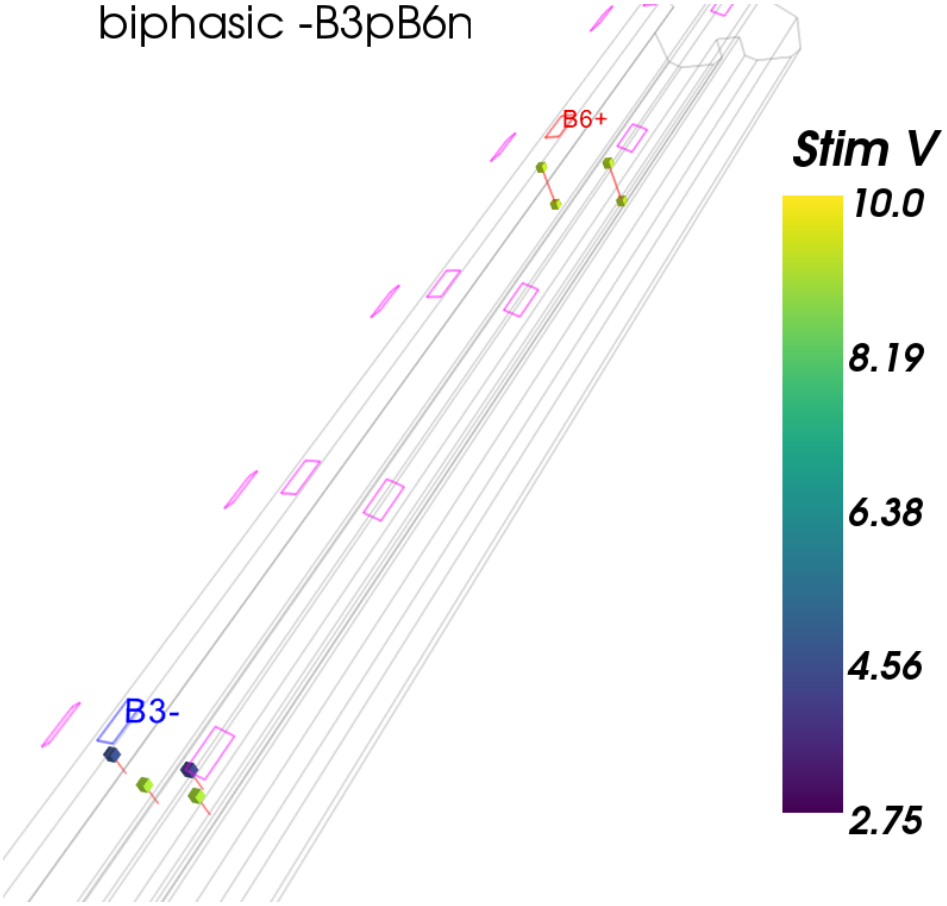

Figure 4.85: Biphasic stimulation using combination -B3pB6n. Electrode B6 has a positive phase first followed by a negative phase and is labeled red. Electrode B3 has a negative phase first followed by a positive phase and is labeled blue. All other electrodes are floating and labeled purple. Soma, AH, IS, and AP are displayed as red lines for those neurons whose axon tip membrane voltage exceeds −10 mV with no more than 10 V of stimulation. Dendrites are not displayed. The color of the cube at each axon tip indicates stimulation voltages required for axon tip to reach $V_m > -10$ mV. List of location, axon direction, and threshold: (GM1_L_r3, Yp, 4.25 V), (GM1_R_r3, Yp, 4.5 V), (GM1_L_r6, Yp, 9.25 V), (GM1_R_r6, Yp, 9.25 V), (GM3_L_r3, Yp, 9.0 V), (GM3_R_r3, Yp, 9.0 V), (GM1_L_r6, Yn, 9.25 V), and (GM1_R_r6, Yn, 9.25 V).

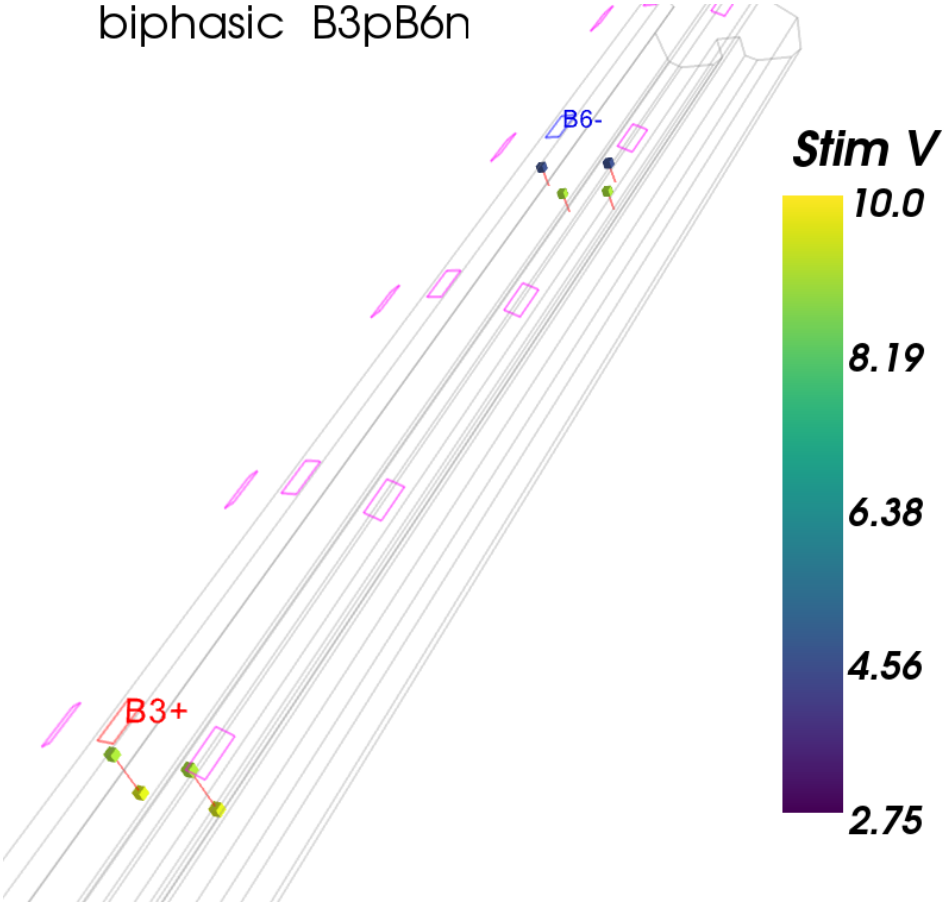

Figure 4.86: Biphasic stimulation using combination B3pB6n. Electrode B3 has a positive phase first followed by a negative phase and is labeled red. Electrode B6 has a negative phase first followed by a positive phase and is labeled blue. All other electrodes are floating and labeled purple. Soma, AH, IS, and AP are displayed as red lines for those neurons whose axon tip membrane voltage exceeds −10 mV with no more than 10 V of stimulation. Dendrites are not displayed. The color of the cube at each axon tip indicates stimulation voltages required for axon tip to reach $V_m > -10$ mV. List of location, axon direction, and threshold: (GM1_L_r3, Yp, 9.0 V), (GM1_R_r3, Yp, 9.0 V), (GM1_L_r6, Yp, 4.5 V), (GM1_R_r6, Yp, 4.5 V), (GM3_L_r6, Yp, 9.0 V), (GM3_R_r6, Yp, 9.0 V), (GM1_L_r3, Yn, 9.5 V), and (GM1_R_r3, Yn, 9.5 V).

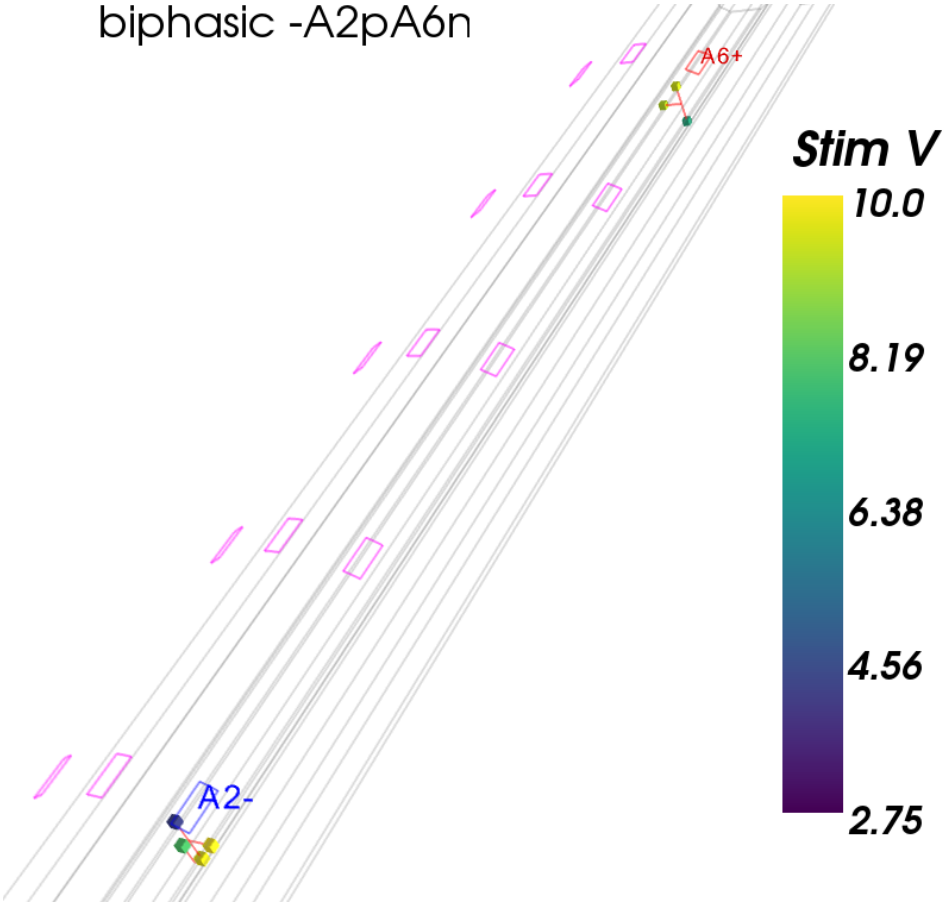

Figure 4.87: Biphasic stimulation using combination -A2pA6n. Electrode A6 has a positive phase first followed by a negative phase and is labeled red. Electrode A2 has a negative phase first followed by a positive phase and is labeled blue. All other electrodes are floating and labeled purple. Soma, AH, IS, and AP are displayed as red lines for those neurons whose axon tip membrane voltage exceeds −10 mV with no more than 10 V of stimulation. Dendrites are not displayed. The color of the cube at each axon tip indicates stimulation voltages required for axon tip to reach $V_m > -10$ mV. List of location, axon direction, and threshold: (GM1_L_r2, Yp, 4.25 V), (GM1_L_r6, Yp, 9.5 V), (GM3_L_r2, Yp, 8.0 V), (GM1_L_r6, Xp, 9.25 V), (GM1_L_r2, Xn, 10.0 V), (GM1_L_r2, Yn, 9.75 V), and (GM1_L_r6, Yn, 7.25 V).

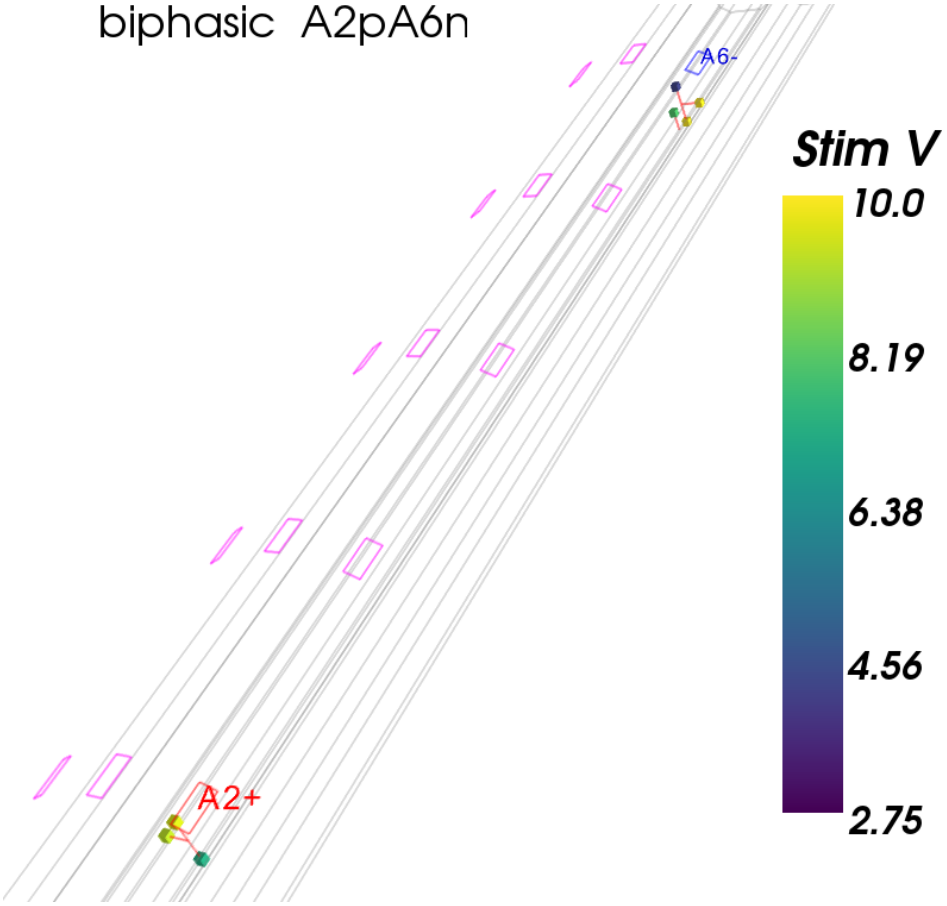

Figure 4.88: Biphasic stimulation using combination A2pA6n. Electrode A2 has a positive phase first followed by a negative phase and is labeled red. Electrode A6 has a negative phase first followed by a positive phase and is labeled blue. All other electrodes are floating and labeled purple. Soma, AH, IS, and AP are displayed as red lines for those neurons whose axon tip membrane voltage exceeds −10 mV with no more than 10 V of stimulation. Dendrites are not displayed. The color of the cube at each axon tip indicates stimulation voltages required for axon tip to reach $V_m > -10$ mV. List of location, axon direction, and threshold: (GM1_L_r2, Yp, 9.5 V), (GM1_L_r6, Yp, 4.25 V), (GM3_L_r6, Yp, 8.0 V), (GM1_L_r2, Xp, 9.25 V), (GM1_L_r6, Xn, 10.0 V), (GM1_L_r2, Yn, 7.25 V), and (GM1_L_r6, Yn, 10.0 V).

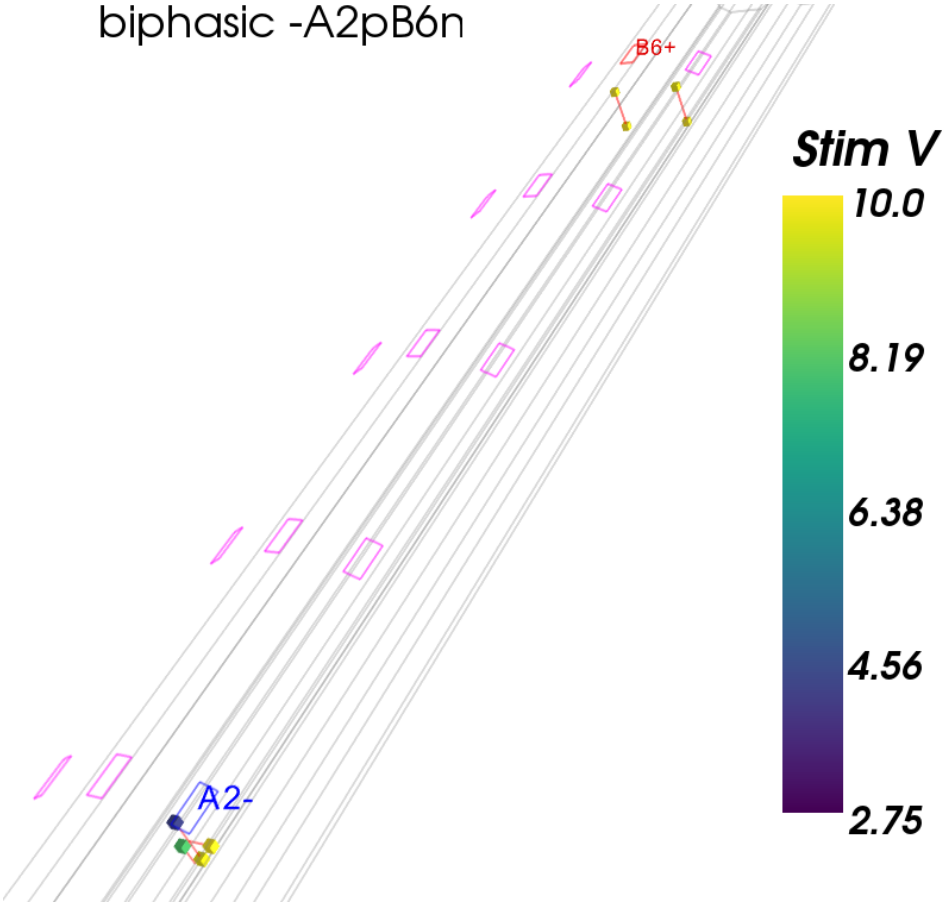

Figure 4.89: Biphasic stimulation using combination -A2pB6n. Electrode B6 has a positive phase first followed by a negative phase and is labeled red. Electrode A2 has a negative phase first followed by a positive phase and is labeled blue. All other electrodes are floating and labeled purple. Soma, AH, IS, and AP are displayed as red lines for those neurons whose axon tip membrane voltage exceeds −10 mV with no more than 10 V of stimulation. Dendrites are not displayed. The color of the cube at each axon tip indicates stimulation voltages required for axon tip to reach $V_m > -10$ mV. List of location, axon direction, and threshold: (GM1_L_r2, Yp, 4.25 V), (GM1_L_r6, Yp, 9.75 V), (GM1_R_r6, Yp, 10.0 V), (GM3_L_r2, Yp, 8.0 V), (GM1_L_r2, Xn, 10.0 V), (GM1_L_r2, Yn, 9.75 V), (GM1_L_r6, Yn, 10.0 V), and (GM1_R_r6, Yn, 10.0 V).

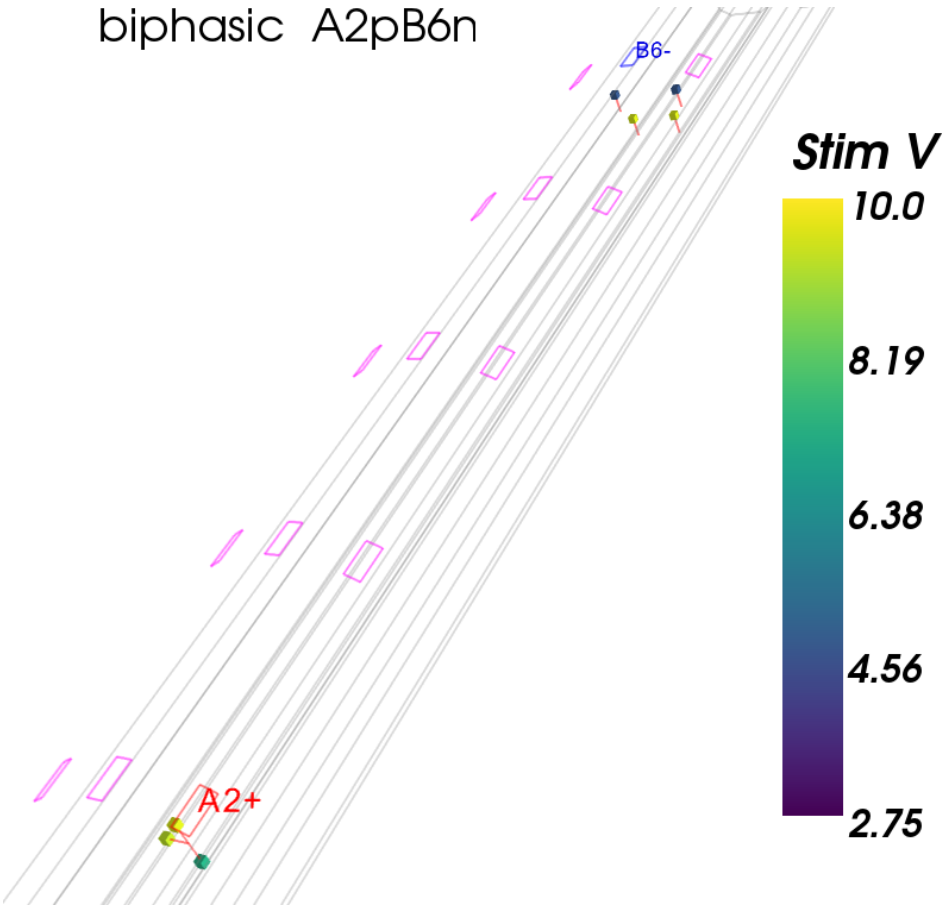

Figure 4.90: Biphasic stimulation using combination A2pB6n. Electrode A2 has a positive phase first followed by a negative phase and is labeled red. Electrode B6 has a negative phase first followed by a positive phase and is labeled blue. All other electrodes are floating and labeled purple. Soma, AH, IS, and AP are displayed as red lines for those neurons whose axon tip membrane voltage exceeds −10 mV with no more than 10 V of stimulation. Dendrites are not displayed. The color of the cube at each axon tip indicates stimulation voltages required for axon tip to reach $V_m > -10$ mV. List of location, axon direction, and threshold: (GM1_L_r2, Yp, 9.5 V), (GM1_L_r6, Yp, 4.75 V), (GM1_R_r6, Yp, 4.75 V), (GM3_L_r6, Yp, 9.5 V), (GM3_R_r6, Yp, 9.5 V), (GM1_L_r2, Xp, 9.25 V), and (GM1_L_r2, Yn, 7.25 V).

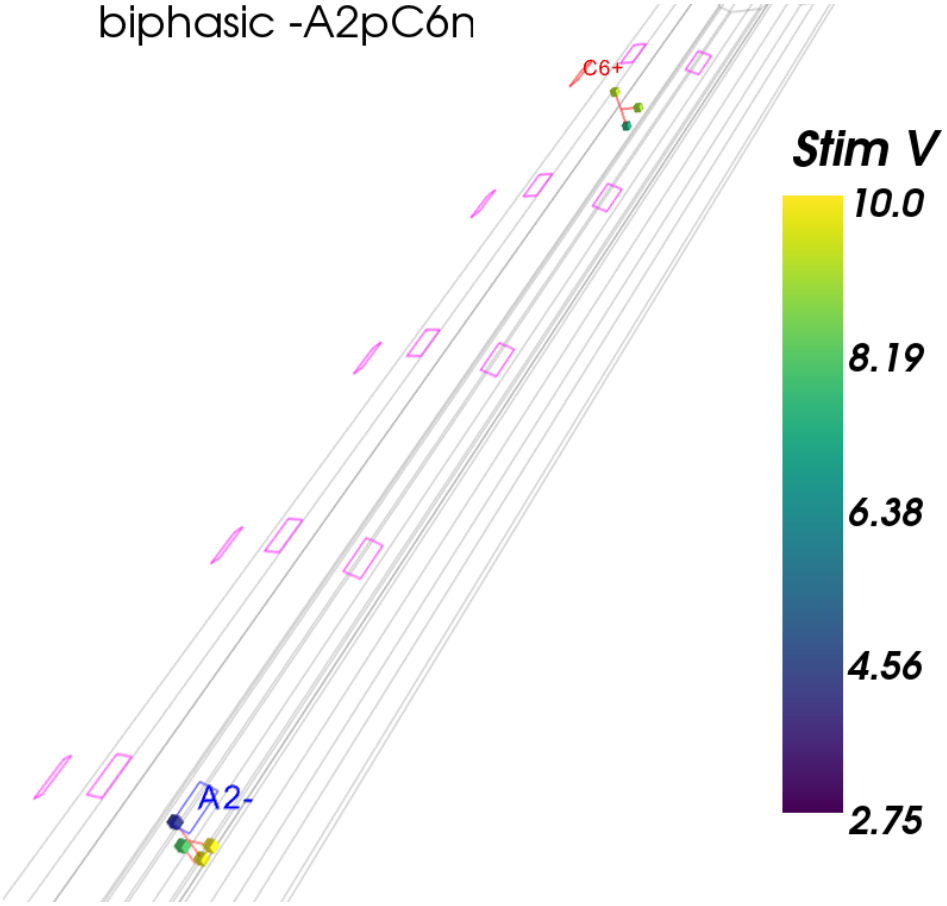

Figure 4.91: Biphasic stimulation using combination -A2pC6n. Electrode C6 has a positive phase first followed by a negative phase and is labeled red. Electrode A2 has a negative phase first followed by a positive phase and is labeled blue. All other electrodes are floating and labeled purple. Soma, AH, IS, and AP are displayed as red lines for those neurons whose axon tip membrane voltage exceeds −10 mV with no more than 10 V of stimulation. Dendrites are not displayed. The color of the cube at each axon tip indicates stimulation voltages required for axon tip to reach $V_m > -10$ mV. List of location, axon direction, and threshold: (GM1_L_r2, Yp, 4.25 V), (GM1_R_r6, Yp, 9.25 V), (GM3_L_r2, Yp, 8.0 V), (GM1_L_r2, Xn, 10.0 V), (GM1_R_r6, Xn, 9.0 V), (GM1_L_r2, Yn, 9.75 V), and (GM1_R_r6, Yn, 7.25 V).

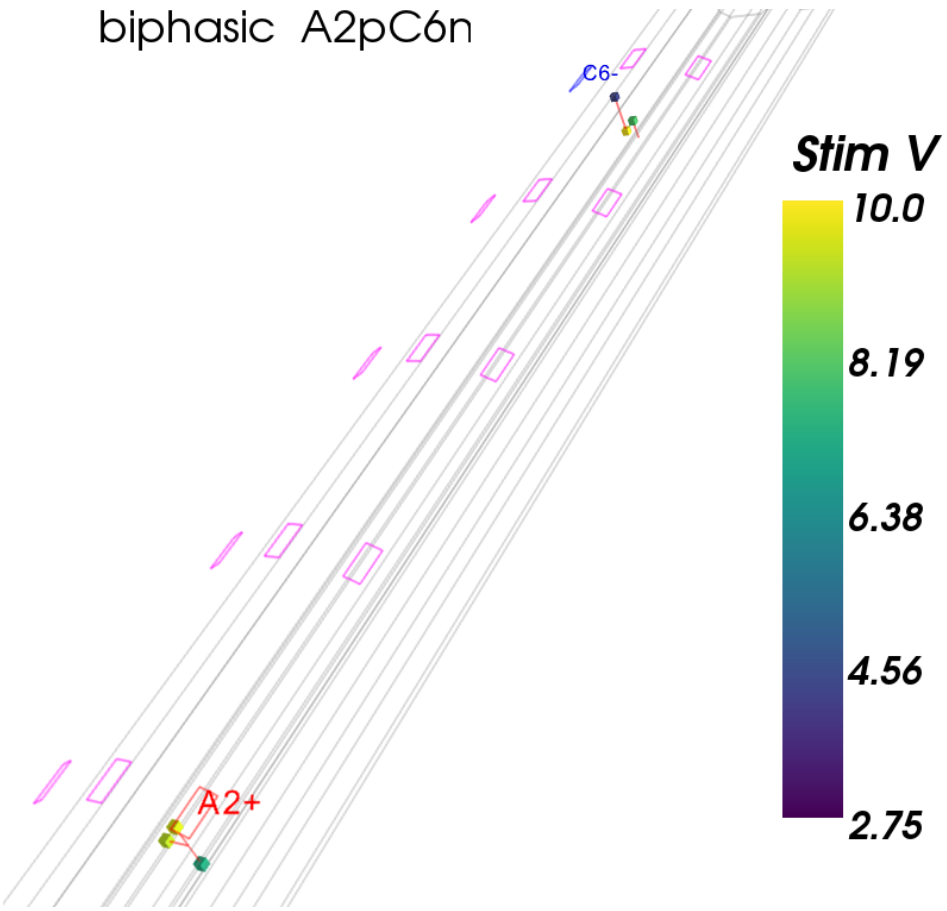

Figure 4.92: Biphasic stimulation using combination A2pC6n. Electrode A2 has a positive phase first followed by a negative phase and is labeled red. Electrode C6 has a negative phase first followed by a positive phase and is labeled blue. All other electrodes are floating and labeled purple. Soma, AH, IS, and AP are displayed as red lines for those neurons whose axon tip membrane voltage exceeds -10 mV with no more than 10 V of stimulation. Dendrites are not displayed. The color of the cube at each axon tip indicates stimulation voltages required for axon tip to reach $V_m > -10$ mV. List of location, axon direction, and threshold: (GM1_L_r2, Yp, 9.5 V), (GM1_R_r6, Yp, 4.25 V), (GM3_R_r6, Yp, 8.0 V), (GM1_L_r2, Xp, 9.25 V), (GM1_L_r2, Yn, 7.25 V), and (GM1_R_r6, Yn, 10.0 V).

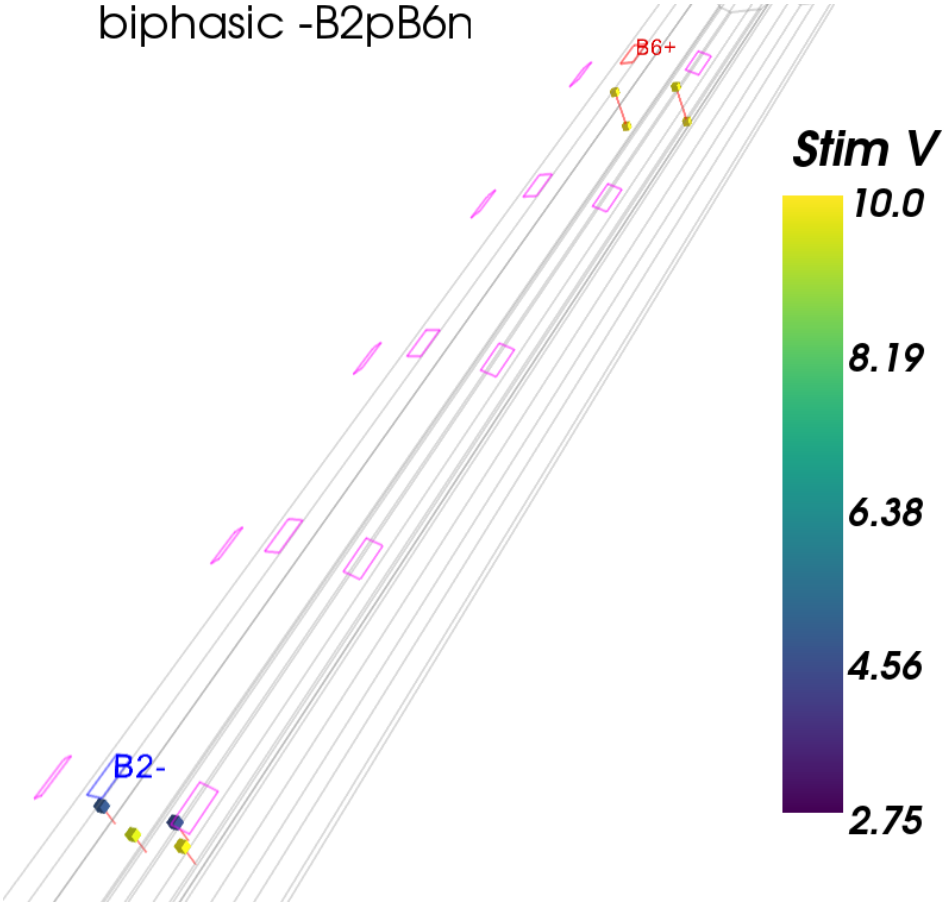

Figure 4.93: Biphasic stimulation using combination -B2pB6n. Electrode B6 has a positive phase first followed by a negative phase and is labeled red. Electrode B2 has a negative phase first followed by a positive phase and is labeled blue. All other electrodes are floating and labeled purple. Soma, AH, IS, and AP are displayed as red lines for those neurons whose axon tip membrane voltage exceeds −10 mV with no more than 10 V of stimulation. Dendrites are not displayed. The color of the cube at each axon tip indicates stimulation voltages required for axon tip to reach $V_m > -10$ mV. List of location, axon direction, and threshold: (GM1_L_r2, Yp, 4.5 V), (GM1_R_r2, Yp, 4.75 V), (GM1_L_r6, Yp, 9.75 V), (GM1_R_r6, Yp, 10.0 V), (GM3_L_r2, Yp, 9.75 V), (GM3_R_r2, Yp, 9.5 V), (GM1_L_r6, Yn, 10.0 V), and (GM1_R_r6, Yn, 10.0 V).

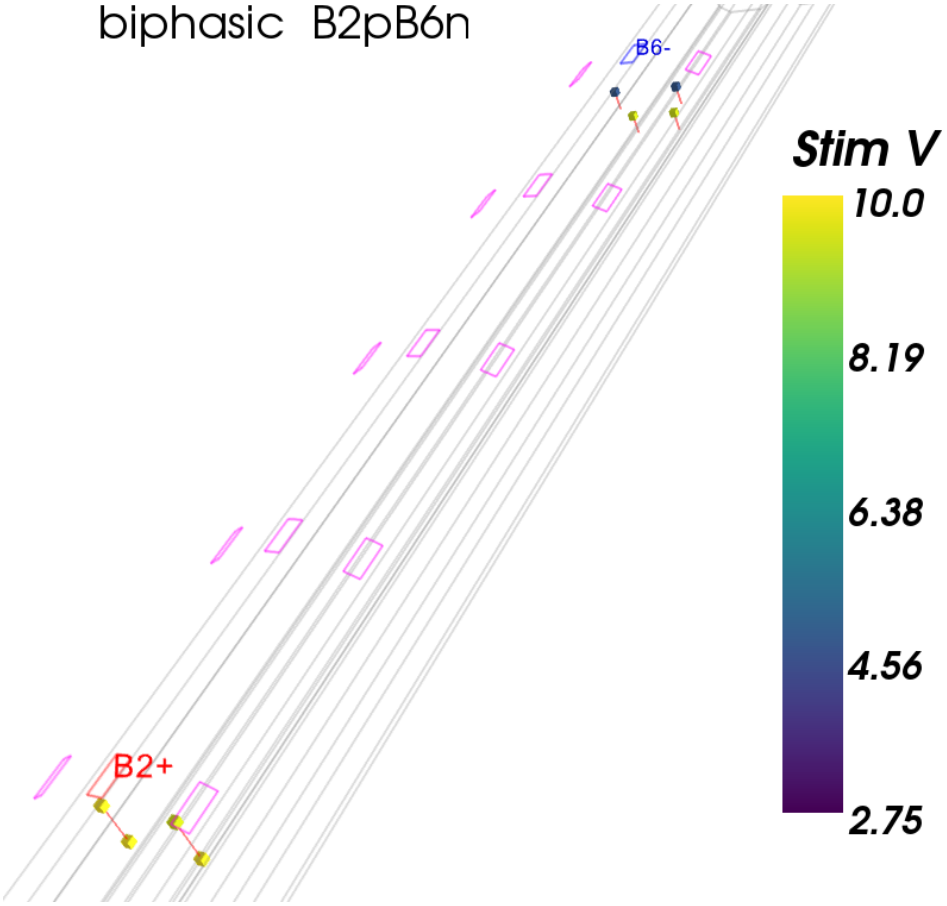

Figure 4.94: Biphasic stimulation using combination B2pB6n. Electrode B2 has a positive phase first followed by a negative phase and is labeled red. Electrode B6 has a negative phase first followed by a positive phase and is labeled blue. All other electrodes are floating and labeled purple. Soma, AH, IS, and AP are displayed as red lines for those neurons whose axon tip membrane voltage exceeds −10 mV with no more than 10 V of stimulation. Dendrites are not displayed. The color of the cube at each axon tip indicates stimulation voltages required for axon tip to reach $V_m > -10$ mV. List of location, axon direction, and threshold: (GM1_L_r2, Yp, 9.5 V), (GM1_R_r2, Yp, 10.0 V), (GM1_L_r6, Yp, 4.75 V), (GM1_R_r6, Yp, 4.75 V), (GM3_L_r6, Yp, 9.5 V), (GM3_R_r6, Yp, 9.5 V), (GM1_L_r2, Yn, 10.0 V), and (GM1_R_r2, Yn, 10.0 V).

Chapter 5

FACILITATING SUB-THRESHOLD SYNAPTIC INPUT USING EPIDURAL STIMULATION TO ACHIEVE NEURON ACTIVATION

After a significant spinal cord injury, the neurons in the spinal cord caudal to the injury often have a decreased amount of connectivity due to the injury and subsequent neural degeneration. But some connectivity and neural activity may remain. Electrical stimulation can of course be used to directly stimulate muscles (Grobelnik and Kralj, 1973; Thrasher, Flett, and Popovic, 2006; Lynch and Popovic, 2008) or activate motor neurons directly (Veraart, W. M. Grill, and Mortimer, 1993), however doing so directly ignores existing neural circuitry in the spinal cord and may also inadvertently activate other undesired neurons. Instead, one hypothesis is to directly facilitate the neuronal activity of existing postural and motor control circuits. Epidural (Edgerton et al., 2008) and transcutaneous (Yury Gerasimenko et al., 2015) electrical stimulation of the spinal cord has proven useful in facilitating the function of existing neural circuitry and even voluntary movement (Harkema et al., 2011; Urban, 2018) in humans and rats with spinal cord injuries.

The experimentally observed facilitation of voluntary movement in subjects with clinically "complete" spinal cord injuries implies that in some of these cases, the brain retains some connectivity with the spinal cord, just not enough to actually move muscles without the aid of spinal stimulation. While there are many existing computational studies of epidural stimulation of the spinal cord (see Section 1.1), to my knowledge there are no existing computational studies exploring how electrical stimulation of the spinal cord could facilitate synaptic input to allow neuron activation. In this chapter, I consider the hypothesis that the electrical stimulation process

somehow facilitates the activation of key neurons in the spinal cord involved in motor control. The anatomical location of these key neurons is still unclear, although recent investigations are shedding light on the possibilities (Asboth et al., 2018; Urban, 2018). It is further unclear how the activity of these neurons is directly facilitated by electrical stimulation. This chapter will consider the possibility that these key neurons are interneurons in the spinal cord that are directly stimulated by the epidural stimulation while being exposed to sub-threshold EPSPs.

The main objective of this chapter is to show that epidural stimulation of a simulated rat spinal cord can facilitate the activation of an interneuron when a sub-threshold EPSP from a synapse on a dendrite is triggered. Of course, in a real biological system, it is possible that multiple EPSPs from sub-threshold synapses in combination with one or more stimulation pulses could result in a facilitated action potential. Understanding single synapse facilitation may lead to principles that are useful in understanding multiple synapse facilitation. Simulations involving multiple stimulation pulses and/or multiple EPSPs could be considered for future work; this thesis will only look at the interaction between a single EPSP and a single stimulation pulse. A number of different synapse weights and stimulation voltages will be used so that the distribution of the number of neurons facilitated vs stimulation voltage and synapse weight can be seen. The properties of this distribution will shed light on the nature of the facilitation process.

Chapter 3 described the interneuron model used in this chapter, and Section 3.4.3 determined the synaptic weights necessary for a single triggered synapse to result in neuron activation without external stimulation. For facilitation, the synaptic weights are required to be less than those thresholds. Chapter 4 explored using epidural stimulation to activate neurons without any triggered synapses. A limited number of neurons were activated by stimulation with a magnitude of less than 5 V, and none were activated using a magnitude of 2.5 V for monophasic stimulation or a

magnitude of 3 V for biphasic stimulation. Chapter 4 also showed that epidural electrical stimulation causes the membrane voltage in the distal tips of the axons and dendrites to have a significantly larger deviation from the resting potential than the proximal parts of the cell. In order to see how this affects the amplitude and propagation of an EPSP from synapses, synapses will be integrated into the model at the distal tips (segment 16) of all dendrites and the middle of the distal section (segment 8) of each dendrite (see locations "A" (segment 8) and "B" (segment 16) in Fig. 3.3). This chapter will consider stimulation magnitudes of 5 V or less, which are biologically relevant. In some of the cases, a few of the neurons will be activated without a synaptic input, but the majority of the neurons will require facilitation by the stimulating field. I found that a synapse triggered within some time window of the stimulation pulse has the greatest opportunity for facilitation. The time window(s) during which the interaction of the stimulation pulse and the synapse response cause neuron activation is referred to as *facilitation window(s)*. After a model neuron is exposed to a subthreshold EPSP (examples seen in Figs. 3.10 and 3.13) the neuron returns to the resting state after some period of time[a]. A subthreshold stimulation pulse (examples shown in Figs. 5.3, 5.3, 5.11 and 5.23) takes less time to return to resting state. Since both the stimulation pulse and the synapse weight are subthreshold by themselves, facilitation cannot occur unless either: (1) a stimulation pulse arrives after a synapse was triggered, but before the neuron's state (V_m, and ion channel state variables) has returned to the resting state, or (2) a synapse is triggered after a stimulation pulse but before the neuron's state has returned to the resting state. Obviously, there are more conditions for facilitation to occur which will be explored a bit in Sections 4.6 and 5.2.

The key finding of this chapter and a contribution of this thesis is that synaptic

[a]For these examples, the neuron takes about 75 ms to 100 ms for the membrane voltage (V_m) and the m ion channel state variables (m_{IKdrSM}, m_{IKaSM}, and m_{INaSM}) to return to the resting state. The h ion channel state variables (h_{IKaSM} and h_{INaSM}) take longer (about 150 ms) to return the resting state.

EPSP inputs that are sub-threshold without stimulation can lead to action potentials with facilitation from epidural stimulation. Prior work (as discussed in Section 1.1) has focused on epidural stimulation of the dorsal roots and myelinated fibers in the white matter. One group of researchers (Capogrosso et al., 2013) have modeled stimulation of interneurons and motor neurons in the spinal cord with epidural stimulation but has not done an intensive study of the interaction of sub-threshold synaptic inputs with epidural stimulation.

Section 5.1 discusses the construction of the simulations and some computational limitations. Section 5.2 shows 8 examples of facilitation using neuron GM1_L_r5_Yn (a neuron in the dorsal horn on the left side under electrode row 5 with an axon pointing in the $-\hat{y}$ direction) and electrode combination A4pA5n (see Section 2.2.1 for electrode combination notation definition) using biphasic and monophasic stimulation. These example sections highlight the facilitation window(s) around a stimulation pulse during which a synaptic input will be facilitated. There is also some evidence that the "least effort" (least magnitude of stimulation and synapse weight) facilitation timing may be dependent on the ion channel states. Section 5.3 summarizes how much facilitation occurs with different stimulation types, synapse locations, stimulation magnitudes, and synapse weights. A significant amount of facilitation occurs when the synapse weight and stimulation magnitude are both large, but sub-threshold. The amount of facilitation decreases as the stimulation magnitude or synapse weight decreases. Section 5.4 finds static voltage features (Section 5.4.1) from static volume conductor simulation and membrane voltage features from stimulation-only (no EPSPs) NEURON simulations (Section 5.4.2) which are useful for separating facilitated neurons (including neurons active with only stimulation) from non-activated neurons. A set of features ($V_{static}^{\text{Synapse}} - V_{static}^{\text{Soma}}$, $V_{static}^{\text{IS}} - V_{static}^{\text{Soma}}$) based on the static volume conductor simulations were better at separating facilitated neurons from

non-activated neurons.

5.1 Modeling of the Facilitation effect

In order to model the mechanism of facilitation, it is necessary to look at the interactions between the effects of a stimulation pulse on a neuron whose synaptic input has been triggered. As shown below, these interactions vary as a function of the time difference between the onset of the stimulation pulse and the onset of synaptic input. In order to study the effect of this time difference, the stimulation pulse onset was fixed in time and the synapse trigger time was varied to include onsets both before and after the stimulation pulse. For each set of parameters (neuron location, orientation, combination, etc.) that would not result in neuron activation without an EPSP, the maximum membrane voltage at the tip of the axon was recorded for each synapse trigger time. A neuron was considered facilitated if the maximum membrane voltage at the axon tip was greater than or equal to $-10\,\text{mV}$, due to the influence of the combined effects of the EPSP and the electrical stimulation and less than $-10\,\text{mV}$ with either alone. The time interval between the onsets that result in facilitation then gives an estimate of how accurately the stimulation pulse must be timed with the existing neuronal activity in order to produce a facilitation effect.

The extracellular voltage was extracted from the volume conductor models and scaled as described in the previous chapter. In addition to the parameters simulated in the last chapter (which yielded 792 simulation configurations for each electrode combination and stimulation type (monophasic or biphasic)), there are 10 synapse locations (distal tip or middle of distal section on 5 dendrites) yielding a total of 7920 simulation parameters. Simulations were conducted using the stimulation voltages and synapse weights in Table 5.1.

In order to understand the temporal interactions between epidural stimulation and the EPSPs, the duration of simulated time was increased from 151 ms to 226 ms,

Table 5.1: Facilitation testing parameters: column $|V_s|$ contains the list of stimulation voltage magnitudes tested, column W_8 contains the list of synapse weights used for the synapse in the middle of the distal section of the dendrite, and W_{16} contains the list of synapse weights used for the synapse of the distal tip of the dendrite.

$\|V_s\|$[mV]	W_8[nS]	W_{16}[nS]
5	3.45	4.783
4	3.443	4.776
3	3.436	4.769
2	3.422	
1	3.394	
0.5	3.337	
	3.225	
	3.0	

and the start of the simulation pulse was moved to $t = 76$ ms to allow for simulation of EPSPs both before, during, and after the stimulation pulse. This time range was believed to be sufficient because the peak of the membrane voltage occurs at a maximum of ~50 ms after synapse trigger, and the maximum membrane voltages due to stimulation pulses occurs within ~25 ms of pulse onset. In each simulation interval, only a single stimulation pulse (at $t = 76$ ms) and a single EPSP (from an Exp2Syn synapse as described in Section 3.3.1) occurred, but the synapse trigger time was selected from the array t_{syn} = [1 ms to 146 ms in steps of 5 ms] (a total of 30 trigger times).

Simulating all of the above parameter configurations would require 792 * (5 dendrites) * (3+8 synapse weights for segments 16 and 8 respectively) * (6 stimulation voltages) * (18 combinations) * (2 stimulation types) * (30 trigger times) =

282,268,800 NEURON simulations, or about 247.5 times the number of simulations required for the previous chapter. Each NEURON simulation for this chapter also can be estimated to take about 1.5 times longer than the simulations in the previous chapter. Since the previous chapter's simulations took on the order of a month to complete, clearly either additional computational resources are required or a smarter sampling algorithm in order to obtain results in a reasonable amount of time. With the goal of reducing computation time while still finding facilitation, a sampling algorithm was written that: (1) avoided simulating synapse firing if the stimulation pulse alone would cause activation, (2) avoided simulations at a particular synapse trigger time if a larger-in-magnitude stimulation voltage or synapse weight did not result in facilitation, unless a neighboring (in time) synapse trigger time did result in facilitation. Using this sampling algorithm, the total number of simulations was reduced to 18,980,825 for monophasic simulations and 10,790,662 for biphasic simulations. The total number of simulations performed (29,771,487) is 10.5% of the number of simulations required to simulate all of the parameter configurations listed earlier. In particular situations, some of the assumptions behind the sampling algorithm could be wrong, and so some facilitation could be missed, but they seem to be true in the cases I specifically examined.

During the NEURON simulations, membrane voltage maxima and minima were recorded at several "probe" locations (axon proper distal tip (seg=16), initial segment ("IS", seg=0), axon hillock ("AH",seg=0), and soma (seg=0). (See Fig. 3.3 for "probe" locations.)

5.2 Examples of facilitation

Before getting to the total amount of facilitation in Section 5.3 or predicting facilitation in Section 5.4, it is necessary to have some understanding of how facilitation occurs and the concept of a facilitation window. A facilitation window is a period

of time near a stimulation pulse during which synaptic input can control the output of the neuron. In this section, I will go through a few examples to help develop a better understanding of the facilitation process.

Consider neuron GM1_L_r5_Yn[b] exposed to stimulation using combination A4pA5n[c] ($V_s^{A4} = V_S G(t)$, $V_s^{A5} = -V_S G(t)$). Based on the data from the last chapter (without synaptic input), biphasic stimulation activates this neuron with stimulation amplitude $V_s = -6\,\text{V}$ or $V_s = 8\,\text{V}$. Using monophasic stimulation it activates using $-4.25\,\text{V}$ of stimulation, and positive monophasic stimulation appears completely ineffective. When synaptic input is present, this situation changes significantly based on the location of the synapse and its synaptic weight. Section 5.2.1 will examine what happens if a synapse is triggered on the distal tip (segment=16) of the distal dendrite pointing in the $+\hat{x}$ direction near the time of a biphasic stimulation pulse. Section 5.2.2 will look at the same situation with 2 polarities of monophasic stimulation. More examples including some with the synapse located in the middle (segment=8) of the distal section are available in Section 5.B.

All of the biphasic examples presented have a "least effort" facilitation window (in terms of least synapse weight and least magnitude of stimulation) for synaptic input ~15-20ms before the stimulation pulse. For the monophasic examples, the facilitation window timing depends on the polarity of the stimulation pulse. With $V_s < 0$, the "least effort" facilitation window for synaptic input is before the stimulation pulse, which is similar to the biphasic examples, but if $V_s > 0$, the facilitation window for synaptic input is mostly after the stimulation pulse.

[b] See Section 4.1 for naming convention. This is a neuron located in the dorsal horn on the left side under electrode row 5 with an axon pointing in the $-\hat{y}$ direction.

[c] See Section 2.2.1 for electrode combination notation definition.

5.2.1 Biphasic stimulation

This section looks an example of facilitation using biphasic stimulation with combination A4pA5n and a negative stimulation ($V_s < 0$) amplitude. Specifically, the facilitation of neuron GM1_L_r5_Yn with a synapse located at segment 16 on the distal dendrite pointing in the $\hat{x}$ direction. Without any synaptic input, the neuron will activate if $V_s = -6\,\mathrm{V}$.

The maximum membrane voltage at the axon tip for the synapse weights, trigger times, and stimulation voltages listed in Section 5.1 can be seen in Fig. 5.1. The stimulation pulse starts at 76 ms. The facilitation window(s) for each pairing of stimulation voltage (V_s) and synapse weight consist of any time that the appropriate line indicating the membrane voltage at the axon tip goes above the red line ($-10\,\mathrm{mV}$). In this case, facilitation window(s) exist both before and after the stimulation pulse, but the "least effort" facilitation occurs before the stimulation pulse.

In this case, the window (in time) of facilitation with $V_s = -2\,\mathrm{V}$ is about 40 ms before the middle of the stimulation pulse and 25 ms after the stimulation pulse for all of the tested synapse weights. Note that there is a reduction in the length of the facilitation time window as V_s approaches 0, especially for the lower values of synapse weight. But there is still some facilitation at the higher synapse weights for $V_s = -0.5\,\mathrm{V}$. For $V_s = -0.5\,\mathrm{V}$ and synapse weight 4.776 nS; there is only an ~15 ms window before the stimulation pulse in which the synapse must fire in order to experience facilitation. Anecdotally, all of the biphasic facilitation plots that I have examined exhibit the same pattern: there exists a "least effort" facilitation window before the stimulation pulse.

Figure 5.2 shows the membrane voltage at the axon tip and the synapse location for $V_s = -2\,\mathrm{V}$ and synapse weight 4.783 nS for all the synapse trigger times shown in Fig. 5.1. The periods of neuron activation are shown in orange-red, while the

synapse trigger time is shown as a dashed cyan line, and the start of the stimulation pulse is depicted as a dotted black line. Any synapse time that results in an activation is part of the facilitation window.

The response of the neuron (membrane voltage and ion-channel state variables) to just the effect of a synaptic input (with synapse weight of 4.783 nS) alone can be found in Fig. 3.13. The response of the neuron to stimulation of level $V_s = -2\,\mathrm{V}$ alone can be found in Fig. 5.3.

When $V_s = -2\,\mathrm{V}$ and the synapse weight takes the value 4.783 nS, a synapse trigger time at $t = 66\,\mathrm{ms}$ maximizes the membrane voltage at the axon tip (compared to other synapse trigger times). Figure 5.4 shows the neuron response to these parameters. Note that this synapse trigger time causes the stimulation pulse to occur when m_{IKdrSM} is at a maximum near the synapse and h_{INaSM} is at a minimum (where m_{IKdrSM} and h_{INaSM} are ion state variables discussed in Section 3.1). These ion channel states may make the neurons more sensitive to biphasic stimulation and explain why the "least effort" facilitation window for biphasic stimulation occurs before the stimulation pulse. Additional examples of biphasic stimulation in Sections 5.B.1 to 5.B.3 show the same behavior.

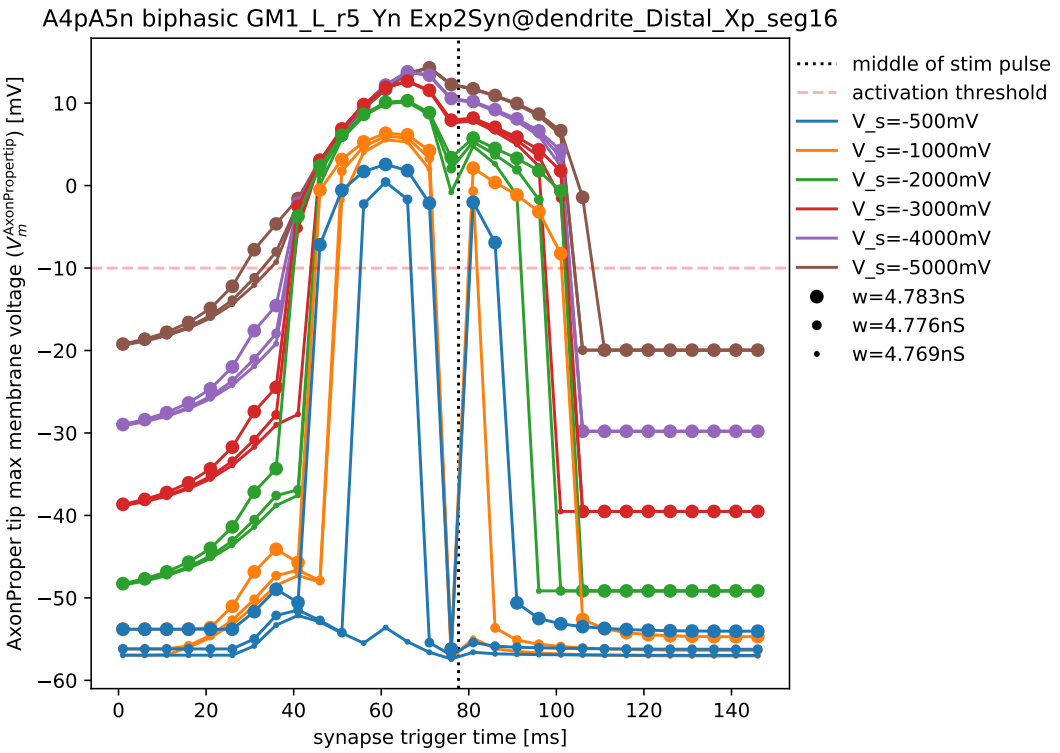

Figure 5.1: Membrane voltage at the axon tip (V_m^{axontip}) vs synapse trigger time for a neuron whose axon points in the $-\hat{y}$ direction located at GM1_L_r5. This neuron's synapse is at segment 16 on the distal dendrite that points in the $+\hat{x}$ direction and is exposed to biphasic epidural stimulation using stimulating electrode combination A4pA5n. The stimulation pulse starts at t=76.0ms and the maximum pulse amplitudes occur at t=77.66ms ± 0.16ms. The following list contains tuples of the form (V_s, w, $\#T_B$, $\#T_A$), where V_s is the stimulation voltage, w is the synapse weight, and ($\#T_B$, $\#T_A$) is the number of synapse trigger time samples (x-axis samples in the above graph) before or after the stimulation pulse, respectively, given the values of V_s and w that result in neuron activation (a value of V_m^{axontip} above $-10\,\text{mV}$) : (-5.0V, 4.783nS, 10, 6), (-5.0V, 4.776nS, 9, 5), (-5.0V, 4.769nS, 9, 5), (-4.0V, 4.783nS, 8, 5), (-4.0V, 4.776nS, 8, 5), (-4.0V, 4.769nS, 8, 5), (-3.0V, 4.783nS, 8, 5), (-3.0V, 4.776nS, 8, 5), (-3.0V, 4.769nS, 7, 4), (-2.0V, 4.783nS, 8, 5), (-2.0V, 4.776nS, 7, 4), (-2.0V, 4.769nS, 7, 3), (-1.0V, 4.783nS, 6, 5), (-1.0V, 4.776nS, 5, 1), (-1.0V, 4.769nS, 5, 0), (-0.5V, 4.783nS, 6, 2), and (-0.5V, 4.776nS, 3, 0).

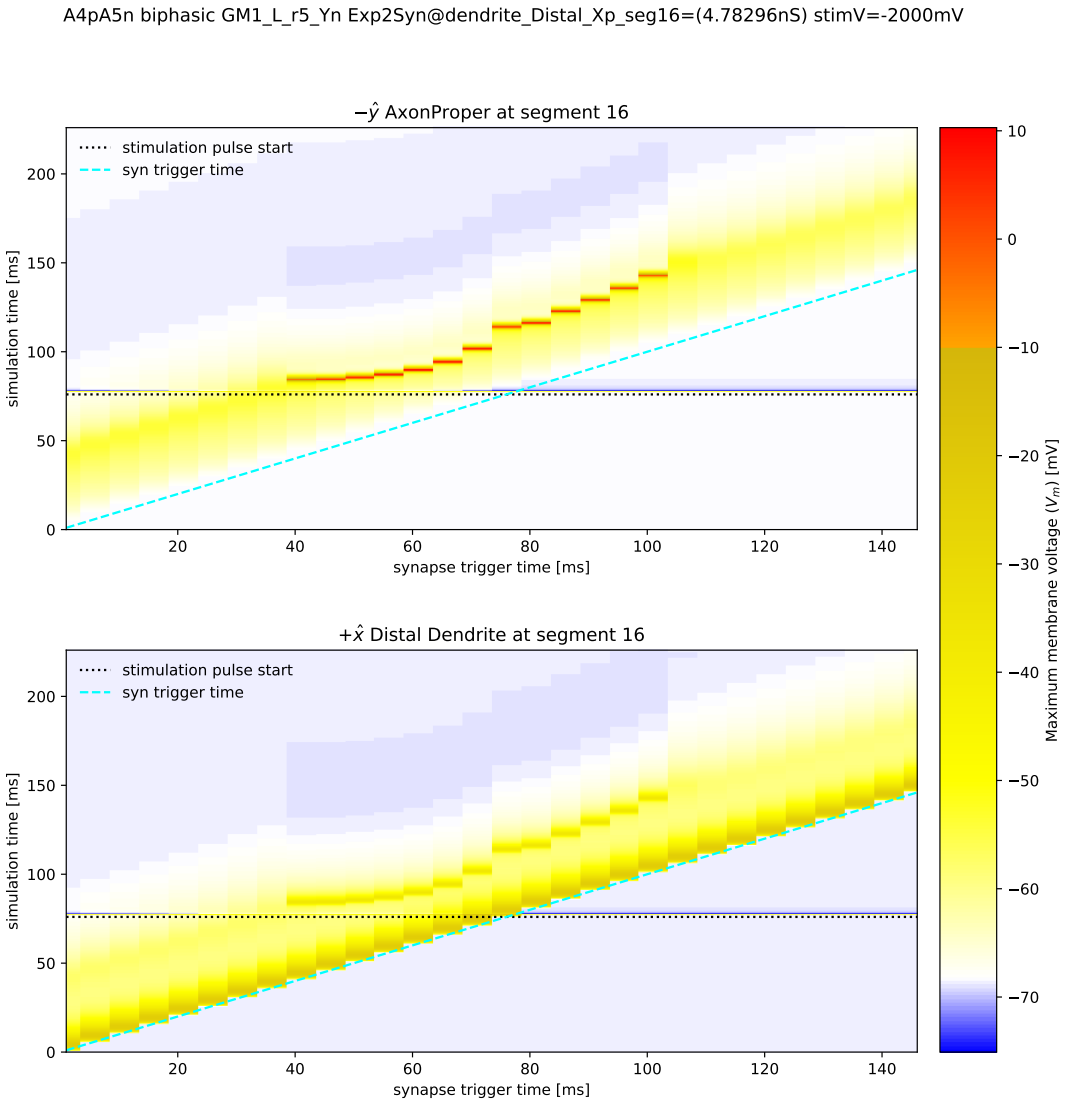

Figure 5.2: Membrane voltage (V_m) (see colormap) at the axon tip (top figure) and at the synapse location (bottom figure) as a function of synapse trigger time (x-axis) and simulation time (y-axis). Measured on neuron GM1_L_r5_Yn exposed to -2.0 V of biphasic epidural stimulation using stimulating electrode combination A4pA5n while a synaptic input with synapse weight=4.783nS is triggered at varying times on the distal dendrite that points in the $+\hat{x}$ direction at segment 16. The electrical stimulation pulse starts at t=76.0ms and the maximum amplitudes of the pulse occur at t=77.66ms ± 0.16ms. The colormap is white when $V_m = -68.31$ mV (the resting membrane voltage for the distal axon tip) and changes from dark yellow to orange at $V_m = -10$ mV to indicate neuron activation. Synapse trigger times that have a dark yellow to orange color above them are a part of the "facilitation window."

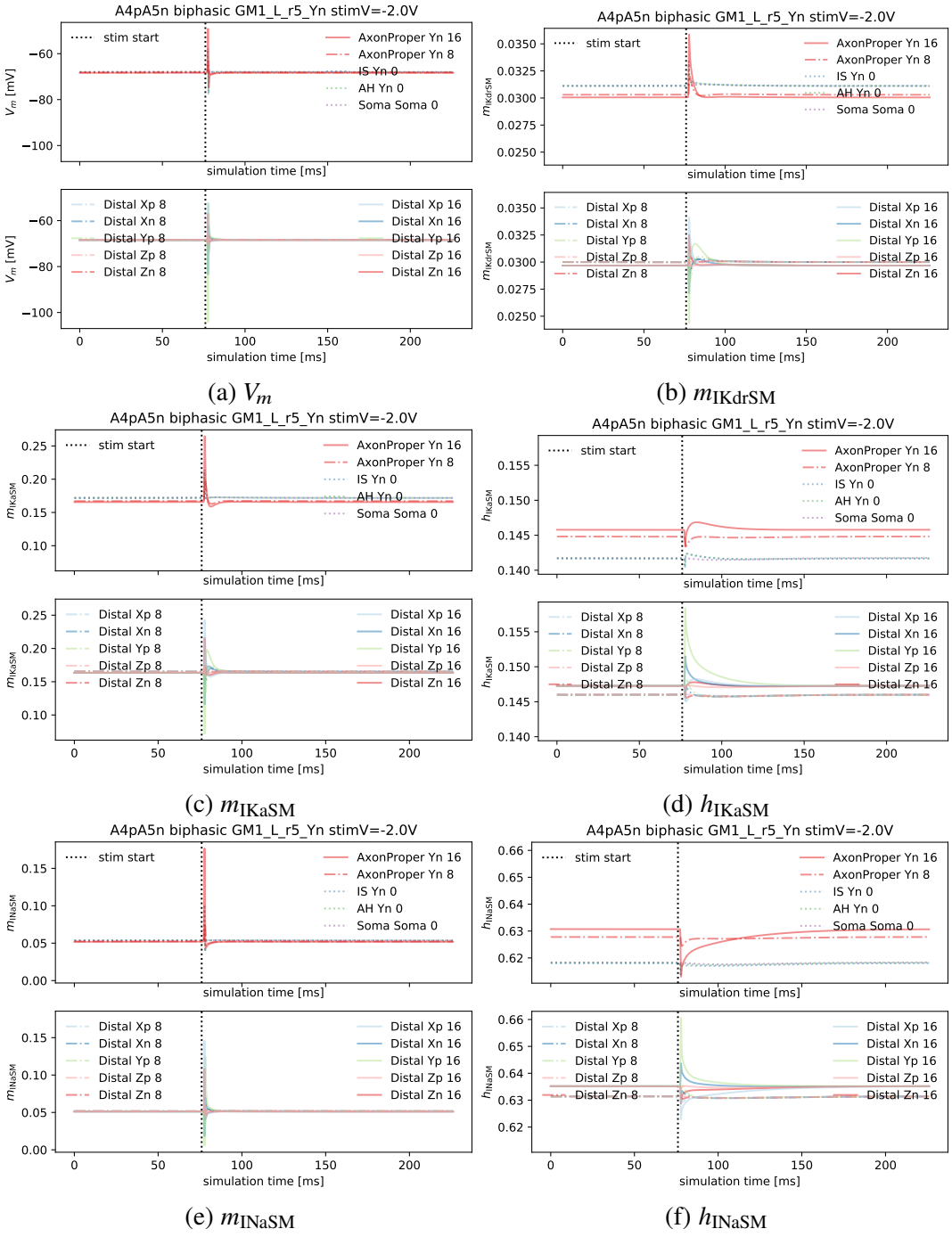

(a) V_m

(b) m_{IKdrSM}

(c) m_{IKaSM}

(d) h_{IKaSM}

(e) m_{INaSM}

(f) h_{INaSM}

Figure 5.3: Stimulation only: Each subplot plots a different variable ((a) V_m, (b) m_{IKdrSM}, (c) m_{IKaSM}, (d) h_{IKaSM}, (e) m_{INaSM}, and (f) h_{INaSM}) against simulation time (ms) for probes on axon-soma (sub-top) and dendrites (sub-bottom). All data measured using neuron GM1_L_r5_Yn exposed to -2.0 V of biphasic stimulation using stimulating electrode combination A4pA5n. The stimulation pulse starts at t=76.0ms and the maximum amplitudes of the pulse occur at t=77.66ms ± 0.16ms.

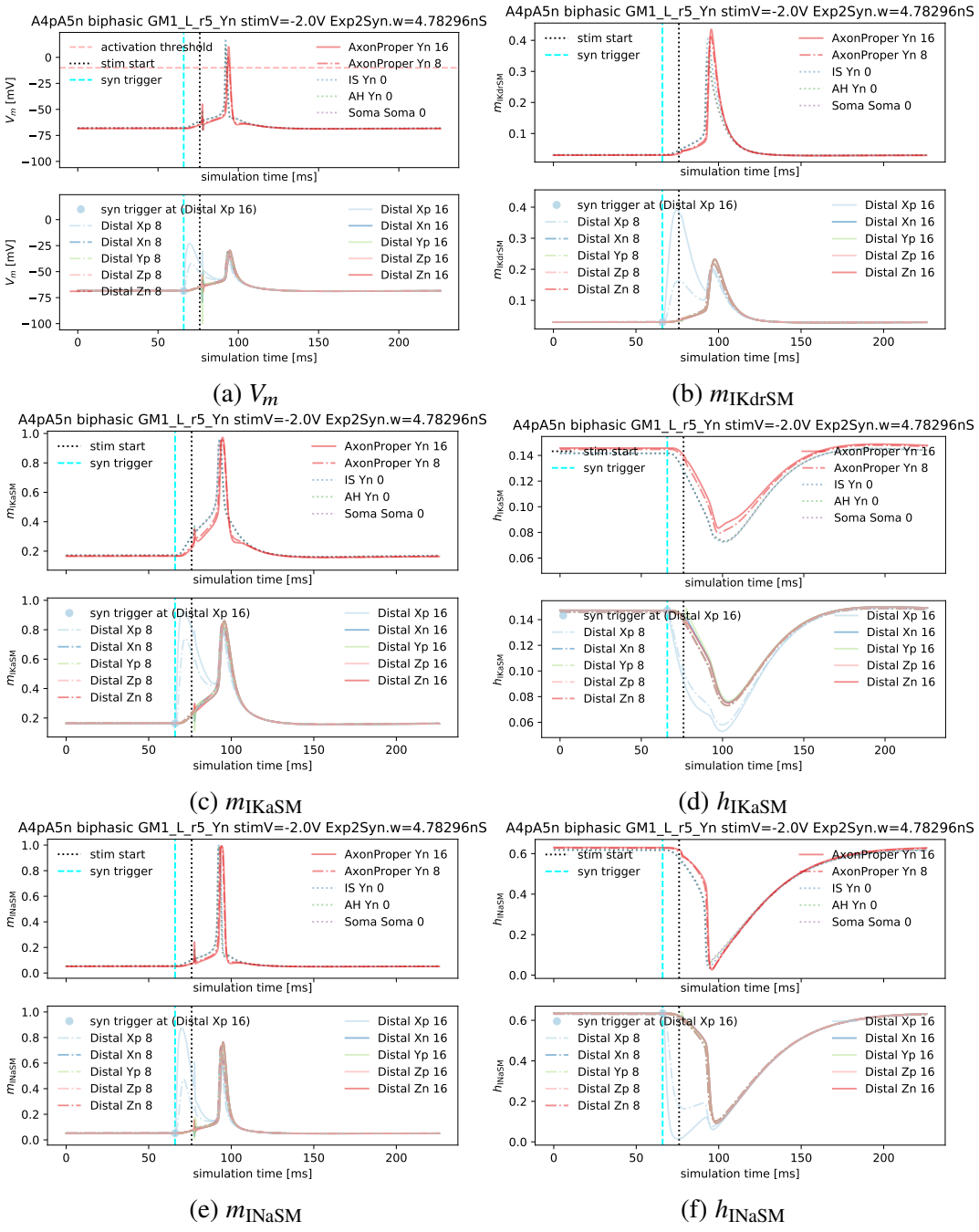

(a) V_m (b) m_{IKdrSM}

(c) m_{IKaSM} (d) h_{IKaSM}

(e) m_{INaSM} (f) h_{INaSM}

Figure 5.4: Stimulation + EPSP: Each subplot plots a different variable ((a) V_m, (b) m_{IKdrSM}, (c) m_{IKaSM}, (d) h_{IKaSM}, (e) m_{INaSM}, and (f) h_{INaSM}) against simulation time (ms) for probes on axon-soma (sub-top) and dendrites (sub-bottom). Measured on neuron GM1_L_r5_Yn exposed to −2.0 V of biphasic stimulation using stimulating electrode combination A4pA5n. The stimulation pulse starts at t=76.0ms and the maximum amplitudes of the pulse occur at t=77.66ms ± 0.16ms. An Exp2Syn synapse was triggered at t=66.0 ms with a synaptic weight of 4.783nS. The synapse was located at segment 16 on the distal dendrite that points in the $+\hat{x}$ direction.

5.2.2 Monophasic stimulation

This section looks at an example of facilitation using monophasic stimulation with combination A4pA5n with both negative and positive stimulation (V_s). Specifically, the facilitation of neuron GM1_L_r5_Yn with a synapse located at segment 16 on the distal dendrite pointing in the $\hat{x}$ direction. Without any synaptic input, the neuron will activate if $V_s \leq -4.25\,\text{V}$.

The maximum membrane voltage at the axon tip for the synapse weights, trigger times, and stimulation voltages listed in Section 5.1 can be seen in Fig. 5.5 for $V_s < 0$ and Fig. 5.9 for $V_s > 0$. Unlike the biphasic stimulation examples, which all have "least effort" facilitation window(s) before the stimulation pulse, in this case if $V_s > 0$, the facilitation window for synaptic input is longer after the stimulation pulse than before the stimulation pulse. The "least effort" facilitation window in this case is when the stimulation pulse occurs. If $V_s < 0$, then the "least effort" facilitation window for synaptic input occurs before the stimulation pulse in the biphasic examples.

With $V_s = -4\,\text{V}$, there are two facilitation windows (one before the stimulation pulse (about 35 ms to 40 ms in width), a gap of about 5 ms to 10 ms of time with no facilitation around the stimulation pulse, and another window after the stimulation pulse with a width of about 35 ms. With $V_s = -3\,\text{V}$, the facilitation window is about 55 ms wide with 40 ms before the stimulation pulse and 15 ms after with no gap in between. For [-2, -1, 0.5]ms, the facilitation windows are all before the stimulation pulse, similar to the biphasic stimulation examples.

Figure 5.6 shows the membrane voltage at the axon tip and the synapse location for $V_s = -2\,\text{V}$ and synapse weight 4.783 nS. Figure 5.10 shows the same for $V_s = 2\,\text{V}$ and the same synapse weight. As in the previous section, the periods of neuron activation are shown in orange-red, while the synapse trigger time is shown as a

dashed cyan line, and the start of the stimulation pulse as a dotted black line.

The response of the neuron (membrane voltage and ion-channel state variables) to just the EPSP (with synapse weight of 4.783 nS) alone can be found in Fig. 3.13. The response of the neuron to $V_s = -2$ V stimulation alone can be found in Fig. 5.7 and $V_s = 2$ V stimulation alone in Fig. 5.11. For $V_s = -2$ V, a synapse trigger time of 71 ms (shown in Fig. 5.8) resulted in the maximum axon tip membrane voltage with a synaptic weight of 4.783 nS. In this case, the stimulation pulse occurs when V_m at the synapse location is a maximum, m_{IKdrSM} is approaching maximum, m_{IKaSM} is close to maximum, m_{INaSM} is near maximum, and h_{INaSM} is approaching minimum. Further study would be required to determine which factors are important for "least effort" timing, but none of the biphasic stimulation examples had "least effort" timing at the maximum of V_m at the synapse.

For the case of $V_s = 2$ V and synapse weight 4.783 nS, the membrane voltage at the axon tip is maximized (compared to other synapse trigger times) when the synapse trigger time coincides with the start of the stimulation pulse. Figure 5.12 shows the neuron response to these parameters.

Additional examples of facilitation with monophasic stimulation and a synapse located in the middle of the distal section of the same dendrite are available in Sections 5.B.4 and 5.B.5. Based on these examples, it appears that the timing of the facilitation window(s) depends on the magnitude, sign, and orientation of the neuron (and likely the orientation of the dendrite with the triggered synapse). There are also differences in the "least effort" facilitation timing between monophasic and biphasic stimulation that should be looked into further.

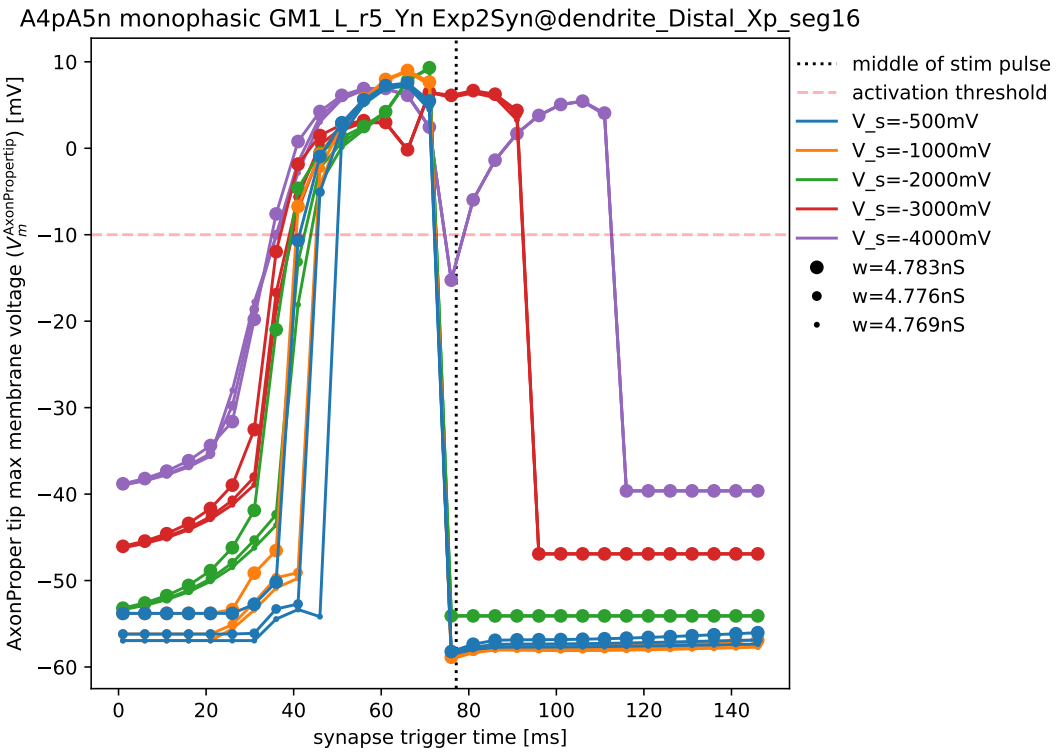

Figure 5.5: Membrane voltage at the axon tip (V_m^{axontip}) vs synapse trigger time for a neuron whose axon points in the $-\hat{y}$ direction located at GM1_L_r5. This neuron has a synapse triggered at segment 16 on the distal dendrite that points in the $+\hat{x}$ direction and is exposed to monophasic epidural stimulation using stimulating electrode combination A4pA5n. The stimulation pulse starts at t=76.0ms and has a maximum amplitude at t=77.13ms. This neuron is active without any EPSPs if exposed to -5.0V of stimulation. The following list contains tuples of the form (V_s, w, $\#T_B$, $\#T_A$) where V_s is the stimulation voltage, w is the synapse weight, and ($\#T_B$, $\#T_A$) is the number of synapse trigger time samples (x-axis samples in the above graph) before or after the stimulation pulse, respectively, given the values of V_s and w that result in neuron activation (a value of V_m^{axontip} above $-10\,\text{mV}$) : (-4.0V, 4.783nS, 8, 7), (-4.0V, 4.776nS, 8, 7), (-4.0V, 4.769nS, 7, 7), (-3.0V, 4.783nS, 8, 3), (-3.0V, 4.776nS, 8, 3), (-3.0V, 4.769nS, 8, 3), (-2.0V, 4.783nS, 7, 0), (-2.0V, 4.776nS, 6, 0), (-2.0V, 4.769nS, 6, 0), (-1.0V, 4.783nS, 7, 0), (-1.0V, 4.776nS, 6, 0), (-1.0V, 4.769nS, 6, 0), (-0.5V, 4.783nS, 6, 0), (-0.5V, 4.776nS, 6, 0), and (-0.5V, 4.769nS, 5, 0).

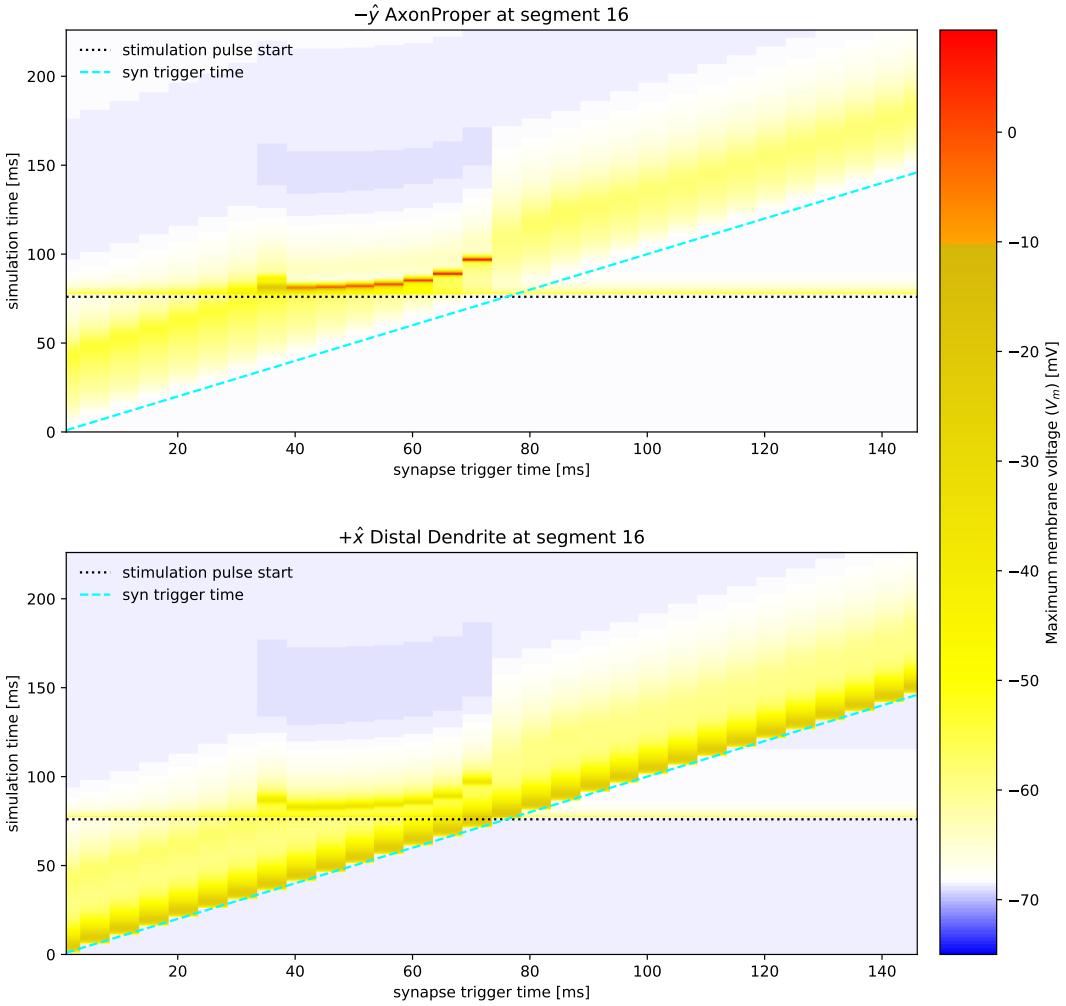

Figure 5.6: Membrane voltage (V_m) (see colormap) at the axon tip (top figure) and at the synapse location (bottom figure) as a function of synapse trigger time (x-axis) and simulation time (y-axis). Measured on neuron GM1_L_r5_Yn exposed to −2.0 V of monophasic epidural stimulation using stimulating electrode combination A4pA5n while a synaptic input with synapse weight=4.783nS is triggered at varying times on the distal dendrite that points in the $+\hat{x}$ direction at segment 16. The electrical stimulation pulse starts at t=76.0ms and has a maximum amplitude at t=77.13ms. The colormap is white when $V_m = -68.31$ mV (the resting membrane voltage for the distal axon tip) and changes from dark yellow to orange at $V_m = -10$ mV to indicate neuron activation.

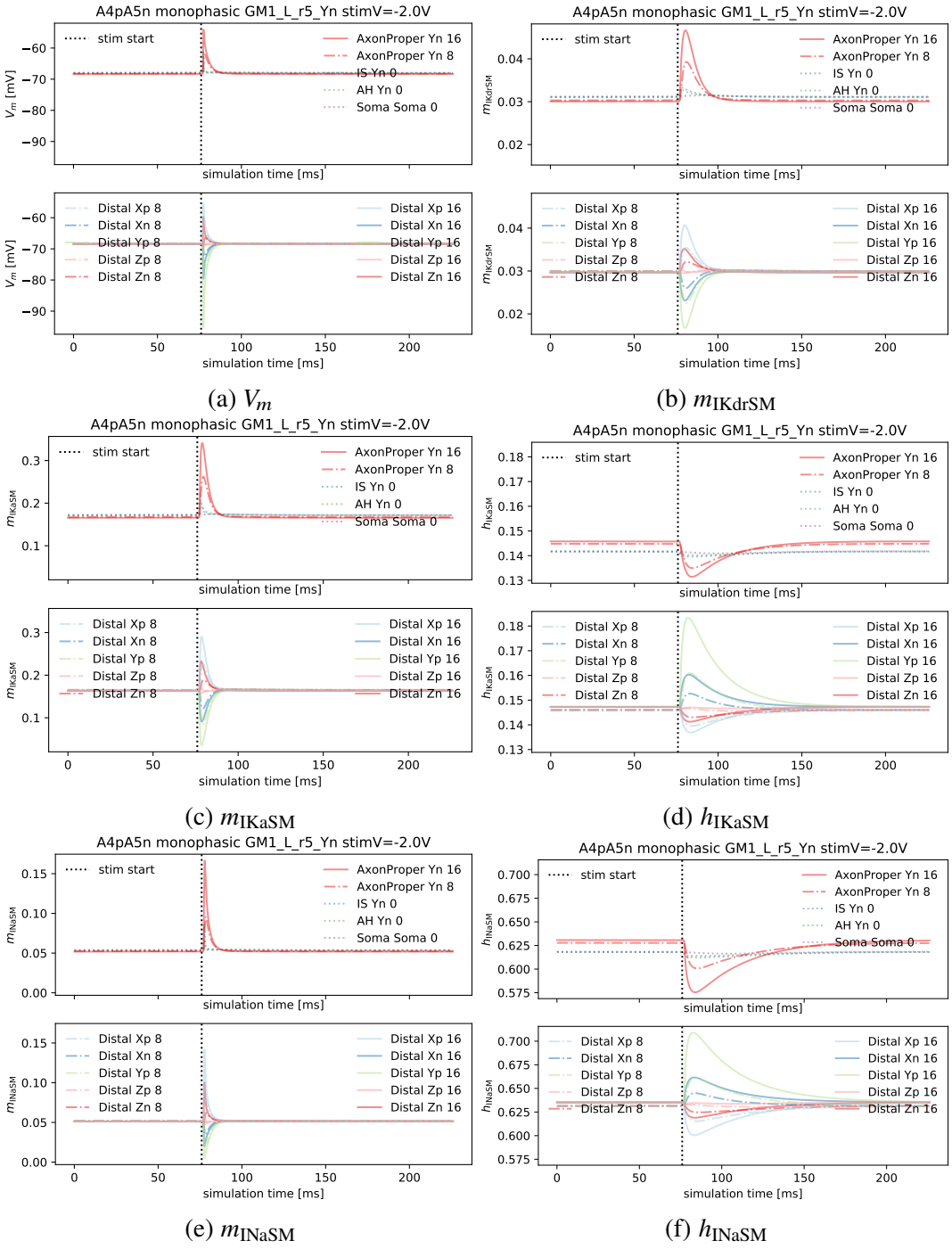

(a) V_m

(b) m_{IKdrSM}

(c) m_{IKaSM}

(d) h_{IKaSM}

(e) m_{INaSM}

(f) h_{INaSM}

Figure 5.7: Stimulation only: Each subplot plots a different variable ((a) V_m, (b) m_{IKdrSM}, (c) m_{IKaSM}, (d) h_{IKaSM}, (e) m_{INaSM}, and (f) h_{INaSM}) against simulation time (ms) for probes on axon-soma (sub-top) and dendrites (sub-bottom). All data measured using neuron GM1_L_r5_Yn exposed to −2.0 V of monophasic stimulation using stimulating electrode combination A4pA5n. The stimulation pulse starts at t=76.0ms and has a maximum amplitude at t=77.13ms.

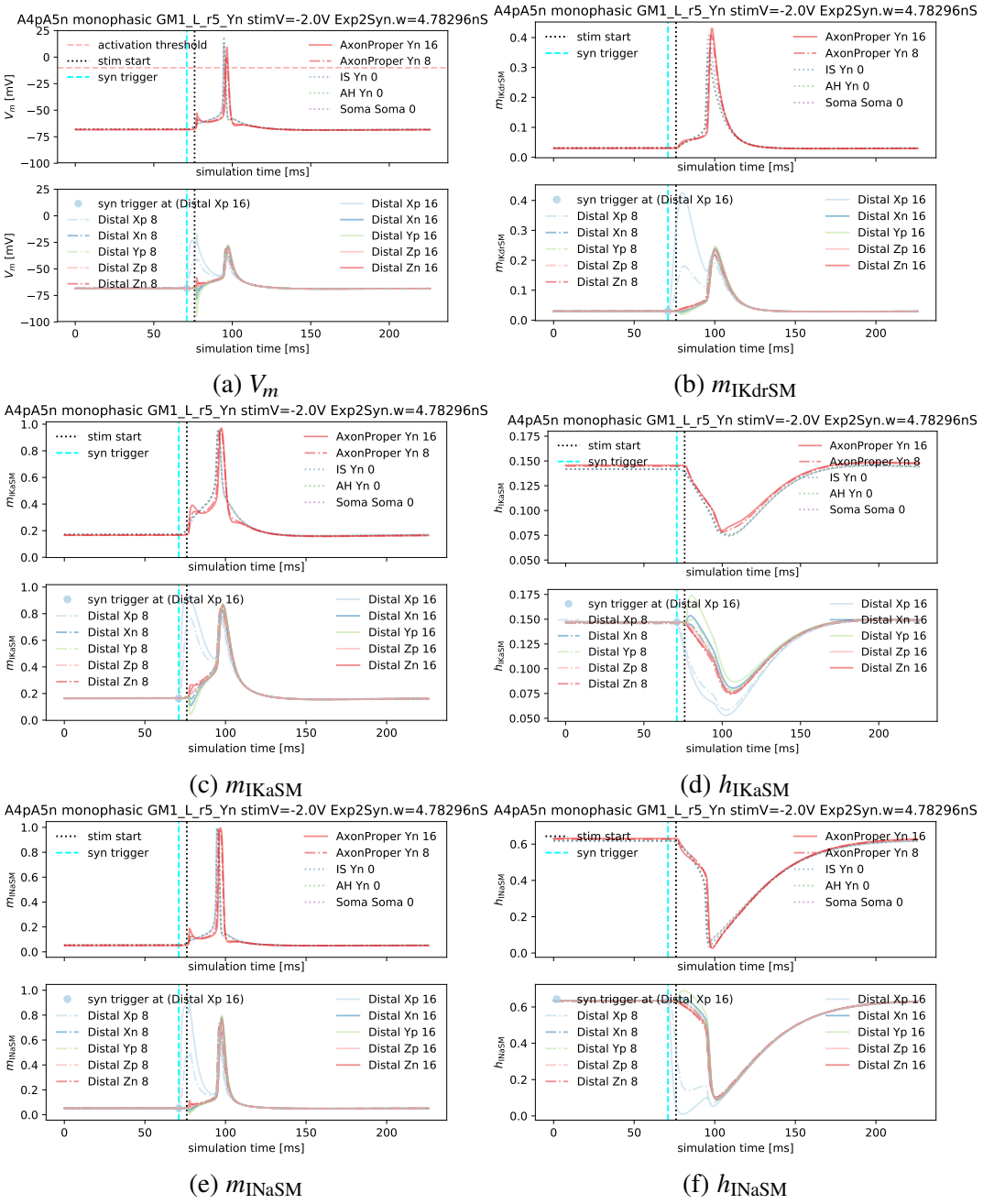

(a) V_m

(b) m_{IKdrSM}

(c) m_{IKaSM}

(d) h_{IKaSM}

(e) m_{INaSM}

(f) h_{INaSM}

Figure 5.8: Stimulation + EPSP: Each subplot plots a different variable ((a) V_m, (b) m_{IKdrSM}, (c) m_{IKaSM}, (d) h_{IKaSM}, (e) m_{INaSM}, and (f) h_{INaSM}) against simulation time (ms) for probes on axon-soma (sub-top) and dendrites (sub-bottom). Measured on neuron GM1_L_r5_Yn exposed to −2.0 V of monophasic stimulation using stimulating electrode combination A4pA5n. The stimulation pulse starts at t=76.0ms and has a maximum amplitude at t=77.13ms. An Exp2Syn synapse was triggered at t=71.0 ms with a synaptic weight of 4.783nS. The synapse was located at segment 16 on the distal dendrite that points in the $+\hat{x}$ direction.

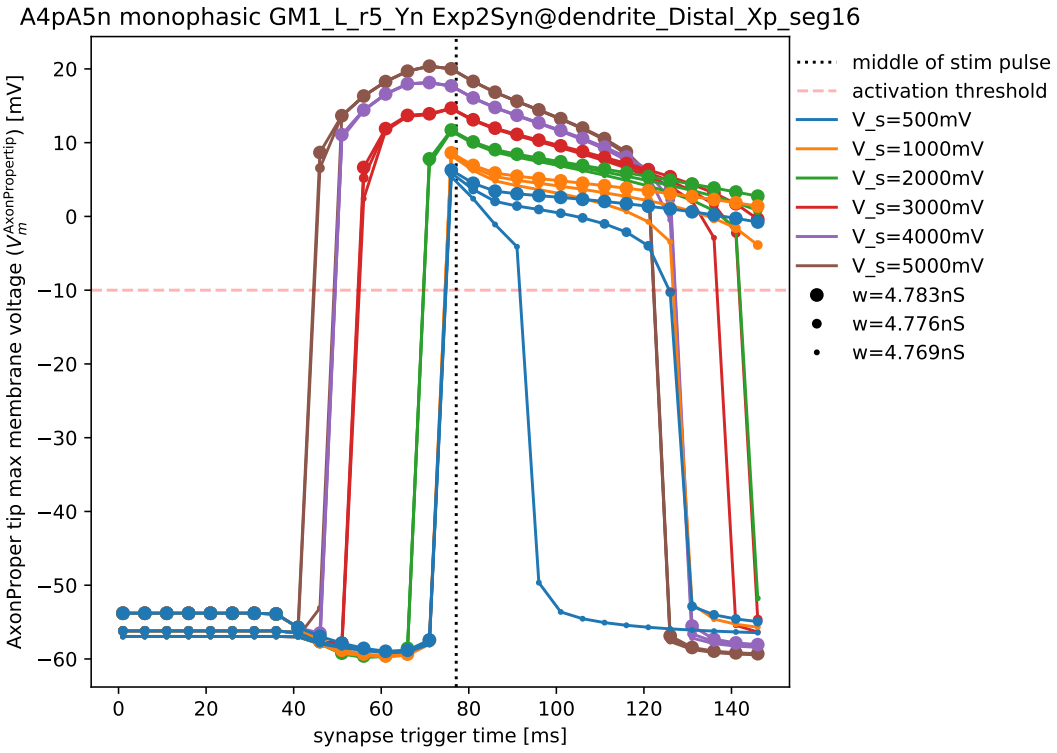

Figure 5.9: Membrane voltage at the axon tip (V_m^{axontip}) vs synapse trigger time for a neuron whose axon points in the $-\hat{y}$ direction located at GM1_L_r5. This neuron has a synapse triggered at segment 16 on the distal dendrite that points in the $+\hat{x}$ direction and is exposed to monophasic epidural stimulation using stimulating electrode combination A4pA5n. The stimulation pulse starts at t=76.0ms and has a maximum amplitude at t=77.13ms. The following list contains tuples of the form (V_s, w, $\#T_B$, $\#T_A$) where V_s is the stimulation voltage, w is the synapse weight, and ($\#T_B$, $\#T_A$) is the number of synapse trigger time samples (x-axis samples in the above graph) before or after the stimulation pulse, respectively, given the values of V_s and w that result in neuron activation (a value of V_m^{axontip} above $-10\,\text{mV}$) : (5.0V, 4.783nS, 7, 9), (5.0V, 4.776nS, 7, 9), (5.0V, 4.769nS, 6, 9), (4.0V, 4.783nS, 6, 10), (4.0V, 4.776nS, 6, 10), (4.0V, 4.769nS, 6, 10), (3.0V, 4.783nS, 5, 14), (3.0V, 4.776nS, 5, 13), (3.0V, 4.769nS, 5, 12), (2.0V, 4.783nS, 2, 14), (2.0V, 4.776nS, 2, 14), (2.0V, 4.769nS, 2, 13), (1.0V, 4.783nS, 1, 14), (1.0V, 4.776nS, 1, 14), (1.0V, 4.769nS, 1, 10), (0.5V, 4.783nS, 1, 14), (0.5V, 4.776nS, 1, 9), and (0.5V, 4.769nS, 1, 3).

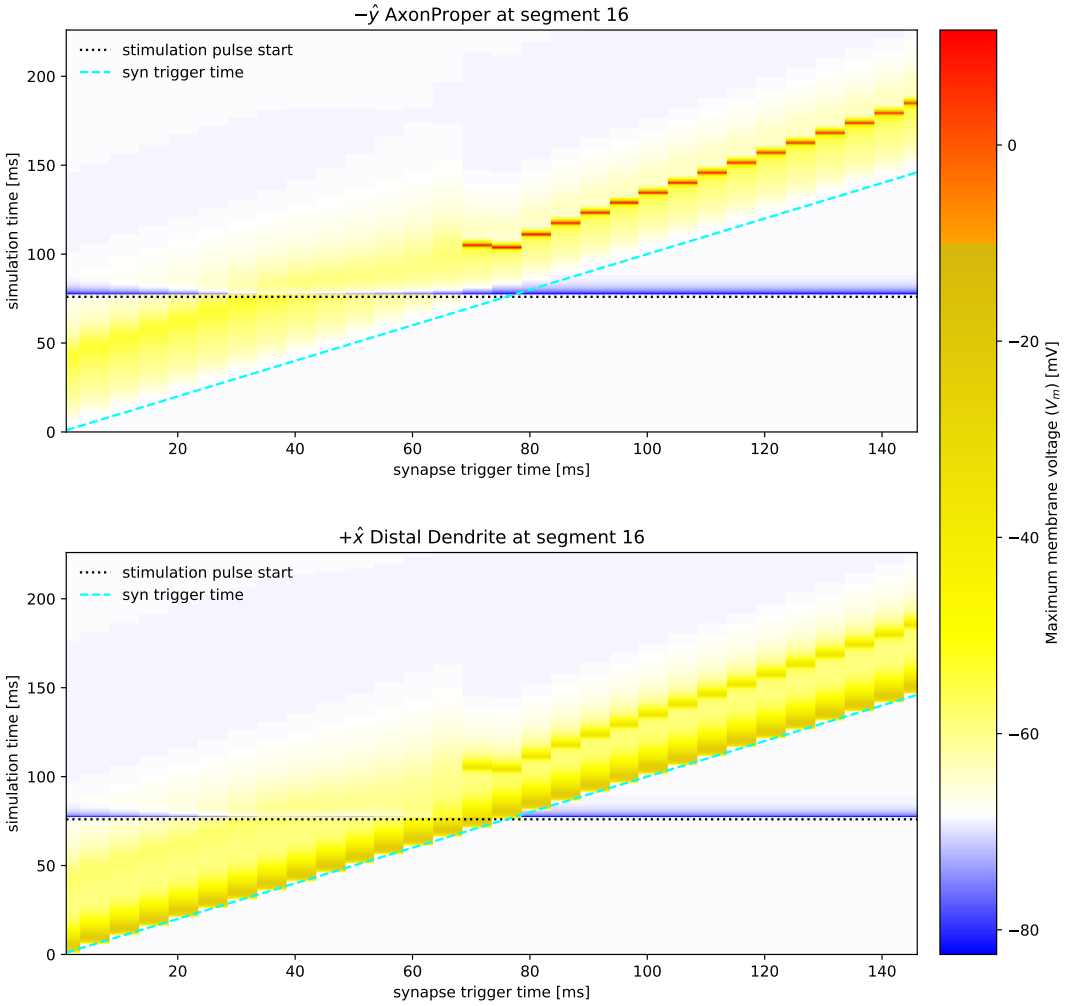

Figure 5.10: Membrane voltage (V_m) (see colormap) at the axon tip (top figure) and at the synapse location (bottom figure) as a function of synapse trigger time (x-axis) and simulation time (y-axis). Measured on neuron GM1_L_r5_Yn exposed to 2.0 V of monophasic epidural stimulation using stimulating electrode combination A4pA5n while a synaptic input with synapse weight=4.783nS is triggered at varying times on the distal dendrite that points in the $+\hat{x}$ direction at segment 16. The electrical stimulation pulse starts at t=76.0ms and has a maximum amplitude at t=77.13ms. The colormap is white when $V_m = -68.31$ mV (the resting membrane voltage for the distal axon tip) and changes from dark yellow to orange at $V_m = -10$ mV to indicate neuron activation.

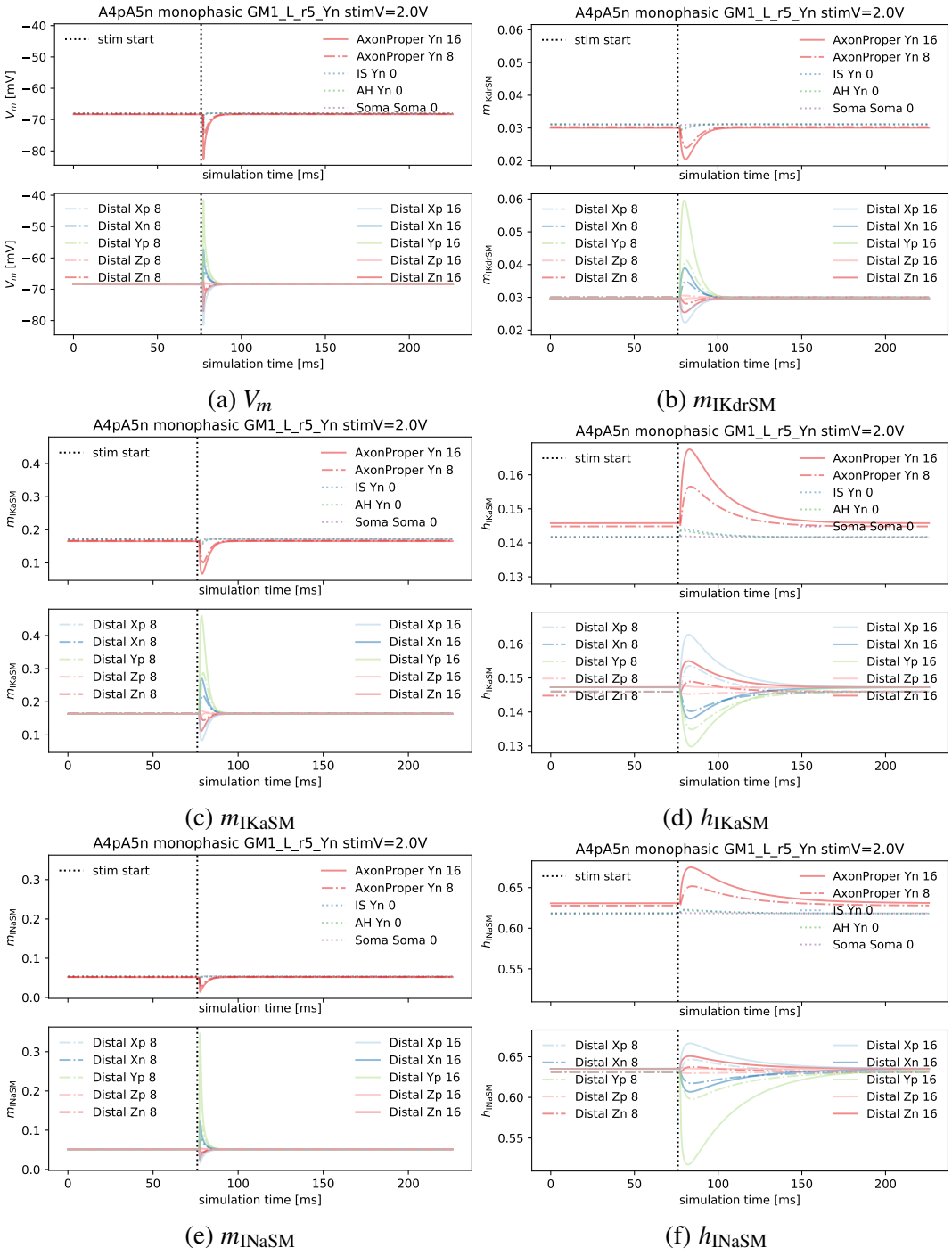

(a) V_m

(b) m_{IKdrSM}

(c) m_{IKaSM}

(d) h_{IKaSM}

(e) m_{INaSM}

(f) h_{INaSM}

Figure 5.11: Stimulation only: Each subplot plots a different variable ((a) V_m, (b) m_{IKdrSM}, (c) m_{IKaSM}, (d) h_{IKaSM}, (e) m_{INaSM}, and (f) h_{INaSM}) against simulation time (ms) for probes on axon-soma (sub-top) and dendrites (sub-bottom). All data measured using neuron GM1_L_r5_Yn exposed to 2.0 V of monophasic stimulation using stimulating electrode combination A4pA5n. The stimulation pulse starts at t=76.0ms and has a maximum amplitude at t=77.13ms.

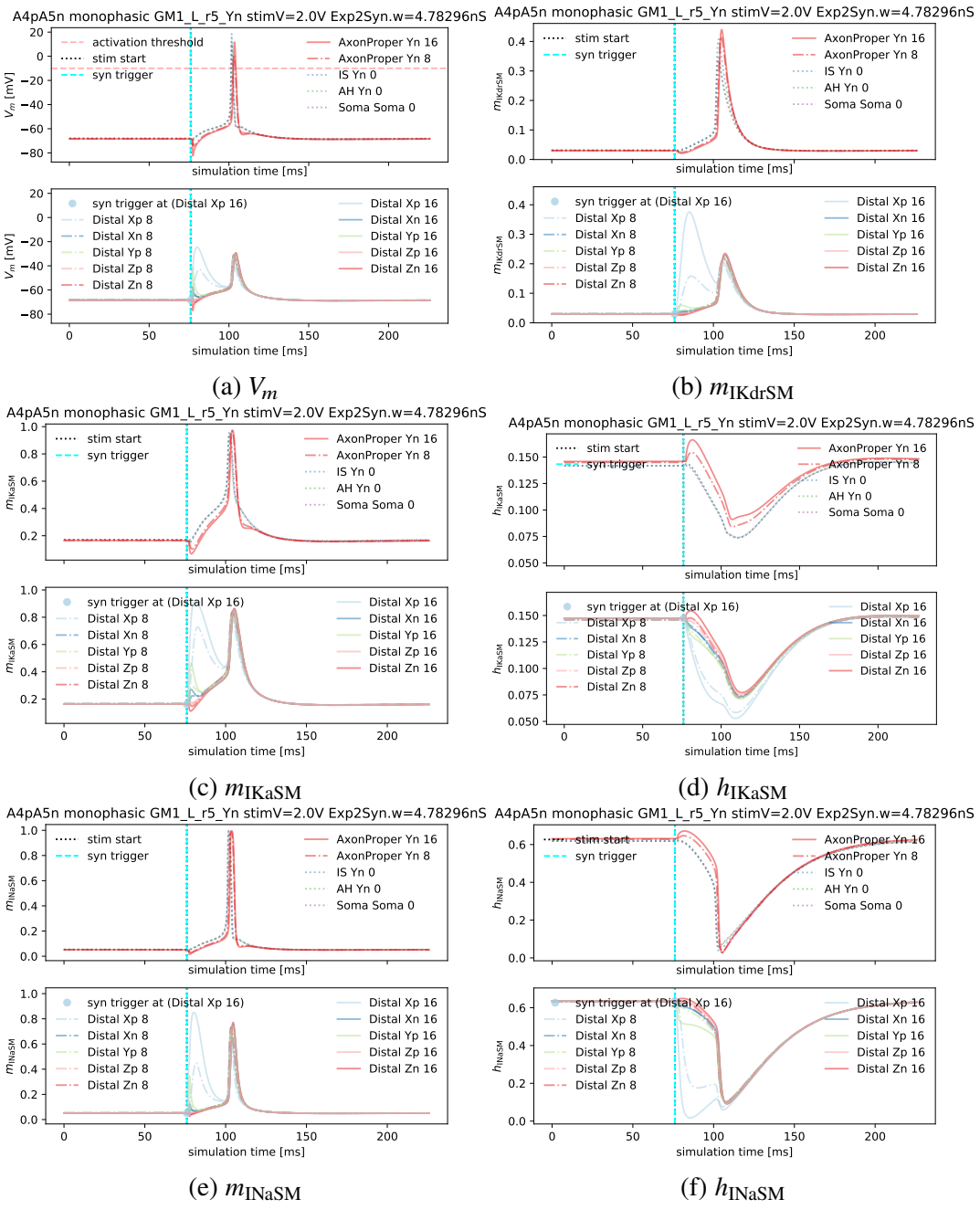

(a) V_m (b) m_{IKdrSM}

(c) m_{IKaSM} (d) h_{IKaSM}

(e) m_{INaSM} (f) h_{INaSM}

Figure 5.12: Stimulation + EPSP: Each subplot plots a different variable ((a) V_m, (b) m_{IKdrSM}, (c) m_{IKaSM}, (d) h_{IKaSM}, (e) m_{INaSM}, and (f) h_{INaSM}) against simulation time (ms) for probes on axon-soma (sub-top) and dendrites (sub-bottom). Measured on neuron GM1_L_r5_Yn exposed to 2.0 V of monophasic stimulation using stimulating electrode combination A4pA5n. The stimulation pulse starts at t=76.0ms and has a maximum amplitude at t=77.13ms. An Exp2Syn synapse was triggered at t=76.0 ms with a synaptic weight of 4.783nS. The synapse was located at segment 16 on the distal dendrite that points in the $+\hat{x}$ direction.

5.3 Total facilitated neurons for monophasic and biphasic stimulation

Section 4.3 discussed the total number of active neurons for monophasic and biphasic stimulation without any EPSPs. When a synapse is triggered close enough in time to interact with the stimulation pulse, this interaction may result in facilitation. As seen in Section 5.2, for each synapse weight and stimulation voltage, there may exist one or more facilitation windows (regions of synapse trigger time for a fixed stimulation time) where the interaction of the EPSP from the synaptic input and the stimulation pulse results in facilitation. Larger facilitation windows means that there is a larger probability that a stimulus pulse will facilitate an EPSP and activate a neuron. The number of synapse trigger times which result in facilitation can be used to summarize the facilitation window(s) for each pair of stimulation voltage and synapse weight.

For each type of stimulation (monophasic and biphasic), electrode stimulation voltage ($|V_s|$), synapse weight, and synapse segment (8 or 16), there are: (6 neuron locations for each constant z plane) * (6 geometry types (axon orientations)) * (5+6 z planes (ignoring neurons under rows 1 and 7)) * (2 positive and negative voltage amplitude) * (18 combinations) * (5 dendrites) = 71280 simulated neurons that could be facilitated.

Two-dimensional histograms of the number of simulated neurons vs the duration of the facilitation window(s), as measured using the number of synapse trigger points resulting in activation vs stimulation and synapse weight were generated by combining the number of synapse trigger times resulting in facilitation for all electrode combinations, neuron locations, and neuron orientations. Figure 5.13 shows the 2d histograms (greyscale squares with colorbar just to the right of each histogram indicate the number of neurons) for monophasic (Fig. 5.13a) and biphasic (Fig. 5.13b) stimulation and synapses located in the middle (segment 8) of the distal section of the dendrites. Figure 5.14 shows the 2d histograms (greyscale squares with colorbar

just to the right of each histogram indicate the number of neurons) for monophasic (Fig. 5.14a) and biphasic (Fig. 5.14b) stimulation and synapses located at the distal tips (segment 16) of the distal section of the dendrites. The y-axis of each 2d histogram shows the number of synapse trigger times which result in facilitation (or stimulation only (stimOnly) if no EPSP is required to activate the neuron at that value of V_s). Understanding the x-axis of each 2d histogram requires looking at the background columns behind the histogram. The magnitude of stimulation voltage ($|V_s|$) is represented by the color of each column (see right color bar (virdis[d]) to the right of each plot). The synapse weight of each column is indicated by the hatching of each column (see legend to the far right of each histogram). The grey-scale colorbar indicating the number of neurons facilitated in each square and the viridis colorbar indicating the magnitude of the stimulation voltage ($|V_s|$) are the same in Figs. 5.13a, 5.13b, 5.14a and 5.14b, allowing for direct comparison.

From Figs. 5.13 and 5.14, it appears that monophasic stimulation in general has wider facilitation windows (with a few exceptions) compared with biphasic stimulation. The histograms also show a general expected trend of increasing facilitation with increasing magnitude of stimulation voltage $|V_s|$ and synapse weight. It also appears that the facilitation windows tend to be a bit larger if the synapse is on the distal tip of the distal dendrite compared with the middle of the distal dendrite. Unfortunately, comparisons between synapse locations are not completely accurate because a larger synaptic weight is required to activate the neuron if the synapse is located further from the soma. I have tried to compensate for this effect by choosing synapse weights for each synapse location as an offset from the synapse activation threshold at each location.

Figures 5.15 and 5.16 show the same data using stacked bars indicating the size

[d]Matplotlib's viridis (yellow-green-blue) colormap is an improvement over traditional rainbow colormaps. See Borland and Ii, 2007 and Liu and Heer, 2018.

of the facilitation windows. The bar charts make it easier to compare the total number of neurons with a facilitation window of various widths. In these plots, the maximum of the y-axis is the total number of neurons so it is easy to see the factions of neurons facilitated. For synapses located in the middle of the distal dendrite (Fig. 5.15), the general trends described above still hold, (monophasic stimulation results in more facilitation than biphasic stimulation, etc.). However, for synapses at the distal tip of the distal dendrite (Fig. 5.15), at the largest synapse weight (4.783 nS), the total number of neurons where at least 1 of the synapse trigger times results in facilitation is actually larger for biphasic than monophasic stimulation if the magnitude of stimulation voltage $|V_s| >= 3$ V.

For both monophasic and biphasic stimulation, there is also an increase in the number of neurons with greater than 4 trigger points that result in facilitation for synapses at the distal tips of the distal dendrites compared with the synapses in the middle of the distal dendrite as seen in Figs. 5.17 and 5.18. This indicates that facilitation of distal synaptic input may be easier than more proximal (to the soma) synaptic input.

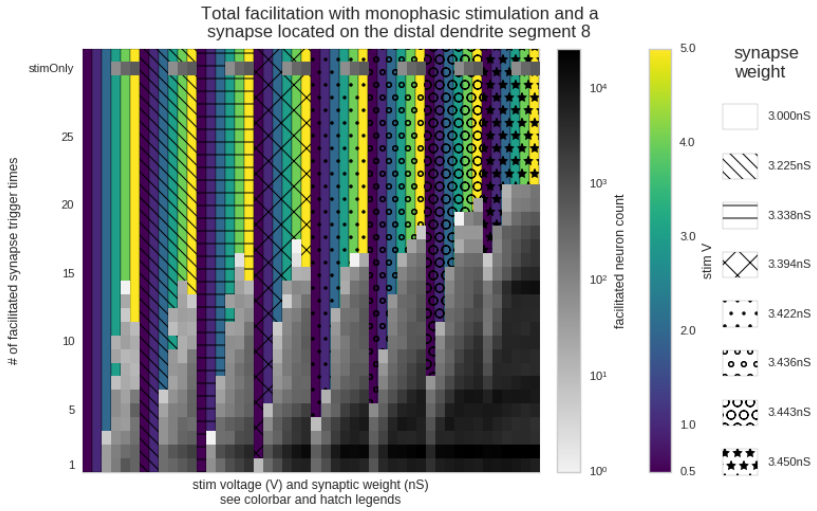

(a) monophasic

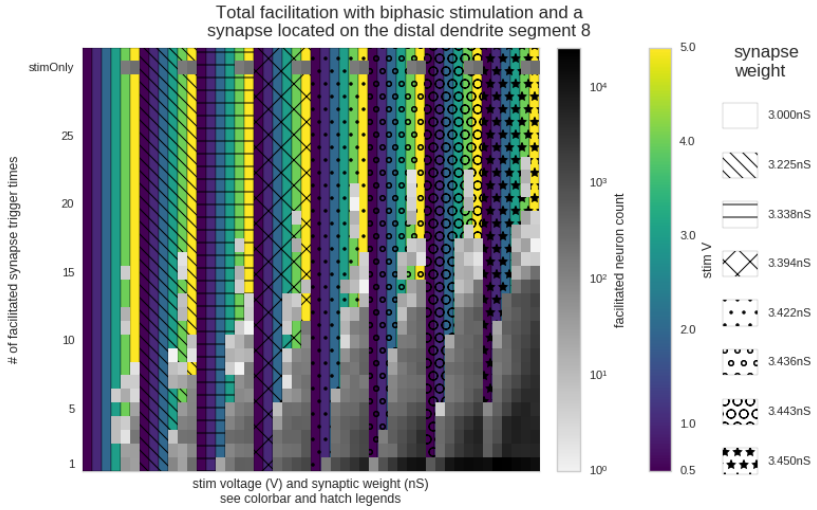

(b) biphasic

Figure 5.13: 2d histogram of the number of facilitated neurons with synapses in the middle (segment 8) of the distal dendrite for: (a) monophasic and (b) biphasic stimulation. The y-axis of each 2d histogram shows the number of synapse trigger times which result in facilitation (or stimOnly if no EPSP is required to activate the neuron at that value of V_s). Understanding the x-axis of each 2d histogram requires looking at the background columns behind the histogram. The magnitude of stimulation voltage ($|V_s|$) is represented by the color of each column (see right color bar to the right of each plot). The synapse weight of each column is indicated by the hatching of each column (see legend to the far right of each histogram). The number of neurons in each square is indicated by the gray-scale colorbar just to the right of the histogram. Each column consists of the results from simulating 71280 neurons under 18 electrode combinations (described in Section 5.3).

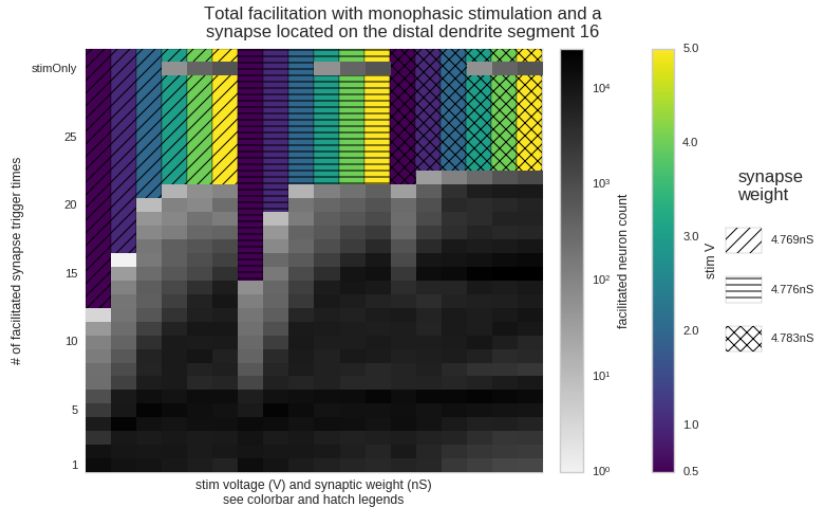

(a) monophasic

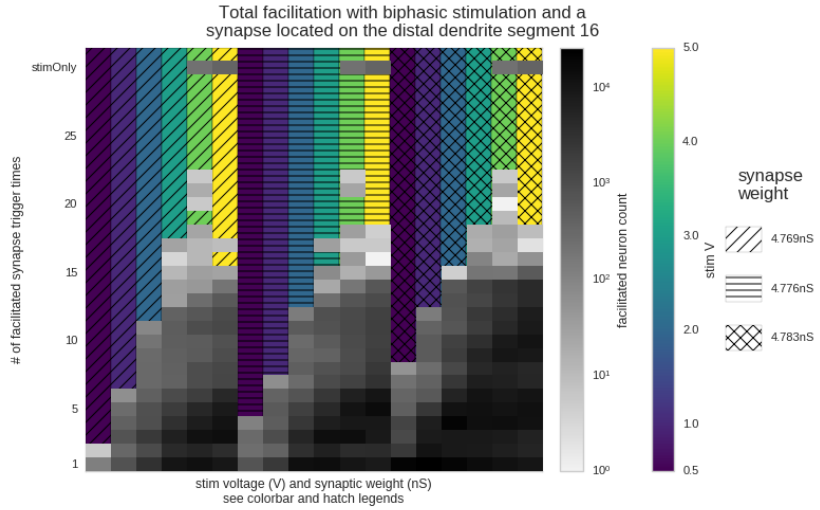

(b) biphasic

Figure 5.14: 2d histogram of the number of facilitated neurons with synapses at the distal tip (segment 16) of the distal dendrite for: (a) monophasic and (b) biphasic stimulation. The y-axis of each 2d histogram shows the number of synapse trigger times which result in facilitation (or stimOnly if no EPSP is required to activate the neuron at that value of V_s). Understanding the x-axis of each 2d histogram requires looking at the background columns behind the histogram. The magnitude of stimulation voltage ($|V_s|$) is represented by the color of each column (see right color bar to the right of each plot). The synapse weight of each column is indicated by the hatching of each column (see legend to the far right of each histogram). The number of neurons in each square is indicated by the gray-scale colorbar just to the right of the histogram. Each column consists of the results from simulating 71280 neurons under 18 electrode combinations (described in Section 5.3).

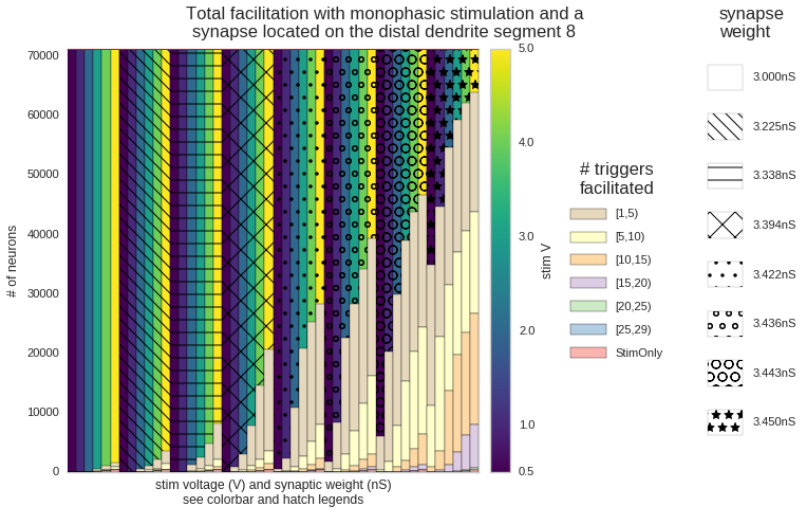

(a) monophasic

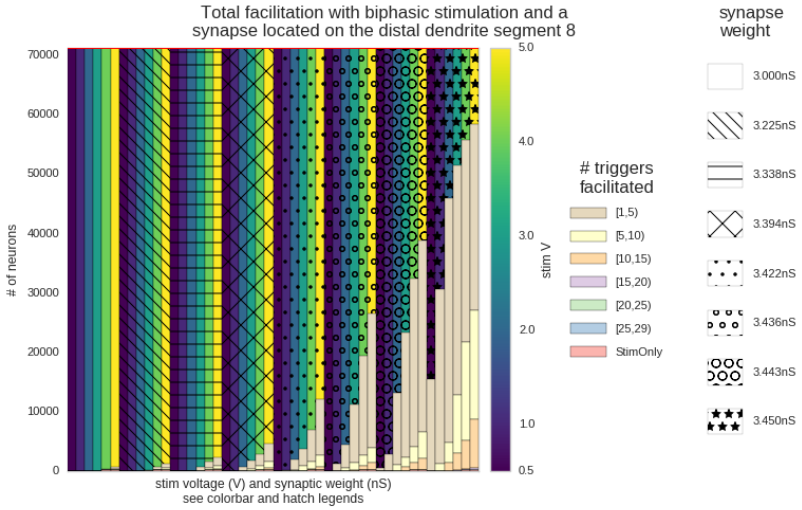

(b) biphasic

Figure 5.15: Stacked bar charts showing the number of active neurons (from facilitation or stimulation-only) where each column corresponds to a different pair of stimulation voltage ($|V_s|$) and synapse weight. These charts are for neurons with synapses in the middle (segment 8) of the distal dendrite and (a) monophasic and (b) biphasic stimulation. Each column consists of the results from simulating 71280 neurons under 18 electrode combinations (described in Section 5.3). Understanding the x-axis of each 2d histogram requires looking at the background columns behind the histogram. The magnitude of stimulation voltage ($|V_s|$) is represented by the color of each column (see virdis (yellow-green-blue color map) color bar to the right of each plot). The synapse weight of each column is indicated by the hatching of each column (see legend to the far right of each histogram). The color of each bar in the stacks (see legend to the right of the colorbar) indicates the number of synapse trigger times which result in facilitation (or stimOnly if the stimulation by itself causes activation). The maximum of the y-axis is the total number of simulated neurons (71280) indicated by a red horizontal line.

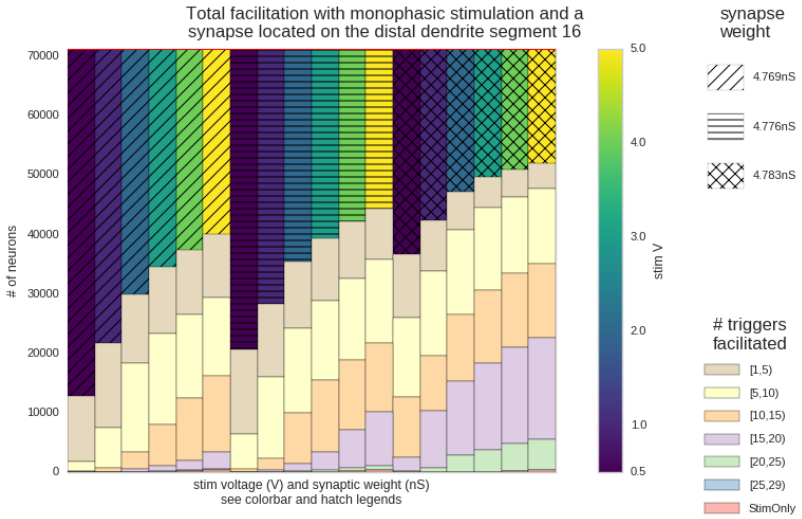

(a) monophasic

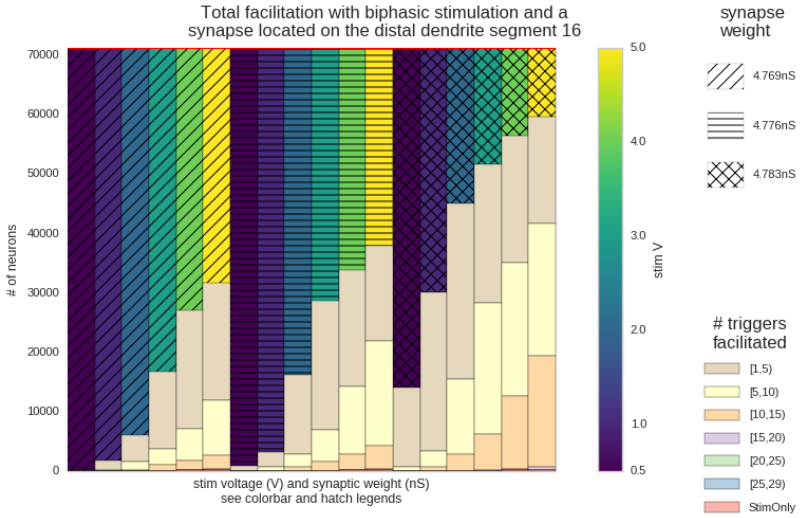

(b) biphasic

Figure 5.16: Stacked bar charts showing the number of active neurons (from facilitation or stimulation-only) where each column corresponds to a different pair of stimulation voltage ($|V_s|$) and synapse weight. These charts are for neurons with synapses at the distal tip (segment 16) of the distal dendrite and (a) monophasic and (b) biphasic stimulation. Each column consists of the results from simulating 71280 neurons under 18 electrode combinations (described in Section 5.3). Understanding the x-axis of each 2d histogram requires looking at the background columns behind the histogram. The magnitude of stimulation voltage ($|V_s|$) is represented by the color of each column (see virdis (yellow-green-blue color map) color bar to the right of each plot). The synapse weight of each column is indicated by the hatching of each column (see legend to the far right of each histogram). The color of each bar in the stacks (see legend to the right of the colorbar) indicates the number of synapse trigger times which result in facilitation (or stimOnly if the stimulation by itself causes activation). The maximum of the y-axis is the total number of simulated neurons (71280) indicated by a red horizontal line.

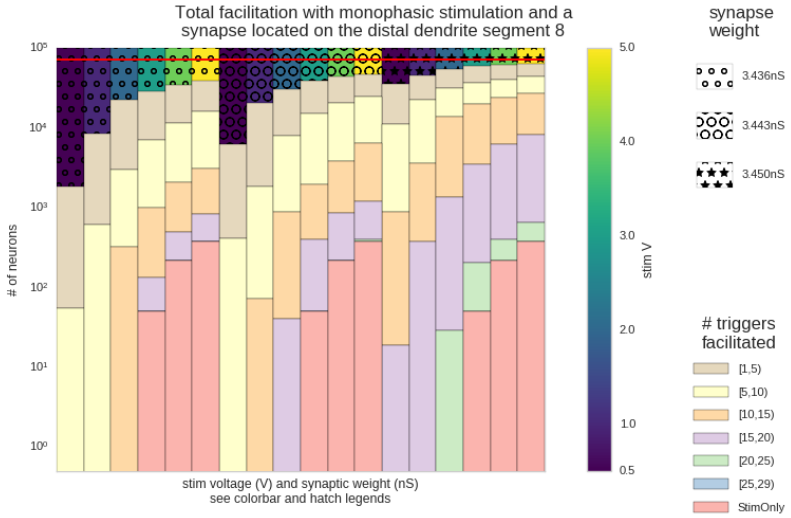

(a) Largest 3 synapse weights with synapse at the middle of the distal dendrite with monophasic stimulation

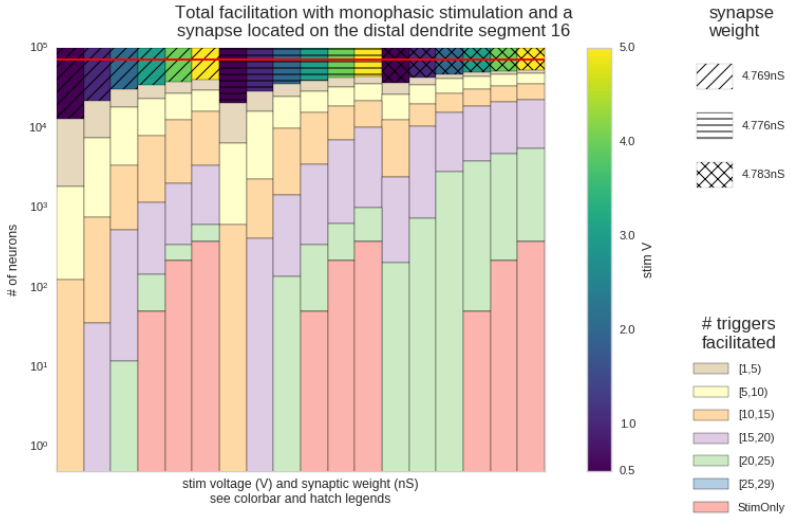

(b) synapse at the distal tip of the distal dendrite with monophasic stimulation

Figure 5.17: These two figures show (a) the largest 3 synapse weights from Fig. 5.15a and (b) Fig. 5.16a. See those figures for detailed description. The y-axis is a $\log_{10}$ scale with the total number of simulated neurons (71280) indicated by a red horizontal line. A greater number of neurons with synapses triggered on the distal tips of the distal dendrites have facilitation windows larger than 2 trigger time samples compared with synapses in the middle of the dendrite for synapse weights that are subthreshold by the same amount.

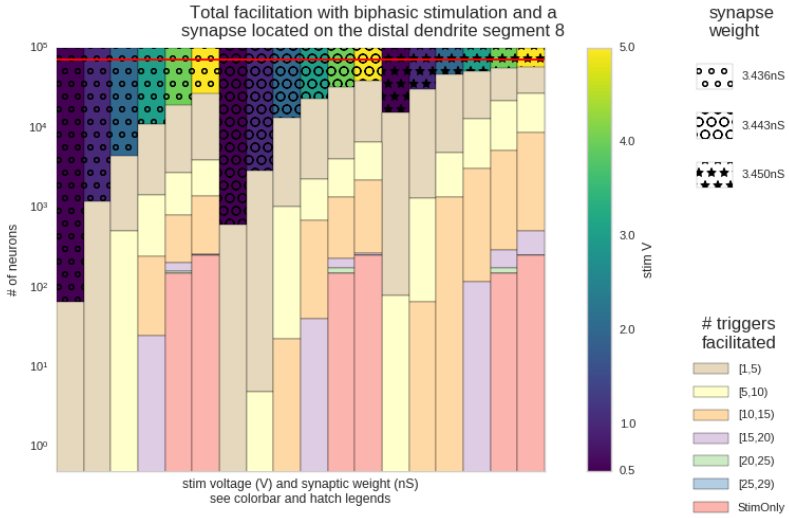

(a) Largest 3 synapse weights with synapse at the middle of the distal dendrite with biphasic stimulation

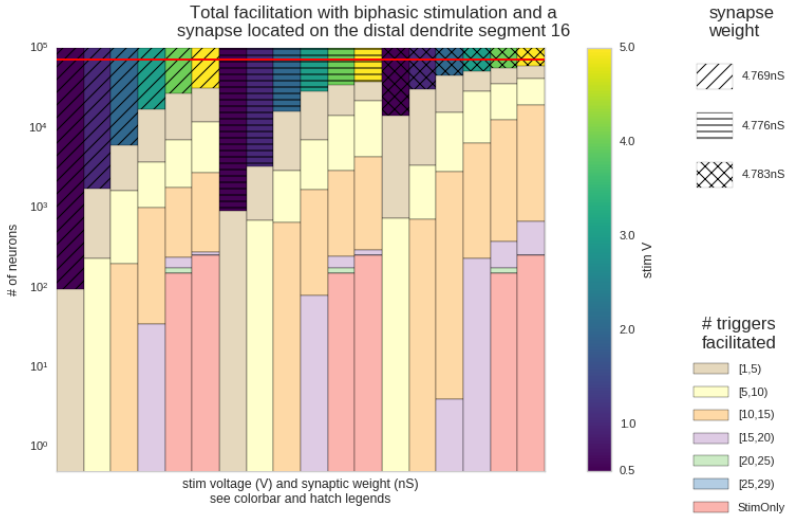

(b) synapse at the distal tip of the distal dendrite with biphasic stimulation

Figure 5.18: These two figures show (a) the largest 3 synapse weights from Fig. 5.15b and (b) Fig. 5.16b. See those figures for detailed description. The y-axis is a $\log_{10}$ scale with the total number of simulated neurons (71280) indicated by a red horizontal line. A greater number of neurons with synapses triggered on the distal tips of the distal dendrites have facilitation windows larger than 2 trigger time samples compared with synapses in the middle of the dendrite for synapse weights that are subthreshold by the same amount.

5.4 Predicting neuron facilitation

Section 4.6 showed that $V_{static}^{\text{AxonTip}} - V_{static}^{\text{Soma}}$ could be useful to estimate if a neuron would be activated by a particular combination of electric fields. Ideally, a similar feature or set of features could be found to estimate neuron facilitation. Additionally, features that are useful for separating facilitated neurons from non-facilitated neurons may indicate which aspects of the neuron's response to stimulation are important.

A dataset including the results from the facilitation simulations, stimulation-only simulations, and static simulations was collected for the 22 facilitation situations (stimulation type, synapse position on the dendrite (middle (iSeg=8) or distal tip (iSeg=16)), and synapse weight). Each of these datasets includes simulations from all 18 bipolar combinations with 6 stimulation voltage levels (0.5V, 1V, 2V, 3V, 4V, 5V). Each data point includes the number of facilitated synapse trigger time samples which, if multiplied by 5 ms (the sampling interval between trigger times), gives an estimate of the width of the facilitation window for that neuron.

In this section, the data is plotted with the number of facilitated synapse trigger time samples vs various features (for illustrative purposes). I have chosen to try to separate the data into three categories referred to by the variable T:

- $T = 0$ or negative – neurons that are not activated by the stimulation, with or without an EPSP,
- $T = 1$ or positive – neurons that are facilitated at 1 or more synapse trigger times or activated with just stimulation, and
- $T = Unknown$ or mixed – neurons cannot be separated or distinguished from others of the opposite category using the current features.

The few neurons that are activated without an EPSP are included in category ($T = 1$) to simplify the analysis.

Attempts to use machine-learning techniques (e.g. random forests) to determine the best features to use and decision boundaries resulted in complicated decision boundaries. These complicated decision boundaries resulted in high true positive rates and low false positive rates using cross-validation. However, the decision boundaries appeared to overfit the data in uncertain regions of the feature space. So a simpler approach (inspired by Fig. 4.22b) was tried with a maximum of 4 decision boundaries.

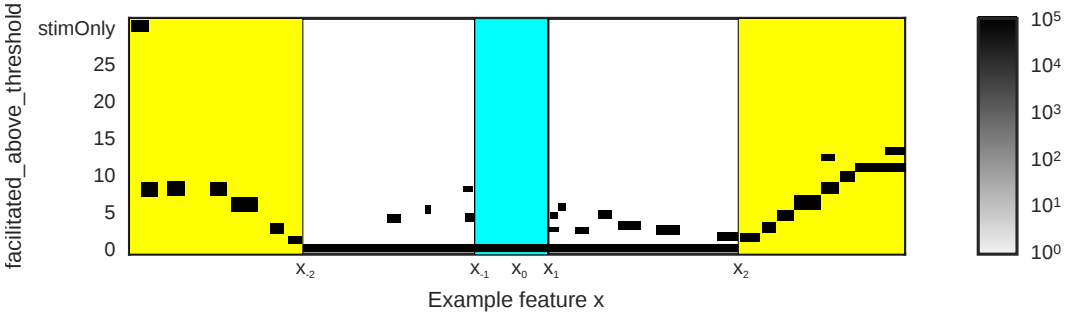

Figure 5.19: Example histogram plot showing the regions of example feature x that can be used for prediction of facilitation. The y-axis is the number of trigger points facilitated above threshold (−10 mV). Each trigger corresponds with about 5 ms of time during which a triggered synapse would cause facilitation. For each feature, active and non-active classification regions of unclassified samples are drawn with a yellow and cyan background respectively. These classification regions are also written as rules below for feature value f_0, where T=1 and T=0 indicates that the neuron is active and non-active respectively.
IF ($f_0 < x_{-2}$) THEN (T=1)
ELIF ($x_{-1} < f_0 < x_1$) THEN (T=0)
ELIF ($x_2 < f_0$) THEN (T=1)
ELSE (T=Unknown)

Consider an arbitrary feature x with value x_0 without stimulation voltage. Since all the neurons have no facilitation without stimulation, there might be a region in feature space around x_0 which contains no facilitated neurons. The decision boundaries for this region (if it exists) are referred to as x_{-1} and x_1 where

$$x_{-1} \leq x_0 \leq x_1 \tag{5.1}$$

and all of the neuron simulations with feature values of x such that $x_{-1} \leq x \leq x_1$ have no facilitation. The last two decision boundaries (if they exist) are referred to as x_{-2} and x_2 where $x_{-2} \leq x_{-1} \leq x_0 \leq x_1 \leq x_2$ and all of the neuron simulations with feature values of x such that $x \leq x_{-2}$ or $x_2 \leq x$ have non-zero size facilitation window(s). Figure 5.19 shows a cartoon example of these facilitation decision boundaries for arbitrary feature x. Custom analysis software was written to find the values x_{-2}, x_{-1}, x_1, and x_2 given a feature dataset and the value of x_0 (the value of the feature without stimulation). For many features, one or more of these decision boundaries do not exist, but the remaining decision boundaries (if any) can be used for classification. A greedy cascading search algorithm was written to find which sequence of features is able to separate the largest number of positive ($T = 1$) neurons and negative ($T = 0$) neurons from the rest. This algorithm evaluates how many neurons each single feature is able to classify as positive and negative, picks the best one (sorted by most identified as positive and then most identified as negative if there are ties) and any neuron samples that are still mixed cascade into the next greedy search over the remaining features until the algorithm has reached the feature limit (a sequence of 4 features). In the next section I will define these features and explain how they are chosen.

The results from these searches are summarized in tables and figures in Sections 5.4.1 and 5.4.2. Each figure shows unclassified data in grey scale, and data classified by earlier stages of the cascade in shades of red (facilitated/activated) and blue (no-activation).

5.4.1 Separating facilitated and non-activated neurons using static features

Predicting facilitation from static (rather than time-domain) volume conductor simulations would imply that time-domain volume conductor simulations are unnecessary (once a predictor is built). In Section 4.6, I showed that the 2nd derivative

of static voltage along the axon and static voltage at the axon tip are not useful for separating active neurons from inactive neurons. Similarly, applying a cascade of 4 static voltage features (V^{L}_{static} for locations L, etc) at individual points[e] or a cascade of 4 second derivative features at individual points[f] did not perform well compared to features based on the static voltage differences between individual points and the soma.

The following features were evaluated by the greedy search algorithm:

- $V^{\text{AxonTip}}_{static} - V^{\text{Soma}}_{static}$,
- $V^{\text{AxonMiddle}}_{static} - V^{\text{Soma}}_{static}$,
- $V^{\text{IS}}_{static} - V^{\text{Soma}}_{static}$,
- $V^{\text{AH}}_{static} - V^{\text{Soma}}_{static}$,
- $\min_{\forall \text{dendrites}}(V^{\text{DistalDendriteTip}}_{static}) - V^{\text{Soma}}_{static}$,
- $\max_{\forall \text{dendrites}}(V^{\text{DistalDendriteTip}}_{static}) - V^{\text{Soma}}_{static}$,
- $\text{avg}_{\forall \text{dendrites}}(V^{\text{DistalDendriteTip}}_{static}) - V^{\text{Soma}}_{static}$,
- $\min_{\forall \text{dendrites}}(V^{\text{DistalDendriteMiddle}}_{static}) - V^{\text{Soma}}_{static}$,
- $\max_{\forall \text{dendrites}}(V^{\text{DistalDendriteMiddle}}_{static}) - V^{\text{Soma}}_{static}$,
- $\text{avg}_{\forall \text{dendrites}}(V^{\text{DistalDendriteMiddle}}_{static}) - V^{\text{Soma}}_{static}$, and
- $V^{\text{Synapse}}_{static} - V^{\text{Soma}}_{static}$,

where V^{L}_{static} is the static voltage at location L, $\min_{\forall \text{dendrites}}(V^{\text{L}}_{static})$ is the minimum static voltage at location L across all of the dendrites for that particular neuron and stimulation parameters, $\max_{\forall \text{dendrites}}(V^{\text{L}}_{static})$ is the maximum static voltage at location L across all of the dendrites for that particular neuron and stimulation parameters, and $\text{avg}_{\forall \text{dendrites}}(V^{\text{DistalDendriteMiddle}}_{static})$ is the average static voltage at location L across all of the dendrites for that particular neuron and stimulation parameters.

[e] only able to classify 0.3% to 16% of facilitated neurons over all 22 datasets

[f] only able to classify 0.2% to 20.8% of facilitated neurons over all 22 datasets

The greedy search algorithm was run using the above features for each type of stimulation (biphasic, monophasic), synapse location (distal tip or middle of distal dendrite), and synapse weight. After all those feature sequences were found, they were evaluated on all the datasets and the feature sequence that did best across all datasets was chosen. The best features overall were:

- $f_0 = V_{static}^{\text{Synapse}} - V_{static}^{\text{Soma}}$,
- $f_1 = V_{static}^{\text{IS}} - V_{static}^{\text{Soma}}$,
- $f_2 = \min_{\forall \text{dendrites}}(V_{static}^{\text{DistalDendriteMiddle}}) - V_{static}^{\text{Soma}}$,
- and $f_3 = \text{avg}_{\forall \text{dendrites}}(V_{static}^{\text{DistalDendriteMiddle}}) - V_{static}^{\text{Soma}}$.

With no stimulation voltage, the value of all of these features is 0 mV.

The results of using these features to separate simulations are shown in supplementary figures in Section 5.C. A summary of the results is available in Table 5.2.

These features are interesting:

- Feature $f_0 = V_{static}^{\text{Synapse}} - V_{static}^{\text{Soma}}$ represents the extracellular voltage difference caused by the stimulation between the synapse location and the soma.
- Feature $f_1 = V_{static}^{\text{IS}} - V_{static}^{\text{Soma}}$ is very similar to the feature $(V_{static}^{\text{AxonTip}} - V_{static}^{\text{Soma}})$ which was used in Fig. 4.22b to predict activation without EPSPs.

In simulations, the initial segment (IS) and the axon hillock (AH) usually have almost the same membrane voltage and the action potential appears to start at both locations almost simultaneously. So, this feature may indicate the amount by which the axon is directly stimulated. The last 2 features likely represent how much other parts of the dendrites are stimulated. The first two features account for most of the

separation of facilitated neurons from the mix of other neurons. In most cases, these features have a low ability to separate non-active neurons from some of the facilitated neurons. This may be because there is a very small difference in feature space between no-activation and a single synapse trigger time that causes facilitation.

Table 5.2: Summary of classification of facilitation for each dataset (labeled by columns stimulation, iSeg, and synapse weight) using features based on the static voltage difference between individual points and the soma at each stage of the cascade. Each stage uses a different feature (f_0, f_1, f_2, and f_3 defined below the table) and has the percent of facilitated neurons identified (id+%) and the percent of non-facilitated neurons identified (id-%) listed. Columns p and n indicate the total number of facilitated and non-facilitated neurons respectively. The Figure column indicates the figure that dataset is plotted in (in the pdf you can click on the figure number to view it).

					Stage f_0		Stage f_1		Stage f_2		Stage f_3		
stimulation	iSeg	synapse weight	p	n	id+%	id-%	id+%	id-%	id+%	id-%	id+%	id-%	Figure
biphasic	8	3.0nS	937	426743	0	4.2	67.24	99.86	67.24	99.86	80.58	99.92	5.47
biphasic	8	3.225nS	2047	425633	4.89	1.26	81.63	22.28	81.63	43.11	88.62	43.57	5.48
biphasic	8	3.337nS	4648	423032	22.16	1.14	84.55	18.4	85.8	35.81	87.74	36.04	5.49
biphasic	8	3.394nS	10070	417610	36.54	1.01	83.82	11.33	87.72	11.42	88.59	11.59	5.50
biphasic	8	3.422nS	24932	402748	51.34	0.47	82.06	4.58	85.24	4.62	85.46	4.73	5.51
biphasic	8	3.436nS	62871	364809	61.96	0.01	84.36	0.79	86.48	0.97	86.65	1.76	5.52
biphasic	8	3.443nS	111204	316476	64.44	0.01	83.94	0.02	85.33	0.05	85.33	0.29	5.53
biphasic	8	3.45nS	257872	169808	79.73	0.01	89.83	0.02	91.05	0.15	91.05	0.15	5.54
biphasic	16	4.769nS	83386	344294	20.66	0.01	75.32	0.03	77.06	0.17	77.34	0.51	5.55
biphasic	16	4.776nS	121016	306664	29.98	0.01	77.98	0.02	79.5	0.1	79.7	0.43	5.56
biphasic	16	4.783nS	257325	170355	40.92	0.01	75.42	0.01	76.67	0.01	76.67	0.03	5.57
monophasic	8	3.0nS	3207	424473	0	0.75	42.25	13.54	42.25	13.78	48.8	13.87	5.58
monophasic	8	3.225nS	7167	420513	28.95	0.66	66.29	1.24	69.02	2.17	73.06	3.77	5.59
monophasic	8	3.337nS	16891	410789	29.93	0.16	67.72	0.52	70.56	0.65	71.36	0.72	5.60
monophasic	8	3.394nS	46967	380713	25.64	0.02	66.05	0.21	68.11	0.26	69.05	0.31	5.61
monophasic	8	3.422nS	88331	339349	33.22	0.01	75.86	0.12	76.9	0.22	77.52	0.24	5.62
monophasic	8	3.436nS	134610	293070	36.38	0.01	74.21	0.08	74.95	0.16	75.8	0.19	5.63
monophasic	8	3.443nS	185932	241748	37.67	0	72.81	0.03	73.4	0.04	73.98	0.06	5.64
monophasic	8	3.45nS	319871	107809	48.17	0	70.56	0	70.87	6.66	70.89	6.66	5.65
monophasic	16	4.769nS	176737	250943	37.15	0	60.03	0.02	60.03	0.02	67.5	0.02	5.66
monophasic	16	4.776nS	210546	217134	40.81	0	60.64	0	60.64	0	70.48	0	5.67
monophasic	16	4.783nS	279199	148481	50.64	0	69.39	0.19	69.39	0.19	72.29	0.21	5.68

$f_0 = V_{static}^{\text{Synapse}} - V_{static}^{\text{Soma}}$
$f_1 = V_{static}^{\text{IS}} - V_{static}^{\text{Soma}}$
$f_2 = \min_{\forall \text{dendrites}}(V_{static}^{\text{DistalDendriteMiddle}}) - V_{static}^{\text{Soma}}$
$f_3 = \text{avg}_{\forall \text{dendrites}}(V_{static}^{\text{DistalDendriteMiddle}}) - V_{static}^{\text{Soma}}$

5.4.2 Separating facilitated and non-activated neurons using stimulation-only membrane voltages

When an electrical stimulation pulse interacts with a neuron, the membrane voltage of the cell deviates from resting potential by different amounts at different locations of the neuron. Predicting whether a neuron would be facilitated based on the membrane voltage changes caused by the stimulation pulse without any EPSP input would reduce the number of NEURON simulations necessary. By using the minimum and the maximum of the membrane voltage at several locations on the neurons as features to separate facilitated neurons from non-activated neurons, I

hope to identify at which locations the membrane voltage changes are most important for facilitation.

The following features were evaluated by the greedy search algorithm:

- $\max_t (V_m^{\text{AxonTip}}(t))$,
- $\max_t (V_m^{\text{AxonMiddle}}(t))$,
- $\max_t (V_m^{\text{IS}}(t))$,
- $\max_t (V_m^{\text{AH}}(t))$,
- $\max_t (V_m^{\text{Soma}}(t))$,
- $\min_{\forall \text{dendrites}} \max_t (V_m^{\text{DistalDendriteTip}}(t))$,
- $\max_{\forall \text{dendrites}} \max_t (V_m^{\text{DistalDendriteTip}}(t))$,
- $\text{avg}_{\forall \text{dendrites}} \max_t (V_m^{\text{DistalDendriteTip}}(t))$,
- $\min_{\forall \text{dendrites}} \max_t (V_m^{\text{DistalDendriteMiddle}}(t))$,
- $\max_{\forall \text{dendrites}} \max_t (V_m^{\text{DistalDendriteMiddle}}(t))$,
- $\text{avg}_{\forall \text{dendrites}} \max_t (V_m^{\text{DistalDendriteMiddle}}(t))$,
- $\max_t (V_m^{\text{Synapse}}(t))$,
- $\min_t (V_m^{\text{AxonTip}}(t))$,
- $\min_t (V_m^{\text{AxonMiddle}}(t))$,
- $\min_t (V_m^{\text{IS}}(t))$,
- $\min_t (V_m^{\text{AH}}(t))$,
- $\min_t (V_m^{\text{Soma}}(t))$,
- $\min_{\forall \text{dendrites}} \min_t (V_m^{\text{DistalDendriteTip}}(t))$,
- $\max_{\forall \text{dendrites}} \min_t (V_m^{\text{DistalDendriteTip}}(t))$,
- $\text{avg}_{\forall \text{dendrites}} \min_t (V_m^{\text{DistalDendriteTip}}(t))$,
- $\min_{\forall \text{dendrites}} \min_t (V_m^{\text{DistalDendriteMiddle}}(t))$,
- $\max_{\forall \text{dendrites}} \min_t (V_m^{\text{DistalDendriteMiddle}}(t))$,
- $\text{avg}_{\forall \text{dendrites}} \min_t (V_m^{\text{DistalDendriteMiddle}}(t))$, and

- $\min_t(V_m^{\text{Synapse}}(t))$,

where $V_m^{\text{L}}(t)$ is the time series of membrane voltage at location L, $\min_t(V_m^{\text{L}}(t))$ is the minimum over time of the membrane voltage at location L, $\max_t(V_m^{\text{L}}(t))$ is the maximum over time of the membrane voltage at location L, and the other functions were defined in Section 5.4.1.

The greedy search algorithm was applied to the above features for each type of stimulation (biphasic, monophasic), synapse location (distal tip or middle of distal dendrite), and synapse weight. After all of those feature sequences were found, they were evaluated on all the datasets, and the feature sequence that had the best minimum performance across all datasets was chosen. The best features overall were:

- $f_0 = \max_t(V_m^{\text{AH}}(t))$,
- $f_1 = \max_t(V_m^{\text{Synapse}}(t))$,
- $f_2 = \min_t(V_m^{\text{Synapse}}(t))$, and
- $f_3 = \max_{\forall \text{dendrites}} \max_t(V_m^{\text{DistalDendriteMiddle}}(t))$.

With no stimulation voltage, the value of these features is just the resting membrane voltages found in Fig. 3.5.

The results of using these features to separate simulations are shown in supplementary figures in Section 5.D. A summary of the results is available in Table 5.3.

As discussed briefly in Section 5.4.1, there is minimal membrane voltage difference between the axon hillock (AH) and the initial segment (IS). So, the first feature ($f_0 = \max_t(V_m^{\text{AH}}(t))$) is almost identical to $\max_t(V_m^{\text{IS}}(t))$, which would correspond with feature $V_{static}^{\text{IS}} - V_{static}^{\text{Soma}}$ from Section 5.4.1. The next two features

($f_1 = \max_t(V_m^{\text{Synapse}}(t))$ and $f_2 = \min_t(V_m^{\text{Synapse}}(t))$) deal with the membrane voltage at the synapse location and would correspond with feature $V_{static}^{\text{Synapse}} - V_{static}^{\text{Soma}}$ from Section 5.4.1. The last feature in the cascade is the maximum membrane voltage in the middle of any dendrite, which seems to measure how much the dendrites in general are stimulated. Compared to the static voltage difference features used in Section 5.4.1, the membrane voltage features tested here seem less able to separate facilitated (and active) neurons from the non-active neurons. These membrane voltage features are better at separating non-active neurons from the rest. The reduced performance on separating facilitated and active neurons from non-active neurons remains even if the cascade is allowed to use 8 features. This seems to indicate that the minimum and maximum of the membrane voltage are not the best choice of features. This may be because of sharp transients in the membrane voltage caused by the stimulation pulse.

Table 5.3: Summary of classification of facilitation for each dataset (labeled by columns stimulation, iSeg, and synapse weight) using membrane voltage features at each stage of the cascade. Each stage uses a different feature (f_0, f_1, f_2, and f_3 defined below the table) and has the percent of facilitated neurons identified (id+%) and the percent of non-facilitated neurons identified (id-%) listed. Columns p and n indicate the total number of facilitated and non-facilitated neurons respectively. The Figure column indicates the figure that dataset is plotted in (in the pdf you can click on the figure number to view it).

					Stage f_0		Stage f_1		Stage f_2		Stage f_3		
stimulation	iSeg	synapse weight	p	n	id+%	id-%	id+%	id-%	id+%	id-%	id+%	id-%	Figure
biphasic	8	3.0nS	937	426743	66.7	99.65	66.7	99.67	66.7	99.67	66.7	99.67	5.69
biphasic	8	3.225nS	2047	425633	76.94	35.88	78.85	36.25	78.85	60.57	78.85	77.17	5.70
biphasic	8	3.337nS	4648	423032	69.6	10.6	81.15	52.38	81.63	71.33	82.98	77.25	5.71
biphasic	8	3.394nS	10070	417610	60.58	4.11	77.41	20.46	81.01	45.8	83.58	61.48	5.72
biphasic	8	3.422nS	24932	402748	42.88	1.43	66.31	22.77	74.41	44.33	76.97	52.13	5.73
biphasic	8	3.436nS	62871	364809	34.4	0.56	64.08	7.2	72.63	16.57	74.09	33.1	5.74
biphasic	8	3.443nS	111204	316476	36.01	0.2	58.95	6.72	70.69	14.09	71.87	26.01	5.75
biphasic	8	3.45nS	257872	169808	43.96	0	58.29	0.19	70.98	4.38	72	13.72	5.76
biphasic	16	4.769nS	83386	344294	60.09	0.59	62.52	0.59	62.56	2.61	63.99	31.45	5.77
biphasic	16	4.776nS	121016	306664	58.65	0.39	61.21	0.4	61.25	1.97	62.74	24.01	5.78
biphasic	16	4.783nS	257325	170355	58.58	0	61.35	0.07	61.43	0.85	62.67	12.07	5.79
monophasic	8	3.0nS	3207	424473	48.8	63.9	48.8	70.95	48.8	92.18	48.8	92.29	5.80
monophasic	8	3.225nS	7167	420513	35.3	42.66	35.82	42.66	62.83	77.44	70.18	78.26	5.81
monophasic	8	3.337nS	16891	410789	32.68	29.38	34.73	29.38	59.22	67.59	64.44	68.49	5.82
monophasic	8	3.394nS	46967	380713	31.93	20.96	34.57	20.96	49.24	61.5	52	62.4	5.83
monophasic	8	3.422nS	88331	339349	37.77	12.27	40.71	12.27	58.21	36.26	59.78	37.31	5.84
monophasic	8	3.436nS	134610	293070	42.74	7.23	47.38	7.23	63.85	25.01	64.89	25.67	5.85
monophasic	8	3.443nS	185932	241748	40.65	3	48.18	3.31	63.92	18.11	64.63	18.49	5.86
monophasic	8	3.45nS	319871	107809	38.11	1.04	50.89	1.73	63.21	9	63.56	13.15	5.87
monophasic	16	4.769nS	176737	250943	20.99	0.99	51.29	0.99	51.29	5.95	51.29	6.18	5.88
monophasic	16	4.776nS	210546	217134	17.62	0.67	47.14	0.67	47.14	4.34	47.14	4.64	5.89
monophasic	16	4.783nS	279199	148481	13.29	0.43	47.92	0.43	47.92	1.44	47.92	1.97	5.90

$f_0 = \max_t(V_m^{\text{AH}}(t))$
$f_1 = \max_t(V_{gt}^{\text{Synapse}}(t))$
$f_2 = \min_t(V_m^{\text{Synapse}}(t))$
$f_3 = \max_{\forall \text{dendrites}} \max_t(V_m^{\text{DistalDendriteMiddle}}(t))$

5.5 Discussion

Simulations of a sub-threshold synaptic input combined with a sub-threshold stimulation pulse showed that time windows where synaptic input would be facilitated existed both before and after a stimulation pulse for a significant number of neurons if the synapse weight and/or the stimulation pulse magnitude is large enough. The location and orientation of both the neuron and the synaptic input also has an effect. As either the stimulation magnitude or the synapse weight is decreased, the size of the facilitation windows (time range that a synapse triggered relative to a fixed stimulation pulse causes neuron activation) is reduced and the number of facilitated neurons is also reduced. For larger synapse weights ([3.45, 3.443, 3.436]nS associated with synapses in the middle of the distal dendrite and [4.783, 4.776, 4.769]nS for synapses located on the distal tip of a dendrite), facilitation is possible for both monophasic and biphasic stimulation pulses of magnitude 0.5 V. With stimulation magnitudes of 5 V or less, monophasic stimulation clearly causes more facilitation compared to biphasic stimulation, with the exception of synapses on the distal tips of dendrites and the largest synapse weight (4.783 nS). However, monophasic stimulation also causes more neuron activation without synaptic input, as seen in Chapter 4, which might be counterproductive for purely facilitating existing circuits.

Based on the examples in Section 5.2, it appears that it takes less magnitude of biphasic stimulation to facilitate a synaptic input if the stimulation pulse occurs within a time window of about 20 ms after the synapse is triggered. For monophasic stimulation, some stimulation combinations and neuron locations show the same behavior as described for biphasic stimulation, but reversing the polarity on those examples caused the facilitation window to be after the stimulation pulse rather than before. For some of the neurons and synapse locations, less magnitude of monophasic stimulation was needed to cause facilitation if the stimulation pulse

occurred at the same time as the synaptic input. These cases also showed a large facilitation window of possibly greater than 75 ms for synaptic input after the stimulation pulse. The exact size of the actual facilitation window in some of these cases is unknown because I underestimated the maximum size of the facilitation window.

The timing of the synaptic input and a biphasic stimulation pulse that results in "least effort" facilitation (lowest magnitude stimulation, and lowest synapse weight) results in the stimulation pulse occurring when m_{IKdrSM} is at a maximum near the synapse and h_{INaSM} is at a minimum. For monophasic stimulation, the "least effort" facilitation timing for the examples shown is either that the synaptic input and the stimulation pulse occur at the same time, or the stimulation pulse occurs after the synaptic input when V_m is at a maximum at the synapse location, m_{IKdrSM} is approaching maximum, m_{IKaSM} is close to maximum, m_{INaSM} is near maximum, and h_{INaSM} is approaching minimum. A more comprehensive study of the facilitation windows and "least effort" facilitation timing could be considered for future work. In particular, the interaction of the ion channel dynamics, synapse dynamics, and stimulation pulses should be examined further.

A method of predicting the probability of facilitation for a given neuron without computing large numbers of time-domain volume conductor simulations and/or NEURON simulations would allow consideration of more complicated electrode patterns and stimulation types. While I have not built a detailed predictor in this thesis, I have found that the features ($V_{static}^{\mathrm{Synapse}} - V_{static}^{\mathrm{Soma}}$, $V_{static}^{\mathrm{IS}} - V_{static}^{\mathrm{Soma}}$) based on the static volume conductor simulations were able to separate many of the facilitated (and activated by stimulation-only) neurons from non-activated neurons. Features based on the minima and maxima of the membrane voltage at various points were also able to separate many of the facilitated neurons from the rest; however, they were not able to separate as many of the neurons as the features based on the difference of static voltage between locations on the neuron and the soma. Features

based on the second derivative of the static voltage were not useful for separating facilitated neurons from non-facilitated neurons.

Additional facilitation simulations using the neurons listed in Tables 4.2 and 4.3 were carried out using passive dendrites instead of active dendrites. When the synapse weights from Table 5.1 were used with the passive dendrite model, I found a significant reduction in the amount of facilitation. This supports the hypothesis that ion channels in the dendrites are important to the facilitation of synaptic input using electrical stimulation.

The next chapter will summarize the main contributions of thesis and discuss possible future work.

5.A Appendix: Position of facilitated neurons

This appendix contains tables of figures showing the width of the facilitation windows (in 5 ms size intervals) for biphasic and monophasic stimulation using electrode combination A3pC5n with synaptic input in the middle (segment 8) of the distal section of each dendrite.

When plotting the activation thresholds in Section 4.A, there was only one number (the activation threshold) for each axon orientation. To plot the width of the facilitation windows for each pair of stimulation voltage and synapse weight, there are 5 dendrites that the synapse could be located on for each axon orientation. The following scheme was used to plot the additional information:

- If the neuron with an axon in that orientation would be activated by stimulation at that voltage without synaptic input, plot the axon as a red line.
- If synaptic input of any of the dendrites (at segment 8) has non-zero facilitation windows then plot the axon as a gray line.
- For each of the synapse locations that have a non-zero facilitation window, plot a cone (colored according to the width of the facilitation window) with a base at the distal tip of the axon and the tip of the cone pointing in the same Euclidean direction as the dendrite the synapse is on.

This scheme allows one to quickly see the amount of facilitation in each location. Figure 5.20 shows an example with biphasic stimulation with combination A3pC5n, a stimulation magnitude of V_s=2 V, and a synapse weight of 3.436 nS.

Tables 5.4 to 5.7 show tiny figures similar to Fig. 5.20 for each pairing of stimulation voltage and synapse weight. All figures in this section have positive electrode voltage indicated by a blue label and negative electrode voltage with a red label.

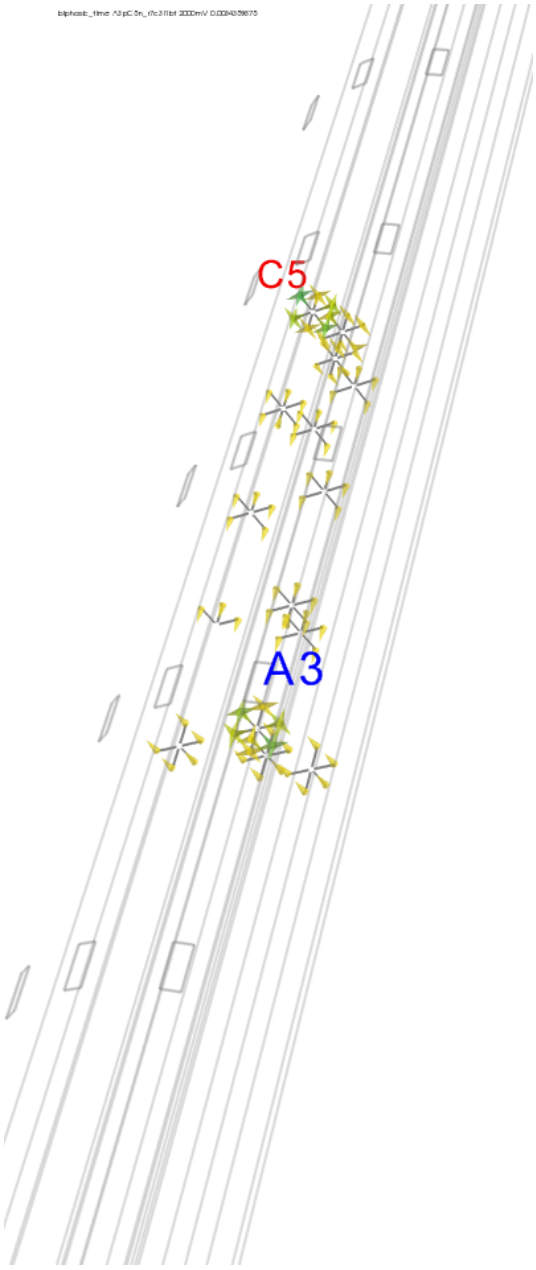

Figure 5.20: Stimulation type: Biphasic, combination: A3pC5n, stimulation magnitude: V_s =2 V. Synapses are on segment 8 of each dendrite with a synapse weight of 3.436 nS. See Section 5.A for more description. Colormap indicating facilitation width can be found in Table 5.4. Darker colors indicate wider facilitation windows.

Table 5.4: Stimulation type: Biphasic, combination: A3pC5n.

Table 5.5: Stimulation type: Biphasic, combination: -A3pC5n.

Table 5.6: Stimulation type: Monophasic, combination: A3pC5n.

Table 5.7: Stimulation type: Monophasic, combination: -A3pC5n.

5.B Appendix: More examples of facilitation

This appendix contains supplementary examples of facilitation similar to those in Section 5.2. Sections 5.B.1 to 5.B.3 contain detailed descriptions of facilitation with biphasic stimulation and Sections 5.B.4 and 5.B.5 for monophasic stimulation. These examples serve to show some of the ways that facilitation can occur. Some interesting findings from these sections are summarized in Section 5.5.

5.B.1 Biphasic stimulation with $V_s > 0$ and a distal tip synapse

For biphasic stimulation using A4pA5n with $V_s > 0$ of neuron GM1_L_r5_Yn with a synapse located at segment 16 on the distal dendrite pointing in the $\hat{x}$ direction, the maximum membrane voltage at the axon tip for the synapse weights, trigger times, and stimulation voltages listed in Section 5.1 can be seen in Fig. 5.21. Without any synaptic activity, the neuron will activate if $V_s = 8\,\text{V}$. As with $V_s < 0$ (described in Section 5.2.1), the duration of the facilitation window is larger for synaptic input occurring before the stimulation pulse. But facilitation also happens for synaptic input occurring after the stimulation pulse. As $|V_s|$ and synapse weight decrease, the facilitation window is only before the stimulation pulse. Even though the baseline stimulation-only membrane voltage at the axon tip is less than with $V_s < 0$ (for the same $|V_s|$), there is a similar amount of facilitation. For $V_s = 0.5\,\text{V}$, all of the facilitation occurs before the stimulation pulse and there is some facilitation with all three tested synapse weights. Figure 5.22 shows the membrane voltage at the axon tip and the synapse location for $V_s = 2\,\text{V}$ and synapse weight $4.783\,\text{nS}$ for all the synapse trigger times shown in Fig. 5.21. The neuron is active in plot regions which are orange-red, while the synapse trigger time is shown as a dashed cyan line, and the start of the stimulation pulse as a dotted black line. The time at which the neuron becomes active generally increases with increasing synaptic trigger time (after an initial decrease).

The response of the neuron (membrane voltage and ion-channel state variables) to just the synaptic input (with synapse weight of 4.783 nS) alone can be found in Fig. 3.13. The response of the neuron to $V_s = 2\,\mathrm{V}$ stimulation alone can be found in Fig. 5.23. Figure 5.24 shows the facilitated response to a synapse triggered before the stimulation pulse. Figure 5.26 shows the facilitated response to a synapse triggered after the stimulation pulse.

As in Section 5.2.1, Figs. 5.24 and 5.26 show many similarities if the synapse trigger times are lined up. The stimulation pulse causes what appear to be minor deviations in the state of the neuron compared to the EPSP by itself, but these deviations are enough to cause activation when combined with the presence of an EPSP.

For the case of $V_s = 2\,\mathrm{V}$ and synapse weight 4.783 nS, a synapse trigger time of $t = 66\,\mathrm{ms}$ (same as with $V_s = -2\,\mathrm{V}$) maximizes the membrane voltage at the axon tip (compared to other synapse trigger times). Figure 5.25 shows the neuron response to these parameters. Note that this synapse trigger time causes the stimulation pulse to occur when m_{IKdrSM} is at a maximum near the synapse and h_{INaSM} is at a minimum. This was also seen in Section 5.2.1.

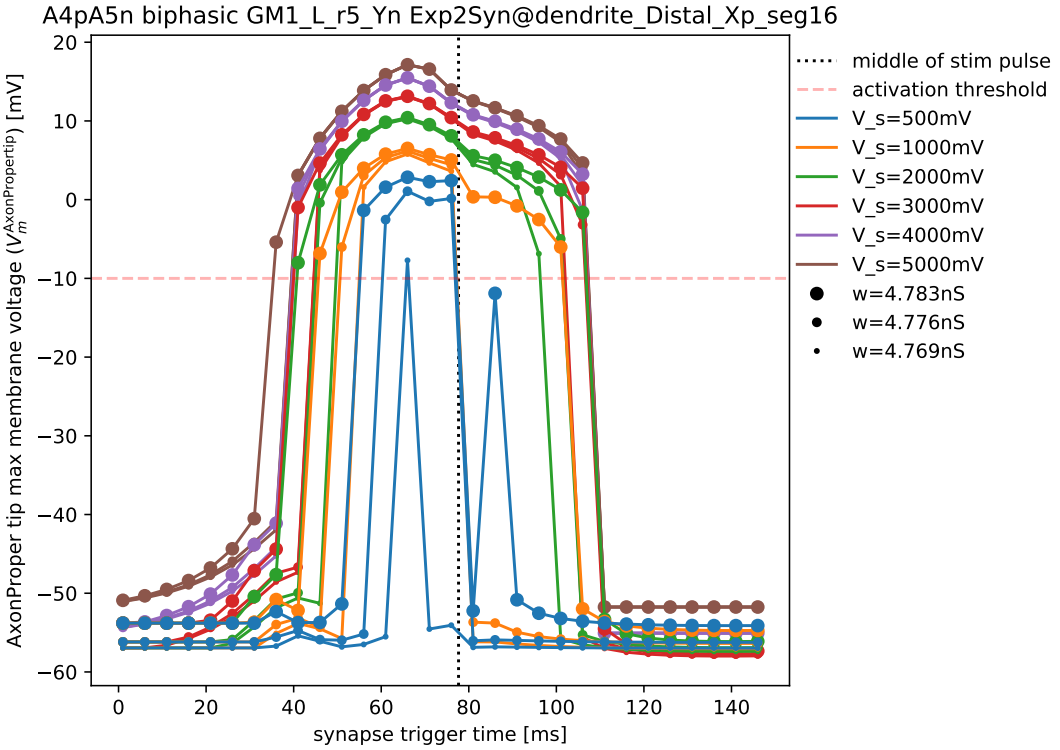

Figure 5.21: Membrane voltage at the axon tip (V_m^{axontip}) vs synapse trigger time for a neuron whose axon points in the $-\hat{y}$ direction located at GM1_L_r5. This neuron has a synapse triggered at segment 16 on the distal dendrite that points in the $+\hat{x}$ direction and is exposed to biphasic epidural stimulation using stimulating electrode combination A4pA5n. The stimulation pulse starts at t=76.0ms and the maximum amplitudes of the pulse occur at t=77.66ms ± 0.16ms. The following list contains tuples of the form (V_s, w, $\#T_B$, $\#T_A$) where V_s is the stimulation voltage, w is the synapse weight, and ($\#T_B$, $\#T_A$) is the number of synapse trigger time samples (x-axis samples in the above graph) before or after the stimulation pulse, respectively, given the values of V_s and w that result in neuron activation (a value of V_m^{axontip} above -10 mV) : (5.0V, 4.783nS, 9, 6), (5.0V, 4.776nS, 8, 6), (5.0V, 4.769nS, 8, 6), (4.0V, 4.783nS, 8, 6), (4.0V, 4.776nS, 8, 6), (4.0V, 4.769nS, 8, 6), (3.0V, 4.783nS, 8, 6), (3.0V, 4.776nS, 7, 6), (3.0V, 4.769nS, 7, 5), (2.0V, 4.783nS, 8, 6), (2.0V, 4.776nS, 7, 5), (2.0V, 4.769nS, 6, 4), (1.0V, 4.783nS, 7, 5), (1.0V, 4.776nS, 6, 0), (1.0V, 4.769nS, 5, 0), (0.5V, 4.783nS, 5, 0), (0.5V, 4.776nS, 4, 0), and (0.5V, 4.769nS, 1, 0).

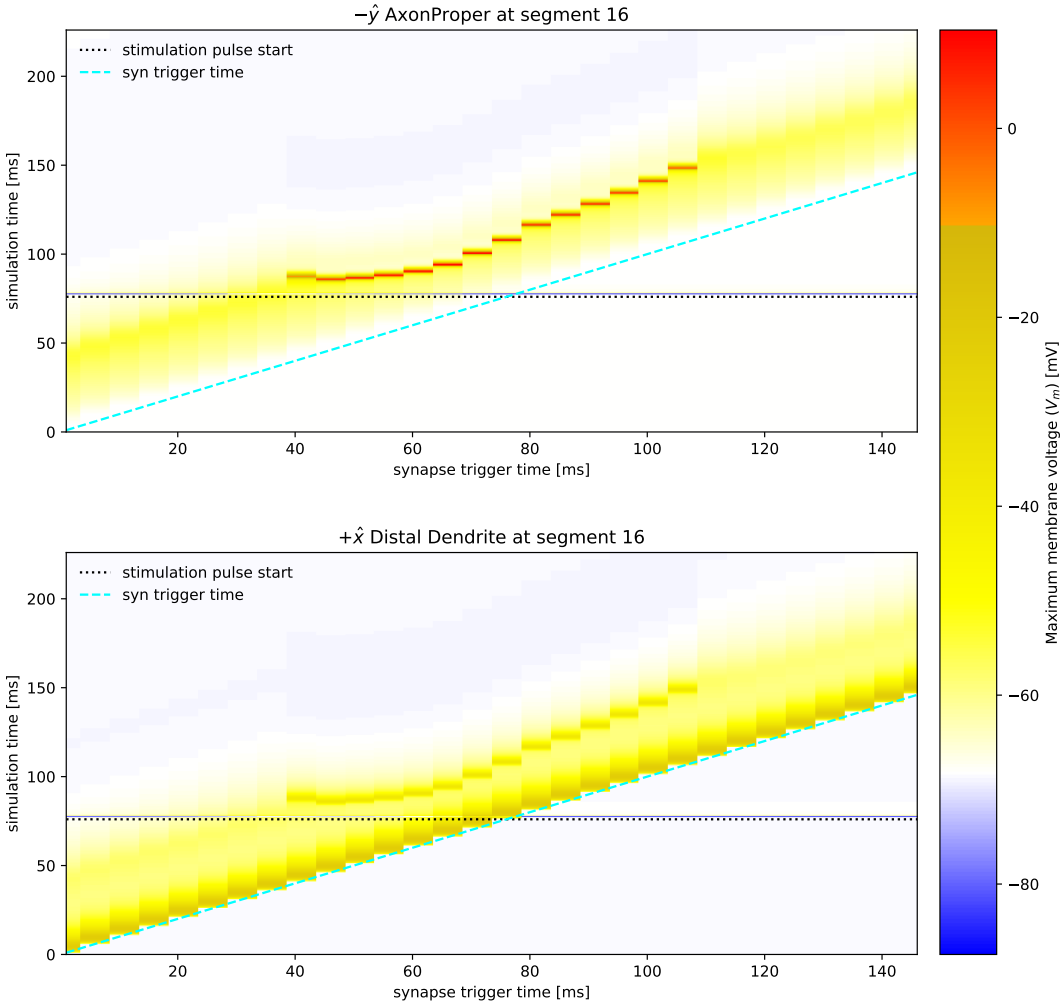

Figure 5.22: Membrane voltage (V_m) (see colormap) at the axon tip (top figure) and at the synapse location (bottom figure) as a function of synapse trigger time (x-axis) and simulation time (y-axis). Measured on neuron GM1_L_r5_Yn exposed to 2.0 V of biphasic epidural stimulation using stimulating electrode combination A4pA5n while a synaptic input with synapse weight=4.783nS is triggered at varying times on the distal dendrite that points in the $+\hat{x}$ direction at segment 16. The electrical stimulation pulse starts at t=76.0ms and the maximum amplitudes of the pulse occur at t=77.66ms ± 0.16ms. The colormap is white when $V_m = -68.31$ mV (the resting membrane voltage for the distal axon tip) and changes from dark yellow to orange at $V_m = -10$ mV to indicate neuron activation.

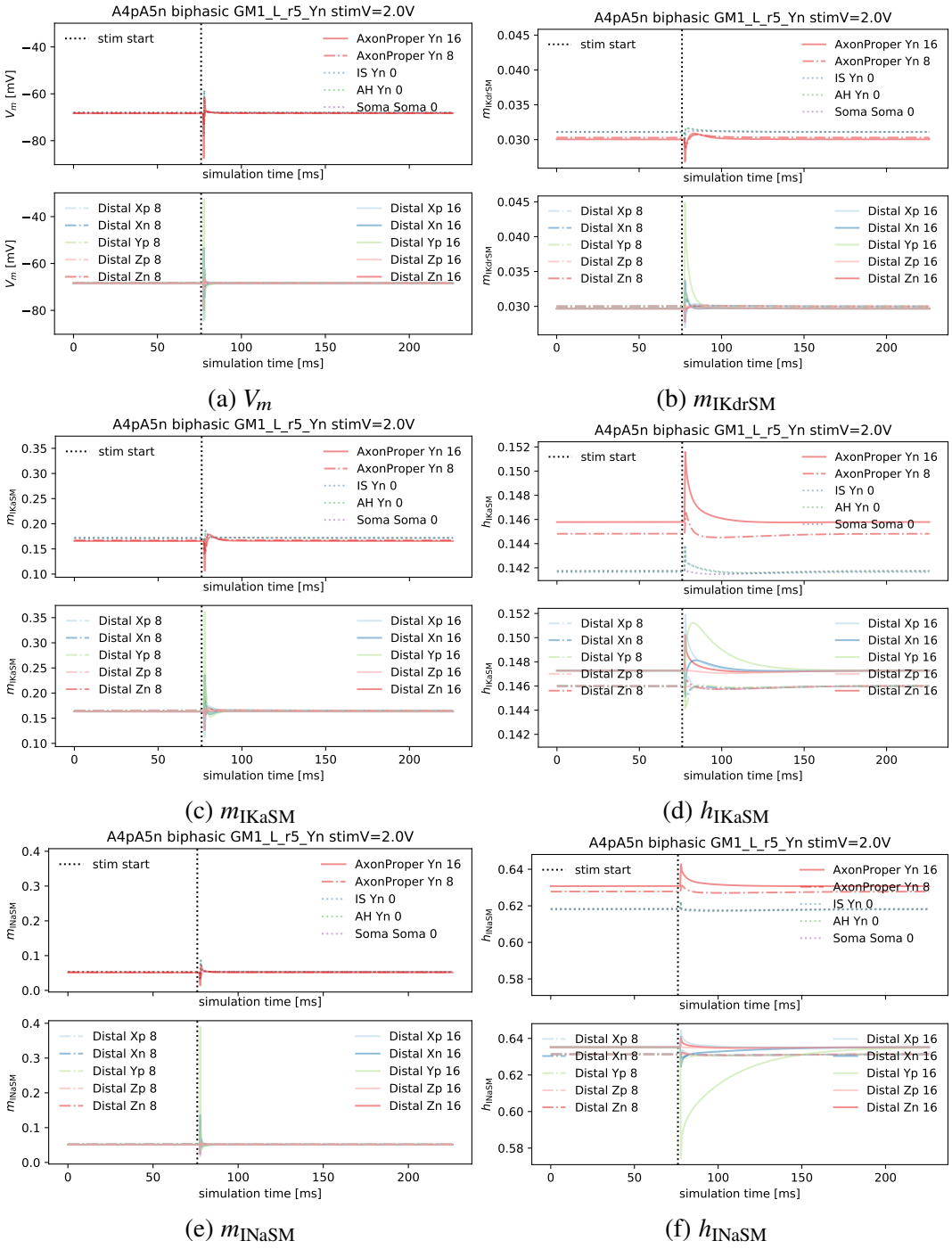

(a) V_m

(b) m_{IKdrSM}

(c) m_{IKaSM}

(d) h_{IKaSM}

(e) m_{INaSM}

(f) h_{INaSM}

Figure 5.23: Stimulation only: Each subplot plots a different variable ((a) V_m, (b) m_{IKdrSM}, (c) m_{IKaSM}, (d) h_{IKaSM}, (e) m_{INaSM}, and (f) h_{INaSM}) against simulation time (ms) for probes on axon-soma (sub-top) and dendrites (sub-bottom). All data measured using neuron GM1_L_r5_Yn exposed to 2.0 V of biphasic stimulation using stimulating electrode combination A4pA5n. The stimulation pulse starts at t=76.0ms and the maximum amplitudes of the pulse occur at t=77.66ms ± 0.16ms.

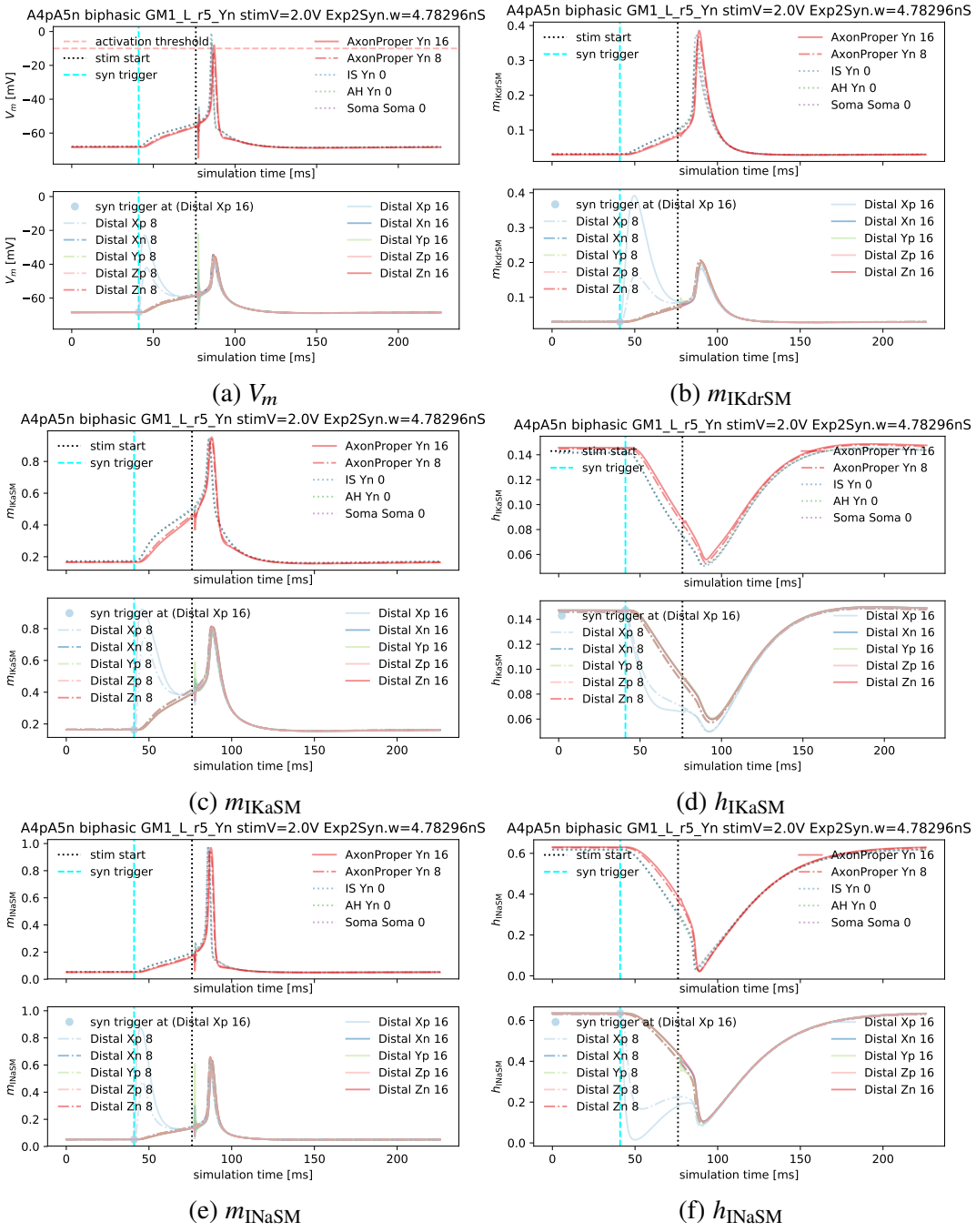

(a) V_m (b) m_{IKdrSM}

(c) m_{IKaSM} (d) h_{IKaSM}

(e) m_{INaSM} (f) h_{INaSM}

Figure 5.24: Stimulation + EPSP: Each subplot plots a different variable ((a) V_m, (b) m_{IKdrSM}, (c) m_{IKaSM}, (d) h_{IKaSM}, (e) m_{INaSM}, and (f) h_{INaSM}) against simulation time (ms) for probes on axon-soma (sub-top) and dendrites (sub-bottom). Measured on neuron GM1_L_r5_Yn exposed to 2.0 V of biphasic stimulation using stimulating electrode combination A4pA5n. The stimulation pulse starts at t=76.0ms and the maximum amplitudes of the pulse occur at t=77.66ms ± 0.16ms. An Exp2Syn synapse was triggered at t=41.0 ms with a synaptic weight of 4.783nS. The synapse was located at segment 16 on the distal dendrite that points in the $+\hat{x}$ direction.

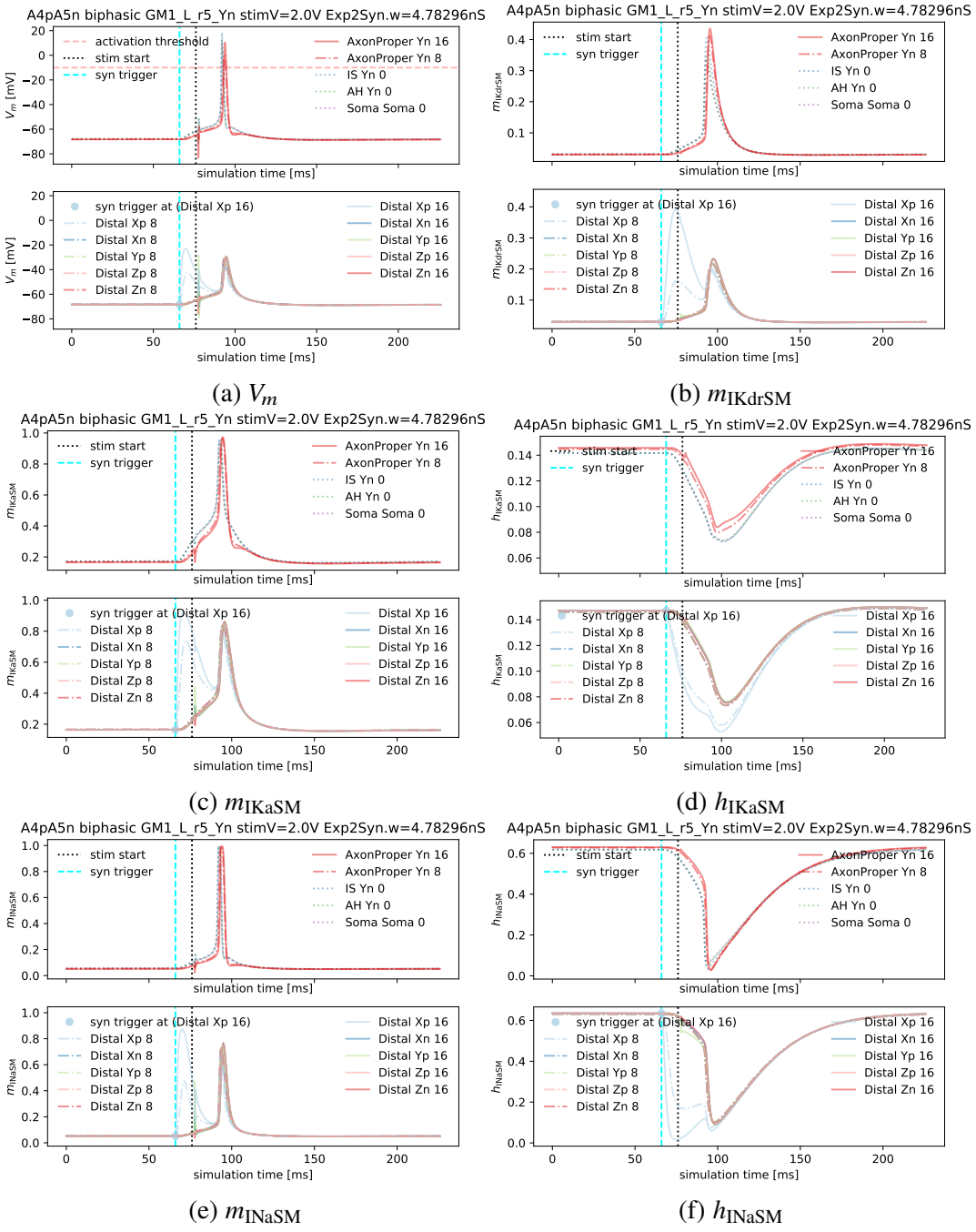

(a) V_m (b) m_{IKdrSM}

(c) m_{IKaSM} (d) h_{IKaSM}

(e) m_{INaSM} (f) h_{INaSM}

Figure 5.25: Stimulation + EPSP: Each subplot plots a different variable ((a) V_m, (b) m_{IKdrSM}, (c) m_{IKaSM}, (d) h_{IKaSM}, (e) m_{INaSM}, and (f) h_{INaSM}) against simulation time (ms) for probes on axon-soma (sub-top) and dendrites (sub-bottom). Measured on neuron GM1_L_r5_Yn exposed to 2.0 V of biphasic stimulation using stimulating electrode combination A4pA5n. The stimulation pulse starts at t=76.0ms and the maximum amplitudes of the pulse occur at t=77.66ms ± 0.16ms. An Exp2Syn synapse was triggered at t=66.0 ms with a synaptic weight of 4.783nS. The synapse was located at segment 16 on the distal dendrite that points in the $+\hat{x}$ direction.

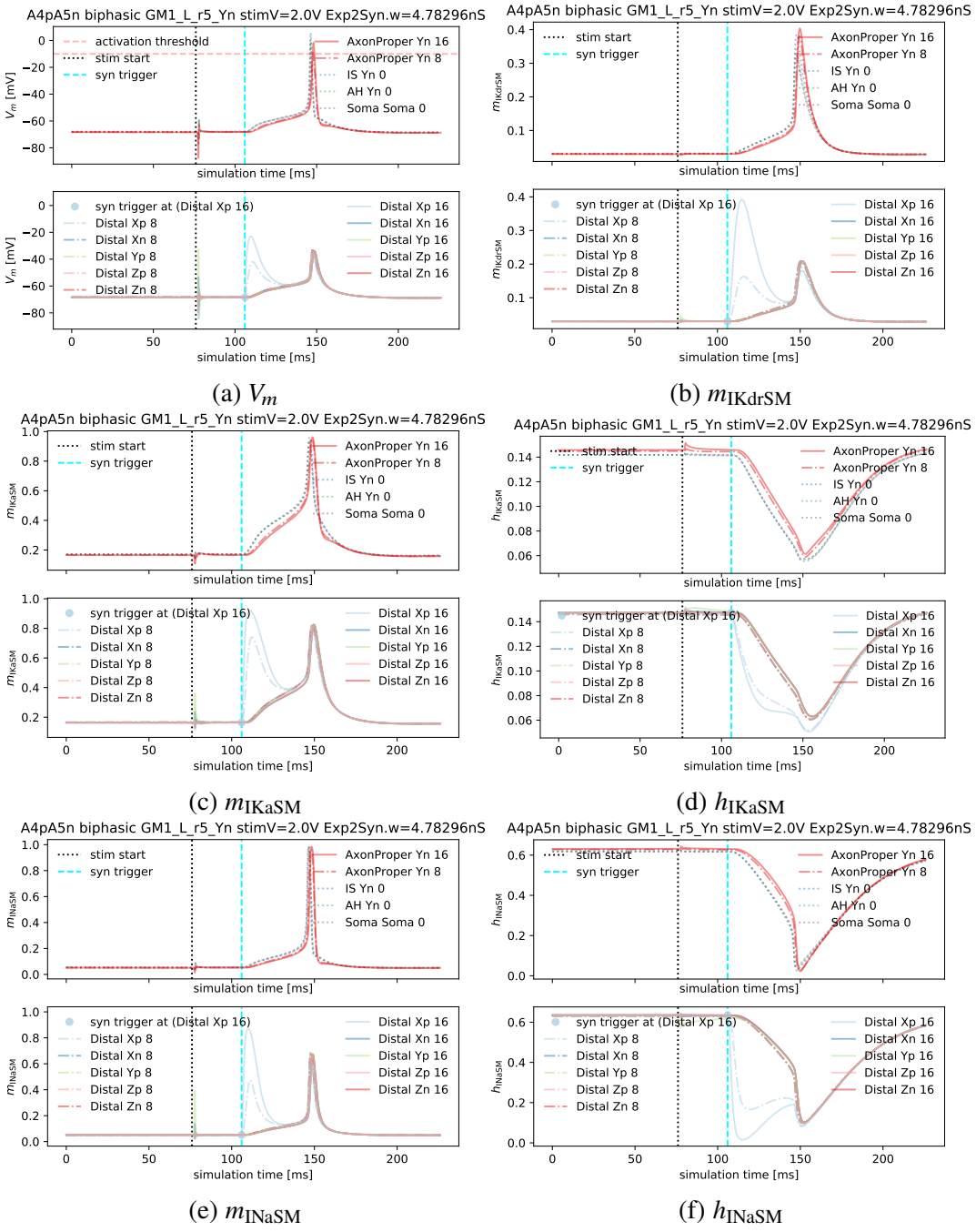

Figure 5.26: Stimulation + EPSP: Each subplot plots a different variable ((a) V_m, (b) m_{IKdrSM}, (c) m_{IKaSM}, (d) h_{IKaSM}, (e) m_{INaSM}, and (f) h_{INaSM}) against simulation time (ms) for probes on axon-soma (sub-top) and dendrites (sub-bottom). Measured on neuron GM1_L_r5_Yn exposed to 2.0 V of biphasic stimulation using stimulating electrode combination A4pA5n. The stimulation pulse starts at t=76.0ms and the maximum amplitudes of the pulse occur at t=77.66ms ± 0.16ms. An Exp2Syn synapse was triggered at t=106.0 ms with a synaptic weight of 4.783nS. The synapse was located at segment 16 on the distal dendrite that points in the $+\hat{x}$ direction.

5.B.2 Biphasic stimulation with $V_s < 0$ and a mid-dendrite synapse

For biphasic stimulation using A4pA5n with $V_s < 0$ of neuron GM1_L_r5_Yn with a synapse triggered on the distal dendrite pointing in the $\hat{x}$ direction at segment 8, the maximum membrane voltage at the axon tip for the synapse weights, trigger times, and stimulation voltages listed in Section 5.1 can be seen in Fig. 5.27. Without any EPSPs, the neuron will activate if $V_s = -6\,\mathrm{V}$. As with the previous biphasic stimulation examples, the window of facilitation is larger before the stimulation pulse. As $|V_s|$ and synapse weight decrease, the facilitation window is only before the stimulation pulse. This implies that it takes less biphasic stimulation and/or synapse weight to facilitate the neuron if the synapse is triggered first and the biphasic stimulation pulse occurs within about 20 ms after.

Figure 5.28 shows the membrane voltage at the axon tip and the synapse location for $V_s = -2\,\mathrm{V}$ and synapse weight 3.45 nS for all the synapse trigger times shown in Fig. 5.27. The neuron activations are shown in orange-red, while the synapse trigger time is shown as a dashed cyan line, and the start of the stimulation pulse as a dotted black line. The time of the neuron activations generally increases with increasing synaptic trigger time (with a gap of no facilitation in the middle), and each of the activations travels back to the synapse location.

The response of the neuron (membrane voltage and ion-channel state variables) to just the EPSP (with synapse weight of 3.45 nS) alone can be found in Fig. 3.10. The response of the neuron to $V_s = 2\,\mathrm{V}$ stimulation alone can be found in Fig. 5.23. Figure 5.29 shows the facilitated response to a synapse triggered before the stimulation pulse. Figure 5.31 shows the facilitated response to a synapse triggered after the stimulation pulse.

As in Sections 5.2.1 and 5.B.1, Figs. 5.29 and 5.31 show many similarities if the synapse trigger times are lined up. The stimulation pulse causes what appear to be

minor deviations in the state of the neuron compared to the EPSP by itself, but these deviations are enough to cause activation when combined with the EPSP.

For the case of $V_s = 2\,\mathrm{V}$ and synapse weight 3.45 nS, a synapse trigger time of $t = 66\,\mathrm{ms}$ (same as with $V_s = -2\,\mathrm{V}$) maximizes the membrane voltage at the axon tip (compared to other synapse trigger times). Figure 5.30 shows the neuron response to these parameters. Note that this synapse trigger time causes the stimulation pulse to occur when m_{IKdrSM} is at a maximum near the synapse and h_{INaSM} is at a minimum. This behavior was also seen in Sections 5.2.1 and 5.B.1.

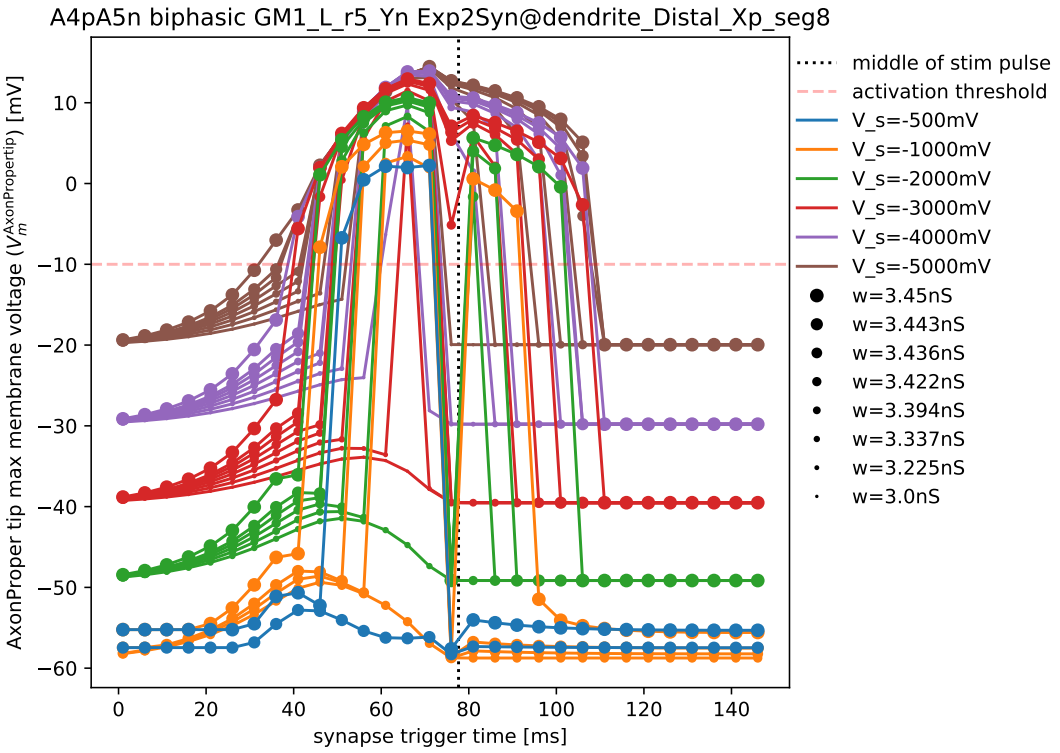

Figure 5.27: Membrane voltage at the axon tip (V_m^{axontip}) vs synapse trigger time for a neuron whose axon points in the $-\hat{y}$ direction located at GM1_L_r5. This neuron has a synapse triggered at segment 8 on the distal dendrite that points in the $+\hat{x}$ direction and is exposed to biphasic epidural stimulation using stimulating electrode combination A4pA5n. The stimulation pulse starts at t=76.0ms and the maximum amplitudes of the pulse occur at t=77.66ms ± 0.16ms. The following list contains tuples of the form (V_s, w, $\#T_B$, $\#T_A$) where V_s is the stimulation voltage, w is the synapse weight, and ($\#T_B$, $\#T_A$) is the number of synapse trigger time samples (x-axis samples in the above graph) before or after the stimulation pulse, respectively, given the values of V_s and w that result in neuron activation (a value of V_m^{axontip} above -10 mV) : (-5.0V, 3.45nS, 9, 6), (-5.0V, 3.443nS, 8, 6), (-5.0V, 3.436nS, 8, 6), (-5.0V, 3.422nS, 7, 5), (-5.0V, 3.394nS, 7, 4), (-5.0V, 3.337nS, 7, 3), (-5.0V, 3.225nS, 6, 1), (-5.0V, 3.0nS, 4, 0), (-4.0V, 3.45nS, 8, 6), (-4.0V, 3.443nS, 7, 5), (-4.0V, 3.436nS, 7, 5), (-4.0V, 3.422nS, 7, 4), (-4.0V, 3.394nS, 6, 2), (-4.0V, 3.337nS, 6, 1), (-4.0V, 3.225nS, 4, 0), (-4.0V, 3.0nS, 2, 0), (-3.0V, 3.45nS, 8, 6), (-3.0V, 3.443nS, 7, 4), (-3.0V, 3.436nS, 7, 3), (-3.0V, 3.422nS, 6, 2), (-3.0V, 3.394nS, 5, 0), (-3.0V, 3.337nS, 4, 0), (-3.0V, 3.225nS, 1, 0), (-2.0V, 3.45nS, 6, 5), (-2.0V, 3.443nS, 5, 2), (-2.0V, 3.436nS, 5, 1), (-2.0V, 3.422nS, 4, 0), (-2.0V, 3.394nS, 3, 0), (-1.0V, 3.45nS, 6, 3), (-1.0V, 3.443nS, 4, 0), (-1.0V, 3.436nS, 3, 0), and (-0.5V, 3.45nS, 5, 0).

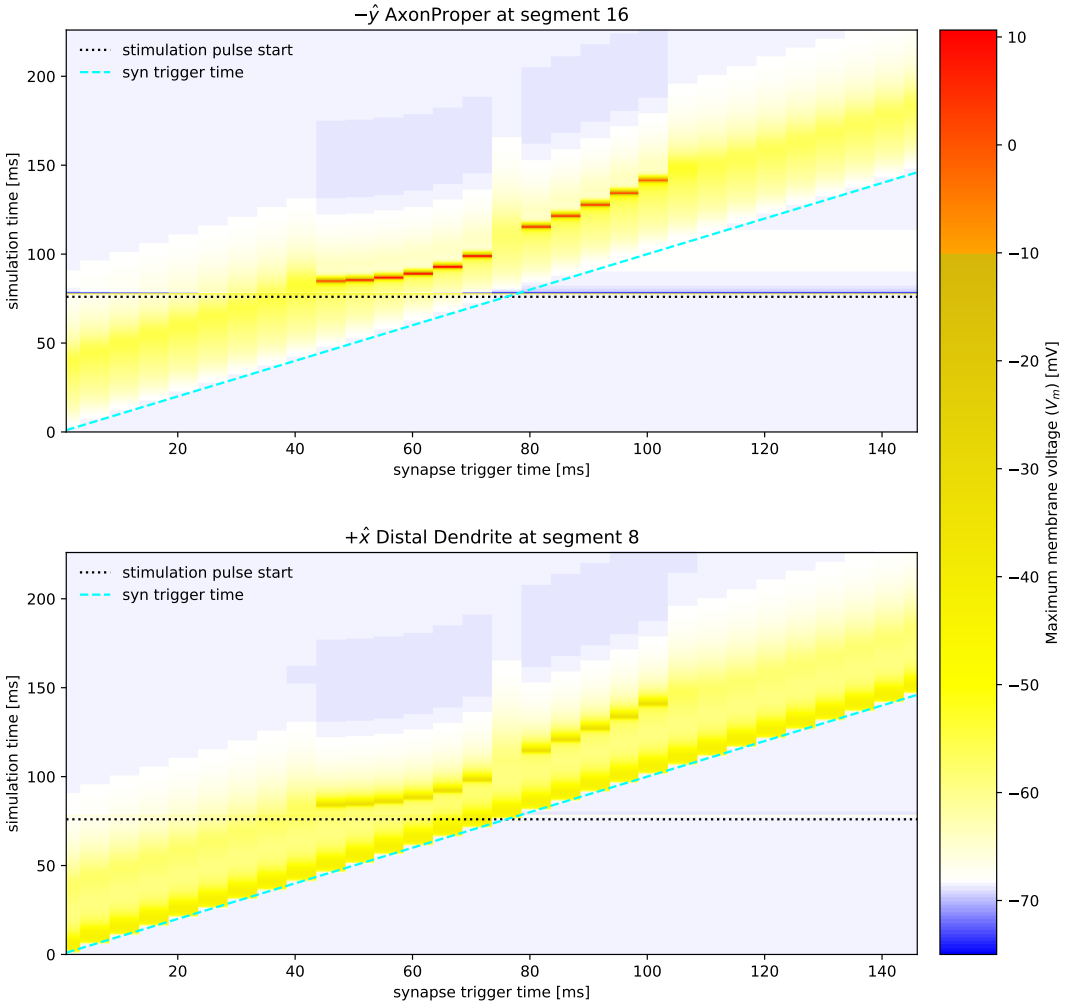

Figure 5.28: Membrane voltage (V_m) (see colormap) at the axon tip (top figure) and at the synapse location (bottom figure) as a function of synapse trigger time (x-axis) and simulation time (y-axis). Measured on neuron GM1_L_r5_Yn exposed to −2.0 V of biphasic epidural stimulation using stimulating electrode combination A4pA5n while a synaptic input with synapse weight=3.45nS is triggered at varying times on the distal dendrite that points in the $+\hat{x}$ direction at segment 8. The electrical stimulation pulse starts at t=76.0ms and the maximum amplitudes of the pulse occur at t=77.66ms ± 0.16ms. The colormap is white when $V_m = -68.31$ mV (the resting membrane voltage for the distal axon tip) and changes from dark yellow to orange at $V_m = -10$ mV to indicate neuron activation.

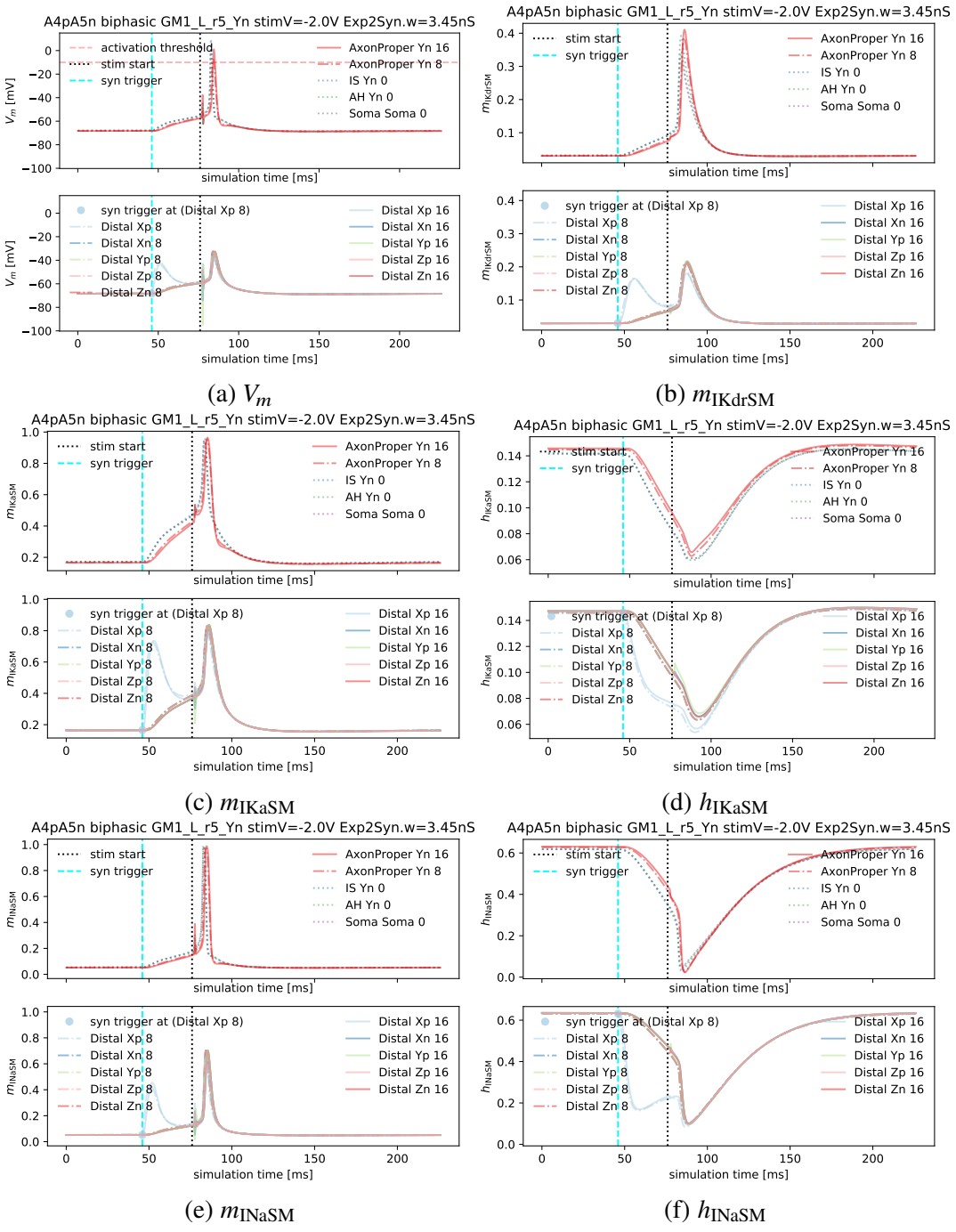

(a) V_m (b) m_{IKdrSM}

(c) m_{IKaSM} (d) h_{IKaSM}

(e) m_{INaSM} (f) h_{INaSM}

Figure 5.29: Stimulation + EPSP: Each subplot plots a different variable ((a) V_m, (b) m_{IKdrSM}, (c) m_{IKaSM}, (d) h_{IKaSM}, (e) m_{INaSM}, and (f) h_{INaSM}) against simulation time (ms) for probes on axon-soma (sub-top) and dendrites (sub-bottom). Measured on neuron GM1_L_r5_Yn exposed to −2.0 V of biphasic stimulation using stimulating electrode combination A4pA5n. The stimulation pulse starts at t=76.0ms and the maximum amplitudes of the pulse occur at t=77.66ms ± 0.16ms. An Exp2Syn synapse was triggered at t=46.0 ms with a synaptic weight of 3.45nS. The synapse was located at segment 8 on the distal dendrite that points in the $+\hat{x}$ direction.

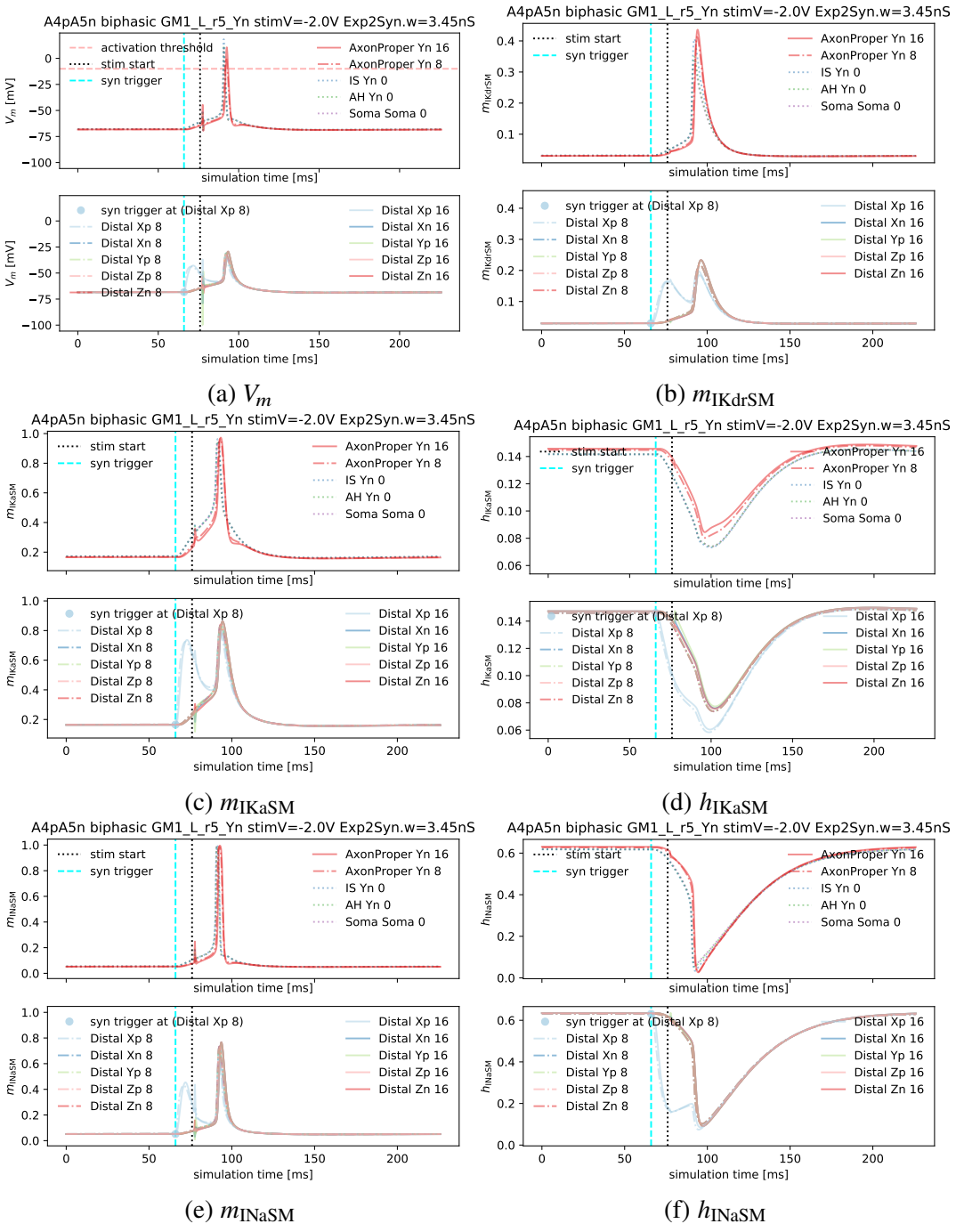

(a) V_m (b) m_{IKdrSM}

(c) m_{IKaSM} (d) h_{IKaSM}

(e) m_{INaSM} (f) h_{INaSM}

Figure 5.30: Stimulation + EPSP: Each subplot plots a different variable ((a) V_m, (b) m_{IKdrSM}, (c) m_{IKaSM}, (d) h_{IKaSM}, (e) m_{INaSM}, and (f) h_{INaSM}) against simulation time (ms) for probes on axon-soma (sub-top) and dendrites (sub-bottom). Measured on neuron GM1_L_r5_Yn exposed to −2.0 V of biphasic stimulation using stimulating electrode combination A4pA5n. The stimulation pulse starts at t=76.0ms and the maximum amplitudes of the pulse occur at t=77.66ms ± 0.16ms. An Exp2Syn synapse was triggered at t=66.0 ms with a synaptic weight of 3.45nS. The synapse was located at segment 8 on the distal dendrite that points in the $+\hat{x}$ direction.

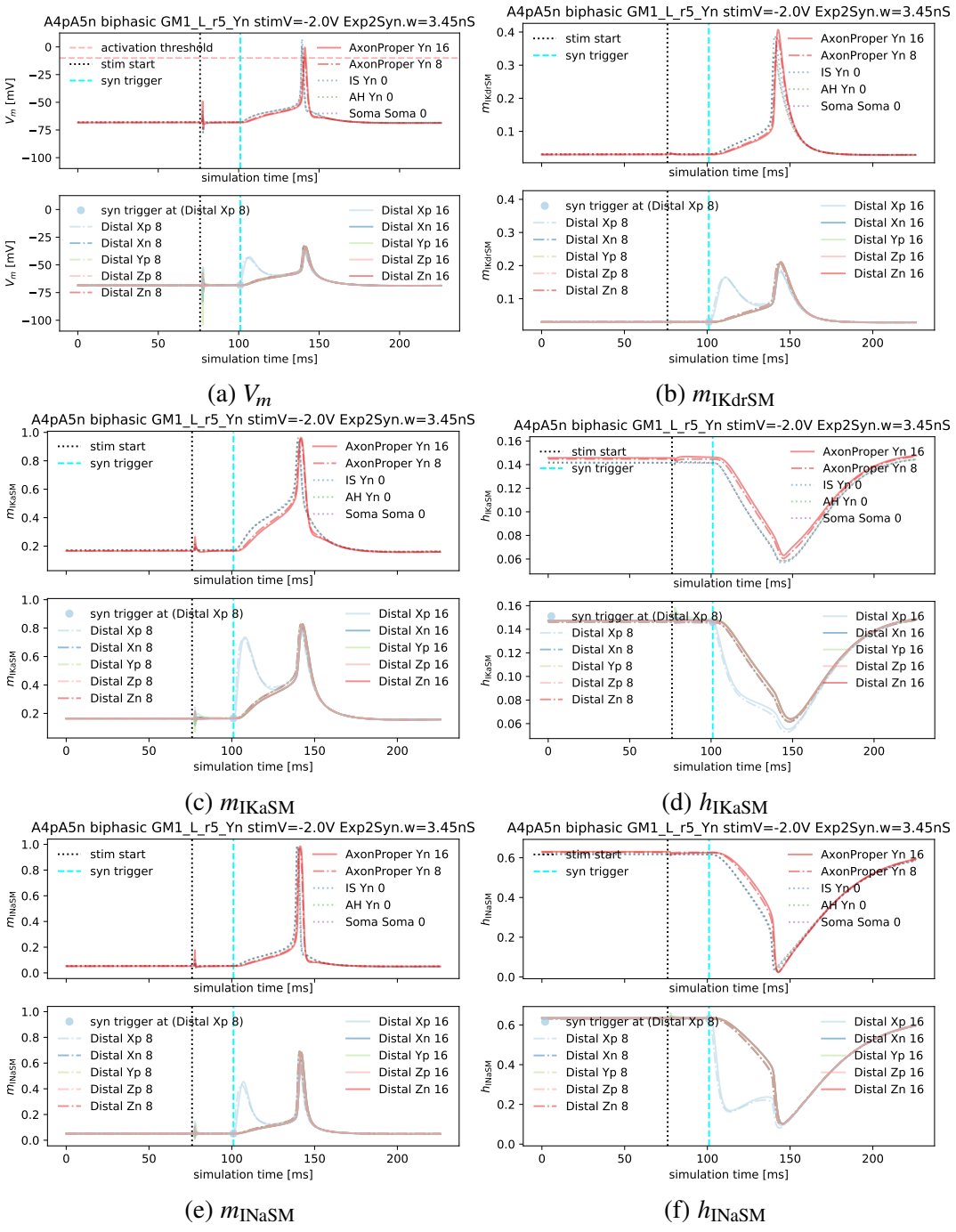

(a) V_m (b) m_{IKdrSM}

(c) m_{IKaSM} (d) h_{IKaSM}

(e) m_{INaSM} (f) h_{INaSM}

Figure 5.31: Stimulation + EPSP: Each subplot plots a different variable ((a) V_m, (b) m_{IKdrSM}, (c) m_{IKaSM}, (d) h_{IKaSM}, (e) m_{INaSM}, and (f) h_{INaSM}) against simulation time (ms) for probes on axon-soma (sub-top) and dendrites (sub-bottom). Measured on neuron GM1_L_r5_Yn exposed to −2.0 V of biphasic stimulation using stimulating electrode combination A4pA5n. The stimulation pulse starts at t=76.0ms and the maximum amplitudes of the pulse occur at t=77.66ms ± 0.16ms. An Exp2Syn synapse was triggered at t=101.0 ms with a synaptic weight of 3.45nS. The synapse was located at segment 8 on the distal dendrite that points in the $+\hat{x}$ direction.

5.B.3 Biphasic stimulation with $V_s > 0$ and a mid-dendrite synapse

For biphasic stimulation using A4pA5n with $V_s > 0$ of neuron GM1_L_r5_Yn with a synapse triggered on the distal dendrite pointing in the $\hat{x}$ direction at segment 8, the maximum membrane voltage at the axon tip for the synapse weights, trigger times, and stimulation voltages listed in Section 5.1 can be seen in Fig. 5.32. Without any EPSPs, the neuron will activate if $V_s = 8\,\mathrm{V}$. As with the previous biphasic stimulation examples, the window of facilitation is larger before the stimulation pulse. As $|V_s|$ and synapse weight decrease, the facilitation window is only before the stimulation pulse. This implies that it takes less biphasic stimulation and/or synapse weight to facilitate the neuron if the synapse is triggered first and the biphasic stimulation pulse occurs within about 20 ms after.

Figure 5.33 shows the membrane voltage at the axon tip and the synapse location for $V_s = 2\,\mathrm{V}$ and synapse weight 3.45 nS for all the synapse trigger times shown in Fig. 5.32. The neuron activations are shown in orange-red, while the synapse trigger time is shown as a dashed cyan line, and the start of the stimulation pulse as a dotted black line. The time of the neuron activations generally increases with increasing synaptic trigger time and each of the activations travels back to the synapse location.

The response of the neuron (membrane voltage and ion-channel state variables) to just the EPSP (with synapse weight of 3.45 nS) alone can be found in Fig. 3.10. Figure 5.34 shows the facilitated response to a synapse triggered before the stimulation pulse. Figure 5.36 shows the facilitated response to a synapse triggered after the stimulation pulse.

As in Sections 5.2.1 to 5.B.2, Figs. 5.34 and 5.36 show many similarities if the synapse trigger times are lined up. The stimulation pulse causes what appear to be minor deviations in the state of the neuron compared to the EPSP by itself, but these deviations are enough to cause activation when combined with the EPSP.

For the case of $V_s = 2\,\mathrm{V}$ and synapse weight 3.45 nS, a synapse trigger time of $t = 66\,\mathrm{ms}$ (same as with $V_s = -2\,\mathrm{V}$) maximizes the membrane voltage at the axon tip (compared to other synapse trigger times). Figure 5.35 shows the neuron response to these parameters. Note that this synapse trigger time causes the stimulation pulse to occur when m_{IKdrSM} is at a maximum near the synapse and h_{INaSM} is at a minimum. The same behavior was also seen in Sections 5.2.1 to 5.B.2.

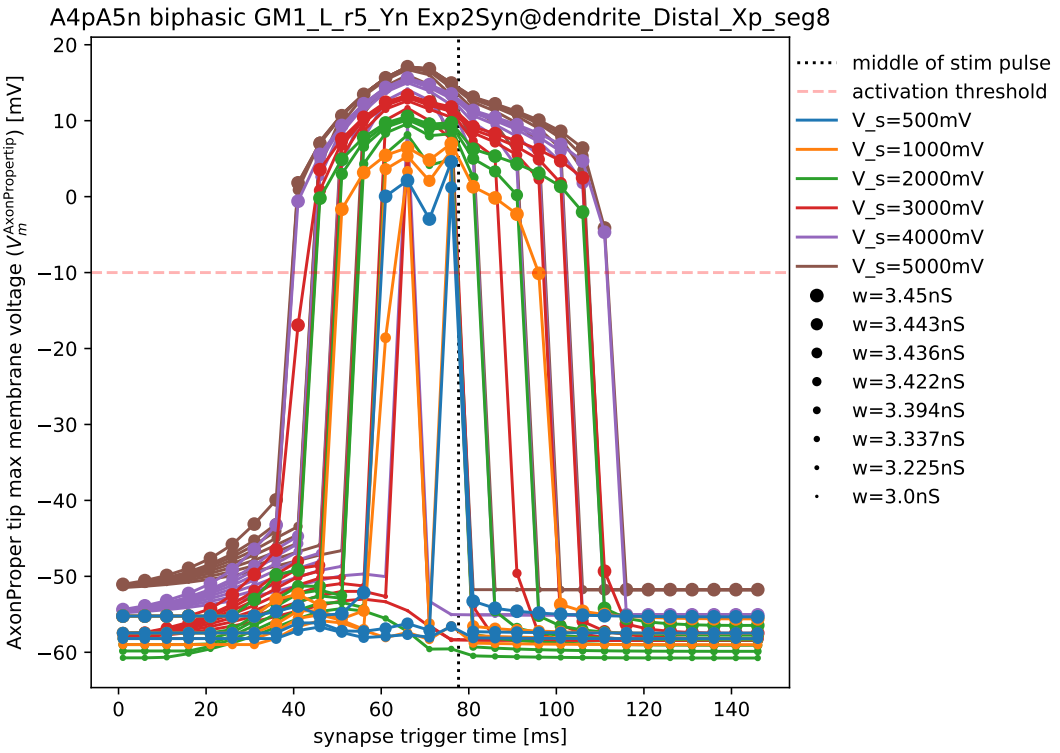

Figure 5.32: Membrane voltage at the axon tip (V_m^{axontip}) vs synapse trigger time for a neuron whose axon points in the $-\hat{y}$ direction located at GM1_L_r5. This neuron has a synapse triggered at segment 8 on the distal dendrite that points in the $+\hat{x}$ direction and is exposed to biphasic epidural stimulation using stimulating electrode combination A4pA5n. The stimulation pulse starts at t=76.0ms and the maximum amplitudes of the pulse occur at t=77.66ms ± 0.16ms. The following list contains tuples of the form (V_s, w, $\#T_B$, $\#T_A$) where V_s is the stimulation voltage, w is the synapse weight, and ($\#T_B$, $\#T_A$) is the number of synapse trigger time samples (x-axis samples in the above graph) before or after the stimulation pulse, respectively, given the values of V_s and w that result in neuron activation (a value of V_m^{axontip} above -10 mV) : (5.0V, 3.45nS, 8, 7), (5.0V, 3.443nS, 8, 6), (5.0V, 3.436nS, 8, 6), (5.0V, 3.422nS, 7, 5), (5.0V, 3.394nS, 7, 4), (5.0V, 3.337nS, 7, 3), (5.0V, 3.225nS, 6, 1), (5.0V, 3.0nS, 5, 0), (4.0V, 3.45nS, 8, 7), (4.0V, 3.443nS, 7, 6), (4.0V, 3.436nS, 7, 5), (4.0V, 3.422nS, 7, 4), (4.0V, 3.394nS, 6, 3), (4.0V, 3.337nS, 6, 1), (4.0V, 3.225nS, 5, 0), (4.0V, 3.0nS, 1, 0), (3.0V, 3.45nS, 7, 6), (3.0V, 3.443nS, 7, 5), (3.0V, 3.436nS, 6, 4), (3.0V, 3.422nS, 6, 2), (3.0V, 3.394nS, 5, 0), (3.0V, 3.337nS, 4, 0), (3.0V, 3.225nS, 1, 0), (2.0V, 3.45nS, 7, 6), (2.0V, 3.443nS, 6, 3), (2.0V, 3.436nS, 5, 1), (2.0V, 3.422nS, 5, 0), (2.0V, 3.394nS, 4, 0), (1.0V, 3.45nS, 6, 3), (1.0V, 3.443nS, 4, 0), (1.0V, 3.436nS, 2, 0), (0.5V, 3.45nS, 4, 0), and (0.5V, 3.443nS, 1, 0).

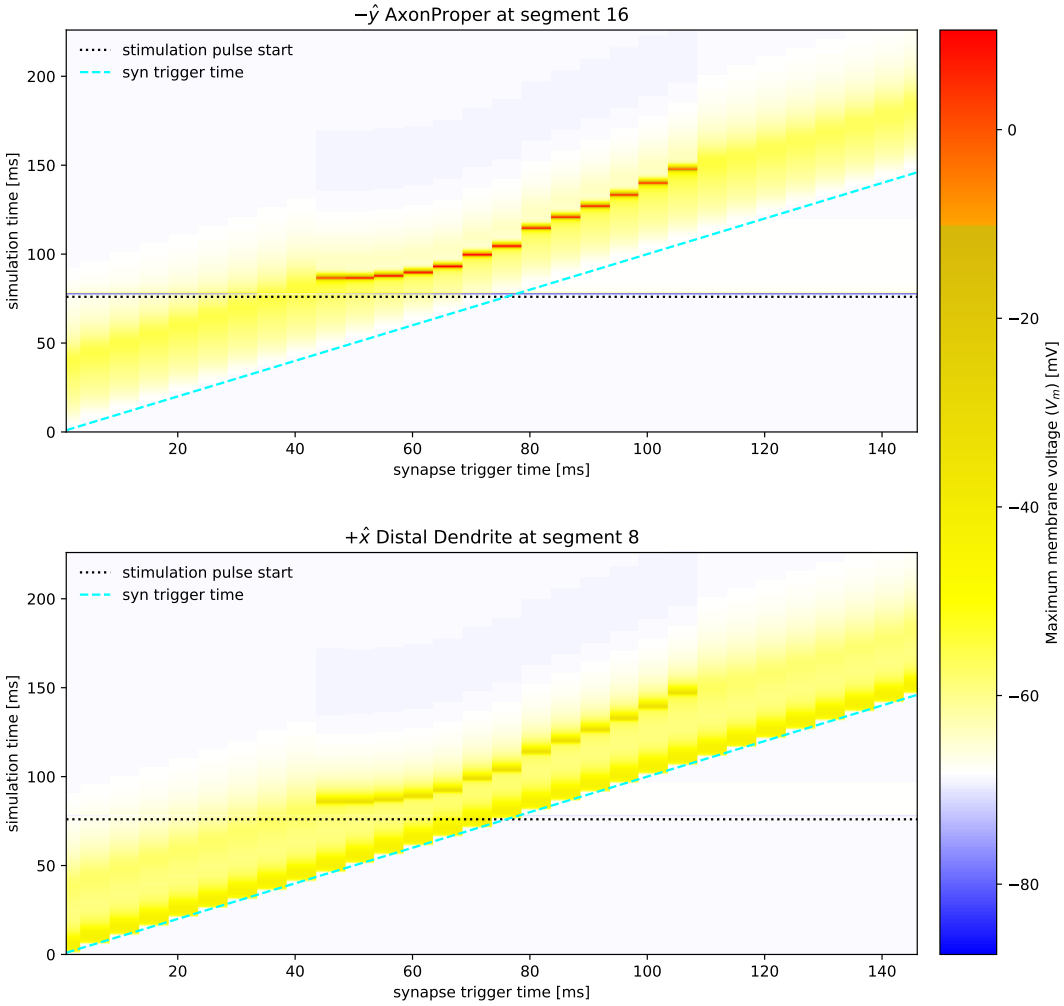

Figure 5.33: Membrane voltage (V_m) (see colormap) at the axon tip (top figure) and at the synapse location (bottom figure) as a function of synapse trigger time (x-axis) and simulation time (y-axis). Measured on neuron GM1_L_r5_Yn exposed to 2.0 V of biphasic epidural stimulation using stimulating electrode combination A4pA5n while a synaptic input with synapse weight=3.45nS is triggered at varying times on the distal dendrite that points in the $+\hat{x}$ direction at segment 8. The electrical stimulation pulse starts at t=76.0ms and the maximum amplitudes of the pulse occur at t=77.66ms ± 0.16ms. The colormap is white when $V_m = -68.31$ mV (the resting membrane voltage for the distal axon tip) and changes from dark yellow to orange at $V_m = -10$ mV to indicate neuron activation.

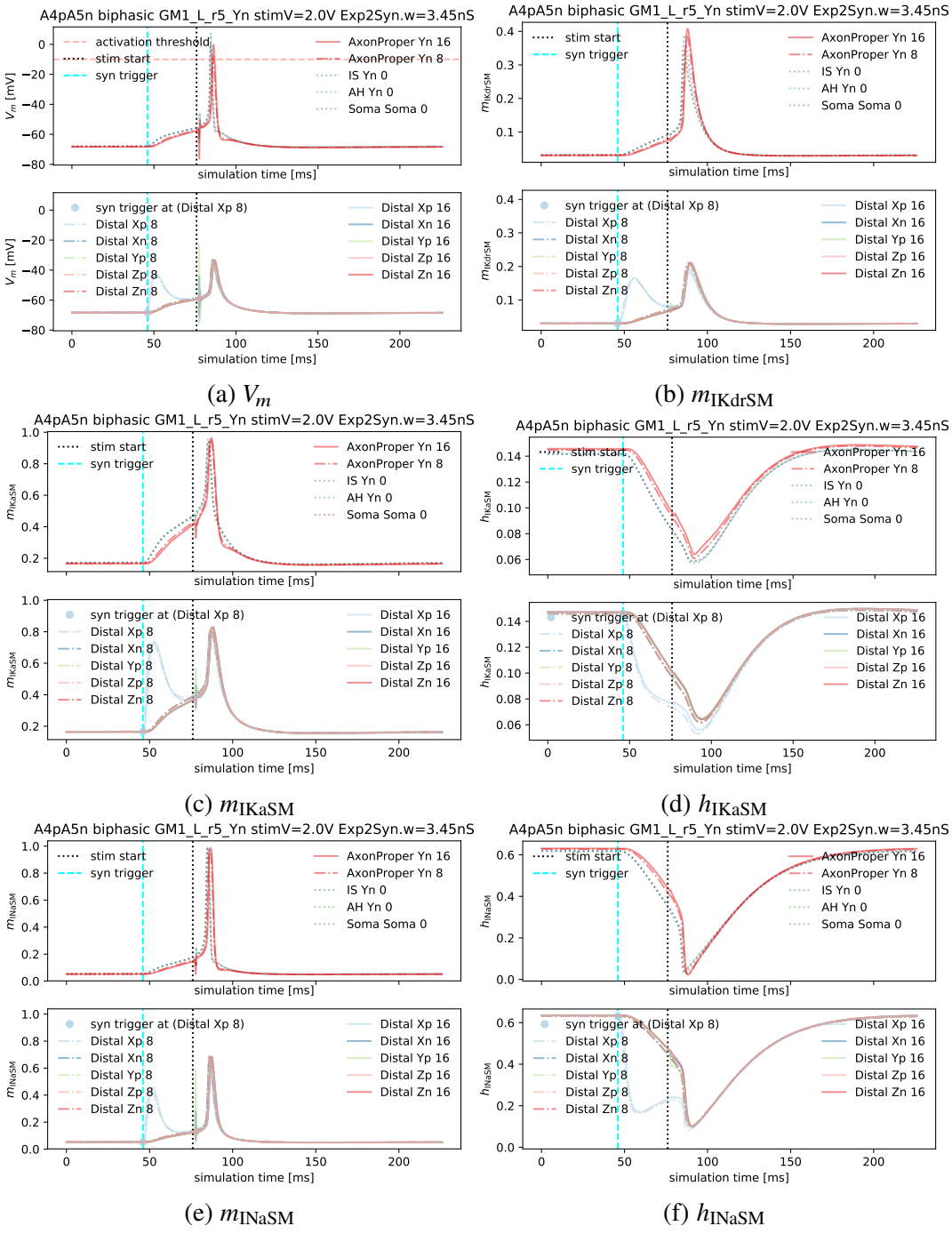

(a) V_m (b) m_{IKdrSM}

(c) m_{IKaSM} (d) h_{IKaSM}

(e) m_{INaSM} (f) h_{INaSM}

Figure 5.34: Stimulation + EPSP: Each subplot plots a different variable ((a) V_m, (b) m_{IKdrSM}, (c) m_{IKaSM}, (d) h_{IKaSM}, (e) m_{INaSM}, and (f) h_{INaSM}) against simulation time (ms) for probes on axon-soma (sub-top) and dendrites (sub-bottom). Measured on neuron GM1_L_r5_Yn exposed to 2.0 V of biphasic stimulation using stimulating electrode combination A4pA5n. The stimulation pulse starts at t=76.0ms and the maximum amplitudes of the pulse occur at t=77.66ms ± 0.16ms. An Exp2Syn synapse was triggered at t=46.0 ms with a synaptic weight of 3.45nS. The synapse was located at segment 8 on the distal dendrite that points in the $+\hat{x}$ direction.

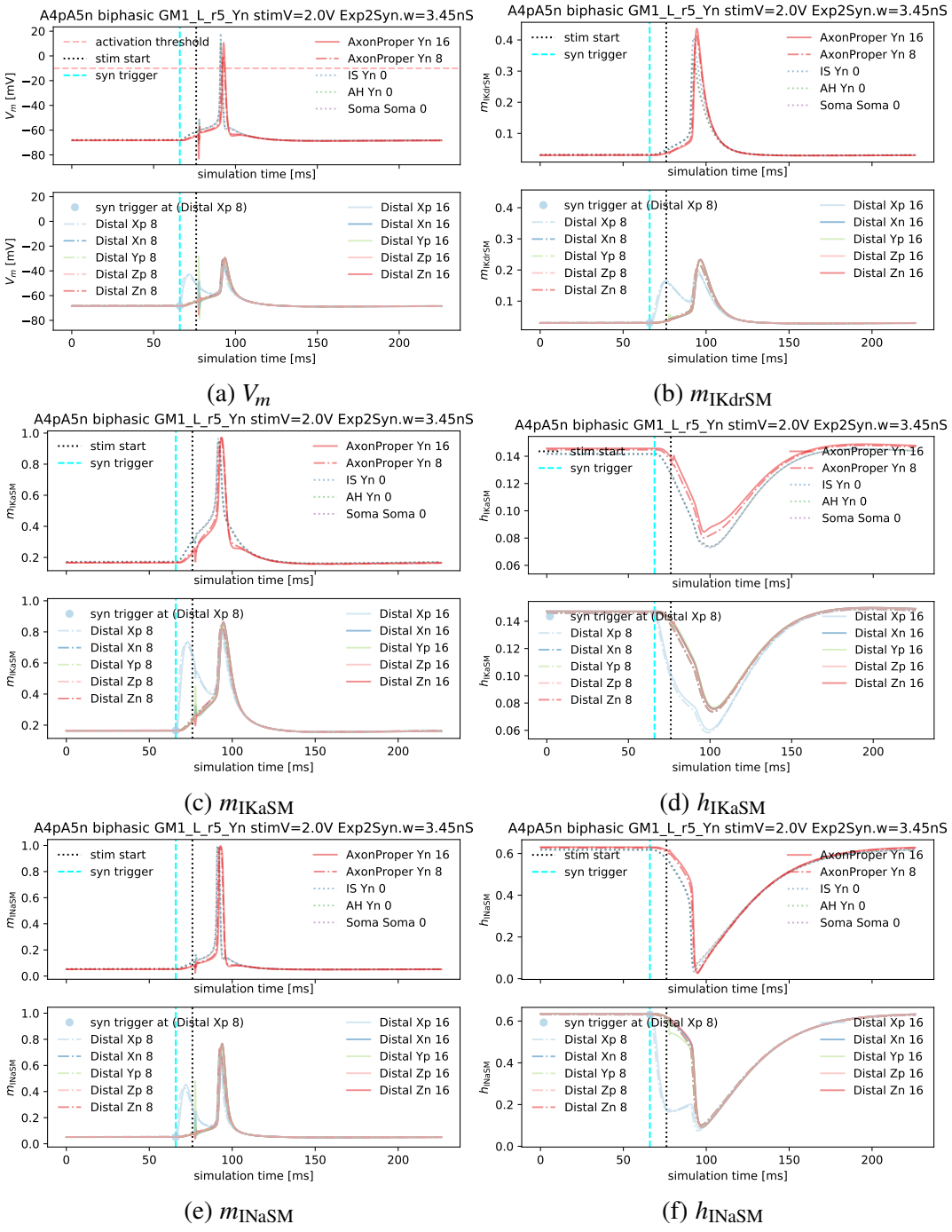

(a) V_m (b) m_{IKdrSM}

(c) m_{IKaSM} (d) h_{IKaSM}

(e) m_{INaSM} (f) h_{INaSM}

Figure 5.35: Stimulation + EPSP: Each subplot plots a different variable ((a) V_m, (b) m_{IKdrSM}, (c) m_{IKaSM}, (d) h_{IKaSM}, (e) m_{INaSM}, and (f) h_{INaSM}) against simulation time (ms) for probes on axon-soma (sub-top) and dendrites (sub-bottom). Measured on neuron GM1_L_r5_Yn exposed to 2.0 V of biphasic stimulation using stimulating electrode combination A4pA5n. The stimulation pulse starts at t=76.0ms and the maximum amplitudes of the pulse occur at t=77.66ms ± 0.16ms. An Exp2Syn synapse was triggered at t=66.0 ms with a synaptic weight of 3.45nS. The synapse was located at segment 8 on the distal dendrite that points in the $+\hat{x}$ direction.

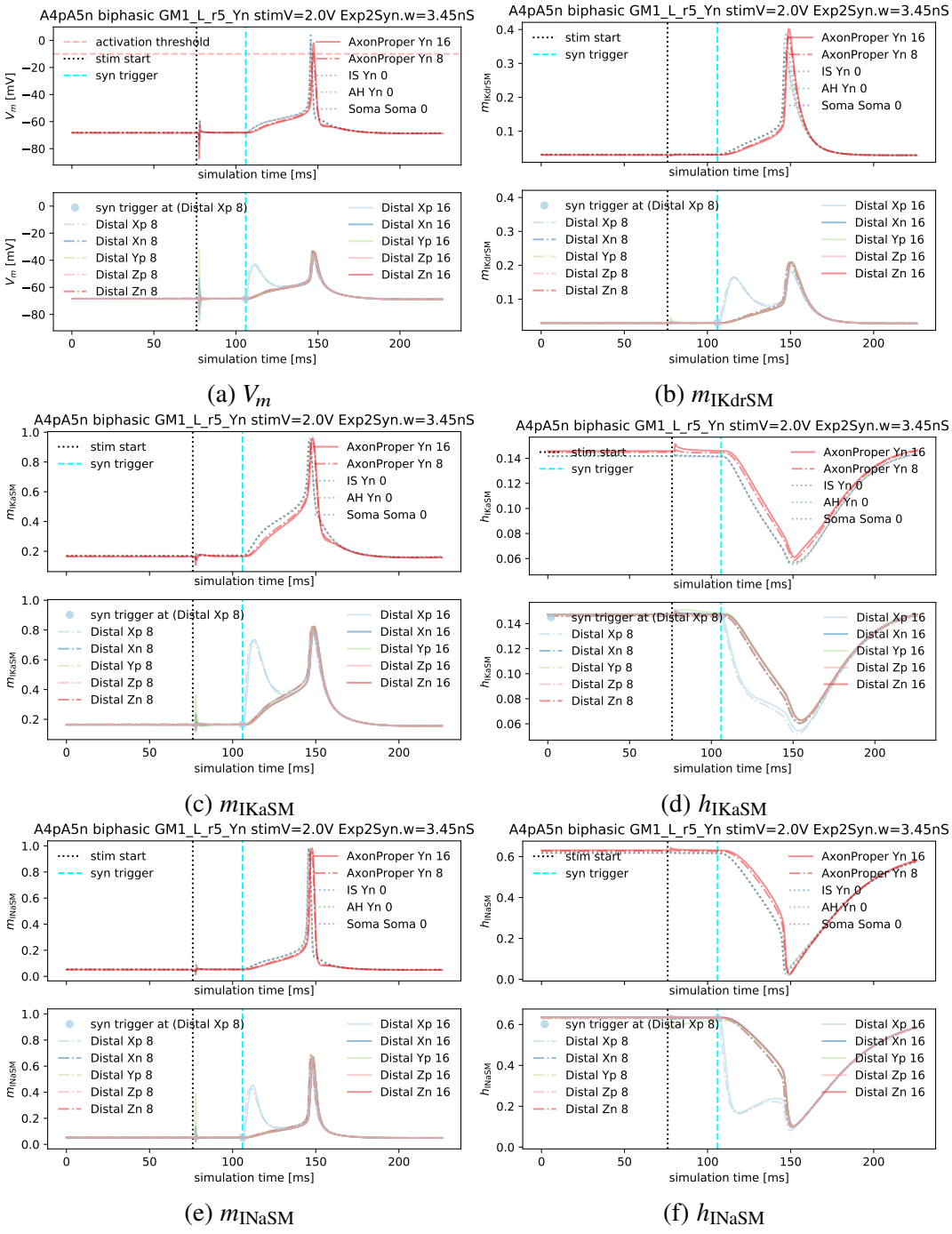

(a) V_m (b) m_{IKdrSM}

(c) m_{IKaSM} (d) h_{IKaSM}

(e) m_{INaSM} (f) h_{INaSM}

Figure 5.36: Stimulation + EPSP: Each subplot plots a different variable ((a) V_m, (b) m_{IKdrSM}, (c) m_{IKaSM}, (d) h_{IKaSM}, (e) m_{INaSM}, and (f) h_{INaSM}) against simulation time (ms) for probes on axon-soma (sub-top) and dendrites (sub-bottom). Measured on neuron GM1_L_r5_Yn exposed to 2.0 V of biphasic stimulation using stimulating electrode combination A4pA5n. The stimulation pulse starts at t=76.0ms and the maximum amplitudes of the pulse occur at t=77.66ms ± 0.16ms. An Exp2Syn synapse was triggered at t=106.0 ms with a synaptic weight of 3.45nS. The synapse was located at segment 8 on the distal dendrite that points in the $+\hat{x}$ direction.

5.B.4 Monophasic stimulation with $V_s < 0$ and a mid-dendrite synapse

For monophasic stimulation using A4pA5n with $V_s < 0$ of neuron GM1_L_r5_Yn with a synapse triggered on the distal dendrite pointing in the $\hat{x}$ direction at segment 8, the maximum membrane voltage at the axon tip for the synapse weights, trigger times, and stimulation voltages listed in Section 5.1 can be seen in Fig. 5.37. Without any EPSPs, the neuron will activate if $V_s = -4.25\,\text{V}$. The window of facilitation is fairly balanced between before and after the stimulation pulse if $V_s = -4\,\text{V}$. If V_s is [0.5, 1, 2, 3]V, there is clearly more facilitation if the synapse is triggered before the stimulation pulse.

Figure 5.38 shows the membrane voltage at the axon tip and the synapse location for $V_s = -2\,\text{V}$ and synapse weight 3.45 nS for all the synapse trigger times shown in Fig. 5.27. The neuron activations are shown in orange-red, while the synapse trigger time is shown as a dashed cyan line, and the start of the stimulation pulse as a dotted black line. The time of the neuron activations generally increases with increasing synaptic trigger time and each of the activations travel back to the synapse location.

The response of the neuron (membrane voltage and ion-channel state variables) to just the EPSP (with synapse weight of 3.45 nS) alone can be found in Fig. 3.10. The response of the neuron to $V_s = -2\,\text{V}$ stimulation alone can be found in Fig. 5.6. Figure 5.39 shows the facilitated response to a synapse triggered before the stimulation pulse. Figure 5.41 shows the facilitated response to a synapse triggered after the stimulation pulse.

For the case of $V_s = -2\,\text{V}$ and synapse weight 3.45 nS, the membrane voltage at the axon tip is maximized (compared to other synapse trigger times) if synapse trigger time is the same as the start of the stimulation pulse ($t = 76\,\text{ms}$). Figure 5.40 shows the neuron response to these parameters.

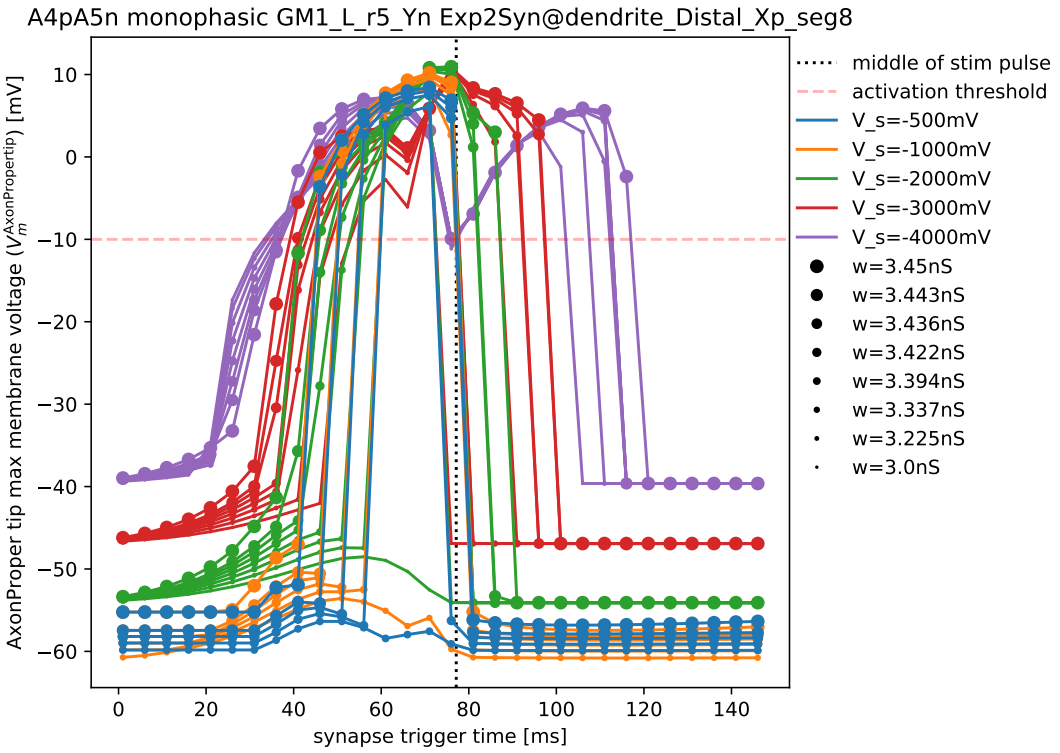

Figure 5.37: Membrane voltage at the axon tip (V_m^{axontip}) vs synapse trigger time for a neuron whose axon points in the $-\hat{y}$ direction located at GM1_L_r5. This neuron has a synapse triggered at segment 8 on the distal dendrite that points in the $+\hat{x}$ direction and is exposed to monophasic epidural stimulation using stimulating electrode combination A4pA5n. The stimulation pulse starts at t=76.0ms and has a maximum amplitude at t=77.13ms. This neuron is active without any EPSPs if exposed to -5.0V of stimulation. The following list contains tuples of the form (V_s, w, $\#T_B$, $\#T_A$) where V_s is the stimulation voltage, w is the synapse weight, and ($\#T_B$, $\#T_A$) is the number of synapse trigger time samples (x-axis samples in the above graph) before or after the stimulation pulse, respectively, given the values of V_s and w that result in neuron activation (a value of V_m^{axontip} above $-10\,\text{mV}$) : (-4.0V, 3.45nS, 8, 8), (-4.0V, 3.443nS, 8, 7), (-4.0V, 3.436nS, 8, 7), (-4.0V, 3.422nS, 7, 7), (-4.0V, 3.394nS, 8, 7), (-4.0V, 3.337nS, 8, 7), (-4.0V, 3.225nS, 8, 6), (-4.0V, 3.0nS, 8, 5), (-3.0V, 3.45nS, 8, 4), (-3.0V, 3.443nS, 8, 4), (-3.0V, 3.436nS, 7, 3), (-3.0V, 3.422nS, 7, 3), (-3.0V, 3.394nS, 7, 2), (-3.0V, 3.337nS, 7, 0), (-3.0V, 3.225nS, 6, 0), (-3.0V, 3.0nS, 4, 0), (-2.0V, 3.45nS, 7, 2), (-2.0V, 3.443nS, 7, 1), (-2.0V, 3.436nS, 6, 1), (-2.0V, 3.422nS, 6, 0), (-2.0V, 3.394nS, 5, 0), (-2.0V, 3.337nS, 5, 0), (-2.0V, 3.225nS, 3, 0), (-1.0V, 3.45nS, 7, 0), (-1.0V, 3.443nS, 6, 0), (-1.0V, 3.436nS, 6, 0), (-1.0V, 3.422nS, 5, 0), (-1.0V, 3.394nS, 4, 0), (-0.5V, 3.45nS, 7, 0), (-0.5V, 3.443nS, 6, 0), (-0.5V, 3.436nS, 5, 0), and (-0.5V, 3.422nS, 3, 0).

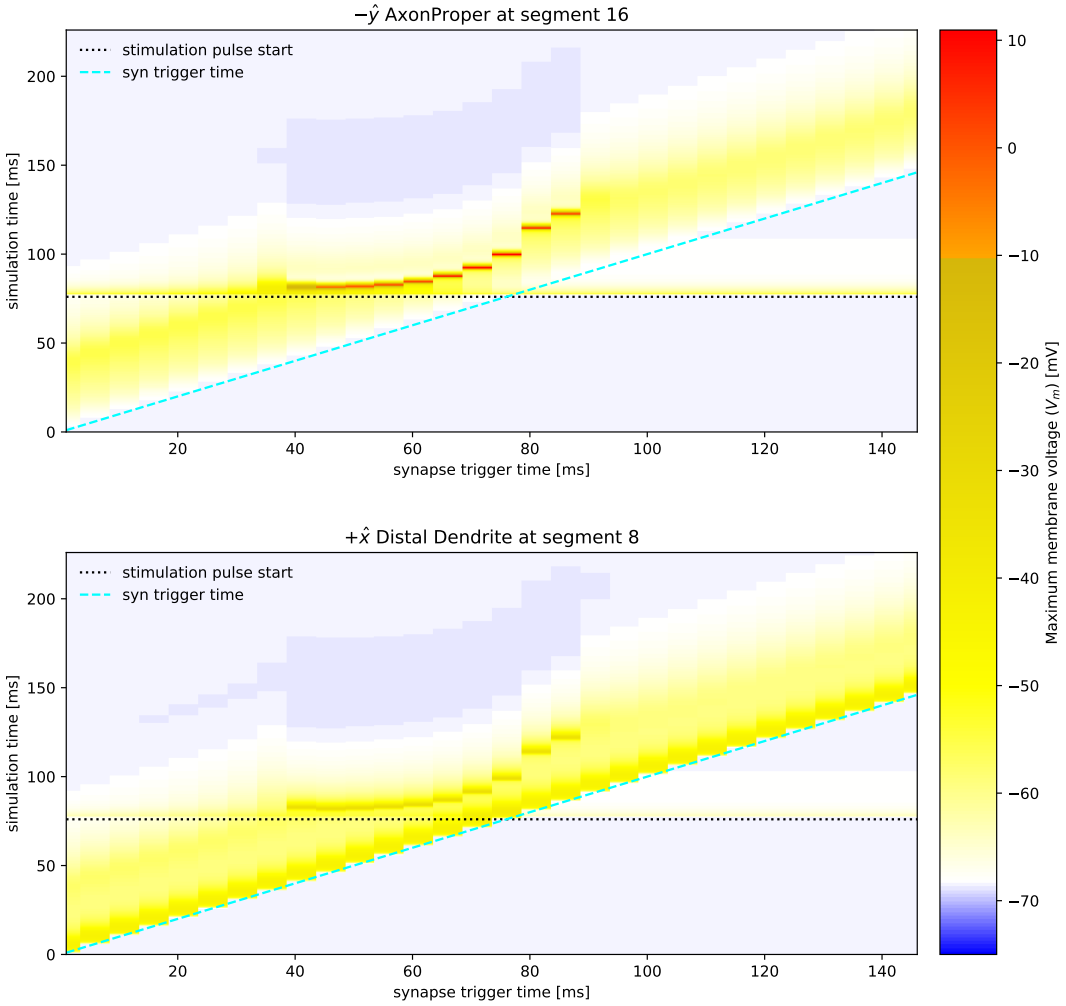

Figure 5.38: Membrane voltage (V_m) (see colormap) at the axon tip (top figure) and at the synapse location (bottom figure) as a function of synapse trigger time (x-axis) and simulation time (y-axis). Measured on neuron GM1_L_r5_Yn exposed to −2.0 V of monophasic epidural stimulation using stimulating electrode combination A4pA5n while a synaptic input with synapse weight=3.45nS is triggered at varying times on the distal dendrite that points in the $+\hat{x}$ direction at segment 8. The electrical stimulation pulse starts at t=76.0ms and has a maximum amplitude at t=77.13ms. The colormap is white when $V_m = -68.31$ mV (the resting membrane voltage for the distal axon tip) and changes from dark yellow to orange at $V_m = -10$ mV to indicate neuron activation.

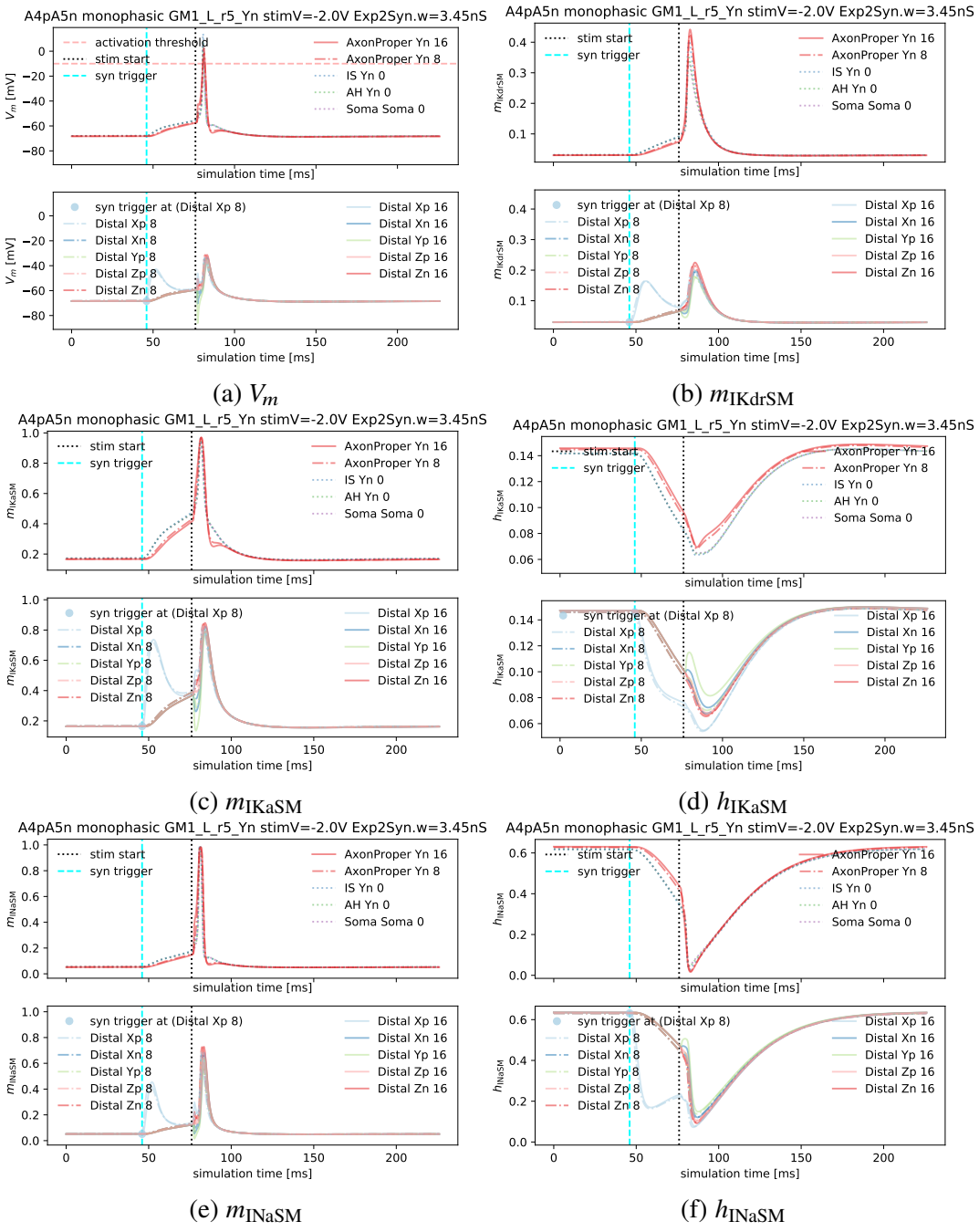

Figure 5.39: Stimulation + EPSP: Each subplot plots a different variable ((a) V_m, (b) m_{IKdrSM}, (c) m_{IKaSM}, (d) h_{IKaSM}, (e) m_{INaSM}, and (f) h_{INaSM}) against simulation time (ms) for probes on axon-soma (sub-top) and dendrites (sub-bottom). Measured on neuron GM1_L_r5_Yn exposed to −2.0 V of monophasic stimulation using stimulating electrode combination A4pA5n. The stimulation pulse starts at t=76.0ms and has a maximum amplitude at t=77.13ms. An Exp2Syn synapse was triggered at t=46.0 ms with a synaptic weight of 3.45nS. The synapse was located at segment 8 on the distal dendrite that points in the $+\hat{x}$ direction.

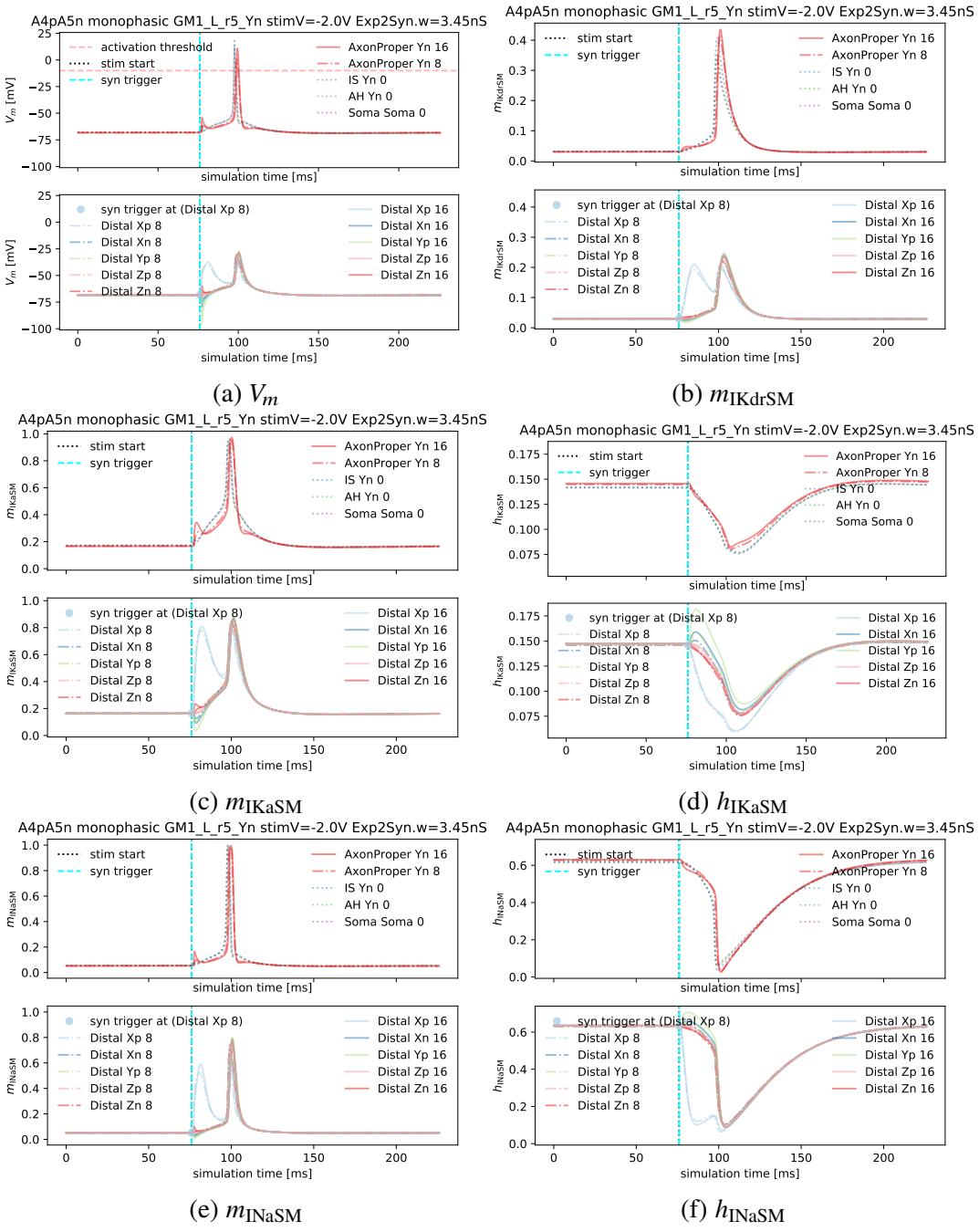

(a) V_m (b) m_{IKdrSM}

(c) m_{IKaSM} (d) h_{IKaSM}

(e) m_{INaSM} (f) h_{INaSM}

Figure 5.40: Stimulation + EPSP: Each subplot plots a different variable ((a) V_m, (b) m_{IKdrSM}, (c) m_{IKaSM}, (d) h_{IKaSM}, (e) m_{INaSM}, and (f) h_{INaSM}) against simulation time (ms) for probes on axon-soma (sub-top) and dendrites (sub-bottom). Measured on neuron GM1_L_r5_Yn exposed to −2.0 V of monophasic stimulation using stimulating electrode combination A4pA5n. The stimulation pulse starts at t=76.0ms and has a maximum amplitude at t=77.13ms. An Exp2Syn synapse was triggered at t=76.0 ms with a synaptic weight of 3.45nS. The synapse was located at segment 8 on the distal dendrite that points in the $+\hat{x}$ direction.

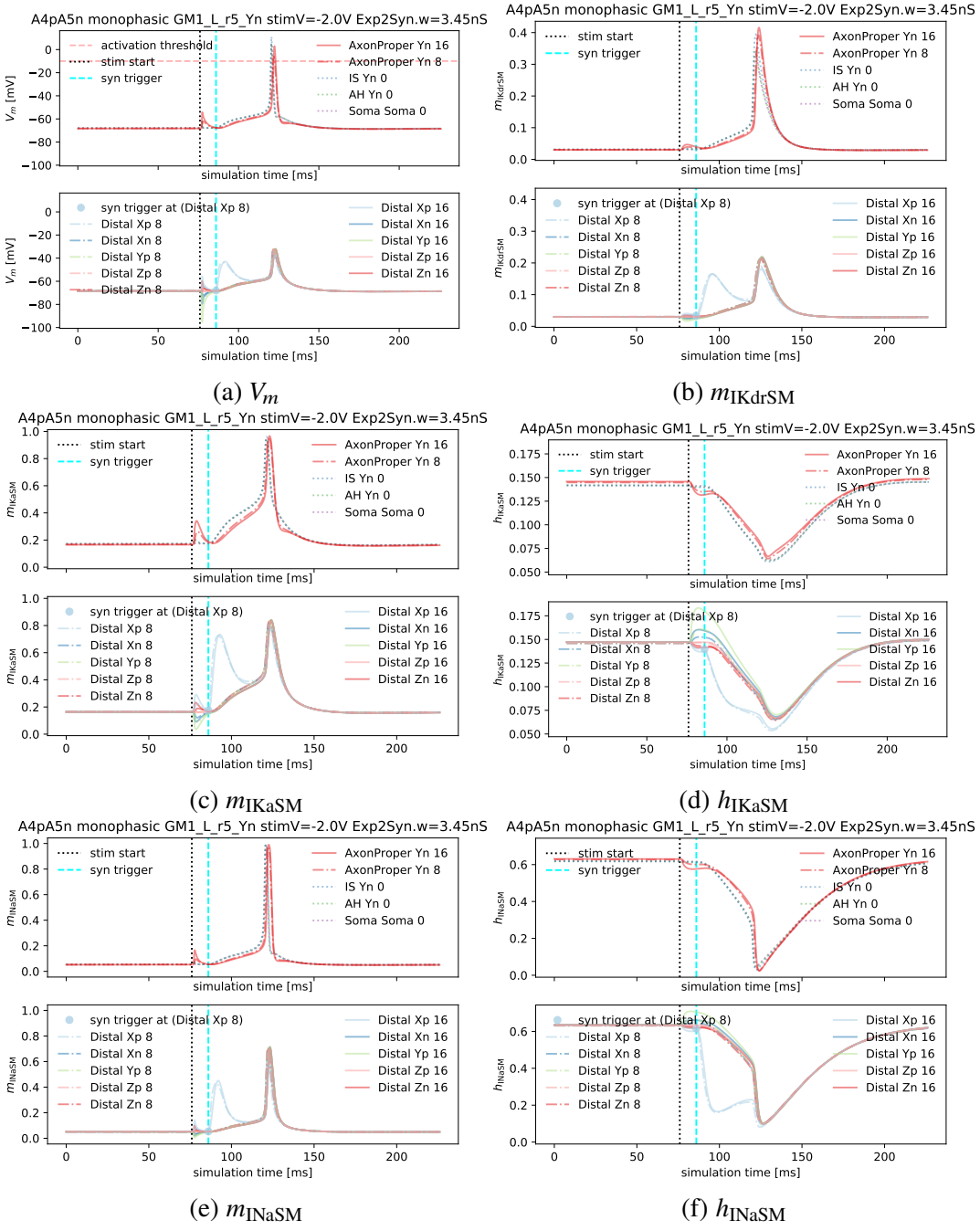

(a) V_m (b) m_{IKdrSM}

(c) m_{IKaSM} (d) h_{IKaSM}

(e) m_{INaSM} (f) h_{INaSM}

Figure 5.41: Stimulation + EPSP: Each subplot plots a different variable ((a) V_m, (b) m_{IKdrSM}, (c) m_{IKaSM}, (d) h_{IKaSM}, (e) m_{INaSM}, and (f) h_{INaSM}) against simulation time (ms) for probes on axon-soma (sub-top) and dendrites (sub-bottom). Measured on neuron GM1_L_r5_Yn exposed to −2.0 V of monophasic stimulation using stimulating electrode combination A4pA5n. The stimulation pulse starts at t=76.0ms and has a maximum amplitude at t=77.13ms. An Exp2Syn synapse was triggered at t=86.0 ms with a synaptic weight of 3.45nS. The synapse was located at segment 8 on the distal dendrite that points in the $+\hat{x}$ direction.

5.B.5 Monophasic stimulation with $V_s > 0$ and a mid-dendrite synapse

For monophasic stimulation using A4pA5n with $V_s > 0$ of neuron GM1_L_r5_Yn with a synapse triggered on the distal dendrite pointing in the $\hat{x}$ direction at segment 8, the maximum membrane voltage at the axon tip for the synapse weights, trigger times, and stimulation voltages listed in Section 5.1 can be seen in Fig. 5.42. Without any EPSPs, it appears that this neuron will not activate with monophasic stimulation if $V_s > 0\,\text{V}$. Unlike the biphasic stimulation examples and the previous example, the facilitation window for the synapse trigger time is clearly larger after the stimulation pulse. If V_s is [2, 1, 0.5]V, the facilitation window is completely after the stimulation pulse starts and goes all the way to the last synapse trigger time tested for the maximum synapse weight (3.45 nS).

Figure 5.43 shows the membrane voltage at the axon tip and the synapse location for $V_s = 2\,\text{V}$ and synapse weight 3.45 nS for all the synapse trigger times shown in Fig. 5.42. The neuron activations are shown in orange-red, while the synapse trigger time is shown as a dashed cyan line, and the start of the stimulation pulse as a dotted black line. The time of the neuron activations increases with increasing synaptic trigger time (after the small decrease in time when the synaptic trigger time coincides with the stimulation pulse start time) and each of the activations travel back to the synapse location.

The response of the neuron (membrane voltage and ion-channel state variables) to just the EPSP (with synapse weight of 3.45 nS) alone can be found in Fig. 3.10. The response of the neuron to $V_s = 2\,\text{V}$ stimulation alone can be found in Fig. 5.11. Figure 5.45 shows the response to the earliest synapse trigger time (t=81 ms) that caused facilitation with $V_s = 2\,\text{V}$ and synapse weight 4.783 nS. A synapse trigger time of 81 ms also maximizes the membrane voltage at the axon tip (compared to other synapse trigger times). Fig. 5.46 shows the response to the latest tested synapse trigger time (t=146 ms) that caused facilitation.

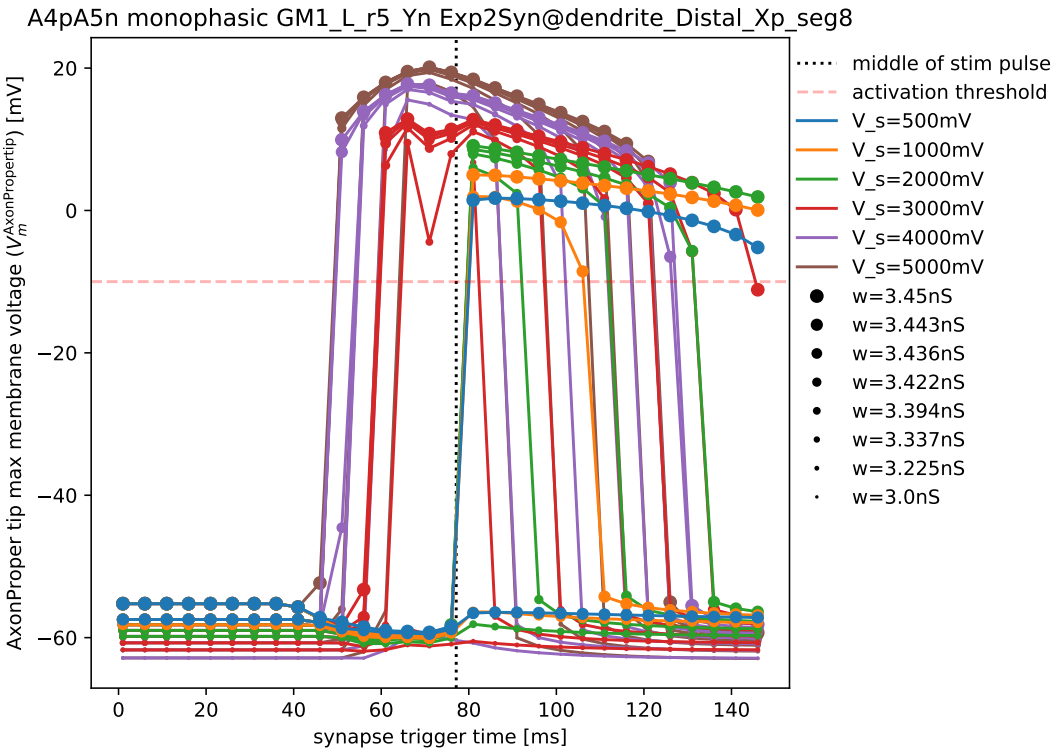

Figure 5.42: Membrane voltage at the axon tip (V_m^{axontip}) vs synapse trigger time for a neuron whose axon points in the $-\hat{y}$ direction located at GM1_L_r5. This neuron has a synapse triggered at segment 8 on the distal dendrite that points in the $+\hat{x}$ direction and is exposed to monophasic epidural stimulation using stimulating electrode combination A4pA5n. The stimulation pulse starts at t=76.0ms and has a maximum amplitude at t=77.13ms. The following list contains tuples of the form (V_s, w, $\#T_B$, $\#T_A$) where V_s is the stimulation voltage, w is the synapse weight, and ($\#T_B$, $\#T_A$) is the number of synapse trigger time samples (x-axis samples in the above graph) before or after the stimulation pulse, respectively, given the values of V_s and w that result in neuron activation (a value of V_m^{axontip} above -10 mV) : (5.0V, 3.45nS, 6, 9), (5.0V, 3.443nS, 6, 9), (5.0V, 3.436nS, 6, 9), (5.0V, 3.422nS, 6, 8), (5.0V, 3.394nS, 5, 7), (5.0V, 3.337nS, 5, 6), (5.0V, 3.225nS, 4, 4), (5.0V, 3.0nS, 3, 2), (4.0V, 3.45nS, 6, 10), (4.0V, 3.443nS, 6, 10), (4.0V, 3.436nS, 5, 9), (4.0V, 3.422nS, 5, 8), (4.0V, 3.394nS, 5, 7), (4.0V, 3.337nS, 4, 5), (4.0V, 3.225nS, 4, 2), (3.0V, 3.45nS, 4, 13), (3.0V, 3.443nS, 4, 11), (3.0V, 3.436nS, 4, 9), (3.0V, 3.422nS, 4, 7), (3.0V, 3.394nS, 3, 4), (3.0V, 3.337nS, 0, 1), (2.0V, 3.45nS, 0, 14), (2.0V, 3.443nS, 0, 11), (2.0V, 3.436nS, 0, 7), (2.0V, 3.422nS, 0, 3), (1.0V, 3.45nS, 0, 14), (1.0V, 3.443nS, 0, 6), and (0.5V, 3.45nS, 0, 14).

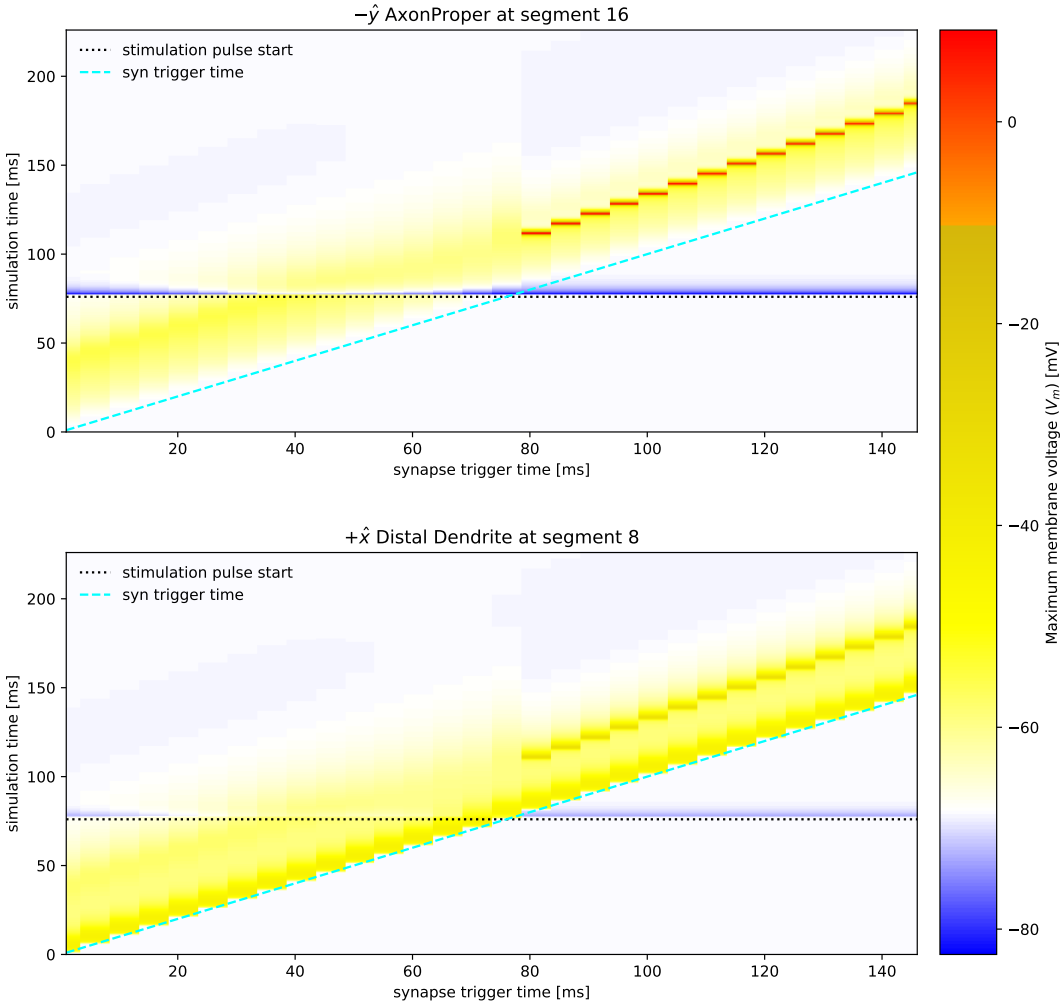

Figure 5.43: Membrane voltage (V_m) (see colormap) at the axon tip (top figure) and at the synapse location (bottom figure) as a function of synapse trigger time (x-axis) and simulation time (y-axis). Measured on neuron GM1_L_r5_Yn exposed to 2.0 V of monophasic epidural stimulation using stimulating electrode combination A4pA5n while a synaptic input with synapse weight=3.45nS is triggered at varying times on the distal dendrite that points in the $+\hat{x}$ direction at segment 8. The electrical stimulation pulse starts at t=76.0ms and has a maximum amplitude at t=77.13ms. The colormap is white when $V_m = -68.31$ mV (the resting membrane voltage for the distal axon tip) and changes from dark yellow to orange at $V_m = -10$ mV to indicate neuron activation.

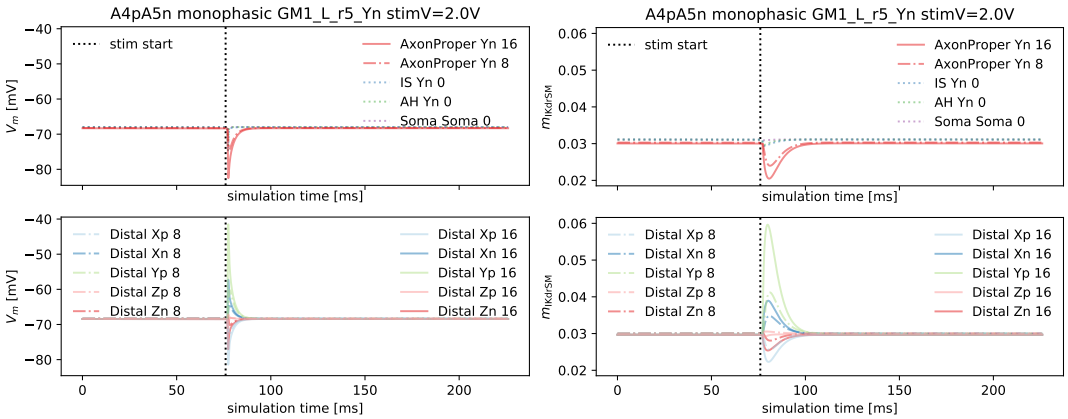

(a) V_m

(b) m_{IKdrSM}

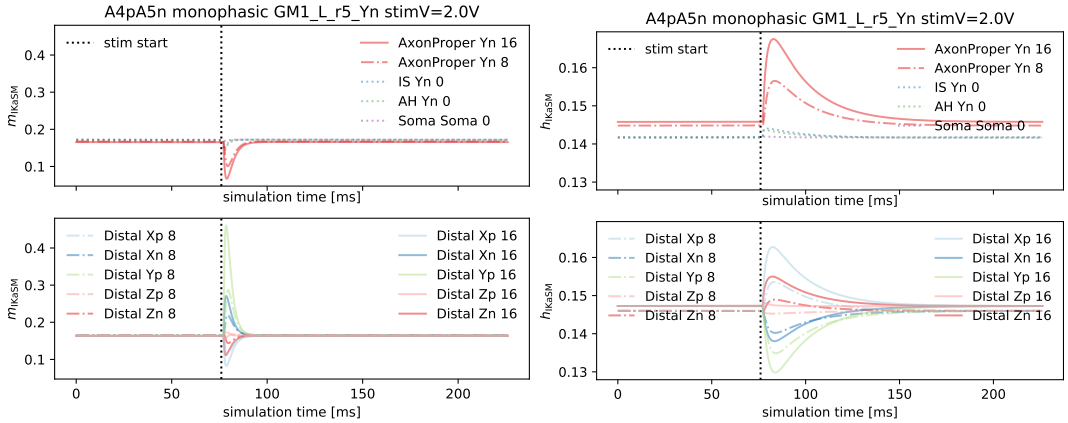

(c) m_{IKaSM}

(d) h_{IKaSM}

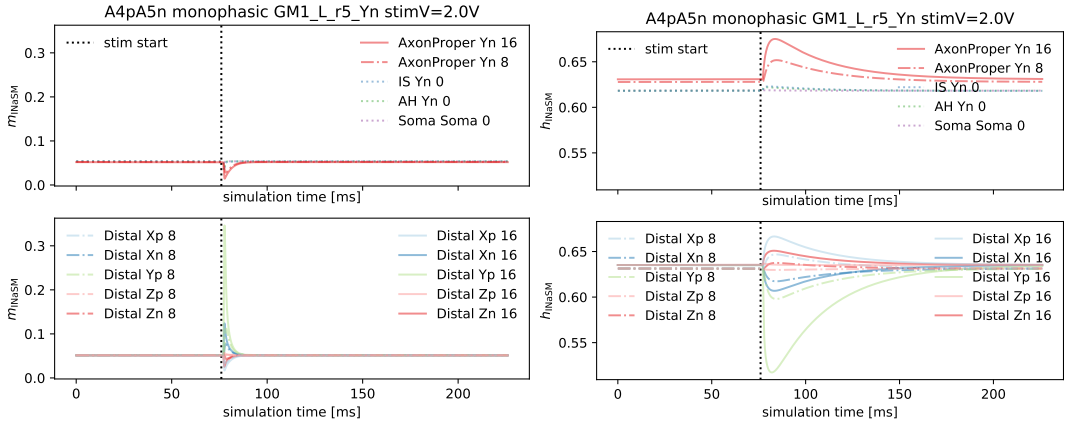

(e) m_{INaSM}

(f) h_{INaSM}

Figure 5.44: Stimulation only: Each subplot plots a different variable ((a) V_m, (b) m_{IKdrSM}, (c) m_{IKaSM}, (d) h_{IKaSM}, (e) m_{INaSM}, and (f) h_{INaSM}) against simulation time (ms) for probes on axon-soma (sub-top) and dendrites (sub-bottom). All data measured using neuron GM1_L_r5_Yn exposed to 2.0 V of monophasic stimulation using stimulating electrode combination A4pA5n. The stimulation pulse starts at t=76.0ms and has a maximum amplitude at t=77.13ms.

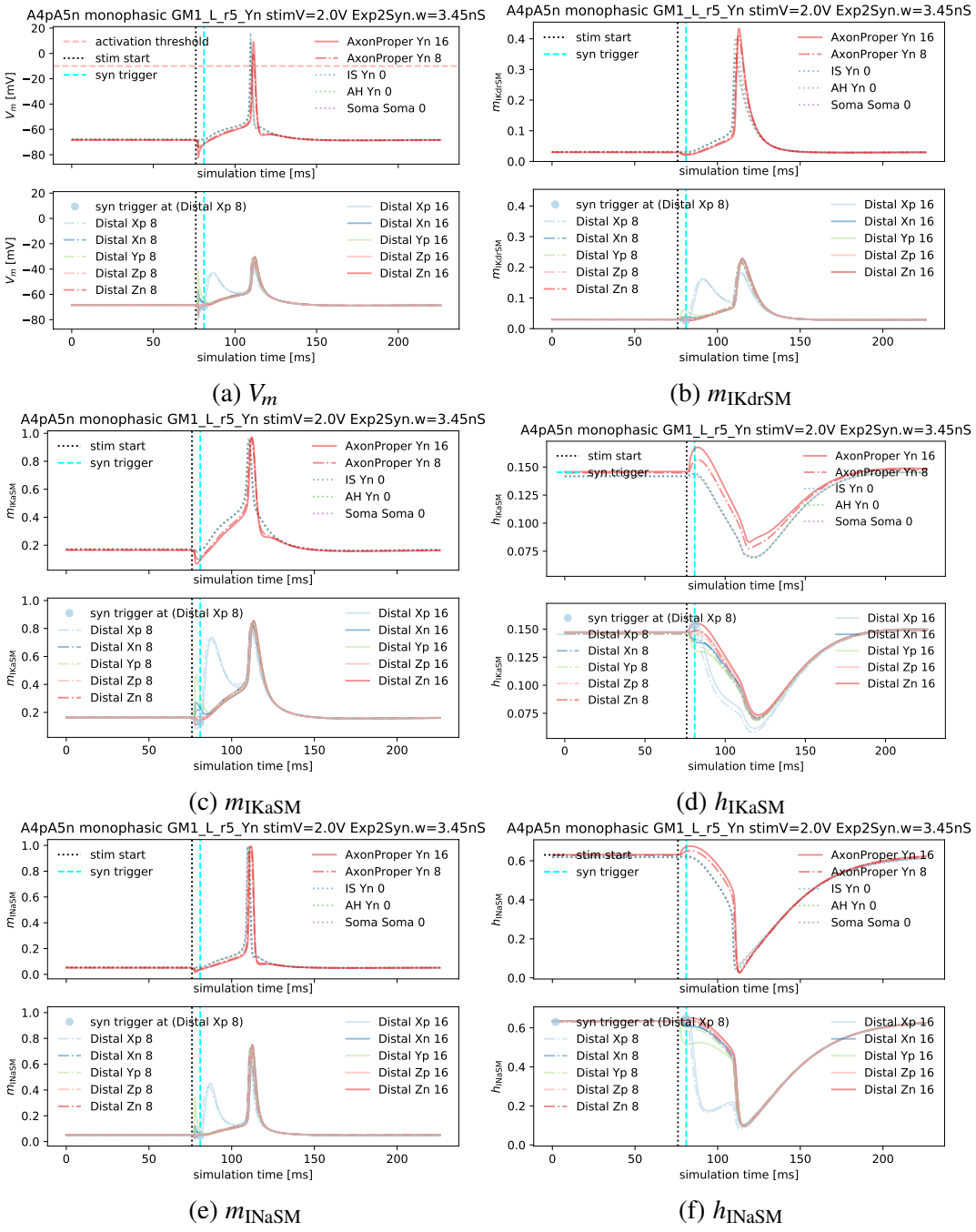

(a) V_m (b) m_{IKdrSM}

(c) m_{IKaSM} (d) h_{IKaSM}

(e) m_{INaSM} (f) h_{INaSM}

Figure 5.45: Stimulation + EPSP: Each subplot plots a different variable ((a) V_m, (b) m_{IKdrSM}, (c) m_{IKaSM}, (d) h_{IKaSM}, (e) m_{INaSM}, and (f) h_{INaSM}) against simulation time (ms) for probes on axon-soma (sub-top) and dendrites (sub-bottom). Measured on neuron GM1_L_r5_Yn exposed to 2.0 V of monophasic stimulation using stimulating electrode combination A4pA5n. The stimulation pulse starts at t=76.0ms and has a maximum amplitude at t=77.13ms. An Exp2Syn synapse was triggered at t=81.0 ms with a synaptic weight of 3.45nS. The synapse was located at segment 8 on the distal dendrite that points in the $+\hat{x}$ direction.

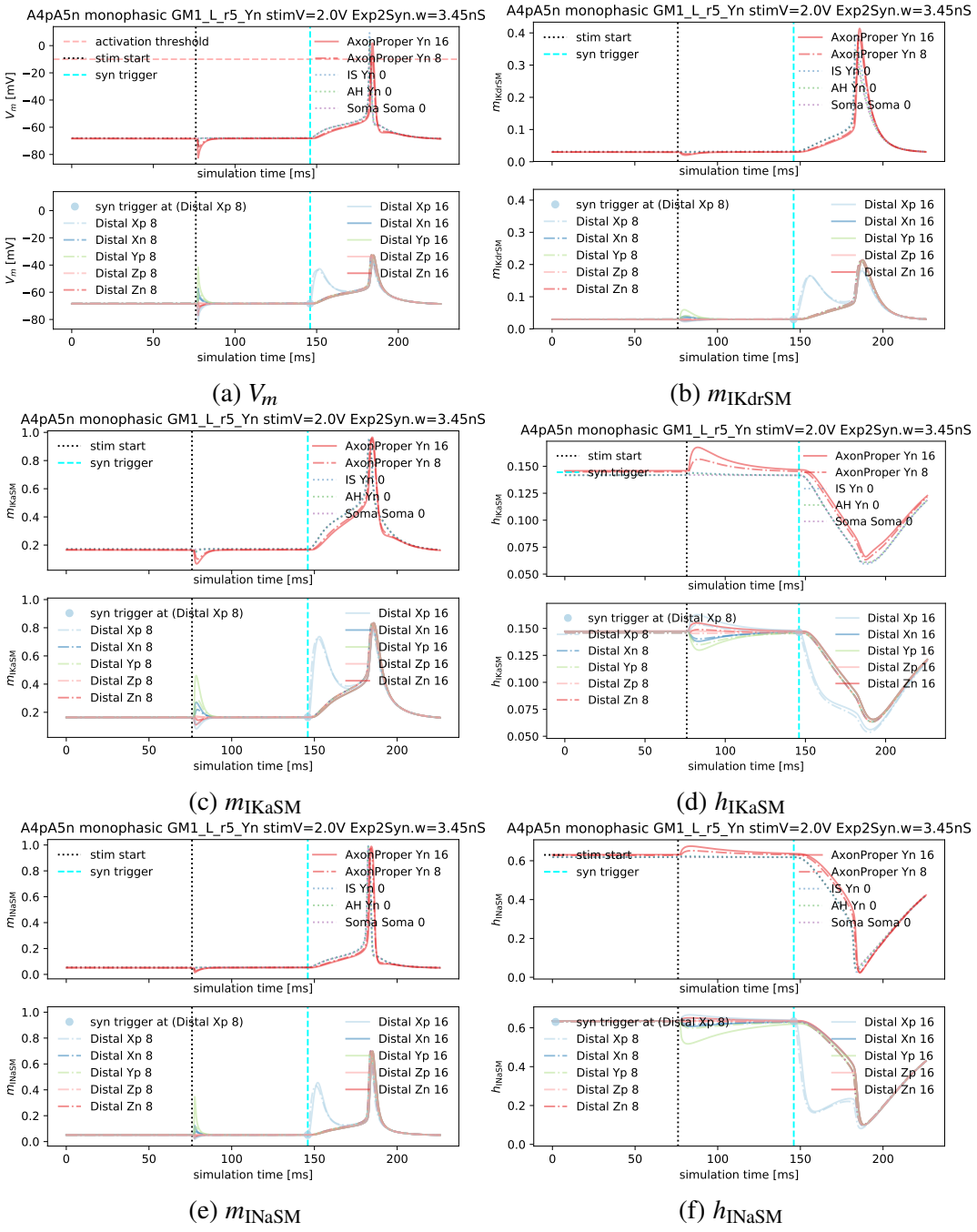

(a) V_m (b) m_{IKdrSM}

(c) m_{IKaSM} (d) h_{IKaSM}

(e) m_{INaSM} (f) h_{INaSM}

Figure 5.46: Stimulation + EPSP: Each subplot plots a different variable ((a) V_m, (b) m_{IKdrSM}, (c) m_{IKaSM}, (d) h_{IKaSM}, (e) m_{INaSM}, and (f) h_{INaSM}) against simulation time (ms) for probes on axon-soma (sub-top) and dendrites (sub-bottom). Measured on neuron GM1_L_r5_Yn exposed to 2.0 V of monophasic stimulation using stimulating electrode combination A4pA5n. The stimulation pulse starts at t=76.0ms and has a maximum amplitude at t=77.13ms. An Exp2Syn synapse was triggered at t=146.0 ms with a synaptic weight of 3.45nS. The synapse was located at segment 8 on the distal dendrite that points in the $+\hat{x}$ direction.

5.C Appendix: Supplementary figures for separating facilitated and non-activated neurons using static features

This appendix contains supplementary figures for Section 5.4.1.

The results of using the best features found in Section 5.4.1 to separate simulations of biphasic stimulation with EPSPs are shown in Figs. 5.47-5.57 and corresponding monophasic stimulation results are displayed in Figs. 5.58-5.68. A summary of these results is available in Table 5.2.

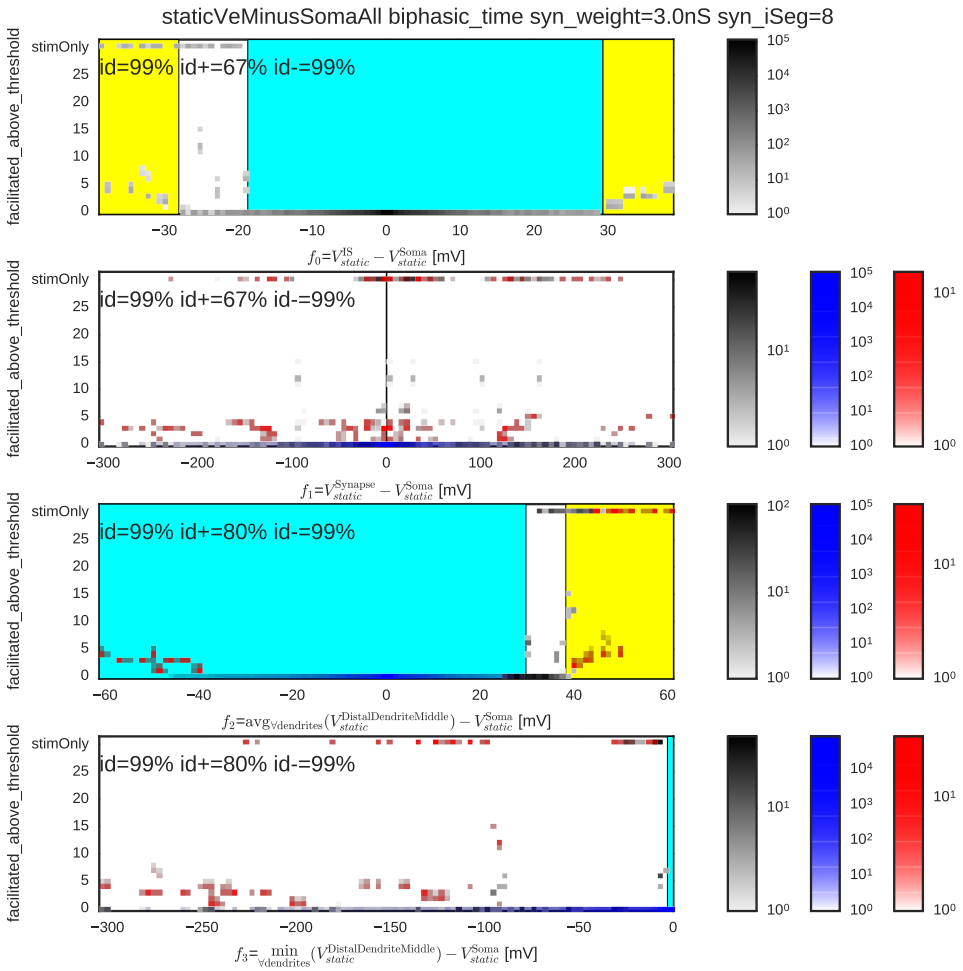

Figure 5.47: Predicting facilitation for all combinations using biphasic epidural stimulation with a synapse triggered on a distal dendrite at segment 8 with weight 3.0 nS using features $f_0 = V^{IS}_{static} - V^{Soma}_{static}$, $f_1 = V^{Synapse}_{static} - V^{Soma}_{static}$, $f_2 = \text{avg}_{\forall dendrites}(V^{DistalDendriteMiddle}_{static}) - V^{Soma}_{static}$, and $f_3 = \min_{\forall dendrites}(V^{DistalDendriteMiddle}_{static}) - V^{Soma}_{static}$. Each feature is on the x-axis in a separate subplot above with the number of trigger points facilitated above threshold (−10 mV) as the y-axis. Each subplot consists of three 2D histograms (showing the number of neuron simulations in each square), shades of grey (unclassified), shades of red (classified as active), and shades of blue (classified as non-active). For each feature active and non-active classification regions of unclassified samples are drawn with a yellow and cyan background respectively. These classification regions are also written as rules below, where T=1 and T=0 indicates that the neuron is active and non-active respectively. The number of samples of neurons caught by each rule is specified in the comment after each rule. Using the decision regions in that subplot and those above, the percent of all samples classified (id), active samples classified (id+), and non-active samples classified (id-) are labeled in each subplot. There are a total of 427680 samples of which 400 are active without the EPSP, 537 are facilitated, and 426743 are non-active.

IF (f_0 < −28.08 mV) THEN (T=1) /* 330 samples */
ELIF (−18.75 mV < f_0 < 29.32 mV) THEN (T=0) /* 426115 samples */
ELIF (29.32 mV < f_0) THEN (T=1) /* 300 samples */
ELIF (−0.045 14 mV < f_1 < 0.5408 mV) THEN (T=0) /* 29 samples */
ELIF (f_2 < 29.8 mV) THEN (T=0) /* 272 samples */
ELIF (38.29 mV < f_2) THEN (T=1) /* 125 samples */
ELIF (−3.031 mV < f_3) THEN (T=0) /* 3 samples */
ELSE (T=Unknown) /* 506 samples */

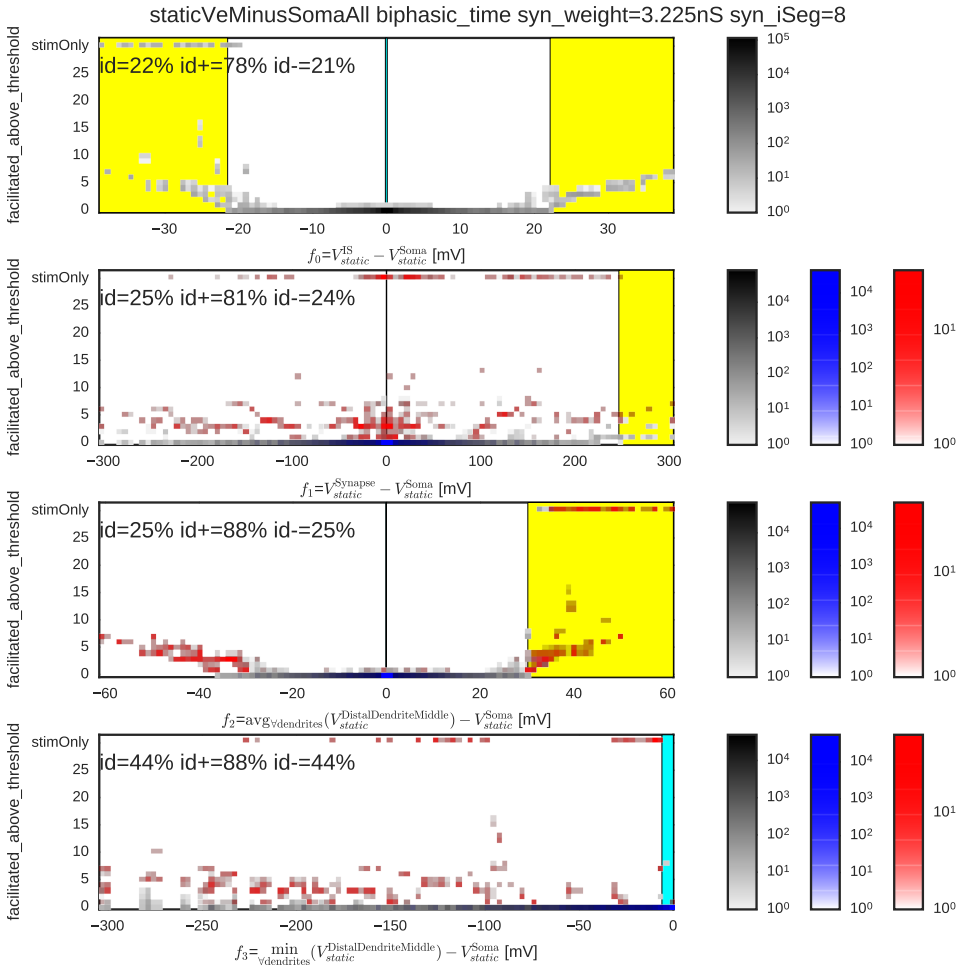

Figure 5.48: Predicting facilitation for all combinations using biphasic epidural stimulation with a synapse triggered on a distal dendrite at segment 8 with weight 3.225 nS using features $f_0 = V^{\text{IS}}_{static} - V^{\text{Soma}}_{static}$, $f_1 = V^{\text{Synapse}}_{static} - V^{\text{Soma}}_{static}$, $f_2 = \text{avg}_{\forall\text{dendrites}}(V^{\text{DistalDendriteMiddle}}_{static}) - V^{\text{Soma}}_{static}$, and $f_3 = \min_{\forall\text{dendrites}}(V^{\text{DistalDendriteMiddle}}_{static}) - V^{\text{Soma}}_{static}$. Each feature is on the x-axis in a separate subplot above with the number of trigger points facilitated above threshold (−10 mV) as the y-axis. Each subplot consists of three 2D histograms (showing the number of neuron simulations in each square), shades of grey (unclassified), shades of red (classified as active), and shades of blue (classified as non-active). For each feature active and non-active classification regions of unclassified samples are drawn with a yellow and cyan background respectively. These classification regions are also written as rules below, where T=1 and T=0 indicates that the neuron is active and non-active respectively. The number of samples of neurons caught by each rule is specified in the comment after each rule. Using the decision regions in that subplot and those above, the percent of all samples classified (id), active samples classified (id+), and non-active samples classified (id-) are labeled in each subplot. There are a total of 427680 samples of which 400 are active without the EPSP, 1647 are facilitated, and 425633 are non-active.

IF (f_0 < −21.47 mV) THEN (T=1) /* 830 samples */
ELIF (−0.1284 mV < f_0 < 0.1284 mV) THEN (T=0) /* 92790 samples */
ELIF (22.17 mV < f_0) THEN (T=1) /* 775 samples */
ELIF (−0.035 48 mV < f_1 < 0.4075 mV) THEN (T=0) /* 12850 samples */
ELIF (246.6 mV < f_1) THEN (T=1) /* 66 samples */
ELIF (−0.1063 mV < f_2 < 0.022 74 mV) THEN (T=0) /* 1935 samples */
ELIF (30.19 mV < f_2) THEN (T=1) /* 143 samples */
ELIF (−5.949 mV < f_3) THEN (T=0) /* 81810 samples */
ELSE (T=Unknown) /* 236481 samples */

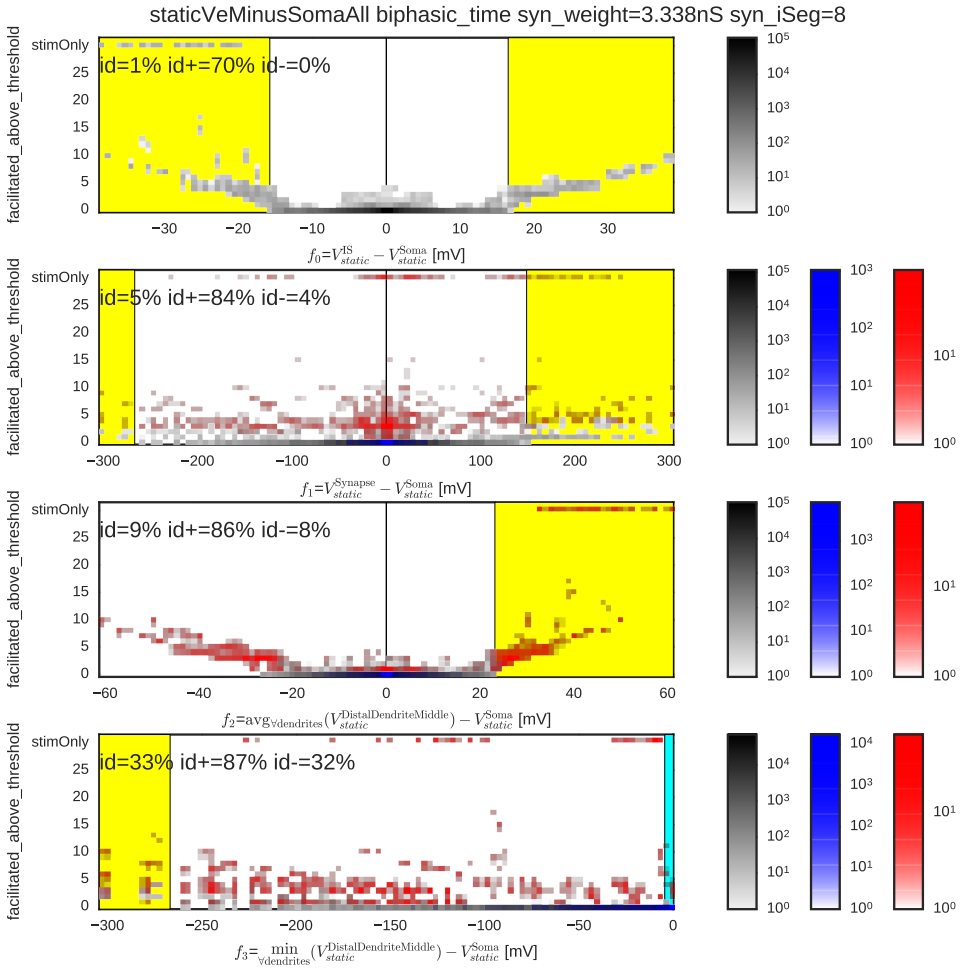

Figure 5.49: Predicting facilitation for all combinations using biphasic epidural stimulation with a synapse triggered on a distal dendrite at segment 8 with weight 3.338 nS using features $f_0 = V^{IS}_{static} - V^{Soma}_{static}$, $f_1 = V^{Synapse}_{static} - V^{Soma}_{static}$, $f_2 = \text{avg}_{\forall dendrites}(V^{DistalDendriteMiddle}_{static}) - V^{Soma}_{static}$, and $f_3 = \min_{\forall dendrites}(V^{DistalDendriteMiddle}_{static}) - V^{Soma}_{static}$. Each feature is on the x-axis in a separate subplot above with the number of trigger points facilitated above threshold (−10 mV) as the y-axis. Each subplot consists of three 2D histograms (showing the number of neuron simulations in each square), shades of grey (unclassified), shades of red (classified as active), and shades of blue (classified as non-active). For each feature active and non-active classification regions of unclassified samples are drawn with a yellow and cyan background respectively. These classification regions are also written as rules below, where T=1 and T=0 indicates that the neuron is active and non-active respectively. The number of samples of neurons caught by each rule is specified in the comment after each rule. Using the decision regions in that subplot and those above, the percent of all samples classified (id), active samples classified (id+), and non-active samples classified (id-) are labeled in each subplot. There are a total of 427680 samples of which 400 are active without the EPSP, 4248 are facilitated, and 423032 are non-active.

IF (f_0 < −15.77 mV) THEN (T=1) /* 1690 samples */
ELIF (−0.000 354 2 mV < f_0 < 0.000 354 2 mV) THEN (T=0) /* 2990 samples */
ELIF (16.49 mV < f_0) THEN (T=1) /* 1600 samples */
ELIF (f_1 < −266.9 mV) THEN (T=1) /* 24 samples */
ELIF (−0.047 31 mV < f_1 < 0.047 31 mV) THEN (T=0) /* 14992 samples */
ELIF (148.8 mV < f_1) THEN (T=1) /* 616 samples */
ELIF (−0.022 93 mV < f_2 < 0.018 34 mV) THEN (T=0) /* 17988 samples */
ELIF (23.16 mV < f_2) THEN (T=1) /* 90 samples */
ELIF (f_3 < −266.9 mV) THEN (T=1) /* 58 samples */
ELIF (−4.462 mV < f_3) THEN (T=0) /* 101971 samples */
ELSE (T=Unknown) /* 285661 samples */

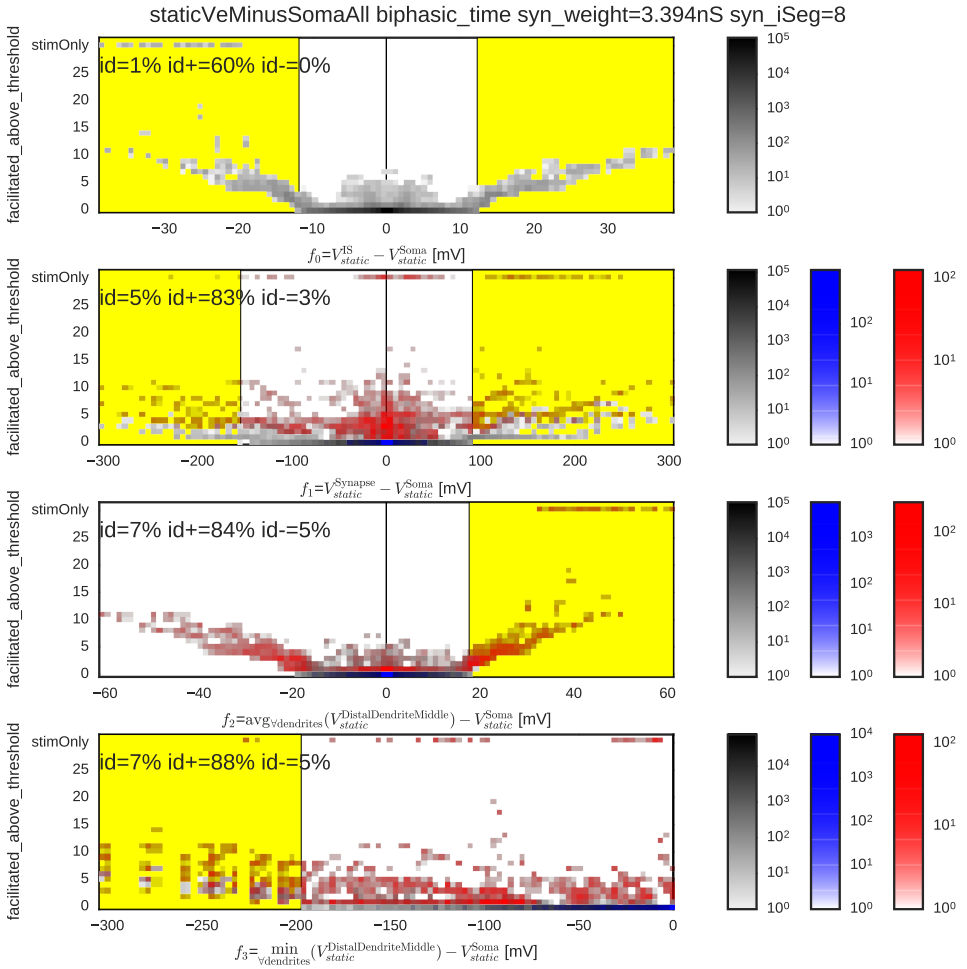

Figure 5.50: Predicting facilitation for all combinations using biphasic epidural stimulation with a synapse triggered on a distal dendrite at segment 8 with weight 3.394 nS using features $f_0 = V^{IS}_{static} - V^{Soma}_{static}$, $f_1 = V^{Synapse}_{static} - V^{Soma}_{static}$, $f_2 = \text{avg}_{\forall dendrites}(V^{DistalDendriteMiddle}_{static}) - V^{Soma}_{static}$, and $f_3 = \min_{\forall dendrites}(V^{DistalDendriteMiddle}_{static}) - V^{Soma}_{static}$. Each feature is on the x-axis in a separate subplot above with the number of trigger points facilitated above threshold (−10 mV) as the y-axis. Each subplot consists of three 2D histograms (showing the number of neuron simulations in each square), shades of grey (unclassified), shades of red (classified as active), and shades of blue (classified as non-active). For each feature active and non-active classification regions of unclassified samples are drawn with a yellow and cyan background respectively. These classification regions are also written as rules below, where T=1 and T=0 indicates that the neuron is active and non-active respectively. The number of samples of neurons caught by each rule is specified in the comment after each rule. Using the decision regions in that subplot and those above, the percent of all samples classified (id), active samples classified (id+), and non-active samples classified (id-) are labeled in each subplot. There are a total of 427680 samples of which 400 are active without the EPSP, 9670 are facilitated, and 417610 are non-active.

IF (f_0 < −11.81 mV) THEN (T=1) /* 3160 samples */
ELIF (−0.000 210 2 mV < f_0 < 0.000 210 2 mV) THEN (T=0) /* 2170 samples */
ELIF (12.3 mV < f_0) THEN (T=1) /* 2975 samples */
ELIF (f_1 < −154.5 mV) THEN (T=1) /* 482 samples */
ELIF (−0.035 48 mV < f_1 < 0.035 48 mV) THEN (T=0) /* 13064 samples */
ELIF (91.31 mV < f_1) THEN (T=1) /* 1824 samples */
ELIF (−0.013 76 mV < f_2 < 0.002 251 mV) THEN (T=0) /* 7826 samples */
ELIF (17.67 mV < f_2) THEN (T=1) /* 88 samples */
ELIF (f_3 < −197.3 mV) THEN (T=1) /* 392 samples */
ELIF (−0.000 796 3 mV < f_3 < 0.0155 mV) THEN (T=0) /* 170 samples */
ELSE (T=Unknown) /* 395529 samples */

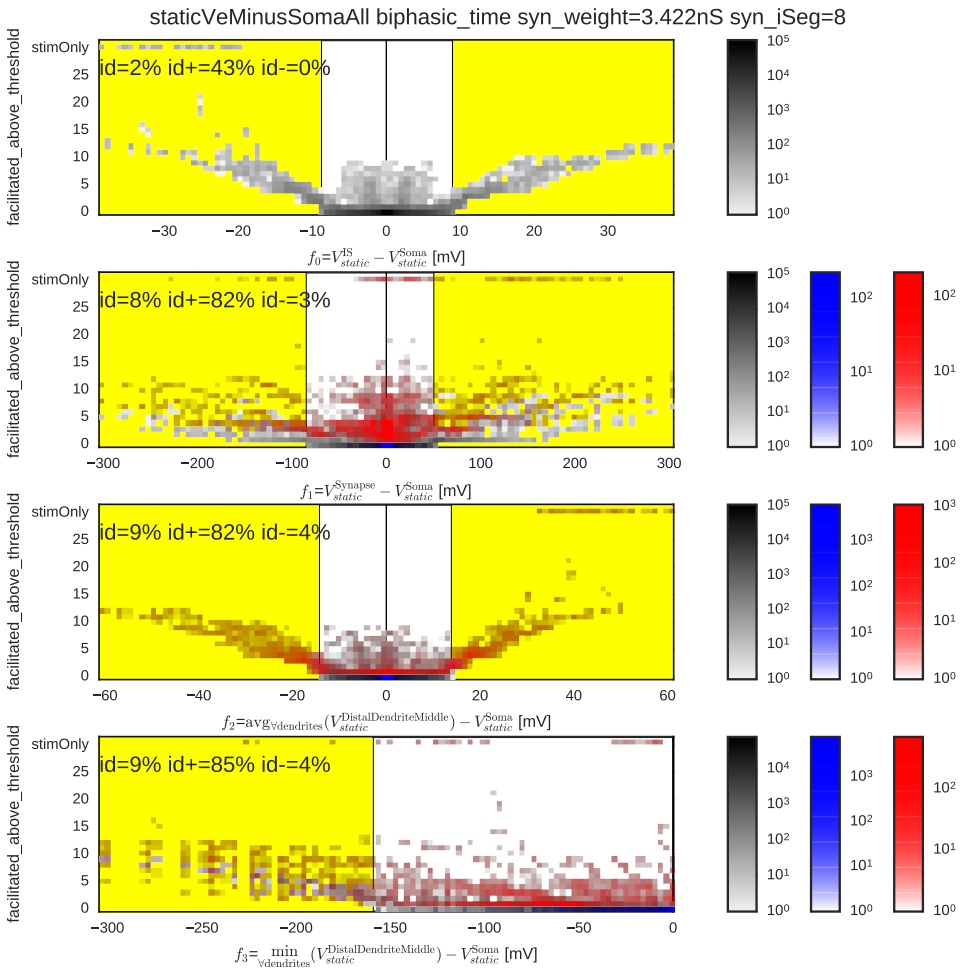

Figure 5.51: Predicting facilitation for all combinations using biphasic epidural stimulation with a synapse triggered on a distal dendrite at segment 8 with weight 3.422 nS using features $f_0 = V^{IS}_{static} - V^{Soma}_{static}$, $f_1 = V^{Synapse}_{static} - V^{Soma}_{static}$, $f_2 = \text{avg}_{\forall\text{dendrites}}(V^{DistalDendriteMiddle}_{static}) - V^{Soma}_{static}$, and $f_3 = \min_{\forall\text{dendrites}}(V^{DistalDendriteMiddle}_{static}) - V^{Soma}_{static}$. Each feature is on the x-axis in a separate subplot above with the number of trigger points facilitated above threshold (−10 mV) as the y-axis. Each subplot consists of three 2D histograms (showing the number of neuron simulations in each square), shades of grey (unclassified), shades of red (classified as active), and shades of blue (classified as non-active). For each feature active and non-active classification regions of unclassified samples are drawn with a yellow and cyan background respectively. These classification regions are also written as rules below, where T=1 and T=0 indicates that the neuron is active and non-active respectively. The number of samples of neurons caught by each rule is specified in the comment after each rule. Using the decision regions in that subplot and those above, the percent of all samples classified (id), active samples classified (id+), and non-active samples classified (id-) are labeled in each subplot. There are a total of 427680 samples of which 400 are active without the EPSP, 24532 are facilitated, and 402748 are non-active.

IF ($f_0 < -8.774$ mV) THEN (T=1) /* 5475 samples */
ELIF (-2.809×10^{-5} mV $< f_0 < 2.809 \times 10^{-5}$ mV) THEN (T=0) /* 620 samples */
ELIF (8.953 mV $< f_0$) THEN (T=1) /* 5285 samples */
ELIF ($f_1 < -84.92$ mV) THEN (T=1) /* 2086 samples */
ELIF (−0.035 48 mV $< f_1 <$ 0.047 31 mV) THEN (T=0) /* 14898 samples */
ELIF (50.4 mV $< f_1$) THEN (T=1) /* 7613 samples */
ELIF ($f_2 < -14.26$ mV) THEN (T=1) /* 39 samples */
ELIF (−0.002 49 mV $< f_2 <$ 0.002 49 mV) THEN (T=0) /* 2941 samples */
ELIF (13.87 mV $< f_2$) THEN (T=1) /* 16 samples */
ELIF ($f_3 < -159.1$ mV) THEN (T=1) /* 792 samples */
ELIF (−0.000 481 2 mV $< f_3 <$ 0.000 711 5 mV) THEN (T=0) /* 66 samples */
ELSE (T=Unknown) /* 387849 samples */

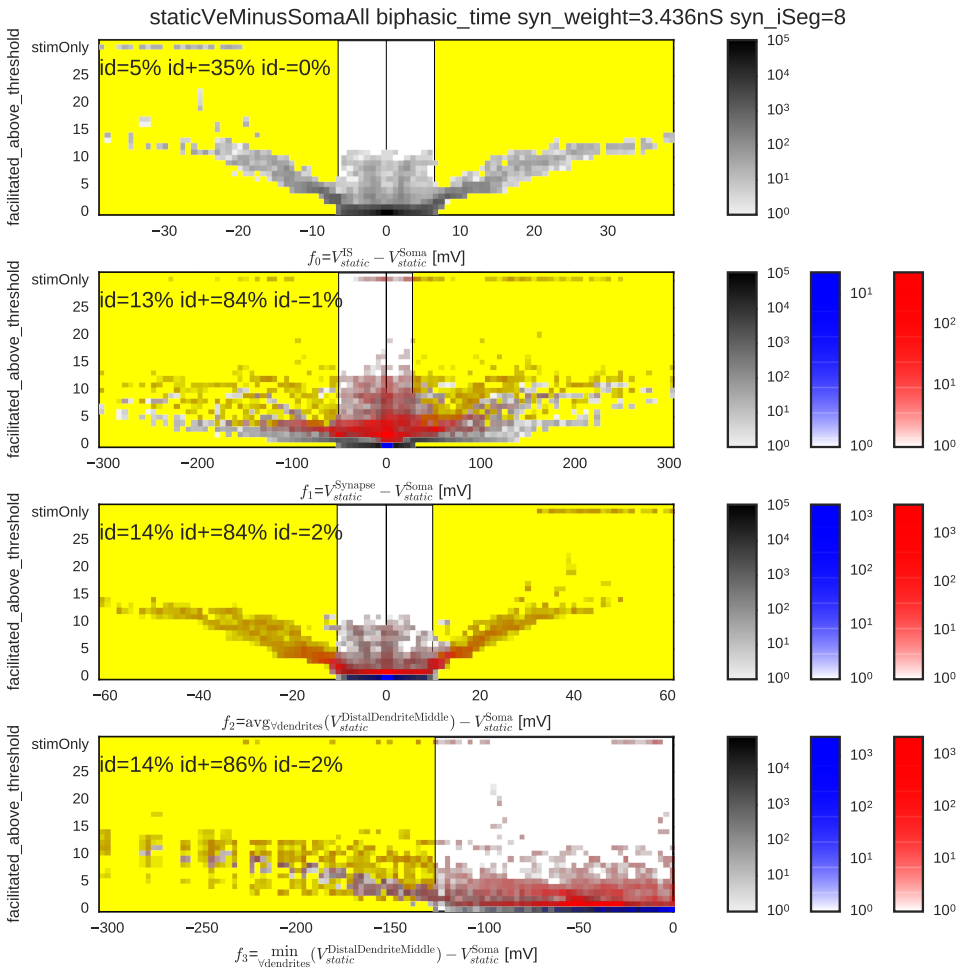

Figure 5.52: Predicting facilitation for all combinations using biphasic epidural stimulation with a synapse triggered on a distal dendrite at segment 8 with weight 3.436 nS using features $f_0 = V^{IS}_{static} - V^{Soma}_{static}$, $f_1 = V^{Synapse}_{static} - V^{Soma}_{static}$, $f_2 = \text{avg}_{\forall dendrites}(V^{DistalDendriteMiddle}_{static}) - V^{Soma}_{static}$, and $f_3 = \min_{\forall dendrites}(V^{DistalDendriteMiddle}_{static}) - V^{Soma}_{static}$. Each feature is on the x-axis in a separate subplot above with the number of trigger points facilitated above threshold (−10 mV) as the y-axis. Each subplot consists of three 2D histograms (showing the number of neuron simulations in each square), shades of grey (unclassified), shades of red (classified as active), and shades of blue (classified as non-active). For each feature active and non-active classification regions of unclassified samples are drawn with a yellow and cyan background respectively. These classification regions are also written as rules below, where T=1 and T=0 indicates that the neuron is active and non-active respectively. The number of samples of neurons caught by each rule is specified in the comment after each rule. Using the decision regions in that subplot and those above, the percent of all samples classified (id), active samples classified (id+), and non-active samples classified (id-) are labeled in each subplot. There are a total of 427680 samples of which 400 are active without the EPSP, 62471 are facilitated, and 364809 are non-active.

IF ($f_0 < -6.521$ mV) THEN (T=1) /* 11095 samples */
ELIF (-4.193×10^{-7} mV $< f_0 < 4.193 \times 10^{-7}$ mV) THEN (T=0) /* 40 samples */
ELIF (6.521 mV $< f_0$) THEN (T=1) /* 11095 samples */
ELIF ($f_1 < -50.57$ mV) THEN (T=1) /* 6487 samples */
ELIF (−0.004 668 mV $< f_1 <$ 0.004 668 mV) THEN (T=0) /* 4788 samples */
ELIF (27.75 mV $< f_1$) THEN (T=1) /* 24361 samples */
ELIF ($f_2 < -10.48$ mV) THEN (T=1) /* 39 samples */
ELIF (−0.001 801 mV $< f_2 <$ 0.002 49 mV) THEN (T=0) /* 3306 samples */
ELIF (9.894 mV $< f_2$) THEN (T=1) /* 114 samples */
ELIF ($f_3 < -126.2$ mV) THEN (T=1) /* 1288 samples */
ELIF (−0.000 881 3 mV $< f_3$) THEN (T=0) /* 249 samples */
ELSE (T=Unknown) /* 364818 samples */

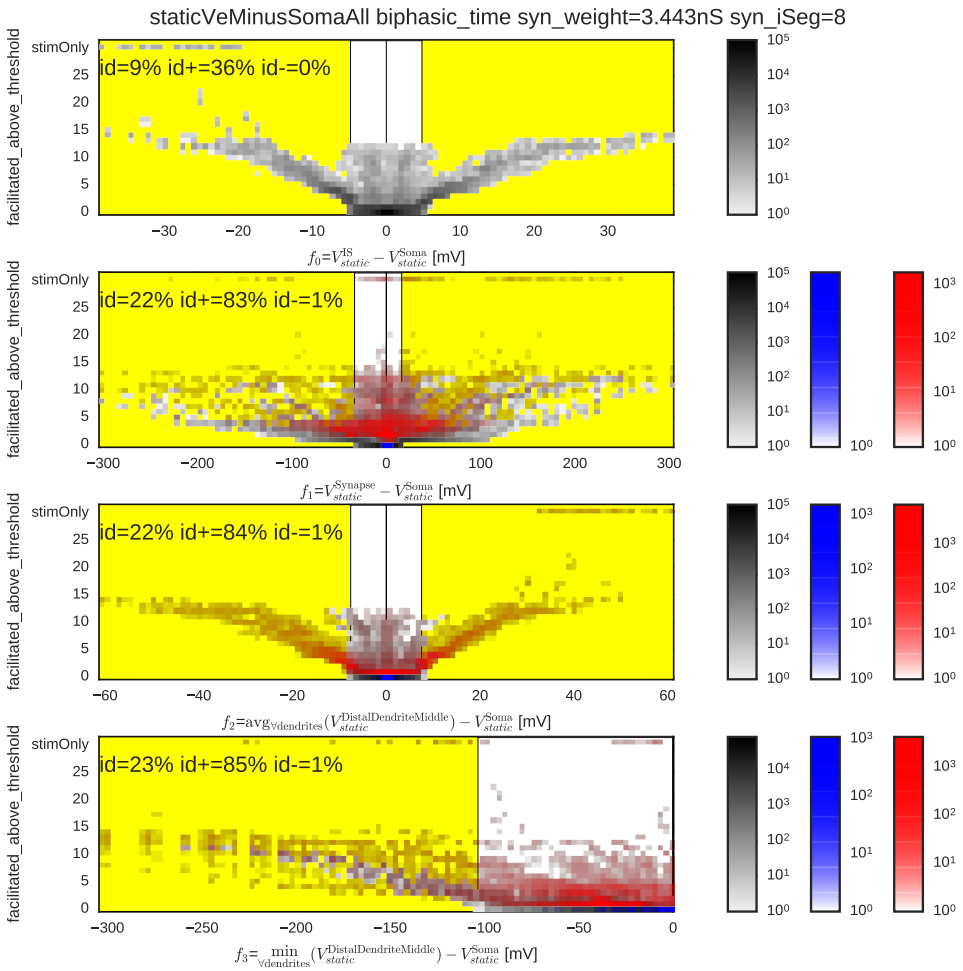

Figure 5.53: Predicting facilitation for all combinations using biphasic epidural stimulation with a synapse triggered on a distal dendrite at segment 8 with weight 3.443 nS using features $f_0 = V^{IS}_{static} - V^{Soma}_{static}$, $f_1 = V^{Synapse}_{static} - V^{Soma}_{static}$, $f_2 = avg_{\forall dendrites}(V^{DistalDendriteMiddle}_{static}) - V^{Soma}_{static}$, and $f_3 = \min_{\forall dendrites}(V^{DistalDendriteMiddle}_{static}) - V^{Soma}_{static}$. Each feature is on the x-axis in a separate subplot above with the number of trigger points facilitated above threshold (−10 mV) as the y-axis. Each subplot consists of three 2D histograms (showing the number of neuron simulations in each square), shades of grey (unclassified), shades of red (classified as active), and shades of blue (classified as non-active). For each feature active and non-active classification regions of unclassified samples are drawn with a yellow and cyan background respectively. These classification regions are also written as rules below, where T=1 and T=0 indicates that the neuron is active and non-active respectively. The number of samples of neurons caught by each rule is specified in the comment after each rule. Using the decision regions in that subplot and those above, the percent of all samples classified (id), active samples classified (id+), and non-active samples classified (id-) are labeled in each subplot. There are a total of 427680 samples of which 400 are active without the EPSP, 110804 are facilitated, and 316476 are non-active.

IF (f_0 < −4.844 mV) THEN (T=1) /* 20460 samples */
ELIF (−1.797 × 10^{-7} mV < f_0 < 1.797 × 10^{-7} mV) THEN (T=0) /* 20 samples */
ELIF (4.823 mV < f_0) THEN (T=1) /* 20600 samples */
ELIF (f_1 < −33.67 mV) THEN (T=1) /* 14472 samples */
ELIF (−0.003 747 mV < f_1 < 0.003 747 mV) THEN (T=0) /* 4186 samples */
ELIF (16.35 mV < f_1) THEN (T=1) /* 37812 samples */
ELIF (f_2 < −7.604 mV) THEN (T=1) /* 59 samples */
ELIF (−0.000 267 9 mV < f_2 < 0.000 267 9 mV) THEN (T=0) /* 396 samples */
ELIF (7.523 mV < f_2) THEN (T=1) /* 89 samples */
ELIF (f_3 < −103.6 mV) THEN (T=1) /* 1476 samples */
ELIF (−0.000 140 4 mV < f_3 < 0.000 202 9 mV) THEN (T=0) /* 20 samples */
ELSE (T=Unknown) /* 328090 samples */

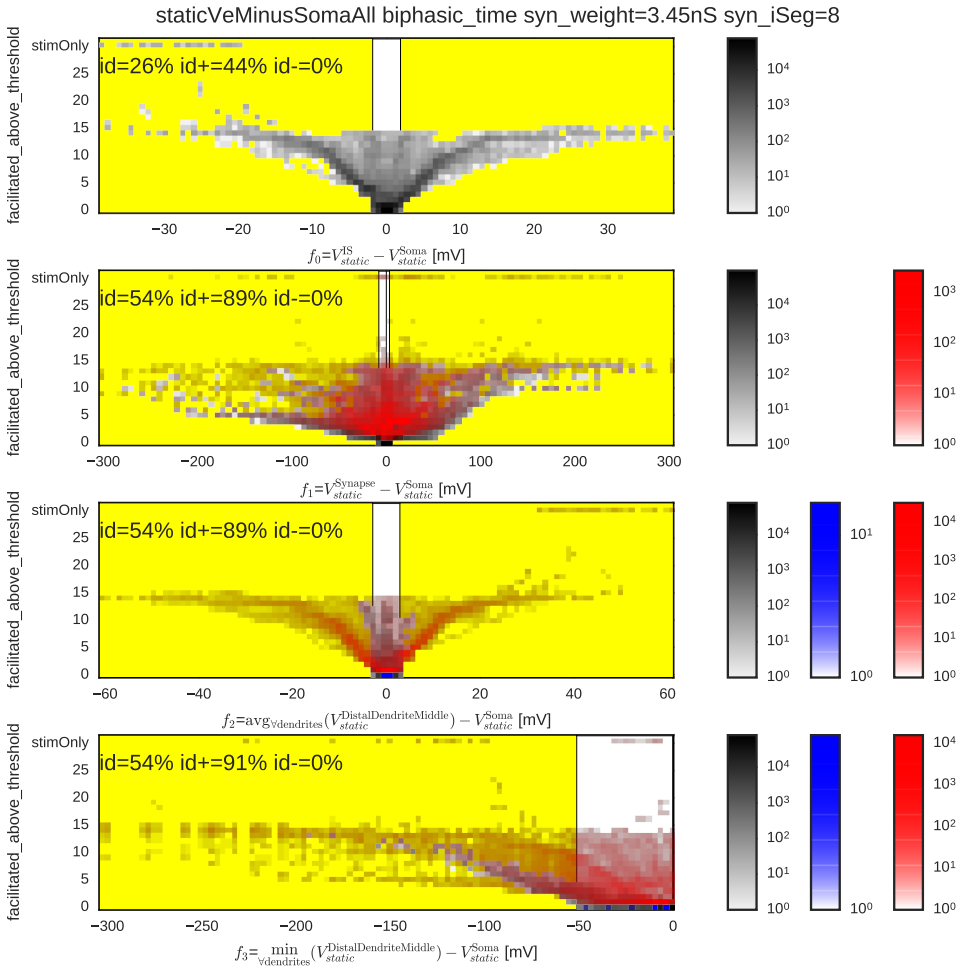

Figure 5.54: Predicting facilitation for all combinations using biphasic epidural stimulation with a synapse triggered on a distal dendrite at segment 8 with weight 3.45 nS using features $f_0 = V^{IS}_{static} - V^{Soma}_{static}$, $f_1 = V^{Synapse}_{static} - V^{Soma}_{static}$, $f_2 = \text{avg}_{\forall dendrites}(V^{DistalDendriteMiddle}_{static}) - V^{Soma}_{static}$, and $f_3 = \min_{\forall dendrites}(V^{DistalDendriteMiddle}_{static}) - V^{Soma}_{static}$. Each feature is on the x-axis in a separate subplot above with the number of trigger points facilitated above threshold (−10 mV) as the y-axis. Each subplot consists of three 2D histograms (showing the number of neuron simulations in each square), shades of grey (unclassified), shades of red (classified as active), and shades of blue (classified as non-active). For each feature active and non-active classification regions of unclassified samples are drawn with a yellow and cyan background respectively. These classification regions are also written as rules below, where T=1 and T=0 indicates that the neuron is active and non-active respectively. The number of samples of neurons caught by each rule is specified in the comment after each rule. Using the decision regions in that subplot and those above, the percent of all samples classified (id), active samples classified (id+), and non-active samples classified (id-) are labeled in each subplot. There are a total of 427680 samples of which 400 are active without the EPSP, 257472 are facilitated, and 169808 are non-active.

IF ($f_0 < -1.848$ mV) THEN (T=1) /* 57880 samples */
ELIF (1.921 mV $< f_0$) THEN (T=1) /* 56210 samples */
ELIF ($f_1 < -7.948$ mV) THEN (T=1) /* 41784 samples */
ELIF (-1.038×10^{-6} mV $< f_1 < 1.038 \times 10^{-6}$ mV) THEN (T=0) /* 38 samples */
ELIF (3.337 mV $< f_1$) THEN (T=1) /* 75768 samples */
ELIF ($f_2 < -2.894$ mV) THEN (T=1) /* 182 samples */
ELIF (2.895 mV $< f_2$) THEN (T=1) /* 86 samples */
ELIF ($f_3 < -51.15$ mV) THEN (T=1) /* 2905 samples */
ELIF (−0.000 634 3 mV $< f_3$) THEN (T=0) /* 223 samples */
ELSE (T=Unknown) /* 192604 samples */

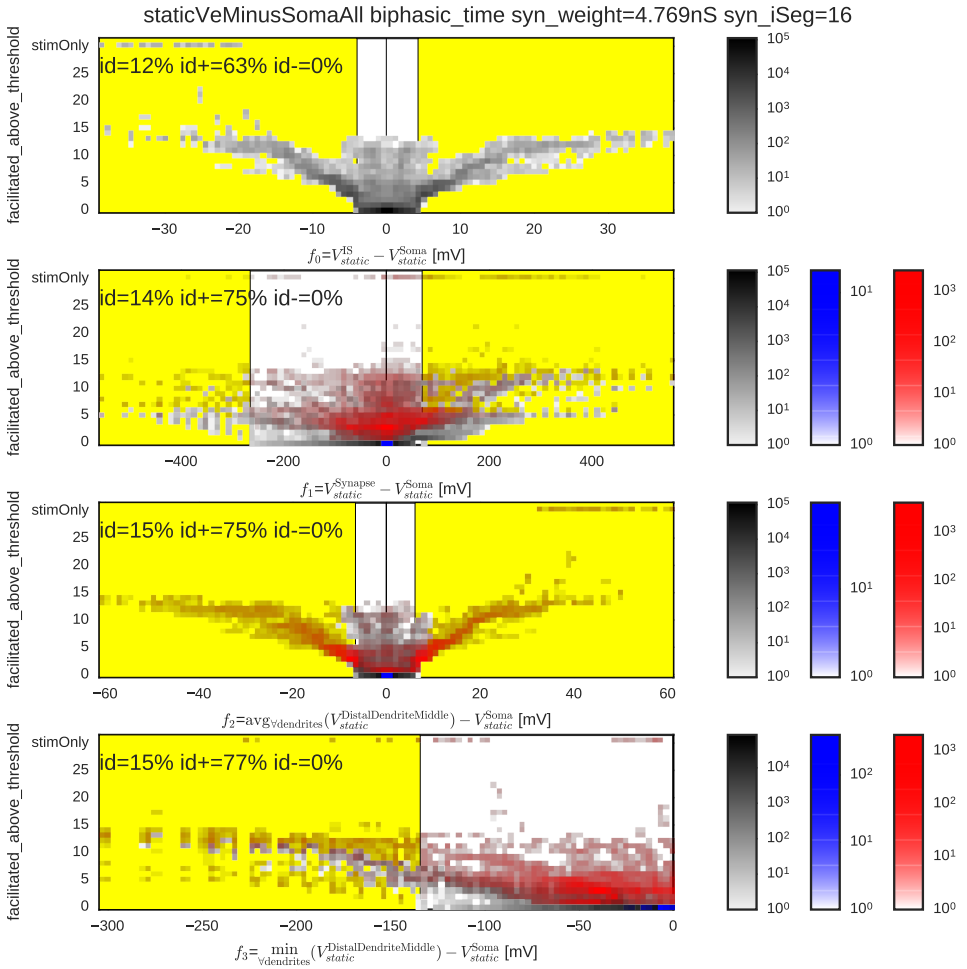

Figure 5.55: Predicting facilitation for all combinations using biphasic epidural stimulation with a synapse triggered on a distal dendrite at segment 16 with weight 4.769 nS using features $f_0 = V^{IS}_{static} - V^{Soma}_{static}$, $f_1 = V^{Synapse}_{static} - V^{Soma}_{static}$, $f_2 = avg_{\forall dendrites}(V^{DistalDendriteMiddle}_{static}) - V^{Soma}_{static}$, and $f_3 = \min_{\forall dendrites}(V^{DistalDendriteMiddle}_{static}) - V^{Soma}_{static}$. Each feature is on the x-axis in a separate subplot above with the number of trigger points facilitated above threshold (−10 mV) as the y-axis. Each subplot consists of three 2D histograms (showing the number of neuron simulations in each square), shades of grey (unclassified), shades of red (classified as active), and shades of blue (classified as non-active). For each feature active and non-active classification regions of unclassified samples are drawn with a yellow and cyan background respectively. These classification regions are also written as rules below, where T=1 and T=0 indicates that the neuron is active and non-active respectively. The number of samples of neurons caught by each rule is specified in the comment after each rule. Using the decision regions in that subplot and those above, the percent of all samples classified (id), active samples classified (id+), and non-active samples classified (id-) are labeled in each subplot. There are a total of 427680 samples of which 400 are active without the EPSP, 82986 are facilitated, and 344294 are non-active.

IF ($f_0 < -3.96$ mV) THEN (T=1) /* 28110 samples */
ELIF (-4.193×10^{-7} mV $< f_0 < 4.193 \times 10^{-7}$ mV) THEN (T=0) /* 40 samples */
ELIF (4.294 mV $< f_0$) THEN (T=1) /* 24770 samples */
ELIF ($f_1 < -265$ mV) THEN (T=1) /* 404 samples */
ELIF (−0.000 174 9 mV $< f_1 <$ 0.000 174 9 mV) THEN (T=0) /* 178 samples */
ELIF (69.75 mV $< f_1$) THEN (T=1) /* 9522 samples */
ELIF ($f_2 < -6.581$ mV) THEN (T=1) /* 223 samples */
ELIF (−0.000 459 6 mV $< f_2 <$ 0.000 459 6 mV) THEN (T=0) /* 1088 samples */
ELIF (6.126 mV $< f_2$) THEN (T=1) /* 183 samples */
ELIF ($f_3 < -134.2$ mV) THEN (T=1) /* 1279 samples */
ELIF (−0.000 881 3 mV $< f_3$) THEN (T=0) /* 491 samples */
ELSE (T=Unknown) /* 361392 samples */

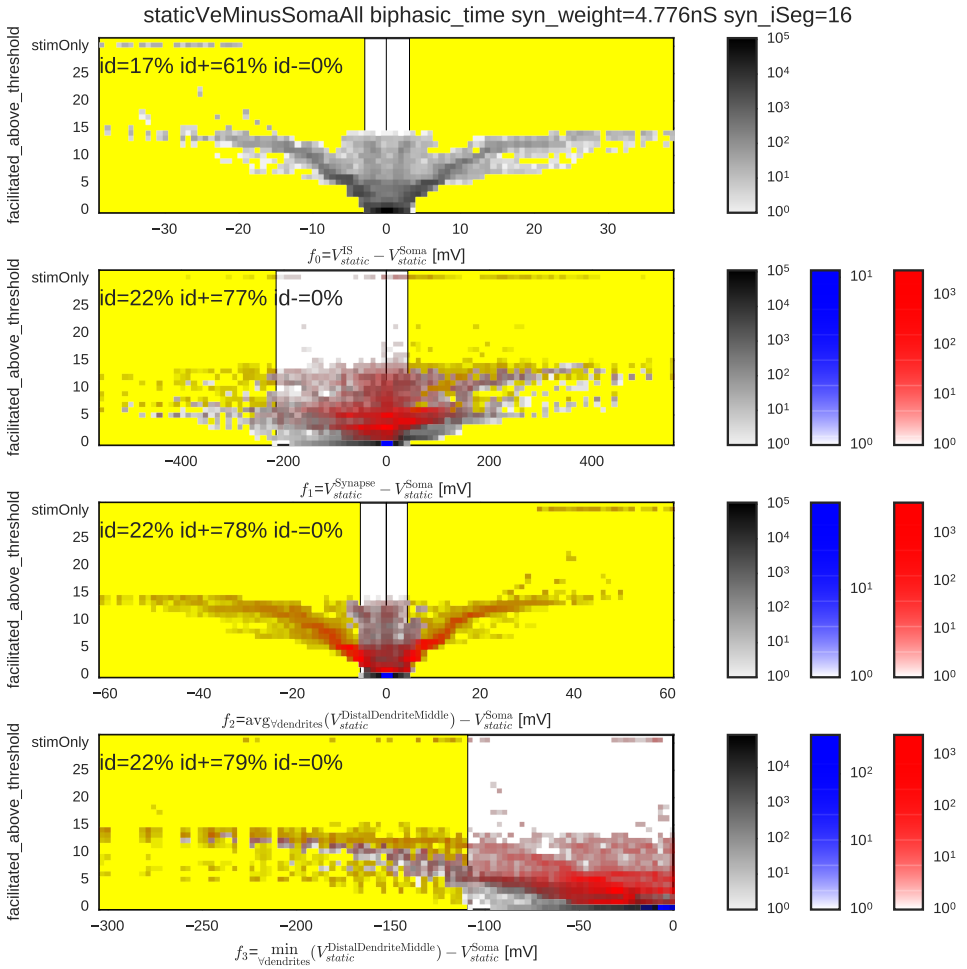

Figure 5.56: Predicting facilitation for all combinations using biphasic epidural stimulation with a synapse triggered on a distal dendrite at segment 16 with weight 4.776 nS using features $f_0 = V^{IS}_{static} - V^{Soma}_{static}$, $f_1 = V^{Synapse}_{static} - V^{Soma}_{static}$, $f_2 = avg_{\forall dendrites}(V^{DistalDendriteMiddle}_{static}) - V^{Soma}_{static}$, and $f_3 = \min_{\forall dendrites}(V^{DistalDendriteMiddle}_{static}) - V^{Soma}_{static}$. Each feature is on the x-axis in a separate subplot above with the number of trigger points facilitated above threshold (−10 mV) as the y-axis. Each subplot consists of three 2D histograms (showing the number of neuron simulations in each square), shades of grey (unclassified), shades of red (classified as active), and shades of blue (classified as non-active). For each feature active and non-active classification regions of unclassified samples are drawn with a yellow and cyan background respectively. These classification regions are also written as rules below, where T=1 and T=0 indicates that the neuron is active and non-active respectively. The number of samples of neurons caught by each rule is specified in the comment after each rule. Using the decision regions in that subplot and those above, the percent of all samples classified (id), active samples classified (id+), and non-active samples classified (id-) are labeled in each subplot. There are a total of 427680 samples of which 400 are active without the EPSP, 120616 are facilitated, and 306664 are non-active.

IF ($f_0 < -2.916$ mV) THEN (T=1) /* 38670 samples */
ELIF (-2.995×10^{-7} mV $< f_0 < 2.995 \times 10^{-7}$ mV) THEN (T=0) /* 30 samples */
ELIF (3.136 mV $< f_0$) THEN (T=1) /* 35855 samples */
ELIF ($f_1 < -214.6$ mV) THEN (T=1) /* 637 samples */
ELIF (−0.000 189 1 mV $< f_1 <$ 0.000 189 1 mV) THEN (T=0) /* 186 samples */
ELIF (41.85 mV $< f_1$) THEN (T=1) /* 19211 samples */
ELIF ($f_2 < -5.537$ mV) THEN (T=1) /* 111 samples */
ELIF (−0.000 404 8 mV $< f_2 <$ 0.000 404 8 mV) THEN (T=0) /* 952 samples */
ELIF (4.493 mV $< f_2$) THEN (T=1) /* 479 samples */
ELIF ($f_3 < -109$ mV) THEN (T=1) /* 1493 samples */
ELIF (−0.000 140 4 mV $< f_3 <$ 0.003 868 mV) THEN (T=0) /* 223 samples */
ELSE (T=Unknown) /* 329833 samples */

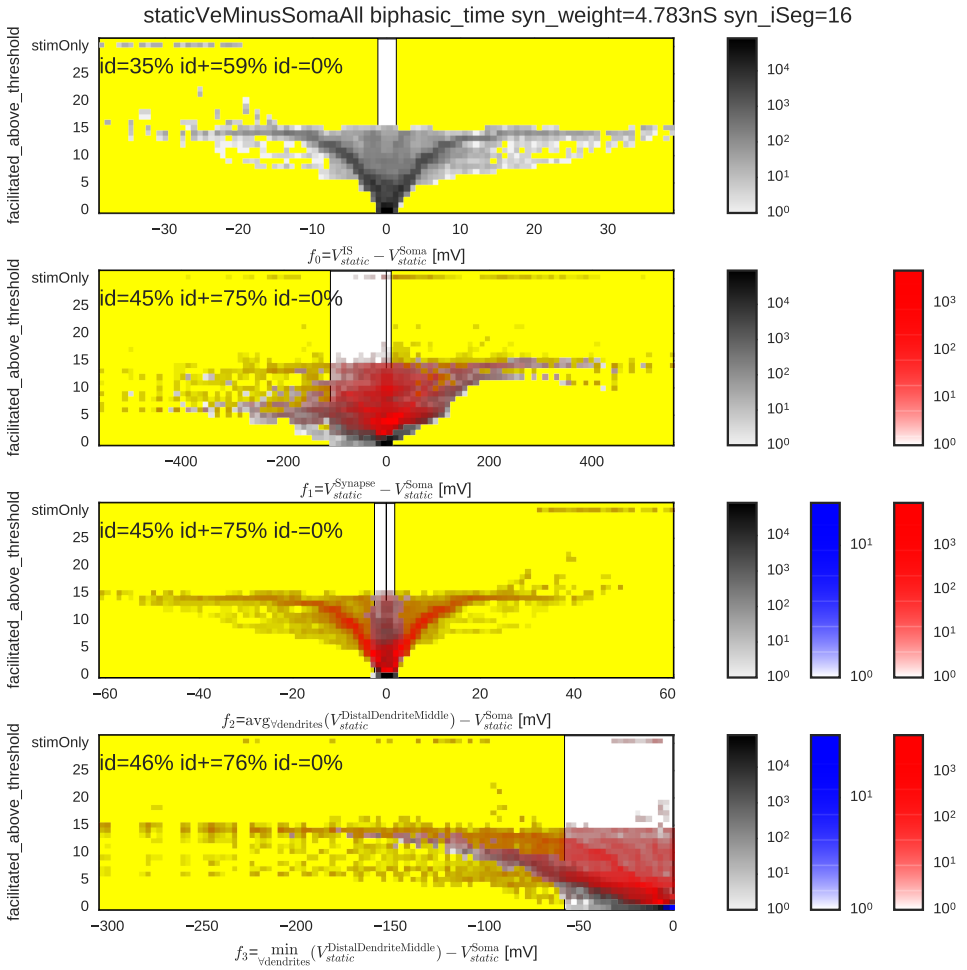

Figure 5.57: Predicting facilitation for all combinations using biphasic epidural stimulation with a synapse triggered on a distal dendrite at segment 16 with weight 4.783 nS using features $f_0 = V^{\text{IS}}_{static} - V^{\text{Soma}}_{static}$, $f_1 = V^{\text{Synapse}}_{static} - V^{\text{Soma}}_{static}$, $f_2 = \text{avg}_{\forall\text{dendrites}}(V^{\text{DistalDendriteMiddle}}_{static}) - V^{\text{Soma}}_{static}$, and $f_3 = \min_{\forall\text{dendrites}}(V^{\text{DistalDendriteMiddle}}_{static}) - V^{\text{Soma}}_{static}$. Each feature is on the x-axis in a separate subplot above with the number of trigger points facilitated above threshold (−10 mV) as the y-axis. Each subplot consists of three 2D histograms (showing the number of neuron simulations in each square), shades of grey (unclassified), shades of red (classified as active), and shades of blue (classified as non-active). For each feature active and non-active classification regions of unclassified samples are drawn with a yellow and cyan background respectively. These classification regions are also written as rules below, where T=1 and T=0 indicates that the neuron is active and non-active respectively. The number of samples of neurons caught by each rule is specified in the comment after each rule. Using the decision regions in that subplot and those above, the percent of all samples classified (id), active samples classified (id+), and non-active samples classified (id-) are labeled in each subplot. There are a total of 427680 samples of which 400 are active without the EPSP, 256925 are facilitated, and 170355 are non-active.

IF ($f_0 < -1.142$ mV) THEN (T=1) /* 80350 samples */
ELIF (1.354 mV $< f_0$) THEN (T=1) /* 72055 samples */
ELIF ($f_1 < -108.8$ mV) THEN (T=1) /* 1203 samples */
ELIF (-3.725×10^{-5} mV $< f_1 < 3.725 \times 10^{-5}$ mV) THEN (T=0) /* 42 samples */
ELIF (9.507 mV $< f_1$) THEN (T=1) /* 40467 samples */
ELIF ($f_2 < -2.521$ mV) THEN (T=1) /* 113 samples */
ELIF (-6.694×10^{-5} mV $< f_2 < 6.694 \times 10^{-5}$ mV) THEN (T=0) /* 46 samples */
ELIF (1.789 mV $< f_2$) THEN (T=1) /* 455 samples */
ELIF ($f_3 < -57.61$ mV) THEN (T=1) /* 2912 samples */
ELSE (T=Unknown) /* 230037 samples */

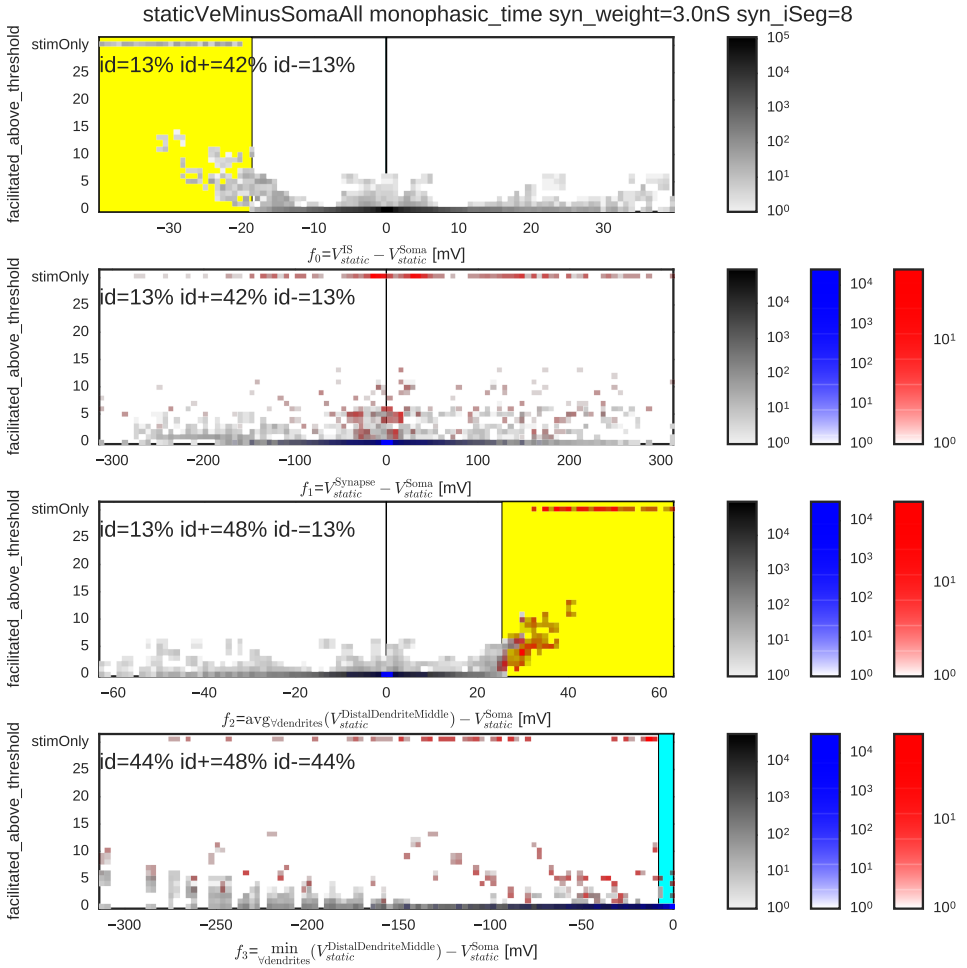

Figure 5.58: Predicting facilitation for all combinations using monophasic epidural stimulation with a synapse triggered on a distal dendrite at segment 8 with weight 3.0 nS using features $f_0 = V^{IS}_{static} - V^{Soma}_{static}$, $f_1 = V^{Synapse}_{static} - V^{Soma}_{static}$, $f_2 = \text{avg}_{\forall dendrites}(V^{DistalDendriteMiddle}_{static}) - V^{Soma}_{static}$, and $f_3 = \min_{\forall dendrites}(V^{DistalDendriteMiddle}_{static}) - V^{Soma}_{static}$. Each feature is on the x-axis in a separate subplot above with the number of trigger points facilitated above threshold (−10 mV) as the y-axis. Each subplot consists of three 2D histograms (showing the number of neuron simulations in each square), shades of grey (unclassified), shades of red (classified as active), and shades of blue (classified as non-active). For each feature active and non-active classification regions of unclassified samples are drawn with a yellow and cyan background respectively. These classification regions are also written as rules below, where T=1 and T=0 indicates that the neuron is active and non-active respectively. The number of samples of neurons caught by each rule is specified in the comment after each rule. Using the decision regions in that subplot and those above, the percent of all samples classified (id), active samples classified (id+), and non-active samples classified (id-) are labeled in each subplot. There are a total of 427680 samples of which 645 are active without the EPSP, 2562 are facilitated, and 424473 are non-active.

IF ($f_0 < -18.55$ mV) THEN (T=1) /* 1355 samples */
ELIF (−0.074 81 mV $< f_0 <$ 0.0561 mV) THEN (T=0) /* 56200 samples */
ELIF (−0.002 051 mV $< f_1 <$ 0.002 051 mV) THEN (T=0) /* 1276 samples */
ELIF (−0.061 48 mV $< f_2 <$ 0.041 36 mV) THEN (T=0) /* 390 samples */
ELIF (25.42 mV $< f_2$) THEN (T=1) /* 210 samples */
ELIF (−7.963 mV $< f_3$) THEN (T=0) /* 131049 samples */
ELSE (T=Unknown) /* 237200 samples */

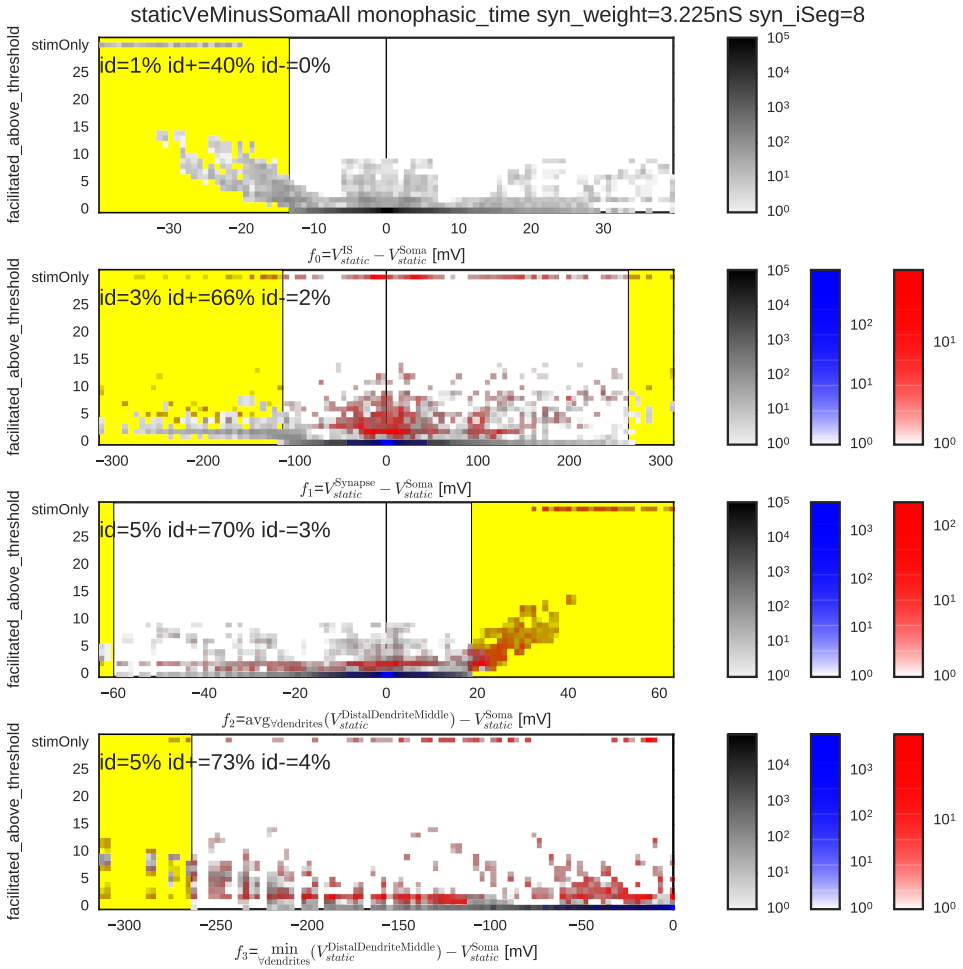

Figure 5.59: Predicting facilitation for all combinations using monophasic epidural stimulation with a synapse triggered on a distal dendrite at segment 8 with weight 3.225 nS using features $f_0 = V^{IS}_{static} - V^{Soma}_{static}$, $f_1 = V^{Synapse}_{static} - V^{Soma}_{static}$, $f_2 = \text{avg}_{\forall dendrites}(V^{DistalDendriteMiddle}_{static}) - V^{Soma}_{static}$, and $f_3 = \min_{\forall dendrites}(V^{DistalDendriteMiddle}_{static}) - V^{Soma}_{static}$. Each feature is on the x-axis in a separate subplot above with the number of trigger points facilitated above threshold (−10 mV) as the y-axis. Each subplot consists of three 2D histograms (showing the number of neuron simulations in each square), shades of grey (unclassified), shades of red (classified as active), and shades of blue (classified as non-active). For each feature active and non-active classification regions of unclassified samples are drawn with a yellow and cyan background respectively. These classification regions are also written as rules below, where T=1 and T=0 indicates that the neuron is active and non-active respectively. The number of samples of neurons caught by each rule is specified in the comment after each rule. Using the decision regions in that subplot and those above, the percent of all samples classified (id), active samples classified (id+), and non-active samples classified (id-) are labeled in each subplot. There are a total of 427680 samples of which 645 are active without the EPSP, 6522 are facilitated, and 420513 are non-active.

IF (f_0 < −13.4 mV) THEN (T=1) /* 2870 samples */
ELIF (−0.000 301 1 mV < f_0 < 0.000 301 1 mV) THEN (T=0) /* 2510 samples */
ELIF (f_1 < −113.1 mV) THEN (T=1) /* 1836 samples */
ELIF (−0.019 84 mV < f_1 < 0.019 84 mV) THEN (T=0) /* 8320 samples */
ELIF (264.6 mV < f_1) THEN (T=1) /* 45 samples */
ELIF (f_2 < −59.92 mV) THEN (T=1) /* 15 samples */
ELIF (−0.007 248 mV < f_2 < 0.007 248 mV) THEN (T=0) /* 5848 samples */
ELIF (18.73 mV < f_2) THEN (T=1) /* 274 samples */
ELIF (f_3 < −263.2 mV) THEN (T=1) /* 196 samples */
ELIF (−0.097 63 mV < f_3) THEN (T=0) /* 2157 samples */
ELSE (T=Unknown) /* 403609 samples */

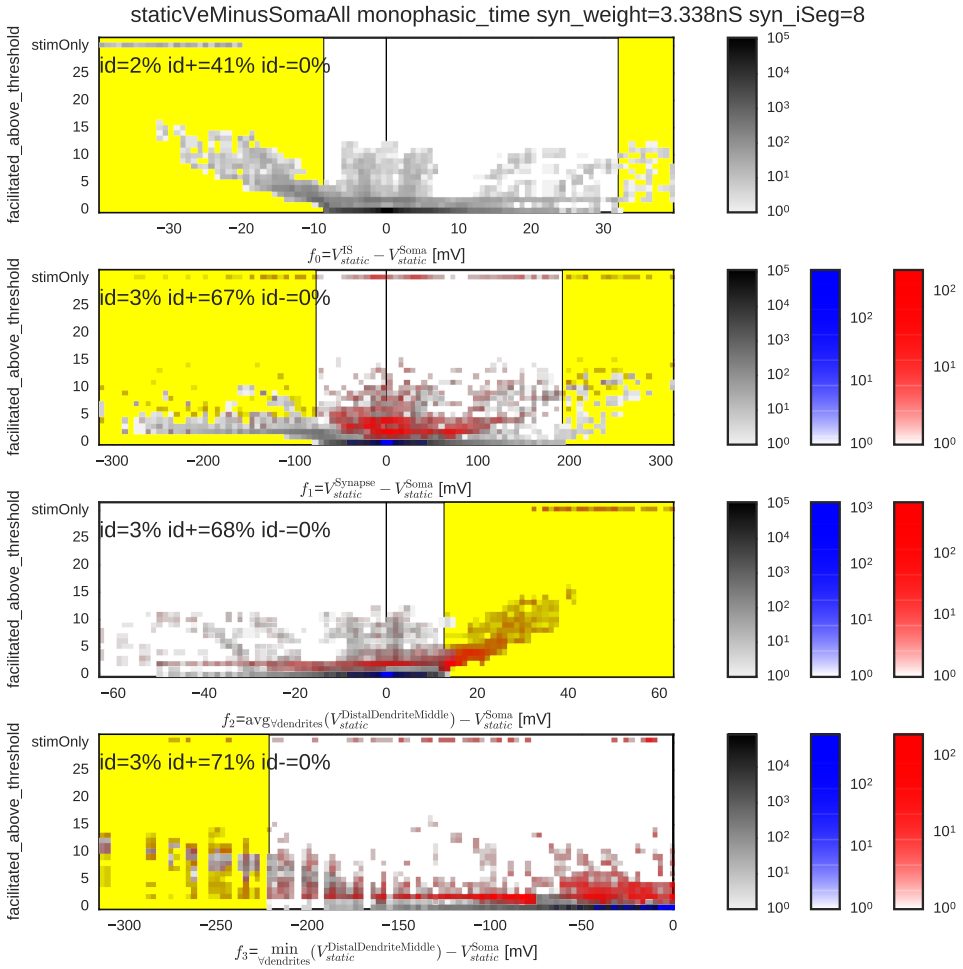

Figure 5.60: Predicting facilitation for all combinations using monophasic epidural stimulation with a synapse triggered on a distal dendrite at segment 8 with weight 3.338 nS using features $f_0 = V^{\text{IS}}_{static} - V^{\text{Soma}}_{static}$, $f_1 = V^{\text{Synapse}}_{static} - V^{\text{Soma}}_{static}$, $f_2 = \text{avg}_{\forall\text{dendrites}}(V^{\text{DistalDendriteMiddle}}_{static}) - V^{\text{Soma}}_{static}$, and $f_3 = \min_{\forall\text{dendrites}}(V^{\text{DistalDendriteMiddle}}_{static}) - V^{\text{Soma}}_{static}$. Each feature is on the x-axis in a separate subplot above with the number of trigger points facilitated above threshold (−10 mV) as the y-axis. Each subplot consists of three 2D histograms (showing the number of neuron simulations in each square), shades of grey (unclassified), shades of red (classified as active), and shades of blue (classified as non-active). For each feature active and non-active classification regions of unclassified samples are drawn with a yellow and cyan background respectively. These classification regions are also written as rules below, where T=1 and T=0 indicates that the neuron is active and non-active respectively. The number of samples of neurons caught by each rule is specified in the comment after each rule. Using the decision regions in that subplot and those above, the percent of all samples classified (id), active samples classified (id+), and non-active samples classified (id-) are labeled in each subplot. There are a total of 427680 samples of which 645 are active without the EPSP, 16246 are facilitated, and 410789 are non-active.

IF ($f_0 < -8.645$ mV) THEN (T=1) /* 6745 samples */
ELIF (−0.000 150 6 mV $< f_0 <$ 0.000 150 6 mV) THEN (T=0) /* 1760 samples */
ELIF (32.04 mV $< f_0$) THEN (T=1) /* 200 samples */
ELIF ($f_1 < -76.77$ mV) THEN (T=1) /* 4177 samples */
ELIF (−0.001 207 mV $< f_1 <$ 0.001 207 mV) THEN (T=0) /* 1582 samples */
ELIF (192.5 mV $< f_1$) THEN (T=1) /* 317 samples */
ELIF (−0.000 236 4 mV $< f_2 <$ 0.000 236 4 mV) THEN (T=0) /* 258 samples */
ELIF (12.69 mV $< f_2$) THEN (T=1) /* 141 samples */
ELIF ($f_3 < -220.9$ mV) THEN (T=1) /* 474 samples */
ELIF (−0.001 754 mV $< f_3 <$ 0.001 632 mV) THEN (T=0) /* 288 samples */
ELSE (T=Unknown) /* 411738 samples */

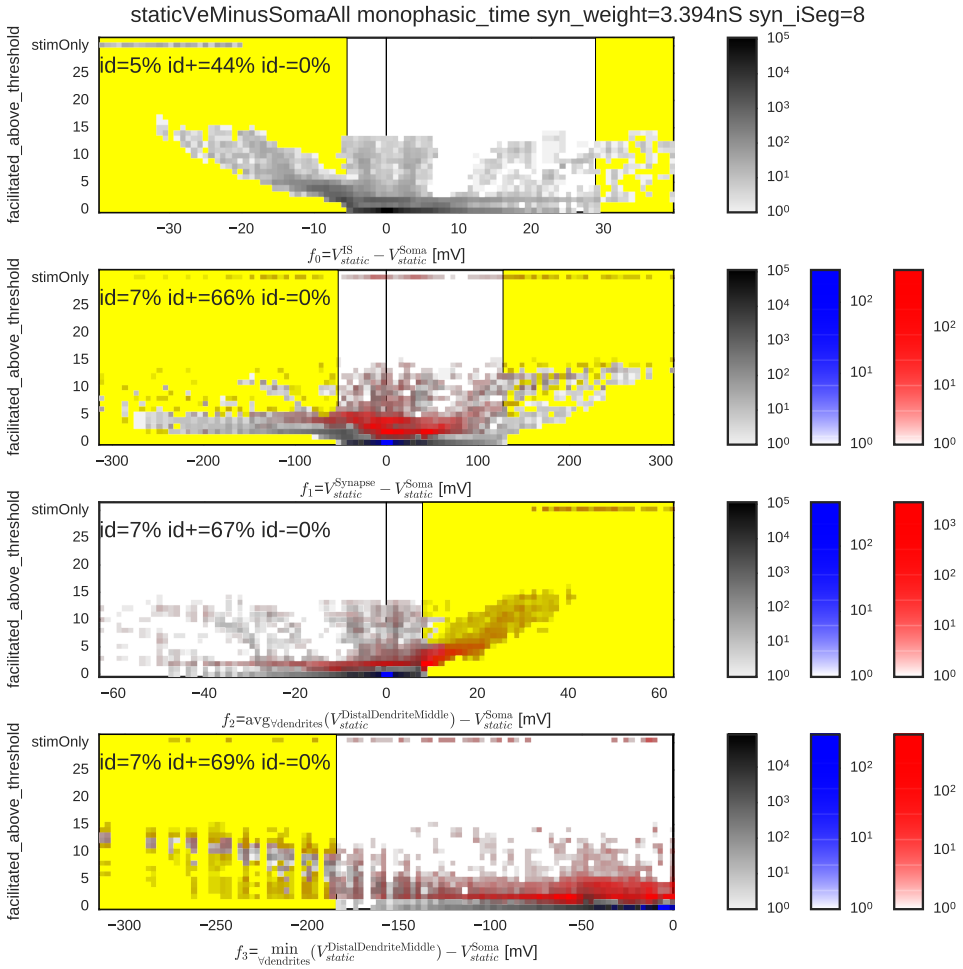

Figure 5.61: Predicting facilitation for all combinations using monophasic epidural stimulation with a synapse triggered on a distal dendrite at segment 8 with weight 3.394 nS using features $f_0 = V^{\text{IS}}_{static} - V^{\text{Soma}}_{static}$, $f_1 = V^{\text{Synapse}}_{static} - V^{\text{Soma}}_{static}$, $f_2 = \text{avg}_{\forall\text{dendrites}}(V^{\text{DistalDendriteMiddle}}_{static}) - V^{\text{Soma}}_{static}$, and $f_3 = \min_{\forall\text{dendrites}}(V^{\text{DistalDendriteMiddle}}_{static}) - V^{\text{Soma}}_{static}$. Each feature is on the x-axis in a separate subplot above with the number of trigger points facilitated above threshold (−10 mV) as the y-axis. Each subplot consists of three 2D histograms (showing the number of neuron simulations in each square), shades of grey (unclassified), shades of red (classified as active), and shades of blue (classified as non-active). For each feature active and non-active classification regions of unclassified samples are drawn with a yellow and cyan background respectively. These classification regions are also written as rules below, where T=1 and T=0 indicates that the neuron is active and non-active respectively. The number of samples of neurons caught by each rule is specified in the comment after each rule. Using the decision regions in that subplot and those above, the percent of all samples classified (id), active samples classified (id+), and non-active samples classified (id-) are labeled in each subplot. There are a total of 427680 samples of which 645 are active without the EPSP, 46322 are facilitated, and 380713 are non-active.

IF ($f_0 < -5.424$ mV) THEN (T=1) /* 20355 samples */
ELIF (-4.263×10^{-5} mV $< f_0 < 4.263 \times 10^{-5}$ mV) THEN (T=0) /* 780 samples */
ELIF (28.91 mV $< f_0$) THEN (T=1) /* 325 samples */
ELIF ($f_1 < -52.6$ mV) THEN (T=1) /* 9370 samples */
ELIF (−0.000 113 1 mV $< f_1 <$ 0.000 113 1 mV) THEN (T=0) /* 266 samples */
ELIF (127.6 mV $< f_1$) THEN (T=1) /* 972 samples */
ELIF (−0.000 116 6 mV $< f_2 <$ 0.000 116 6 mV) THEN (T=0) /* 172 samples */
ELIF (7.952 mV $< f_2$) THEN (T=1) /* 457 samples */
ELIF ($f_3 < -184.1$ mV) THEN (T=1) /* 953 samples */
ELIF (−0.000 265 3 mV $< f_3 <$ 0.000 347 5 mV) THEN (T=0) /* 147 samples */
ELSE (T=Unknown) /* 393883 samples */

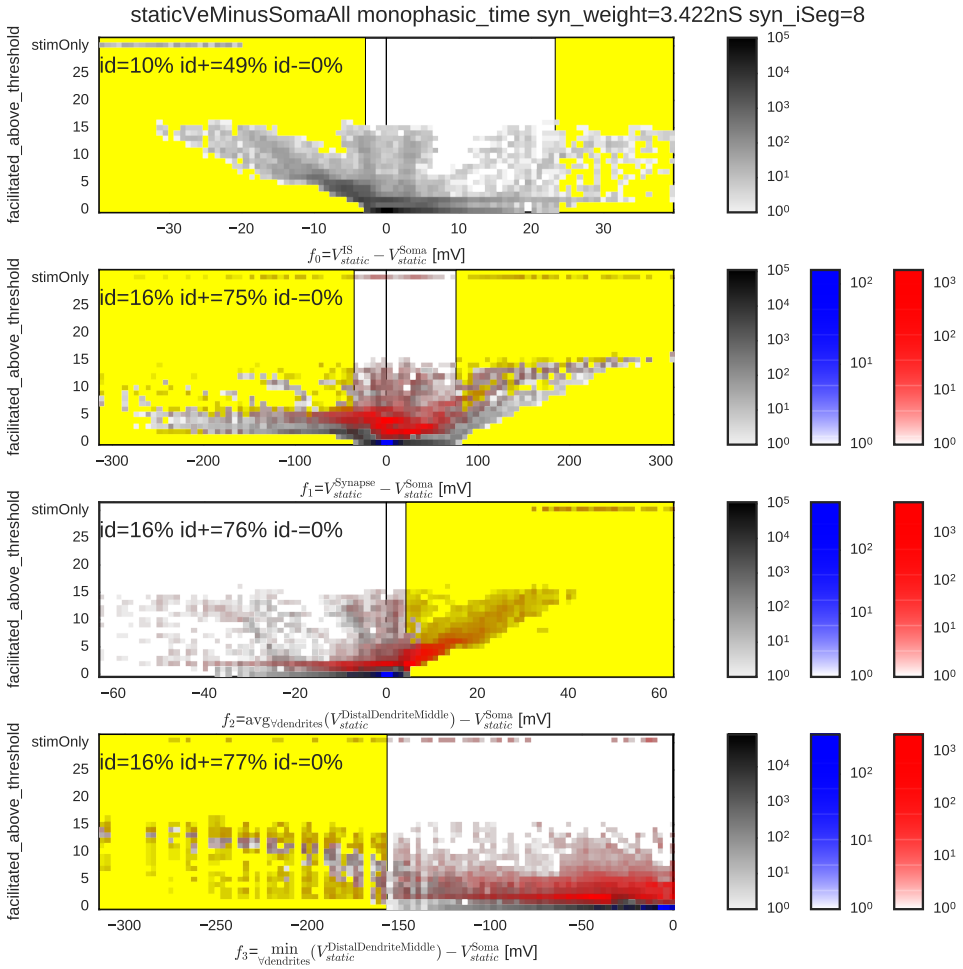

Figure 5.62: Predicting facilitation for all combinations using monophasic epidural stimulation with a synapse triggered on a distal dendrite at segment 8 with weight 3.422 nS using features $f_0 = V^{\text{IS}}_{static} - V^{\text{Soma}}_{static}$, $f_1 = V^{\text{Synapse}}_{static} - V^{\text{Soma}}_{static}$, $f_2 = \text{avg}_{\forall\text{dendrites}}(V^{\text{DistalDendriteMiddle}}_{static}) - V^{\text{Soma}}_{static}$, and $f_3 = \min_{\forall\text{dendrites}}(V^{\text{DistalDendriteMiddle}}_{static}) - V^{\text{Soma}}_{static}$. Each feature is on the x-axis in a separate subplot above with the number of trigger points facilitated above threshold (−10 mV) as the y-axis. Each subplot consists of three 2D histograms (showing the number of neuron simulations in each square), shades of grey (unclassified), shades of red (classified as active), and shades of blue (classified as non-active). For each feature active and non-active classification regions of unclassified samples are drawn with a yellow and cyan background respectively. These classification regions are also written as rules below, where T=1 and T=0 indicates that the neuron is active and non-active respectively. The number of samples of neurons caught by each rule is specified in the comment after each rule. Using the decision regions in that subplot and those above, the percent of all samples classified (id), active samples classified (id+), and non-active samples classified (id-) are labeled in each subplot. There are a total of 427680 samples of which 645 are active without the EPSP, 87686 are facilitated, and 339349 are non-active.

IF ($f_0 < -2.88$ mV) THEN (T=1) /* 43085 samples */
ELIF (-1.937×10^{-5} mV $< f_0 < 1.937 \times 10^{-5}$ mV) THEN (T=0) /* 370 samples */
ELIF (23.34 mV $< f_0$) THEN (T=1) /* 755 samples */
ELIF ($f_1 < -35.16$ mV) THEN (T=1) /* 20543 samples */
ELIF ($-0.000\,584\,4$ mV $< f_1 < 0.000\,584\,4$ mV) THEN (T=0) /* 1100 samples */
ELIF (76.18 mV $< f_1$) THEN (T=1) /* 2626 samples */
ELIF (-5.332×10^{-5} mV $< f_2 < 5.332 \times 10^{-5}$ mV) THEN (T=0) /* 70 samples */
ELIF (4.31 mV $< f_2$) THEN (T=1) /* 565 samples */
ELIF ($f_3 < -156.4$ mV) THEN (T=1) /* 900 samples */
ELIF ($-0.000\,552\,6$ mV $< f_3$) THEN (T=0) /* 227 samples */
ELSE (T=Unknown) /* 357439 samples */

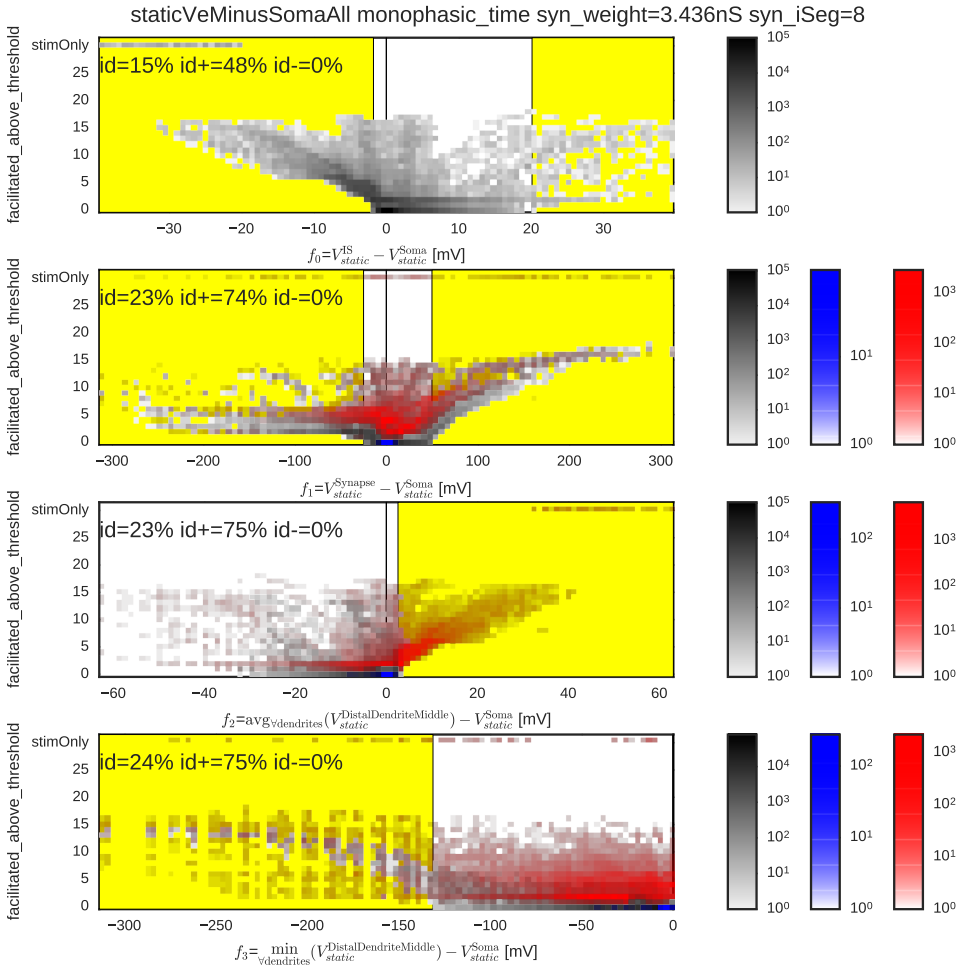

Figure 5.63: Predicting facilitation for all combinations using monophasic epidural stimulation with a synapse triggered on a distal dendrite at segment 8 with weight 3.436 nS using features $f_0 = V^{\text{IS}}_{static} - V^{\text{Soma}}_{static}$, $f_1 = V^{\text{Synapse}}_{static} - V^{\text{Soma}}_{static}$, $f_2 = \text{avg}_{\forall \text{dendrites}}(V^{\text{DistalDendriteMiddle}}_{static}) - V^{\text{Soma}}_{static}$, and $f_3 = \min_{\forall \text{dendrites}}(V^{\text{DistalDendriteMiddle}}_{static}) - V^{\text{Soma}}_{static}$. Each feature is on the x-axis in a separate subplot above with the number of trigger points facilitated above threshold (−10 mV) as the y-axis. Each subplot consists of three 2D histograms (showing the number of neuron simulations in each square), shades of grey (unclassified), shades of red (classified as active), and shades of blue (classified as non-active). For each feature active and non-active classification regions of unclassified samples are drawn with a yellow and cyan background respectively. These classification regions are also written as rules below, where T=1 and T=0 indicates that the neuron is active and non-active respectively. The number of samples of neurons caught by each rule is specified in the comment after each rule. Using the decision regions in that subplot and those above, the percent of all samples classified (id), active samples classified (id+), and non-active samples classified (id-) are labeled in each subplot. There are a total of 427680 samples of which 645 are active without the EPSP, 133965 are facilitated, and 293070 are non-active.

IF ($f_0 < -1.776$ mV) THEN (T=1) /* 64145 samples */
ELIF (-1.268×10^{-5} mV $< f_0 < 1.268 \times 10^{-5}$ mV) THEN (T=0) /* 230 samples */
ELIF (20.14 mV $< f_0$) THEN (T=1) /* 1095 samples */
ELIF ($f_1 < -24.89$ mV) THEN (T=1) /* 28472 samples */
ELIF ($-0.000\,239$ mV $< f_1 < 0.000\,239$ mV) THEN (T=0) /* 578 samples */
ELIF (49.9 mV $< f_1$) THEN (T=1) /* 6178 samples */
ELIF (-4.675×10^{-5} mV $< f_2 < 4.675 \times 10^{-5}$ mV) THEN (T=0) /* 66 samples */
ELIF (2.565 mV $< f_2$) THEN (T=1) /* 1146 samples */
ELIF ($f_3 < -131.3$ mV) THEN (T=1) /* 993 samples */
ELIF ($-0.000\,926$ mV $< f_3 < 0.001\,075$ mV) THEN (T=0) /* 157 samples */
ELSE (T=Unknown) /* 324620 samples */

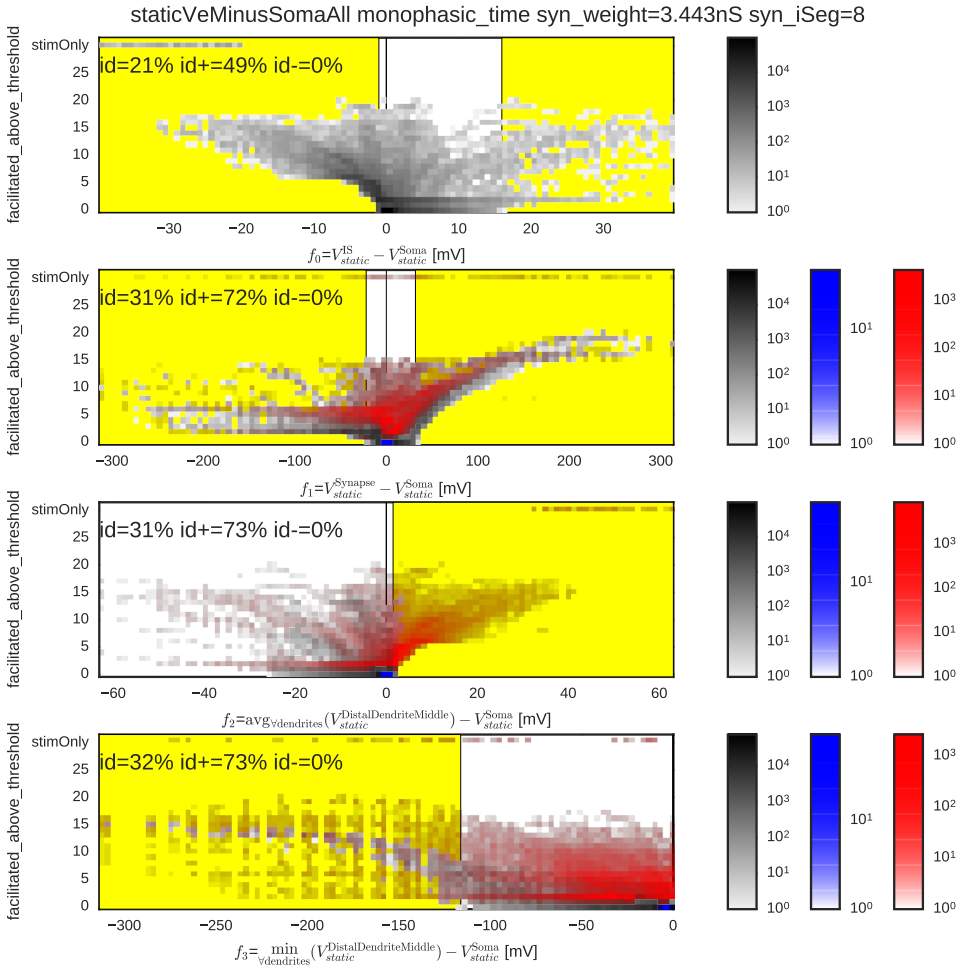

Figure 5.64: Predicting facilitation for all combinations using monophasic epidural stimulation with a synapse triggered on a distal dendrite at segment 8 with weight 3.443 nS using features $f_0 = V^{\text{IS}}_{static} - V^{\text{Soma}}_{static}$, $f_1 = V^{\text{Synapse}}_{static} - V^{\text{Soma}}_{static}$, $f_2 = \text{avg}_{\forall \text{dendrites}}(V^{\text{DistalDendriteMiddle}}_{static}) - V^{\text{Soma}}_{static}$, and $f_3 = \min_{\forall \text{dendrites}}(V^{\text{DistalDendriteMiddle}}_{static}) - V^{\text{Soma}}_{static}$. Each feature is on the x-axis in a separate subplot above with the number of trigger points facilitated above threshold (−10 mV) as the y-axis. Each subplot consists of three 2D histograms (showing the number of neuron simulations in each square), shades of grey (unclassified), shades of red (classified as active), and shades of blue (classified as non-active). For each feature active and non-active classification regions of unclassified samples are drawn with a yellow and cyan background respectively. These classification regions are also written as rules below, where T=1 and T=0 indicates that the neuron is active and non-active respectively. The number of samples of neurons caught by each rule is specified in the comment after each rule. Using the decision regions in that subplot and those above, the percent of all samples classified (id), active samples classified (id+), and non-active samples classified (id-) are labeled in each subplot. There are a total of 427680 samples of which 645 are active without the EPSP, 185287 are facilitated, and 241748 are non-active.

IF ($f_0 < -1.028$ mV) THEN (T=1) /* 90650 samples */
ELIF (-6.339×10^{-6} mV $< f_0 < 6.339 \times 10^{-6}$ mV) THEN (T=0) /* 70 samples */
ELIF (15.96 mV $< f_0$) THEN (T=1) /* 1830 samples */
ELIF ($f_1 < -22.01$ mV) THEN (T=1) /* 28829 samples */
ELIF (-1.885×10^{-5} mV $< f_1 < 1.885 \times 10^{-5}$ mV) THEN (T=0) /* 88 samples */
ELIF (31.85 mV $< f_1$) THEN (T=1) /* 14065 samples */
ELIF (-2.666×10^{-5} mV $< f_2 < 2.666 \times 10^{-5}$ mV) THEN (T=0) /* 40 samples */
ELIF (1.484 mV $< f_2$) THEN (T=1) /* 1101 samples */
ELIF ($f_3 < -116.2$ mV) THEN (T=1) /* 1079 samples */
ELIF (-3.4×10^{-5} mV $< f_3 < 5.135 \times 10^{-5}$ mV) THEN (T=0) /* 17 samples */
ELSE (T=Unknown) /* 289911 samples */

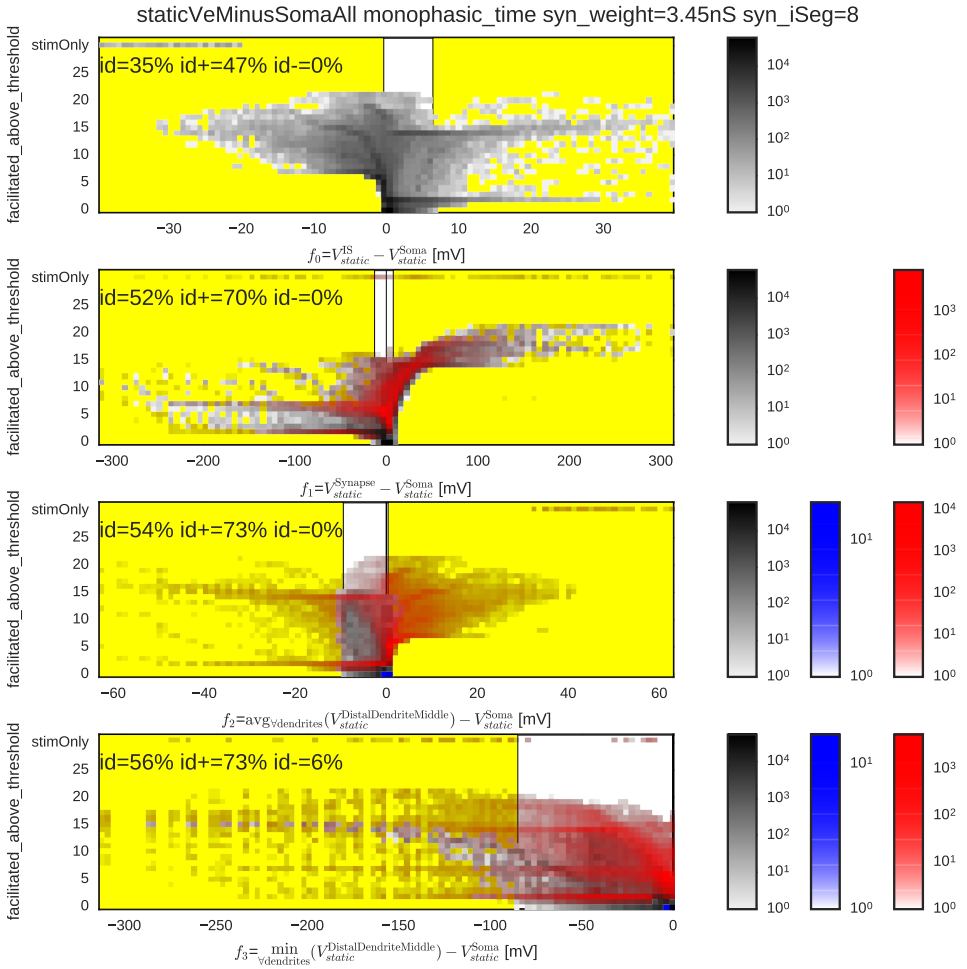

Figure 5.65: Predicting facilitation for all combinations using monophasic epidural stimulation with a synapse triggered on a distal dendrite at segment 8 with weight 3.45 nS using features $f_0 = V^{IS}_{static} - V^{Soma}_{static}$, $f_1 = V^{Synapse}_{static} - V^{Soma}_{static}$, $f_2 = \text{avg}_{\forall dendrites}(V^{DistalDendriteMiddle}_{static}) - V^{Soma}_{static}$, and $f_3 = \min_{\forall dendrites}(V^{DistalDendriteMiddle}_{static}) - V^{Soma}_{static}$. Each feature is on the x-axis in a separate subplot above with the number of trigger points facilitated above threshold (−10 mV) as the y-axis. Each subplot consists of three 2D histograms (showing the number of neuron simulations in each square), shades of grey (unclassified), shades of red (classified as active), and shades of blue (classified as non-active). For each feature active and non-active classification regions of unclassified samples are drawn with a yellow and cyan background respectively. These classification regions are also written as rules below, where T=1 and T=0 indicates that the neuron is active and non-active respectively. The number of samples of neurons caught by each rule is specified in the comment after each rule. Using the decision regions in that subplot and those above, the percent of all samples classified (id), active samples classified (id+), and non-active samples classified (id-) are labeled in each subplot. There are a total of 427680 samples of which 645 are active without the EPSP, 319226 are facilitated, and 107809 are non-active.

IF ($f_0 < -0.355$ mV) THEN (T=1) /* 139035 samples */
ELIF (6.437 mV $< f_0$) THEN (T=1) /* 13775 samples */
ELIF ($f_1 < -12.83$ mV) THEN (T=1) /* 35623 samples */
ELIF (-7.299×10^{-6} mV $< f_1 < 7.299 \times 10^{-6}$ mV) THEN (T=0) /* 40 samples */
ELIF (7.584 mV $< f_1$) THEN (T=1) /* 37256 samples */
ELIF ($f_2 < -9.452$ mV) THEN (T=1) /* 87 samples */
ELIF (-1.293×10^{-5} mV $< f_2 < 1.293 \times 10^{-5}$ mV) THEN (T=0) /* 10 samples */
ELIF (0.3935 mV $< f_2$) THEN (T=1) /* 8296 samples */
ELIF ($f_3 < -84.92$ mV) THEN (T=1) /* 962 samples */
ELIF (-0.238 mV $< f_3$) THEN (T=0) /* 7175 samples */
ELSE (T=Unknown) /* 185421 samples */

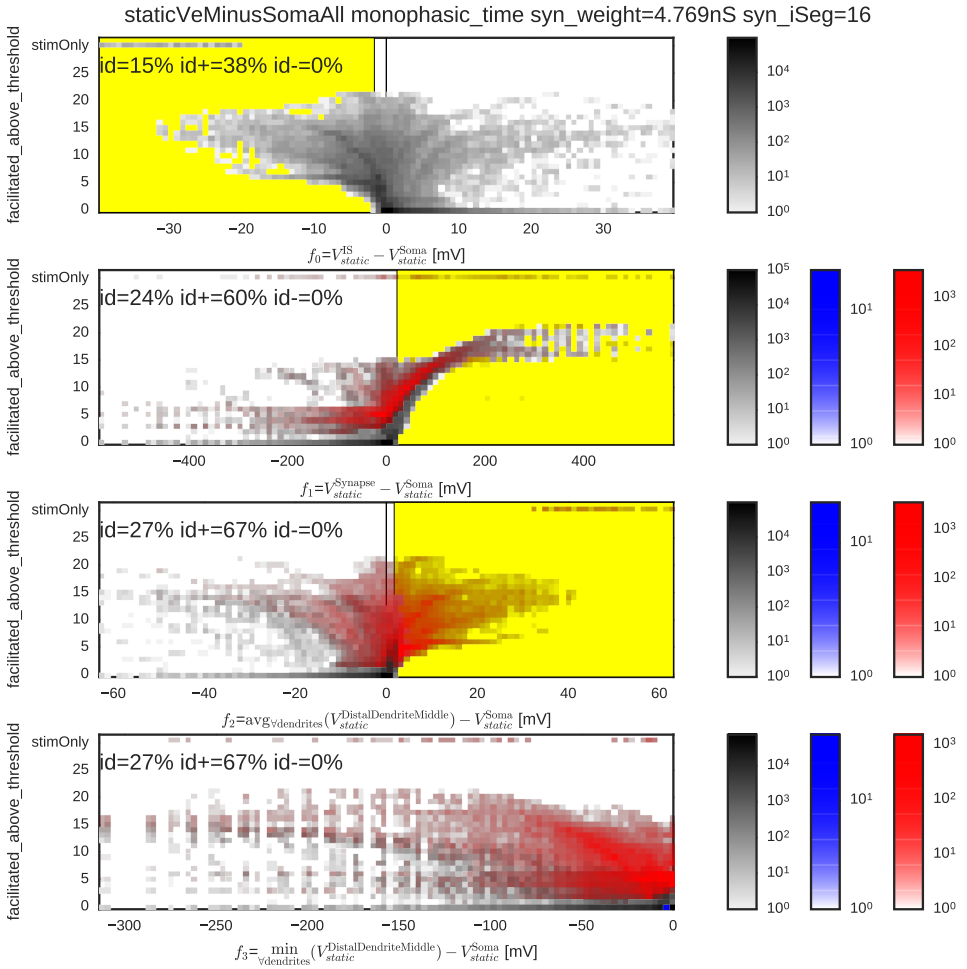

Figure 5.66: Predicting facilitation for all combinations using monophasic epidural stimulation with a synapse triggered on a distal dendrite at segment 16 with weight 4.769 nS using features $f_0 = V^{IS}_{static} - V^{Soma}_{static}$, $f_1 = V^{Synapse}_{static} - V^{Soma}_{static}$, $f_2 = \text{avg}_{\forall dendrites}(V^{DistalDendriteMiddle}_{static}) - V^{Soma}_{static}$, and $f_3 = \min_{\forall dendrites}(V^{DistalDendriteMiddle}_{static}) - V^{Soma}_{static}$. Each feature is on the x-axis in a separate subplot above with the number of trigger points facilitated above threshold (−10 mV) as the y-axis. Each subplot consists of three 2D histograms (showing the number of neuron simulations in each square), shades of grey (unclassified), shades of red (classified as active), and shades of blue (classified as non-active). For each feature active and non-active classification regions of unclassified samples are drawn with a yellow and cyan background respectively. These classification regions are also written as rules below, where T=1 and T=0 indicates that the neuron is active and non-active respectively. The number of samples of neurons caught by each rule is specified in the comment after each rule. Using the decision regions in that subplot and those above, the percent of all samples classified (id), active samples classified (id+), and non-active samples classified (id-) are labeled in each subplot. There are a total of 427680 samples of which 645 are active without the EPSP, 176092 are facilitated, and 250943 are non-active.

IF ($f_0 < -1.649$ mV) THEN (T=1) /* 67650 samples */
ELIF (-5.329×10^{-6} mV $< f_0 < 5.329 \times 10^{-6}$ mV) THEN (T=0) /* 40 samples */
ELIF (21.64 mV $< f_1$) THEN (T=1) /* 38439 samples */
ELIF (-1.293×10^{-5} mV $< f_2 < 1.293 \times 10^{-5}$ mV) THEN (T=0) /* 10 samples */
ELIF (1.729 mV $< f_2$) THEN (T=1) /* 13201 samples */
ELSE (T=Unknown) /* 308340 samples */

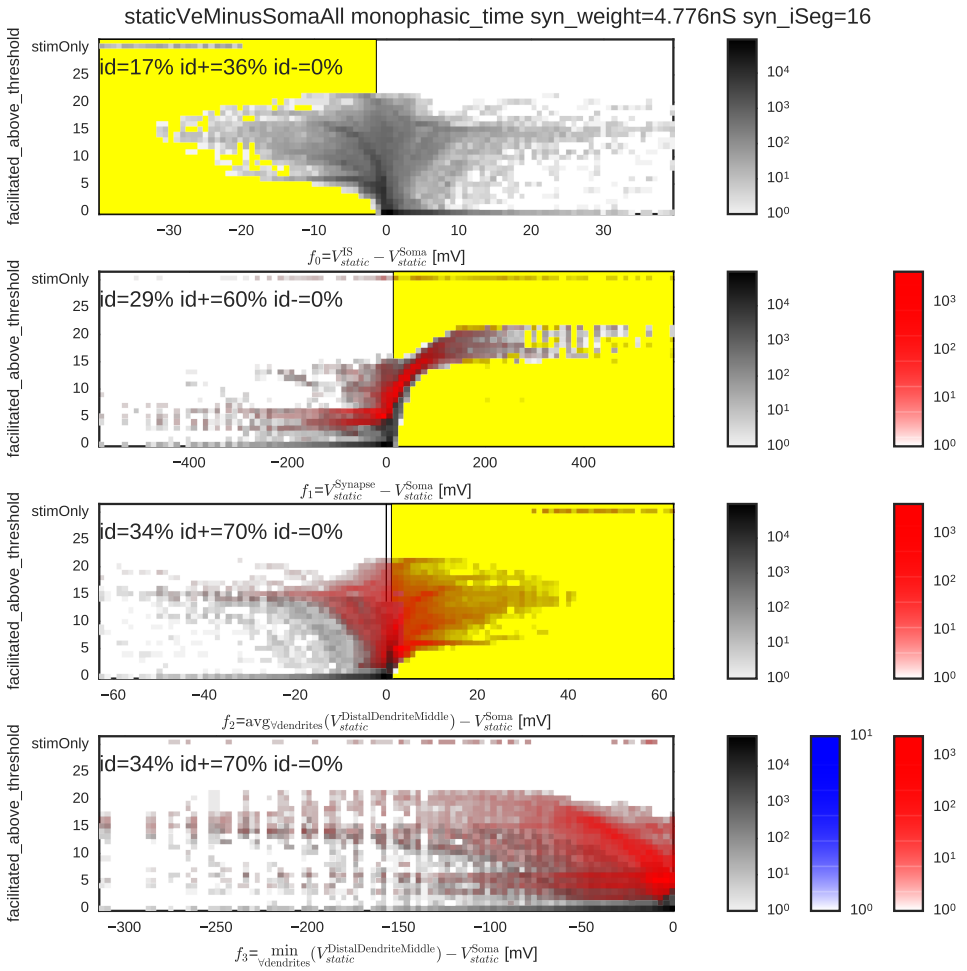

Figure 5.67: Predicting facilitation for all combinations using monophasic epidural stimulation with a synapse triggered on a distal dendrite at segment 16 with weight 4.776 nS using features $f_0 = V^{IS}_{static} - V^{Soma}_{static}$, $f_1 = V^{Synapse}_{static} - V^{Soma}_{static}$, $f_2 = avg_{\forall dendrites}(V^{DistalDendriteMiddle}_{static}) - V^{Soma}_{static}$, and $f_3 = \min_{\forall dendrites}(V^{DistalDendriteMiddle}_{static}) - V^{Soma}_{static}$. Each feature is on the x-axis in a separate subplot above with the number of trigger points facilitated above threshold (−10 mV) as the y-axis. Each subplot consists of three 2D histograms (showing the number of neuron simulations in each square), shades of grey (unclassified), shades of red (classified as active), and shades of blue (classified as non-active). For each feature active and non-active classification regions of unclassified samples are drawn with a yellow and cyan background respectively. These classification regions are also written as rules below, where T=1 and T=0 indicates that the neuron is active and non-active respectively. The number of samples of neurons caught by each rule is specified in the comment after each rule. Using the decision regions in that subplot and those above, the percent of all samples classified (id), active samples classified (id+), and non-active samples classified (id-) are labeled in each subplot. There are a total of 427680 samples of which 645 are active without the EPSP, 209901 are facilitated, and 217134 are non-active.

IF ($f_0 < -1.378$ mV) THEN (T=1) /* 76010 samples */
ELIF (14.14 mV $< f_1$) THEN (T=1) /* 51673 samples */
ELIF (-1.293×10^{-5} mV $< f_2 < 1.293 \times 10^{-5}$ mV) THEN (T=0) /* 10 samples */
ELIF (1.121 mV $< f_2$) THEN (T=1) /* 20700 samples */
ELSE (T=Unknown) /* 279287 samples */

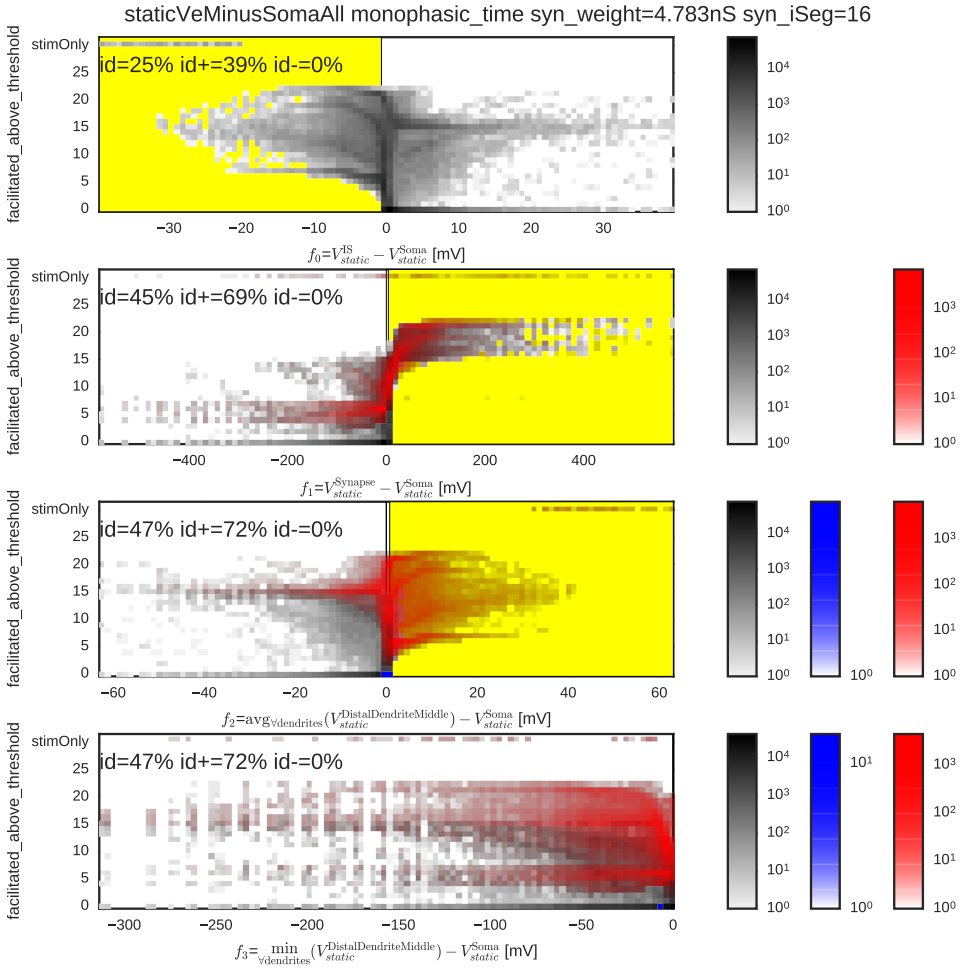

Figure 5.68: Predicting facilitation for all combinations using monophasic epidural stimulation with a synapse triggered on a distal dendrite at segment 16 with weight 4.783 nS using features $f_0 = V^{IS}_{static} - V^{Soma}_{static}$, $f_1 = V^{Synapse}_{static} - V^{Soma}_{static}$, $f_2 = \text{avg}_{\forall dendrites}(V^{DistalDendriteMiddle}_{static}) - V^{Soma}_{static}$, and $f_3 = \min_{\forall dendrites}(V^{DistalDendriteMiddle}_{static}) - V^{Soma}_{static}$. Each feature is on the x-axis in a separate subplot above with the number of trigger points facilitated above threshold (−10 mV) as the y-axis. Each subplot consists of three 2D histograms (showing the number of neuron simulations in each square), shades of grey (unclassified), shades of red (classified as active), and shades of blue (classified as non-active). For each feature active and non-active classification regions of unclassified samples are drawn with a yellow and cyan background respectively. These classification regions are also written as rules below, where T=1 and T=0 indicates that the neuron is active and non-active respectively. The number of samples of neurons caught by each rule is specified in the comment after each rule. Using the decision regions in that subplot and those above, the percent of all samples classified (id), active samples classified (id+), and non-active samples classified (id-) are labeled in each subplot. There are a total of 427680 samples of which 645 are active without the EPSP, 278554 are facilitated, and 148481 are non-active.

IF ($f_0 < -0.6751$ mV) THEN (T=1) /* 110560 samples */
ELIF (-3.574×10^{-5} mV $< f_1 < 3.574 \times 10^{-5}$ mV) THEN (T=0) /* 16 samples */
ELIF (4.074 mV $< f_1$) THEN (T=1) /* 83187 samples */
ELIF (-1.854×10^{-5} mV $< f_2 < 1.854 \times 10^{-5}$ mV) THEN (T=0) /* 18 samples */
ELIF (0.7406 mV $< f_2$) THEN (T=1) /* 8076 samples */
ELIF (−0.062 25 mV $< f_3$) THEN (T=0) /* 710 samples */
ELSE (T=Unknown) /* 225113 samples */

5.D Appendix: Supplementary figures for separating facilitated and non-activated neurons using stimulation-only membrane voltages

This appendix contains supplementary figures for Section 5.4.2.

Figures 5.69-5.79 show the result of the greedy search using membrane voltage features for biphasic stimulation and Figs. 5.80-5.90 show the result for monophasic stimulation. A summary of the results is available in Table 5.3.

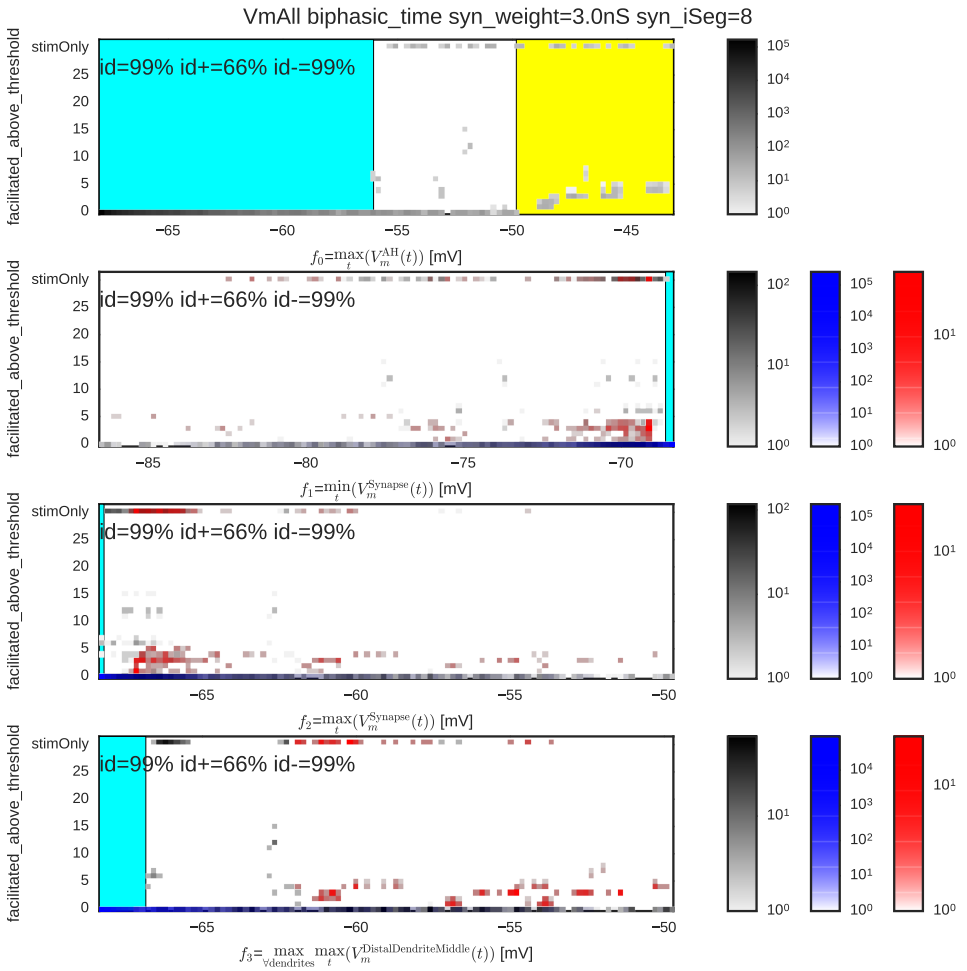

Figure 5.69: Predicting facilitation for all combinations using biphasic epidural stimulation with a synapse triggered on a distal dendrite at segment 8 with weight 3.0 nS using features $f_0 = \max_t(V_m^{\mathrm{AH}}(t))$, $f_1 = \min_t(V_m^{\mathrm{Synapse}}(t))$, $f_2 = \max_t(V_m^{\mathrm{Synapse}}(t))$, and $f_3 = \max_{\forall \mathrm{dendrites}} \max_t(V_m^{\mathrm{DistalDendriteMiddle}}(t))$. Each feature is on the x-axis in a separate subplot above with the number of trigger points facilitated above threshold (−10 mV) as the y-axis. Each subplot consists of three 2D histograms (showing the number of neuron simulations in each square), shades of grey (unclassified), shades of red (classified as active), and shades of blue (classified as non-active). For each feature active and non-active classification regions of unclassified samples are drawn with a yellow and cyan background respectively. These classification regions are also written as rules below, where T=1 and T=0 indicates that the neuron is active and non-active respectively. The number of samples of neurons caught by each rule is specified in the comment after each rule. Using the decision regions in that subplot and those above, the percent of all samples classified (id), active samples classified (id+), and non-active samples classified (id-) are labeled in each subplot. There are a total of 427680 samples of which 400 are active without the EPSP, 537 are facilitated, and 426743 are non-active.

IF ($f_0 < -56.03$ mV) THEN (T=0) /* 425230 samples */
ELIF (-49.81 mV $< f_0$) THEN (T=1) /* 625 samples */
ELIF (-68.58 mV $< f_1$) THEN (T=0) /* 111 samples */
ELIF ($f_2 < -68.18$ mV) THEN (T=0) /* 2 samples */
ELIF ($f_3 < -66.82$ mV) THEN (T=0) /* 6 samples */
ELSE (T=Unknown) /* 1706 samples */

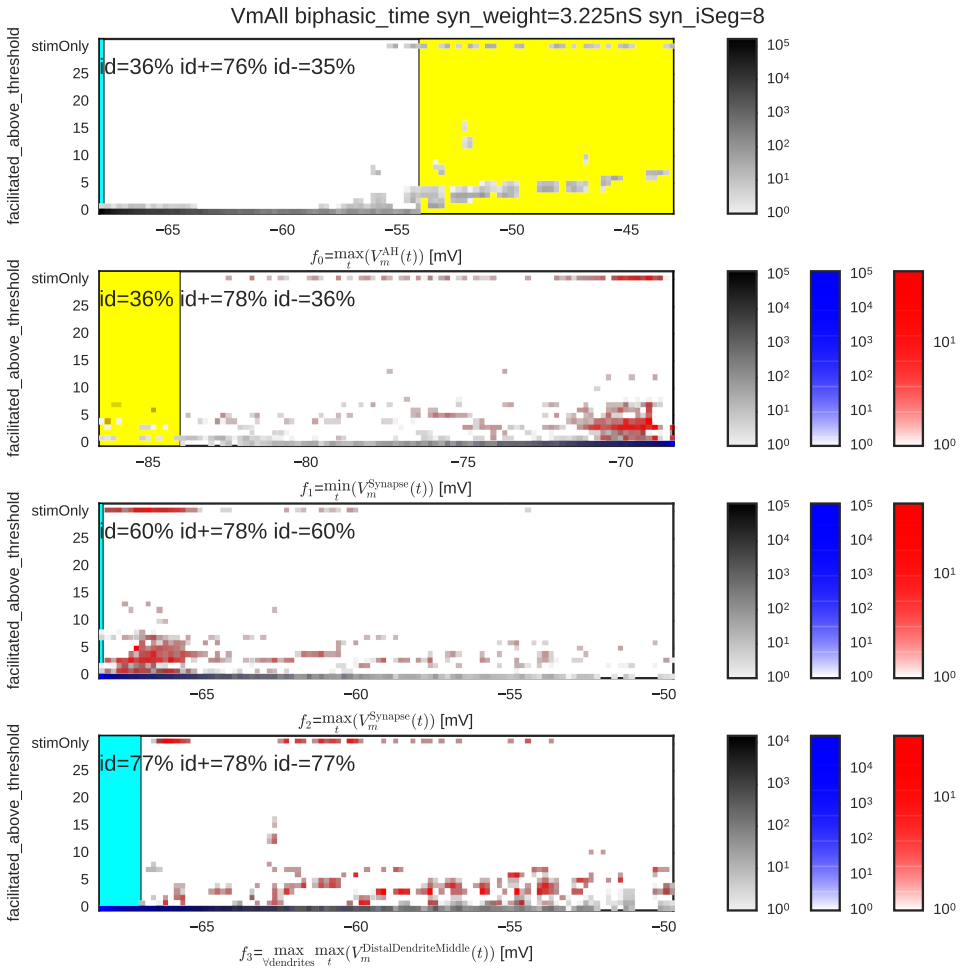

Figure 5.70: Predicting facilitation for all combinations using biphasic epidural stimulation with a synapse triggered on a distal dendrite at segment 8 with weight 3.225 nS using features $f_0 = \max_t(V_m^{AH}(t))$, $f_1 = \min_t(V_m^{Synapse}(t))$, $f_2 = \max_t(V_m^{Synapse}(t))$, and $f_3 = \max_{\forall dendrites} \max_t(V_m^{DistalDendriteMiddle}(t))$. Each feature is on the x-axis in a separate subplot above with the number of trigger points facilitated above threshold (−10 mV) as the y-axis. Each subplot consists of three 2D histograms (showing the number of neuron simulations in each square), shades of grey (unclassified), shades of red (classified as active), and shades of blue (classified as non-active). For each feature active and non-active classification regions of unclassified samples are drawn with a yellow and cyan background respectively. These classification regions are also written as rules below, where T=1 and T=0 indicates that the neuron is active and non-active respectively. The number of samples of neurons caught by each rule is specified in the comment after each rule. Using the decision regions in that subplot and those above, the percent of all samples classified (id), active samples classified (id+), and non-active samples classified (id-) are labeled in each subplot. There are a total of 427680 samples of which 400 are active without the EPSP, 1647 are facilitated, and 425633 are non-active.

IF (f_0 < −67.78 mV) THEN (T=0) /* 152735 samples */
ELIF (−54.06 mV < f_0) THEN (T=1) /* 1575 samples */
ELIF (f_1 < −83.99 mV) THEN (T=1) /* 39 samples */
ELIF (−68.34 mV < f_1) THEN (T=0) /* 1536 samples */
ELIF (f_2 < −68.21 mV) THEN (T=0) /* 103534 samples */
ELIF (f_3 < −66.98 mV) THEN (T=0) /* 70643 samples */
ELSE (T=Unknown) /* 97618 samples */

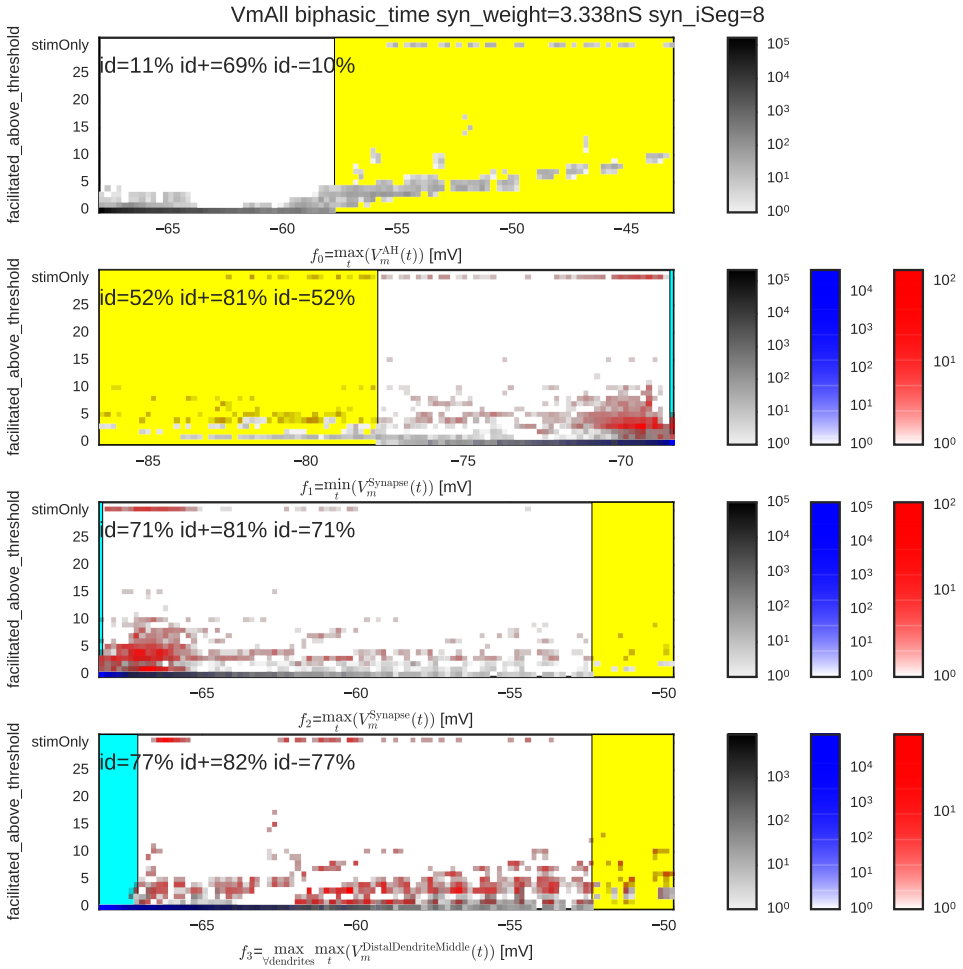

Figure 5.71: Predicting facilitation for all combinations using biphasic epidural stimulation with a synapse triggered on a distal dendrite at segment 8 with weight 3.338 nS using features $f_0 = \max_t(V_m^{\mathrm{AH}}(t))$, $f_1 = \min_t(V_m^{\mathrm{Synapse}}(t))$, $f_2 = \max_t(V_m^{\mathrm{Synapse}}(t))$, and $f_3 = \max_{\forall \mathrm{dendrites}} \max_t(V_m^{\mathrm{DistalDendriteMiddle}}(t))$. Each feature is on the x-axis in a separate subplot above with the number of trigger points facilitated above threshold (−10 mV) as the y-axis. Each subplot consists of three 2D histograms (showing the number of neuron simulations in each square), shades of grey (unclassified), shades of red (classified as active), and shades of blue (classified as non-active). For each feature active and non-active classification regions of unclassified samples are drawn with a yellow and cyan background respectively. These classification regions are also written as rules below, where T=1 and T=0 indicates that the neuron is active and non-active respectively. The number of samples of neurons caught by each rule is specified in the comment after each rule. Using the decision regions in that subplot and those above, the percent of all samples classified (id), active samples classified (id+), and non-active samples classified (id-) are labeled in each subplot. There are a total of 427680 samples of which 400 are active without the EPSP, 4248 are facilitated, and 423032 are non-active.

IF ($f_0 < -67.97$ mV) THEN (T=0) /* 44845 samples */
ELIF (-57.74 mV $< f_0$) THEN (T=1) /* 3235 samples */
ELIF ($f_1 < -77.72$ mV) THEN (T=1) /* 537 samples */
ELIF (-68.45 mV $< f_1$) THEN (T=0) /* 176734 samples */
ELIF ($f_2 < -68.23$ mV) THEN (T=0) /* 80163 samples */
ELIF (-52.33 mV $< f_2$) THEN (T=1) /* 22 samples */
ELIF ($f_3 < -67.08$ mV) THEN (T=0) /* 25044 samples */
ELIF (-52.33 mV $< f_3$) THEN (T=1) /* 63 samples */
ELSE (T=Unknown) /* 97037 samples */

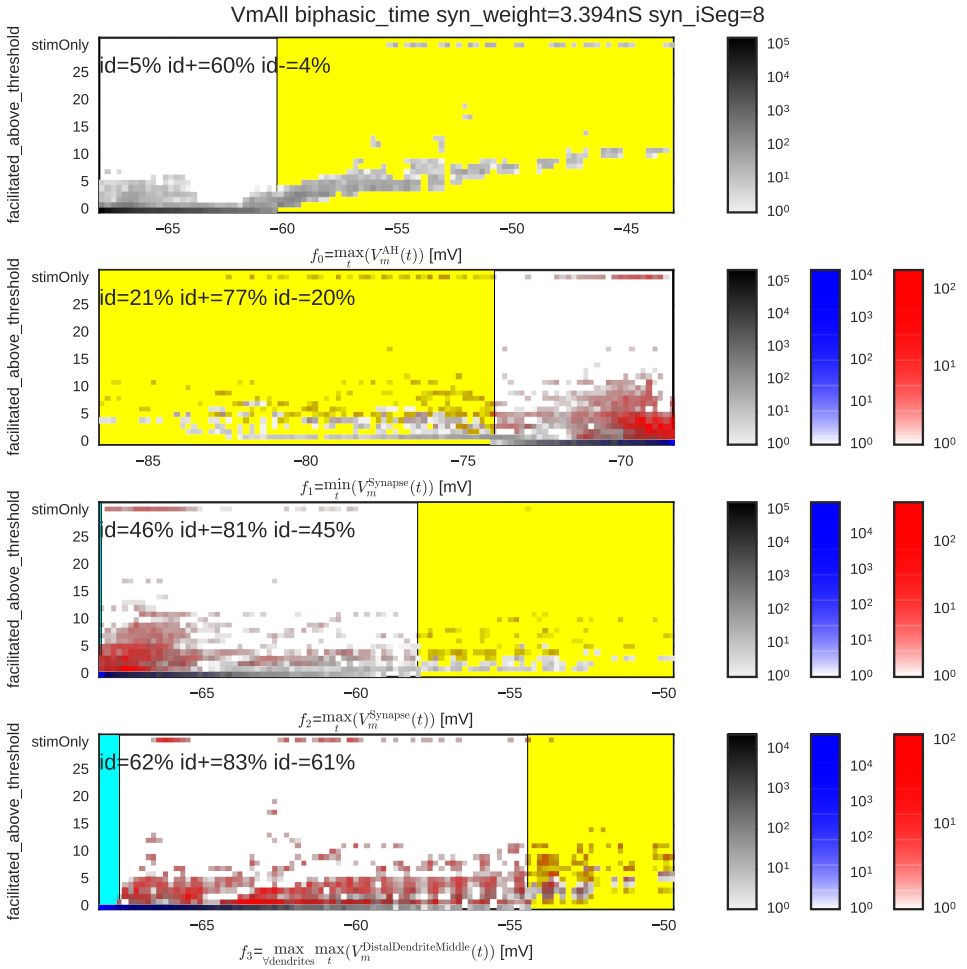

Figure 5.72: Predicting facilitation for all combinations using biphasic epidural stimulation with a synapse triggered on a distal dendrite at segment 8 with weight 3.394 nS using features $f_0 = \max_t(V_m^{\mathrm{AH}}(t))$, $f_1 = \min_t(V_m^{\mathrm{Synapse}}(t))$, $f_2 = \max_t(V_m^{\mathrm{Synapse}}(t))$, and $f_3 = \max_{\forall \mathrm{dendrites}} \max_t(V_m^{\mathrm{DistalDendriteMiddle}}(t))$. Each feature is on the x-axis in a separate subplot above with the number of trigger points facilitated above threshold (−10 mV) as the y-axis. Each subplot consists of three 2D histograms (showing the number of neuron simulations in each square), shades of grey (unclassified), shades of red (classified as active), and shades of blue (classified as non-active). For each feature active and non-active classification regions of unclassified samples are drawn with a yellow and cyan background respectively. These classification regions are also written as rules below, where T=1 and T=0 indicates that the neuron is active and non-active respectively. The number of samples of neurons caught by each rule is specified in the comment after each rule. Using the decision regions in that subplot and those above, the percent of all samples classified (id), active samples classified (id+), and non-active samples classified (id-) are labeled in each subplot. There are a total of 427680 samples of which 400 are active without the EPSP, 9670 are facilitated, and 417610 are non-active.

IF ($f_0 < -67.98$ mV) THEN (T=0) /* 17160 samples */
ELIF (-60.24 mV $< f_0$) THEN (T=1) /* 6100 samples */
ELIF ($f_1 < -74.01$ mV) THEN (T=1) /* 1695 samples */
ELIF (-68.35 mV $< f_1$) THEN (T=0) /* 68263 samples */
ELIF ($f_2 < -68.27$ mV) THEN (T=0) /* 105836 samples */
ELIF (-58 mV $< f_2$) THEN (T=1) /* 363 samples */
ELIF ($f_3 < -67.68$ mV) THEN (T=0) /* 65502 samples */
ELIF (-54.42 mV $< f_3$) THEN (T=1) /* 259 samples */
ELSE (T=Unknown) /* 162502 samples */

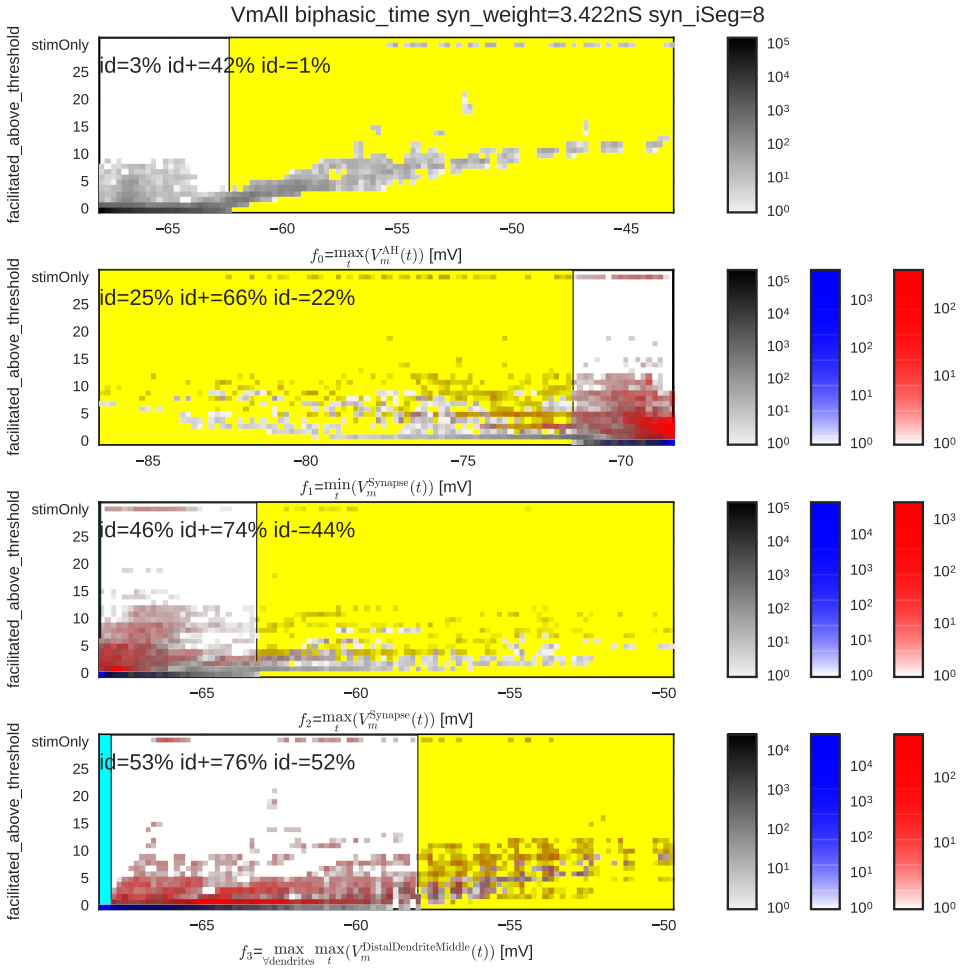

Figure 5.73: Predicting facilitation for all combinations using biphasic epidural stimulation with a synapse triggered on a distal dendrite at segment 8 with weight 3.422 nS using features $f_0 = \max_t(V_m^{\mathrm{AH}}(t))$, $f_1 = \min_t(V_m^{\mathrm{Synapse}}(t))$, $f_2 = \max_t(V_m^{\mathrm{Synapse}}(t))$, and $f_3 = \max_{\forall \mathrm{dendrites}} \max_t(V_m^{\mathrm{DistalDendriteMiddle}}(t))$. Each feature is on the x-axis in a separate subplot above with the number of trigger points facilitated above threshold (−10 mV) as the y-axis. Each subplot consists of three 2D histograms (showing the number of neuron simulations in each square), shades of grey (unclassified), shades of red (classified as active), and shades of blue (classified as non-active). For each feature active and non-active classification regions of unclassified samples are drawn with a yellow and cyan background respectively. These classification regions are also written as rules below, where T=1 and T=0 indicates that the neuron is active and non-active respectively. The number of samples of neurons caught by each rule is specified in the comment after each rule. Using the decision regions in that subplot and those above, the percent of all samples classified (id), active samples classified (id+), and non-active samples classified (id-) are labeled in each subplot. There are a total of 427680 samples of which 400 are active without the EPSP, 24532 are facilitated, and 402748 are non-active.

IF ($f_0 < -67.99$ mV) THEN (T=0) /* 5740 samples */
ELIF (−62.33 mV $< f_0$) THEN (T=1) /* 10690 samples */
ELIF ($f_1 < -71.52$ mV) THEN (T=1) /* 5843 samples */
ELIF (−68.36 mV $< f_1$) THEN (T=0) /* 85974 samples */
ELIF ($f_2 < -68.29$ mV) THEN (T=0) /* 86844 samples */
ELIF (−63.22 mV $< f_2$) THEN (T=1) /* 2019 samples */
ELIF ($f_3 < -67.95$ mV) THEN (T=0) /* 31397 samples */
ELIF (−57.99 mV $< f_3$) THEN (T=1) /* 639 samples */
ELSE (T=Unknown) /* 198534 samples */

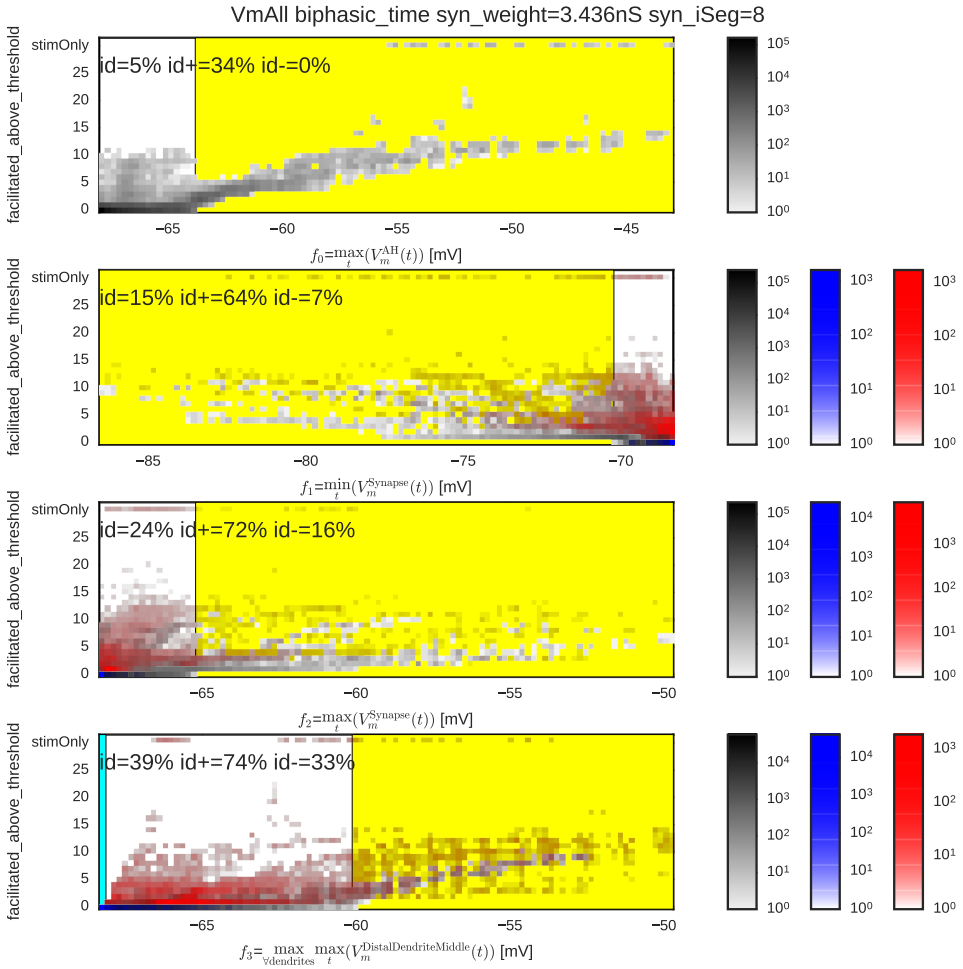

Figure 5.74: Predicting facilitation for all combinations using biphasic epidural stimulation with a synapse triggered on a distal dendrite at segment 8 with weight 3.436 nS using features $f_0 = \max_t(V_m^{\mathrm{AH}}(t))$, $f_1 = \min_t(V_m^{\mathrm{Synapse}}(t))$, $f_2 = \max_t(V_m^{\mathrm{Synapse}}(t))$, and $f_3 = \max_{\forall \mathrm{dendrites}} \max_t(V_m^{\mathrm{DistalDendriteMiddle}}(t))$. Each feature is on the x-axis in a separate subplot above with the number of trigger points facilitated above threshold (−10 mV) as the y-axis. Each subplot consists of three 2D histograms (showing the number of neuron simulations in each square), shades of grey (unclassified), shades of red (classified as active), and shades of blue (classified as non-active). For each feature active and non-active classification regions of unclassified samples are drawn with a yellow and cyan background respectively. These classification regions are also written as rules below, where T=1 and T=0 indicates that the neuron is active and non-active respectively. The number of samples of neurons caught by each rule is specified in the comment after each rule. Using the decision regions in that subplot and those above, the percent of all samples classified (id), active samples classified (id+), and non-active samples classified (id-) are labeled in each subplot. There are a total of 427680 samples of which 400 are active without the EPSP, 62471 are facilitated, and 364809 are non-active.

IF ($f_0 < -67.99$ mV) THEN (T=0) /* 2035 samples */
ELIF (-63.8 mV $< f_0$) THEN (T=1) /* 21630 samples */
ELIF ($f_1 < -70.22$ mV) THEN (T=1) /* 18660 samples */
ELIF (-68.34 mV $< f_1$) THEN (T=0) /* 24218 samples */
ELIF ($f_2 < -68.33$ mV) THEN (T=0) /* 34178 samples */
ELIF (-65.21 mV $< f_2$) THEN (T=1) /* 5375 samples */
ELIF ($f_3 < -68.12$ mV) THEN (T=0) /* 60313 samples */
ELIF (-60.12 mV $< f_3$) THEN (T=1) /* 918 samples */
ELSE (T=Unknown) /* 260353 samples */

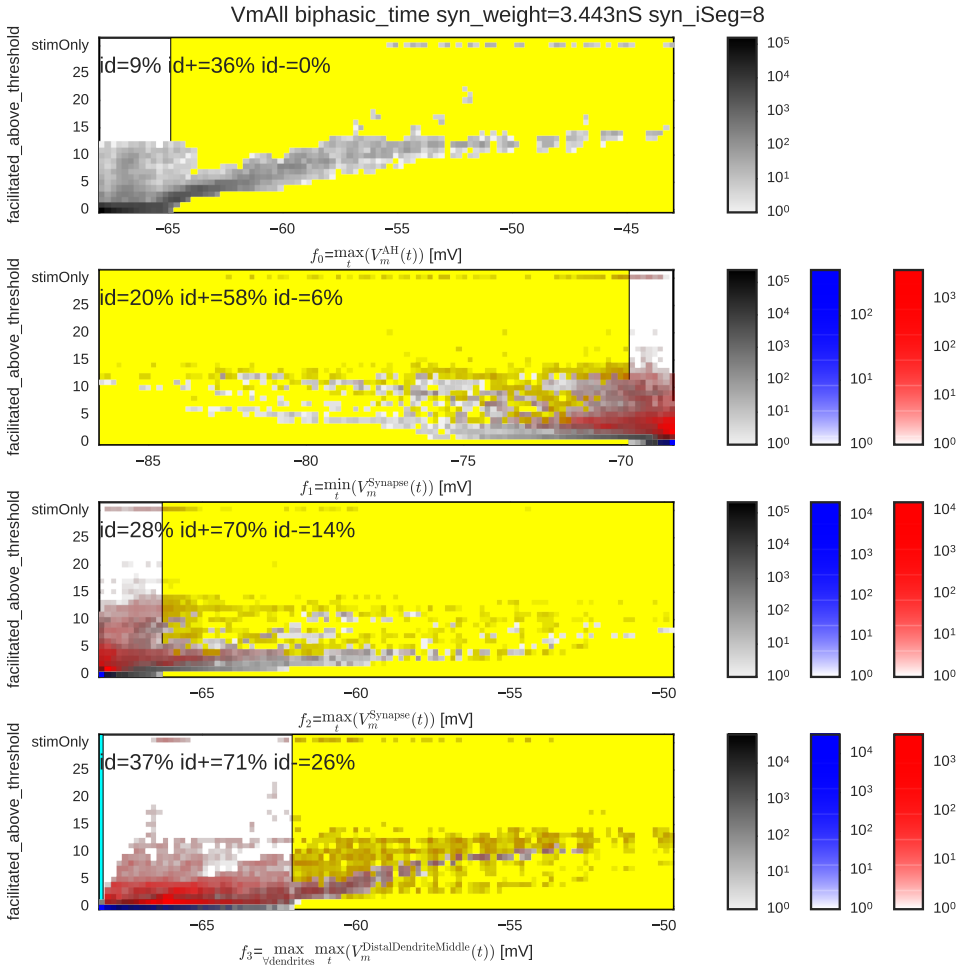

Figure 5.75: Predicting facilitation for all combinations using biphasic epidural stimulation with a synapse triggered on a distal dendrite at segment 8 with weight 3.443 nS using features $f_0 = \max_t(V_m^{\mathrm{AH}}(t))$, $f_1 = \min_t(V_m^{\mathrm{Synapse}}(t))$, $f_2 = \max_t(V_m^{\mathrm{Synapse}}(t))$, and $f_3 = \max_{\forall \mathrm{dendrites}} \max_t(V_m^{\mathrm{DistalDendriteMiddle}}(t))$. Each feature is on the x-axis in a separate subplot above with the number of trigger points facilitated above threshold (−10 mV) as the y-axis. Each subplot consists of three 2D histograms (showing the number of neuron simulations in each square), shades of grey (unclassified), shades of red (classified as active), and shades of blue (classified as non-active). For each feature active and non-active classification regions of unclassified samples are drawn with a yellow and cyan background respectively. These classification regions are also written as rules below, where T=1 and T=0 indicates that the neuron is active and non-active respectively. The number of samples of neurons caught by each rule is specified in the comment after each rule. Using the decision regions in that subplot and those above, the percent of all samples classified (id), active samples classified (id+), and non-active samples classified (id-) are labeled in each subplot. There are a total of 427680 samples of which 400 are active without the EPSP, 110804 are facilitated, and 316476 are non-active.

IF ($f_0 < -67.99$ mV) THEN (T=0) /* 640 samples */
ELIF (−64.87 mV < f_0) THEN (T=1) /* 40050 samples */
ELIF ($f_1 < -69.74$ mV) THEN (T=1) /* 25504 samples */
ELIF (−68.34 mV < f_1) THEN (T=0) /* 20618 samples */
ELIF ($f_2 < -68.33$ mV) THEN (T=0) /* 23330 samples */
ELIF (−66.29 mV < f_2) THEN (T=1) /* 13057 samples */
ELIF ($f_3 < -68.21$ mV) THEN (T=0) /* 37738 samples */
ELIF (−62.07 mV < f_3) THEN (T=1) /* 1309 samples */
ELSE (T=Unknown) /* 265434 samples */

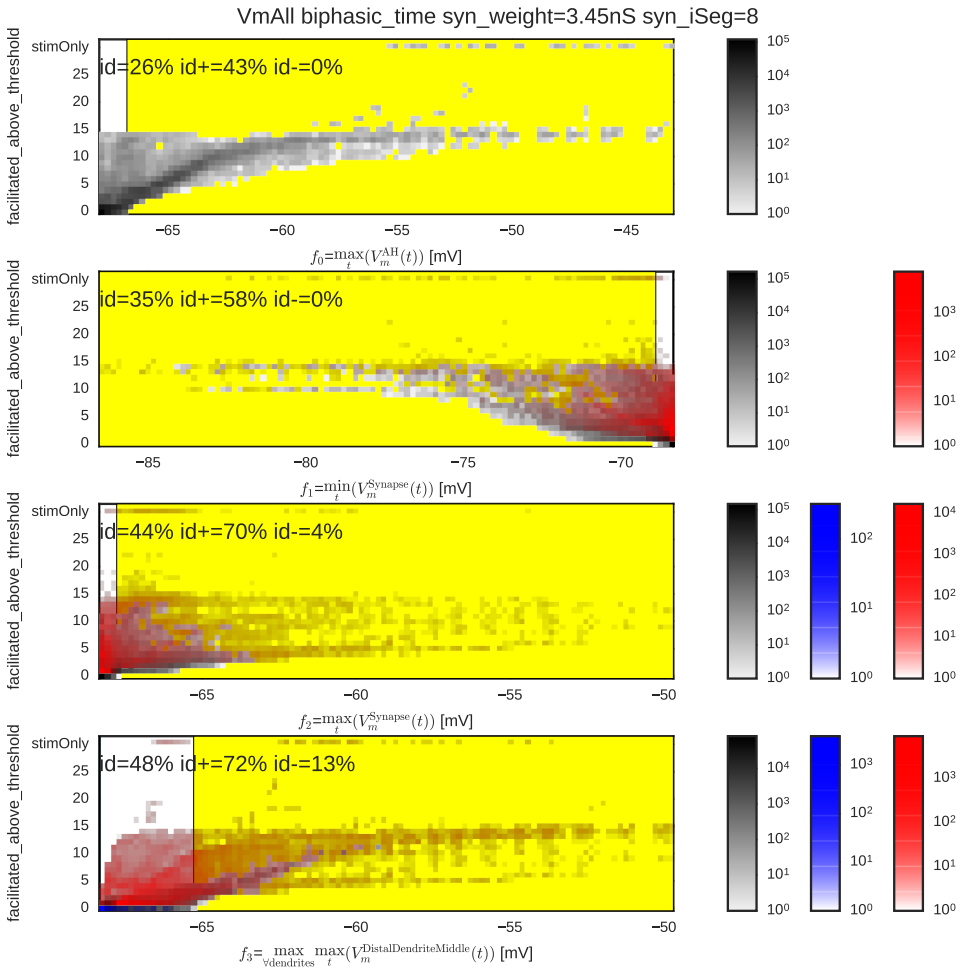

Figure 5.76: Predicting facilitation for all combinations using biphasic epidural stimulation with a synapse triggered on a distal dendrite at segment 8 with weight 3.45 nS using features $f_0 = \max_t(V_m^{\mathrm{AH}}(t))$, $f_1 = \min_t(V_m^{\mathrm{Synapse}}(t))$, $f_2 = \max_t(V_m^{\mathrm{Synapse}}(t))$, and $f_3 = \max_{\forall \mathrm{dendrites}} \max_t(V_m^{\mathrm{DistalDendriteMiddle}}(t))$. Each feature is on the x-axis in a separate subplot above with the number of trigger points facilitated above threshold (−10 mV) as the y-axis. Each subplot consists of three 2D histograms (showing the number of neuron simulations in each square), shades of grey (unclassified), shades of red (classified as active), and shades of blue (classified as non-active). For each feature active and non-active classification regions of unclassified samples are drawn with a yellow and cyan background respectively. These classification regions are also written as rules below, where T=1 and T=0 indicates that the neuron is active and non-active respectively. The number of samples of neurons caught by each rule is specified in the comment after each rule. Using the decision regions in that subplot and those above, the percent of all samples classified (id), active samples classified (id+), and non-active samples classified (id-) are labeled in each subplot. There are a total of 427680 samples of which 400 are active without the EPSP, 257472 are facilitated, and 169808 are non-active.

IF (−66.78 mV < f_0) THEN (T=1) /* 113350 samples */
ELIF (f_1 < −68.89 mV) THEN (T=1) /* 36955 samples */
ELIF (−68.34 mV < f_1) THEN (T=0) /* 323 samples */
ELIF (f_2 < −68.34 mV) THEN (T=0) /* 7123 samples */
ELIF (−67.77 mV < f_2) THEN (T=1) /* 32725 samples */
ELIF (f_3 < −68.31 mV) THEN (T=0) /* 15857 samples */
ELIF (−65.27 mV < f_3) THEN (T=1) /* 2643 samples */
ELSE (T=Unknown) /* 218704 samples */

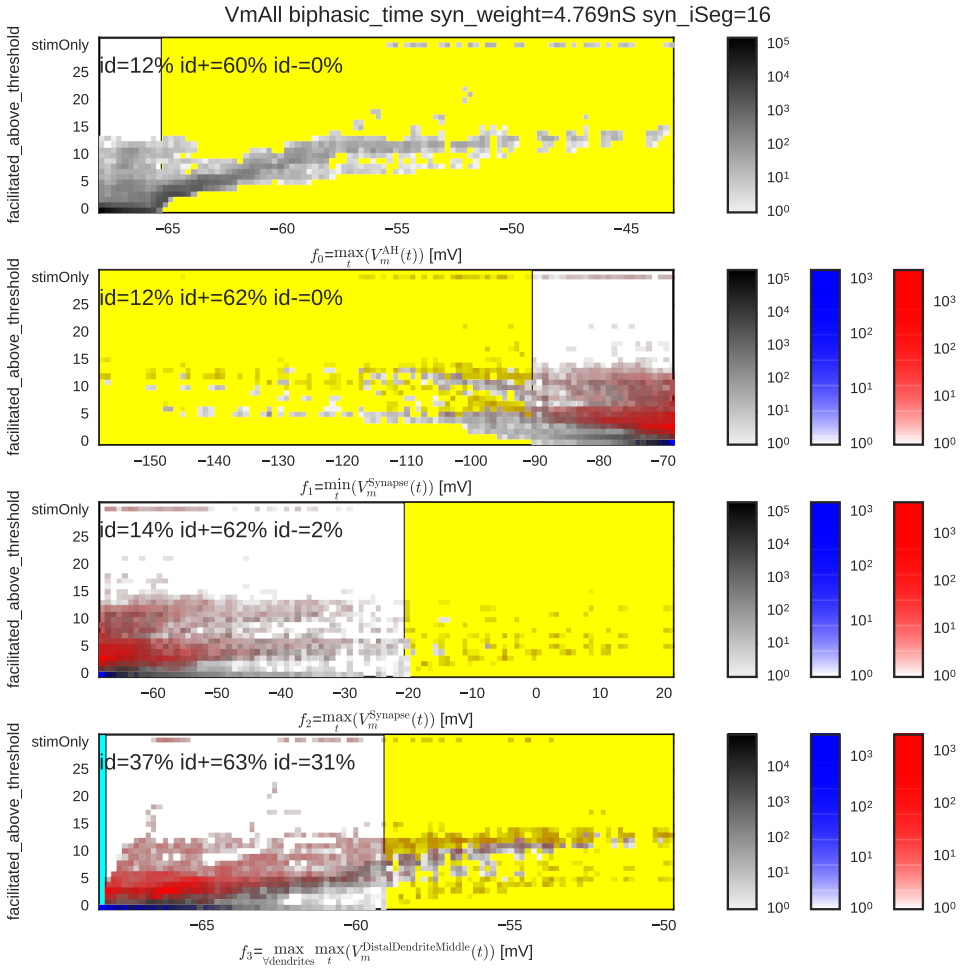

Figure 5.77: Predicting facilitation for all combinations using biphasic epidural stimulation with a synapse triggered on a distal dendrite at segment 16 with weight 4.769 nS using features $f_0 = \max_t(V_m^{\mathrm{AH}}(t))$, $f_1 = \min_t(V_m^{\mathrm{Synapse}}(t))$, $f_2 = \max_t(V_m^{\mathrm{Synapse}}(t))$, and $f_3 = \max_{\forall \mathrm{dendrites}} \max_t(V_m^{\mathrm{DistalDendriteMiddle}}(t))$. Each feature is on the x-axis in a separate subplot above with the number of trigger points facilitated above threshold (−10 mV) as the y-axis. Each subplot consists of three 2D histograms (showing the number of neuron simulations in each square), shades of grey (unclassified), shades of red (classified as active), and shades of blue (classified as non-active). For each feature active and non-active classification regions of unclassified samples are drawn with a yellow and cyan background respectively. These classification regions are also written as rules below, where T=1 and T=0 indicates that the neuron is active and non-active respectively. The number of samples of neurons caught by each rule is specified in the comment after each rule. Using the decision regions in that subplot and those above, the percent of all samples classified (id), active samples classified (id+), and non-active samples classified (id-) are labeled in each subplot. There are a total of 427680 samples of which 400 are active without the EPSP, 82986 are facilitated, and 344294 are non-active.

IF ($f_0 < -67.99$ mV) THEN (T=0) /* 2035 samples */
ELIF (-65.28 mV $< f_0$) THEN (T=1) /* 50105 samples */
ELIF ($f_1 < -90.43$ mV) THEN (T=1) /* 2032 samples */
ELIF (-68.44 mV $< f_1$) THEN (T=0) /* 7 samples */
ELIF ($f_2 < -68.44$ mV) THEN (T=0) /* 6938 samples */
ELIF (-20.68 mV $< f_2$) THEN (T=1) /* 29 samples */
ELIF ($f_3 < -68.12$ mV) THEN (T=0) /* 99306 samples */
ELIF (-59.09 mV $< f_3$) THEN (T=1) /* 1189 samples */
ELSE (T=Unknown) /* 266039 samples */

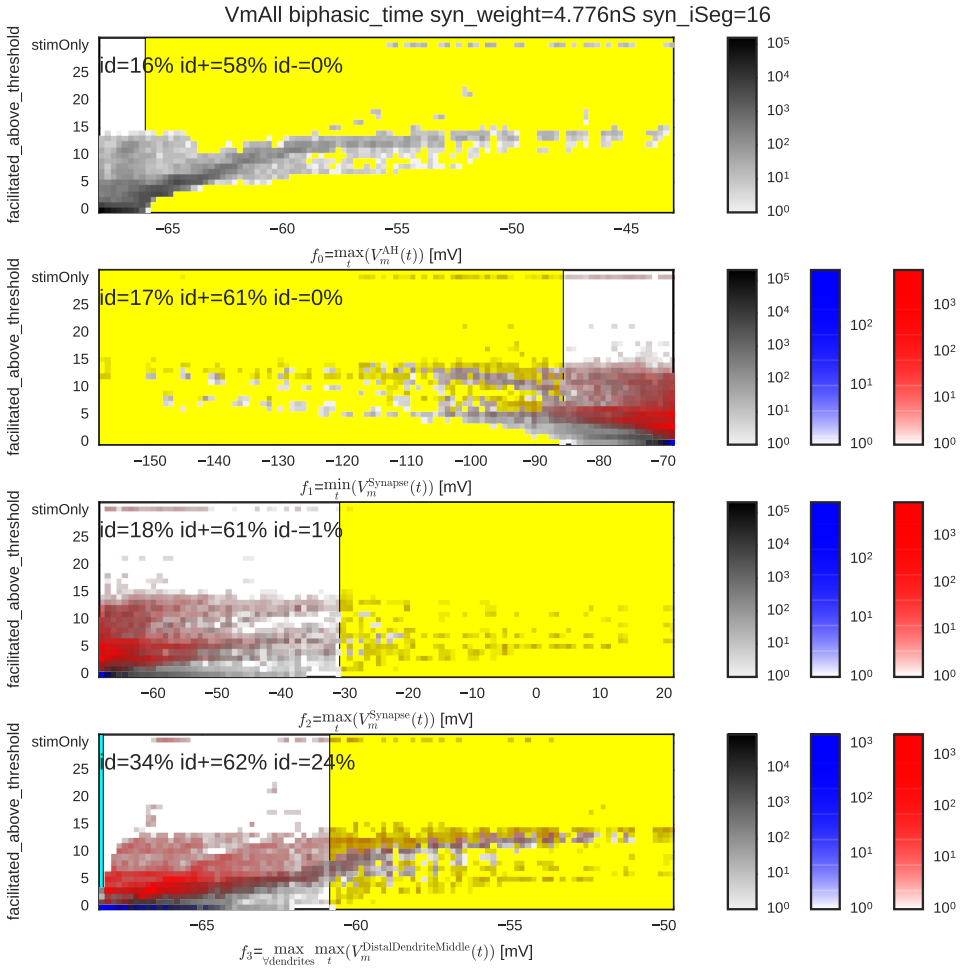

Figure 5.78: Predicting facilitation for all combinations using biphasic epidural stimulation with a synapse triggered on a distal dendrite at segment 16 with weight 4.776 nS using features $f_0 = \max_t(V_m^{\mathrm{AH}}(t))$, $f_1 = \min_t(V_m^{\mathrm{Synapse}}(t))$, $f_2 = \max_t(V_m^{\mathrm{Synapse}}(t))$, and $f_3 = \max_{\forall \mathrm{dendrites}} \max_t(V_m^{\mathrm{DistalDendriteMiddle}}(t))$. Each feature is on the x-axis in a separate subplot above with the number of trigger points facilitated above threshold (−10 mV) as the y-axis. Each subplot consists of three 2D histograms (showing the number of neuron simulations in each square), shades of grey (unclassified), shades of red (classified as active), and shades of blue (classified as non-active). For each feature active and non-active classification regions of unclassified samples are drawn with a yellow and cyan background respectively. These classification regions are also written as rules below, where T=1 and T=0 indicates that the neuron is active and non-active respectively. The number of samples of neurons caught by each rule is specified in the comment after each rule. Using the decision regions in that subplot and those above, the percent of all samples classified (id), active samples classified (id+), and non-active samples classified (id-) are labeled in each subplot. There are a total of 427680 samples of which 400 are active without the EPSP, 120616 are facilitated, and 306664 are non-active.

IF ($f_0 < -67.99$ mV) THEN (T=0) /* 1200 samples */
ELIF (-65.98 mV $< f_0$) THEN (T=1) /* 70970 samples */
ELIF ($f_1 < -85.59$ mV) THEN (T=1) /* 3104 samples */
ELIF (-68.44 mV $< f_1$) THEN (T=0) /* 33 samples */
ELIF ($f_2 < -68.44$ mV) THEN (T=0) /* 4818 samples */
ELIF (-30.8 mV $< f_2$) THEN (T=1) /* 51 samples */
ELIF ($f_3 < -68.21$ mV) THEN (T=0) /* 67587 samples */
ELIF (-60.85 mV $< f_3$) THEN (T=1) /* 1795 samples */
ELSE (T=Unknown) /* 278122 samples */

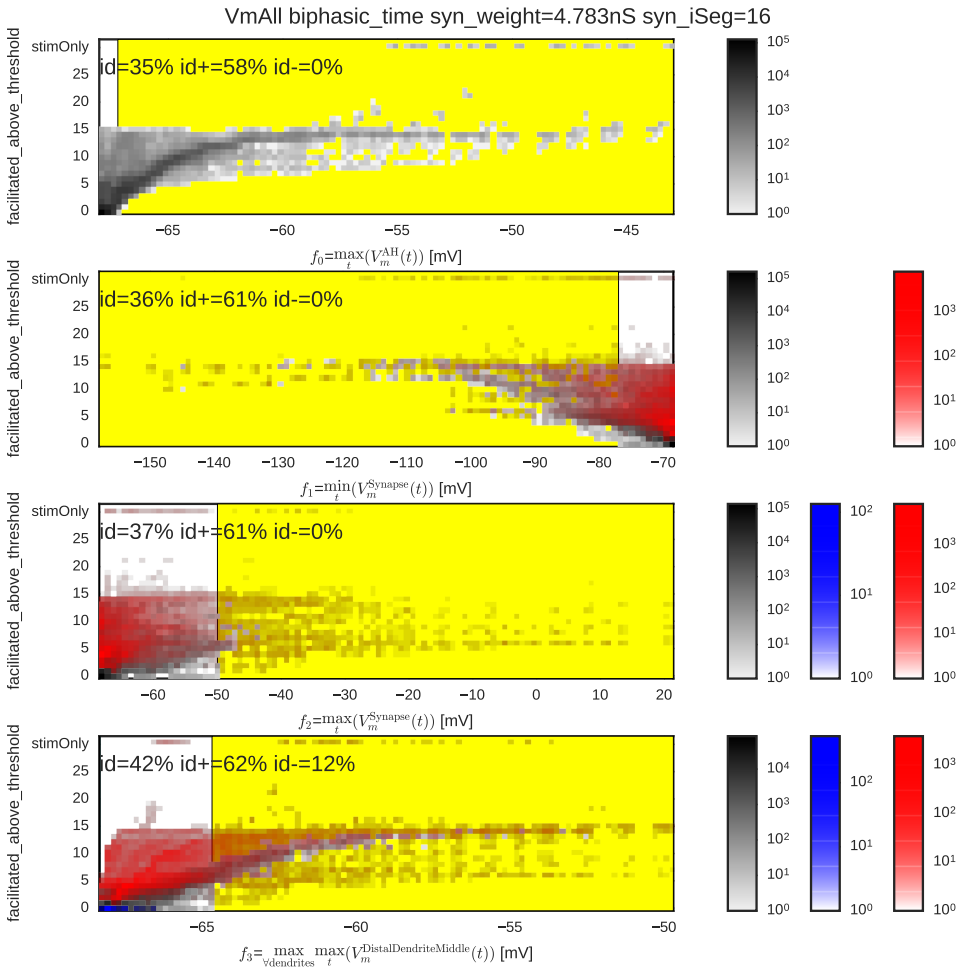

Figure 5.79: Predicting facilitation for all combinations using biphasic epidural stimulation with a synapse triggered on a distal dendrite at segment 16 with weight 4.783 nS using features $f_0 = \max_t(V_m^{\mathrm{AH}}(t))$, $f_1 = \min_t(V_m^{\mathrm{Synapse}}(t))$, $f_2 = \max_t(V_m^{\mathrm{Synapse}}(t))$, and $f_3 = \max_{\forall \mathrm{dendrites}} \max_t(V_m^{\mathrm{DistalDendriteMiddle}}(t))$. Each feature is on the x-axis in a separate subplot above with the number of trigger points facilitated above threshold (−10 mV) as the y-axis. Each subplot consists of three 2D histograms (showing the number of neuron simulations in each square), shades of grey (unclassified), shades of red (classified as active), and shades of blue (classified as non-active). For each feature active and non-active classification regions of unclassified samples are drawn with a yellow and cyan background respectively. These classification regions are also written as rules below, where T=1 and T=0 indicates that the neuron is active and non-active respectively. The number of samples of neurons caught by each rule is specified in the comment after each rule. Using the decision regions in that subplot and those above, the percent of all samples classified (id), active samples classified (id+), and non-active samples classified (id-) are labeled in each subplot. There are a total of 427680 samples of which 400 are active without the EPSP, 256925 are facilitated, and 170355 are non-active.

IF (−67.18 mV < f_0) THEN (T=1) /* 150740 samples */
ELIF (f_1 < −76.98 mV) THEN (T=1) /* 7124 samples */
ELIF (−68.44 mV < f_1) THEN (T=0) /* 126 samples */
ELIF (f_2 < −68.44 mV) THEN (T=0) /* 1314 samples */
ELIF (−49.93 mV < f_2) THEN (T=1) /* 222 samples */
ELIF (f_3 < −68.31 mV) THEN (T=0) /* 19128 samples */
ELIF (−64.67 mV < f_3) THEN (T=1) /* 3171 samples */
ELSE (T=Unknown) /* 245855 samples */

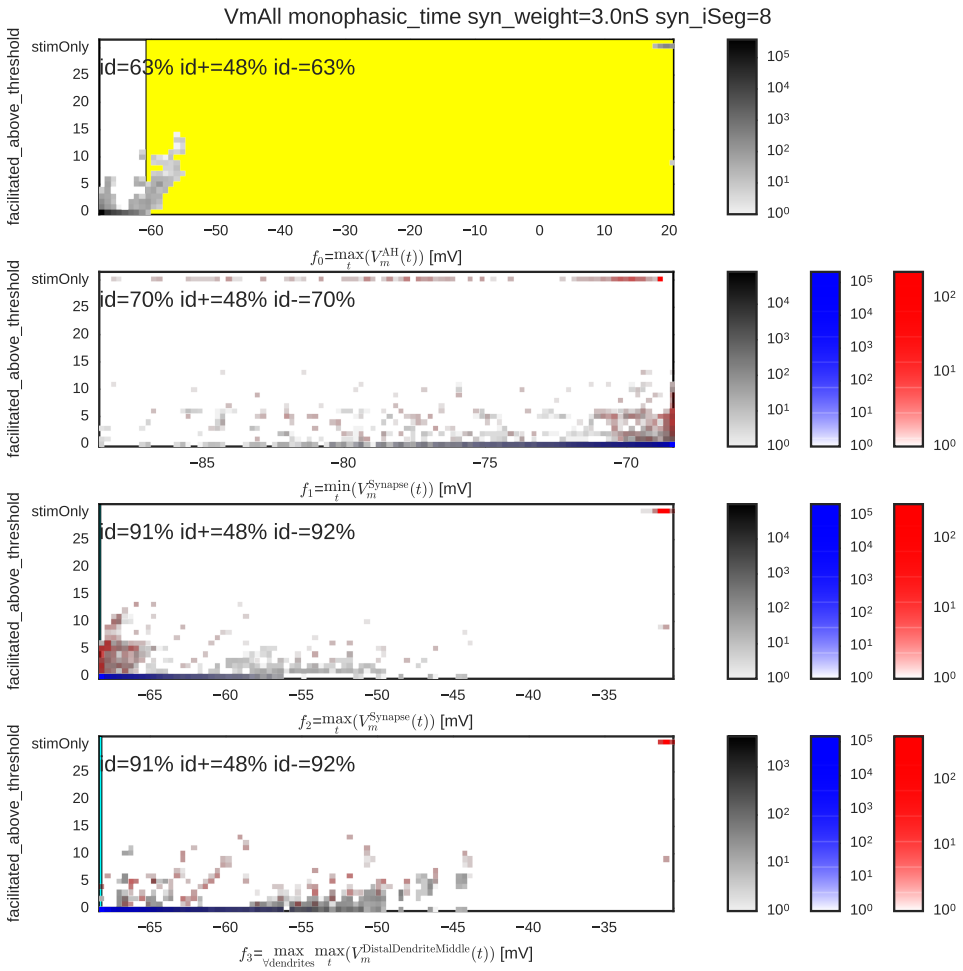

Figure 5.80: Predicting facilitation for all combinations using monophasic epidural stimulation with a synapse triggered on a distal dendrite at segment 8 with weight 3.0 nS using features $f_0 = \max_t(V_m^{\mathrm{AH}}(t))$, $f_1 = \min_t(V_m^{\mathrm{Synapse}}(t))$, $f_2 = \max_t(V_m^{\mathrm{Synapse}}(t))$, and $f_3 = \max_{\forall \mathrm{dendrites}} \max_t(V_m^{\mathrm{DistalDendriteMiddle}}(t))$. Each feature is on the x-axis in a separate subplot above with the number of trigger points facilitated above threshold (−10 mV) as the y-axis. Each subplot consists of three 2D histograms (showing the number of neuron simulations in each square), shades of grey (unclassified), shades of red (classified as active), and shades of blue (classified as non-active). For each feature active and non-active classification regions of unclassified samples are drawn with a yellow and cyan background respectively. These classification regions are also written as rules below, where T=1 and T=0 indicates that the neuron is active and non-active respectively. The number of samples of neurons caught by each rule is specified in the comment after each rule. Using the decision regions in that subplot and those above, the percent of all samples classified (id), active samples classified (id+), and non-active samples classified (id-) are labeled in each subplot. There are a total of 427680 samples of which 645 are active without the EPSP, 2562 are facilitated, and 424473 are non-active.

IF ($f_0 < -67.92$ mV) THEN (T=0) /* 271235 samples */
ELIF (−60.77 mV $< f_0$) THEN (T=1) /* 1565 samples */
ELIF (−68.34 mV $< f_1$) THEN (T=0) /* 29915 samples */
ELIF ($f_2 < -68.24$ mV) THEN (T=0) /* 90119 samples */
ELIF ($f_3 < -68.16$ mV) THEN (T=0) /* 494 samples */
ELSE (T=Unknown) /* 34352 samples */

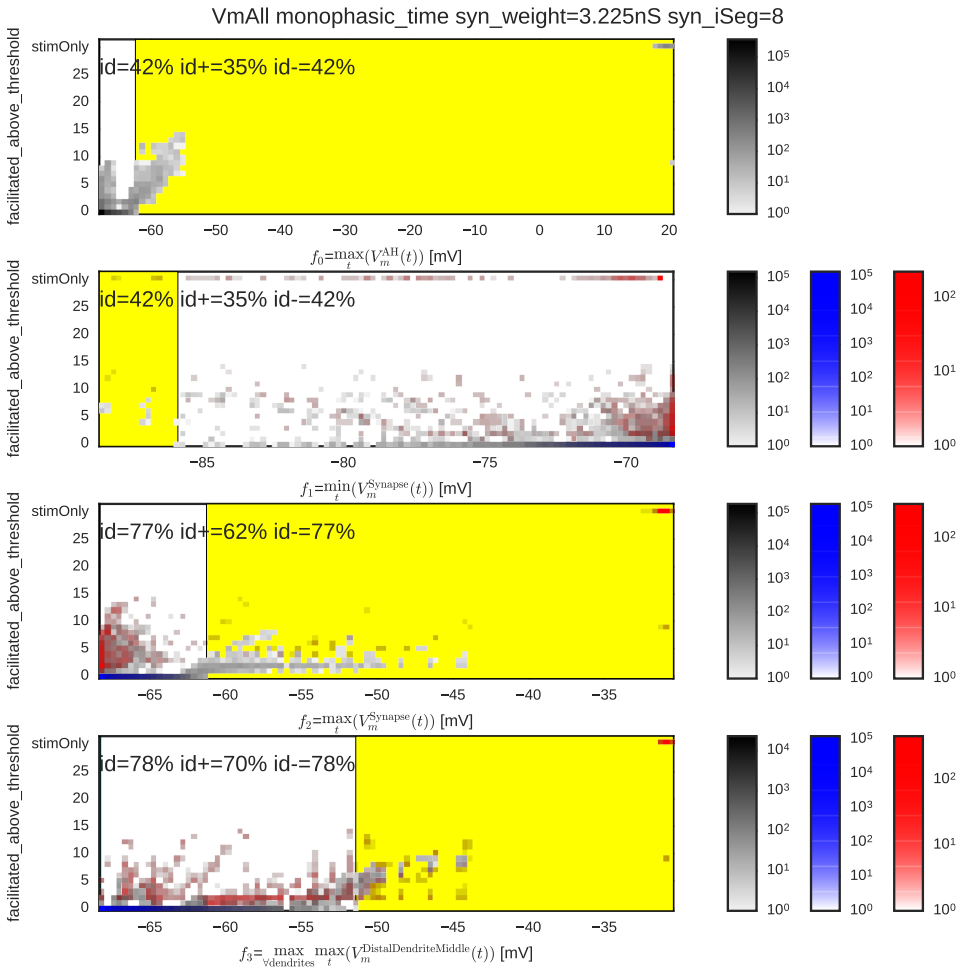

Figure 5.81: Predicting facilitation for all combinations using monophasic epidural stimulation with a synapse triggered on a distal dendrite at segment 8 with weight 3.225 nS using features $f_0 = \max_t(V_m^{\mathrm{AH}}(t))$, $f_1 = \min_t(V_m^{\mathrm{Synapse}}(t))$, $f_2 = \max_t(V_m^{\mathrm{Synapse}}(t))$, and $f_3 = \max_{\forall \mathrm{dendrites}} \max_t(V_m^{\mathrm{DistalDendriteMiddle}}(t))$. Each feature is on the x-axis in a separate subplot above with the number of trigger points facilitated above threshold (−10 mV) as the y-axis. Each subplot consists of three 2D histograms (showing the number of neuron simulations in each square), shades of grey (unclassified), shades of red (classified as active), and shades of blue (classified as non-active). For each feature active and non-active classification regions of unclassified samples are drawn with a yellow and cyan background respectively. These classification regions are also written as rules below, where T=1 and T=0 indicates that the neuron is active and non-active respectively. The number of samples of neurons caught by each rule is specified in the comment after each rule. Using the decision regions in that subplot and those above, the percent of all samples classified (id), active samples classified (id+), and non-active samples classified (id-) are labeled in each subplot. There are a total of 427680 samples of which 645 are active without the EPSP, 6522 are facilitated, and 420513 are non-active.

IF ($f_0 < -67.99$ mV) THEN (T=0) /* 179395 samples */
ELIF (-62.41 mV $< f_0$) THEN (T=1) /* 2530 samples */
ELIF ($f_1 < -85.86$ mV) THEN (T=1) /* 37 samples */
ELIF ($f_2 < -68.29$ mV) THEN (T=0) /* 146246 samples */
ELIF (-61.26 mV $< f_2$) THEN (T=1) /* 1936 samples */
ELIF ($f_3 < -68.24$ mV) THEN (T=0) /* 3440 samples */
ELIF (-51.41 mV $< f_3$) THEN (T=1) /* 527 samples */
ELSE (T=Unknown) /* 93569 samples */

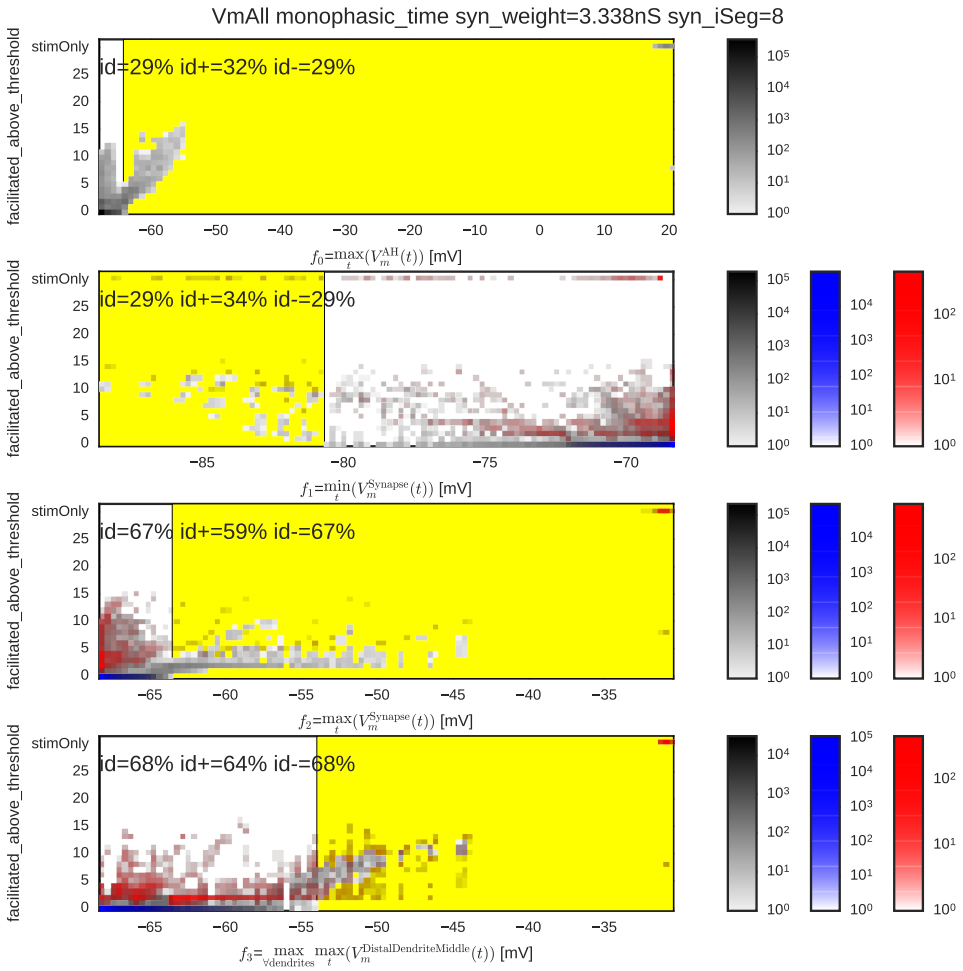

Figure 5.82: Predicting facilitation for all combinations using monophasic epidural stimulation with a synapse triggered on a distal dendrite at segment 8 with weight 3.338 nS using features $f_0 = \max_t(V_m^{\mathrm{AH}}(t))$, $f_1 = \min_t(V_m^{\mathrm{Synapse}}(t))$, $f_2 = \max_t(V_m^{\mathrm{Synapse}}(t))$, and $f_3 = \max_{\forall \mathrm{dendrites}} \max_t(V_m^{\mathrm{DistalDendriteMiddle}}(t))$. Each feature is on the x-axis in a separate subplot above with the number of trigger points facilitated above threshold (−10 mV) as the y-axis. Each subplot consists of three 2D histograms (showing the number of neuron simulations in each square), shades of grey (unclassified), shades of red (classified as active), and shades of blue (classified as non-active). For each feature active and non-active classification regions of unclassified samples are drawn with a yellow and cyan background respectively. These classification regions are also written as rules below, where T=1 and T=0 indicates that the neuron is active and non-active respectively. The number of samples of neurons caught by each rule is specified in the comment after each rule. Using the decision regions in that subplot and those above, the percent of all samples classified (id), active samples classified (id+), and non-active samples classified (id-) are labeled in each subplot. There are a total of 427680 samples of which 645 are active without the EPSP, 16246 are facilitated, and 410789 are non-active.

IF ($f_0 < -67.99$ mV) THEN (T=0) /* 120685 samples */
ELIF (-64.26 mV $< f_0$) THEN (T=1) /* 5520 samples */
ELIF ($f_1 < -80.68$ mV) THEN (T=1) /* 346 samples */
ELIF ($f_2 < -68.32$ mV) THEN (T=0) /* 156974 samples */
ELIF (-63.52 mV $< f_2$) THEN (T=1) /* 4137 samples */
ELIF ($f_3 < -68.28$ mV) THEN (T=0) /* 3682 samples */
ELIF (-53.98 mV $< f_3$) THEN (T=1) /* 881 samples */
ELSE (T=Unknown) /* 135455 samples */

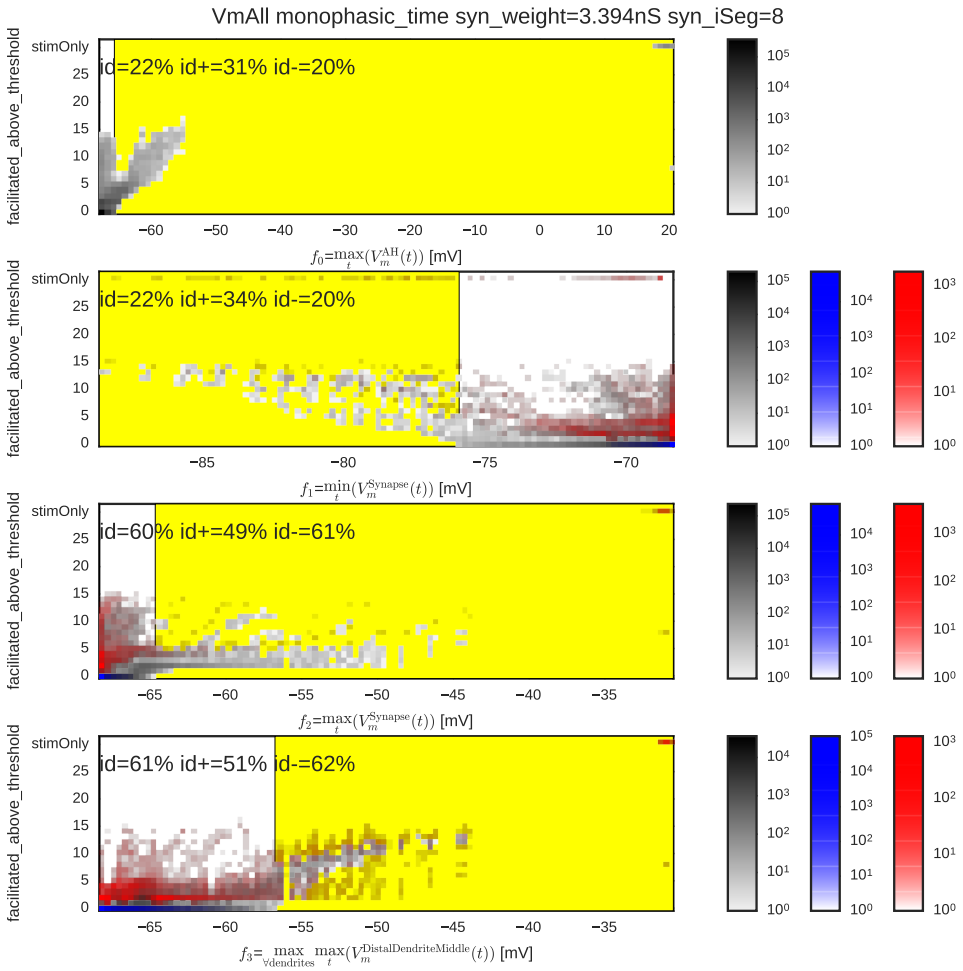

Figure 5.83: Predicting facilitation for all combinations using monophasic epidural stimulation with a synapse triggered on a distal dendrite at segment 8 with weight 3.394 nS using features $f_0 = \max_t(V_m^{\mathrm{AH}}(t))$, $f_1 = \min_t(V_m^{\mathrm{Synapse}}(t))$, $f_2 = \max_t(V_m^{\mathrm{Synapse}}(t))$, and $f_3 = \max_{\forall \mathrm{dendrites}} \max_t(V_m^{\mathrm{DistalDendriteMiddle}}(t))$. Each feature is on the x-axis in a separate subplot above with the number of trigger points facilitated above threshold (−10 mV) as the y-axis. Each subplot consists of three 2D histograms (showing the number of neuron simulations in each square), shades of grey (unclassified), shades of red (classified as active), and shades of blue (classified as non-active). For each feature active and non-active classification regions of unclassified samples are drawn with a yellow and cyan background respectively. These classification regions are also written as rules below, where T=1 and T=0 indicates that the neuron is active and non-active respectively. The number of samples of neurons caught by each rule is specified in the comment after each rule. Using the decision regions in that subplot and those above, the percent of all samples classified (id), active samples classified (id+), and non-active samples classified (id-) are labeled in each subplot. There are a total of 427680 samples of which 645 are active without the EPSP, 46322 are facilitated, and 380713 are non-active.

IF ($f_0 < -67.99$ mV) THEN (T=0) /* 79800 samples */
ELIF (−65.65 mV $< f_0$) THEN (T=1) /* 14995 samples */
ELIF ($f_1 < -75.91$ mV) THEN (T=1) /* 1243 samples */
ELIF ($f_2 < -68.33$ mV) THEN (T=0) /* 154338 samples */
ELIF (−64.64 mV $< f_2$) THEN (T=1) /* 6889 samples */
ELIF ($f_3 < -68.3$ mV) THEN (T=0) /* 3433 samples */
ELIF (−56.74 mV $< f_3$) THEN (T=1) /* 1294 samples */
ELSE (T=Unknown) /* 165688 samples */

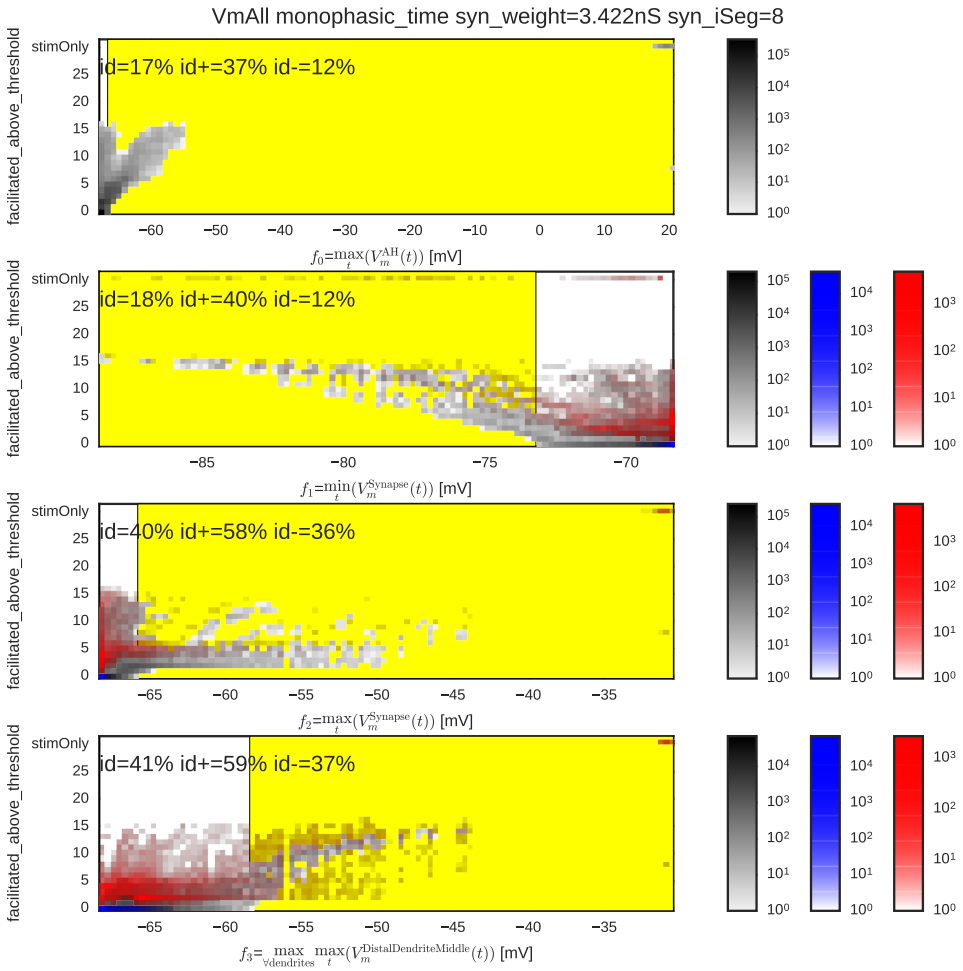

Figure 5.84: Predicting facilitation for all combinations using monophasic epidural stimulation with a synapse triggered on a distal dendrite at segment 8 with weight 3.422 nS using features $f_0 = \max_t(V_m^{\mathrm{AH}}(t))$, $f_1 = \min_t(V_m^{\mathrm{Synapse}}(t))$, $f_2 = \max_t(V_m^{\mathrm{Synapse}}(t))$, and $f_3 = \max_{\forall \mathrm{dendrites}} \max_t(V_m^{\mathrm{DistalDendriteMiddle}}(t))$. Each feature is on the x-axis in a separate subplot above with the number of trigger points facilitated above threshold (−10 mV) as the y-axis. Each subplot consists of three 2D histograms (showing the number of neuron simulations in each square), shades of grey (unclassified), shades of red (classified as active), and shades of blue (classified as non-active). For each feature active and non-active classification regions of unclassified samples are drawn with a yellow and cyan background respectively. These classification regions are also written as rules below, where T=1 and T=0 indicates that the neuron is active and non-active respectively. The number of samples of neurons caught by each rule is specified in the comment after each rule. Using the decision regions in that subplot and those above, the percent of all samples classified (id), active samples classified (id+), and non-active samples classified (id-) are labeled in each subplot. There are a total of 427680 samples of which 645 are active without the EPSP, 87686 are facilitated, and 339349 are non-active.

IF ($f_0 < -67.99$ mV) THEN (T=0) /* 41635 samples */
ELIF (−66.7 mV $< f_0$) THEN (T=1) /* 33365 samples */
ELIF ($f_1 < -73.2$ mV) THEN (T=1) /* 2591 samples */
ELIF ($f_2 < -68.34$ mV) THEN (T=0) /* 81426 samples */
ELIF (−65.8 mV $< f_2$) THEN (T=1) /* 15461 samples */
ELIF ($f_3 < -68.32$ mV) THEN (T=0) /* 3562 samples */
ELIF (−58.41 mV $< f_3$) THEN (T=1) /* 1389 samples */
ELSE (T=Unknown) /* 248251 samples */

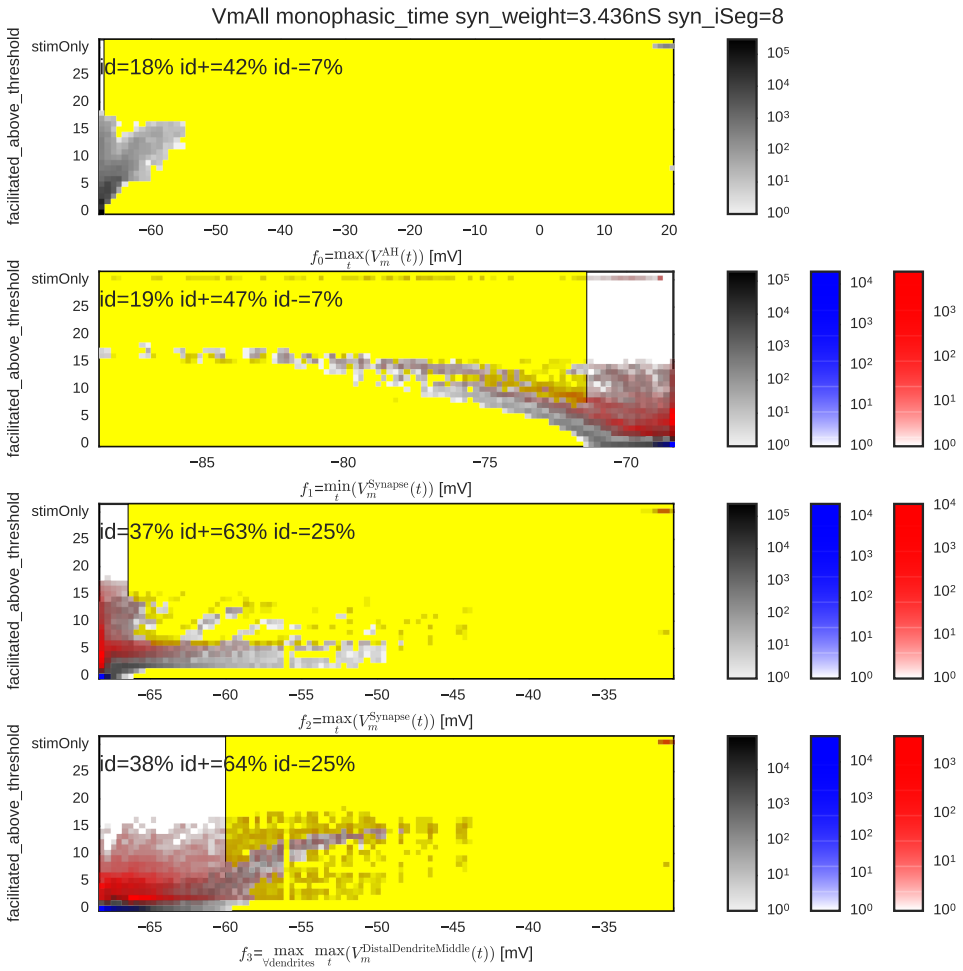

Figure 5.85: Predicting facilitation for all combinations using monophasic epidural stimulation with a synapse triggered on a distal dendrite at segment 8 with weight 3.436 nS using features $f_0 = \max_t(V_m^{\mathrm{AH}}(t))$, $f_1 = \min_t(V_m^{\mathrm{Synapse}}(t))$, $f_2 = \max_t(V_m^{\mathrm{Synapse}}(t))$, and $f_3 = \max_{\forall \mathrm{dendrites}} \max_t(V_m^{\mathrm{DistalDendriteMiddle}}(t))$. Each feature is on the x-axis in a separate subplot above with the number of trigger points facilitated above threshold (−10 mV) as the y-axis. Each subplot consists of three 2D histograms (showing the number of neuron simulations in each square), shades of grey (unclassified), shades of red (classified as active), and shades of blue (classified as non-active). For each feature active and non-active classification regions of unclassified samples are drawn with a yellow and cyan background respectively. These classification regions are also written as rules below, where T=1 and T=0 indicates that the neuron is active and non-active respectively. The number of samples of neurons caught by each rule is specified in the comment after each rule. Using the decision regions in that subplot and those above, the percent of all samples classified (id), active samples classified (id+), and non-active samples classified (id-) are labeled in each subplot. There are a total of 427680 samples of which 645 are active without the EPSP, 133965 are facilitated, and 293070 are non-active.

IF ($f_0 < -67.99$ mV) THEN (T=0) /* 21180 samples */
ELIF (−67.26 mV $< f_0$) THEN (T=1) /* 57530 samples */
ELIF ($f_1 < -71.4$ mV) THEN (T=1) /* 6249 samples */
ELIF ($f_2 < -68.34$ mV) THEN (T=0) /* 52115 samples */
ELIF (−66.43 mV $< f_2$) THEN (T=1) /* 22165 samples */
ELIF ($f_3 < -68.33$ mV) THEN (T=0) /* 1924 samples */
ELIF (−60 mV $< f_3$) THEN (T=1) /* 1400 samples */
ELSE (T=Unknown) /* 265117 samples */

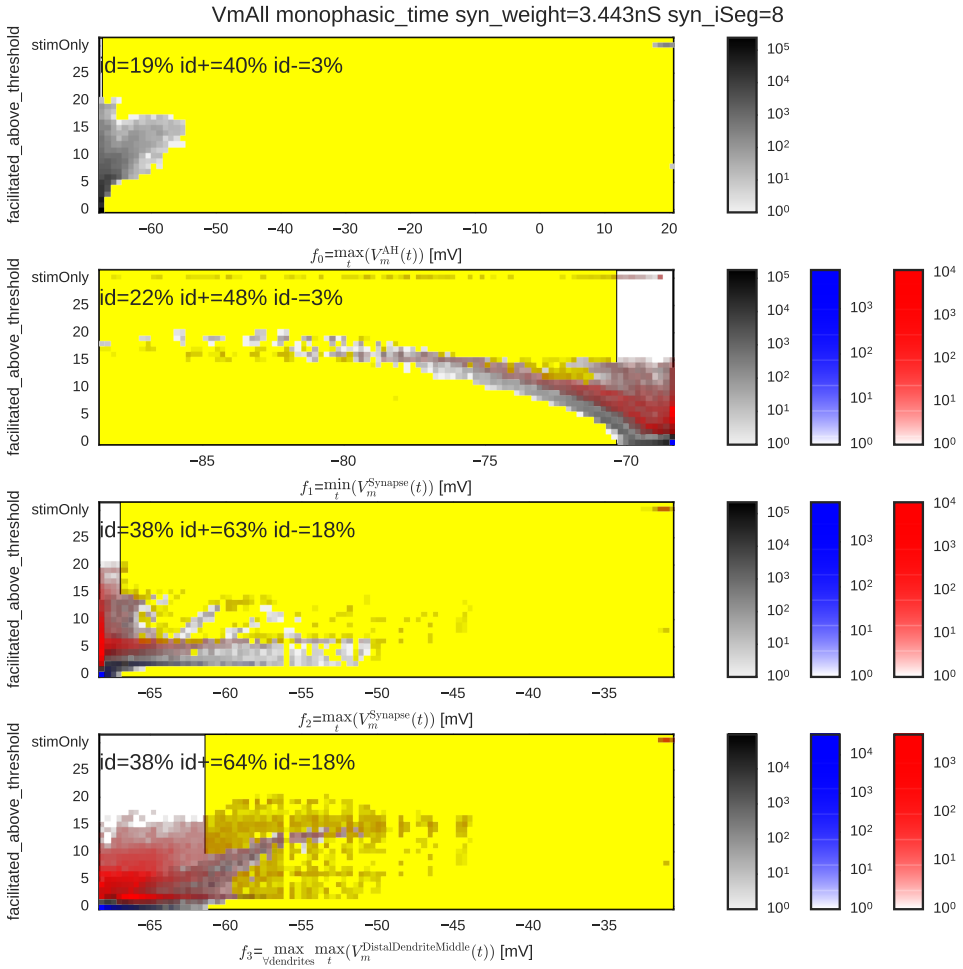

Figure 5.86: Predicting facilitation for all combinations using monophasic epidural stimulation with a synapse triggered on a distal dendrite at segment 8 with weight 3.443 nS using features $f_0 = \max_t(V_m^{AH}(t))$, $f_1 = \min_t(V_m^{Synapse}(t))$, $f_2 = \max_t(V_m^{Synapse}(t))$, and $f_3 = \max_{\forall dendrites} \max_t(V_m^{DistalDendriteMiddle}(t))$. Each feature is on the x-axis in a separate subplot above with the number of trigger points facilitated above threshold (−10 mV) as the y-axis. Each subplot consists of three 2D histograms (showing the number of neuron simulations in each square), shades of grey (unclassified), shades of red (classified as active), and shades of blue (classified as non-active). For each feature active and non-active classification regions of unclassified samples are drawn with a yellow and cyan background respectively. These classification regions are also written as rules below, where T=1 and T=0 indicates that the neuron is active and non-active respectively. The number of samples of neurons caught by each rule is specified in the comment after each rule. Using the decision regions in that subplot and those above, the percent of all samples classified (id), active samples classified (id+), and non-active samples classified (id-) are labeled in each subplot. There are a total of 427680 samples of which 645 are active without the EPSP, 185287 are facilitated, and 241748 are non-active.

IF ($f_0 < -67.99$ mV) THEN (T=0) /* 7255 samples */
ELIF (-67.51 mV $< f_0$) THEN (T=1) /* 75585 samples */
ELIF ($f_1 < -70.34$ mV) THEN (T=1) /* 13998 samples */
ELIF (-68.34 mV $< f_1 < -68.34$ mV) THEN (T=0) /* 9 samples */
ELIF ($f_2 < -68.34$ mV) THEN (T=0) /* 35775 samples */
ELIF (-66.95 mV $< f_2$) THEN (T=1) /* 29475 samples */
ELIF ($f_3 < -68.33$ mV) THEN (T=0) /* 936 samples */
ELIF (-61.36 mV $< f_3$) THEN (T=1) /* 1368 samples */
ELSE (T=Unknown) /* 263279 samples */

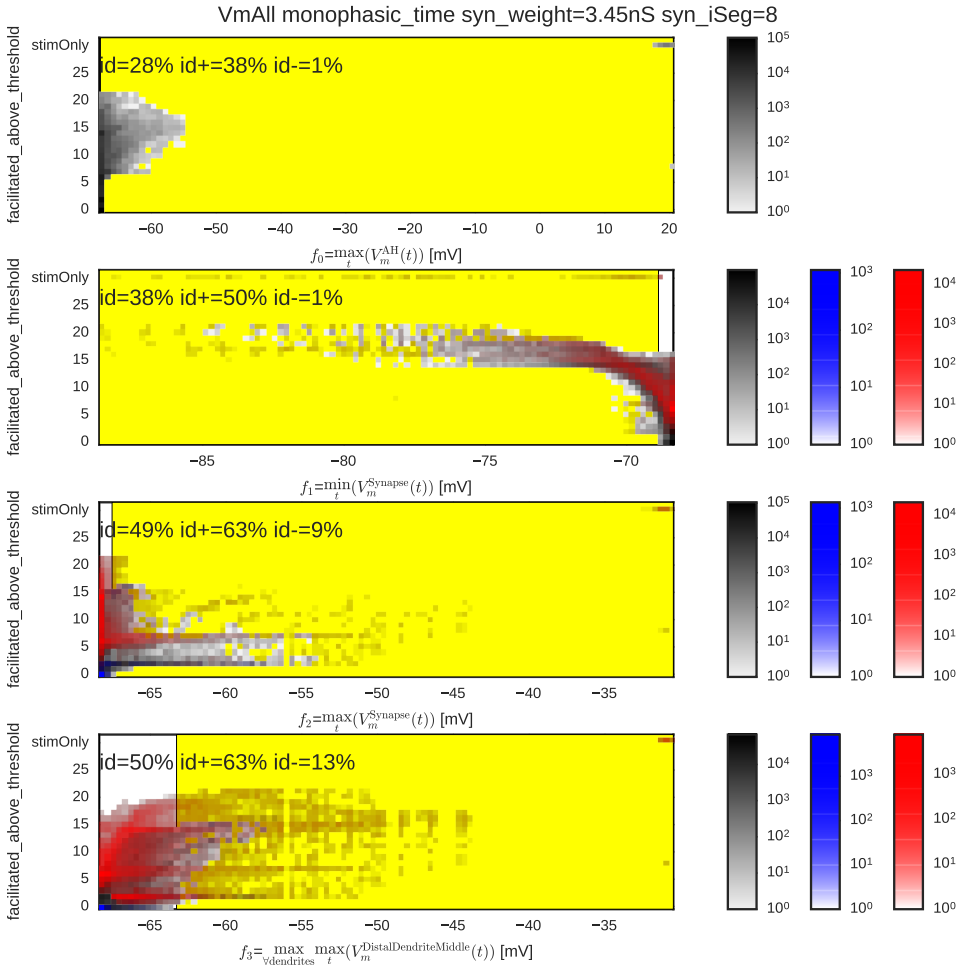

Figure 5.87: Predicting facilitation for all combinations using monophasic epidural stimulation with a synapse triggered on a distal dendrite at segment 8 with weight 3.45 nS using features $f_0 = \max_t(V_m^{\mathrm{AH}}(t))$, $f_1 = \min_t(V_m^{\mathrm{Synapse}}(t))$, $f_2 = \max_t(V_m^{\mathrm{Synapse}}(t))$, and $f_3 = \max_{\forall \mathrm{dendrites}} \max_t(V_m^{\mathrm{DistalDendriteMiddle}}(t))$. Each feature is on the x-axis in a separate subplot above with the number of trigger points facilitated above threshold (−10 mV) as the y-axis. Each subplot consists of three 2D histograms (showing the number of neuron simulations in each square), shades of grey (unclassified), shades of red (classified as active), and shades of blue (classified as non-active). For each feature active and non-active classification regions of unclassified samples are drawn with a yellow and cyan background respectively. These classification regions are also written as rules below, where T=1 and T=0 indicates that the neuron is active and non-active respectively. The number of samples of neurons caught by each rule is specified in the comment after each rule. Using the decision regions in that subplot and those above, the percent of all samples classified (id), active samples classified (id+), and non-active samples classified (id-) are labeled in each subplot. There are a total of 427680 samples of which 645 are active without the EPSP, 319226 are facilitated, and 107809 are non-active.

IF ($f_0 < -67.99$ mV) THEN (T=0) /* 1125 samples */
ELIF (−67.81 mV $< f_0$) THEN (T=1) /* 121900 samples */
ELIF ($f_1 < -68.86$ mV) THEN (T=1) /* 40879 samples */
ELIF (−68.34 mV $< f_1 <$ −68.34 mV) THEN (T=0) /* 2 samples */
ELIF ($f_2 < -68.34$ mV) THEN (T=0) /* 7846 samples */
ELIF (−67.49 mV $< f_2$) THEN (T=1) /* 39693 samples */
ELIF ($f_3 < -68.32$ mV) THEN (T=0) /* 4468 samples */
ELIF (−63.24 mV $< f_3$) THEN (T=1) /* 1145 samples */
ELSE (T=Unknown) /* 210622 samples */

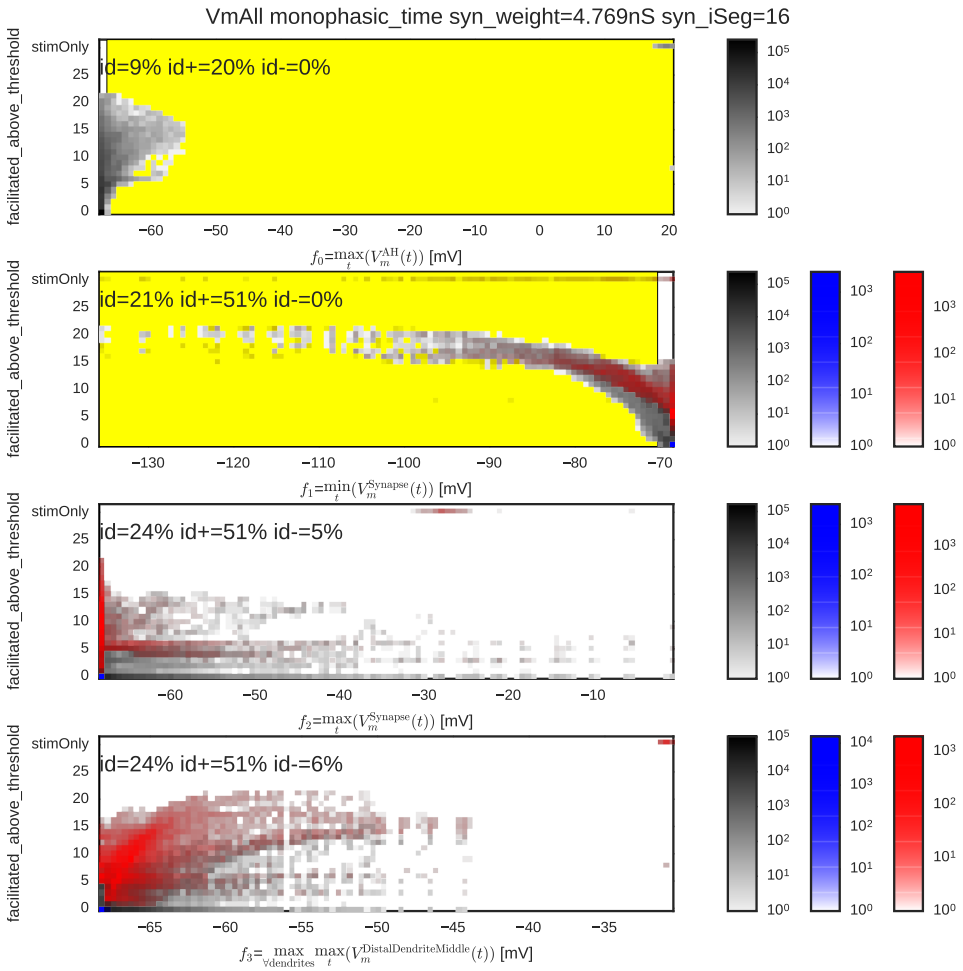

Figure 5.88: Predicting facilitation for all combinations using monophasic epidural stimulation with a synapse triggered on a distal dendrite at segment 16 with weight 4.769 nS using features $f_0 = \max_t(V_m^{\mathrm{AH}}(t))$, $f_1 = \min_t(V_m^{\mathrm{Synapse}}(t))$, $f_2 = \max_t(V_m^{\mathrm{Synapse}}(t))$, and $f_3 = \max_{\forall \mathrm{dendrites}} \max_t(V_m^{\mathrm{DistalDendriteMiddle}}(t))$. Each feature is on the x-axis in a separate subplot above with the number of trigger points facilitated above threshold (−10 mV) as the y-axis. Each subplot consists of three 2D histograms (showing the number of neuron simulations in each square), shades of grey (unclassified), shades of red (classified as active), and shades of blue (classified as non-active). For each feature active and non-active classification regions of unclassified samples are drawn with a yellow and cyan background respectively. These classification regions are also written as rules below, where T=1 and T=0 indicates that the neuron is active and non-active respectively. The number of samples of neurons caught by each rule is specified in the comment after each rule. Using the decision regions in that subplot and those above, the percent of all samples classified (id), active samples classified (id+), and non-active samples classified (id-) are labeled in each subplot. There are a total of 427680 samples of which 645 are active without the EPSP, 176092 are facilitated, and 250943 are non-active.

IF ($f_0 < -67.99$ mV) THEN (T=0) /* 2495 samples */
ELIF (−66.81 mV $< f_0$) THEN (T=1) /* 37100 samples */
ELIF ($f_1 < -70.29$ mV) THEN (T=1) /* 53545 samples */
ELIF ($f_2 < -68.44$ mV) THEN (T=0) /* 12443 samples */
ELIF ($f_3 < -68.33$ mV) THEN (T=0) /* 561 samples */
ELSE (T=Unknown) /* 321536 samples */

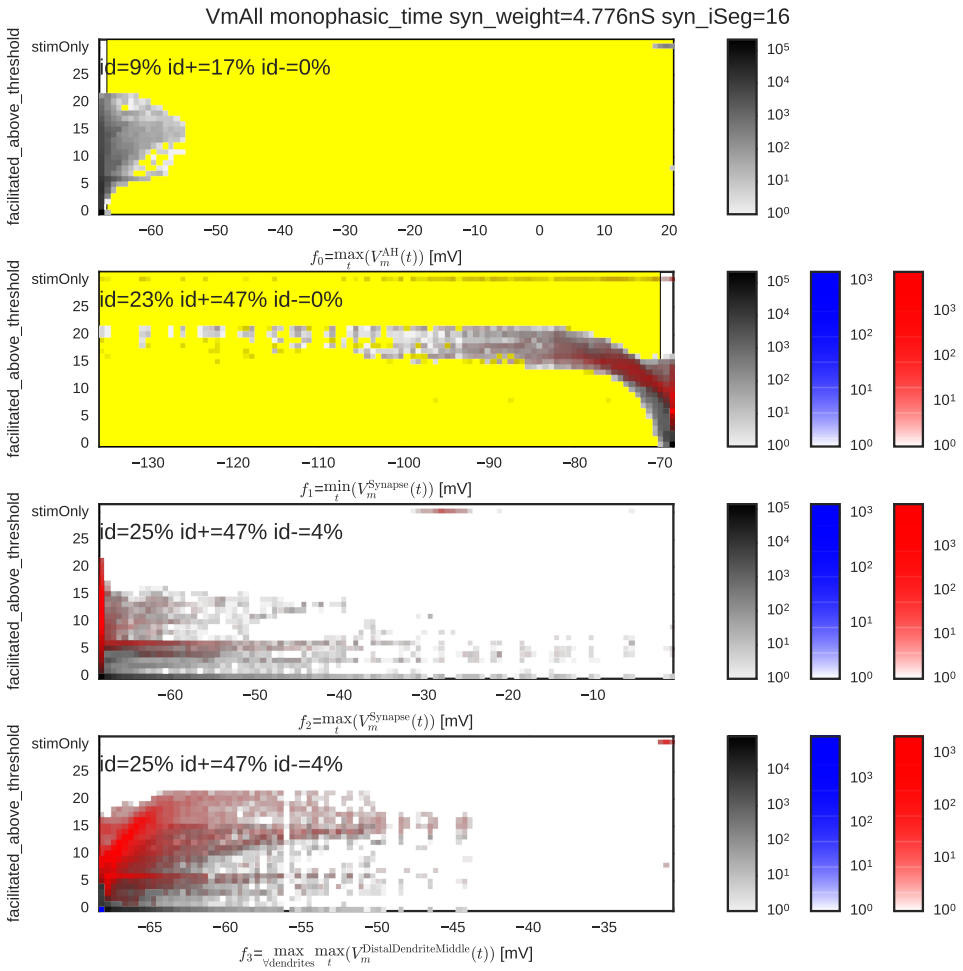

Figure 5.89: Predicting facilitation for all combinations using monophasic epidural stimulation with a synapse triggered on a distal dendrite at segment 16 with weight 4.776 nS using features $f_0 = \max_t(V_m^{\mathrm{AH}}(t))$, $f_1 = \min_t(V_m^{\mathrm{Synapse}}(t))$, $f_2 = \max_t(V_m^{\mathrm{Synapse}}(t))$, and $f_3 = \max_{\forall \mathrm{dendrites}} \max_t(V_m^{\mathrm{DistalDendriteMiddle}}(t))$. Each feature is on the x-axis in a separate subplot above with the number of trigger points facilitated above threshold (−10 mV) as the y-axis. Each subplot consists of three 2D histograms (showing the number of neuron simulations in each square), shades of grey (unclassified), shades of red (classified as active), and shades of blue (classified as non-active). For each feature active and non-active classification regions of unclassified samples are drawn with a yellow and cyan background respectively. These classification regions are also written as rules below, where T=1 and T=0 indicates that the neuron is active and non-active respectively. The number of samples of neurons caught by each rule is specified in the comment after each rule. Using the decision regions in that subplot and those above, the percent of all samples classified (id), active samples classified (id+), and non-active samples classified (id-) are labeled in each subplot. There are a total of 427680 samples of which 645 are active without the EPSP, 209901 are facilitated, and 217134 are non-active.

IF ($f_0 < -67.99$ mV) THEN (T=0) /* 1460 samples */
ELIF (−66.81 mV $< f_0$) THEN (T=1) /* 37100 samples */
ELIF ($f_1 < -69.96$ mV) THEN (T=1) /* 62159 samples */
ELIF ($f_2 < -68.44$ mV) THEN (T=0) /* 7970 samples */
ELIF ($f_3 < -68.33$ mV) THEN (T=0) /* 645 samples */
ELSE (T=Unknown) /* 318346 samples */

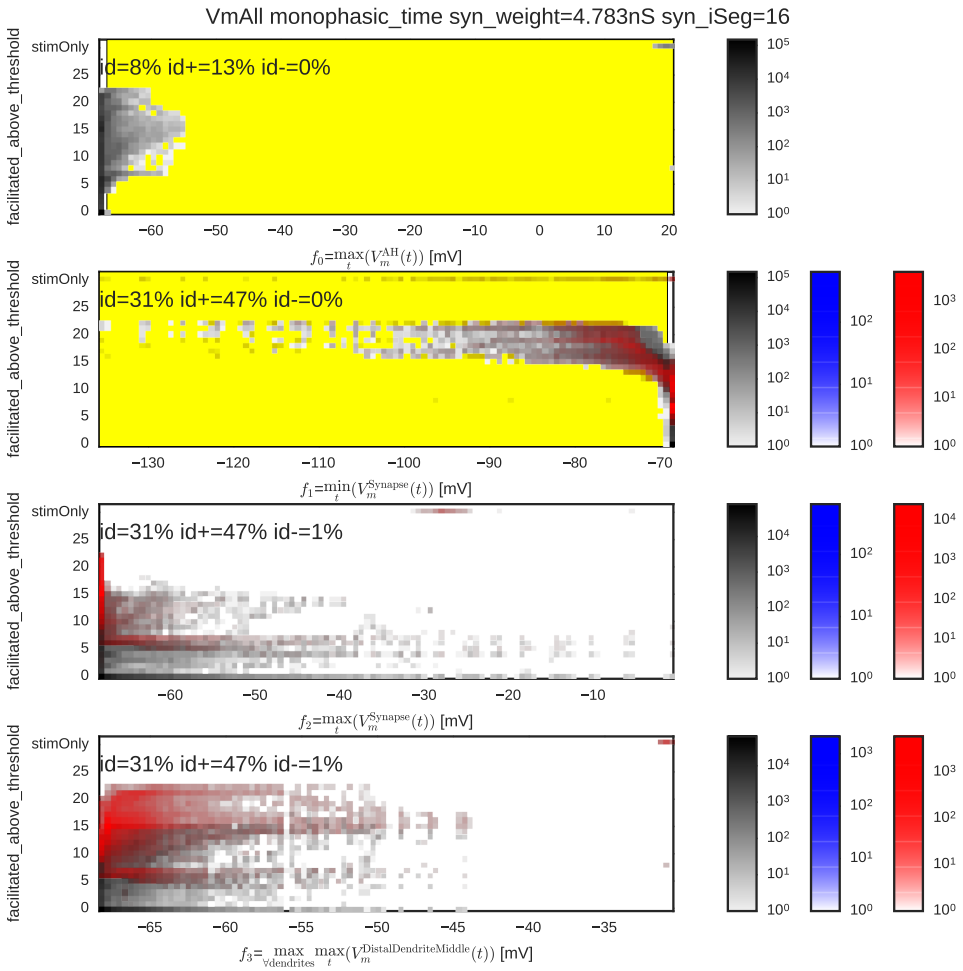

Figure 5.90: Predicting facilitation for all combinations using monophasic epidural stimulation with a synapse triggered on a distal dendrite at segment 16 with weight 4.783 nS using features $f_0 = \max_t(V_m^{AH}(t))$, $f_1 = \min_t(V_m^{Synapse}(t))$, $f_2 = \max_t(V_m^{Synapse}(t))$, and $f_3 = \max_{\forall dendrites} \max_t(V_m^{DistalDendriteMiddle}(t))$. Each feature is on the x-axis in a separate subplot above with the number of trigger points facilitated above threshold (−10 mV) as the y-axis. Each subplot consists of three 2D histograms (showing the number of neuron simulations in each square), shades of grey (unclassified), shades of red (classified as active), and shades of blue (classified as non-active). For each feature active and non-active classification regions of unclassified samples are drawn with a yellow and cyan background respectively. These classification regions are also written as rules below, where T=1 and T=0 indicates that the neuron is active and non-active respectively. The number of samples of neurons caught by each rule is specified in the comment after each rule. Using the decision regions in that subplot and those above, the percent of all samples classified (id), active samples classified (id+), and non-active samples classified (id-) are labeled in each subplot. There are a total of 427680 samples of which 645 are active without the EPSP, 278554 are facilitated, and 148481 are non-active.

IF (f_0 < −67.99 mV) THEN (T=0) /* 645 samples */
ELIF (−66.81 mV < f_0) THEN (T=1) /* 37100 samples */
ELIF (f_1 < −69.13 mV) THEN (T=1) /* 96685 samples */
ELIF (f_2 < −68.44 mV) THEN (T=0) /* 1492 samples */
ELIF (f_3 < −68.33 mV) THEN (T=0) /* 787 samples */
ELSE (T=Unknown) /* 290971 samples */

Chapter 6

CONCLUSIONS

Epidural electrical stimulation has been shown to facilitate the recovery of motor function and voluntary movement in humans (Harkema et al., 2011) and rats (Urban, 2018). Computational studies have aimed to better understand the mechanism underlying this motor recovery. Early work focused on stimulation of the dorsal fibers and roots (J Ladenbauer et al., 2010). More recently, studies (Capogrosso et al., 2013; Moraud et al., 2016) have emphasized the role of feedback pathways driven by the muscle spindle feedback. In this thesis, I have shown in simulation that facilitation of synaptic input to interneurons in the rat spinal cord is possible with both biphasic and monophasic epidural stimulation, using voltage magnitudes consistent with those used in biological experiments.

A 3D volume conductor model of the rat spinal cord and a 3-column by 7-row electrode array was constructed based on a transverse slice of an MRI image of a rat spinal cord. Biphasic and monophasic stimulation pulses were analyzed for frequency content. Material conductivity and permittivity values (anisotropic for white matter and muscle, isotropic for CSF, platinum, parylene C, gray matter, and bone) were found as close as possible to the dominant frequencies of Gaussian biphasic and monophasic stimulation pulses. A simple 3D model of an interneuron in the rat spinal cord was constructed based on data from (Ostroumov, 2007; Thurbon et al., 1998; Santos et al., 2009). Based on (Destexhe, Mainen, and Sejnowski, 1994), a threshold of -10 mV for the membrane voltage at the axon tip was chosen to indicate that a neuron had activated (released neurotransmitters from the tip of the axon). The synapse weight necessary for a single presynaptic event to generate an EPSP large enough to achieve neurotransmitter release from the axon tip was

determined for synapse locations along the length of each dendrite (see Fig. 3.6). Synapse weights less than this amount were used in Chapter 5 to allow for the possibility of facilitation rather than causing neurotransmitter release directly.

Static and time-domain solutions to the volume conductor models were found for biphasic and monophasic stimulation of 18 characteristic (unique under translation and mirroring across the x=0 and z=0 planes) bipolar combinations (Section 2.2.1). Static voltages and voltage time-series were extracted from these simulations at locations corresponding to neuron locations under and between each row of electrodes at 3 different depths (see Figs. 4.1 and 4.2) and used with different voltage scaling factors to obtain the extracellular voltages used in the NEURON simulations.

NEURON simulations of neurons exposed to a single stimulation pulse without any synaptic activity (for each type of stimulation (biphasic or monophasic) and all 18 characteristic combinations) were conducted. The minimum amount of stimulation to activate a neuron was 2.75 V for monophasic stimulation and 3.75 V for biphasic stimulation. This is within range of stimulation voltages used in actual experiments (i.e. 1 V to 8 V from Parag Gad, Roy, Choe, Zhong, et al., 2015), so this implies that direct stimulation of at least some of the interneurons in the spinal cord should be expected. For monophasic stimulation, the stimulation pulse causes activation of the neuron and also results in an action potential which spreads throughout the neuron (by orthodromic and antidromic propagation). Biphasic stimulation, on the other hand, only causes an action potential in some neurons at or above 8 V of stimulation. Activation of some neurons may occur with stimulation magnitudes less than 8 V without generating a traditional action potential because the membrane voltage at the axon tip exceeds -10 mV, resulting in at least some neurotransmitter release. The locations of neurons electrically stimulated sufficiently to release neurotransmitters using an amplitude of less than 5 V of stimulation were presented in Tables 4.2 and 4.3. Results for neurotransmitter release using an amplitude of less

than 10 V were presented graphically (see Sections 4.A, 4.3 and 4.4).

Axon tip membrane voltage for all the NEURON simulations without synaptic input were plotted against the voltage from static simulations at the axon tip ($V_{static}^{\text{AxonTip}}$) and the second derivative of the static voltage at the axon tip along the axon. Activated neurons were found to be scattered across a wide range of ($V_{static}^{\text{AxonTip}}$) and the second derivative of the static voltage without any obvious clustering. However, plotting the difference in the static voltage between the axon tip and the soma ($V_{static}^{\text{AxonTip}} - V_{static}^{\text{soma}}$) vs axon tip membrane voltage resulted in some interesting relationships (see Fig. 4.22) which would be useful for predicting neuron activation. While the exact behavior seen in Fig. 4.22 is likely dependent on the neuron parameters and geometry defined in Chapter 3, based on the large number of neuron locations and electrode configurations, it seems likely that similar behavior could be found for other neuron parameters.

Modeling facilitation was done with NEURON simulations that included a single sub-threshold synaptic input arriving at times before, during, and after a stimulation pulse. Synaptic input was modeled at the distal tip and middle of each dendrite. A significant amount of facilitation of neuron activation occurred when the synapse weight and/or the stimulation pulse magnitude was sufficiently large. This facilitation was dependent on both the orientation of the axon and the dendrite on which the synaptic input was located.

A significant contribution of this thesis is the discovery of an interval which I call the facilitation window. The stimulus pulse and the synaptic input need not occur simultaneously for facilitation to occur, instead the onset of the synaptic input may occur at any time inside the facilitation window and still experience a facilitation effect. This window is a function of synaptic weight, the stimulating field strength, which is itself a function of electrode positions and neuron geometry. As either the

stimulation magnitude or the synapse weight decreased, the size of the facilitation windows reduced and the number of facilitated neurons also reduced. For the parameters studied in this thesis, the facilitation windows can be as large as 115 ms wide. Some neurons were facilitated at the lowest stimulation voltage magnitude tested (0.5 V) when tested with some of the largest synapse weights. With stimulation magnitudes of 5 V or less, monophasic stimulation produced more facilitation compared with biphasic stimulation with the exception of synapses on the distal tips of dendrites and the largest synapse weight (4.783 nS).

Examples of facilitation using biphasic and monophasic stimulation were shown, including the facilitation windows. Each of these examples showed facilitation windows with the synapse triggered both before and after the stimulation pulse. However, for all the examples, there exists an optimal time delay between the synaptic input and the stimulation pulse which results in the "least effort" facilitation (lowest magnitude stimulation and lowest synapse weight). For the biphasic examples, the "least effort" timing occurs if the synaptic input occurs before the stimulation pulse and the stimulation pulse occurs when the ion channel variable m_{IKdrSM} is at a maximum for ion channels near the synapse and h_{INaSM} is at a minimum near the synapse. For some of the monophasic examples, the "least effort" facilitation timing is such that the synaptic input and the stimulation pulse occur at the same time. For the rest of the monophasic examples, the "least effort" facilitation occurs when the stimulation pulse occurs after the synaptic input and when V_m is at a maximum at the synapse location, m_{IKdrSM} is approaching maximum, m_{IKaSM} is close to maximum, m_{INaSM} is near maximum, and h_{INaSM} is approaching minimum. A more comprehensive study of the facilitation windows and "least effort" facilitation timing is an important future issue to be considered.

A search for features which separate simulations of neurons resulting in facilitation from simulations that did not result in facilitation was conducted. I found that the

features ($V_{static}^{\text{Synapse}} - V_{static}^{\text{Soma}}$, $V_{static}^{\text{IS}} - V_{static}^{\text{Soma}}$) based on the static volume conductor simulations were able to separate many of the facilitated (and activated by stimulation only) neurons from non-activated neurons. These static voltage features are much more readily computed than the time-domain volume conductor simulations and NEURON simulations, so a machine learning algorithm could likely be built around these or similar features to find optimal facilitation configurations while reducing computation time.

6.1 Discussion

This is the first large scale computational study of facilitation of synaptic input with electrical stimulation. Direct activation and robust facilitation of interneurons in the spinal cord were found to occur at biologically relevant stimulation thresholds. The facilitation occurs as a result of the temporal interaction between the synapse conductance, the stimulation pulse, and the ion channel dynamics (particularly the ion channels close to the synaptic input). After a stimulation pulse or synaptic input, the ion channel dynamics are slower to return to a resting state than the membrane voltage. These dynamics lead to facilitation window(s) (or periods of time) before and/or after a stimulation pulse during which a sub-threshold synaptic input is able to control the output of a neuron. This means that there is no strict requirement that the synapse input occur exactly at the same time as the stimulation pulse. The size of these facilitation windows depends on the stimulation voltage, synapse weight, geometry and orientation of the neuron, stimulation geometry, and synapse location. The maximum width of these facilitation windows is ~115 ms for the models that were studied and a significant amount of the facilitation window(s) are at least 25 ms wide. A facilitation window with a width of 25 ms means that if the sub-threshold stimulation pulses occur with a frequency of 40 Hz, some of the neurons in the spinal cord will be almost continuously facilitated. Current rodent model

stimulation experiments have found that stepping is best recovered with stimulation pulse frequencies of 40-60Hz (Parag Gad, Roy, Choe, Creagmile, et al., 2015). One hypothesis for the narrow frequency tuning of good motor recovery is that this is due to a network effect (Jilge et al., 2004). The discovery of the facilitation window in this thesis suggests another hypothesis: the optimum stimulation frequency is the one that results in near constant facilitation of synaptic input without causing too much direct activation of neurons. Further in vivo or slice experiments with single neuron recording could test this hypothesis.

This thesis is also the first large scale comparison of monophasic vs biphasic electrical stimulation of interneurons in the spinal cord. Monophasic stimulation resulted in more interneuron activation and facilitation compared with the same magnitude of biphasic stimulation. However, the decreased amount of direct activation of interneurons from biphasic stimulation may actually allow for a wider range of stimulation voltages to be used for facilitation without causing direct interneuron activation. There are also some differences in the timing of the facilitation windows for biphasic and monophasic stimulation (summarized earlier in this chapter). It remains to be seen whether this effect could be used intelligently to modulate response to sensory input as a function of step cycle or some other function. Phase dependent modulation of spinal neurons has been found to improve balance and gait in spinal rodent models (Moraud et al., 2016). This study also suggests an additional control parameter which could be used for precise modulation of key spinal neurons during a gait cycle.

For this application, the activating function (Rattay, 1999) is not as useful a predictor of facilitation or activation compared with other features such as gradients of voltage along different parts of the neuron's geometry. The activating function is still used as a standard predictor of neuron activation in the field, but others have noticed that the activation function was less predictive (Zierhofer, Feb./2001).

6.2 Comparing with the literature

There are very few studies that use comprehensive computational models to study epidural stimulation in spinal cord injury. None of these studies have considered the facilitation effect. Previous studies used direct activation (as measured by action potential generation) of a neuron without synaptic input as the criteria for neuron recruitment. Previous models have used computational models to support specific hypotheses about the primary neural mechanisms of epidurally stimulated recovery. The discovery of the facilitation mechanism supports alternative explanations for the roles of key neural populations in spinally stimulated recovery.

As mentioned in Section 1.1, Capogrosso et al., 2013 concluded that activation of interneurons in the spinal cord was not possible in commonly used stimulation ranges. There are significant differences in our models (most of which are described in Section 1.1). In particular, their model uses a neuron with a larger dendritic arbor, larger diameter axon, and larger soma, all of which would make direct activation harder. The size of the neuron that I have modeled is in the distribution of neurons presented in Thurbon et al., 1998 Table 3 (see Section 3.2 for more details).

An important difference is their use of passive dendrites with limited support of synaptic input. My results indicate that the behavior of the ion channels in the dendrites is critical to the facilitation effect. I propose that the facilitation effect is an important consideration for determining the activity, the role, and the relative importance of particular spinal neural populations.

The computational work in this thesis suggests that facilitation of interneurons in the postural control circuitry may be an important, if not critical, part of motor recovery. This implies that multi-electrode epidural stimulating arrays should be designed to facilitate the functions of interneurons in the gray matter of the spinal cord. The absence of this facilitation may hamper the neural pathways that transmit

critical information from muscle spindle feedback, which has been proposed as a key mechanism for epidural stimulation in SCI (Moraud et al., 2016). This observation also suggests that future epidural stimulating arrays should be designed to provide adequate facilitation of these critical pathways.

6.3 Future work

While multi-electrode epidural stimulating arrays were originally designed for reducing and/or blocking pain, there has been little study of electrode design that is specialized for spinal cord injury recovery. With current array designs, it is likely that facilitation of interneurons plays a role in recovery of motor function. As researchers design new stimulation arrays, it may be important to design them to optimize the facilitation of interneurons rather than just focusing on the dorsal roots. Otherwise, the new designs may make it harder to facilitate interneurons. The work in this thesis can provide a starting point for the computational design of new electrode arrays. A simple, but computationally intensive, approach could use the following cycle. First, propose a multi-electrode geometry, the methods introduced in this thesis can then be used to determine the degree of facilitation in a spinal region of interest. The gradient of a function which measures the quality of the facilitation is then used to adjust the array design parameters. The updated array is then used to restart the cycle.

There may also be ways to tune the stimulation waveform to optimize the effect on the ion channels or perhaps precondition the ion channel states so that they are more responsive to future stimuli. One approach to study this problem would be to use linear quasi-active approximations to the ion channels similar to that found in Remme and Rinzel, 2011. Remme and Rinzel, 2011 studied the role of active ion channels found that each ion channel conductance propagation and summation of excitatory postsynaptic potentials (EPSPs) without external stimulation. They

found that ion channels can contribute to either a regenerative membrane current which amplifies the effect of the EPSP, or a restorative current, which accelerates the decay of the EPSP. The extension of their model to include external stimulation could provide a starting point for the analysis of the optimal stimulating waveform shape. This linearized model would have to be augmented with numerical simulations to obtain the truly optimal waveform. The detailed time domain simulations in this thesis would support the computational study of new waveform shapes. An optimization cycle analogous to the one described above could be used. Another way to alter ion channel states would be with pharmacological methods.

BIBLIOGRAPHY

Aló, Kenneth M. and Jan Holsheimer (2002). "New Trends in Neuromodulation for the Management of Neuropathic Pain". In: *Neurosurgery* 50.4, pp. 690–704. ISSN: 0148-396X, 1524-4040. DOI: 10.1097/00006123-200204000-00003. URL: https://academic.oup.com/neurosurgery/article/50/4/690/2757151 (visited on 09/06/2018).

Anastassiou, Costas A et al. (2011). "Ephaptic Coupling of Cortical Neurons". In: *Nature Neuroscience* 14.2, pp. 217–223. ISSN: 1097-6256, 1546-1726. DOI: 10.1038/nn.2727. URL: http://www.nature.com/doifinder/10.1038/nn.2727 (visited on 05/21/2012).

Asboth, Leonie et al. (2018). "Cortico–Reticulo–Spinal Circuit Reorganization Enables Functional Recovery after Severe Spinal Cord Contusion". In: *Nature Neuroscience* 21.4, pp. 576–588. ISSN: 1546-1726. DOI: 10.1038/s41593-018-0093-5. URL: https://www.nature.com/articles/s41593-018-0093-5 (visited on 09/25/2018).

Borland, D. and R. M. Taylor Ii (2007). "Rainbow Color Map (Still) Considered Harmful". In: *IEEE Computer Graphics and Applications* 27.2, pp. 14–17. ISSN: 0272-1716. DOI: 10.1109/MCG.2007.323435.

Cahill, Anthony, Heidi Fredine, and Luciana Zilberman (2009). "Initial briefing: Prevalence of paralysis including spinal cord injuries in the United States, 2008". In: *Technical Document* 41609, pp. 1–60.

Capogrosso, Marco et al. (2013). "A Computational Model for Epidural Electrical Stimulation of Spinal Sensorimotor Circuits". In: *The Journal of Neuroscience* 33.49, pp. 19326–19340. ISSN: 0270-6474, 1529-2401. DOI: 10.1523/JNEUROSCI.1688-13.2013. pmid: 24305828. URL: http://www.jneurosci.org/content/33/49/19326 (visited on 06/03/2014).

Chemical Rubber Company (2012). *CRC handbook of chemistry and physics*. Electronic ed. Boca Raton: CRC Press. URL: http://sfx.caltech.edu:8088/caltech?sid=III:innopac&svc.fulltext=yes&sfx.ignore%20date%20threshold=1&pid=id=1539-2244 (visited on 11/25/2012).

Coburn, B. (1980). "Electrical Stimulation of the Spinal Cord: Two-Dimensional Finite Element Analysis with Particular Reference to Epidural Electrodes". In: *Medical and Biological Engineering and Computing* 18.5, pp. 573–584. ISSN: 1741-0444. DOI: 10.1007/BF02443129. URL: https://doi.org/10.1007/BF02443129 (visited on 09/13/2018).

– (1988). "Theoretical Modelling of Neurostimulation". In: *Engineering Design for the Disabled, IEE Colloquium On*, pp. 4–1.

Coburn, Barry (1985). “A Theoretical Study of Epidural Electrical Stimulation of the Spinal Cord - Part II: Effects on Long Myelinated Fibers”. In: *IEEE Transactions on Biomedical Engineering* BME-32.11, pp. 978–986. ISSN: 0018-9294. DOI: 10.1109/TBME.1985.325649. URL: http://ieeexplore.ieee.org/document/4121976/ (visited on 09/06/2018).

Coburn, Barry and Wing Kee Sin (1985). “A Theoretical Study of Epidural Electrical Stimulation of the Spinal Cord Part I: Finite Element Analysis of Stimulus Fields”. In: *IEEE Transactions on Biomedical Engineering* BME-32.11, pp. 971–977. ISSN: 0018-9294. DOI: 10.1109/TBME.1985.325648. URL: http://ieeexplore.ieee.org/document/4121975/ (visited on 09/12/2018).

Cole, Kenneth S. and Robert H. Cole (1941). “Dispersion and Absorption in Dielectrics I. Alternating Current Characteristics”. In: *The Journal of Chemical Physics* 9.4, p. 341. ISSN: 00219606. DOI: 10.1063/1.1750906. URL: http://link.aip.org/link/JCPSA6/v9/i4/p341/s1&Agg=doi (visited on 05/31/2012).

Cook, A. W. and S. P. Weinstein (1973). “Chronic Dorsal Column Stimulation in Multiple Sclerosis. Preliminary Report.” In: *New York state journal of medicine* 73.24, pp. 2868–2872.

Courtine, Grégoire et al. (2009). “Transformation of Nonfunctional Spinal Circuits into Functional States after the Loss of Brain Input”. In: *Nature Neuroscience* 12.10, pp. 1333–1342. ISSN: 1097-6256, 1546-1726. DOI: 10.1038/nn.2401. URL: http://www.nature.com/doifinder/10.1038/nn.2401 (visited on 11/29/2012).

De Geeter, N. et al. (2012). “A DTI-based model for TMS using the independent impedance method with frequency-dependent tissue parameters”. In: *Physics in Medicine and Biology* 57, p. 2169.

Desautels, Thomas et al. (2015). “An Active Learning Algorithm for Control of Epidural Electrostimulation”. In: *IEEE transactions on bio-medical engineering* 62. DOI: 10.1109/TBME.2015.2431911.

Destexhe, Alain, Zachary F. Mainen, and Terrence J. Sejnowski (1994). “Synthesis of models for excitable membranes, synaptic transmission and neuromodulation using a common kinetic formalism”. In: *Journal of computational neuroscience* 1.3, pp. 195–230. URL: http://link.springer.com/article/10.1007/BF00961734 (visited on 03/22/2017).

Edgerton, V. Reggie et al. (2008). “Training Locomotor Networks”. In: *Brain research reviews* 57.1, pp. 241–254. ISSN: 0165-0173. DOI: 10.1016/j.brainresrev.2007.09.002. pmid: 18022244. URL: https://www.ncbi.nlm.nih.gov/pmc/articles/PMC2288528/ (visited on 09/06/2018).

ElBasiouny, Sherif M. and Vivian K. Mushahwar (2007). "Suppressing the Excitability of Spinal Motoneurons by Extracellularly Applied Electrical Fields: Insights from Computer Simulations". In: *Journal of Applied Physiology* 103.5, pp. 1824–1836. ISSN: 8750-7587, 1522-1601. DOI: 10.1152/japplphysiol.00362.2007. URL: http://jap.physiology.org/content/103/5/1824 (visited on 12/24/2012).

Gabriel, C. (1996). *Compilation of the Dielectric Properties of Body Tissues at RF and Microwave Frequencies.* Tech. rep. DTIC Document.

Gabriel, C. and S. Gabriel (1997). *Compilation of the Dielectric Properties of Body Tissues at RF and Microwave Frequencies*. URL: http://niremf.ifac.cnr.it/docs/DIELECTRIC/Title.html (visited on 09/05/2018).

Gabriel, C., S. Gabriel, and E. Corthout (1996). "The Dielectric Properties of Biological Tissues: I. Literature Survey". In: *Physics in medicine and biology* 41, p. 2231.

Gad, Parag, Jaehoon Choe, et al. (2013). "Development of a multi-electrode array for spinal cord epidural stimulation to facilitate stepping and standing after a complete spinal cord injury in adult rats". In: *Journal of NeuroEngineering and Rehabilitation* 10, p. 2. ISSN: 1743-0003. DOI: 10.1186/1743-0003-10-2. URL: http://dx.doi.org/10.1186/1743-0003-10-2 (visited on 06/24/2016).

Gad, Parag, Roland R. Roy, Jaehoon Choe, Jack Creagmile, et al. (2015). "Electrophysiological Biomarkers of Neuromodulatory Strategies to Recover Motor Function after Spinal Cord Injury". In: *Journal of Neurophysiology* 113.9, pp. 3386–3396. ISSN: 0022-3077. DOI: 10.1152/jn.00918.2014. URL: https://www.physiology.org/doi/abs/10.1152/jn.00918.2014 (visited on 09/12/2018).

Gad, Parag, Roland R. Roy, Jaehoon Choe, Hui Zhong, et al. (2015). "Electrophysiological Mapping of Rat Sensorimotor Lumbosacral Spinal Networks after Complete Paralysis". In: *Progress in brain research* 218, pp. 199–212. ISSN: 0079-6123. DOI: 10.1016/bs.pbr.2015.01.005. pmid: 25890138. URL: https://www.ncbi.nlm.nih.gov/pmc/articles/PMC4512743/ (visited on 09/12/2018).

Gad, P. et al. (2012). "Forelimb EMG-Based Trigger to Control an Electronic Spinal Bridge to Enable Hindlimb Stepping after a Complete Spinal Cord Lesion in Rats". In: *Journal of NeuroEngineering and Rehabilitation* 9.1, p. 38. ISSN: 1743-0003. URL: http://www.jneuroengrehab.com/content/pdf/1743-0003-9-38.pdf.

Gerasimenko, Yury et al. (2015). "Initiation and Modulation of Locomotor Circuitry Output with Multisite Transcutaneous Electrical Stimulation of the Spinal Cord in Noninjured Humans". In: *Journal of Neurophysiology* 113.3, pp. 834–842. ISSN: 0022-3077, 1522-1598. DOI: 10.1152/jn.00609.2014. URL:

http://www.physiology.org/doi/10.1152/jn.00609.2014 (visited on 09/25/2018).

Gill, Megan L. et al. (2018). "Neuromodulation of Lumbosacral Spinal Networks Enables Independent Stepping after Complete Paraplegia". In: *Nature Medicine*, p. 1. ISSN: 1546-170X. DOI: 10.1038/s41591-018-0175-7. URL: https://www.nature.com/articles/s41591-018-0175-7 (visited on 09/26/2018).

Gold, Carl et al. (2009). "High-Amplitude Positive Spikes Recorded Extracellularly in Cat Visual Cortex". In: *Journal of neurophysiology* 102.6, pp. 3340–3351.

Grobelnik, Slobodan and A. Kralj (1973). "Functional Electrical Stimulation—a New Hope for Paraplegic Patients". In: *Bull. Prosthet. Res* 20, pp. 75–102.

Gudjonsson, Sk. V. (1932). "The body temperature in rats on normal and deficient diets". In: *The Journal of Physiology* 74.1. PMID: 16994260 PMCID: PMC1394435, pp. 73–80. ISSN: 0022-3751. URL: http://www.ncbi.nlm.nih.gov/pmc/articles/PMC1394435/ (visited on 10/04/2012).

Gulani, Vikas et al. (1997). "A multiple echo pulse sequence for diffusion tensor imaging and its application in excised rat spinal cords". In: *Magnetic Resonance in Medicine* 38.6, pp. 868–873. ISSN: 1522-2594. DOI: 10.1002/mrm.1910380603. URL: http://onlinelibrary.wiley.com/doi/10.1002/mrm.1910380603/abstract (visited on 02/17/2017).

Harkema, S. et al. (2011). "Effect of Epidural Stimulation of the Lumbosacral Spinal Cord on Voluntary Movement, Standing, and Assisted Stepping after Motor Complete Paraplegia: A Case Study". In: *Lancet* 377.9781, pp. 1938–1947. ISSN: 01406736. DOI: 10.1016/S0140-6736(11)60547-3. URL: http://www.sciencedirect.com/science/article/pii/S0140673611605473.

Hines, M. L. and N. T. Carnevale (2001). "Neuron: A Tool for Neuroscientists". In: *The Neuroscientist* 7.2, pp. 123–135. ISSN: 1073-8584, 1089-4098. DOI: 10.1177/107385840100700207. URL: http://journals.sagepub.com/doi/10.1177/107385840100700207 (visited on 09/28/2018).

Hines, Michael L. and Nicholas T. Carnevale (1997). "The NEURON Simulation Environment". In: *Neural computation* 9.6, pp. 1179–1209.

Holsheimer, J. and J. J Struijk (1992). "Electrode Geometry and Preferential Stimulation of Spinal Nerve Fibers Having Different Orientations: A Modeling Study". In: *Engineering in Medicine and Biology Society, 1992 14th Annual International Conference of the IEEE*. Vol. 4, pp. 1374–1375.

Holt, Gary R. and Christof Koch (1999). "Electrical Interactions via the Extracellular Potential near Cell Bodies". In: *Journal of computational neuroscience* 6.2, pp. 169–184.

Hosobuchi, Yoshio, John E. Adams, and Rita Linchitz (1977). "Pain Relief by Electrical Stimulation of the Central Gray Matter in Humans and Its Reversal by Naloxone". In: *Science* 197.4299, pp. 183–186.

Illis, L. S., E. M. Sedgwick, and R. C. Tallis (1980). "Spinal Cord Stimulation in Multiple Sclerosis: Clinical Results." In: *Journal of Neurology, Neurosurgery & Psychiatry* 43.1, pp. 1–14. ISSN: 0022-3050, 1468-330X. DOI: 10.1136/jnnp.43.1.1. pmid: 7354351. URL: https://jnnp.bmj.com/content/43/1/1 (visited on 09/13/2018).

Jilge, Bernhard et al. (2004). "Frequency-dependent selection of alternative spinal pathways with common periodic sensory input". In: *Biological Cybernetics* 91.6, pp. 359–376. ISSN: 0340-1200, 1432-0770. DOI: 10.1007/s00422-004-0511-5. URL: http://www.springerlink.com/index/10.1007/s00422-004-0511-5 (visited on 05/17/2012).

Kahouli, A et al. (2012). "Effect of O2, Ar/H2 and CF4 plasma treatments on the structural and dielectric properties of parylene-C thin films". In: *Journal of Physics D: Applied Physics* 45.21, p. 215306. ISSN: 0022-3727, 1361-6463. DOI: 10.1088/0022-3727/45/21/215306. URL: http://iopscience.iop.org/0022-3727/45/21/215306 (visited on 09/19/2012).

Ladenbauer, Josef (2008). "Simulation of the Excitation of Human Lower Spinal Cord Structures with Surface Electrodes". In: p. 86.

Ladenbauer, J et al. (2010). "Stimulation of the Human Lumbar Spinal Cord With Implanted and Surface Electrodes: A Computer Simulation Study". In: *IEEE Transactions on Neural Systems and Rehabilitation Engineering* 18.6, pp. 637–645. ISSN: 1534-4320, 1558-0210. DOI: 10.1109/TNSRE.2010.2054112. URL: http://ieeexplore.ieee.org/lpdocs/epic03/wrapper.htm?arnumber=5497186 (visited on 05/20/2012).

Lempka, Scott F. et al. (2015). "Computational Analysis of Kilohertz Frequency Spinal Cord Stimulation for Chronic Pain Management". In: *Anesthesiology: The Journal of the American Society of Anesthesiologists* 122.6, pp. 1362–1376. ISSN: 0003-3022. DOI: 10.1097/ALN.0000000000000649. URL: http://anesthesiology.pubs.asahq.org/article.aspx?articleid=2235353 (visited on 09/12/2018).

Leseal, C (1982). "Electronic and Ionic Polarizabilities of Silicate Minerals". In: *American Mineralogist* 67, pp. 328–334.

Liu, Yang and Jeffrey Heer (2018). "Somewhere Over the Rainbow: An Empirical Assessment of Quantitative Colormaps". In: *Proceedings of the 2018 CHI Conference on Human Factors in Computing Systems*. CHI '18. Montreal QC, Canada: ACM, 598:1–598:12. ISBN: 978-1-4503-5620-6. DOI: 10.1145/3173574.3174172. URL: http://doi.acm.org/10.1145/3173574.3174172.

Lynch, C. L. and M. R. Popovic (2008). "Functional Electrical Stimulation". In: *IEEE Control Systems Magazine* 28.2, pp. 40–50. ISSN: 1066-033X. DOI: 10.1109/MCS.2007.914689.

McIntyre, Cameron C and Warren M Grill (2002). "Extracellular stimulation of central neurons: influence of stimulus waveform and frequency on neuronal output". In: *Journal of neurophysiology* 88.4, pp. 1592–1604. ISSN: 0022-3077.

Moraud, Eduardo Martin et al. (2016). "Mechanisms Underlying the Neuromodulation of Spinal Circuits for Correcting Gait and Balance Deficits after Spinal Cord Injury". In: *Neuron* 89.4, pp. 814–828. ISSN: 0896-6273. DOI: 10.1016/j.neuron.2016.01.009. URL: http://www.sciencedirect.com/science/article/pii/S0896627316000106 (visited on 10/03/2018).

Nunes, Daniel et al. (2017). "Mapping Axonal Density and Average Diameter Using Non-Monotonic Time-Dependent Gradient-Echo MRI". In: *Journal of Magnetic Resonance* 277, pp. 117–130.

Orfanidis, Sophocles J (2016). *Electromagnetic Waves and Antennas*. URL: http://www.ece.rutgers.edu/orfanidi/ewa (visited on 09/05/2018).

Ostroumov, Konstantin (2007). "A new stochastic tridimensional model of neonatal rat spinal motoneuron for investigating compartmentalization of neuronal conductances and their influence on firing". In: *Journal of Neuroscience Methods* 163.2, pp. 362–372. ISSN: 0165-0270. DOI: 10.1016/j.jneumeth.2007.03.003. URL: http://www.sciencedirect.com/science/article/pii/S0165027007001343 (visited on 12/22/2012).

Ranck Jr., James B. and Spencer L. BeMent (1965). "The specific impedance of the dorsal columns of cat: An anisotropic medium". In: *Experimental Neurology* 11.4, pp. 451–463. ISSN: 0014-4886. DOI: 10.1016/0014-4886(65)90059-2. URL: http://www.sciencedirect.com/science/article/pii/0014488665900592 (visited on 06/10/2015).

Rattay, F. (1999). "The Basic Mechanism for the Electrical Stimulation of the Nervous System". In: *Neuroscience* 89.2, pp. 335–346. ISSN: 03064522. DOI: 10.1016/S0306-4522(98)00330-3. URL: http://linkinghub.elsevier.com/retrieve/pii/S0306452298003303 (visited on 09/12/2018).

Remme, Michiel W. H. and John Rinzel (2011). "Role of Active Dendritic Conductances in Subthreshold Input Integration". In: *Journal of Computational Neuroscience* 31.1, pp. 13–30. ISSN: 0929-5313, 1573-6873. DOI: 10.1007/s10827-010-0295-7. URL: http://link.springer.com/10.1007/s10827-010-0295-7 (visited on 10/29/2018).

Richardson, A. G., C. C. McIntyre, and W. M. Grill (2000). "Modelling the Effects of Electric Fields on Nerve Fibres: Influence of the Myelin Sheath". In: *Medical and Biological Engineering and Computing* 38.4, pp. 438–446. URL: http://

www.springerlink.com/index/EH30T5X34WH93013.pdf (visited on 12/17/2012).

Rubinstein, J.T. (1991). "Analytical Theory for Extracellular Electrical Stimulation of Nerve with Focal Electrodes. II. Passive Myelinated Axon". In: *Biophysical Journal* 60.3, pp. 538–555. ISSN: 00063495. DOI: 10.1016/S0006-3495(91)82084-7. URL: http://linkinghub.elsevier.com/retrieve/pii/S0006349591820847 (visited on 09/12/2018).

Rubinstein, J.T. and F.A. Spelman (1988). "Analytical Theory for Extracellular Electrical Stimulation of Nerve with Focal Electrodes. I. Passive Unmyelinated Axon". In: *Biophysical Journal* 54.6, pp. 975–981. ISSN: 00063495. DOI: 10.1016/S0006-3495(88)83035-2. URL: http://linkinghub.elsevier.com/retrieve/pii/S0006349588830352 (visited on 09/12/2018).

Safronov, Boris V., Matthias Wolff, and Werner Vogel (2000). "Excitability of the Soma in Central Nervous System Neurons". In: *Biophysical Journal* 78.6, pp. 2998–3010. ISSN: 0006-3495. DOI: 10.1016/S0006-3495(00)76838-X. URL: http://www.sciencedirect.com/science/article/pii/S000634950076838X (visited on 09/18/2018).

Saliani, Ariane et al. (2017). "Axon and Myelin Morphology in Animal and Human Spinal Cord". In: *Frontiers in Neuroanatomy* 11. ISSN: 1662-5129. DOI: 10.3389/fnana.2017.00129. URL: http://journal.frontiersin.org/article/10.3389/fnana.2017.00129/full (visited on 09/12/2018).

Santos, Sónia F. A. et al. (2009). "Transmission Efficacy and Plasticity in Glutamatergic Synapses Formed by Excitatory Interneurons of the Substantia Gelatinosa in the Rat Spinal Cord". In: *PLOS ONE* 4.11, e8047. ISSN: 1932-6203. DOI: 10.1371/journal.pone.0008047. URL: http://journals.plos.org/plosone/article?id=10.1371/journal.pone.0008047 (visited on 05/25/2017).

Saywell, S. A. et al. (2011). "Electrophysiological and Morphological Characterization of Propriospinal Interneurons in the Thoracic Spinal Cord". In: *Journal of Neurophysiology* 105.2, pp. 806–826. ISSN: 0022-3077, 1522-1598. DOI: 10.1152/jn.00738.2010. URL: http://www.physiology.org/doi/10.1152/jn.00738.2010 (visited on 09/14/2018).

Scheffler, Marc et al. (2005). "Extremely Slow Drude Relaxation of Correlated Electrons". In: *Nature* 438.7071, pp. 1135–1137. ISSN: 1476-4687. DOI: 10.1038/nature04232. URL: https://www.nature.com/articles/nature04232 (visited on 08/31/2018).

Shealy, C. Norman, J. T. Mortimer, and J. B. Reswick (1967). "Electrical Inhibition of Pain by Stimulation of the Dorsal Columns". In: *Anesth Analg* 46.4, pp. 489–491.

Struijk, J.J., J. Holsheimer, G.G. van der Heide, et al. (Sept./1992). "Recruitment of Dorsal Column Fibers in Spinal Cord Stimulation: Influence of Collateral Branching". In: *IEEE Transactions on Biomedical Engineering* 39.9, pp. 903–912. ISSN: 00189294. DOI: 10.1109/10.256423. URL: http://ieeexplore.ieee.org/document/256423/ (visited on 09/06/2018).

Struijk, J.J., J. Holsheimer, B.K. van Veen, et al. (Jan./1991). "Epidural Spinal Cord Stimulation: Calculation of Field Potentials with Special Reference to Dorsal Column Nerve Fibers". In: *IEEE Transactions on Biomedical Engineering* 38.1, pp. 104–110. ISSN: 00189294. DOI: 10.1109/10.68217. URL: http://ieeexplore.ieee.org/document/68217/ (visited on 09/06/2018).

Struijk, Johannes J., Jan Holsheimer, and Herman BK Boom (1993). "Excitation of Dorsal Root Fibers in Spinal Cord Stimulation: A Theoretical Study". In: *IEEE Transactions on Biomedical Engineering* 40.7, pp. 632–639. URL: http://doc.utwente.nl/15352/ (visited on 06/09/2015).

Thrasher, T. A., H. M. Flett, and M. R. Popovic (2006). "Gait Training Regimen for Incomplete Spinal Cord Injury Using Functional Electrical Stimulation". In: *Spinal Cord* 44.6, pp. 357–361. ISSN: 1476-5624. DOI: 10.1038/sj.sc.3101864. URL: https://www.nature.com/articles/3101864 (visited on 09/24/2018).

Thurbon, David et al. (1998). "Passive Electrical Properties of Ventral Horn Neurons in Rat Spinal Cord Slices". en. In: *Journal of Neurophysiology* 79.5, pp. 2485–2502. ISSN: 0022-3077, 1522-1598. URL: http://jn.physiology.org/content/79/5/2485 (visited on 12/24/2012).

Tranchina, D. and C. Nicholson (1986). "A Model for the Polarization of Neurons by Extrinsically Applied Electric Fields". In: *Biophysical Journal* 50.6, pp. 1139–1156. ISSN: 00063495. DOI: 10.1016/S0006-3495(86)83558-5. URL: http://linkinghub.elsevier.com/retrieve/pii/S0006349586835585 (visited on 09/06/2018).

Urban, Luke Stuart (2018). "An Electrophysiological Study Of Voluntary Movement and Spinal Cord Injury". phd. California Institute of Technology. DOI: 10.7907/K6P2-ZH75. URL: http://resolver.caltech.edu/CaltechTHESIS:06012018-140912331 (visited on 09/03/2018).

Veraart, C., W. M. Grill, and J. T. Mortimer (1993). "Selective Control of Muscle Activation with a Multipolar Nerve Cuff Electrode". In: *IEEE Transactions on Biomedical Engineering* 40.7, pp. 640–653. ISSN: 0018-9294. DOI: 10.1109/10.237694.

Ye, Hui and Amanda Steiger (2015). "Neuron Matters: Electric Activation of Neuronal Tissue Is Dependent on the Interaction between the Neuron and the Electric Field". In: *Journal of NeuroEngineering and Rehabilitation* 12.1. ISSN: 1743-

0003. DOI: 10.1186/s12984-015-0061-1. URL: http://www.jneuroengrehab.com/content/12/1/65 (visited on 10/03/2018).

Yushkevich, Paul A. et al. (2006). “User-Guided 3D Active Contour Segmentation of Anatomical Structures: Significantly Improved Efficiency and Reliability”. In: *Neuroimage* 31.3, pp. 1116–1128.

Zhang, Xiaowei et al. (2010). “Increased anatomical detail by in vitro MR microscopy with a modified Golgi impregnation method”. eng. In: *Magnetic Resonance in Medicine* 63.5, pp. 1391–1397. ISSN: 1522-2594. DOI: 10.1002/mrm.22322.

Zierhofer, C.M. (Feb./2001). “Analysis of a Linear Model for Electrical Stimulation of Axons-Critical Remarks on the "Activating Function Concept"”. In: *IEEE Transactions on Biomedical Engineering* 48.2, pp. 173–184. ISSN: 00189294. DOI: 10.1109/10.909638. URL: http://ieeexplore.ieee.org/document/909638/ (visited on 10/02/2018).

INDEX